The First European Seminar on

Computerised Axial Tomography in Clinical Practice

Edited by
G. H. du Boulay and I. F. Moseley

With 335 Figures

Springer-Verlag
Berlin Heidelberg New York 1977

Professor Dr. GEORGE DU BOULAY and Dr. IVAN F. MOSELEY
Lysholm Radiological Department, The National Hospital, Queen Square,
London WC1N 3BG

ISBN-13: 978-3-540-08116-6 e-ISBN-13: 978-3-642-66594-3
DOI: 10.1007/978-3-642-66594-3

Library of Congress Cataloging in Publication Data. European Seminar on Computerised Axial Tomography in Clinical Practice, 1st, London, 1976. The First European Seminar on Computerised Axial Tomography in Clinical Practice. Includes index. 1. Tomography--Congresses. I. Du Boulay, G. H., II. Moseley, Ivan F., 1940-. RC78.7.T6E93. 1976. 616.07'572. 77-1618.

Printing and bookbinding: Beltz Offsetdruck, Hemsbach.

Introduction

The publication of proceedings of conferences has often been so delayed that they are useless both to active workers in the field and for currently appropriate teaching. Rapid publication on the other hand may impose very difficult conditions upon authors and demand unwelcome sacrifices. We wish to thank the many speakers at ESCAT for their cooperation in providing manuscripts and to apologise to those unable for reasons beyond their control to fall in with the rigorous editorial policy. To get this book out at the earliest possible moment we have also cut the normal consultation between editors and authors to a minimum. One decision made in the interests of uniformity was to replace the various terms used by different writers by one, C.A.T., consistent with the title of the Seminar of which the book is a record.

The organisers of ESCAT decided upon a largely didactic meeting with as little overlap as was practicable between contributions and a determined attempt to view computerised axial tomography in the light of its clinical usefulness. As consequence, the purpose of this book is to provide a comprehensive introduction to the whole field for clinicians as well as radiologists.

The editors wish to acknowledge the very efficient help and encouragement of the publishers and the hard secretarial work of Miss G. JOHNS, as well as the editorial assistance of Dr. DEREK KINGSLEY.

London, Spring 1977 G.H. DU BOULAY · I.F. MOSELEY

Foreword

It is a pleasure to write the Foreword to the Proceedings of the European Seminar on computerised axial tomography held recently in London.

It seems incredible that it is still less than 5 years since Dr. GODFREY HOUNSFIELD described to the world his revolutionary radiological technique whereby the very first patient ever examined by his machine was shown to have a brain tumour. Until his discovery X-ray photography had not advanced fundamentally since RÖNTGEN X-rayed his wife's hand in his laboratory at Würzburg in 1895.

The result of HOUNSFIELD'S discovery has been to transform investigative medicine (especially of the nervous system), and his method is already being used in all the continents of the world.

It may be asked why London (the home of the discovery) has held back in staging a conference while other places have not shown this hesitation. The answer is that the local organisers felt that enough time should elapse to allow judgement of some maturity to be made of the value of both the brain and the body scanner. HOUNSFIELD'S first machine was designed for the brain and it is only recently that the rest of the body has been investigated satisfactorily by his technique. For this reason the Seminar was planned so that about two thirds of the week was devoted to the brain and orbits and one third to the body.

The papers which follow are mostly from Europe and a few from America. The contributors are to be congratulated on the high quality of their texts. It can be confidently stated that the contents provide the most up-to-date information available anywhere on this new discipline.

Lastly, great credit is due to the Editors, Professor DU BOULAY and Dr. MOSELEY, who not only played a very large part in the planning of the Seminar but also, with the aid of the publishers, expedited the publication with a rapidity seldom seen.

J.W.D. BULL

Contents

Diseases of the Brain Parenchyma, Atrophy and Hydrocephalus

Vascular Conditions

Measurements: Physical Considerations

C. A. T. of the Head

Anatomy

Computerised Axial Tomography and the Normal Brain

P. A. Roberts*, L. E. Claveria, and I. F. Moseley

Computerised axial tomography provides a means of examining the intracranial contents expressed as a series of 'slices' through the skull taken in a transaxial plane. The plane of slices may be varied from case to case, depending upon the suspected location of the lesion. Commonly employed angles of the slice are parallel to Reid's base line (R.B.L.), 10° to R.B.L., and 25° to R.B.L. (1). The appearance of the brain prepared in this manner presents a view not normally depicted in most atlases of neuroanatomy. Several authors (1, 2, 3) have published works which include a series of brain slices taken in a particular plane, but comparison of normal anatomy between various different planes of section seems to be lacking.

A series of three brains was prepared in order to make this comparison. 7 mm slices were taken of the fixed brains, one brain being sliced parallel to R.B.L., one at 10° to this plane, and another at 25°. The relative angulation of the slices is shown in Figure 1, projected over the lateral and midline aspects of the brain.

These brain slices were matched with normal tomograms, prepared at similar angles with respect to R.B.L.

Representative views appear in Figures 2, 3 and 4 of the 25° angle. The 10° angle is illustrated in Figures 5, 6 and 7. Planes parallel to R.B.L. are shown in Figures 8, 9 and 10.

In comparing the lowest levels of brain slices, which pass through th posterior fossa, the difference between the appearance of such slices from one angulation to another is apparent. The slice taken at 25° to R.B.L. (Fig. 2A) includes the hemispheres of the cerebellum at the point of their greatest width. The fourth ventriclte is well seen, also at its widest extent. The inferior cerebellar vermis and part of the cisterna magna can be identified. The section passes through the pons at the level of attachment of the trigeminal nerves. The supratentorial regions seen at this level include the inferior surface of the temporal lobes, just above the floor of the middle cranial fossa, but not high enough to include the temporal horns of the lateral ventricles. Anteriorly, the lower portions of the frontal lobes are evident, showing the medially placed rectus gyri and a portion of the slightly higher, laterally located orbital gyri, overlying the upwardly convex roof of the orbit. The accompanying C.A.T. scan shows these features, and, in addition, the high densities due to the presence of part of the orbital roofs, the sphenoid wings separating the frontal lobes from the temporal lobes, and also the petrous bones demarcating the anterior limits of the posterior fossa and the posterior limits of the middle cranial fossa containing the temporal lobes.

The lowermost slice in the series which parallels R.B.L. (Fig. 8A) presents a somewhat different appearance. The cerebellum and fourth

*University of Oklahoma, Health Science Center, Oklahoma City, OK/USA and National Hospital for Nervous Diseases, Queen Square, London W.C.I.

ventricle are transected in their more anterior regions (note the configuration of the fourth ventricle compared with the 25° slice). The pons is cut at less of an oblique angle, the cisterna magna is only seen at its upper extent and the section passes through the superior vermis. The supratentorial structures are not represented at this level. The C.A.T. scan of this region is seen to include the inferior part of the orbits, and thus passes below the frontal lobes; it also just grazes the floor of the middle fossa and traverses the sphenoid air sinuses on the midline.

The brain slice angled at 10° to R.B.L. (parallel to the orbitomeatal line, Fig. 5A), shows the fourth ventricle just anterior to its widest point. Only the most inferior portions of the frontal lobes are present, namely the rectus gyri, adjacent to the midline. The slice passes just above the floor of the middle cranial fossa and thus includes the lowest parts of the temporal lobes. These features may be identified on the lowermost C.A.T. scan at this angulation.

At the next highest level the slice which parallels R.B.L. (Fig. 8B), includes the inferior part of the temporal lobes, but still does not traverse the frontal lobes. The fourth ventricle is shown at its most anterior end, where it is continuous with the posterior portion of the aqueduct. The comparable C.A.T. scan, in addition to these structures, also passes through the midportion of the orbits. Note also the density in the midline near the medial limits of the sphenoid wings. This probably represents the bone density of the dorsum sellae.

The next level of the series, taken at 25° to R.B.L. (Fig. 2B), still displays an excellent view of the posterior fossa structures. The fourth ventricle is still apparent just anterior to its widest point. The cisterna magna is still well shown. Almost the full width of the cerebellar hemispheres are present (note the dentate nuclei are still seen in the deep white matter of the hemispheres).

Supratentorially, the slice is high enough to pass through the superior, middle and inferior frontal gyri. The temporal regions now include the temporal horn of the lateral ventricle, parts of the superior and middle temporal gyri, the medially placed parahippocampal gyri and the uncus. On the midline, the slice passes through the region of the superior portion of the optic chiasm, and also the infundibular recess of the third ventricle, just posterior to the chiasm. The most anterior part of the Sylvian fissure between the frontal lobe and the temporal lobe may also be seen at this level.

The brain slice taken at 10° to R.B.L. (Fig. 5B) differs from the 25° angle mainly in that the fourth ventricle configuration is different due to the slice passing through the anterior, and smaller, portion of the ventricle. The frontal lobes include parts of the orbital gyri, and the inferior part of the optic chiasm appears in the midline.

The temporal lobes display the anterior tips of the temporal horns of the lateral ventricles.

C.A.T. scans of both the 25° and 10° angles indicate the diminished density of the chiasmatic cisterns on the midline, bounded by the brainstem posteriorly, the uncus laterally, and the posterior portion of the frontal lobes, anteriorly.

The next higher level of brain slices in both the 25° (Fig. 3A) and 10° (Fig. 6A) to R.B.L. series have numerous features in common. Both slices are high enough to include the frontal horns of the lateral ventricles, the head of the caudate nucleus (forming the lateral bound-

ary of the frontal horns), and the genu of the corpus callosum. The medial border of the frontal horns in the 25° slice is represented by the septum pellucidum. In the 10° angle slice, the section passes below the septum pellucidum, and, in this instance, the medial border of the frontal horn is formed by the subcallosal gyrus. Both angles of slice show the third ventricle in the midline, as well as the anterior portion of the aqueduct as it traverses the midbrain. The internal capsule is well seen, with the lenticular nucleus, comprising the putamen and globus pallidus, located just lateral to the limbs of the capsule, and the thalamus seen medial to the posterior limb. External capsule, claustrum, extreme capsule and insula cortex are seen on both brain slices, lateral to the lenticular nucleus. The superior colliculus appears on both slices, as do the quadrigeminal cisterns and wings of the ambient cisterns.

The 25° angle slice includes more of the anterior portion of the cerebellum than does the 10° angle cut, which barely grazes the superior vermis. The columns of the fornix are seen near the midline in the steeper angle slice, at the posterior limits of the septum pellucidum, indicating the presence of the foramina of Monroe. In the 10° slice, the cut passes through the anterior commissure on the midline, below the foramen of Monro. Some of these features may be seen on the corresponding C.A.T. scans; particularly the frontal horns, the quadrigeminal cisterns, Sylvian fissures, and the posterior limb of the internal capsule.

The brain slice in the R.B.L. series (Fig. 9A) does not pass through either the third ventricle or the frontal horns of the lateral ventricles. The frontal lobes are represented primarily by the rectus gyri. The optic chiasm appears on this slice, and a small portion of the most superior cerebellum. The C.A.T. scan of this level passes through the superior parts of the orbits and the posterior portion of the optic foramina.

Higher slices in all three series (Figs. 3B, 6B and 9B) pass through the region of the pineal organ, seen in all brain slices in the midline, adjacent to the posterior portions of the thalamus. The series paralleling R.B.L. (Fig. 9B) shows the splenium of the corpus callosum, the parieto-occipital fissure and the visual cortex on the medial side of the occipital lobes posterior to this fissure. The trigone region of the lateral ventricles is also seen, containing the glomus of the choroid plexus. C.A.T. scans at these levels display the densities of the pineal, and choroid plexus and also the reduced density of the retropulvinar cisterns. (Note that the C.A.T. scan of the 10° series does not correspond exactly to the brain slice and does not show the pineal.)

The higher brain slices pass just below the bodies of the lateral ventricles, grazing the superior aspect of the thalamus, but still traversing the frontal horns and the superior part of the trigone, in the 25° (Fig. 4A) and 10° (Fig. 7A) series of slices. In the R.B.L. series (Fig. 10A), the slice still traverses a large part of the lenticular nuclei and the main body of the thalamus. The C.A.T. scan at the 25° angle shows the reduced density of the body of the lateral ventricles. The 10° angle scan shows the pineal density (shining through the overlying splenium of the corpus callosum). The thalamic masses and the internal capsule are seen in the C.A.T. scan of the R.B.L. series.

In the highest cuts illustrated (Figs. 4B, 7B and 10B), all slices except the 10° angle series pass above the bodies of the lateral ventricles. The 10° slice just grazes the body of the ventricles. In the

25° angle slice the central sulcus is located quite anteriorly, consequently more of the parietal lobe is seen than in the other two angles of slice.

The angle at which the C.A.T. scan is taken with respect to R.B.L. does significantly alter the appearance of the intracranial anatomy encountered.

Steeper angles (25° or even greater) offer more views of the posterior fossa and also illustrate the lower portions of this region. However, the upper parts of the parietal and occipital lobes may possibly be better visualized at less angulation. In any event, the differing appearance due to angulation of the scans should be considered in interpretation of these studies.

References

1. GAWLER, J., BULL, J.W.D., DU BOULAY, G.H., MARSHALL, J.: Computerized axial tomography: The normal EMI scan. Journal of Neurology, Neurosurgery and Psychiatry. 38, 935-947 (1975).
2. NEW, P.F.J., SCOTT, W.R.: Computed Tomography of the Brain and Orbit. Baltimore: Williams and Wilkins 1975.
3. SCHOULTZ, T.W., MORRISON, J.R., CALHOUN, J.D.: Atlas of the human brain for use in diagnosis by computer assisted tomography. Surgical Neurology 5, 255-266 (1976).

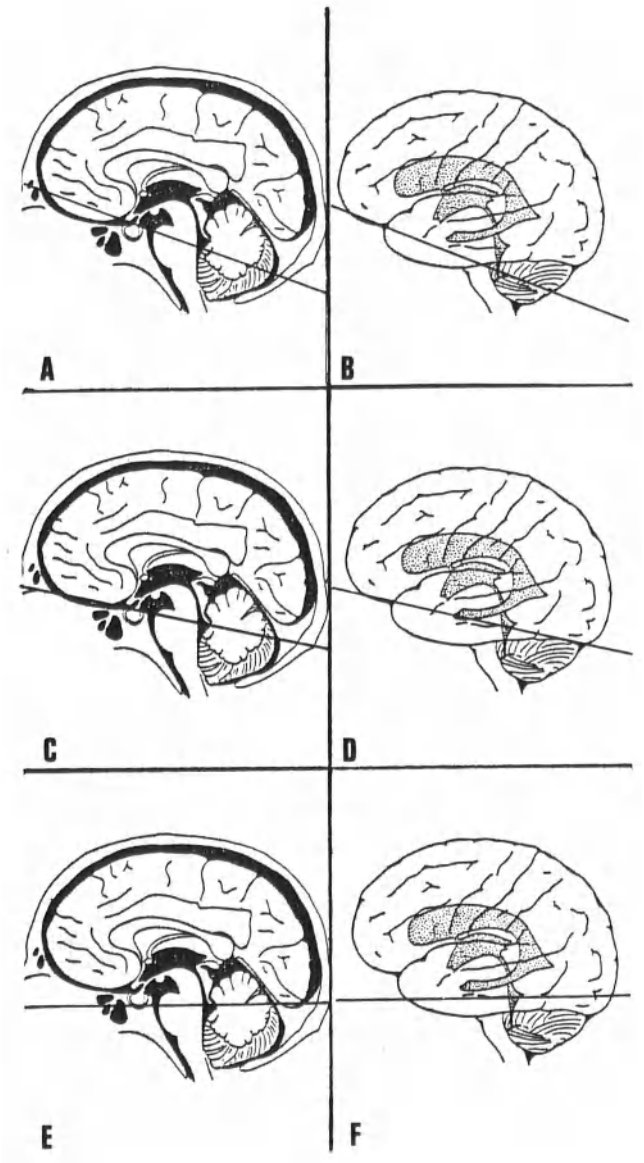

Fig. 1. Planes of Section projected on midline and lateral views of the brain. A and B 25° to R.B.L. C and D 10° to R.B.L. E and F parallel to R.B.L.

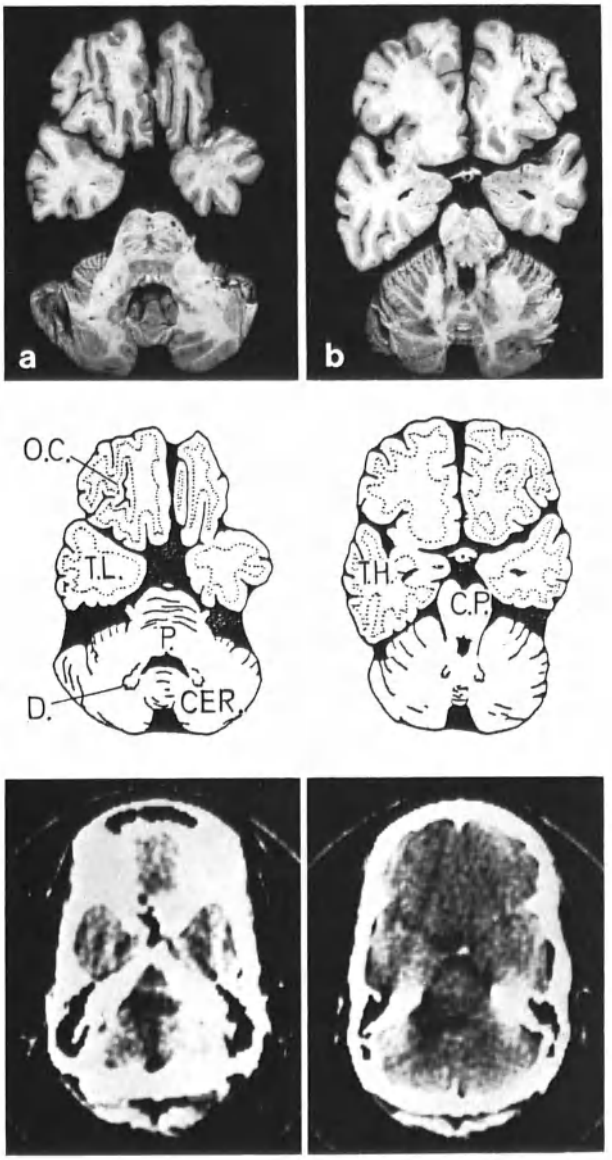

Fig. 2. Brain slices and C.A.T. scans at 25° to R.B.L.; C.P.- cerebral peduncle; CER. cerebellar hemisphere; D.- dentate nucleus; T.L.- temporal lobe; T.H.- temporal horn of lateral ventricle

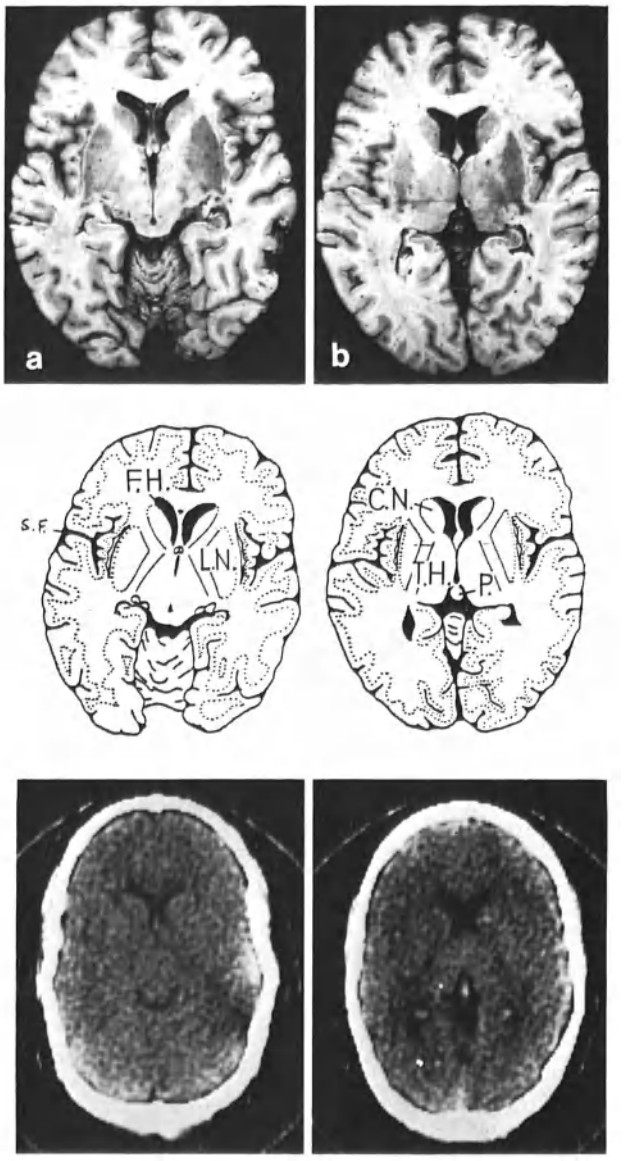

Fig. 3. Brain slices and C.A.T. scans at 25° to R.B.L. C.N.-caudate nucleus; F.H.-frontal horn of lateral ventricle; L.N.-lenticular nucleus; P.-pineal; TH.-thalamus; S.F.-Sylvian fissure

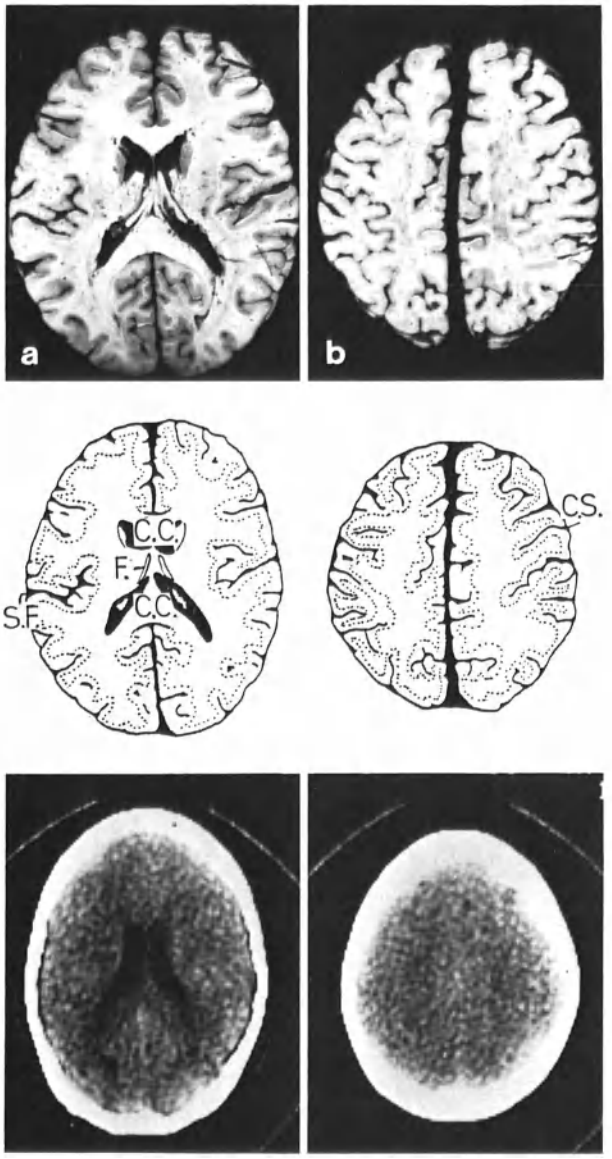

Fig. 4. Brain slices and C.A.T. scans at 25° to R.B.L. C.C.- corpus callosum; C.S.- central sulcus; F.- fornix; S.F.- Sylvian fissure

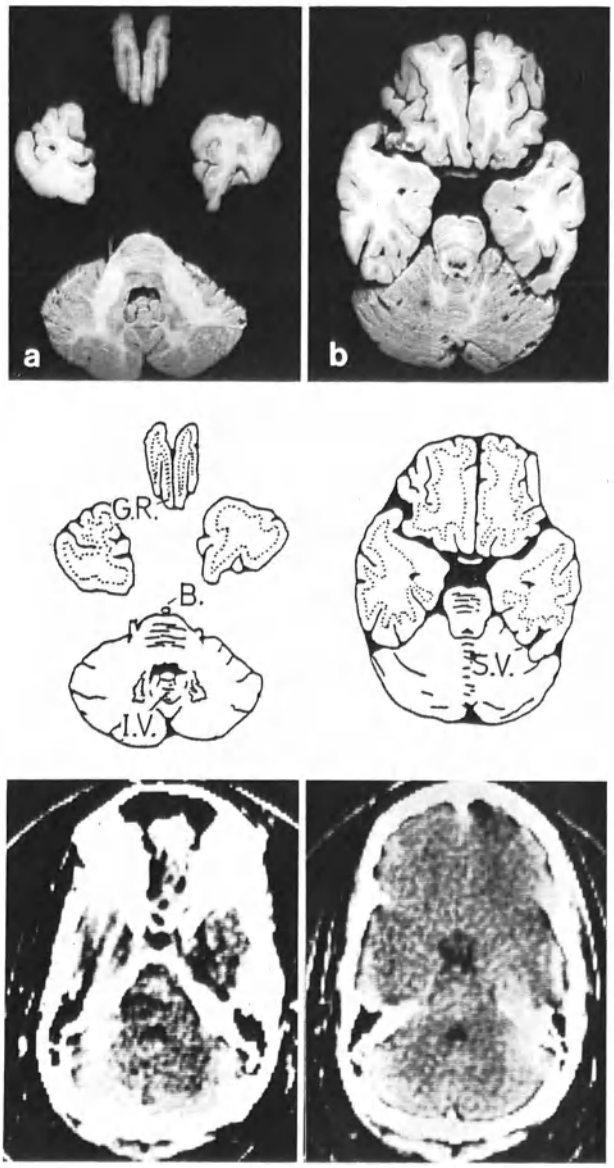

Fig. 5. Brain slices and C.A.T. scans at 10° to R.B.L. B.- basilar artery; G.R.- gyrus rectus; I.V.- inferior cerebellar vermis; S.V.- superior cerebellar vermis

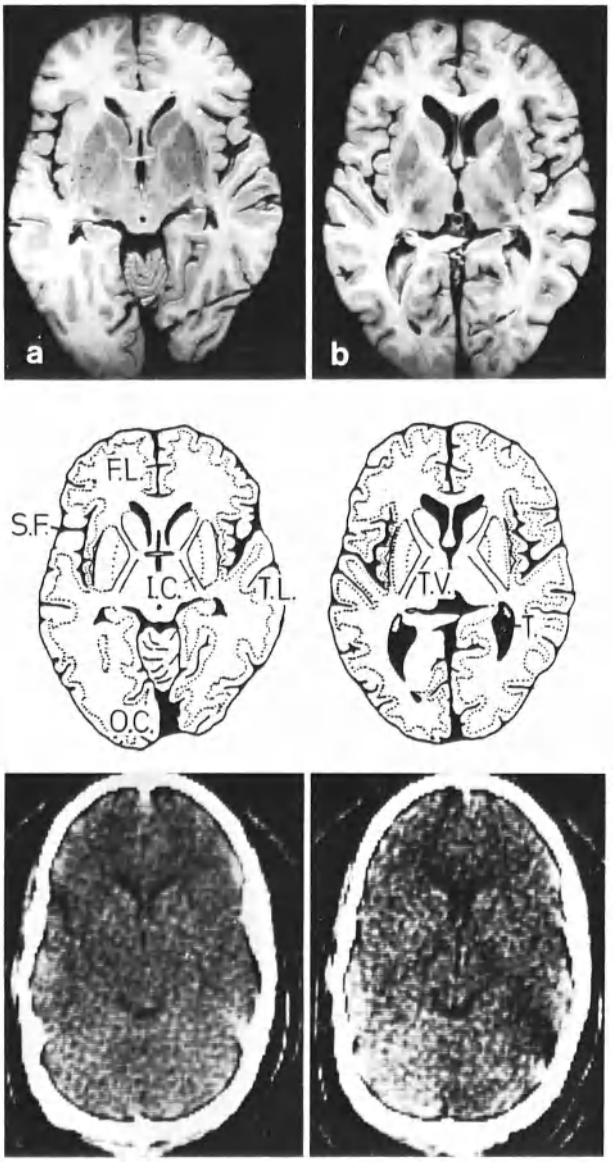

Fig. 6. Brain slices and C.A.T. scans at 10° to R.B.L. F.L.- frontal lobe; I.C.- internal capsule; O.C.- occipital lobe; T.- trigone of lateral ventricle; T.L.- temporal lobe; T.V.- third ventricle; S.F.- Sylvian fissure

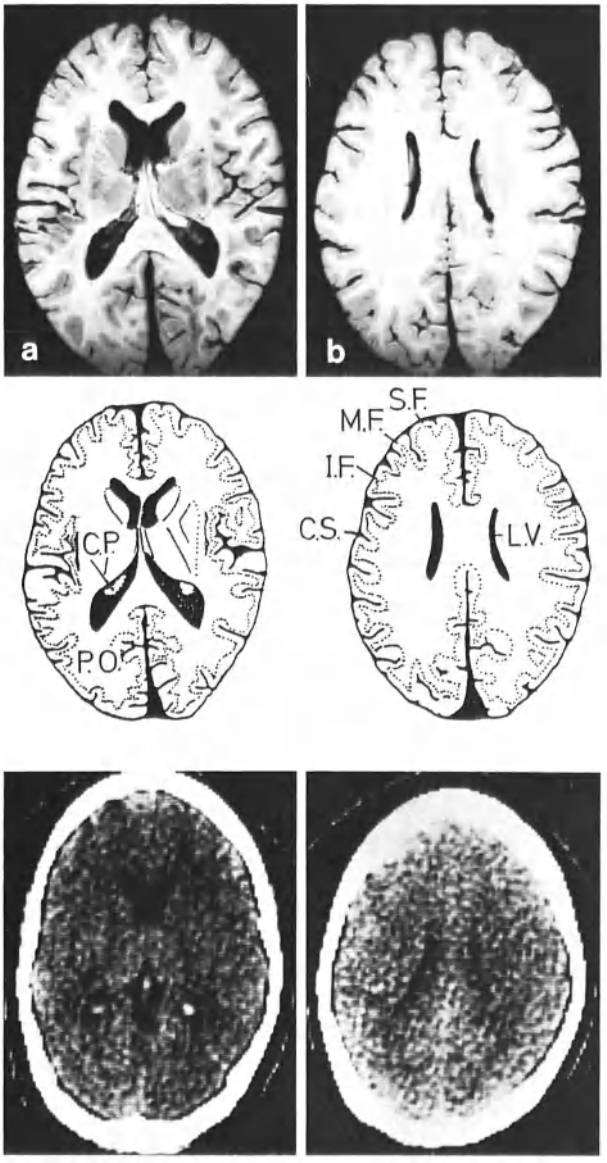

Fig. 7. Brain slices and C.A.T. scans at 10° to R.B.L. C.P.- choroid plexus; M.F.- middle frontal gyrus; C.S.- central sulcus; I.F.- inferior frontal gyrus; P.O.- parieto-occipital fissure; S.F.- Sylvian fissure

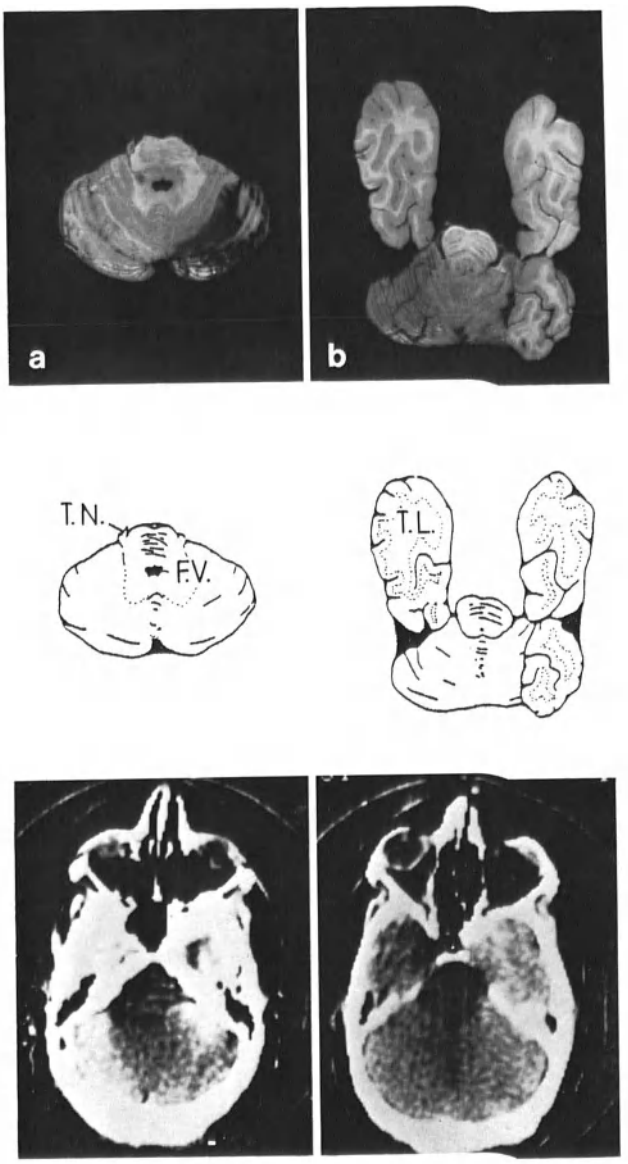

Fig. 8. Brain slices and C.A.T. scans parallel to R.B.L. F.V.- fourth ventricle; T.L.- temporal lobe; T.N.- trigeminal nerve

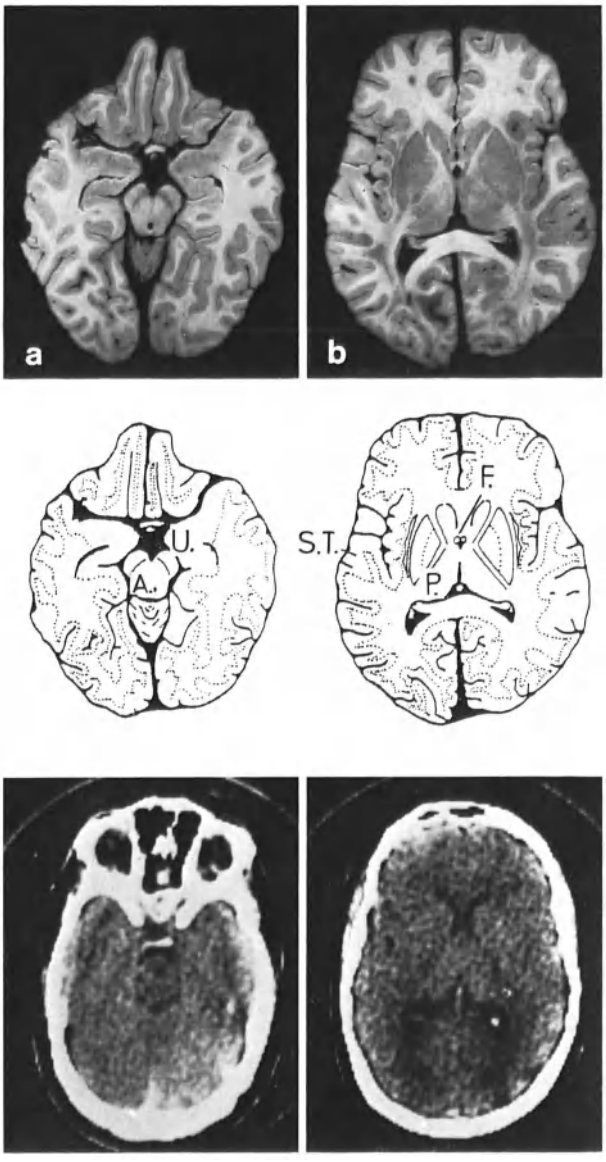

Fig. 9. Brain slices and C.A.T. scans parallel to R.B.L. A.- aqueduct; F.- columns of fornix; P.- pulvinar of thalamus; S.T.- superior temporal gyrus; U.- uncus

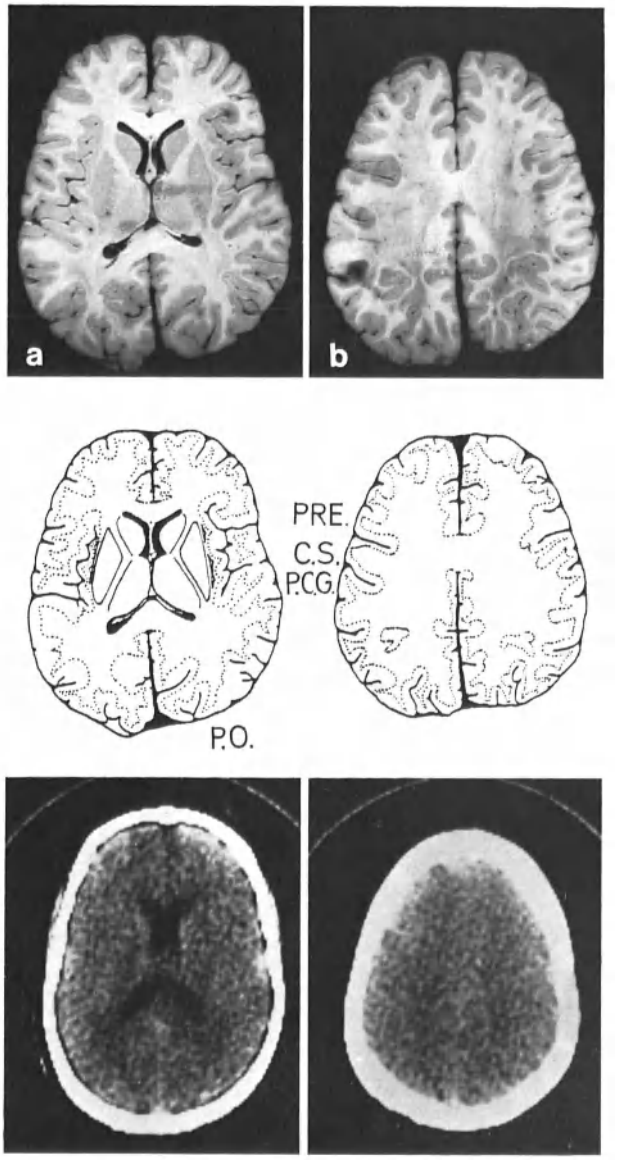

Fig. 10. Brain slices and C.A.T. scans parallel to R.B.L. C.S.- central sulcus; P.C.G.- postcentral gyrus; P.O.- parieto-occipital fissure; PRE-precentral gyrus

C.A.T. Scanning: Correlations with Vascular and Topographical Anatomy

G. Salamon, G. Lecaque, K. Hall, and J. M. Corbaz*

For this paper an attempt was made to assess the following questions:

1. How is the arterial anatomy of the brain orientated in the horizontal plane, as used for C.A.T. scanning? Is this vascular pattern shown on the C.A.T. scan after contrast medium administration, and is this demonstration of any practical use?

2. How accurately can the cortical structures of the brain (lobes, lobules and gyri) be localised on the C.A.T. scan?

What is the effect of flexion and extension of the head, from the orbitomeatal plane, on this topographical localisation?

3. Which is the more accurate, cerebral angiography or C.A.T. scanning, for the topographical localisation of the cerebral cortex and the deeper structures of the brain?

Brain sections, cut in the same horizontal planes used for C.A.T. scanning, were used to answer these questions, and these were compared with normal C.A.T. scans.

Vascular Anatomy of the Brain as Seen on the C.A.T. Scan

A brain, in which all the major arteries had been injected with a radiopaque medium, was cut in horizontal sections, 10 mm thick, in a plane parallel to the orbitomeatal (O.M.) line. Radiographs of these sections were then studied.

The cortical branches of the three main cerebral arteries, anterior, middle and posterior cerebral arteries, supply the grey matter of the medial, lateral and posterior aspects of the cerebrum respectively. The central white matter is relatively avascular. The deep basal nuclei, being grey matter as well, have a prominent arterial supply; the lenticulostriate arteries and the recurrent artery of Heubner (from the middle and anterior cerebral arteries respectively) supply the caudate and lentiform nuclei; the thalamoperforate and thalamogeniculate arteries (from the posterior communicating and posterior cerebral arteries) supply the thalamus.

The cerebellum and brainstem have a prominent arterial supply as well. The arrangement of the arteries in the cerebellum is characteristically in parallel lines, at about 45° to the midline of the brain.

The C.A.T. scan, after contrast administration, may show enhancement of the cortex and deep basal nuclei, so that they are more easily de-

* Neuroradiology Department, INSERM, Marseille/France

lineated. The circle of Willis is often well seen, as it outlines the surasellar cistern, especially when the contrast medium is slowly infused during the scanning procedure. Sometimes the cerebellum shows a streakiness, produced by the parallel arteries in its substance.

From a thorough knowledge of the cerebral anatomy in the horizontal plane, the distribution of the major cerebral arteries can be appreciated, and from this the sites of vascular pathology may be localised. When the circle of Willis is visualised, it may show displacements by adjacent masses, and aneurysms are sometimes identified.

Topographical Anatomy of the Cerebral Cortex

Three normal brains were taken, and on each the major gyri and lobules were marked with different coloured inks, so that they could be recognised when the brains were sectioned. The sections were 10 mm thick and in one brain the sections were parallel to the O.M. line; in the other two brains, the sections were produced as if the head were either flexed or extended 25° to the O.M. line.

When the sections were parallel to the O.M. line (Fig. 1):

1. Frontal and occipital lobes are of approximately equal size.

2. Junction between frontal and parietal lobes (the central fissure, with the motor cortex in front and the sensory cortex behind) is fairly anteriorly placed, but becomes more posterior on the upper sections.

3. Junction between temporal and parietal lobes is about at the 3A/3B level.

4. Junction between parietal/temporal lobes and occipital lobe is very indistinct.

When the sections were as if the head was flexed 25° to the O.M. line (Fig. 2):

1. Frontal lobes are prominent in lower sections, becoming smaller (and even absent) in the upper ones.

2. Occipital lobes are the reverse - small at first, but more prominent later; again junction with parietal and temporal lobes is very indistinct.

3. Junction between frontal and parietal lobes (the central fissure) is anteriorly placed, but becomes more anteriorly placed, as the frontal lobes get smaller in the upper sections.

4. Junction between temporal and parietal lobes is about at the 3B level.

When the sections were as if the head was extended 25° to the O.M. line (Fig. 3):

1. Frontal lobes are absent or small in the lower sections, becoming prominent later.

2. Occipital lobes are the reverse; their anterior boundaries are again indistinct.

3. Junction between frontal and parietal lobes (the central fissure) is fairly posteriorly placed, becoming more posterior in the upper sections.

4. Junction between temporal and parietal lobes is about at the 2B level, a little lower than before.

Precise delineation of the lobes of the cerebrum is difficult in the C.A.T. scan, and changes in position of the head do not help. Some rough guides are:

1. Frontal lobe-temporal lobe junction: pterion (bone landmark) on the lower sections, Sylvian fissure on the higher ones.

2. Temporal/parietal lobe-occipital lobe junction: usually impossible (depends on level of section and position of head).

3. Frontal lobe-parietal lobe junction: again very difficult, being very dependant on the flexion or extension of the head as described; in sections parallel to the O.M. line, the frontal lobe is about the anterior third of the brain, but is more like the anterior half in the upper sections.

4. Temporal lobe-parietal lobe junction: very difficult: roughly 3A cut (range 2B-3B), but little effect from angulation of head.

Separate gyri and lobules cannot be identified. On the other hand, by using the appropriate landmarks, the deep nuclei can usually be well defined - head of caudate nucleus, lentiform nucleus and thalamus - as well as internal capsule.

Comparison between Cerebral Angiography for Defining the Topographical Anatomy of the Brain

As already demonstrated, the lobes of the brain are hard to define, let alone the gyri and lobules. This applies to all three surfaces of the brain - medial, lateral and inferior.

On the other hand, many of the sulci on these three surfaces (and hence the adjacent gyri) can be identified by careful analysis of the cerebral angiogram:

Medial surface - the anterior cerebral artery branches can show the pericallosal cistern, the cingulate sulcus and the boundaries of the paracentral lobule.

Lateral surface (convexity) - the middle cerebral artery branches can show the superior and inferior frontal and the superior and middle temporal sulci; also the central fissure can be shown, as well as the precentral and postcentral sulci, the outlines of the angular gyrus and the Sylvian fissure.

Inferior surface (posterior part) - the posterior cerebral artery branches can show the collateral and inferior temporal sulci; these can often be seen on the AP vertebral angiogram.

The deep structures of the cerebral hemisphere are, however, not well demonstrated on a cerebral angiogram (carotid or vertebral) in the same three-dimensional manner in which they can be demonstrated on the

C.A.T. scan. The lenticulostriate arteries are well shown on the a-p or Towne's view at carotid angiography, but not on the lateral view (being overlapped by the middle cerebral artery branches). The thalamoperforate and thalamogeniculate arteries are usually well shown on a lateral vertebral angiogram, but not on an a-p or Towne's view.

Conclusions

1. The vascular anatomy of the brain can be appreciated on the C.A.T. scan, and may even be demonstrable, to some extent, after contrast administration.

2. The cerebral cortical structures are not well shown on the C.A.T. scan, and it is usually even difficult to accurately identify the lobes; cerebral angiography is better in this respect.

3. The deep structures of the cerebral hemisphere are well shown on the C.A.T. scan, but are not so well shown by cerebral angiography.

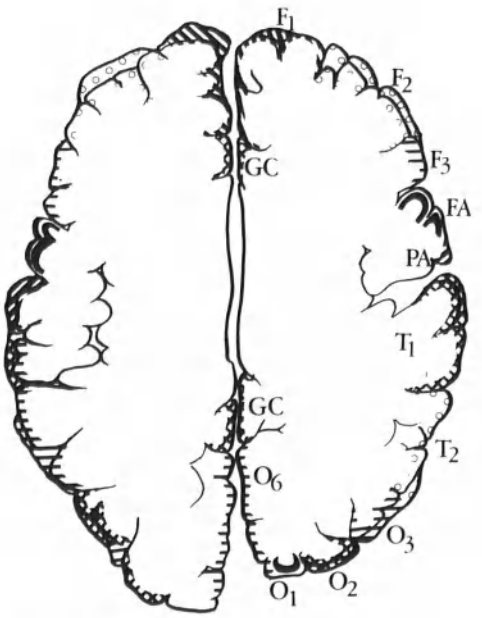

OM 3A

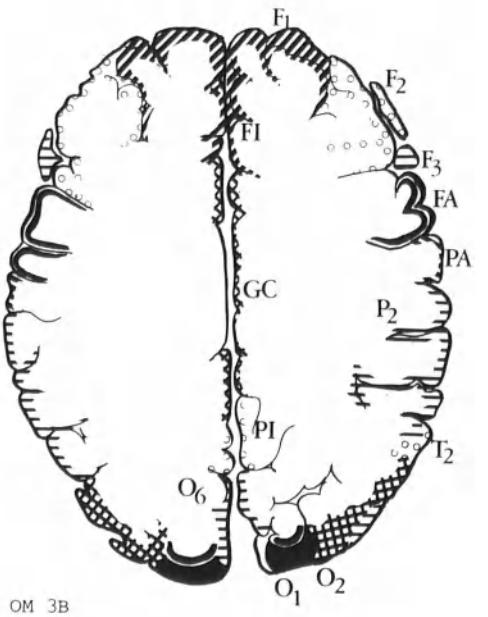

OM 3B

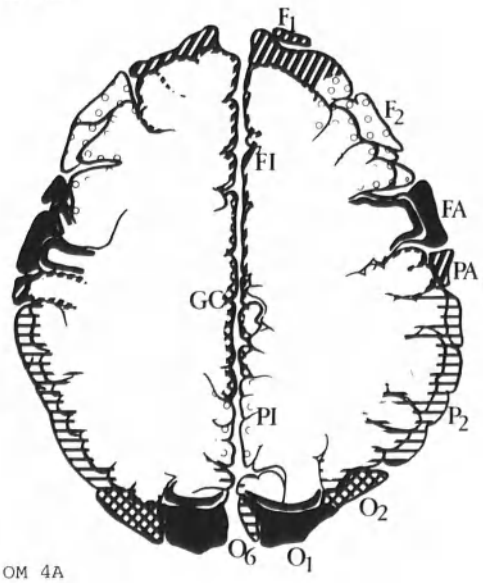

OM 4A

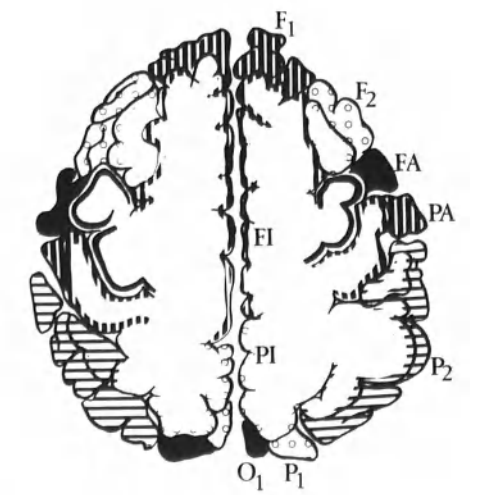

OM 4B

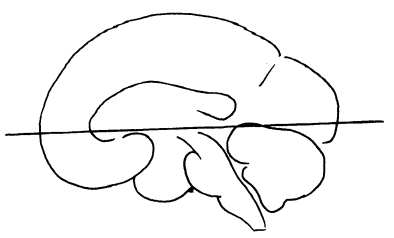

Fig. 1. Projection of the cerebral cortex on cuts done in a plane parallel to orbitomatal line (Abbreviations see next page)

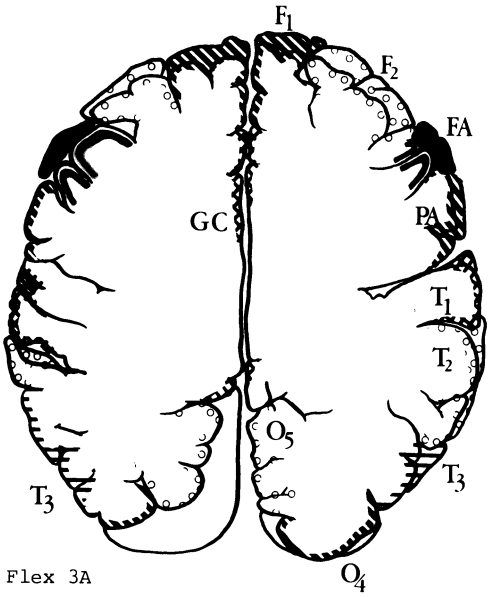

Flex 3A

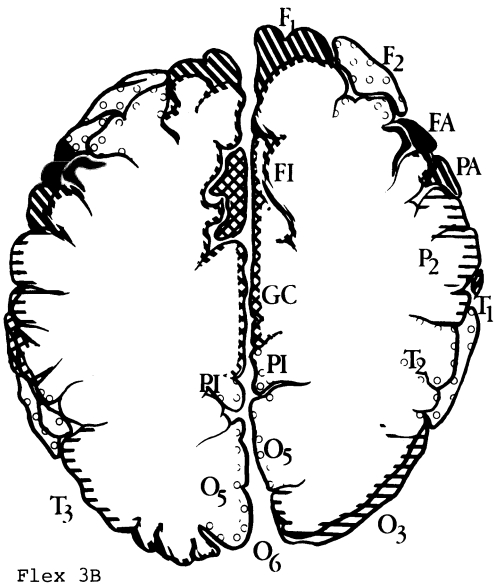

Flex 3B

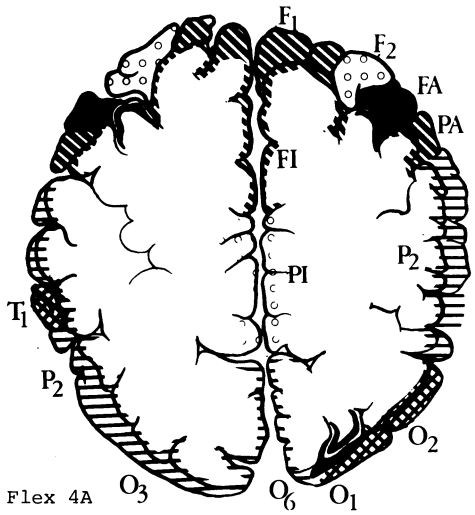

Flex 4A

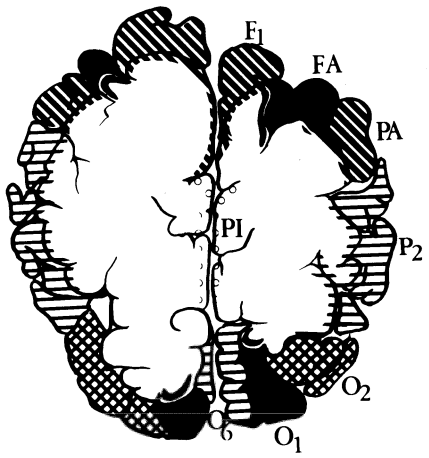

Flex 4B

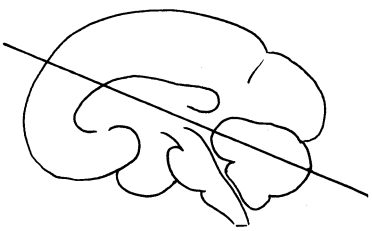

Fig. 2. Projection of the cerebral cortex on cuts done in flexion (25°). For key to figure, see Figure 1

F_1 - Superior frontal gyrus, F_2 - Middle frontal gyrus, F_3 - Inferior frontal gyrus, FA - Precentral gyrus (motor cortex), PA - Postcentral gyrus (sensory cortex), P_1 - Superior parietal lobule, P_2 - Inferior parietal lobule, O_1 - Superior occipital gyrus, O_2 - Middle occipital gyrus, O_3 - Inferior occipital gyrus, O_4 - Fusiform gyrus, O_5 - Lingual gyrus, O_6 - Cuneus, T_1 - Superior temporal gyrus, T_2 - Middle temporal gyrus, T_3 - Inferior temporal gyrus, GC - Cingulate gyrus

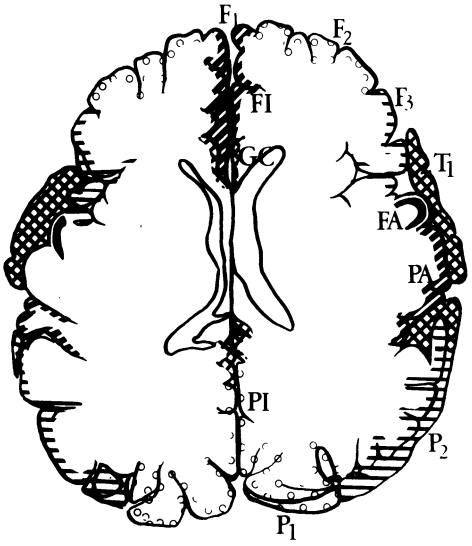

Ext 3A

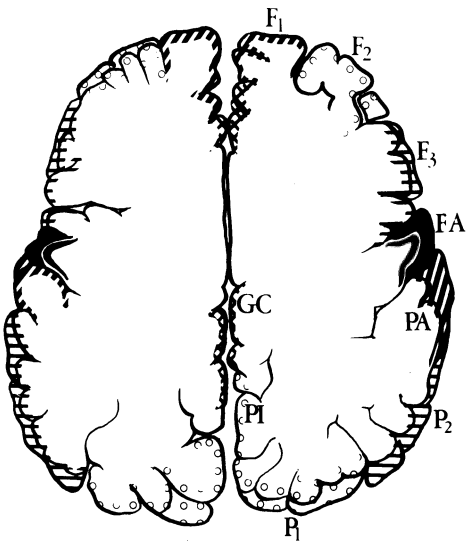

Ext 3B

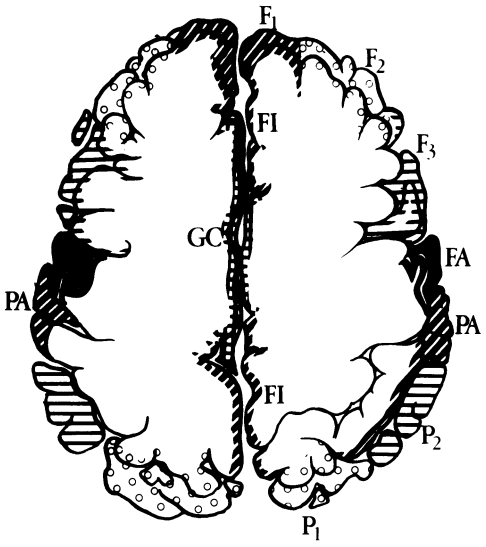

Ext 4A

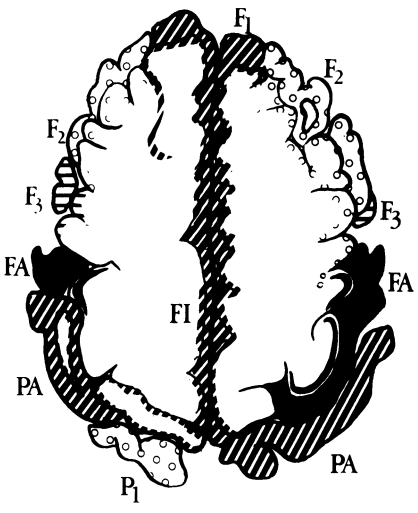

Ext 4B

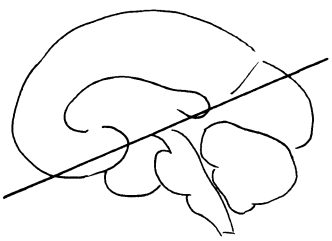

Fig. 3. Projection of the cerebral cortex on cuts done in extension (25°). For key to figure, see Figure 1

C.A.T. Investigation of the Subarachnoid Space

A. Grepe and T. Greitz*

The attenuation of the normal C.S.F. is lower than that of the brain, about 5 Hounsfield units as compared to 15 and 18 for the white and grey matter respectively. This fact makes possible visualization of the ventricular system, the subarachnoid cisterns and the cerebral sulci. However, these latter spaces are usually very narrow in normal patients and therefore few of them are seen. As we have been able to demonstrate earlier, the C.S.F. spaces may be enhanced following lumbar injection of metrizamide (1, 5, 3). The introduction of a finer matrix and an improved algorithm has allowed a more detailed study of the anatomy of the subarachnoid space.

Material and Methods

This report is mainly based on experiences of computed cisternography in 10 patients who were examined following lumbar myelography using the first version EMI head scanner and the new matrix. As these patients were examined following lumbar myelography, our approach has been somewhat different from that used for computed cisternography (3, 5), mainly because the patients were kept in a slightly upright position following myelography as opposed to patients with suspected hydrocephalus, in whom the contrast medium was purposely brought up to the cervicodorsal junction. However, the position of the patient, the amount and concentration of the contrast medium used and its mode of application seem to be less critical. One to two grams of Amipaque is usually sufficient. Scanning was usually carried out before and 3, 6, 12 and 24 h after the injection. Normally, contrast medium appears in the basal cisterns after 3 h and reaches the sulci over the cerebral hemispheres after 12 h (for details see *Hydrocephalus, atrophy and their differential diagnosis* by HINDMARSH and GREITZ in this issue). The appearances of the cisterns in computed tomograms were compared with those obtained at postmortem cisternography (2), using the same orientation of the cuts as those employed at C.A.T.

Results

The cisterns and cerebral sulci are usually very narrow in the normal patient and therefore few of them are visualized on a plain C.A.T. scan. The only cistern which always appears on a C.A.T. examination is the quadrigeminal cistern. The cistern of the velum interpositum is also frequently seen. The suprasellar cisterns are less constant. Their visualization depends on the level of the cut. If the structures of the sella are included in a basal cut, the limits of chiasmatic

*Department of Neuroradiology, Karolinska Sjukhuset, S-10401 Stockholm/Sweden

and interpeduncular cisterns are not seen, due to the preponderance of bone, and a cut at a superior level may then pass above the suprasellar cisterns. The pontine and cerebellopontine cisterns may often be difficult to identify with certainty due to frequent occurrence of streak-like artefacts in this area. The narrow cerebral sulci are barely visible in a normal case.

Following enhancement of the subarachnoid space using metrizamide (Amipaque), one is usually able to demonstrate, in addition to the cisterns mentioned, the cisterna magna, the lateral extension of the suprasellar cisterns, the Sylvian and interhemispheric fissures, the sulci of the cerebral and cerebellar hemispheres, the ambient cistern and the subarachnoid space over the cerebellum.

In fact, computer assisted cisternography allows rather detailed analysis of the anatomy of the subarachnoid space. As can be demonstrated in serial cuts starting from the level of the foramen magnum (Figs. 1-6), a cut at this level does not demonstrate the spinal cord in a plain C.A.T. scan. However, following enhancement of the CSF using metrizamide, the shape and the position of the cord may be studied (Fig. 1). A cut at a slightly higher level (Fig. 2) occasionally demonstrates the medial aspects of the tonsils and the inferior part of the fourth ventricle as well as the cisterna magna. However, these structures are more clearly and more frequently visualized at C.A. cisternography, which may demonstrate these structures and in addition more minute details such as the lateral recesses of the fourth ventricle. The restiform bodies, which form the floor of the fourth ventricle, may also be seen, and are best shown in cuts perpendicular to the clivus (Fig. 3). In the more customary cuts taken parallel to the floor of the anterior fossa, the cerebellopontine cisterns are usually seen at the same level as the fourth ventricle. These cisterns are outlined by the lateral aspects of the pons and are limited posteriorly by the cerebellar hemispheres. Like the pontine cistern, they are also seen at the level of the superior part of the fourth ventricle (Fig. 4). A cut at this level demonstrates the infratentorial part of the ambient cistern limited anteriorly and medially by the cerebellar peduncles and laterally and posteriorly by the cerebellar hemisphere. The orientation of this cistern is familiar to those acquainted with the course of the brachial vein.

The suprasellar cistern is referred to by HILAL (4) and is now classically known as the pentagon-shaped cistern (Figs. 5 and 6). It is limited posteriorly by the belly of the pons and the cerebral peduncles, laterally by the uncus of the temporal lobe and anteriorly by the posterior aspect of the straight gyrus of the frontal lobe. In a plain C.A. tomogram small filling defects suggestive of the chiasm and the optical tracts may occasionally be seen. However, using C.A. cisternography these tiny structures are indisputably demonstrated. In addition to the basilar artery C.A. cisternography demonstrates the pituitary stalk, the optic tracts, the optic nerves and the trigeminal nerves (Fig. 5).

As mentioned, the quadrigeminal cistern is a constant observation in a plain C.A. tomogram through the inferior part of the frontal horns and the superior part of the third ventricle. The posterior aspects of the ambient cisterns are also usually seen in the same cut. The anterior part of the ambient cistern and the cerebral peduncles are less constant. They usually have a quite symmetrical appearance.

In the normal case, only the most anterior extension of the sylvian fissure is seen without contrast enhancement. It appears as a triangular area with a narrow, anteriorly directed base close to the vault just

above the pterion. This level is identified by the inward bulging of the bone at this level. Only small streaks of the more superiorly and posteriorly located parts of the sylvian fissures are seen without contrast enhancement, unless these parts of the fissure are dilated. There should be no difficulty in distinguishing the sylvian fissures from the temporal horns (7) as the temporal horns are remote from the anterior wall of the middle fossa and have a fairly close relationship to the uncus and the brain stem.

C.A. cisternography demonstrates the full extent of the sylvian fissure. Its floor, formed by the insula, is clearly demonstrated.

The quadrigeminal cistern is superiorly and anteriorly continuous with the cistern of the velum interpositum. This latter cistern may be seen in a plain C.A. tomogram as a triangle with a pointed corner directed anteriorly in the midline. The pineal body may be included in a cut passing through the posterior aspect of this cistern. At C.A. cisternography the third ventricle may be seen protruding as a defect into this cistern, which posteriorly is continuous with the subarachnoid space over the vermis (Fig. 6).

Discussion

In the case of isodense lesions, evaluation of deformities and displacements of the C.S.F.-containing spaces may be of decisive importance for diagnosis. This applies not only to the ventricular system but also to the cisterns and sulci. Accordingly, it has been pointed out that displacement of the ventricular system may be the only sign of an isodense subdural hematoma. A compression of the suprasellar cisterns from behind may be the only significant change in an isodense pontine glioma (4). Such changes of the cisterns may be observed without the use of contrast medium. Deformities and filling defects seen in the suprasellar cisterns may give a clear indication of a suprasellar tumour. In fact, most of the classical changes observed at pneumoencephalography in posterior fossa tumours may be recognized on a plain C.A. tomogram. In the case of an acoustic neuroma we have been able to observe not only displacement of the fourth ventricle but also a dilatation of the medial portion of the ipsilateral cerebellopontine cistern, a filling defect in its lateral part and compression of the contralateral cerebellopontine cistern, i.e. all the changes typical of an acoustic neuroma as seen at pneumoencephalography. As pointed out earlier, (3) C.A. cisternography affords a means of demonstrating extracerebral lesions in the posterior fossa as well as in the sellar area.

In patients with subarachnoid haemorrhage an excellent visualization of the cisterns is sometimes obtained due to the high attenuation of the patient's blood which fills the subarachnoid spaces. The demonstration of displaced cisterns and sulci in these cases may sometimes contribute to a more accurate localization of concomitant infarcts and haematomas. Sometimes the only observation in the case of a subarachnoid bleed is the fact that the cisterns have become isodense and therefore not visible.

As most of the cerebral sulci and gyri are not seen in normal cases, C.A. cisternography affords new means of accurate mapping of these anatomical structures. This provides new possibilities, in addition to cerebral angiography, to make more accurate anatomico-physiological correlative studies.

References

1. GREITZ, T., HINDMARSH, T.: Computer assisted tomography of intracranial CSF circulation using a water-soluble contrast medium. Acta Radiol. (Diagnosis) 15, 497-507 (1974).
2. GREPE, A.: Anatomy of the cranial nerves in the basal cisterns. A radiologic post-mortem investigation. Acta Radiol. (Diagnosis) 16, 17-38 (1975).
3. GREPE, A., GREITZ, T., NORÉN, G.: Computer cisternography of extracerebral tumours using lumbar injection of water-soluble contrast medium. Acta Radiol. Suppl. 346, 51-62 (1975).
4. HILAL, S.: Discussion of paper on C.T. in posterior fossa lesions, International Symposium and Course on Computerized Tomography, San Juan, Puerto Rico, 1976.
5. HINDMARSH, T., GREITZ, T.: Computer cisternography in the diagnosis of communicating hydrocephalus. Acta Radiologica Suppl. 346, 91-97 (1975).
6. HINDMARSH, T., GREITZ, T.: Hydrocephalus, atrophy and their differential diagnosis. This issue, p.
7. RUGGIERO, G., NUZZO, G., SABATTINI, L.: Computerized axial tomography and encephalography. Paper presented at the 5th Congress of the European Society of Neuroradiology, Geilo, Norway 1975.

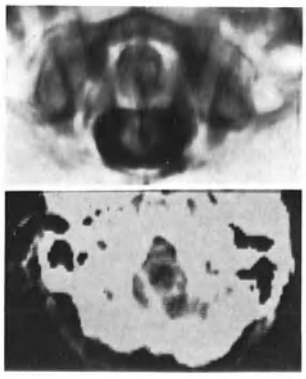

Fig. 1

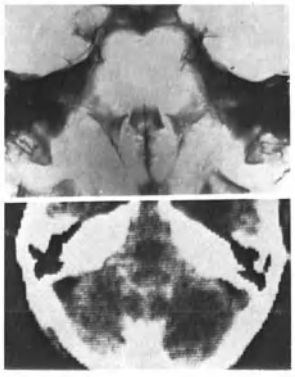

Fig. 2

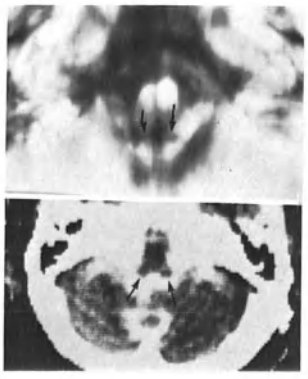

Fig. 3

Figs. 1-6. Each figure illustrates the appearance of the subarachnoid space as seen in a tomographic cut at post-mortem cisternography (*top*) and at in vivo C.A. cisternography (*bottom*) at the same level

Fig. 1. Cut at the level just below foramen magnum demonstrates spinal cord

Fig. 2. Cut at a higher adjacent level shows (from behind) cisterna magna, intertonsillar space and posterior part of fourth ventricle surrounding tonsils. The medullary cisterns (fossae olivares) being slightly inferior to fourth ventricle are seen to outline upper medulla and to be continuous laterally anteriorly with cerebellopontine fissure

Fig. 3. A cut perpendicular to brain stem may visualize floor of fourth ventricle formed inferiorly by restiform bodies (*arrow*). These are surrounded laterally by lateral recesses of fourth ventricle

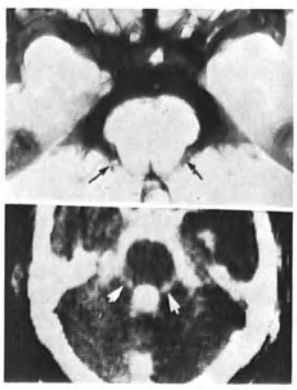

Fig. 4

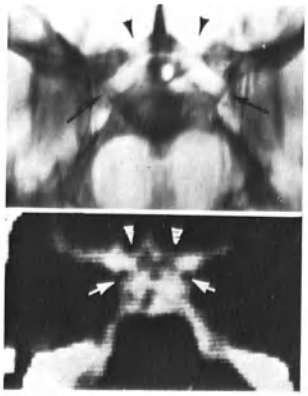

Fig. 5

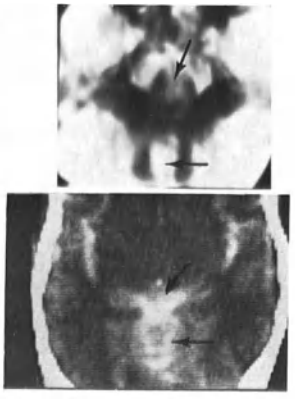

Fig. 6

Fig. 4. Cut at the level of upper part of fourth ventricle showing infratentorial portions of ambient cisterns as well as lateral extension of chiasmatic cistern

Fig. 5. At C.A. cisternography, infundibular stalk and chiasm are frequently visualized. Occasionally the optic tracts (*arrow*) and optic nerves (*arrowhead*) may be seen. Basilar artery is anterior to pons and trigeminal nerves may sometimes be identified lateral to pons

Fig. 6. Cut through Sylvian fissures, inferior part of cisterna veli interpositi and through subarachnoid space over vermis. Defects caused by posterior part of third ventricle and by superior part of vermis (*arrows*)

Computerised Tomography of the Tentorium Cerebelli

T. P. Naidich*, I. I. Kricheff**, and N. E. Leeds*

Introduction

NEWTON et al. (5), GOODING et al. (3), and GADO et al. (2), have demonstrated that iodinated radiographic contrast agents accumulate in the intravascular and extravascular spaces of the dura mater. Computerised tomography in the axial plane (C.A.T.) permits routine identification of this falx and tentorial blush after intravenous administration of contrast agent. Familiarity with the normal C.A.T. appearance and anatomic relationships of the tentorium provides a basis for understanding the C.A.T. manifestations of many non-neoplastic disease processes.

Anatomy of the Tentorium

The tentorium cerebelli is a double fold of dura which forms the tent-shaped roof of the posterior fossa (5). Laterally, the tentorium attaches to the occipital and petrous bones along the transverse and superior petrosal sinuses, and then continues forward to the posterior clinoid processes as the petroclinoid ligaments (6). Medially, the tentorium fuses with the falx along the straight sinus and then continues forward to the anterior clinoid processes as two crescentic, medially concave, free tentorial borders which define the tentorial notch or incisura (1, 6). The midbrain usually occupies the anterior half of the tentorial incisura (1). The posterior half may be occupied by the superior vermis or the splenium of the corpus callosum (1). The remaining space is filled by the cerebrospinal fluid, blood vessels and nerves within the perimesencephalic and superior vermian cisterns.

The tentorium is highest medially at the apex of the incisura and falls off posteriorly toward the torcula and laterally towards the transverse and petrosal sinuses. Because the slope of this descent is steepest medially and less steep laterally, the side walls of the tentorium are concave superolaterally over much of their surface. However, when viewed from above, the uppermost portion of the tentorium around and below the incisura is slightly convex laterally.

In a sequential series of 100 *contrast-enhanced* C.A.T. scans of good quality, the tentorium was visualized in 99% of cases. It was well seen in two-thirds of those and faint but visible in an additional third.

*Montefiore Hospital and Medical Center, Department of Radiology, New York.
**New York University Medical Center, Department of Radiology, New York.

C.A.T. Appearance of the Tentorium

The tentorial image seen on C.A.T. is that of coverging or diverging bands of density which vary in configuration depending on the inclination of the C.A.T. slice, its level relative to the torcula and the anatomical configuration of the individual tentorium. In most cases, however, the tentorial image assumes one of three basic configurations:

1. "V" Configuration. A fortuitous section in the plane of the incisura will show the full contour of the tentorial margin from the anterior clinoid processes to the apex of the incisura. Less well-placed cuts will show the tentorium piecemeal and with varying configuration at each level.

Above a plane through the torcula, the tentorial leaves converge medially to the midline. Any section through the tentorium which exits above the torcula will demonstrate converging V-shaped tentorial bands (Fig. 1).

2. Diverging Bands. Below the plane through the torcula, the tentorial leaves diverge laterally. A C.A.T. section which passes through the incisura and exits from the tentorium below the torcula demonstrates tentorial bands which diverge posterolaterally toward the lateral tentorial attachments (Fig. 2). The diverging bands often appear to increase in width as they pass posterolaterally, because the same 13 mm thickness of the section includes a greater width of the gently sloping lateral portion of the tentorium.

3. "M" Configuration. A C.A.T. section which passes directly through the torcula creates a distinct M-shaped tentorial image (Fig. 3). Because the section through the torcula is 13 mm thick, the top of the section lies above the torcula and forms the V-shaped image that is the midportion or lower point of the M. The bottom of the 13 mm-thick section lies beneath the torcula and forms the two diverging bands that are the uprights of the M. At the normal scanning angle, serial cuts in a single patient will show the V, M and diverging band configurations.

When the C.A.T. section enters the tentorium inferior to the incisura, the anterior gap represents only the width of the roof of the posterior fossa at the level of section. Almost always, however, the relationship of the tentorial bands to the midbrain, superior vermis and quadrigeminal cistern permits ready identification of the true incisura.

A number of pathological states may make the tentorium more evident on *unenhanced* C.A.T. Calcification of the tentorium causes a focal or diffuse increase in density (Fig. 4) which lies along and conforms to the tentorial bands shown on contrast-enhanced C.A.T. Subarachnoid haemorrhage accumulated on the surface of the tentorium creates converging and diverging bands of density that are identical in configuration with the tentorial bands seen on normal *contrast-enhanced* C.A.T. scans (Fig. 5). The relationship of the blood density to the known tentorial contours permits differentiation of subarachnoid supratentorial blood from intraparenchymal haemorrhage in most cases.

Tumour Localisation

On C.A.T. after contrast medium enhancement, medial posterior temporal lesions lie anterolateral to the opacified band of the tentorium and

may show flattening of their posteromedial contour to conform to the tentorium (Fig. 6). Occipital lesions present further posteriorly but will also be lateral to the tentorial bands and may be flattened medially. Lateral cerebellar lesions lie posteromedial to the opacified lateral edge of the tentorium and may show flattening of their anterolateral border (Fig. 7).

Masses which lie on the bands may not be localised as to their supratentorial or infratentorial position unless medial or lateral flattening are observed or the lesion is large enough to be seen on other slices to project medial or laterally to the bands. In such cases coronal sections may be helpful.

When the "V" configuration is seen, lesions lateral or anterior to the "V" are supratentorial, whereas masses within the limbs of the V are incisural (Fig. 8).

The criteria for diagnosis of an extra-axial posterior fossa mass include sharp definition and confluence with the walls or roof of the posterior fossa. On cuts above the level of the petrous pyramid, flattening of the tentorial border of the lesion indicates confluence with the roof of the posterior fossa (Fig. 9). In our experience such flattened margins indicate that the masses are growing upwards towards the incisura.

Infratentorial extra-axial lesions that grow upward toward the *incisura* often assume a 'comma' configuration: The infratentorial portion of the tumour, constrained by the tentorium, exhibits posterolateral flattening. The supratentorial component, free to grow in all directions, forms the rounded contour of a tumour ball.

Summary

Appreciation of the anatomical relationships of the opacified tentorial bands permits accurate localisation of supratentorial, infratentorial and incisural lesions on most contrast-enhanced C.A.T. scans. Lesions that overlie the tentorial bands, particularly those that fall within the broad M blush, may be indeterminate in position. Transincisural extension of meningiomas is readily identified. It is not always possible to differentiate between upward bulging of the tentorium and tentorial invasion with transtentorial growth.

References

1. BULL, J.W.D.: Tentorium cerebelli. Proc. roy. Soc. Med. 62, 1301-1310 (1969).
2. GADO, M.H., PHELPS, M.E., COLEMAN, R.E.: An extravascular component of contrast enhancement in cranial computed tomography. Part II: Contrast enhancement and the blood tissue barrier. Radiology 117, 595-597 (1975).
3. GOODING, C.A., PRICE, D.C., NEWTON, T.H.: Experimental studies of falx and tentorial opacification during cerebral angiography. Radiology 102, 77-82 (1972).
4. KAPLAN, H.A., BOWDER, J., KRIEGER, A.J.: Venous channels within the intracranial dural partitions. Radiology 115, 641-645 (1975).

5. NEWTON, T.H., GOODING, C.A., PRICE, D.C.: Opacification of falx and tentorium during cerebral angiography. Preliminary report. Invest. Radiol. 5, 348-354 (1970).
6. SUNDERLAND, S.: The tentorial notch and complications produced by herniations of the brain through that aperture. Brit. J. Surg. 45, 422-438 (1958).

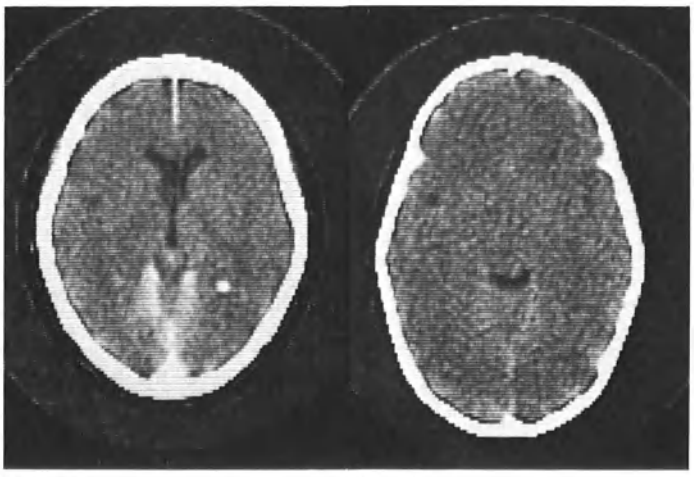

Fig. 1a Fig. 1b

Fig. 1a and b. While the entire incisural portion of the tentorium is occassionally visualised, this area of the tentorium is usually seen only in part as a dense "V" with attached falx frequently converting the "V" to a "Y". Usually the "V" is faint (a); however it may normally be thick and dense, perhaps augmented by contrast-filled veins (b)

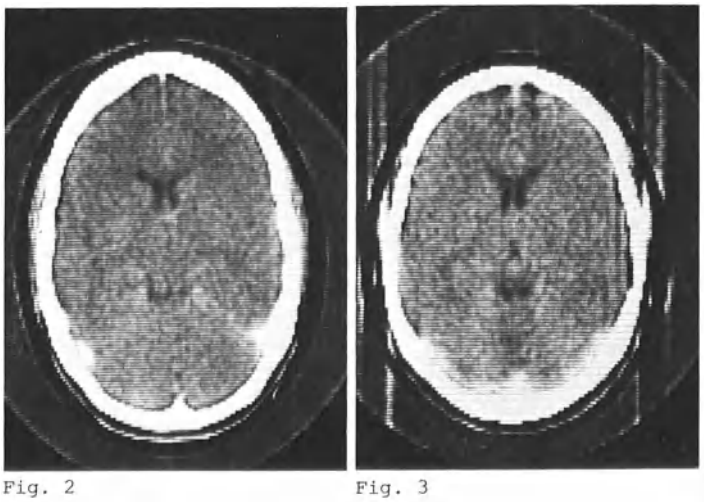

Fig. 2 Fig. 3

Fig. 2. Faint laterally broadening bands of enhanced tentorium pass, at a 45^{o} angle, from edge of quadrigeminal cistern to calvarium

Fig. 3. "M" configuration. Note enhanced torcular and lateral sinuses

Fig. 4

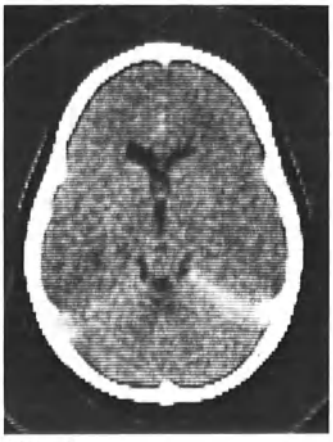

Fig. 5

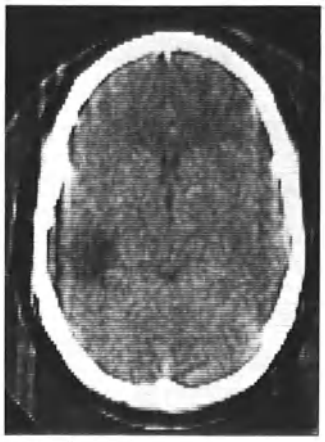

Fig. 6

Fig. 4. Multiple calcific densities delineate free margin of tentorium

Fig. 5. Subarachnoid blood conforms to superior surface of left side of tentorium

Fig. 6. A posterior temporal infarct (lucent) is lateral to the tentorial bands and is flattened medially

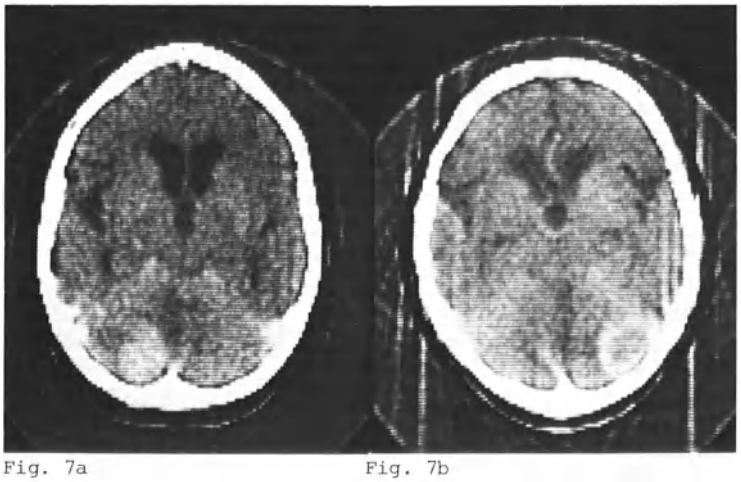

Fig. 7a

Fig. 7b

Fig. 7a and b. Cerebellar metastases are visualised medial to the tentorial bands: (a) demonstrates lateral flattening against the tentorium; (b) projects over band, but extends well medial to it

Fig. 8

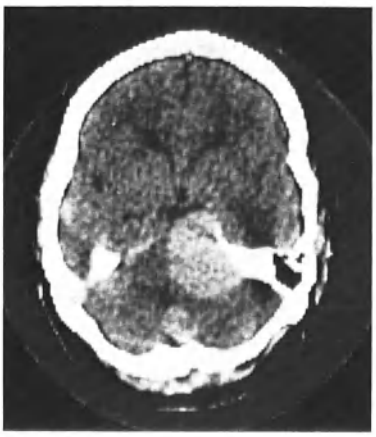

Fig. 9

Fig. 8. Incisural extension of a vermian metastasis that projects between the "V" of tentorial margins

Fig. 9. A left tentorial meningioma is flattened laterally against upper petrous bone and tentorium. As it grows through the incisura, that part of the tumour becomes rounded, producing a comma shaped density

Technical Operation

Computer Tomographic Artefacts Using the CT 1000

D. P. E. Kingsley*

Artefacts

Artefacts are defined as areas of the display which are not true representations of the actual densities of the same areas within the scanned object.

Sometimes the amount of artefact is small and may not be obviously artefactual. In such cases errors of diagnosis may be made. At other times artefact may be present but not sufficiently gross to alter the value of the scan. Frequently, artefacts occur as a result of surgery and other investigatory procedures and occasionally the artefact is of such a nature that the scan is not just valueless but the display is bizarre. Although the list is by no means complete it is the purpose of this paper to demonstrate some of the commoner artefacts and also some of the less common ones.

Artefacts can be divided into two broad categories: those occurring because of the patient's state and those due to the machinery.

Patient Artefacts

Artefacts can really be divided into those which, although present, do not alter the scan significantly and those which reduce the level of diagnostic usefulness of the scan, and which therefore should be avoided where possible. Table 1 lists the causes of artefacts which should be avoided.

Table 1. Causes of major patient artefacts

1. Movement	Nodding
	Horizontal
	Rotational
	Mixed
	Violent short-lived
	Extreme
2. Barium	
3. Air	
4. Metallic objects	
5. Myodil	

*Lysholm Radiological Department, The National Hospital, Queen Square, London WC1N 3BG.

By far the most important factor in the production of an increase in artefactual content of a scan is movement of the patient's head. Movement occurs in different directions and each produces a definite type of artefact. Firstly there is the nodding type of artefact produced by flexion and extension of the head (Fig. 1). The artefact is seen mainly in the base cuts, and consists of low density shadows opposite the mastoid air cells and high density opposite the dense petrous ridge. On lower cuts vertical low density artefacts may be seen in the posterior fossa in the midline due to the paranasal air sinuses.

Horizontal movement (Fig. 2) produces artefact mainly on either side, consisting of vertical extracranial streaks of alternating high and low density, since the bone is at one position at the start of the scan and at another at the end. This may reduce the overall quality of the scan by adding to 'edge blur' but does not necessarily reduce the diagnostic value.

Rotational movement (Fig. 3) procudes streaks tangential to the skull vault. These streaks are both within and outside the display area of the skull. Minor degrees of rotation may not reduce the overall quality of the scan, but more persistent movement in all directions produces a scan which is undiagnostic, particularly in the low cuts.

Sudden violent movement such as sneezing appears to distort the picture more than continuous but less violent movement, and the appearances may become completely undiagnostic even when the movement is short-lived.

Finally, extremes of movement need only occur for a short period to distort the display totally. Removal of the patient's head from the scanner within 5^{o} of the end of the scan results in a very bizarre appearance.

Barium within abscess cavities produces very high density readings. A certain amount of overshoot occurs at the edges and this may produce problems during follow-up when the development of further loculi may occur. Enhancement of new loculi may be overshadowed by the residual barium. It is therefore essential that barium and other persistent radio-opaque materials should not be put into abscess cavities.

Air by itself is relatively innocuous in small quantities and only produces computer overshoot (Fig. 4). This is a white line around the margin of the air or in the case of the bony vault a black line immediately deep to the bone. With the 160 × 160 matrix the overshoot is 1-2%. Any patient movement of the head, however, produces very marked artefact (Fig. 5).

Metallic objects such as surgical clips or metallic plates, however, present a greater problem. Surgical clips almost invariably produce severe streaking radiating outwards from the clip. A single clip is relatively easy to avoid by scanning above or below or by angling the cut. Multiple clips, particularly when accompanied by movement, are a different matter. Larger metallic objects such as a plate at first sight produces a completely undiagnostic scan. Alteration of the window levels can reduce the artefact considerably and, although detail is poor, such structures as the lateral ventricles and choroid plexuses may become visible and this may be sufficiently diagnostic, particularly in a follow-up scan.

Myodil only produces problematic artefacts by reason of its most frequent situation in the posterior fossa, already a difficult area to scan. Large amounts of Myodil may, however, render the posterior fossa undiagnostic.

Table 2. Causes of minor patient artefacts

1. Posterior fossa-IAMs
2. Air cell distortion
3. Asymmetry
4. Hair and deflation of trapped air
5. Shunt tubes
6. Intracranial calcification

Table 2 lists the types of artefacts which if recognised do not cause a problem in diagnosis.

A common artefact is a linear horizontal low density artefact in the posterior fossa situated between the internal auditory meatuses (Fig. 6). This is usually seen on one cut only, although occasionally it obscures a small fourth ventricle.

Artefacts may occur between areas of similar extremes of density, for example between the ethmoid and mastoid air cells (Fig. 7). They should not cause problems of diagnosis since the artefact extends between the two, but alteration of the window may be required before the artefact becomes obvious.

Slight asymmetry of the skull may result in the occurrence of low density areas, the commonest one being in the temporal fossa. It is only present on the lowest temporal scan, and may represent overshoot related to bone in the orbital plate.

A similar-looking artefact is seen in the frontal region, sometimes extending into the temporal region, but in that case always involving the frontal region as well (Fig. 8). This is due to hair, and to air trapped between the head bag and the skull deflating during the course of the scan. Shunt tubes and calcification within the skull vault do not usually produce much artefact unless patient movement occurs. Such artefact as does occur is related to computer overshoot but does appear to depend upon the shape of the artefact. Sudden changes in absorption coefficients produce greater artefact.

Machine Artefacts

Machine artefacts may arise from many different sources and can be adequately divided into those due to the scan machine, those due to the viewer or diagnostic console, and those due to the computer itself.

Table 3. Scanning unit artefacts

1. Indexing-less than 5^{o}
greater than 5^{o}
2. Head box movement
3. Faulty high tension cable to detector
4. Tube wear
5. Air bubbles in head box
6. Burst head bag

Table 3 is a list of some of the artefacts which can occur with the scanning unit.

Irregular indexing, that is, failure of the normal 1^{o} rotation may occur. Most commonly there is intermittent indexing of up to 5^{o} and this produces low density artefacts which are most prominent in the periphery of the scan. The centre of the scan is usually reasonably normal and ventricles and other midline structures can be interpreted without much difficulty. Occasionally, indexing faults as great at 10^{o} or more may occur. This produces a far greater degree of artefact and involves all areas of the scan. It is to be noted, however, that the shape of the skull vault is formed in a normal manner.

Movement of the whole head-box unit produces a rather bizarre appearance. Vertical and horizontal artefacts occur, both inside and outside the skull vault, and it is impossible to define even the ventricles. However, the outline of the skull vault remains intact.

A faulty high tension cable to the scan detectors may produce intermittent high voltage to the detectors. This may occur only during part of the scan and the linear streaks produced are present in only part of the display. A more persistent faulty contact produces streaking over the whole scan.

Tube wear results in a marked increase in the overall noise-to-signal ratio and this has the effect of producing a loss of definition without completely obliterating the scan information. The development of this particular artefact is insidious, and the quality of the scans is only gradually reduced. The diagnostic quality of the scan is only impaired at the end of the tube life.

Small bubbles of air occasionally remain in the head-box and are situated during the scan between the tube and the detectors. This produces a quite characteristic artefact, there being an inverted horseshoe-shaped low-density shadow within the display area extending over the scanned angle of 180^{o} or 225^{o}. The position of the artefact is constant whatever the position of the patient.

The last of this group of artefacts involving the scanning unit is due to a burst head bag occurring at the end of the scan. The outline of the bony vault is visible but no intracranial structures can be seen. The whole scan has a grey quality and an air bubble is present at the top of the scan.

Viewer Artefacts

The types of artefact which may occur due to problems with the viewer are shown in Table 4. They are due either to high tension circuit,

Table 4. Viewer artefacts

1. High tension cable fault
2. Vertical drive fault
3. Photographic fault

vertical drive faults or photographic faults. A faulty high tension lead produces a make-and-break contact artefact on the screen. The artefact lines are parallel and horizontal. If the fault is intermittent, part of the image may be acceptable. However, if the cable fault is more persistent, then the quality of the image becomes totally un-

satisfactory. Naturally, a complete break in the high-tension cable results in no picture.

Partial interruption of the 30-V power supply to the vertical drive of the cathode ray tube results in part of the display being absent over the period of the interruption. If the cathode ray tube oscilloscope is used for photographing the scans, it is important to switch from 'view' to 'photograph' when the image is complete. Failure to do this results in a horizontal artefact, the upper part of the picture being more exposed than the lower (Table 5).

Table 5. Computer artefacts

1. Dirty disc head
2. Disc head controller fault
3. Disc corruption
4. Integrator fault
5. Memory board fault

Artefacts Due to the Computer

Many artefacts may occur in the computer itself. They may be divided into those involving the disc head or the disc itself and more complicated ones involving the memory boards and integrators in the scan electronics. Failure to clean the disc head may result in one or both images being unacceptable, with increased noise-to-signal ratio similar to that seen with tube wear. If only part of the disc head is dirty it is possible to separate the two artefacts, since one scan is relatively normal while the other scan is of poor quality. Faults in the disc head controller may result in malformation of the display image. The normal ring of the bony vault is not complete and two overlapping half circles occur. Corruption of the disc may occur resulting in artefact. The display image may be relatively unharmed but almost any display abnormality may occur.

Faults in the integrators in the scan electronics converting the signal from the photomultiplier tube to digital form may occur. If 'bits' are lost the quality of the scan is impaired, the display appearing as a rippling effect seen on still water.

Faults on the memory boards again vary, and the appearance can be very bizarre. A display is produced which may bear no resemblance to the correct one.

Summary

Artefacts are either man made or machine made. The machine artefacts are interesting and may produce very bizarre appearances; but so abnormal are they that they cannot produce any confusion in radiological diagnosis.

Man-made artefacts on the other hand are rather more subtle and frequently can be corrected or avoided. It is therefore important to be aware of the possibilities, so that errors of judgement and diagnosis do not occur.

Fig. 1

Fig. 2

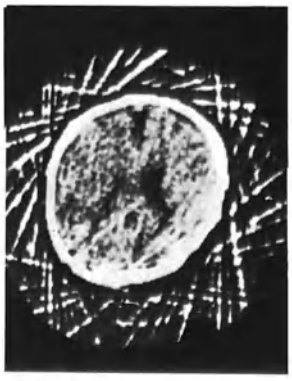

Fig. 3

Fig. 1. Nodding movement artefact
Fig. 2. Horizontal movement artefact
Fig. 3. Rotational movement artefact

Fig. 4

Fig. 5

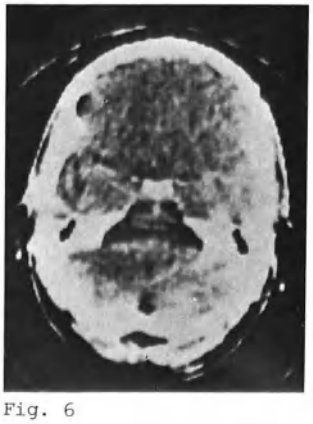

Fig. 6

Fig. 4. Air in ventricles. Small artefact due to computer overshoot, with patient still
Fig. 5. Air in ventricles. Patient movement producing marked artefact
Fig. 6. Posterior fossa artefact due to petrous bones and mastoid air cells

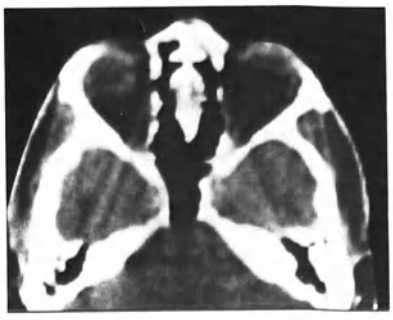

Fig. 7

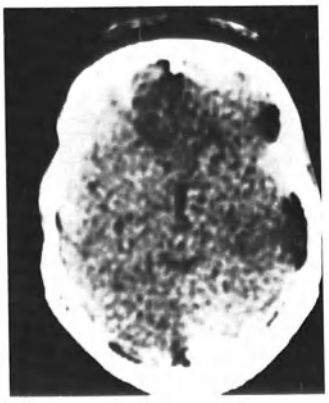

Fig. 8

Fig. 7. Left orbital and temporal artefact due to air cells
Fig. 8. Left frontal and right fronto-temporal artefact due to trapped hair and air

C.A.T. Under Stereotaxic Conditions

J. M. Caillé*, F. Cohadon, P. Constant, and J. P. Campagne

C.A.T. provides a direct three-dimensional picture of the head. Lesions situated near easily-identifiable anatomical landmarks can be localised with only a small margin of error. However, for certain lesions situated away from these landmarks, localisation is more problematical. This is the case for lesions of the centrum ovale, those close to the vertex, parasagittal lesions, intra-axial lesions of the posterior fossa, etc.

Moreover, the slice angle varies from one examination to another, even with the same patient. The parallelism of the slice planes to the orbitomeatal plane is not stable because the head is not held with sufficient rigidity. In the axial slice alone, angular variations can cause errors of from one to several centimeters for lesions away from the easily-identifiable landmarks. It is thus very difficult exactly to locate small lesions of several centimetres in diameter, to compare one slice with the preceding one, and to follow with precision the evolution of ventricular dilation, an infarct or a tumour receiving radiotherapy.

It is possible with certain machines (Total Body Scanner) to supplement the axial slices with coronal ones. These frontal slices give some help in the localisation of small lesions but there is still considerable imprecision. The slice is rarely perpendicular to the axial slice and the angular variations already mentioned introduce a considerable cause of error.

For all of these reasons we decided to do C.A.T. under stereotaxic conditions using a frame derived from Talaraich's stereotaxic frame fixed rigidly to the examination table. The slices are strictly parallel to the plane of the frame, which serves as reference.

The fixation points of the frame are the bridge of the nose and the external auditory meatus. For each patient the coordinates of these points are noted (Fig. 1).

For any given patient it then becomes possible to repeat the C.A.T. under conditions which, if not absolutely identical, are at least very similar. Angular variation is of the order of 1^{o} and linear error of the order of 1 to 2 mm.

In order to eliminate the partial volume phenomenon the slices are done every 7.5 mm (Acta Scanner gives 2 slices 7.5 mm thick and 3 mm apart). The polaroids are then enlarged (photographically) to bring the picture to its true dimensions. Immediately after the examination a cylindrical phantom of known diameter is scanned in order to determine the enlargement coefficient to be applied to the polaroids. It is then easy to

*Service de Neuro-Radiologie, Centre Jean-Abadie, 89, rue des Sablières, 3300 Bordeaux (France).

determine the coordinates of a point in three dimensions using the stereotaxic frame as reference.

The stability of the slice orientation then allows one to compare one examination with another for the same patient so as to determine precisely the localisation and volume of any tumour whether large or small.

This stereotaxic technique has obvious applications:

1. The scans provide exactly superimposable pictures which can be used to follow the evolution of all pathological processes, ventricular dilatation, haematoma, softening, tumour undergoing radiotherapy or chemotherapy.

2. It allows one to locate and to determine exactly the volume of a large tumour being treated by radiotherapy.

3. It is of use also in the diagnosis and treatment of small lesions. A second frame identical to the one used with the scanner is used in the Neurosurgery Department. By reproducing the conditions of the C.A.T. examination and doing an angiogram in stereotaxic conditions the biopsy of small lesions (of the order of 1 cm diameter) is possible without a risk of error.

After histological analysis, the precision of localisation of the target volume allows surgery or radiotherapy to be undertaken. After calculation of the dose it is possible to carry out interstitial radiotherapy with iridium strands for small lesions deep in the brain.

Conclusion

The relative imprecision of C.A.T. in locating and determining the volume of tumours led us to perform the examination under stereotaxic conditions.

By the use of this technical device, the evolution of pathological processes can be followed, the histological diagnosis of small lesions can be facilitated and possible surgical or radiotherapeutic treatment rendered more precise and thus more effective.

Reference

1. BERGSTRÖM, M., GREITZ, T.: Stereotaxic computed tomography. Amer. J. Roentgenol. 127, 143-155 (1976).

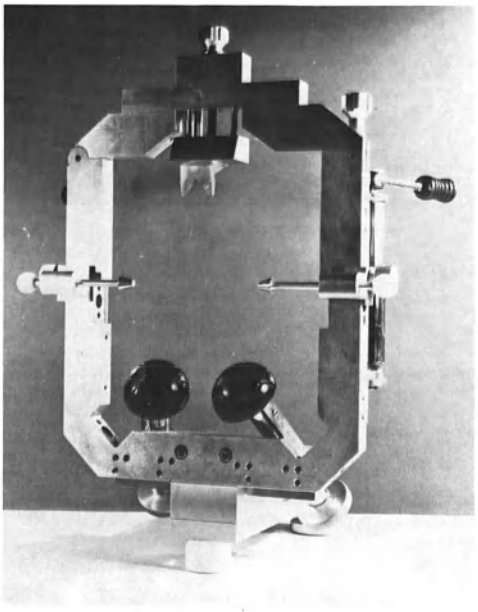

Fig. 1. Talaraich's stereotactic frame

The Application of Receiver Operating Charateristic Curve Data in the Evaluation of Hard Copy and an Interactive Display from an EMI Scanner

B. R. Pullan* and I. Isherwood**

Introduction

The basic principles of signal detection and decision theory have previously been applied to the problem of evaluating quantitatively and objectively the ability of observers to detect signals or image features in the presence of noise (1-5).

In a simple signal detection exercise the observer is presented with a series of images only some of which, usually 50%, contain a signal against a background of noise. The remainder contain only noise. The observer is then required to decide whether a signal is present or not. Clearly a 'confidence threshold' or 'level of conservatism' must be taken into account if the observer's response is to be meaningful. The frequency of correct, i.e. true positive or true negative, or incorrect, i.e. false positive and false negative, decisions will depend on such a threshold.

A receiver operating characteristic curve (R.O.C.) at its simplest is a graph plotting conditional probability of true positive against false positive responses, as the level of conservatism is varied. An analysis of observer or detection performance is then possible from this data.

If pure guesswork is employed, e.g. a blindfold observer, then the response should be independent of the actual presence or absence of the signal. The R.O.C. curve is then a straight line at 45^{o} to the abscissae. If information about the presence or absence of a signal is actually present in the image and perceived then the conditional probability of a true positive response will be greater when the signal is actually present. A typical R.O.C. curve is therefore in the upper left-hand half of the graph (Fig. 1). The technique can be further elaborated by recording the position of the signal within the noise.

The aim of the present investigation has been to set up the technique in Manchester to enable a quantitative comparison to be made of display techniques. This paper describes such an application of the method and the results obtained in the comparison of hard copy on polaroid film and an interactive display on a Diagnostic Display Console (D.D.C.) from an EMI brain scanner during observations of marginally detectable changes in a phantom object.

*Department of Medical Biophysics, University of Manchester.
**Department of Diagnostic Radiology, University of Manchester.

Material and Methods

Five objects were made from acetate sheet. Each object was a 1 cm diameter disc of 0.125 mm thickness with a density of 1.2 g per cc.

Five such objects were spaced at 1.2 cm intervals on nylon threads stretched parallel to the axis of the scanner in a specially devised frame. The nylon thread was of 0.008 in. diameter. Each object had a small hole in the middle with a slit from the hole to the edge of the disc to enable easy threading. A spacing of 1.2 cm was chosen in order that two objects never appeared on a single section. The frame and objects were then immersed in gas-free water (fresh distilled water from a still).

A total of 28 computer tomographic sections were then obtained at random. The assumption was made that each section would contain a positive object but of variable detectability. The objects were then moved to the top of the suspending wires and eight further sections obtained through water only, at different positions, but with the frame in the same orientation. The orientatation of the frame could not then be used to detect the presence or absence of objects.

The computer tomographic section numbers were then placed in random sequence by reference to random number tables. An equal number of positive and normal sections were then arranged at random (Figs. 2a and 2b).

Sequences of eight such random sections were then transferred to each of seven floppy discs making a total of 56 sections.

Polaroids were obtained from the D.D.C.'s small monitor for each section at a fixed window width, selected by an independent observer. The window level employed was 2 and the window width 30, for all polaroids.

A form was devised requiring the observer to record the presence or absence of any abnormality on a confidence scale of 0-9. The score 9 indicated absolute confidence that a lesion was present. Score 0 indicated absolute confidence that a lesion was not present. The forms were completed for both polaroid and interactive displays with two observers.

All polaroid prints were viewed with the observer sitting at a desk under normal office lighting. The D.D.C. was viewed in two ways:

1. With the observer sitting close to the screen, in the normal viewing position and being allowed to alter window width and window level settings at will.

2. With the D.D.C. display at 12 ft from the observer so that the display screen subtended about the same angle at the eye as the polaroid prints. No interaction with the display was allowed in this case.

Data Analysis

Histograms were obtained of all numbers recorded by each observer and for each experiment. The histograms were divided into sections containing equal numbers of responses. The criteria were such that 10, 25, 40 and then all numbers of responses were positive. This technique

enabled the normalisation of four levels of conservatism to be achieved for different observers and the same observer on different occasions (Figs. 3a and 3b).

The response sheets were analysed and coded into correct and incorrect responses. Each score at each level of conservatism was summed. With knowledge of the total number of objects and the total number of normals, the percentage of correct and incorrect observations could be calculated. All data from repeated runs were pooled for each observer and the total percentages calculated.

The percentage of correct observations was then plotted against the percentage of incorrect observations for the different levels of conservatism, thus generating the R.O.C. curve.

Results

The R.O.C. curves for the interactive display indicate a difference between the two observers (Fig. 4a and 4b). Observer B showed more random observations as the conservatism level was reduced.

The detectability of the abnormality was better when using polaroid prints than the D.D.C. with interaction and close viewing conditions. The same result was obtained for both observers. When the D.D.C. was used without interaction and at a large viewing distance, the detectability of the lesion was at its highest. This was true for both observers (Fig. 5a and 5b).

Discussion and Conclusions

The R.O.C. curve is relative to the observer and display. Comparison between displays using observers is possible when the same object and observer are used for all observations, i.e. the display is the only variable.

In these experiments an attempt has been made to stabilise the test objects and observers so that the results will indicate differences between the display methods tested.

It can be concluded that under the conditions of the experiment, with uniform background and free interaction with the display and close viewing, that the polaroid prints allowed better detection of the abnormality then the D.D.C.

Possible explanations of this are:

1. The high display contrast which can be achieved using the D.D.C. may allow false positive results to be generated from noise by over manipulation of data. This was not possible with the polaroid prints.

2. The image of the abnormality on the polaroid prints subtends a much smaller angle at the eye under normal viewing conditions than does the D.D.C. when viewed sitting at the display console. The smaller viewing angle in the case of the polaroid prints leads to a suppression of irrelevant detail such as scan lines and pixel edges and also an averaging of the noisy data leading to better detectability.

The second suggestion is supported by the results obtained using a long viewing distance. The improvement in detectability over polaroid prints in this case can be accounted for by the degrading effect of the photographic process.

These experiments indicate that there may be dangers in overmanipulation of data or digital display consoles, particularly when the observer sits close to the display.

Acknowledgments

The authors would like to thank Dr. R.A. Fawcitt and Mr. R. A. Rutherford for their valuable assistance and the Department of Medical Illustration and Mrs. G.E.H. Shawcross for preparation of illustrative material. They would also like to thank Mrs. M. Tipton for her secretarial support.

References

1. GOODENOUGH, D.J., ROSSMANN, K., LUSTED, L.B.: Radiographic applications of signal detection theory. Radiology 105, 199 (1972).
2. GOODENOUGH, D.J., ROSSMANN, K., LUSTED, L.B.: Radiographic applications of receiver operating characteristic (R.O.C.) curves. Radiology 110, 89 (1974).
3. LUSTED, L.B.: Receiver operating characteristic analysis. In: Current Concepts in Radiology, POTCHEN, E.J. (ed.). St. Louis, Missouri: C.V. Mosby Co. 1975, Vol. II, p. 117.
4. METZ, C.E., GOODENOUGH, D.J., ROSSMANN, K.: Evaluation of receiver operating characteristic curve data in terms of information theory with applications in radiography. Radiology 109, 297 (1973).
5. STARR, S.J., METZ, C.E., LUSTED, L.B., GOODENOUGH, D.J.: Visual detection and localisation of radiographic images. Radiology 116, 533 (1975).

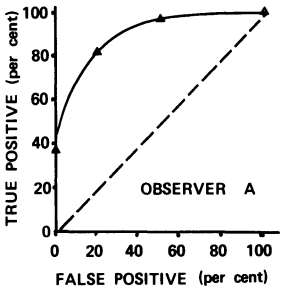

Fig. 1. Typical R.O.C. curve

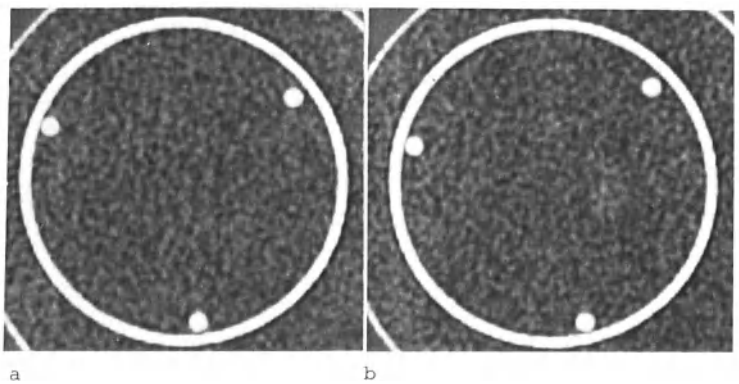

Fig. 2a and b. Polaroid prints of computer tomographic sections of test object. (a) Normal, (b) Positive

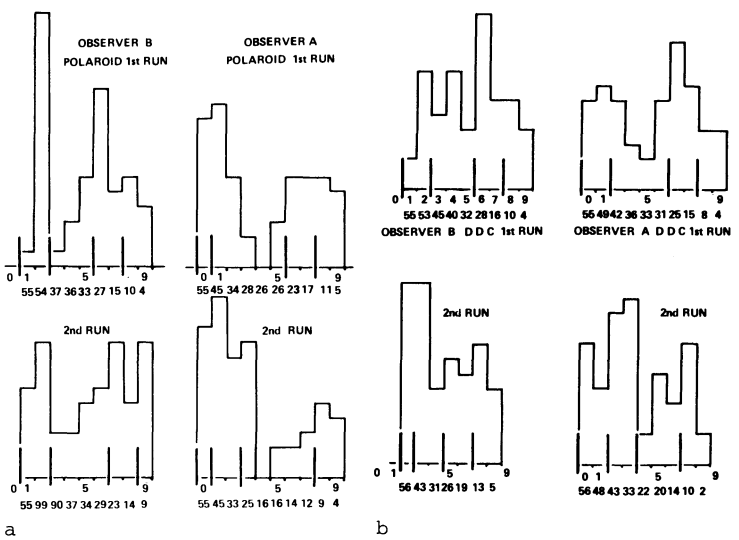

Fig. 3a and b. Histograms of recorded confidence scale numbers. (a) First run. (b) Second run

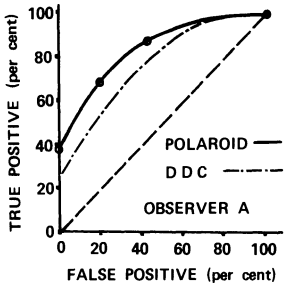

a

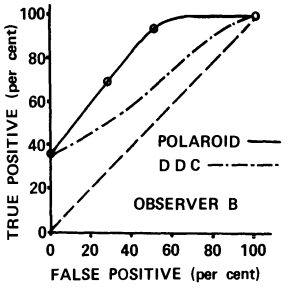

b

Fig. 4a and b. R.O.C. curves for polaroid prints and interactive display (D.D.C.). (a) Observer A. (b) Observer B

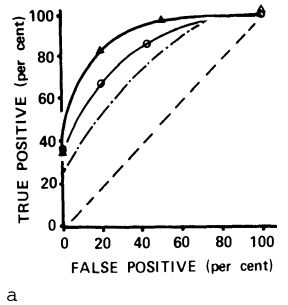

a

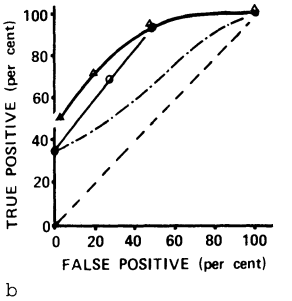

b

Fig. 5a and b. R.O.C. curve for polaroid copy interactive display and D.D.C. viewed from a distance. (a) Observer A. (b) Observer B

Costing and Logistics

Departmental Logistics: C.A.T. in a Neurological Hospital

G. H. du Boulay*

How Does a Neurological Hospital Differ?

How does the work of a neurological hospital differ from that of the neurological services of a general hospital?

1. It is likely that all, rather than only a proportion, of the X-ray staff can take their turn in the C.A.T. scan rooms.

2. It is probable that the case load will be especially heavy.

3. There may be a greater commitment and obligation to carry out research.

4. Unpaid help may be available for research and even for part of the service commitment from postgraduates attached to the hospital.

For more than a year the case load at Queen Square was so great that only in-patients could be scanned, but this probably ensured that the apparatus was used on the iller or more urgent patients (as borne out by the very low proportion of normal scans - 10-15%).

The installation of a second scanner has allowed us to scan out-patients again (about two-thirds in-patients to one-third out-patients at the moment).

In-patient C.A.T. scanning involved an average wait of 3 days. No doubt for some this time was well spent, but for those for whom the admission to hospital was purely for the purpose of getting a scan it represented an extra charge on the Health Service. Subsequent experience suggests that up to about one-third of the patients were admitted for this reason alone, involving 3,500 in-patient-days, costing £47.71 × 3500 (nearly £167,000). This was almost the cost of another EMI scanner spent simply on bed-occupancy.

Estimating the Cost of a Service

Estimation of the approximate cost of installing and running a C.A.T. scanner is a simple though rather tedious calculation. The exercise is much more difficult when one attempts to set savings brought about by C.A.T. scanning against these costs.

First of all a philosophy has to be adopted. For example, there is at the moment no doubt that C.A.T. scanning is replacing many air-studies. For the moment, then, it is helpful and realistic to set the saved cost

*Lysholm Radiological Department, The National Hospital, Queen Square, London WC1N 3BG.

of an appropriate number of air-studies against the cost of a similar number of C.A.T. scans, but for how long may one go on calculating like that? If one were not to change the method after a while one would now still be allowing for savings in the Health Service on phasing out leeches.

It seems to me reasonable to set the costs of one type of examination. against the other only when looking for the effects of bringing a C.A.T. service up, more or less, to maximum use - a phase which with us is now nearly over.

After that, though one may monitor small shifts in the usage of alternative examinations, it is likely to be more useful simply to state the costs without accounting savings on other studies and shorter bed-occupancy.

To judge from our experience it takes at least 3 years to appreciate how best to use a C.A.T. scanner, and we are still making a few significant changes in our investigatory regimes. I have therefore chosen to assume that after 5 years a more or less stable situation will have been reached. The diminution of pneumoencephalograms and scintigrams over that time is, however, more or less exponential. I have assumed that the decrease in these examinations at the half-way point (2 1/2 years) is near its maximum, and as this 2 1/2 years' point for us has already passed we can apply actual experience to the calculations.

Cost-benefit analysis at 2 1/2 years is likely therefore to be roughly applicable up to the end of the first 5 years, but increasingly thereafter, benefits will be in the form of more information per patient and a service for more of the population. Both of these benefits are in general quantified as changes in bed-occupancy and greater departmental through-put (15% in our case).

Depreciation of apparatus is also difficult to estimate during a time when many improvements are being made in design. I have assumed not only that a significant sum will be spent yearly on updating the old apparatus, but that after 5 years it will be so obsolete that its secondhand value is no more than £25,000.

We have been able to cost these X-ray examinations from historical data. A summary is given in Table 1 where it is shown that one patient examination costs £30.9. This applies, however, only to 1975/76. The cost changes. For example, we are at the moment operating two head scanners in adjacent rooms without any increase in staff. The price of this second scanner, borne by Research and Development, was greater than the first, and other costs have escalated too, notably service charges. The net result, however, is that the cost of a single scan has very slightly dropped (£30). (In order to make this calculation I have counted both cost and servicing as though paid by the hospital rather than the DHSS's Research and Development budget). Our patient examinations are rather more elaborate and take longer, so that we are probably working at the rate of about 3000 a year on each machine. Updating to Mark II standards will change the cost again, presumably in a downward direction.

Savings on Other Examinations

In 1973 we were carrying out 750 angiograms, 700 pneumoencephalograms and 3600 scintigrams a year. As in costing C.A.T. scanning, every item

Table 1. Costs of C.A.T. scanning 1975/6

Capital		
Depreciation of capital investment (less resale price)	£25,000.00	
Proportion of installation cost	8,000.00	
Annual updating	15,000.00	
Total	£48,000.00	£48,000.00
Salaries		
Radiologists	7,250.00	
Radiographers (including training)	12,475.00	
Nurses	1,100.00	
Anaesthesist	200.00	
Reception, typing and filing	6,430.00	
Porter	3,000.00	
Cleaner	150.00	
Total	£30,650.00	£78,605.00
Expendables		
Polaroid film	10,000.00	
Contrast medium	5,000.00	
Servicing and repairs	7,500.00	
Major replacements (e.g. tubes)	5,000.00	
Tapes	320.00	
Miscellaneous	1.700.00	
Total	£29,520.00	£108,125.00
= 3500 patient examinations at £30.9 each		

of expenditure relating to the X-ray Department has been taken into account, including costs of installation, depreciation and a due proportion of all salaries, not forgetting something for supervision, in-service teaching, filing and reporting.

Table 2 shows the approximate monetary cost of an individual angiogram, pneumoencephalogram (AEG) and scintigram.

Table 2. 1973 Costs of examinations per patient (£ sterling)

Investigation	No. performed	Capital	Salaries	Expendables	Total
Angiogram	750	11.6	16.4	25.7	53.7
AEG	700	7.3	20.7	9.99	38.0
Scintigram	3600	1.8	16.8	2.5	20.1

Changes take place continuously, however.

Decreases in the numbers of angiograms, AEGs and scintigrams have released radiographers for duties which have increased - C.A.T. scanning particularly, but the nursing side has not undergone the same redeployment so that the nursing contribution to individual examinations costs a little more.

We were also able to sell our rectilinear scanner for £1,500 (it cost £12,000 in 1971) and carry out all scintigraphy with a single gamma

camera. Inflation has had its effects. Costs of individual examinations in 1976 are shown in Table 3.

Table 3. 1976 Cost of individual examinations

	No. performed	Total cost of one (£/sterling)
Angiogram	500	69.3
AEG	260	45.7
Scintigram	1200	25.00

At 1973 prices the contrast investigations avoided in 1 year would have cost £78,385 and the cost of associated extra bed-occupancy avoided was of the order of £32,590 (£78,385 + £32,590 = £110,975).

Research

Research is a major occupation of the National Hospital, but it is very difficult to estimate the proportion of salaries devoted to research when so many people are involved in their space time; I have counted 5 hours of consultant time a week and 3 hours of senior registrar time, as paid for by the National Health Service and used during normal working hours, in addition to the staff employed for research from research funds. In total research and travel really costs about £15,000 a year. We receive in grants and salaries about £12,000 a year.

The difference has been partly made up from a discretionary fund derived from private patient fees, but most of it represents time which was given free by the staff for research activities outside normal working hours.

Logistics: A Neuroradiological Service. The Cost-Effectiveness of an EMI Brain Scanner

J. L. G. Thomson*

An EMI Brain Scanner has been fully operational at Frenchay Hospital since June 1st, 1974. An attempt is made to assess the cost-effectiveness of the machine during the first 2 years of use, by balancing the estimated cost of the machine and its operation, in relation to the amount of work done, against the savings made in the same period. Some assumptions have to be made, but it is considered that these are if anything on the conservative side for the purposes of the paper.

Frenchay Hospital is a District Hospital serving a local population of about one-quarter of a million people, with regional units for plastic surgery, thoracic surgery and neurosurgery in addition, serving a much greater population of about two and a quarter million people. The neurosurgical unit has 53 beds, in the care of four consultant neurosurgeons, and there are also 30 neurological beds in the care of two neurologists. The X-ray department is staffed by a superintendent radiographer and 21 radiographers, meeting the demands of the whole hospital, the regional units, and a busy accident and emergency unit, with a full daytime and evening service and overnight and weekend cover. In 1975/76 there were 49,500 patient attendances in the whole X-ray department.

Against this background an EMI brain scanner was installed in 1974 and became fully operational on June 1st of that year, although for the first four months, only a daytime service was provided until all the radiographers had been taught to use the machine. Thereafter inpatients and outpatients, both of our hospital and of others in the region, were accepted for examination on an appointment system. In the year 1974/75, 2102 scans were carried out on 1520 patients and in 1975/76, 4012 scans were carried out on 2559 patients. Of these, 570 and 786 patients attended the department as outpatients either of our hospital or other hospitals in the region, respectively. These patients, who would previously have had to be admitted to hospital for traditional investigatory techniques, e.g. cerebral angiography and pneumoencephalography, represent a considerable saving to the hospital and the taxpayer by no longer requiring a bed for a diagnosis to be obtained.

Furthermore, as a result of the accuracy of the information provided by the scanner, there was a significant reduction in the demands for traditional investigations, so that the numbers of cerebral angiograms have reduced to about 50%, pneumographies to about 25% and isotope studies to about 33% of those obtaining in the previous years. An incidental finding is that the average length of inpatient stay of 18 days in 1970 has become 13.2 days in 1975, although the contribution played by the scanner towards this reduction would be difficult to evaluate.

Concerning the cost of installing and running the machine, which is regarded as having a 10-year life, to include a service contract, spare

---

*Frenchay Hospital, Bristol, Great Britain.

parts allowance, the engagement of an extra senior radiographer, an extra secretary, a part-time physicist, and allowing for overtime payments, Conray injections, telephone, heat, light, power etc, tables show that in 1974/75 the total was nearly £30,000 and for '75/'76 was nearly £50,000. The virtual doubling of the work-load in the 2 years meant in fact that the absolute minimum cost per scan remained at about the same level, i.e. £12-15. It should be understood that this represents the extra cost over and above money used on the X-ray department before the introduction of the scanner and still needed in 1974-76 for such items as for example radiologists' salaries.

However, the savings which accrued from the use of the machine more than balanced out the above figures for extra expenditure. The savings arose from two main sources, the traditional investigations no longer required, and the beds saved by outpatient attendances. In the first group, the savings on the arteriograms, pneumoencephalograms and isotope scans were calculated to be of the order of £14,000, and in the second group the savings were thought to be between £25,000 and £70,000 taking the lowermost figure for 1974/75 and the uppermost figure for 1975/76 calculated on a patient stay of either half a weak or a whole week in hospital.

It is assessed, therefore, that the savings which arise from the installation of such a machine, certainly in an environment such as that in existence at Frenchay Hospital, more than outweigh the expenditure involved. Greater detail of the figures quoted will be found in *Health Trends* (1).

Reference

1. THOMSON, J.L.G.: Cost-effectiveness of an EMI Brain Scanner. In: Health Trends (in press).

C.A.T. of Brain and Body in a General Hospital

M. Collard*

Organisation and logistic planning of a radiology service, particularly of a C.A.T. service, is currently made more difficult by rapid technical progress. Thus, when James Ambrose gave the first results of cerebral C.A.T. in Madrid in 1973 (8th International Congress of Radiology), he did so to a very small audience; scarcely 3 years ago this technique hardly aroused any interest in radiologists or neuroradiologists, despite its truly revolutionary nature. To have planned a department in 1973 without giving due thought to such a technological advance would have been risky indeed.

This notion indicates very well the fundamental change through which our discipline is passing today. Perhaps we should therefore discuss 'diagnosis by physical methods' rather than 'radiology', for radiology has recently grown to encompass thermometry, ultrasound, dynamic ultrasound (Doppler flow recordings), bone densitometry and a number of other techniques.

For the first time, these various methods have been taken up by several different disciplines: thus, ultrasound imaging is employed by gynaecologists, cardiologists, neurologists, etc. At the same time, by virtue of the exponential development of technology, it seems desirable to concentrate technical investment in a centralised department which is open to the various specialities and subspecialities. Since the indications and role of these techniques are so rapidly changing, it is obviously preferable to make use of such a complex installation on a pluri-disciplinary basis, and to adapt it to technological advances rather than to duplicate identical facilities within a single hospital.

Apart from its purely medical aspects, continuing development of physical diagnostic methods in a centralised service entails ever closer and more efficient collaboration with engineers and physicists alike.

Placement of a C.A.T. Department

It may be useful to attempt a definition of the objective criteria governing the installation of a C.A.T. apparatus within a hospital. In most countries, at the present time, the need for some such installation appears self-evident, although that need may often arise for reasons other than purely medical (e.g. prestige).

Experience in Belgium has proved interesting: during 1974 and 1975 our own C.A.T. brain machine was the sole apparatus not only in Belgium, but in the neighbouring countries as well: a study of the location of

*Agrégé, Chargé de Cours a L'Université Libre de Bruxelles, C.G.T.R., B-6110 Montignies le Tilleul.

the referring physicians would therefore allow us to suggest objectively where C.A.T. devices could be usefully placed in Belgium. In fact, during those two years, our patients came from four specific groups of Belgians only, while, at present, some 20 groups are asserting a need for such apparatus, occasionally for more than one machine.

This demographic study related clearly to a need per capita: siting of C.A.T. machines is justified not by the presence of a hospital (be it university linked or not: the difference in the end result is becoming less and less apparent) but by the patient population concerned. In fact, as with any piece of heavy equipment, the important factors in placement of C.A.T. machines are related to regional needs, to the size of the patient population, and also to communications and access.

Referral Pattern of Patients

The patients referred during our first 2 years with the brain C.A.T. apparatus came essentially from neurological specialists, but, increasingly, we have noted that patients are being referred directly by general practitioners, without a previous neurological consultation. We are not in a position to refuse patients referred directly for C.A.T. by general practitioners; and we feel it somewhat unreasonable to insist that patients should undergo a neurological examination. In addition to these theoretical considerations, our experience has shown that the proportion of cases with positive C.A.T. findings among those referred by general practitioners has increased, which we think reflects the growing interest in a reliable, non-traumatic means of investigation.

Organisation of a C.A.T. Department

Referring Doctors

The medical staff, specialised or with general interests, who may order C.A.T. examinations must be fully aware of the possibilities and, particularly, the limitations of the method.

As a result of the publicity the technique has received, the medical profession may have gained the impression that C.A.T. is almost infallible, and capable of diagnosing any condition. We are currently trying to rectify this by describing the specific indications for this type of investigation, its limitations and the possible types of error to general practitioners by means of a series of meetings organised at their request.

For any more specialised groups, the problem may sometimes be aggravated by unwillingness to admit that a new method may permit older ones to be replaced. Thus, it has been difficult to establish the correct role for the EEG (as a functional test), or to show the limited applications of cerebral ultrasound studies. This reluctance is not unique to clinicians, and over the last few years a number of neuroradiologists have denigrated the contribution of C.A.T. seemingly in an attempt to defend conventional neuroradiology.

Thus, those who find themselves in charge of a C.A.T. department must apply themselves to educating the referring staff, with the end view of reducing the burden of superfluous or poorly-indicated examinations.

Paramedical Personnel

These personnel have three functions:

1. To deal with the patients
2. To manipulate the apparatus
3. To maintain the apparatus in good working order

The first of these is easily carried out by the previously existing staff, and is basically no different from their role in conventional radiology. On the other hand, the manipulation and maintenance of a C.A.T. machine involve an increase in technical staff. Trained nurses have no role in a modern radiology department except when minor surgical procedures are involved (catheterisation, punctures, etc), but technical staff are increasingly needed. It is simpler to teach anatomy or certain basic clinical concepts to technical personnel than to teach nurses technology. This being so, it would seem more logical to recruit graduates of an industrial college and then train them in radiography.

Medical Personnel

Interpretation of the results of C.A.T. falls naturally within the general training of a radiologist, and it is best not to over-specialise the individual doctor; this also applies to ultrasound or any other physical diagnostic method.

The development of radiology since the advent of C.A.T. makes a precise knowledge of each method of examination and their synthesis more necessary than ever. Hyperspecialisation tends to increase the number of investigations carried out regardless of the efficiency with which radiology is then being employed for the patients' good.

The development of C.A.T. has meant that a good understanding of radiological anatomy is more important than it was previously.

Computer Engineers

A computer expert will become an indispensable part of a radiological service, dealing with the ever-increasing possibilities of memory, subtraction, etc., posed by developments in C.A.T. In a large general hospital, each radiological service has specific problems which can be approached by a computer expert; it seems highly desirable that he should be attached to the department itself so as to best appreciate its problems and provide adequate solutions, working with a computer belonging to the radiological service, or integrated with a central hospital computer.

C.A.T. Brain/Body

The great medical difference between brain and body C.A.T. at present would seem to lie in the sequence of radiological investigation which each imposes. For the brain, C.A.T. is a first-step procedure, conventional procedures such as pneumoencephalography or angiography being used secondarily, as indicated by C.A.T.

It is generally noted (and our experience would confirm) that the numbers of conventional neuroradiological investigations have undoubtedly

decreased since the advent of C.A.T. This does not reduce the neuro-radiologist's contribution, but enables him to concentrate his efforts on more problem-orientated examinations.

Conversely, C.A.T. examination of the body is carried out only when a problem has exhausted the resources of general radiology or its associated techniques such as ultrasound. This inverse relationship derives from the obvious need to centre the body C.A.T. on a particular region, which is in turn made necessary by the importance of keeping the radiation dose to a minimum. Dosimetric studies show, in fact, that the dose resulting from C.A.T. of the body extends beyond the tomographic cut itself, and that adjacent tissues may receive between 15% and 30% of the dose delivered to the slice under examination.

Quite independently of this biological consideration, the cost of a C.A.T. study of the body imposes a prior selection of patients.

These differences between the brain and body C.A.T. devices raise a difficult problem as regards the equipment of the radiological services of a large general hospital.

From the Technical Viewpoint

Technically, the brain C.A.T. machine is the best suited to the examination of the brain because of its higher powers of resolution and the reproducibility of the results (in EMI numbers). Moreover, the radiation dose is less than when a whole-body device is used to study the brain.

From the Medical Viewpoint

Whether it is necessary to dedicate a machine solely to study of the brain will depend on the neurological or psychiatric case-load of the hospital concerned.

These two factors may argue in favour of the acquisition of a brain C.A.T. device. However, even if the technical differences between brain and body machines have been clearly established by the Manchester School, further work is required to determine whether such differences are significant also at a clinical level. The work begun by Gado, in comparing the diagnostic studies of a single patient performed on different machines but on the same day, in the same service and with the same personnel must be continued.

In a service possessing both types of apparatus, an independent viewing and analysis console (such as EMI's I.V.C.) should be provided, so that the routine clinical work may be kept separate from research. In such a way the radiologist can use this complex machinery not only for routine diagnosis, but to bring radiology to a competitive position in research.

Head Injuries

The Role of C.A.T. in the Diagnosis and Management of Traumatic Intracranial Haematoma

B. Jennett, G. Teasdale, S. Galbraith, and T. L. Steven*

Head injuries are an important aspect of health care which impose considerable burdens on the hospital service; in the UK they comprise 1 in every 10 new patients in accident and emergency departments, and account for 150,000 hospital admissions every year. In Europe most admissions are to accident or general surgery wards, only the minority of obviously serious injuries coming to neurosurgeons. Even after mild injury there is the threat of serious complications which can develop rapidly, and are associated with considerable mortality and morbidity rates. The reason why so many mildly injured patients are admitted to hospital is in the hope that clinical observation will result in early detection of complications.

The Clinical Problem

There is good evidence that this policy often fails, and that there is considerable preventable mortality and morbidity in patients whose initial injury was relatively mild - as indicated by the patient's ability to talk, at some stage after the impact.

One-third of head injury survivors referred to the Glasgow Institute in coma had talked before going into coma: and a third of fatal head injuries had talked at some time after injury before they died (9). Intracranial haematoma was found in 75% of patients who talked and died. Investigation of patients coming to the notice of the medico-legal organisations in Great Britain following head injury revealed that most were 'talk and die' cases; many had intracranial haematoma (7). Yet another survey revealed that a third of patients referred to neurosurgeons in Glasgow with intracranial haematoma had been deteriorating for 12 h or more before transfer - often because they were mistakenly believed to have suffered a stroke or to be drunk (3). One reason for this is that skilled clinical observation of head-injured patients is not available in all general surgical and accident wards; another is that the clinical syndrome is often atypical and investigations are necessary. However, until the introduction of the EMI scanner there was no reliable and safe method of investigation. Echo-encephalography and isotope encephalography have very limited value in this particular situation; even when patients are referred to special units, where angiography and ventriculography are available, it can be difficult to decide when to use these invasive methods, which carry considerable risk of aggravating the intracranial condition when the brain has recently been damaged. For this reason exploratory burr holes are sometimes recommended as a primary measure; but in one large series 40% of haematomas were missed on initial exploration, only to be revealed later by contrast radiology or autopsy (6).

*Institute of Neurological Sciences, GB Glasgow G51 4TF.

Our experience with C.A.T. accords with that in other preliminary reports - namely that it is indeed a useful means of diagnosing intracranial haematoma; and that since its introduction other invasive investigations are rarely needed (2). In the first 150 consecutive cases investigated in our Institute there were 60 with haematoma (4). Whilst it is easy enough for even a junior radiographer to diagnose an obvious extradural haematoma on the C.A.T., a more important question is how reliable the method is in a consecutive series of cases when the diagnosis is made by the surgical staff involved in making clinical decisions. Intracranial haematoma is liable to present at unsocial hours, when interpretation by a neuroradiologist is often not possible; and immediate action is usually required following investigation.

Investigation into the Reliability of C.A.T.

We therefore decided to determine the reliability of interpretation by young neurosurgeons, who are those most concerned in the practical application of the method (5). Three senior registrars, (two are now consultants) participated in an investigation in which one of them reviewed the records of 150 patients who had had C.A.T., and classified them into those with and without an acute intracranial haematoma (within 14 days of injury) on the basis of clinical, operative and autopsy evidence. From these cases 51 patients were selected *with* and 46 *without* haematoma; about half of each group was on the 80 × 80 matrix and the other with the 160 × 160. The other two neurosurgeons then read the scans of these patients 'blind' - without access to the case notes or to the patient's name.

Detection of Haematoma

There was agreement between the two neurosurgeons about the presence or absence of a significant haematoma on the scan in all but two cases (Table 1). There were two cases about which the neurosurgeons disagreed;

Table 1. Interpretation of C.A.T. of 97 head injured patients

C.A.T. diagnosis			
Neurosurgeon A	Neurosurgeon B	Number of cases	Final diagnosis
Haematoma	Haematoma	49	Haematoma
Haematoma	Uncertain	1	
Uncertain	No haematoma	1	No haematoma
No haematoma	No haematoma	46	

in one case with a haematoma one surgeon was uncertain about it, and in one without a haematoma the other surgeon was uncertain. In practice management is likely to depend on the opinion of the more certain of two clinicians; the more certain diagnosis was correct in both these cases. If these two are recorded as correctly diagnosed, then there were no false positives and no false negatives in the 97 cases reviewed.

Intradural haematomas were commoner than extradural, but some patients had both. Many of the intradural haematomas had both intracerebral and subdural collections; pure subdural haematomas are unusual during this active stage, which is why we use the term intradural. Ten of 13 extradural haematomas and 28 of 34 intradural haematomas were correctly placed in these sites (Table 2); each of the 11 discrete intracerebral haematomas was correctly identified as in this site by both surgeons.

Table 2. C.A.T. in distinguishing different types of traumatic haematoma

Type of haematoma	Number of cases		Accurate C.A.T. diagnosis	
Extradural only	13		10	
Intradural only	34		28	
Intracerebral only		11		11
Subdural + intracerebral		23		17
Extra and intradural	3		1	
Total	50		39	(78%)

In most cases haematoma was diagnosed on the basis of locally increased density, but in four cases the diagnosis was based on midline shift and ventricular distortion, there being no local increase of density. Except for one intracerebral clot all haematomas which showed up locally were associated with midline shift; this was not seen in any of the patients judged clinically not to have a haematoma.

Practical Problems in Using C.A.T. for Acute Head Injuries

At the stage when intracranial haematoma is suspected patients are often restless and unco-operative, and many of our patients therefore had to have general anaesthesia, sometimes after an unsuccessful attempt at scanning without. Quicker scanning and dispensing with the water bag in newer models of the scanner should reduce the need for anaesthesia, although other means of sedation might have to be considered; however, in patients with acute brain damage it is doubtful whether the widespread use of sedation would be acceptable to neurosurgeons. Another problem is patient selection. Patients already deteriorating, with a haematoma or brain swelling suspected, are obviously in need of scanning, although if the patient is already in a critical condition the surgeon may consider that the delay involved in arranging a scan (out of normal working hours) is unjustified. But what about the patient in the early hours after head injury who is already improving, or the patient 24-48 h later who is clinically stable, though perhaps not improving as quickly as was expected. Given that the facilities are available, should all such patients have a scan, and if so when?

Some further observations in Glasgow suggest that more widespread use of C.A.T. soon after injury may pose a new problem for surgeons. We have begun to find sizeable haematomas in some patients in whom the clinician would not have any reason to suspect this complication on clinical grounds. Should such a patient then be submitted to surgery? Colleagues in one American university hospital think the answer should always be yes, in order to keep ahead of events and to avoid the development of clinical deterioration; they carry out C.A.T. soon after admission on all patients who have impaired consciousness. We are not

so sure about this. Already in several cases found unexpectedly to have an intracranial haematoma we have pursued an expectant policy (8); these patients have recovered satisfactorily, and the C.A.T. abnormality has disappeared (Figs. 1, 2). We have had the confidence to do this largely because intracranial pressure monitoring is available in our Institute; we have used this to decide whether or not an unsuspected haematoma represents a threat and requires treatment, or is a compensated lesion which will resolve spontaneously. More cases will need to be studied before we can determine if and when this decision can safely be made on clinical grounds alone. Meanwhile we foresee a problem in management if C.A.T. becomes more widely available in general hospitals. The price of earlier detection of life-threatening haematomas could well be a number of false alarms about compensated clots. This could cause difficulties for neurosurgeons with restricted facilities, who might have to accept patients whose clinical condition would not previously have justified transfer, but who have been found to have an abnormal C.A.T. scan. Such a situation has already arisen as other non-invasive techniques have become available in the context of limited specialist experience; e.g. isotope scans and echoencephalograms both yield a number of false positives from general hospitals. But in the investigations of 'cold' conditions, such as epilepsy of late onset, this does not cause a problem of the kind which could arise in the more pressing situation of recent head injury.

C.A.T. in Patients without Haematoma

The main contribution of C.A.T. to the reduction of mortality and morbidity in head-injured patients seems likely to derive from earlier, safer and more reliable detection of intracranial haematoma. But C.A.T. scanning may also show the development of cerebral oedema and its response to treatment; contusions may be seen, and brain shifts due to local swelling or oedema may be detected. What part serial studies may play in the management and prognosis of head injury in general remains to be seen, and must await the accumulation of many scans in association with careful clinical assessment and follow-up. It is already apparent that some seriously brain-damaged patients have a normal scan, probably when the condition is due to widespread axonal shearing in white matter with minimal gross pathology; this is also the type of injury which occurs without skull fracture (1). For these reasons caution is needed in forecasting too much from this new investigation in the management of the patient with diffuse injury.

References

1. ADAMS, J.H.: Handbook of Clinical Neurology. Amsterdam: North-Holland Publishing Co. 1975, Vol. 23, p. 35.
2. AMBROSE, J., GOODING, M.R., UTTLEY, D.: EMI scan in the management of head injuries. Lancet 1976/I, 847-848.
3. GALBRAITH, S.: Misdiagnosis and delayed diagnosis in traumatic intracranial haematoma. Brit. med. J. 1976/I, 1438-1439.
4. GALBRAITH, S., BLAIKLOCK, C.T., JENNETT, B., STEVEN, J.L.: The reliability of computerised transaxial tomography in diagnosing acute traumatic intracranial haematoma. Brit. J. Surg. 63, 157-159 (1976).
5. GALBRAITH, S., TEASDALE, G., BLAIKLOCK, C.: EMI scanner diagnosis of acute traumatic intracranial haematoma. Reliability of neurosurgeons' interpretations. Brit. med. J. (1976) in press.

6. HOFF, J.T., SPETZLER, R., WINESTOCK, D.: Head injury patients with early signs of tentorial herniation: a management dilemma. J. Trauma (1976) in press.
7. JENNETT, B.: Some medicolegal aspects of the management of acute head injury. Brit. med. J. 1976/I, 1383-1385.
8. JENNETT, B., GALBRAITH, S.L., TEASDALE, G.M., STEVEN, J.L.: EMI scan and head injuries. Lancet 1976/I, 1026.
9. REILLY, P.I., GRAHAM, D.I., ADAMS, J.H., JENNETT, B.: Patients with head injury who talk and die. Lancet 1975/II, 375.

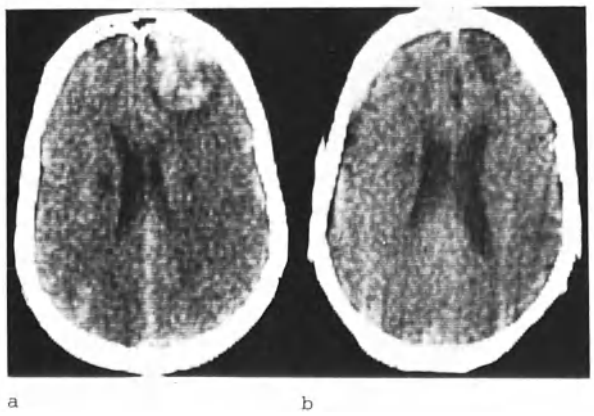

a b

Fig. 1. Man of 66 years. a) C.A.T. 30 h after injury when already recovering consciousness; right frontal intracerebral haematoma. Intracranial pressure normal during next 48 h with continued clinical improvement. b) C.A.T. 7 weeks later; no clinical signs; regarded as normal by the family

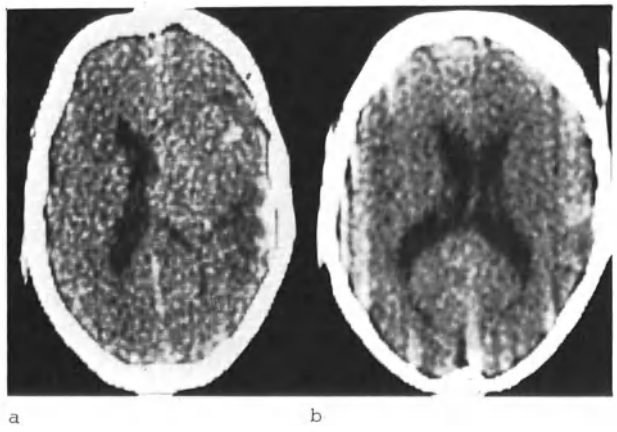

a b

Fig. 2. Man of 37 years. a) EMI scan 5 days after injury when still disorientated but improving; right temporal intracerebral and subdural haematoma; intracranial pressure elevated but resolved over next 48 h. b) EMI scan 2 months later when well recovered

C.A.T. and Angiography in Cranial Trauma

J. M. Caillé, F. Cohadon, S. Becke, and P. Constant*

The possibilities and the limitations of C.A.T. in pathology of the brain, vascular, tumoral pathology, etc. are now well known. Certain authors hold that C.A.T. is the ideal method for the investigation of cranial trauma and that angiography is no longer necessary. We therefore compare the respective merits of angiography and C.A.T. in traumatic pathology.

Material and Methods

All the C.A.T.s were done on a first generation machine (Acta Scanner) equipped with a 160 × 160 matrix. Each rotation gives two slices 7.5 mm thick and 3 mm apart. Rotation time is 4 1/2 min, which is of course much too long for this category of patient. No contrast medium injection was given.

The angiograms were all carried out in the same way: direct puncture of the carotid, injection of 8 to 10 ml of contrast agent, rapid serial radiography.

We excluded patients with recent trauma who presented extradural hematoma and patients suffering from previous trauma being treated for ventricular dilatation or post-traumatic epilepsy.

In all, 102 patients were examined, upon whom 102 C.A.T.s and 53 angiograms were carried out.

Analysis of 102 C.A.T.s (Fig. 1)

1st week	48
2nd week	22
3rd week	17
4th week	5
2nd month	4

Analysis of 53 angiograms (Fig. 2)

1st week	18
2nd week	20
3rd week	9
4th week	4
2nd month	3

In traumatology the different physical parameters characterising trauma (force, direction, point of impact, etc.) are of capital importance.

*Service de Neuro-Radiologie Centre Jean Abadie, Bordeaux (France).

It is unfortunately never possible to assess them accurately, much less to quantify them precisely.

We thus chose our 102 patients from four clinical varieties using as a criterion for selection the state of consciousness and its evolution.

First presentation: 34 cases

Initial loss of consciousness followed by a rapid return to consciousness, with or without focal signs.

C.A.T.: 30		Angiograms: 13
1st week	19	6
2nd week	6	5
3rd week	4	2
4th week	1	0

Second presentation: 27 cases

Initial loss of consciousness followed by obtundation lasting several days and gradual return to normal consciousness.

C.A.T.: 22		Angiograms: 15
1st week	8	2
2nd week	9	8
3rd week	4	5

Third presentation: 19 cases

Initial coma with secondary aggravation requiring continuous mechanical respiratory assistance.

C.A.T.: 19		Angiograms: 12
1st week	10	5
2nd week	2	4
3rd week	6	1
4th week	1	2

Fourth presentation: 22 cases

Initial deep coma requiring immediate mechanical respiratory assistance.

C.A.T.: 13		Angiograms: 14
1st week	9	5
2nd week	5	3
3rd week	3	0
4th week	2	1
2nd month	4	3

Results

1. Overall C.A.T. Results

6 C.A.T.s were uninterpretable because of movement artefacts.
7 were normal.

13 were considered normal, although the clinical examination suggested a hemispheric lesion. We considered these cases as false negatives.

5 were positive but the lesions found did not correspond with the clinical picture (incomplete positive C.A.T.).

In all, 71 cases were positive, 69 with a supratentorial lesion and two with lesions in the brain stem.

The nature of the lesions revealed by C.A.T. was: (Fig. 3)

Oedematous contusion	40
Haemorrhagic swelling	12
Intracerebral haematoma	9
Subdural Haematoma	6
Ventricular collapse	4

In 16 cases the lesions were multiple; in 7 cases they were bilateral. The vast majority of the lesions were in the temporal, frontal or fronto-temporal regions.

2. Overall Results of Angiography

In 9 cases angiography was normal despite a clinical picture suggesting contusion (9 false negatives: 17%).

In 8 cases it showed a traumatic lesion but did not determine its nature (haemorrhagic contusion, intra-cerebral haematoma).

In 4 cases it did not show multiple lesions, showing only the most obvious.

On the other hand, it easily confirmed 11 subdural haematomas although C.A.T., carried out twice as often, showed only 6.

3. Results Related to the Clinical Forms: C.A.T.

First presentation: 34 cases

2 haemorrhagic swellings
18 oedematous contusions
7 normal C.A.T.s

Second presentation: 27 cases

4 haemorrhagic swellings
14 oedematous contusions
1 intracerebral haematoma
1 subdural haematoma
2 multiple lesions

Third presentation: 19 cases

4 haemorrhagic contusions
9 oedematous contusions
4 subdural haematomas
2 ventricular collapses
7 bilateral lesions

Fourth presentation: 22 cases

5 intracerebral haematomas
1 haemorrhagic swelling
8 oedematous contusions
6 subdural haematomas
7 multiple lesions
2 ventricular collapses
2 haemorrhagic lesions of the brain stem

Discussion

With supratentorial lesions C.A.T. is incontestably more effective than angiography:

71% positive results vs. 61%
14% false negatives vs. 17%
17% incomplete positives vs. 24%

Moreover, in none of our cases could angiography distinguish between oedematous contusion, swelling and haematoma while C.A.T. made the distinction without possibility of error.

In 16% of cases C.A.T. showed unambiguously the haemorrhagic nature of the lesion and indicated exactly its extent and volume, while angiography showed only the vascular displacements.

Multiple or bilateral oedematous or haemorrhagic lesions are easily shown by C.A.T.

After the 10th day it is very difficult to assess lesions using angiography alone. There are by then few, if any major vascular displacements (28% of angiograms are normal after the 10th day).

C.A.T. also allows one to follow the evolution of size of the ventricles: in four children with deep coma there was ventricular collapse, caused not by diffuse oedema but by an increase in cerebral blood volume.

However, there are several points about this technique to go on the debit side: subdural haematomas are at certain stages of their evolution difficult to recognise: although initially hyperdense, they become isodense and then hypodense. After the 2nd week, if they are associated with a contusion, or if they are bilateral, it is impossible to recognise them. We missed five cases of subdural haematoma in this way.

C.A.T. showed only intratentorial lesions. In our series we found haemorrhagic lesions of the brain stem only twice, although 22 patients presented clinical pictures very suggestive of primary brain stem lesions (fourth presentation: deep coma necessitating urgent respiratory assistance).

The quality of the C.A.T. does not always allow a precise analysis; six of our C.A.T.s were uninterpretable and numerous others had movement artefacts. In these conditions only intracerebral haemorrhagic lesions are identifiable. Administration of general anaesthetic which is sometimes necessary reduces the advantages of this technique.

However, C.A.T. does allow the establishment of certain clinicoanatomical correlations.

First presentation (initial loss of consciousness followed by rapid return to normal consciousness) is characterised by the reduced volume of the contusion, the small number of haemorrhagic swellings, the high number of normal C.A.T.s (7). (Fig. 4).

Second presentation (loss of consciousness followed by obtundation) is characterised essentially by oedematous temporal or frontal contusions of small volume - in five cases haemorrhagic swelling or haematoma. Shift of the midline structures remains moderate (Fig. 5).

Third presentation (coma with secondary aggravation) is characterised by very grave hemispheric lesions which are both large and numerous (7 cases of multiple lesions, 7 cases of bilateral lesions).

The two-phase clinical evolution, C.A.T. and angiographic findings suggest that the lesions of the brain-stem are secondary to large hemispheric lesions which compress the brain stem by the shifts which they provoke (Fig. 6).

Fourth presentation (initial deep coma) most probably corresponds to a primary lesion of the brain stem. Hemispheric lesions shown by C.A.T. indicate the gravity of the trauma but would seem to be only coincidental (Fig. 7).

A previous angiographic study of cerebral contusions showed the same clinicoanatomical correlations but with vastly inferior precision as to the number, volume and especially the nature of the lesions.

Conclusion

Though C.A.T. constitutes an undeniable progress in the means of studying the number, volume and the oedematous or haemorrhagic nature of intracranial lesions, considerable progress remains to be made before we could be said to possess a completely satisfactory means of investigating this area: brain stem lesions are shown only exceptionally and false negatives remain numerous. Technological progress will doubtless allow improved performance through such changes as more rapid rotation and improved spatial and densitometric definition.

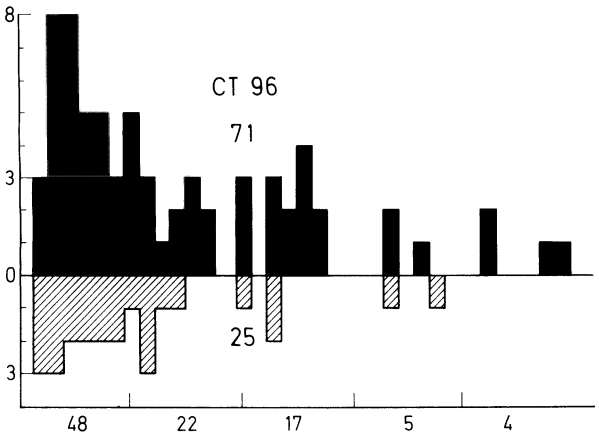

Fig. 1

Fig. 1. Time distribution of C.A.T. examinations after head trauma: each block represents 1 day. Cases above horizontal axis: positive results; cases below axis: negative results. Lowest figure: number of cases per week

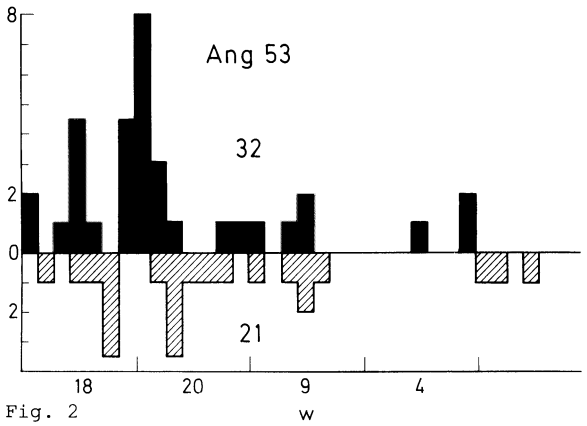

Fig. 2

Fig. 2. Time distribution of angiograms after head trauma (see Fig. 1 for explanation)

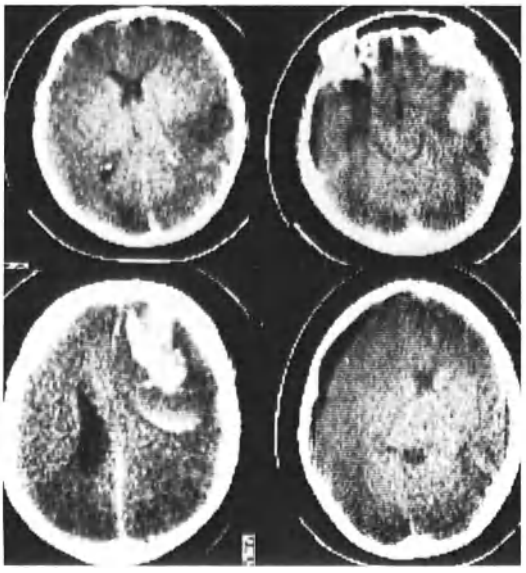

Fig. 3

Fig. 3. Examples of traumatic lesions seen at C.A.T.: *top left:* oedematous contusion; *top right:* haemorrhagic contusion; *bottom left:* intracerabral haematoma; *bottom right:* hypodense subdural haematoma

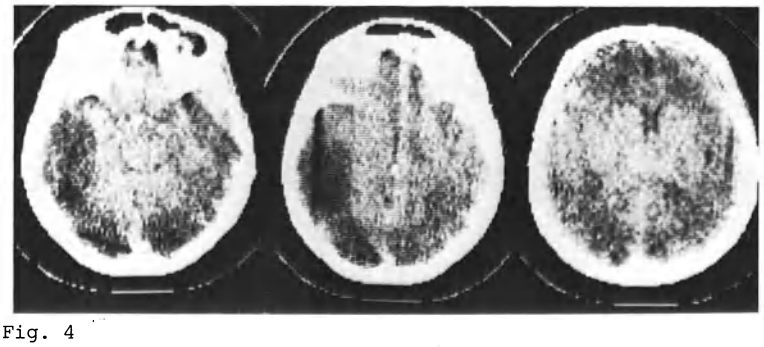

Fig. 4

Fig. 4. Typical C.A.T. findings in 'first presentation' (*see text*): left temporo-occipital contusion with little swelling

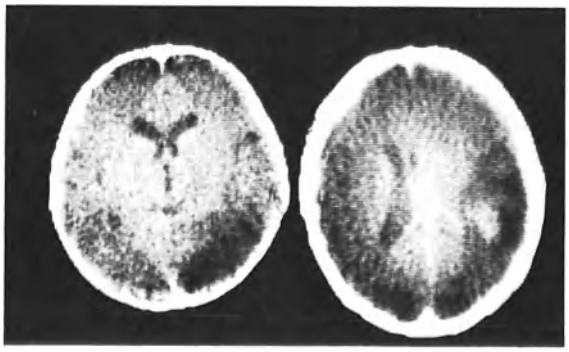

Fig. 5

Fig. 5. Typical C.A.T. findings in 'second presentation' (*see text*): right parieto-occipital haemorrhagic contusion with moderate displacement of the bodies of the lateral ventricles

Fig. 6

Fig. 6. Typical C.A.T. findings in 'third presentation' (*see text*): facial fractures (fluid level right antrum), facial soft tissue swelling; haemorrhagic contusion left temporal lobe and multiple intracerebral haemorrhages

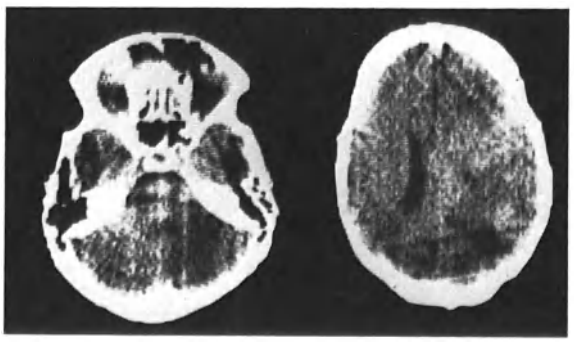

Fig. 7

Fig. 7. Typical C.A.T. findings in 'fourth presentation' (*see text*): brain stem haemorrhage accompanied by contusion of the parietal lobe

Tumours Above and Below the Tentorium

The Radiological Management of Cerebral Tumours

V. Logue*

I have been asked to describe the radiological management of intracranial tumours and the methods used in subjecting the clinical assessment to radiodiagnostic analysis and the order in which the tests are employed.

From the point of view of diagnostic requirements, there are two different breeds of neurosurgeon. On the one hand, there are those who tend to apply a single radiological test and are mainly concerned with the diagnosis of the site and possible size of the tumour, its anatomical and vascular relationships being less relevant. On the result of the one investigation, perhaps C.A.T., they are prepared to explore the lesion and deal with, as they go along, its potential excessive vascularity; its involvement with major arterial branches; possibly through an access which may be limited by evocative brain or from what is later proved to be the wrong side of the chiasm in suprasellar lesions.

I have a great deal of admiration for the spirit of adventure shown by these talented surgeons, but I belong to a different school, which wants to know as much as is possible about a mass lesion before embarking on surgery.

I would agree that in many cases a single examination may be adequate, whether it be an arteriogram, air study or C.A.T., but when one is performing precision surgery striving to reduce the mortality rate, for instance among benign tumours, to less than 2% for the convexity meningiomas, 2.5% for the pituitary adenomas, and to under 5% for the acoustic neuromas, the very large, large and small, then one must have precision radiodiagnosis.

It is the tumour with unusual features relating to its blood supply, or its relationship to large vessels or evocative brain that tends to add to mortality and morbidity rates and it is by knowing these peculiarities beforehand that one can avoid the pitfalls. One cannot always recognise from one test these odd features in a particular case and so the need to perform further contrast studies arises, and in anatomical areas of particular difficulty one must employ them in addition, as a routine, in virtually all cases. It is typical, with increasing use of C.A.T., to emphasise the risks and morbidity of the invasive investigations, namely arteriography (particularly vertebral) and pneumoencephalography, whereas previously it was popular to minimise them. These still remain as small risks, but I should emphasise that arteriography remains less invasive than any craniotomy and less even than a burr-hole biopsy, and if it reduces the magnitude of the surgical procedure or eliminates the need for it altogether, this has been a gain for the patient.

---

*Gough Cooper Department of Neurological Surgery, The National Hospital, Queen Square, London, WC1 (Great Britain).

The real crux of radiological management therefore remains in the weighing up of the small risks of arteriography and pneumoencephalography as additional investigations against the advantages to be gained for the patient at the time of surgery, and the extra risk to the patient if these tests are not performed.

I will now describe my own particular methods of management as an ideal which stems from these personal prejudices, and for the attainment of which I am assuming two things: unrestricted access to C.A.T. and unlimited co-operation from my neuroradiological colleagues.

Computerised Axial Tomography

Computerised axial tomography has been available at the National Hospitals for just 3 years and of a total of over 1100 brain tumours both supra- and subtentorial which have been investigated during this time, about 70% (and this is a very rough estimate) have been subjected to C.A.T., so one is now able to begin to assess its reliability and its accuracy and how it is being integrated into the radiodiagnostic armamentarium. The statistics on which I base my observations are provided by my radiological colleagues, to whom I am greatly indebted.

Diagnostic Management

I shall deal with the diagnostic management in this order:

1. Tumours involving cerebral hemispheres, intra- and extra-axial

2. Suprasellar and third ventricular areas, which I find provide particular difficulties

3. The posterior fossa

Finally, I shall describe the increasing application of radiodiagnostic measures to management of the postoperative phase.

Tumours in the Cerebral Hemispheres

The first specific radiological investigation is that of C.A.T., always both with and without enhancement in all tumour suspects. It is hardly necessary at this stage to emphasise that the introduction of C.A.T. has not altered in any way the initial clinical approach to diagnosis comprising the general, physical and neurological examinations with skull and chest radiography.

The appearance on initial examination by C.A.T., excluding the rarer tumours, are twofold, as shown in Table 1.

The ability to demonstrate multiple metastases or multiple gliomas is a particularly valuable advantage of C.A.T., this single scan rendering further cerebral investigations unnecessary for patients who are often seriously ill and for whom there is little therapeutic help. However, in a specialised neurological hospital one sees few of these cases:

Table 1. Initial appearances of tumours of the cerebral hemispheres on C.A.T.

Multiple tumours	
	Metastatic with or without known 1^{o} neoplasm elsewhere
	Gliomas
	Meningiomas
Solitary tumours	
	Metastatic with (54%) or without known 1^{o} elsewhere
	Glioma
	Meningioma

only five cases of multiple metastases, eight of multiple glioma in the author's experience.

Multiple Meningiomas

Out of a series of 100 meningiomas analysed in some detail there was a total of five cases of multiple meningiomas; the scan appearances and the tendency for the tumours to be sited parasagittally or on the falx rendered the diagnosis clear.

Solitary Tumours

Glioma

Metastasis (in 54% of cases in my series, the presence of a primary tumour was known at the time of the scan).

In the surgical management of the cerebral hemisphere gliomas the surgeon has to live with two facts:

1. With the malignant gliomas of histological grades 3 and 4, radical surgery and radiotherapy prolong life, in some cases only, by at most 2-3 months, thus increasing life expectation from the average of 8 months to 10, so there is little therapeutic scope for this group.

2. With the more benign gliomas, grades 1 and 2, treatment by partial removal or lobectomy, often combined with radiotherapy, frequently achieves a comfortable existence lasting up to many years.

In the radiodiagnostic management there are three questions to be answered:

1. The site and size of the tumour and its relationship to evocative brain

2. The precise nature of the neoplasm, if possible

3. The intrinsic vascularity of the neoplasm, and the relationship of the major vessels in the vicinity - mainly a surgical requirement.

C.A.T. answers the first question in nearly every patient. It can answer the second question in a number of cases, distinguishing between the metastasis and glioma in a proportion of them, in addition to the 54% of metastases when the primary tumour is already known to be present. It cannot however, distinguish reliably between gliomas grade 1, 2, 3 or 4.

In order to recognise those malignant tumours associated with an increased malignant vascular pattern one must use arteriography. Accepting that 50% of the malignant gliomas present as avascular masses on arteriogram, it is nevertheless of great value in the remaining 50%, and if one sees a malignant pattern with arteriovenous shunting, one tries to avoid any surgery, including biopsy, and the patient has gained a little; although in a few of the cases one is forced into palliative action.

In addition, the arteriogram in those cases suitable for surgery will delineate the neighbouring major vessels as well as the tumour supply.

Bearing these points in mind, my present philosophy is for lesions shown by C.A.T. to lie in the frontal lobes or postparietal zones, relatively non-evocative areas not closely involved with the major arterial trunks, there is usually no need for further radiological tests and one can proceed to surgery. However, for a tumour in or near evocative areas (the motor-sensory strip, speech zone, temporal or occipital lobes) arteriography, I find, is essential to show the blood supply of the tumour and the relationship of major vessels in the vicinity.

Radionuclide Scanning

The gamma scan I also find occasionally helpful in two situations. In dealing with a solid tumour, glioma or metastasis which on C.A.T. has the same density as the extensive peritumoral oedema and by which its outline is obscured, the isotope scan may often delineate precisely the tumour mass and make needle biopsy, or indeed excision, more accurately sited.

Secondly, with a high convexity tumour, the variable obliquity of the C.A.T. cut may apparently falsify the position in relationship to the skull, and the gamma scan may relate the mass more accurately to the topography of the cranium.

Air studies are never used.

Meningiomas

Out of a series of 100 cases analysed in detail with C.A.T. 3 were missed altogether and there were 11 false positive diagnosis, a different sort of tumour being present in each case. With the diagnosis rate as accurate as this, many surgeons may operate without further investigations. However, in my view, factors other than the stark diagnosis need to be considered before proceeding to surgery.

Arteriography, with magnification if possible, is used to demonstrate the features shown in Table 2.

With these investigations supplementing C.A.T., I find the surgical approach and the manipulations required to remove the tumour rendered much easier and thereby much safer.

Table 2. Meningioma

The place of arteriography (with magnification) in surgical management:
1. To indicate the degree of vascularity with the resulting potential technical difficulties.
2. To delineate the local major arterial channels and their relationship to the capsule so as to avoid damage during surgery.
3. To demonstrate the vascular supply of the dural attachment, thus defining the tumour origin, particularly helpful with parasagittal, sphenoidal ridge and posterior fossa tumours, (CP angle, clivus and foramen magnum) and to permit embolisation in selected cases as a preliminary to surgery.
4. To define the relationship of parasagittal and falx tumours to the sagittal sinus and the degree of obstruction; the course of the sagittal veins and the collateral venous anastomosis on the surface of the hemispheres, which must be preserved; with sphenoidal ridge tumours, the course of Sylvian veins and middle cerebral arteries and constriction of the internal carotid.
5. To confirm the nature of the tumour by its vascular pattern.

Suprasellar and Third Ventricular Zone

This is an area in which inadequate radiographic delineation may well influence the outcome of surgery very adversely.

The clinical probability of a lesion in the suprasellar-third ventricular zone will have been suggested by the history, the examination of the visual and ocular function in combination with metabolic studies of the pituitary gland and the hypothalamus, together with the plain X-rays of the skull. Again, C.A.T. as the first investigation will show general features of the zone and the presence of a tumour in 80-85% of cases as a result of density of the tumour and its propensity in some cases to enhance, its encroachment on the suprasellar cistern and displacement of the third ventricle. This ratio may be higher still with more detailed examination by multiple overlapping cuts. The precise nature of the lesion, however, is not recognised so readily and, more importantly, C.A.T. will not define adequately the essential features of the local pathological anatomy which, from the point of view of the surgical approach, are more important.

One needs to know the precise relationships of these tumours to three structures, as shown in Table 3.

Table 3. Prerequisites for surgical treatment of suprasellar tumours

Knowledge of the relationship of the tumour to:
1. The anterior cerebral-anterior communicating artery complex a) to avoid damage to important branches; b) to confirm that the dome of the tumour, although it may have extended in front of the chiasm, is not situated above the anterior communicating vessel - when perforating and recurrent branches might be in the line of surgical approach
2. The floor and cavity of the third ventricle
3. The chiasm and if possible (in association with the charting of the field defect) to determine the former's degree of prefixation which will indicate whether a sub-chiasmatic approach or a posterolateral one below or across the temporal lobe is appropriate

Table 4. Pneumoencephalography in suprasellar and third venticular tumours

To delineate:

1. The optic chiasm and its relationship to the tumour
2. The degree of involvement of the third ventricle floor
3. The extent of the mass occupying the retrochiasmatic space

To determine:

4. Whether the neoplasm originates within the third ventricle or from below it in the suprasellar zone
5. Whether the suprasellar extension (particularly with the cystic lesions) has intruded into the third ventricle and whether this is accessible through the foramen of Monro

Bilateral arteriography will give all the vascular information and will also exclude the rare unsuspected aneurysm.

Pneumoencephalography with tomography is required in addition for the reasons shown in Table 4. In my view, the pneumoencephalogram and very occasionally the ventriculogram remain the final diagnostic arbiters of the sella and the parasellar zone.

Posterior Fossa Tumours

The clinical presentation of a posterior fossa tumour needs no description. In this situation C.A.T. in adults is not as helpful as in the supratentorial compartment.

Artefact is, for obvious reasons, more frequent, and although the failure rate to recognise the presence of a tumour is low, nevertheless fourth ventricular and paraventricular neoplasms, if small, may be missed. The recognition of the nature of the neoplasm and the differentiation between metastasis, astrocytoma, ependymoma and medulloblastoma is frequently unclear, owing to their variable density and variable enhancement.

Cystic neoplasms are readily recognised with, in many cases, a mural nodule. This however may be a haemangioblastoma and as 20% of these are small multiple lesions, which C.A.T. may not identify, arteriography is essential to locate all the tumours, to give the opportunity of their removal at the same time as the cystic tumour.

Again, in the management of extrinsic tumours, particularly of the cerebellopontine angle, the actual diagnosis is only one part of the problem. In the surgery of these neoplasms the cause of death and morbidity is usually interference with the vascular supply, particularly the anterior and posterior inferior cerebellar vessels, occasionally the superior cerebellar. I personally like to know the situation of these arteries in relationship to an acoustic neuroma and meningioma and also to recognise the anomalies in their distribution, particularly the presence of a dominant posterior or anterior inferior cerebellar arteries supplying both territories, which occurs in over 20% of our cases, when interference with the main vessel carries a much greater hazard. I also wish to know the degree of tumour vascularity, as this will modify the surgical technique.

For all these reasons I find it important to have vertebral arteriography performed and this test still remains for the present the essential investigation in all posterior fossa tumours.

However, neoplasms within the fourth ventricle or paraventricular may only eventually be recognised by pneumoencephalography or ventriculography and these tumours with obstruction in the aqueduct constitute the few remaining indications for this latter test.

Postoperative Management

1. Immediate: first 24 h postoperatively
2. Intermediate: 24 h to 1 month
3. Long term: 1 month onwards

C.A.T. has an increasingly important part to play in postoperative management. However, this does not apply during the first 24 h after operation when deterioration of conscious level usually indicates compression by haematoma or massive oedema of an infarction, complications best dealt with by immediate reopening of the wound and evacuation of the clot or the removal of infarcted brain. Events usually happen too quickly for C.A.T. or any other radiological investigation to play any part.

Intermediate Phase - 24 h to 1 Month

The possible causes of failure of the patient to improve or of actual deterioration during this stage are well known:

1. Haematoma in the tumour cavity, subdural space or extradurally
2. Obstructive hydrocephalus following third ventricular or posterior fossa surgery
3. Communicating hydrocephalus
4. Rapid tumour recurrence
5. Persisting oedema from an infarction

All these are easily recognisable by C.A.T.

C.A.T. has taken over completely from arteriography or ventriculography in this analysis, and although it must be accepted that much artefact may be present due to metal clips, elevated or depressed bone flaps and shunt tubes, it is nonetheless invaluable.

The important feature in monitoring the postoperative recovery is that C.A.T. gives the opportunity of investigation at the very first sign of interruption of the recovery course or at the slightest evidence of deterioration.

Long Term Management

Apart from hydrocephalus, this is largely concerned with recurrent growth of gliomas and meningiomas. In the daunting field of glioma surgery, C.A.T. may well change our attitude to recurrent growth of those astrocytomas of pathological grades 1 and 2 (little can be done for the really malignant tumours, as mentioned earlier) and also perhaps for the oligodendroglioma. Previously long-term management of patients with gliomas had not been very dynamic in this country because

confirmation of recurrent tumour growth required hospital admission and invasive neuroradiological investigations. For this reason reinvestigation was usually delayed until tumour extension was massive enough to raise intracranial pressure and produce progressive neurological signs, or both. At this late stage surgery was either not feasible or, if carried out, often produced a fatality or increased morbidity. As a result, very little re-explorative surgery was performed.

With C.A.T. to demonstrate tumour recurrence at an early stage one is in the position to propose reoperation before major symptoms reappear. In some cases, of course, tumour infiltrates the surrounding brain widely, but in others it tends to grow largely into the cavity created by previous surgery and may be removed without necessarily adding to the disability.

The protocol I have adopted is to perform the C.A.T. about 1 month postoperatively when the healing processes are completed, and this can be compared with subsequent scans taken at regular intervals, say 6-monthly depending on the previous history of the tumour, and surgery can be proposed before major symptoms reappear. It will take time to work out the long-term value of this approach.

The main problem, if uncommon, is that of radionecrosis, which may show exactly the same attenuation features as glioma recurrence and may enhance. However, a radionecrotic area often presents as an expanding lesion when surgical removal is often beneficial.

Gamma Scan

The radionuclide scan has been of little help in this field in the past owing to the permanent and misleading changes following surgery seen around the bone flap and in the brain itself.

Meningiomas

With these tumours C.A.T. is of greater value and this is exemplified for instance in the well-known problem of the recurrent parasagittal tumour. A patient goes for several years postoperatively and then develops headache, or fits for the first time, or seizures which, having been present since surgery, become more frequent or more severe, often unaccompanied by neurological signs. These symptoms are not necessarily indicative of tumour regrowth. Arteriography, on which we previously relied for diagnosis was notoriously fallible in this situation, but C.A.T. can show unequivocally the site and size of any recurrence.

Again, the protocol is to take a scan at 1 month postoperatively and then repeat it at 6-monthly intervals. I am prepared to reoperate long before any fresh signs or symptoms appear in an attempt to avoid further tumour involvement of the sagittal sinus, when the whole outlook for further recurrence and indeed survival is rendered significantly worse, and I am now prepared to reoperate in recurrent meningiomas in any site, before major symptoms reappear and when it is easier and safer to remove them.

These trends may well alter our whole attitude to tumour follow-up.

Conclusion

These are times of great change in the field of neuroradiology, with the promise of greater changes to come. However, for the foreseeable future there will remain a great deal of work for the neuroradiologist as the surgeon will still require his sophisticated arteriograms and air studies for selected areas.

I would even suggest we do not take out all the radionuclide scanners; there are some aspects of diagnosis in which they are still useful as a complement to C.A.T. I think it also wise for any neurosurgical department to ensure that they retain one surgeon on the staff who is capable of performing a competent ventriculogram.

My personal views on radiological management of brain tumours are summarised in Table 5.

Table 5. Radiological management of cerebral tumours

Initial examination
C.A.T. scan, with and without enhancement in all tumour suspects
Complementary examinations
Arteriography
For: solitary intra-axial, hemispheral tumours in evocative regions To show degree of vascularity and relationship to major arteries
Sellar and suprasellar tumours: To demonstrate relationship to anterior cerebral/anterior communicating arteries To exclude aneurysm
All meningiomas
All posterior fossa tumours: To reveal degree of vascularity; vascular supply, relationship of major arterial branches
Pneumoencephalography
For: sellar and suprasellar tumours: To show relationship of third ventricle and chiasm, and any intraventricular extension Third ventricular tumours Fourth ventricular tumours
Radionuclide scan
For: locating a neoplasm in an area of peritumoral oedema as shown on C.A.T. localising a tumour on the high convexity of hemisphere and relating it to skull topography
Ventriculography: air/positive contrast
Occasionally for third ventricular tumours, aqueduct stenosis, fourth ventricular tumours

Computerised Axial Tomography in Supratentorial Gliomas and Metastases

L. E. Claveria, B. E. Kendall, and G. H. du Boulay*

It is now well established that Computerised Axial Tomography (C.A.T.) is a highly sensitive system and its non-invasive characteristics have made it a better method of investigation in tumour suspects than any other conventional technique. The purpose of this study was to analyse the reliability of C.A.T. in the diagnosis of intrinsic cerebral tumours in detecting the presence of a lesion within the cerebrum, in defining its localisation and in predicting the specific nature of the tumour.

Material and Methods

We reviewed the first 6500 C.A.T. scans performed in the National Hospital with a 160 × 160 matrix scanner. The scans and notes of those patients in which the original radiological reports had suggested a glioma or metastasis were selected as were the records of all other patients with a pathologically proven diagnosis of glioma or carcinoma.

1. All these C.A.T. scans were reassessed without any other information.

2. All scans were then again reviewed with full clinical information and the findings correlated with the results of other studies and the histological diagnosis.

The gliomas were classified according to their pathological type and gliomas were subdivided into benign (Kernohan Grades I and II) and malignant (Kernohan Grades III and IV). The morphological appearances on the C.A.T. scans were recorded and, depending on the dominant feature, the tumours were classified as cystic (Fig. 1), solid (Fig. 2), mixed (Fig. 3) (i.e. both cystic and solid components) and infiltrating. The term 'cystic' was used to describe a well-defined region of low attenuation, and does not necessarily imply fluid content, (3), because, for example, necrotic solid tissue may also show low attenuation coefficients. Infiltrating tumours were those where the margins of the tumour were illdefined both before and after intravenous contrast injection. Depending on their behaviour after the administration of intravenous contrast medium, the tumours were also subdivided into four groups, viz - those with irregular enhancement (Fig. 1), homogeneous anhancement (Fig. 2), a mixture of both the former types of enhancement and finally those in which no enhancement occurred. On the original radiological reports and again on the retrospective analysis the tumours were reclassified into those in which a correct diagnosis had been made, those which the correct histology had been suggested as part of a differential diagnosis and those in which the diagnosis was incorrect.

---

*Lysholm Radiological Department, The National Hospital, Queen Square, London WC1N 3BG. (Great Britain).

The results are shown in Tables 1-7. An attempt has been made to correlate the pathology with the morphological characteristics and enhancement patterns, and each of these has been assessed in relation to the accuracy in predicting a specific histological diagnosis on C.A.T.

Table 1. Material analysed

	No. of cases	(%)
A. Computerised axial tomography series		
Total number of C.A.T. scans performed: 6500		
C.A.T. diagnosis of glioma	242	100
Glioma verified histologically	163	67
Unverified by biopsy	47	19
Another pathology confirmed (false positive)	32	13
C.A.T. diagnosis of metastasis	62	100
Metastasis verified histologically	17	27
Unverified, but primary malignancy proven	4	6
Another pathology confirmed (false positive)	41	66
B. Pathology Series		
Histologically verified gliomas	179	100
Accurately diagnosed on C.A.T.	163	91
Lesion shown on C.A.T., but another pathology predicted (false negative)	15	8.4
No lesion shown on C.A.T.	1	0.6
Histologically verified metastases	25	100
Accurately diagnosed on C.A.T.	17	68
Lesion shown on C.A.T., but another pathology predicted (false negative)	8	32

Table 2. Gliomas: Incidence of manifestations in each type and grade of tumour

	Astrocytoma (%)		Oligodendroglioma (%)		Total	(%)
	I-II	III-IV	I-II	III-IV		
Calcification	11 (31)	9 (8)	7 (70)	5 (45)	32	18
Oedema	30 (83)	106 (90)	5 (50)	10 (91)	151	84
Midline shift	31 (86)	95 (81)	8 (80)	9 (82)	143	80
Obliteration of ventricle	34 (94)	109 (92)	8 (80)	11 (100)	163	91
Hydrocephalus	22 (61)	37 (31)	6 (60)	3 (27)	68	38
High attenuation	7 (19)	18 (15)	2 (20)	1 (9)	28	17

Discussion

Detection of a Lesion

From our analysis it is obvious that it is rare to overlook an intracerebral supratentorial neoplastic lesion, (Table 1). There was only one such proven case in our series and we are aware of only two other similar cases since this study was completed. However, the period of follow-up is too short (6-18 months) to exclude latent lesions unde-

Table 3. Gliomas: Incidence of types related to contrast enhancement (130 cases)

	Astrocytoma (%)		Oligodendroglioma (%)		Total	(%)
	I-II	III-IV	I-II	III-IV		
Irregular	14 (61)	74 (80)	5 (63)	5 (71)	98	75
Homogeneous	4 (17)	14 (15)	2 (25)	2 (29)	22	17
Mixed	1 (4)	1 (1)	-	-	2	2
Negative	4 (17)	3 (3)	1 (13)	-	8	6
Total number of cases	23	92	8	7		

Contrast not given 49

Table 4. Metastases: Incidence of manifestations

	No. of cases	(%)
Systemic neoplasm evident	19	66
Multiple	9	31
Oedema	27	93
Midline shift	20	69
Obliteration of ventricle	27	93
Hydrocephalus	5	17
High attenuation	18	62
Low attenuation	8	29
Irregular attenuation	8	29
Calcification	0	0
Enhancement		
Homogeneous	17	61
Irregular	6	21
Negative	0	0
Not given	5	18
Tumour components		
Cystic	7	25
Solid	19	68
Mixed	2	7
Infiltrating	0	0

Table 5. Supratentorial gliomas: Comparison of initial radiological and retrospective C.A.T. diagnosis without clinical information

Initial C.A.T. Diagnosis	Correct	119 (66%)
	Within differential diagnosis	44 (25%)
	Incorrect	16 (9%)
Retrospective C.A.T. Diagnosis	Correct	163 (91%)
	Within differential diagnosis	11 (6%)
	Incorrect	5 (3%)

tected by C.A.T. scan, which may later become obvious from progression of clinical signs. It should be noted that we have not attempted in this study to analyse those cases in which an equivocal report has been given, usually because of artefact or minor anatomical asymmetry, failing to exclude the presence of a tumour. In these cases tumour was

Table 6. Retrospective diagnoses[a]

Enhancement	Tumour component		Correct (C)	Differential (D) diagnosis	Incorrect (I)	Overall accuracy		
Irregular 98 (75%)	Cystic	38 (39%)	37 (97%)	1 (3%)	-	C 95%	D 4%	I 1%
	Solid	10 (10%)	9 (90%)	-	1 (10%)			
	Mixed	38 (39%)	35 (92%)	3 (8%)	-			
	Infil.	12 (11%)	12(100%)	-	-			
Homogeneous 22 (17%)	Solid	22(100%)	17 (77%)	3 (14%)	2 (9%)	77%	14%	9%
Mixed 2 (2%)	Cyst	1 (50%)	1(100%)	-	-	50%	50%	-
	Infil.	1 (50%)	-	1 (100%)	-			
Negative 8 (6%)	Cystic	3 (38%)	3(100%)	-	-	100%	-	-
	Solid	2 (25%)	2(100%)	-	-			
	Mixed	1 (13%)	1(100%)	-	-			
	Infil.	2 (25%)	2(100%)					
Not given 49	Cystic	15	15(100%)	-	-			
	Solid	11	8 (73%)	2 (18%)	1 (9%)			
	Mixed	11	10 (91%)	1 (9%)	-			
	Infil.	11	10 (91%)	1 (9%)	-			
	Normal	1			x			

[a]More detailed analysis of retrospective diagnosis of glioma related to enhancement and morphological features. All cases in column C were correctly diagnosed as gliomas on retrospective review. In column D are cases in which the correct tumour type was identified as one of several given in differential diagnosis.

Table 7. Supratentorial metastases: Comparison of initial radiological and retrospective C.A.T. diagnosis without clinical information

Initial C.A.T. diagnosis	Correct	9 (31%)
	Within differential diagnosis	12 (41%)
	Incorrect	8 (28%)
Retrospective C.A.T. diagnosis	Correct	17 (59%)
	Within differential diagnosis	3 (10%)
	Incorrect	9 (31%)

excluded either by clinical correlation or by a normal follow-up scan. We estimate that such cases constitute no more than 5% of our negative material.

These results endorse the view that as a screening procedure for suspected tumour within the supratentorial compartment, C.A.T. performed both before and after contrast injection is the most accurate single diagnostic procedure available. (2)

Localisation and Extent of Tumour

For accurate localisation of a lesion it is important to be able to relate the position and angle of the head to the internal structure of the brain. We have as yet no reliable method of precisely indicating head position and have relied on the documentation of the angle of the

cut and measurements taken from the orbitomeatal line. With this information, it is usually possible to localise the tumour with a sufficient degree of accuracy for management. In certain regions, such as the high parietofrontal, surgeons may experience difficulty in localisation, and other procedures such as isotope scanning and angiography have been requested for this purpose. We now find it useful to place a plastic marker (which is visible on the scans) over the approximate line of the coronal suture in these cases to indicate the position on the patient's head. The precise location and extent of tumour tissue may not be demonstrable in lesions which do not enhance after contrast injection and are infiltrating, so that the tumour cannot be demarcated from adjacent brain or, if it is of low attenuation, from surrounding oedema. In these cases isotope scanning and angiography may provide the localising information necessary for a burr-hole biopsy to be taken.

In this series, however, 8 patients with infiltrating tumours on C.A.T. had isotope scans, of which 4, including one Grade III astrocytoma, were negative. Angiography was performed in 10 of these patients but only 1 had pathological circulation.

Surgeons planning resection of a lesion may require angiography, not for localisation or pathological diagnosis but merely to show the relationship of major vessels to the lesion, especially if the tumour involves an evocative cortical area. It is often difficult in retrospect to decide precisely why studies other than C.A.T. have been requested. The fact that such studies were performed in 80% of our supratentorial tumours is certainly not a measure of lack of confidence in C.A.T. diagnosis.

Specific Diagnosis of Nature of Tumour

Re-scanning after intravenous contrast was performed in 80% of these cases. On scans prior to contrast an accurate diagnosis of glioma was made in 71%; this was increased to 90% after contrast. Enhancement had its greatest value, however, in displaying the components of the neoplasms. For example 'cysts' were evident in 37% of gliomas before enhancement and in 64% after enhancement and the proportion of apparently infiltrating gliomas was reduced from 34% before enhancement to 10% after it. Intravenous contrast was also valuable in displaying further unsuspected metastases when a solitary tumour was shown on the plain scan.

We attempted to predict the histology of tumour from C.A.T. appearances by consideration of their morphological features and their enhancement patterns (Tables 2, 3, 4 and 6). This work has previously been reported in some detail (1) and will only be briefly summarised.

The great majority of our glial tumours have shown as masses of mixed attenuation in which the Hounsfield unit values were within or below the normal range. Enhancement also tends to be irregular; it is usually of greater degree than normal brain but less than that of meningiomas and many metastases.

Metastases were usually homogeneous, well-demarcated masses with surrounding oedema and 62% were of increased attenuation compared with only 17% of gliomas. However, comparison of the tables shows that there is a considerable number of cases of each type of tumour with C.A.T. features more commonly found in the others and distinction between some of them on C.A.T. findings alone is not possible. Failure to appreciate this fact was a major cause of misdiagnosis, accounting for

the high rate of false positives in the metastatic group (Fig. 4) (and false negatives in the glioma group) on the original reports due to the inclusion of many of those gliomas with a homogeneous pattern of increased attenuation (13 cases) in this group. Similarly, the false negatives among the metastases were tumours showing features more commonly found in gliomas, such as irregular attenuation (8 cases) or large neoplastic cavities (5 cases) (Fig. 5) which often led to false positive diagnosis of glioma (5 cases).

An important factor in distinguishing metastases, which should decrease the number of incorrect diagnoses on clinical correlation, was that a primary neoplasm was evident in two-thirds of these lesions. After due consideration of other pathologies, such as multiple infarcts and inflammatory lesions, multiple intracerebral masses were always considered to be metastases; this premise caused an error in diagnosis in two multifocal gliomas.

Calcification in gliomas was helpful in excluding metastases, but in two cases dense calcification in peripheral tumours made angiography necessary for exclusion of meningioma. Three peripheral metastases were indistinguishable from meningiomas and conversely four meningiomas with atypical features, such as marked cystic degeneration, irregular enhancement, excavation into the brain to a degree suggesting an intracerebral tumour or extremely marked intracerebral oedema, could not be reliably categorised on C.A.T.

Although oedema was present in 93% of metastases and 84% of gliomas, in general, though by no means invariably, it was more marked with metastatic tumours in proportion to their size. Midline shift was slightly less common in metastases, because of the balancing effect of bilateral lesions. Ventricular narrowing, which is also a manifestation of mass effect, was equally common with both types of tumour.

Cerebral swelling in non-tumourous conditions sometimes caused diagnostic difficulties. Thus, infarcts during the first 2 weeks after onset resulted in false positive diagnosis of tumour in four cases and glioma was included in differential diagnosis in four others. There was considerable mass effect in all these cases and all showed enhancement (Fig. 6). These features of infarction are now well documented (4) and they caused little difficulty in retrospective diagnosis. This important error is usually at least suspected on clinical correlation and doubt can be resolved by angiography in a proportion of cases in which typical vascular changes are shown.

The only other major source of error was radionecrosis, which in three cases caused the partial enhancement of mass lesions indistinguishable from progression of growth in gliomas which had previously been treated. Angiography showed only avascular swelling and is unhelpful in specific diagnosis prior to excision which is the recommended curative therapy in regions where this is applicable.

Other false positive diagnosis were made in isolated examples of many pathologies. None of these were typical of tumour which was usually only mentioned in differential diagnosis and in none of them was the C.A.T. diagnosis accepted as the basis of specific clinical management.

Hydrocephalus in the gliomas was usually due to obvious involvement of the supratentorial midline CSF pathways. In metastases it was most frequently associated with further lesions in the posterior fossa.

Distinction between Types and Grades of Glioma

Tables 4 and 6 show that calcification and homogeneous enhancement were more frequent in oligodendrogliomas and that oedema was less likely in low grade oligodendrogliomas. Calcification and hydrocephalus due to encroachment on CSF pathways were also more frequent in low grade gliomas and irregular enhancement in high grade astrocytomas. However, distinction between the various primary cerebral tumours was unsatisfactory in individual cases on C.A.T. alone. Consideration of age, clinical course up to time of C.A.T. and plain X-ray changes increased considerably the likelihood of correct diagnosis.

During the period of this study the influence of C.A.T. on the management of patients has been changing. In the early stages, most cases were also subjected to angiography and biopsy, the latter procedure carrying a considerable morbidity. Now many high grade gliomas, especially in evocative areas are diagnosed without surgical intervention, unless this is indicated as part of the therapy; the proportion of cases investigated by C.A.T. alone has increased from the average of 20% up to 25% in the last 9 months of the study. The value of follow-up C.A.T. in differential diagnosis of tumour from non-progressive or resolving lesions has also become established and has to some extent replaced angiography when the clinical problem does not demand urgent solution.

References

1. CLAVERIA, L.E., DU BOULAY, G.H., KENDALL, B.E.: The diagnostic limitations of computerised axial tomography in hemispheric tumours. Round Table on C.A.T., 6th Congress of the European Society of Neuroradiology, Dijon 17-18 September, 1976.
2. GREITZ, T.: Computer tomography for diagnosis of intracranial tumours compared with other neurological procedures. Acta radiol. (Stockh.) Suppl 346, 14-20 (1975).
3. NORMAN, D., ENZMANN, D.R., LEVIN, V.A., WILSON, C.B., NEWTON, T.H.: Computer tomography in the evaluation of malignant glioma before and after therapy. Radiology 121, 85-88 (1976).
4. WING, S.D., NORMAN, D., POLLOCK, J.A., NEWTON, T.H.: Contrast enhancement of cerebral infarcts in computed tomography. Radiology 121, 89-92 (1976).

a b

Fig. 1a and b. Cystic astrocytoma. (a) Plain scan. Right posterior temporal tumour, of mixed, but mainly low attenuation causing marked mass effect. (b) After intravenous contrast. Irregular marginal enhancement

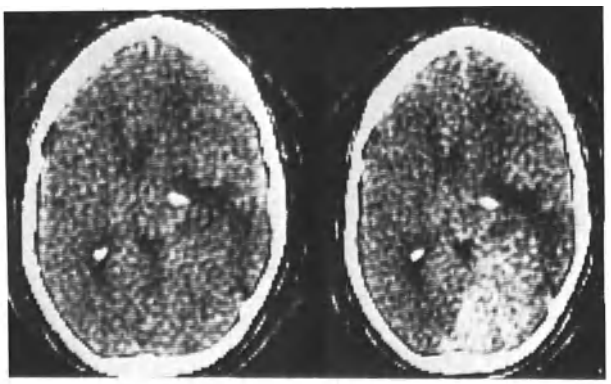

a b

Fig. 2a and b. Solid astrocytoma. (a) Plain scan. Mass of brain density displacing calcified right choroid plexus anteriorly. (b) After intravenous contrast. Homogeneous enhancement

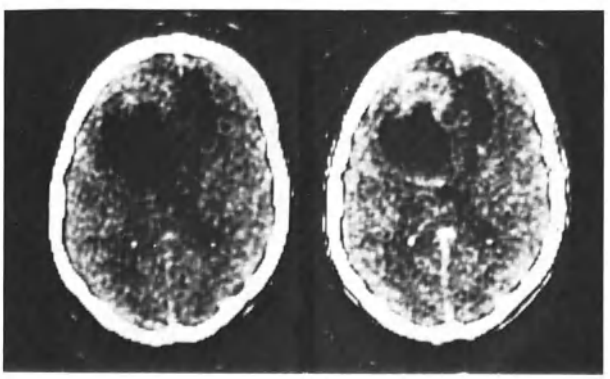

a b

Fig. 3a and b. Mixed solid and cystic astrocytoma. (a) Plain scan. In left frontal lobe, mass of higher attenuation than brain anteriorly and low attenuation posteriorly. (b) After intravenous contrast. Enhancement anterior part of mass and rim enhancement of cystic posterior component

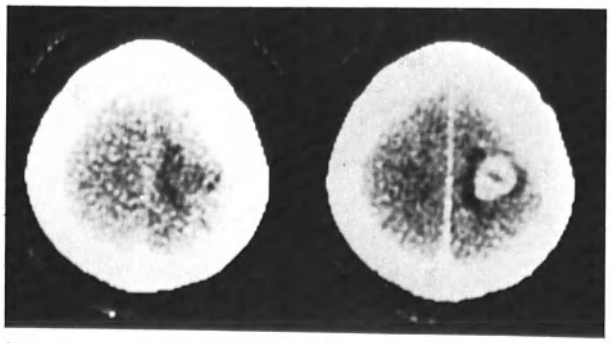

a b

Fig. 4a and b. Glioma. (a) Plain scan. Low density lesion right parietal lobe. (b) After intravenous contrast. Well demarcated enhancement with small central low attenuation region and surrounding oedema

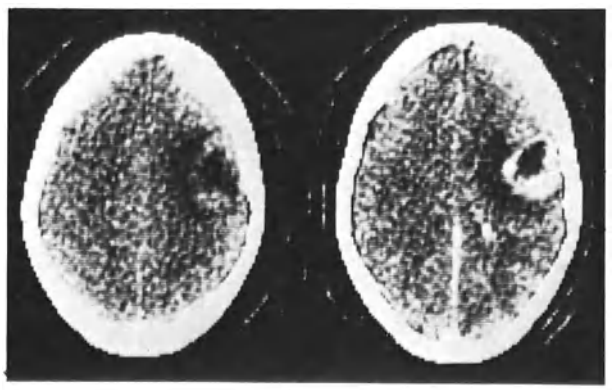

a b

Fig. 5a and b. Metastasis, originally diagnosed as glioma on C.A.T. (a) Plain scan. Thick-walled ring shadow of slightly increased attenuation with surrounding low attenuation in right parietal lobe. (b) After intravenous contrast. Enhancement of ring showing irregular thickness characteristic of malignant neoplasm

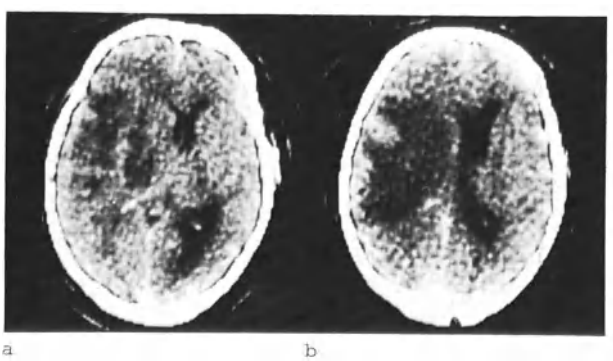

a b

Fig. 6a and b. Infarct left temporal and posterior frontal lobes 14 days after onset. (a) and (b) After intravenous contrast. Large low attenuation mass with patchy enhancement

Intracranial Epidermoid and Dermoid Tumours

R. A. Fawcitt and I. Isherwood*

Introduction

It is proposed to discuss intracranial epidermoid and dermoid tumours, emphasising the radiological appearances demonstrated on plain radiography of the skull, contrast examinations and computerised axial tomography.

The first record of such a tumour is that of VERATTUS (19) in 1745 who recorded at necropsy a brain tumour containing masses of hair. In 1829 CRUVELHIER (3) described a growth in the basal cisterns of the brain with an external surface of "metallic sheen like silver or a pearl of the finest water". The contents of the growth "presented all the characters of cholesterin". Because of their striking appearance he called them pearly tumours. MÜLLER (12) in 1838 reported another two examples and because of their content named them cholesteatomas. VIRCHOW (20) in 1855 favoured again the term pearly tumours. VON REMACK (14) in 1854 suggested that these tumours arose from misplaced epithelial tissue; this was substantiated by BÖSTROEM in 1897 (1).

The origin of what DANDY (5) described as "the most beautiful tumour in the body" is generally accepted to be due to abnormalities of closure of the neural tube in the 3rd to 5th weeks of embryonic life.

Histologically, epidermoids and dermoids are cystic tumours with a thin capsule of epidermis or dermis. Desquamation fills the epidermoid tumour with epithelial debris and cholesterin crystals, while the dermoid includes also sebaceous material and hair within its cavity. Dermoids more commonly than epidermoids may show mural calcification.

Incidence and Distribution

CUSHING (4) cited epidermoids and dermoids as constituting 0.75% of his series of 2023 intracranial tumours. CASTELLANO and RUGGIERO (2), quoting Olivecrona's series, reported a similar incidence of 0.85%. Intracranial epidermoids usually present in the fourth, fifth and sixth decades of life, whereas the dermoids are reputed to be most frequent in the first decade of life.

Pearly tumours occur in four sites intracranially:

1. In the region of the petrous apex and cerebellopontine angle
2. In the suprasellar region
3. In the cerebral hemispheres
4. Associated with the cerebellum and fourth ventricle

---

*Department of Neuroradiology, Manchester Royal Infirmary.

Material and Method

We have recently reviewed 22 intracranial dermoids and epidermoids in adolescents and adults collected over the last 20 years from the Department of Neuroradiology, Manchester Royal Infirmary. The anatomical distribution of these tumours is listed:

1. Cerebellopontine angle and petrous bone:		7 dermoids	(7)
2. Suprasellar:		4 epidermoids	
		1 dermoid	(5)
3. Intracerebral (including intraventricular):			
	Frontal	3 epidermoids	
		2 dermoids	
	Parietal	1 epidermoid	
	Temporal	2 epidermoids	(8)
4. Cerebellum and fourth ventricle:		2 epidermoids	(2)

Age distribution by decades is:

	11-20	21-30	31-40	41-50	51-60	61-70
Epidermoids	1	2	4	7	4	1
Dermoids	-	1	-	-	2	-

Previous reviews include those by LOVE and KERNOHAN (9), MAHONEY (11), TYTUS and PENNYBACKER (18) and McCARTHY et al. (10).

Present Series

Radiological Investigations

All patients had plain films of the skull and underwent further neuroradiological examinations according to the site of the suspected tumour.

Two patients have been investigated by means of C.A.T. preoperatively and six patients postoperatively. This investigation has, we believe, demonstrated typical appearances which will be described below.

Radiological Appearances

The radiological appearances of the intracranial dermoid and epidermoid will be considered according to site.

Cerebellopontine Angle and Petrous Bone

Of the seven cases encountered, four displayed marked erosion of the petrous bone, but of these three showed negative air encephalograms or Myodil ventriculograms.

Only 1 showed the typical appearance of the cerebellopontine angle epidermoid, bony erosion with the irregular tumour mass. This was in a 55-year-old woman with a right cerebellopontine angle syndrome. Plain film showed smooth erosion of the petrous apex and air encephalography showed the irregularly outlining 'cauliflower' mass, with air in the interstices of the tumour, displacing the midbrain and cerebellum.

C.A.T. of a similar case after several postoperative recurrences showed an extensive cerebrospinal fluid density area containing an ill-defined area of slightly higher density with marginal calcification extending from the right cerebellopontine angle to the temporal and occipital lobes (Fig. 1). At post mortem an extensive epidermoid tumour was demonstrated throughout this region.

Bone erosion may occur either in the apex or in the middle third of the petrous bone where Stenver's view and a-p tomography show a smooth defect in the mid portion of the right petrous bone with no sclerosis. Air encephalography was essentially negative. The bone erosion of the petrous apex may be demonstrable on C.A.T.

In the three cases showing no bony erosion, the radiological appearances were those of a non-specific cerebellopontine angle tumour.

Suprasellar Tumours

Of five cases, three were confined to the suprasellar region. The two suprasellar epidermoids showed flattening of the tuberculum sellae or erosion of the posterior clinoids, this not being shown by the more distantly placed dermoid. In only one case (on post-operative follow-up) was the irregular tumour outline seen which would give any radiological clue to the diagnosis.

In that particular case:

1960 - Skull radiograph showed flattening of the tuberculum sellae and erosion of posterior clinoids. A right carotid angiogram showed elevation of the anterior cerebral artery. An air encephalogram demonstrated a suprasellar mass. At operation a right suprasellar primary epidermoid was found.

1973 - Follow-up air encephalogram demonstrated an irregularly outlining suprasellar mass extending anteriorly and bilaterally, demonstrated on coronal and sagittal tomography. This lady died recently, 15 years after her first investigations, with a recurrence of the tumour extending throughout the suprasellar subarachnoid cisterns and into the Sylvian fissures. C.A.T. in the later stages of her illness showed extensive low (CSF) density areas throughout the basal cisterns corresponding to the extent of the tumour (Fig. 2).

Of the two epidermoids with an intrasellar component, one showed on plain films calcification in an expanded sella. Air encephalogram demonstrated tumour extending superiorly through basal cistern into the third ventricle on sagittal and coronal tomography. At operation the tumour was tethered to the hypothalamus with collagenous elements and calcification in its wall. C.A.T. on a patient with a similar suprasellar epidermoid showed an extensive suprasellar mass of CSF density corresponding to a recurrence (Fig. 3).

Intracerebral Tumours

Of the eight tumours, six showed definite vascular displacement but no pathological circulation. Three (one postoperatively) showed the classical irregular outlining of the interstices of the tumour by air. Both dermoids and one epidermoid showed irregular calcification. The two dermoids showed distinctive appearances on pre-operative C.A.T. and these cases are described in more detail.

Case E.B.

A 54-year-old female had been 44 years in a mental institution. Plain skull radiographs showed curvilinear irregular calcification in the left frontal region with an associated low density area. At air encephalography air passed initially only over the surface of the brain. Delayed films showed air within a partially calcified mass in the left anterior fossa which extended to displace the anterior horn of the left lateral ventricle. Ventricular dilatation was present. Coronal anterior fossa tomography showed erosion of the lesser wing of sphenoid with air surrounding the irregular tumour mass. Horizontal beam films revealed an air/fat/CSF level in the right lateral ventricle, confirmed on tomography. C.A.T. showed a low density area in the left frontal region with calcification peripherally and a fluid level in the right frontal horn (Fig. 4). By altering window width and levels it was possible to demonstrate the heterogenous low density tumour (μm = -10 to -40) adjacent to the left frontal horn and one can separate out the fat/CSF level in the right frontal horn (μm of fat = -60 to -70).

At operation there was a communication between this left frontal dermoid tumour and the left lateral ventricle, through which fluid fat flowed from the ventricular system. We believe that these radiological appearances of intraventricular fluid fat have not been previously published and are unique to this type of tumour.

Case R.A.

A 22-year-old male presented with what was clinically thought to be a post-traumatic epileptic fit. C.A.T. showed a well-circumscribed low-density area in the right frontal region with a small area of calcification on the anteriomedial border. The density of the cyst was less than CSF (Fig. 5). Analysis of the C.A.T. showed much of the mass to be approximately -16 Hounsfield units. A smaller area of -30 Hounsfield units is demonstrable, representing fat (Fig. 6). At operation this lesion was confirmed to be an extensive, pearly white dermoid tumour in the right frontal lobe, arising from the midline.

Calcification in the parietal epidermoid was readily demonstrable on C.A.T. but there was no associated low density lesion either of CSF of fat density.

Cerebellum and Fourth Ventricle

Both patients showed obstruction to outflow of CSF from the fourth ventricle, one by a tumour in the vermis, the other due to an intraventricular tumour within the fourth ventricle. The intraventricular epidermoid in a 69-year-old woman produced dilated lateral ventricles and fourth ventricle with an irregular filling defect within the enlarged fourth ventricle.

Discussion

In the investigation of a lesion occupying intracranial space a small proportion, e.g. not more than 0.5-1%, of tumours will be due to intracranial epidermoids or dermoids.

In two areas debate has arisen on the nature or origin of 'cholesteatomas'. Firstly, in the region of the petrous bone, where differentiation must be made between those arising as a result of middle ear disease producing local erosion of the attic or tympanic spur, and the true primary epidermoid tumour.

The second area for debate has arisen in the differentiation of cystic craniopharyngiomas and suprasellar epidermoids (15). Histologically, however, the craniopharyngiomas show a typical reaction in the surrounding glia with tadpole-shaped Rosenthal bodies in the astrocytic cells. They also show a histochemical differentiation, with the presence of high alkaline phosphatase activity in the epithelium (absent in that of the epidermoid) (16, 17).

Summary

Finally, what are the best radiological investigations to carry out on the patient with a suspected dermoid or epidermoid tumour? On plain skull films, calcification is an inconstant feature (visible in 7 of our 22 cases) (8, 10). At certain sites, bone erosion may occur. Angiography may demonstrate an avascular space occupying lesion, so providing no valid indication of pathology. The air encephalogram produces the 'typical' appearance in only a small proportion of cases of intraventricular (7) and extraventricular tumours (five cases in our series).

Of the patients with epidermoid tumours who underwent C.A.T. three patients showed extensive low (CSF) density lesions commensurate with the recurrent tumour (6). In one of these, an area of slightly higher density within this low density was seen. Two patients showed no evidence of recurrence on C.A.T., while the final patient showed only parietal intracerebral calcification. In the case of the intracranial dermoid tumour, we believe that C.A.T. may produce pathognomonic appearances, as we have demonstrated above.

Acknowledgments

The authors are grateful to Mr. R.T. Johnson and the Department of Neurosurgery, Manchester Royal Infirmary, for permission to study patients under their care. Thanks are due to Miss H. Jarvis, Superintendent Radiographer and the Radiographic staff of the Department of Neuroradiology, Manchester Royal Infirmary, and also to the Department of Medical Illustration and Mrs. G.E.H. Shawcross for the preparation of illustrative material. Finally, our thanks are extended to Mrs. M. Tipton for her secretarial assistance.

References

1. BÖSTROEM, E.: Über die pialen Epidermode, Dermoide und Lipome und duralen Dermoide. Zbl. allg. Path. paht. Anat. 8, 1 (1897). Cited by CRITCHLEY and FERGUSON.
2. CASTELLANO, F., RUGGIERO, G.: Meningiomas of the posterior fossa. Acta radiol. (Stockh.) Suppl. 104, 7 (1953).

3. CRUVELHIER, J.: Anatomie Pathologique du Corps Humain. Paris: Bailliere 1829.
4. CUSHING, H.: Intracranial Tumours. Notes upon a series of two thousand verified cases with surgical mortality percentages pertaining thereto. London: Bailliere, Tindall and Cox 1932, p. 8.
5. DANDY, W.E.: The Brain. Hagerstown, Maryland: W.F. Prior Co. 1966, pp. 626-633.
6. DAVIS, K.R., ROBERSON, G.H., TAVERAS, J.M., NEW, P.F.J., TREVOR, R.: Diagnosis of epidermoid tumour by computed tomography. Radiology 119, 347-353 (1976).
7. DYKE, C.G., DAVIDOFF, L.M.: Encephalographic appearance of an intraventricular epidermoid. Bull. Inst. N.Y. 6, 489-493 (1937).
8. LINDGREN, E., DI CHIRO, G.: Suprasellar tumours with calcification. Acta Radiol. (Stockh.) 36, 173-195 (1951).
9. LOVE, J.G., KERNOHAN, J.W.: Dermoid and epidermoid tumours (cholesteatomas) of the central nervous system. J. Amer. med. Ass. 23, 1876-1883 (1936).
10. MACCARTY, C.S., LEARENS, M.E., LOVE, J.G., KERNOHAN, J.W.: Dermoid and epidermoid tumours in the central nervous system of adults. Surg. Gynaec. Obstet. 108, 191-198 (1959).
11. MAHONEY, W.: Die Epidermoide des zentralen Nervensystems. Z. ges. Neurol. Psychiat. 155, 416-471 (1936).
12. MÜLLER, J.: Über den feineren Bau und die Formen der krauschafen Geschwülste. Berlin: Reimer 1838, p. 50. Cited by CRITCHLEY and FERGUSON.
13. PEYTON, W.B., BAKER, A.B.: Epidermoid, dermoid and terratomatous tumours of the central nervous system. Arch. Neurol. Psychiat. (Chicago) 47, 890-917 (1942).
14. REMACK, VON. (1854). Cited by CRITCHLEY and FERGUSON.
15. RUSSELL, D.S., RUBINSTEIN, L.J.: Pathology of Tumours of the Nervous System. 3rd ed. London: Edward Arnold 1971, pp. 24-25.
16. TIMPERLEY, W.R.: Histochemistry of Rathke Pouch tumours. J. Neurol. Neurosurg. Psychiat. 31, 589-595 (1968).
17. TIMPERLEY, W.R., TURNER, P., DAVIES, S.: Alkaline phosphatase in craniopharyngiomas. J. Path. 103, 257-262 (1971).
18. TYTUS, J.S., PENNYBACKER, J.: Pearly tumours in relation to the central nervous system. J. Neurol. Neurosurg. Psychiat. 19, 241-259 (1956).
19. VERATTUS: De bononiensie scientiarum et artium institute atque academia commentarii. 2. Pt. 1 (1745). Cited by CRITCHLEY and FERGUSON.
20. VIRCHOW: Über Perlgeschwülste. Virchow's Arch. path. Anat. 8, 371 (1855). Cited by CRITCHLEY and FERGUSON.

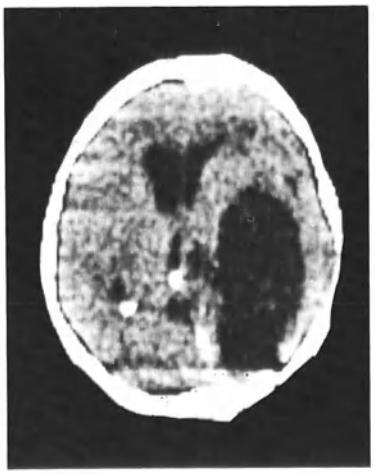

Fig. 1

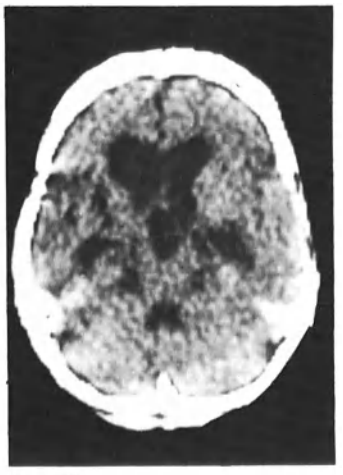

Fig. 2

Fig. 1. Recurrence of right cerebellopontine angle epidermoid, extending into temporal and occipital lobes

Fig. 2. Recurrence of a suprasellar epidermoid, extending bilaterally into both sylvian fissures

Fig. 3

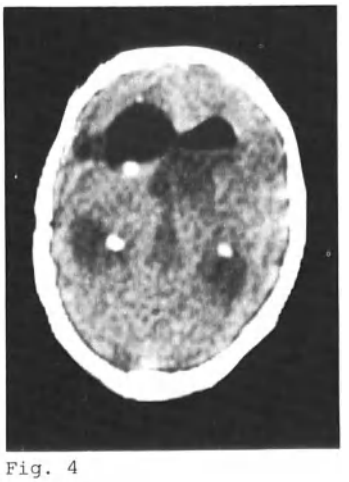

Fig. 4

Fig. 3. Recurrent suprasellar epidermoid, confined to suprasellar region

Fig. 4. Left frontal dermoid, with mural calcification and fat/CSF level in the right frontal horn

Fig. 5

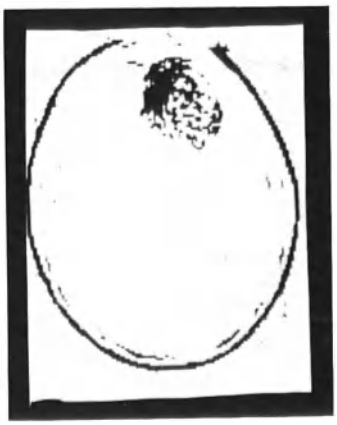

Fig. 6

Fig. 5. Right frontal dermoid of less than CSF density

Fig. 6. Same tumour as in Fig. 5 with altered window level and window width showing heterogeneity. Densities measured at -16 and -30 Hounsfield units

Meningiomas Diagnosed by Scanning: A Review of 100 Intracranial Cases

D. Sutton and L. E. Claveria*

Meningiomas are among the commonest intracranial tumours. The diagnosis is frequently suspected on clinical grounds, but specific proof has up to now depended on radiological investigations and in very recent years on isotope scanning. There have been several previous reviews on the accuracy of these methods of investigation.

Plain X-rays will diagnose some 30-50% of intracranial meningiomas, while they may confirm suspicion of the presence of an intracranial tumour in 60-75% of cases (3, 5, 6, 7, 13, 14).

Pneumography, which was widely practised before the days of angiography, was said to localise 95% of meningiomas, although, of course, specific diagnosis of the pathology was only possible in a small proportion of cases where the tumour was clearly shown to be extracerebral.

Angiography, which has been so widely used in the last 20 years, enables a definitive diagnosis to be made in a high proportion of cases and thus not only will the presence of a tumour be diagnosed in over 90% of cases, but specific diagnosis of meningioma is possible in over 70% of cases (2, 8, 15).

Brain scanning by isotopes will diagnose the presence of an intracranial tumour in up to 90% of meningioma cases and the pattern of uptake will suggest the actual pathology in a good proportion of these (5, 11, 12, 16).

In the last 3 years the advent of computerised axial tomography (C.A.T.) has given us the opportunity to analyse a large series of meningiomas investigated by both the new and old techniques and to assess their relative value.

Material

One hundred proven intracranial meningiomas have now been investigated by C.A.T. with a high resolution matrix (160 × 160) and by various other methods. We have analysed and attempted to compare the values of the different methods used in this service. A description of the first 70 cases has already been given (4), and this paper is an extension of that work.

*National Hospitals for Nervous Diseases, Queen Square and Maida Vale, London (Great Britain).

Findings

Table 1 shows the distribution of our 100 intracranial cases and Table 2 the analyses of our findings.

Plain X-ray. The diagnosis of intracranial tumour was made in 48 out of 74 cases where the plain X-rays taken at original presentation were available for review (65%). Our series contained 24 recurrences, so that plain X-rays at the time of admission were not relevant or readily available in most of these. A specific diagnosis of meningioma was made in 28 of the cases (38%).

Specific diagnosis was possible on the presence of such well-known features as hyperostosis in a typical meningioma site, locally increased meningeal markings leading to a meningioma, or characteristic meningioma calcification.

Angiography. Arteriography was performed in 63 of our cases. It was diagnostic of tumour in 60 cases (96%) and diagnostic of meningioma in 47 of the cases (75%). It was considered normal in 3 cases (5%).

Angiography was frequently undertaken in cases where a diagnosis of meningioma was already certain on other investigations. This is because many neurosurgeons wish to define the exact relationship of the tumour to veins and arteries and to determine the exact blood supply before operation. Meningiomas can infiltrate around arteries and can invade veins and this is particularly important with sphenoidal ridge and suprasellar meningiomas, which may involve the middle or anterior cerebral arteries. It is also important where the tumour is parasagittal since the sagittal sinus can be involved or obstructed.

Pneumography

This was only undertaken in four cases in our series and there now usually have to be special indications for such air studies. Thus with a small suprasellar mass which is avascular and not obvious at angiography the full extent of the tumour has been better shown by air. It has also been used in this series in a case of meningioma near the petrous apex to show the relationships to the middle and posterior fossa.

There is no doubt, however, that pneumography will now rarely be required, and has been largely replaced by the newer techniques.

Isotope Brain Scanning

Fifty-two of our intracranial cases were investigated by this method. Tumour was diagnosed in 48 (92%). The specific diagnosis of meningioma was suggested in 29 (56%). In the literature the percentage of accuracy of tumour diagnosed in meningioma cases is given variously as from 70% to over 90%. The features which suggest meningioma on an isotope scan are heavy uptake by the tumour showing a circumscribed or rounded lesion at a typical meningioma site, i.e. parasagittal or on the convexity or along the sphenoidal ridge.

We have, however, several times suggested the diagnosis of meningioma on these grounds and have been proved wrong when the lesion was found to be a superficial malignant tumour.

We have not used serial scanning and sequential measurements of uptake in attempting to recognise tumour type.

C.A.T. Review of our material shows that the overall accuracy of the new method in making a specific diagnosis of meningioma is higher than any of the other methods, including the invasive ones. This is also already suggested by figures of small series published in the last 2 years. Thus BAKER claims 21/23 (91%), PAXTON and AMBROSE 34/35 (97%) GREITZ 16/18 (92%) and NEW 11/11 (100%) (1, 7, 9, 10). It is clear from this and our own material that the presence of a tumour can be diagnosed with an accuracy approaching 100%.

However, it is important to stress that careful evaluation of the clinical history and signs is vital before scanning since a small lesion can easily be missed if the appropriate area is not included. The cases we failed to diagnose include two small tuberculum sellae meningiomas which were less than 1 cm in size. Review showed that in one of these the cuts did not have the correct angulation to visualise the region accurately. In the second case the lesion was identified on the polaroid print at retrospective review. The third case which we failed to identify was a small parasagittal recurrence (under 1 cm in diameter) in which there was a large amount of artefact from residual surgical clips.

All tumours more than 1 cm in diameter were adequately demonstrated. The localisation of the meningiomas in our series is shown in Table 1.

Table 1. Localisation of meningiomas

Convexity	frontal	15
	parietal	5
	temporal	9
	occipital	3
Parasagittal		26
Subfrontal		3
Tuberculum sellae		13
Sphenoidal ridge		12
Cerebellopontine angle		8
Tentorium		2
Cerebellar convexity		3
Intraventricular		1
Total		100

Among the 100 cases listed there were 5 with multiple meningiomas and 24 admitted with recurrence of previously operated meningiomas. Suspected postoperative recurrence may be difficult to diagnose when small. Nevertheless it has been our impression that C.A.T. is more accurate than the other methods in this particular problem, and this material will be presented in a further communication.

The multiple meningiomas diagnosed in five cases were all parasagittal and all clinically unsuspected.

The Unenhanced Scan

Unenhanced scans of meningiomas have very characteristic features. The tumours appear as homogeneous high-density areas with well-defined round borders. The attenuation values are slightly more than that of normal brain and average 20-36 Hounsfield units if uncalcified. However, if calcification is present the density can be as high as 270 or 300 units. Normal brain tissue measures only 16-20 units.

Contrast Enhancement

This is an important feature of C.A.T. diagnosis and significantly increases the specific identification rate. Once the simple scan has been performed the procedure is repeated immediately following intravenous injection of 60-80 ml of Conray 420, given as a bolus. With this technique, meningiomas show contrast enhancement in a striking fashion. The whole tumour increases homogeneously in density both visually and as measured by Hounsfield units. In only two cases was contrast enhancement less extreme. In most cases the tumour edge was well defined by the enhancement pictures and the exact extension of the tumour was clear.

Table 2. Intracranial meningioma - radiology

	No.	Diagnostic	Tumour non-specific	Normal
Skull X-ray	74	28 (38%)	20 (27%)	26 (35%)
Isotope scan	52	29 (56%)	19 (37%)	4 (8%)
Angiography	63	47 (75%)	13 (21%)	3 (5%)
Pneumography	4	-	4 (100%)	-
C.A.T.	100	90 (90%)	7 (7%)	3 (3%)

Table 3. Meningiomas - C.A.T. features

Hyperostosis	marked	4
	slight	8
Bone destruction		3
Calcification		16
Cystic component	major	4
	minor	3
Oedema	severe	2
	moderate	11
	minimal	51
Mass effect	marked	8
	slight	44
	minimal	20

Radiological features which assist in plain X-ray diagnosis of meningioma are rarely visualised on C.A.T. However, four cases did clearly (Table 3) demonstrate *hyperostosis* and in another eight cases there was a suggestion of its presence.

Bone destruction is also a rare plain X-ray manifestation, but it was identified in three cases by C.A.T., as well as being obvious on the plain X-rays.

Calcification within the tumour was identified as a density greater than 45 Hounsfield units. This was present in 16 cases and varied from calcification of the whole tumour to irregular or scanty calcification within it.

Cystic components to the tumour are relatively rare in meningiomas, but they are occasionally seen. In seven of our cases such cystic components were identified and in four of these they were a major feature.

One of these cases seemed to resemble a glioma (Fig. 4). The pathology, however, was unique in that the meningioma was associated with an adjacent tuberculoma which was presumably responsible for the cystic appearance.

Oedema surrounding the tumour tended to be minimal and circumscribed. Only very occasionally did it appear extensive and with the characteristic digital elongation of more malignant tumours. We saw only 2 cases of this type and 11 cases with moderate oedema. Fifty-one cases showed minimal oedema around the tumour and the rest showed none. Oedema was usually absent in subfrontal, suprasellar and cerebellopontine angle tumours.

Mass effect, with displacement of the ventricles, was marked in 8 cases, moderate in 44, minimal in 20 and absent in the rest.

Table 4 includes 20 cases listed as false positives. These were abnormalities incorrectly diagnosed as meningiomas, although correctly localised. The figures are derived from an analysis of 8000 cases including over 1000 tumours. Furthermore, some of these diagnoses were made at an early stage, before our experience had grown; and they were made by a variety of observers.

Table 4. C.A.T. performed: 8000

C.A.T. meningioma	120		
False positive	20		
Histology verified	100	False negative	3
Recurrence	24		
Multiple	5		

Table 5. Meningioma - false positive

Metastasis	5
Glioma	2
Lymphosarcoma	1
Cavernous angioma	1
Craniopharyngioma	1
Pituitary adenoma	1

The 11 cases with a wrong final diagnosis of meningioma are shown in Table 5, and the 9 cases where meningioma was put forward as one of several suggestions are shown in Table 6.

Table 6. Meningioma suggested as a differential diagnosis

Metastasis	4
Pituitary adenoma	2
Glioma	2
A.V.M. (thrombosed)	1

Even allowing for unproved technique there will still be a residuum of cases where a confident specific diagnosis is not possible though it should be suggested as part of a differential.

These include high-density tumours in the *cerebellopontine angle* with similar appearances to meningioma and similar behaviour following con-

trast enhancement. They would include deposits, gliomas, and some trigeminal neurinomas. We do not think that acoustic neurinomas present a problem in this context. Some workers have suggested that these tumours can appear as high density lesions but in our material nearly all have been low density lesions before contrast enhancement. As noted from our tables the main problems are with vascular metastases.

In the suprasellar region both pituitary adenomas and craniopharyngiomas may present a similar picture to meningiomas as they frequently show increased density on simple C.A.T. and contrast enhancement. Differentiation again depends on the clinical presentation and other radiological features, but a meningioma should always be considered in the differential diagnosis. A pinealoma can also resemble a meningioma.

We had only one intraventricular meningioma in our series and this was readily identified. We have, however, encountered intraventricular gliomas which showed similar features. In some cases the irregular margins and infiltrations of the glioma may help to differentiate it. Intraventricular ependymoma or papilloma may also show similar features. Another area where in our experience it is unwise to make a specific diagnosis of meningioma on C.A.T. alone is in the orbit and the retro-ocular region (4).

In conclusion, we present a review of the impact of C.A.T. on the radiological diagnosis of meningiomas. This new non-invasive method is undoubtedly the most accurate diagnostic tool yet available. Using contrast enhancement, it provided a specific diagnosis of meningioma in 90% of our 100 intracranial cases, and diagnosed the presence of a tumour in a further 7%. Even without Conray, the specific diagnostic rate of meningioma was nearly 80%. The false negative rate was only 3%. False positives - in the restricted sense that a specific diagnosis of meningioma can only be offered as part of a differential diagnosis - may occasionally occur, and usually involve vascular gliomas or metastases. Such equivocations should be rare when the clinical and other features are considered in context.

References

1. BAKER, H.L., CAMPBELL, J.K., HOUSER, D.W.: Computer assisted tomography of the head. An early evaluation. Mayo Clin. Proc. 49, 17-27 (1974).
2. BANNA, M., APPLEBY, A.: Some observations on the angiography of supratentorial meningiomas. Clin. Radiol. 20, 375-386 (1969).
3. BUTCHTEL, B.C., JOHNSON, D.E., Jr., SAAL, B.M.: Radiographic diagnosis of meningiomas. S. Med. J. (Bgham, Ala.) 64, 973-977 (1971).
4. CLAVERIA, L.E., SUTTON, D., TRESS, B.M.: The radiological diagnosis of meningiomas. Brit. J. Radiol. (1976) (in press).
5. DU BOULAY, G.H., McALLISTER, V.L.: The choice between carotid angiography and brain scanning in the investigation of tumour suspects. Proc. Roy. Soc. Med. 63, 46-50 (1970).
6. GOLD, L.H., KIEFFER, S.A., PETERSON, H.O.: Intracranial meningiomas: a retrospective analysis of the diagnostic value of plain skull films. Neurology (Minneap.) 19, 873 (1969).
7. GREITZ, T.: Computed tomography for diagnosis of intracranial tumours compared with other neuroradiologic procedures. Acta Radiol. (Stockh.) Suppl. 346, 14-21 (1975).
8. JACOBSON, H.E., LUBETZKY, H.W., SHAPIRO, J.E., CARTON, C.: Intracranial meningiomas: a Roentgen study of 126 cases. Radiology 72, 356 (1959).

9. NEW, P.F.J., SCOTT, W.R.: Computed Tomography of the Brain and Orbit. Baltimore: Williams and Wilkins 1975.
10. PAXTON, R., AMBROSE, J.: The EMI Scanner - a brief review of the first 650 patients. Brit. J. Radiol. 47, 530-565 (1974).
11. SAUER, J., FIEBACK, O., OTTO, H., LOHR, E., STROTGES, H.W., BERTAG, W.: Comparative studies of cerebral scintigraphy, angiography and encephalography for diagnosis of meningioma. Neuroradiology 2, 102-106 (1971).
12. SCHUNK, H., DAVIES, M., DRAKE, M.: A study of meningiomas with correlation of hyperostosis and tumour vascularity. Amer. J. Roentgenol. 91 (1964).
13. SHELDON, J.J., SMOAK, W., GARGANO, F.P., WATSON, D.D.: Dynamic scintigraphy in intracranial meningiomas. Radiology 109, 109-115 (1973).
14. TRAUB, S.P.: Roentgenology of Intracranial Meningiomas. Springfield, Ill.: Charles C. Thomas 1961.
15. WICKBOM, I., STATTIN, S.: Fifth Symposium Neurodiologique. Acta Radiol. (Stockh.) 50, 175 (1958).
16. WITCOFSKI, R.L., MAYNARD, C.D., ROPER, T.J.: A comparative analysis of the accuracy of the brain scan. J. Nucl. Med. 8, 187-196 (1967).

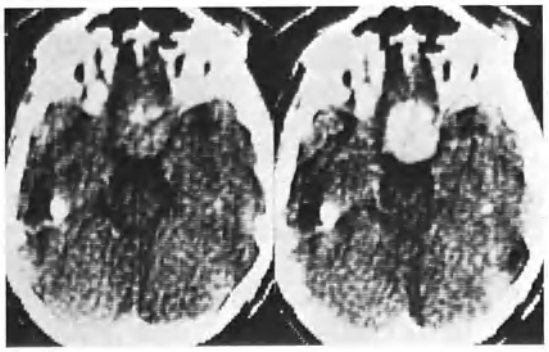

Fig. 1. Tuberculum sellae meningioma. Well-delineated spherical mass with attenuation coefficients higher than normal brain tissue, encroaching upon the chiasmatic cistern, (a) before, (b) after intravenous contrast administration. Note homogeneous enhancement, outlining full extent of tumour

Fig. 2. Sphenoidal ridge meningioma. Note large homogeneous dense tumour implanted on outer third of sphenoidal wing (a) before, (b) after intravenous contrast administration, demonstrating characteristic enhancement pattern

Fig. 3. Tentorial meningioma. Similar appearances to Fig. 2. Because of its localisation a tumour of the pineal should be considered in differential diagnosis

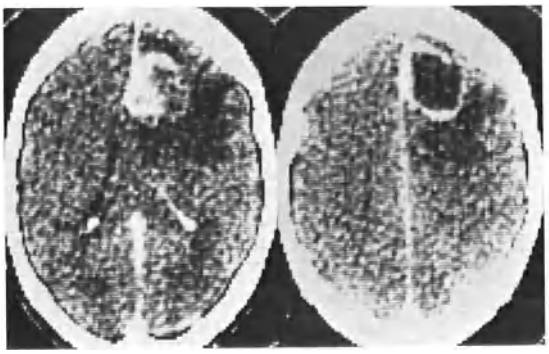

Fig. 4. Atypical frontal parafalcine cystic meningioma after administration of intravenous contrast medium. This tumour had been originally diagnosed as a glioma, but note the attachment to the falx. Histology demonstrates features of a meningioma combined with granulomatous tissue resembling a tuberculoma

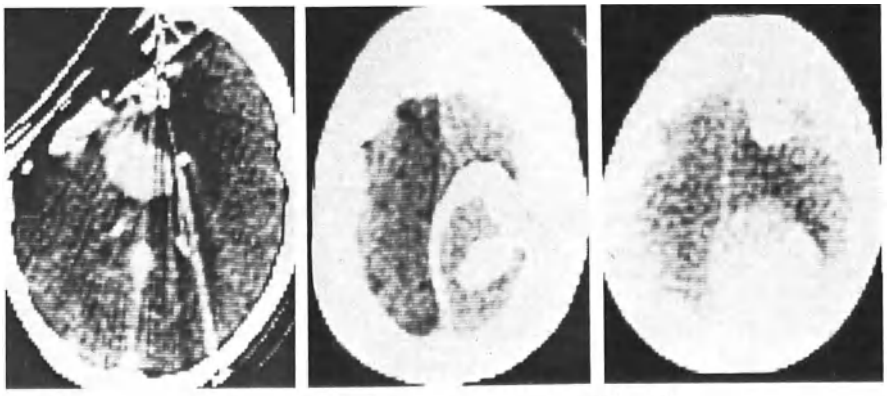

Fig. 5 Fig. 6 Fig. 7

Fig. 5. Recurrent parasagittal meningioma. Note surgical defect; bone flap from previous craniotomy had been removed. Artefacts due to surgical clips interfere with quality of scan, but enhancement of recurrent tumour is easily shown

Fig. 6. Calcified parasagittal meningioma. Homogeneously dense mass with high attenuation coefficients is demonstrated in an unenhanced scan by virtue of calcium in the outer surface and in the centre of tumour. This was visible on plain skull X-ray

Fig. 7. Parasagittal and parafalcine meningiomata after administration of intravenous contrast medium

A German Multicentre Study of Intracranial Tumours

S. Wende**, A. Aulich, E. Schindler, T.Grumme, W. Meese, S. Lange, E. Kazner, H. Steinhoff, and W. Lanksch*

This cooperative study of the CT-groups of Berlin, Mainz and Munich includes the investigations on 1304 patients with intracranial neoplasms.

Table 1 gives a survey of the number of cases of the different tumour groups and the detection rate in the plain as well as in the post-contrast scan. Of the tumours studied, 15.3% were isodense in the plain scan compared to normal brain tissue. Isodensity of tumour tissue was most frequent in acoustic neuromas amounting to 58% of the cases. A percentage of isodense tumours higher than the average was observed in astrocytomas of grade II, glioblastomas, spongioblastomas, metastases and craniopharyngiomas. Of all tumours 6.4% were not detectable in the plain scan. In 115 isodense tumours, localisation became possible through the recognition of indirect signs of a space-occupying process.

Table 1. Isodense intracranial tumours

Type of neoplasms	No.	Tumour isodense (plain scan)	Tumour negative (plain scan)	Tumour negative (post-contrast scan)
Astrocytoma gr. I	72	1	-	-
Astrocytoma gr. II	64	11	4	-
Glioblastoma	251	38	8	-
Oligodendroglioma	66	3	-	-
Spongioblastoma	27	8	3	-
Meningioma	205	28	11	3
Sarcoma	23	3	1	-
Epidermoid	7	-	-	-
Metastases	159	31	12	4
Pituitary adenoma	118	14	2	-
Craniopharyngioma	32	5	5	1
Ependymoma	20	2	-	-
Medulloblastoma	30	4	-	-
Plexuspapilloma	4	-	-	-
Acoustic neurinoma	62	36	31	2
Angioblastoma	14	-	-	-
Other tumours	48	5	3	3
Unclassified tumours	102	10	4	4
Total	1304	199	84	17
%	100	15.3	6.4	1.3

By contrast enhancement 67 primarily negative neoplasms, among them 29 acoustic neuromas, could also be recognized. Only 1.3% of all tumours (17 cases) remained undetectable in the post-contrast scan (Table 2).

*Cooperative study of the University Clinics of Berlin, Mainz and Munich.
**Dept. of Neuroradiology, University Hospital Mainz, Langenbeckstraße 1, 6500 Mainz (FRG).

Table 2. Intracranial tumours not visualized in the contrast scan: an evaluation of 1304 neoplasms

Type of neoplasm	No.
Craniopharyngioma	1
Meningioma	3
Acoustic neurinoma	2
Neurofibroma	1
Pinealocytoma	1
Clivus chordoma	1
Metastases	4
Unclassified tumours	4
Total	17 (1.3%)

We find that the various masses exhibit differing absorptions and we differentiate between an increased, a decreased, an equal and a mixed density of the tumour compared to cerebral tissue. After contrast injection the density may either increase or remain unchanged.

Gliomas of Grades I and II (Astrocytomas and Oligodendrogliomas) (202 Cases)

It is shown that astrocytomas of grade I nearly always exhibit a decreased density both before and after contrast injection. On the contrary, astrocytomas of grade II give an inhomogeneous image in the plain scan. Contrast enhancement occurred in 90% of the cases (Figs. 1, 2).

Glioblastomas (251 cases)

In 65% of the cases the plain scan revealed a mixed density. There was a combination of increased and decreased density. Following intravenous contrast injection, the density in the tumour region nearly always increased. In the cases in which a ring-shaped pattern is visible there is likely to be central tumour necrosis (Figs. 3, 4).

Meningiomas

A decreased density is never shown on the plain scan; the density is slightly increased. After contrast injection a distinct increase of density develops. Meningiomas are relatively homogeneous in density and well-defined.

Metastases (Figs. 5, 6)

Absorption is extremely variable in the plain scan. After contrast injection a considerable increase in density occurs. Here too, there are

different images of metastases. There may be ring-shapes, nodular formations, mixed forms and metastases which become observable only through the perifocal oedema. There are quite typical small tumour foci with very pronounced perifocal oedemas.

Our group 'other tumours' also contains pinealomas. Figure 7 deals with a prolonged follow up study during and after X-ray therapy.

Examination on *January 8:* Pronounced dilatation of both lateral ventricles. Tumour in the pineal region with compression of the third ventricle.

Examination on *February 3* after X-ray therapy: Regression of the dilatation of ventricles. No enhancement of the pinealoma. The third ventricle is not identifiable.

Examination on *February 18:* No alteration of the size of ventricles. The third ventricle is recognizable again.

Examination on *March 10:* No alteration of the size of ventricles, distinct visualization of the third ventricle. Slight tumour enhancement in the dorsal part of the third ventricle. Slight nodular indentation of the medial wall of the left anterior horn.

Examination of *April 22:* Compression of the third ventricle. Intensified tumour stain in both the regions of the left anterior horn and the septum.

Examination of *May 24:* Tumour stain of both lateral ventricles showing distinct hyperdensity.

Examination of *June 24:* The tumour extent in both lateral ventricles has increased. The ventricles are dilated. No visualization of the third ventricle. Repeated X-ray therapy.

Examination on *August 6:* Following X-ray therapy distinct tumour regression. Both lateral ventricles and the third ventricle have regained normal size.

Follow-up studies on *August 22* and *September 22* do not display proven changes in findings. However, the inadequate visualization of the third ventricle is evident.

This case shows that follow-up studies are of crucial relevance for the demonstration of the development of a brain tumour as well as in cases of questionable tumour recurrences and for the demonstration of the therapeutic success.

Differential diagnosis on brain tumours by means of C.A.T. is limited. In some cases it is not possible to distinguish between astrocytomas grade II, sarcomas, metastases, malignant melanomas and meningiomas. An inhomogeneous contrast enhancement with a ring-shaped pattern may be similar to cases of metastases, glioblastomas and abscesses.

The mean attenuation of the tumour tissue in the plain scan does not provide further information for differential diagnosis in many tumour groups. Also the quantitative values of attenuation enhancement do not contribute to a differential tumour diagnosis as they are similar in different tumour groups.

On critical inspection of the examination findings of 1304 cerebral tumours, we established that at C.A.T. brain tumours are detectable

in 98.7% of cases by means of direct and indirect tumour signs in the plain scan and by additional contrast application. This high diagnostic accuracy cannot be achieved by any other neuroradiological method of examination. In many cases, however, only follow-up studies enable the exact diagnosis of a cerebral tumour to be made.

We should, however, bear in mind that C.A.T. can lead to considerable misinterpretation unless history and clinical findings are carefully considered. The differential diagnosis between the various tumour types is limited; a tumour, moreover, may not always be distinguished from an abscess. Follow-up studies assist the final differential diagnosis between brain infarct and brain tumour. One single C.A.T. investigation does not always lead to a final statement on the tumour histology. A positive tumour demonstration in C.A.T. should, however, always give rise to angiography for further elucidation of the diagnosis.

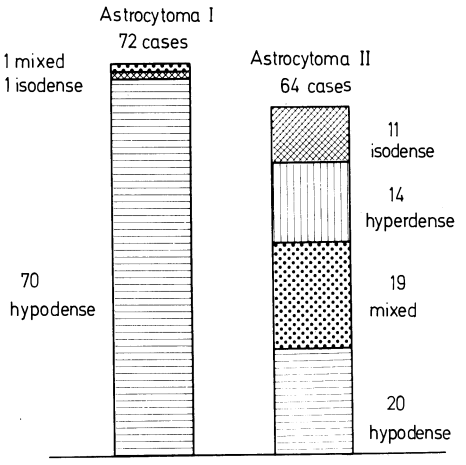

Fig. 1

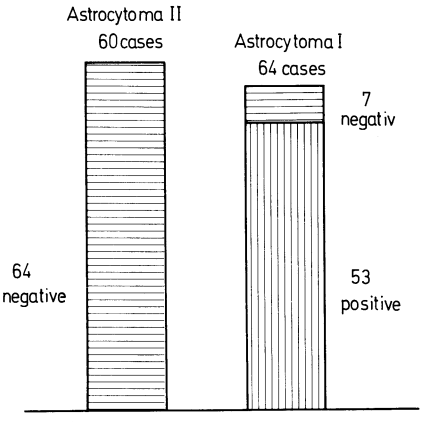

Fig. 2

Fig. 1. Astrocytomas; tumour density before enhancement
Fig. 2. Astrocytoma; enhancement

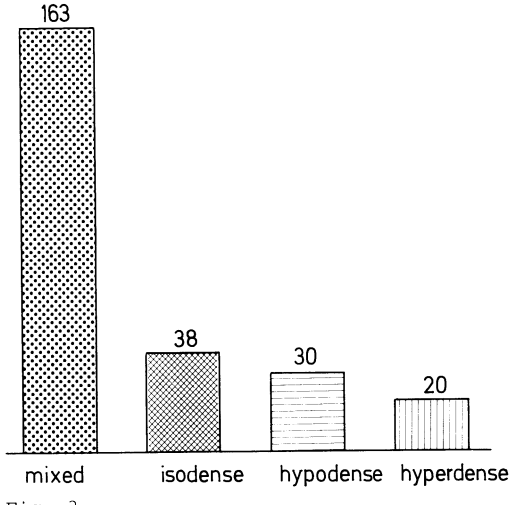

Fig. 3

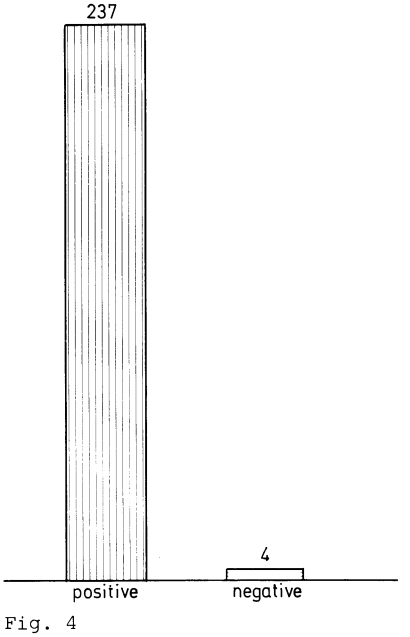

Fig. 4

Fig. 3. Glioblastoma (251 cases); tumour density before enhancement
Fig. 4. Glioblastomas; enhancement (241 cases)

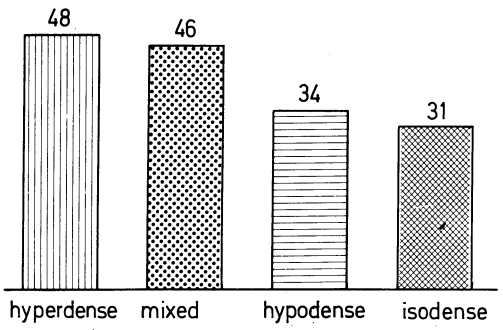

Fig. 5

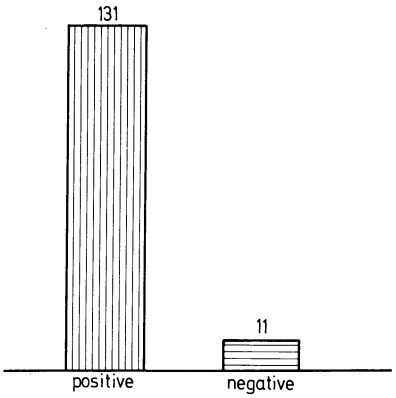

Fig. 6

Fig. 5. Metastases (159 cases); tumour density before enhancement

Fig. 6. Metastases; enhancement (142 cases)

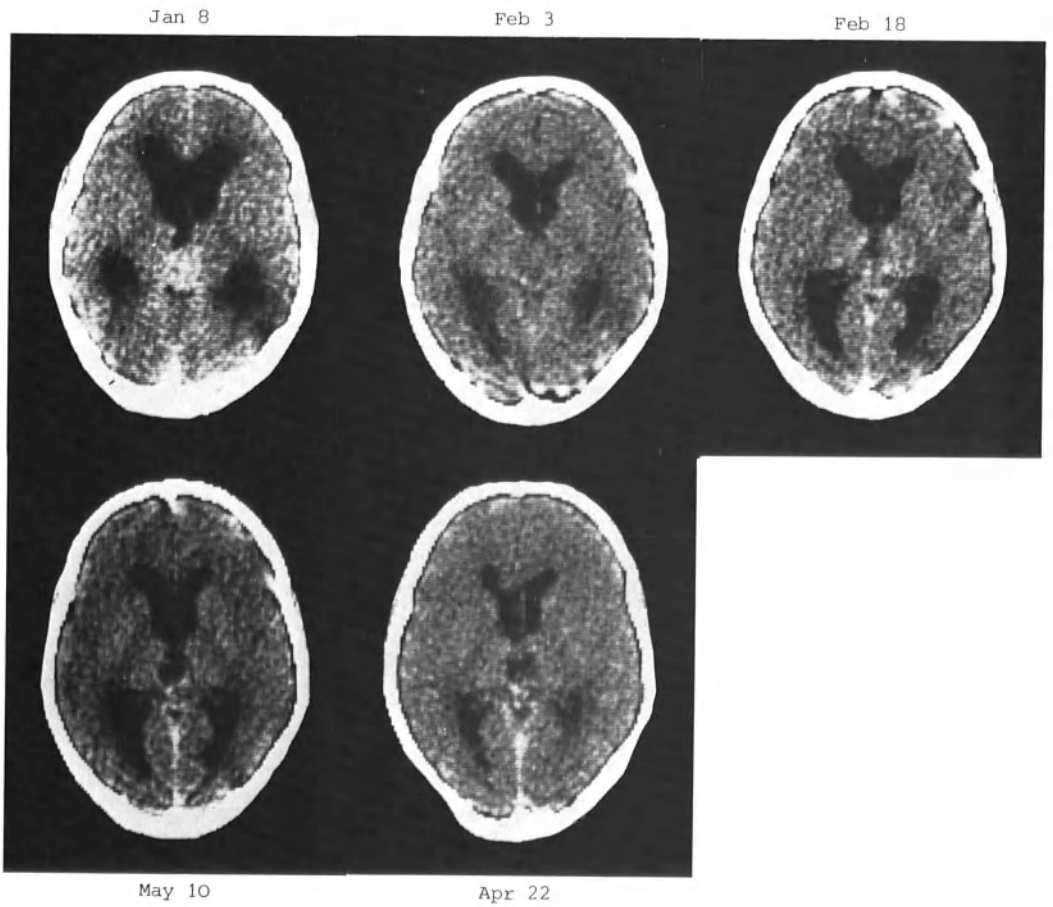

Fig. 7a

Fig. 7a and b. Follow-up study of a patient with a pinealoma (see text)

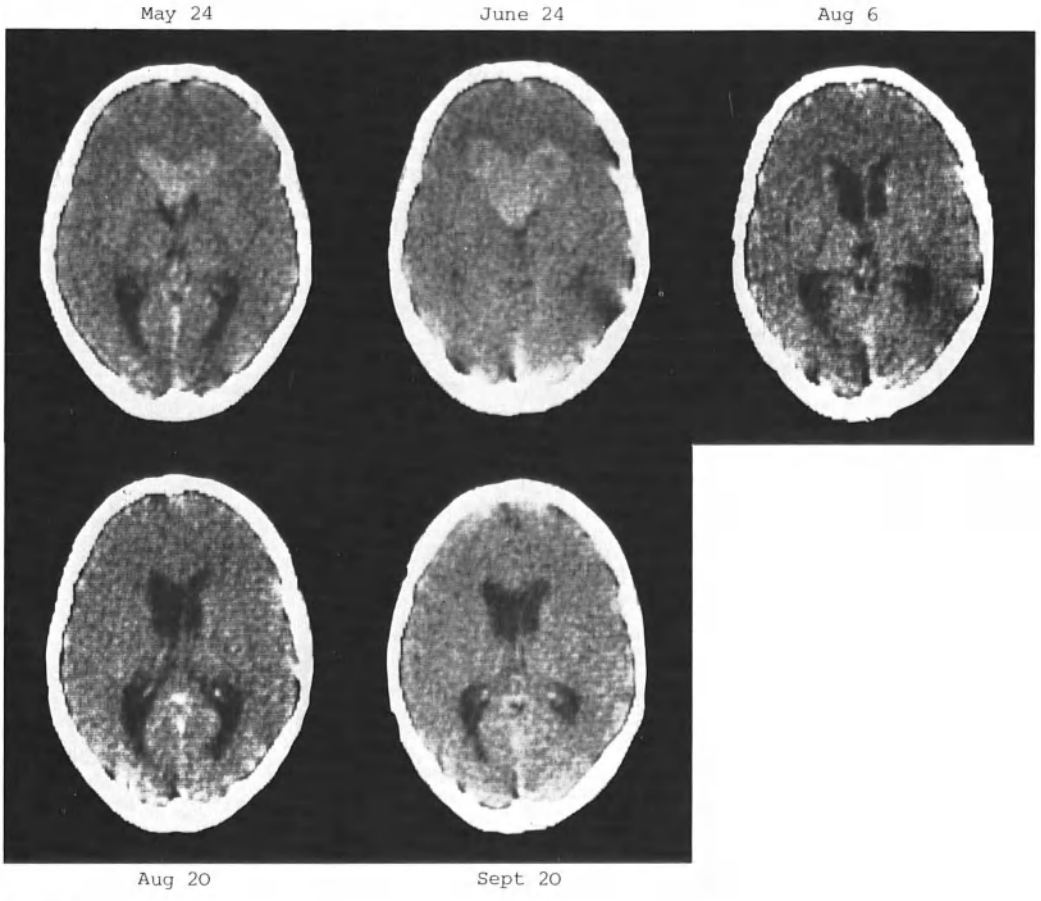

Fig. 7b

C.A.T. Investigations of the Development of Cerebral Oedema and the Effects of its Treatment in Patients with Brain Tumours*

S. Wende, A. Aulich, K. Kretschmar, S. Lange, T. Grumme, W. Meese, W. Lanksch, E. Kazner, and H. Steinhoff**

The use of computerised axial tomography makes it possible to study the expansion of perifocal oedema in patients with cerebral tumours. C.A.T. opened up the possibility of visualizing the outline of this oedema and the effect of dexamethasone treatment.

Our experiences leads us to believe that by means of follow-up studies (1) new information on the pathophysiological or biological process may be obtained and (2) the therapeutic effect may be controlled objectively.

Owing to the increased water content, oedema appears as an area of low density at C.A.T. The use of Hounsfield units does not facilitate the differentiation between tumour and infarct oedemas. Shape and localisation, however, as well as extent and development revealed typical differences.

In a cooperative study of the University Clinics of Berlin, Mainz and Munich, 724 ischaemic infarcts and 1304 brain tumours were examined.

Since cerebral oedemas can reach different extents, gradation appears to be useful. As an oedema of grade 1 we define a perifocal oedematous margin up to 2 cm in diameter. If half a hemisphere is encroached by a cerebral oedema, there is a case of oedema of grade 2. More extensive oedemas we quantify as grade 3.

On comparison of the different images of perifocal oedema with the appropriate anatomical cuts, it becomes obvious that the localisation of the oedema as shown in C.A.T. corresponds to the region of the white matter. The extension of perifocal oedema seems to be determined by the topography of the white matter which leads to the formation of characteristic oedematous images according to the tumour localisation.

The oedema of a frontal tumour terminates funnel-shaped into the narrow pass formed by the basal ganglia and the Sylvian fissure. Following contrast enhancement the tumour may be distinctly visualized. In the case of bilateral development of such an oedema, e.g. olfactory meningiomas, the typical 'poodle face' appears.

In the case of temporal and occipital tumour localization, one recognizes a finger-shaped extension towards the front where three spread-out fingers may always be outlined. These consist of the oedematous extension to the internal capsule, the external capsule and the white matter of the temporal lobe (Fig. 1).

In the region of the Sylvian fissure, two cortical zones join. Here a large area of tissue, when cut out by extensive oedema in the white matter may be mistaken for a tumour.

---

*Cooperative study of the University Clinics of Berlin, Mainz and Munich.

**Dept. of Neuroradiology, University Hospital Mainz, Langenbeckstraße 1, 6500 Mainz (FRG).

Cerebral oedema occurs most frequently in glioblastomas (90% of cases), metastases (82%), astrocytomas grade 2 (66%), meningiomas (64%), sarcomas (60%), oligodendrogliomas grade 2 (42%) (Table 1).

Table 1. Brain oedema; 1304 patients with brain tumours

251	Glioblastomas	90%
159	Metastases	82%
64	Astrocytomas grade 2	66%
205	Meningiomas	64%
23	Sarcomas	60%
66	Oligodendrogliomas grade 2	42%

In those cases of astrocytoma of grade 1 which show a decreased tissue density and which, due to their poor vascularisation, do not absorb any contrast medium, one cannot distinguish between tumour and oedema.

The extent of perifocal oedema does not depend at all on the size of the tumour. Small metastases may be surrounded by oedema which spreads through half a hemisphere. On the other hand, large meningiomas may appear without any oedema or only with a slight oedematous margin.

Not only do tumours of different kind and localisation occur with or without perifocal oedema but also histologically identical masses in the same localisation. C.A.T. is not able to display the factors responsible for the differing oedema reactions of development. In some cases, however, there seems to be a correlation between the malignancy and rapidity of the tumour growth and the extent of the oedema. Nearly all tumour patients with the history of a rapidly progressive clinical deterioration exhibit extensive oedema. Entirely calcified tumours, pituitary adenomas, craniopharyngiomas, pinealomas and most of the intraventricular tumours never show any oedema.

It is rarer for tumours of the posterior cranial fossa to show oedema. This is traceable to the volume of the white matter in proportion to the preponderant volume of the grey matter and to the resolution of the scanner available.

Our follow-up studies on the treatment of tumour-dependent cerebral oedema were made on more than 100 patients.

Short-term treatment with dexamethasone or aldosterone from 3 to 5 days using doses between 16 and 24 mg/day resulted in only a few cases in which a significant change of the oedema was shown on C.A.T., although clinical improvement was obvious.

During long-term therapy with dexamethasone for several weeks, however, even small doses (4 mg/day) are obviously capable of reducing the tumour-dependent oedema visibly. This, according to our observations made so far is, however, only recognizable in cases of malignant masses.

In another group of patients treatment was carried out with dexamethasone combined with furosemide (120 mg/day). Here too, one should differentiate between short-term and long-term therapy. In some cases, we could already observe an effect of therapy on C.A.T. after 3 to 5 days. At first, a regression of the mass effect becomes apparent. The ventricle compressed on the tumour side re-expands slowly. In the region of the visualized oedema too there is a tendency towards regression (Fig. 2).

If this therapy is performed during a period of several weeks, complete regression of the cerebral oedema can be achieved. On discontinuation of therapy, the oedema re-appears. We therefore believe that a proven influence on the cerebral oedema due to a tumour can only be achieved through prolonged treatment using dexamethasone or dexamethasone combined with furosemide.

Contrary to the perifocal oedema in cerebral tumours, oedemas due to acute vascular processes are demonstrable by C.A.T. both in white and grey matter. Following occlusions of larger arteries, the entire vascular supply area is visualized as a dark homogenous zone of decreased X-ray absorption. The diffuse extension of oedema into the white and grey matter is based on the pathomechanism of the vasogenous oedema. Such oedematous patterns are already observable in adults a few hours after the acute event. The shortest interval of time in children was 3 h. On comparison of the average absorption value of tumour oedema with that of pure vascular oedema, no essential differences occur. In both oedemas we measure 10 to 12 EMI units. However, shape and localisation as well as extent and development display typical differences. In cases of tumours and cerebral infarcts, larger areas of oedema are space-occupying, with displacement of midline structures and ventricular compression. Signs of a space-occupying process for more than 3 weeks lead to suspicion of a tumour.

At the earliest 3 to 4 days after insult, changes are visible in C.A.T. after enhancement, which point to disturbance of the blood-brain barrier. The maximum is between the 12th and 21th days. In the contrast scan we found that the low-density area could disappear and give way to a deceptive normal finding (Fig. 3).

In cases of uncertain differential diagnosis, follow-up studies are crucial.

Fig. 1

Fig. 2a

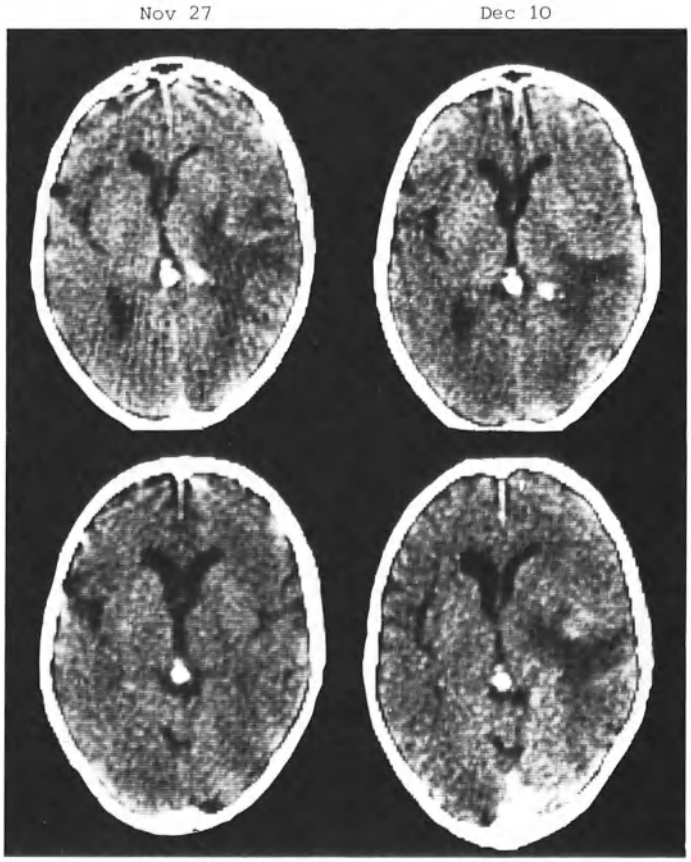

Fig. 2b

Fig. 1. Extension of the oedema in cases of temporal and occipital tumour (three fingers)

Fig. 2. (a) Glioblastoma right parietal (proven by autopsy). (b) Same patient as (a). Regression of tumour oedema. November 27, 1975 before therapy with dexamethasone/ furosamide. December 10, 1975: after 13 days' therapy. January 26, 1976: of therapy 60 days. April 22, 1976: after cessation of therapy, oedema reappears

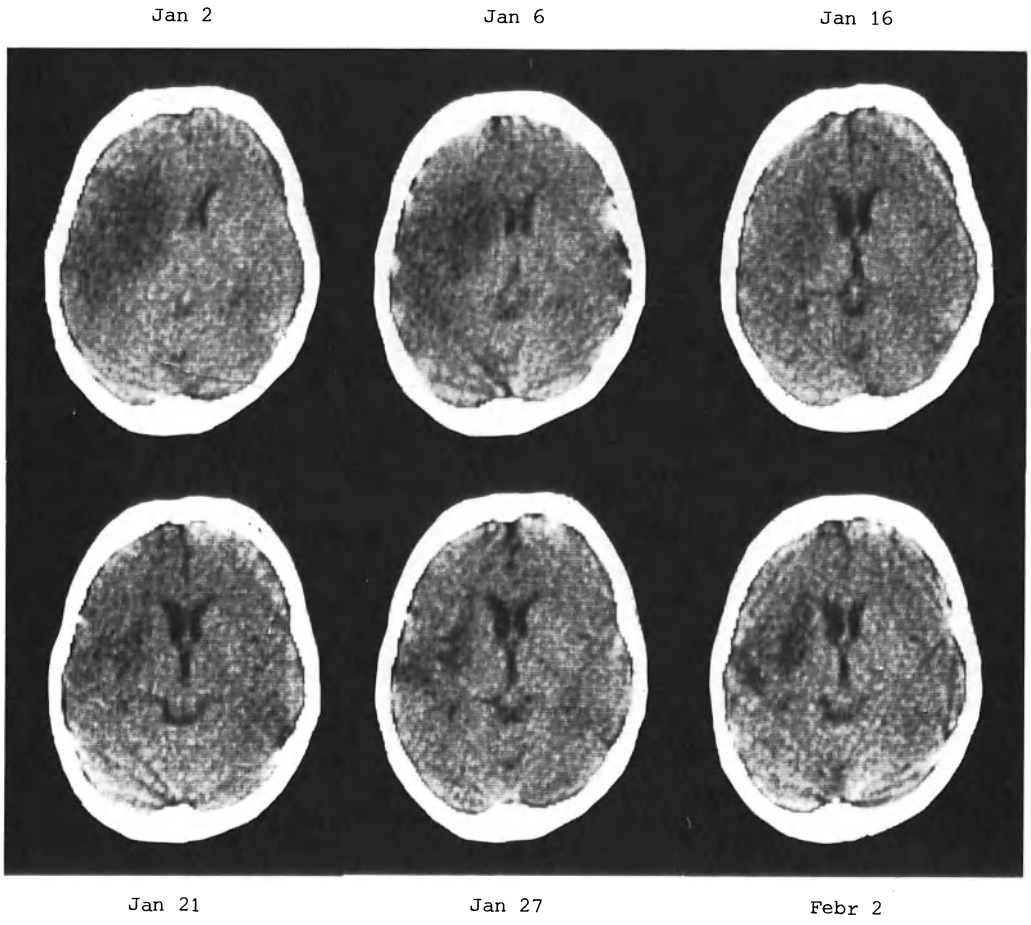

Fig. 3. Follow-up studies of oedema in a patient with an infarct

A Diagnostic Approach to Cerebellar Lesions

J. L. Wilson and I. F. Moseley*

The computerised axial tomograms C.A.T. of 105 patients with cerebellar lesions have been analysed in an attempt to determine the characteristics of the different lesions commonly encountered in this situation, with particular reference to differential diagnosis (1, 2).

Method

All C.A.T. scans in which a posterior fossa lesion had originally been reported were analysed. Extra-axial lesions or those involving primarily the brainstem were excluded (4, 5). The remaining cerebellar lesions were studied with reference to the following features:

1. Modification in the size, shape and position of the fourth ventricle

2. Areas of abnormal density, greater or lesser than surrounding brain, and their shape, position, extent and size in cm (corrected)

3. The effects of intravenous contrast enhancement

4. Cisterns: normal, widened, narrowed or obliterated

5. Hydrocephalus: absent, slight, moderate or severe

6. The presence or absence of periventricular lucency and the visibility and size of the temporal horns

7. The presence or absence of other abnormalities, related or unrelated to the cerebellar lesion

These data were correlated with the final diagnosis which, when possible, was obtained from histological reports. Cases which did not come to biopsy or post-mortem were excluded unless a firm conclusion could be reached on clinical, laboratory and radiological grounds.

Results

The analyses of the lesions analysed are shown in Tables 1-7.

*Lysholm Radiological Department, The National Hospital, Queen Square, London WC1N 3BG.

Table 1. Results: final diagnosis

Astrocytoma	23
Medulloblastoma	15
Haemangioblastoma	11
Ependymoma	5
Metastasis	26
Infarct	13
Haemorrhage	3
Angioma	2
Demyelination	2
Dermoid	2
Infection	3
Normal	1
	106

(One patient had dual pathology).

Table 2. Astrocytoma

Grade I	6
II	9
III	4
IV	1
Ungraded	3

Table 3. Metastasis

Type:	
Adenocarcinoma	11
Squamous carcinoma	10
Melanoma	1
Undifferentiated	4

Table 4. Age and sex distribution

Diagnosis	Number	Male	Female	Age	Mean age
Astrocytoma	23	17	6	2-70 years	20
Medulloblastoma	15	10	5	2-47 years	14
Haemangioblastoma	11	6	5	5-71 years	48
Ependymoma	5	4	1	2 months - 40 years	14
Metastasis	26	21	5	19-79 years	56
Infarct	13	9	4	28-79 years	51
Haematoma	3	2	1	7, 50, 71 years	
Angioma	2	2	-	21 and 33 years	
Demyelination	2	-	2	5 1/2 and 11 years	
Infection	3	1	2	2, 20, 42 years	
Dermoid	2	-	2	2 and 6 1/2 years	
Normal	1	1	-	10 years	

Astrocytoma (23 cases)

The lesion was of lower than brain density in 16 cases, higher in 3 cases and had mixed high and low density in 4 cases. The tumour was located in a cerebellar hemisphere in 14 cases, and in 2 of these it involved the adjacent cerebellar peduncle. In 6 cases the tumour was situated in the midline, while in 2 cases both hemisphere and midline structures were affected. Contrast medium was given in 17 cases; 11 tumours showed enhancement, 4 in a ring pattern, 6 homogeneously and 3 patchily. Presence and degree of enhancement was not clearly related to tumour grade (Figs. 1, 2). Hydrocephalus was moderate or severe in 17 cases and absent or slight in 6 cases. The degree of ventricular

Table 5. Size, density, position and contrast enhancement of lesions

Diagnosis	Size range in cm^2	Density			Situation			Contrast enhancement			
		Reduced	Increased	Mixed	Hemi	Midline	Both	None	Homogeneous	Patchy	Ring
Astrocytoma	1.0 × 1.5 to whole hemisphere	16	3	4	14	6	3	6/17	6	3	4
Medulloblastoma	1.8 to 5.0	4	11	-	5	10	-	2/15	4	4	-
Haemangioblastoma	2.3 to 5.0	11	-	-	7	3	1	3	Nodule 7	-	1
Ependymoma	2.0 to 4.5	-	1	4	-	3	2	-	1	3	-
Metastasis	1.0 to 4.0	11	10	5	17	2	6	4/22	10	5	4
Infarct	1.25 to whole cerebellum	12	-	1	12	1	-	6	-	4	-
Haemorrhage	2.0 to 6.0 × 1.0	-	3	-	1	1	1	1	-	-	-
Angioma	1.0 to whole hemisphere	-	2	-	2	-	-	-	-	2	-
Demyelination	2.0 and 1.0 × 2.0	2	-	-	2	-	-	1/1	-	-	-
Infection	1.5 to 5.0	1	-	2	1	2	-	-	1	1	1
Dermoid	4.0 × 3.0 + 5.0	-	-	2	-	2	-	-	-	-	2

Table 6. Secondary effects of cerebellar lesions

Diagnosis	Fourth Ventricle				Hydrocephalus				Periventricular lucency	Cisterns				Other Lesions	
	Displaced	Dilated	Compressed	Obliterated	None	Slight	Moderate	Severe		Normal	Wide	Narrow	Obliterated	Related	Unrelated
Astrocytoma	10	2	4	11	3	3	14	3	6	2	-	-	14	-	-
Medulloblastoma	8	1	9	3	4	3	7	1	4	5	1	-	8	2	-
Haemangioblastoma	3	-	6	4	1	-	8	2	4	-	-	1	10	-	-
Ependymoma	2	2	-	2	-	1	2	2	3	-	-	1	4	1	-
Metastasis	-	-	17	8	5	10	11	-	12	6	-	-	11	7	-
Infarct	-	-	4	-	6	6	1	-	1	5	2	-	2	6	2
Haemorrhage	-	-	-	3	-	1	2	-	1	-	-	-	3	-	-
Angioma	-	-	2	-	2	-	-	-	-	1	-	1	-	-	-
Demyelination	-	-	-	-	2	-	-	-	-	2	-	-	-	-	-
Infection	-	-	-	3	-	1	2	-	2	-	-	-	3	-	-
Dermoid	1	-	1	1	-	-	2	-	1	-	-	-	2	-	-
Normal	-	-	-	-	1	-	-	-	-	1	-	-	-	-	-

Table 7. Relationship of ventricular size, temporal horn size and periventricular lucency to presence or absence of papilloedema

	Hydrocephalus				Temporal horns			Periventricular lucency			
	None	Slight	Moderate	Severe	Not visible	Just visible	Enlarged	Absent	Slight	Moderate	Severe
Papilloedema	3	4	17	-	2	4	19	9	8	8	-
No papilloedema	10	5	5	1	13	2	6	15	-	4	2

enlargement was not related to tumour grade or size, but to position: all midline tumours had at least moderate hydrocephalus, but the 6 cases in which the hydrocephalus was absent or slight were all hemisphere lesions.

Medulloblastoma (15 cases)

The density of the lesion was increased in relation to normal brain in 11 cases and reduced in 4. Ten of the tumours were situated in the midline and 5 in a hemisphere. Size varied from 1.8 cm to 5.0 cm and shape was usually circular or oval. Contrast medium was given in 10 cases, of which 4 showed patchy enhancement (Fig. 3), 4 homogeneous enhancement and 2 equivocal change only. A ring pattern was not observed. Since enhancement was often slight or patchy, the extent of associated oedema was difficult to asses. Hydrocephalus was moderate or severe in 8 cases but slight only, or absent, in seven, and was generally associated with obvious compression of the fourth ventricle. Periventricular lucency was seen in 4 cases, all of which had dilated ventricles. Two patients had supratentorial tumours in addition to the posterior fossa lesion. These were regarded as evidence of metastatic or multifocal medulloblastomas. Obliteration of the basal cisterns was the rule with all types of tumour but in one case of medulloblastoma the cerebellar cisterns were widened over the surface of the hemisphere containing the tumour.

Haemangioblastoma (11 cases)

All tumours were low in density and two showed a mural nodule of less reduced density. Seven tumours were in a cerebellar hemisphere, three lay in the midline and one affected both locations. Contrast medium was given in all cases: seven showed enhancement of a nodule (Fig. 4). No enhancement was seen in three cases and one case showed ring enhancement. Two cases proved to be solid tumours: one of these showed homogeneous enhancement anterior to a low density area (presumably oedema) and the other case showed ring enhancement. In at least two cases small additional tumours near the base, subsequently shown angiographically, were not identified on C.A.T. Hydrocephalus was moderate in eight cases, gross in two and absent in one. Periventricular lucency was seen in four cases.

Ependymoma (5 cases)

Three lesions were of patchy high and low density, one of increased density and the last was a tumour having the same density as the surrounding brain. All tumours were situated in the midline, but two also spread to both hemispheres. Contrast medium was given in four cases and showed homogeneous enhancement in one and patchy enhancement in three. Hydrocephalus was moderate or severe in four cases and slight in only one. Periventricular lucency was seen in three patients, including the one in whom the hydrocephalus was slight. The fourth ventricle appeared dilated in two cases, both of whom had hydrocephalus involving also the third and lateral ventricles. In one case with a malignant ependymoma a mass was seen in the right lateral ventricle, presumably representing a metastasis.

Metastasis (26 cases)

Eleven cases showed reduced density, 10 increased and 5 were of patchy high and low density. Alterations in density were not clearly related to the histology of the tumour. In 17 cases the tumours were in the hemispheres: of these, 1 had bilateral tumours (Fig. 5a) and in another the tumour also involved the peduncle. Six lesions also involved the vermis; only two tumours were confined to the midline structures. Contrast medium was given in 22 cases, producing no enhancement in 4, homogeneous enhancement in 10 (Fig. 5b), patchy enhancement in 5 and ring enhancement in 4. Hydrocephalus was absent or slight in 15 cases and moderate in 11, despite the fact that the fourth ventricle was obliterated in 8 cases and compressed in 16. The degree of ventricular dilatation was only loosely related to tumour size. Definite periventricular lycency was seen in 9 cases, all but one of which involved moderate hydrocephalus. The basal cisterns were obliterated in 11 cases. Seven involved multiple tumours; in 5 of these the other lesions were in the cerebral hemispheres, while 2 cases each had two cerebellar deposits.

Infarct (13 cases)

Twelve of these lesions were reduced in density and 1 showed patchy mixed and normal density (Fig. 6a). In 12 cases the hemispheres were affected and in 4 of these there was also involvement of the peduncle. The remaining case was a midline infarct. Contrast medium was given in 10 cases, producing slight enhancement of the border of the lesion in 4. Hydrocephalus was absent in 6 cases and slight in 6, but the remaining patient (with an infarct of the upper hemisphere and peduncle) did show moderate third and lateral ventricular dilatation with periventricular lucency. In this latter case the fourth ventricle was displaced and compressed; it was also seen to be compressed in 3 other cases. The cisterns were normal or widened in 7 cases and obliterated only in 2. Three patients also showed low density in the brainstem, consistent with infarction (Fig. 6b), and 3 had cerebral infarcts. Cerebral atrophy was present in 2 cases, 1 of which also showed cerebellar atrophy.

Haemorrhage (3 cases)

All these showed the typical high-density appearance of clotted blood, situated in the hemisphere, midline and in both respectively. The fourth ventricle and cisterns were obliterated in all three cases, and hydrocephalus was moderate in two cases and mild in one. One case showed, in addition, blood in the third and lateral ventricles. Contrast medium was given to one patient, but showed no additional abnormality.

Angioma (2 cases)

One lesion occupied the whole of one hemisphere, while the other, 1 cm in diameter, lay alongside the fourth ventricle. Despite the fact that the fourth ventricle was distorted in both cases, neither showed hydrocephalus. Both angiomata were originally higher than normal brain density and enhanced markedly after Conray injection.

Demyelination (2 cases, both children)

The abnormality showed as a low density involving the white matter of the cerebellum and adjacent peduncle. There was no mass effect and no enhancement. In both cases the difference in density might have been thought to be artefactual, but in the first case the abnormality correlated well with the clinical picture and was present on three separate examinations. In the second case a follow-up scan 20 days later, at a time when there had been clinical improvement, showed resolution to normal.

Infection (3 cases)

One tuberculoma showed patchy low density in the middle of the posterior fossa, with enhancement after contrast medium injection. An aspergilloma showed as a large mass in the right hemisphere, of patchy high and low density with slight patchy enhancement. One infected dermoid presented a large midline, low density containing a ring of less reduced density representing the capsule, which enhanced markedly. All cases showed obliteration of the fourth ventricle and cisterns, but only two showed moderate hydrocephalus.

Dermoid (2 cases; 1 infected, see above)

Both lesions were of mixed density and both showed some enhancement.

Normal (1 case)

This case has been included as representing a true false positive. The patient, a child of 10, had ataxia and papilloedema. C.A.T. scan showed a very striking increased density in the inferior vermis, with moderate homogeneous enhancement after Conray injection. There was no displacement or compression of the fourth ventricle and no hydrocephalus. At surgery no lesion was found. The appearances seen in this case have subsequently been observed fairly frequently and may be due to a combination of a prominent choroid plexus blush, the dense grey matter of the inferior vermis and artefact resulting from the proximity of the base of the skull.

Hydrocephalus

Recognisable ventricular enlargement was seen in 75 of the 88 cases with a space-occupying lesion (85%) (Table 5). In contrast, hydrocephalus was recognised in 7 of the 17 cases with non-space-occupying conditions (41%) (infarcts, demyelination, angioma). Periventricular lucency was seen in 33 of the 88 cases with a space-occupying lesion (40%), as compared to 1 of 17 of the other group (6%). In the various tumour categories periventricular lucency was most common in the metastases, in spite of the relative lack of severe hydrocephalus in this group. In 46 cases the results of retinoscopy were obtained. Twenty-five patients had papilloedema and of these 21 had hydrocephalus (84%). Twenty-three patients with papilloedema had visible or definitely enlarged temporal horns (92%), and only 2 had temporal horns of normal size. Periventricular lucency was seen in 16 of the cases with papilloedema (64%). In 21 patients without papilloedema 11 had enlarged ventricles (52%), 8 had visible or enlarged temporal horns (38%) and 6 had periventricular lucency (28%).

Discussion

It is thus possible to construct a paradigm of each of the tumour types seen (3, 6):

1. Medulloblastoma: a teenage boy, showing a midline tumour of increased density, enhancing homogeneously or patchily; hydrocephalus may or may not be present

2. Astrocytoma: a young man having a low density lesion in one hemisphere, showing homogeneous or ring enhancement and causing moderate hydrocephalus

3. Ependymoma: a boy with a midline lesion as dense or denser than normal brain; which enhances patchily and is associated with hydrocephalus

4. Haemangioblastoma: a patient of either sex and any age with a hemispheric low density lesion, showing considerable enhancement of a nodule and causing moderately severe hydrocephalus

5. Metastasis: an elderly man with a rather small lesion of any density in the cerebellar hemisphere, enhancing homogeneously or patchily and unassociated with marked hydrocephalus: a second lesion may be present

There is, however, sufficient overlap, as regards not only single cases but also general characteristics (compare the medulloblastoma and the ependymoma above), to make a definitive tissue diagnosis impossible in the majority of cases.

Infarcts were usually easy to distinguish from tumours because of their low density and lack of mass effect, but one case had patchy high and low density. Several were causing compression of the fourth ventricle and one caused moderate hydrocephalus. In a number of cases there were infarcts in other parts of the brain. In most cases the clinical diagnosis of an infarct was obvious; however, C.A.T. is the only investigative method which actually shows the lesion. The pattern of enhancement of lesions after the injection of intravenous contrast was variable; the only specific type of enhancement was the dense homogeneous mural nodule seen in patients with haemangioblastoma. It is worth noting that this nodule was not seen in three of the cases and overlapping sections are necessary to avoid overlooking a single nodule or to detect the presence of multiple nodules. It is therefore probably still necessary to perform angiography to determine the exact number and the site of the haemangioblastoma nodules.

Ventricular dilatation was seen in a high proportion of the patients with a space-occupying lesion. Marked enlargement was less common in the metastases than in the primary brain tumours. Hydrocephalus was also seen in the great majority of patients with papilloedema; however, in a few of these cases the only sign of ventricular enlargement was temporal horn dilatation. Hydrocephalus was much less frequent in the patients with conditions which do not usually have a space-occupying effect. The notable exception was the infarct where there was moderate ventricular dilatation in one case and slight dilatation in six. Periventricular lucency was much commoner in patients with a space-occupying lesion and was particularly common in patients with metastases, in spite of the absence of severe hydrocephalus in this group (Table 7). The appearance is thought to represent transependymal absorption of CSF and, when present, is a reliable sign of obstruction to the CSF pathways. Hydrocephalus and temporal horn enlargement were seen in a smaller number of patients without papilloedema. At least some of these probably did have raised intracranial pressure without papilloedema. Unfortunately, it was not possible to correlate the C.A.T. appearances with the CSF pressure data.

Summary

In the analysis of cerebellar lesions certain patterns emerge. It is possible to distinguish between various types of pathology according to site, size and density and on behaviour after contrast injection. However, the overlap between the various categories is such as to make a definitive tissue diagnosis impossible in the tumour group. Infarcts are usually easy to recognise and haemorrhage, when fresh, should give no problem.

References

1. AMBROSE, J.: Computerised transverse axial scanning (tomography). Part 2. Clinical application. British Journal of Radiology 46, 1023-1047 (1973).
2. GAWLER, J., DU BOULAY, G.H., BULL, J.W.D., MARSHALL, J.: Computer assisted tomography (EMI scanner). Lancet 1974II, 419-423.
3. GREITZ, T.: Computer tomography for diagnosis of intracranial tumours compared with other neuroradiological procedures. Acta Radiol. Suppl. 346, 14-20 (1975).
4. GYLDENSTED, C., LESTER, J., THOMSEN, J.: Computer tomography in the diagnosis of cerebello-pontine angle tumours. Neuroradiology 11, 191-197 (1976).
5. NAIDICH, T.P., LIN, J.P., LEEDS, N.E., KRICHEFF, I.I., GEORGE, A.E., CHASE, N.E., PUDLOWSKE, R.M., PASSALAGWA, A.: Computer tomography in the diagnosis of extra-axial posterior fossa masses. Radiology 120, 333 (1976).
6. PAXTON, R., AMBROSE, J.: The EMI scanner, a brief review of the first 560 patients. British Journal of Radiology 47, 530-565 (1974).

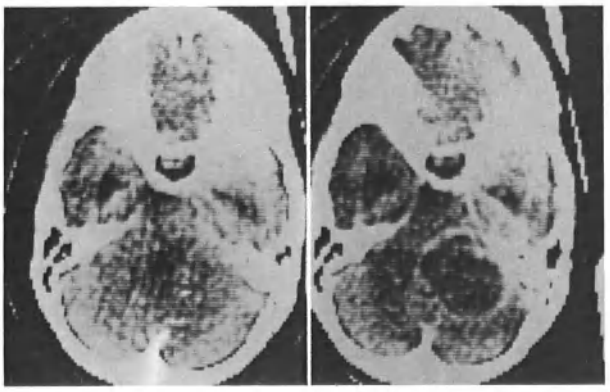

a b

Fig. 1a and b. Grade II astrocytoma: a) before contrast, b) after contrast

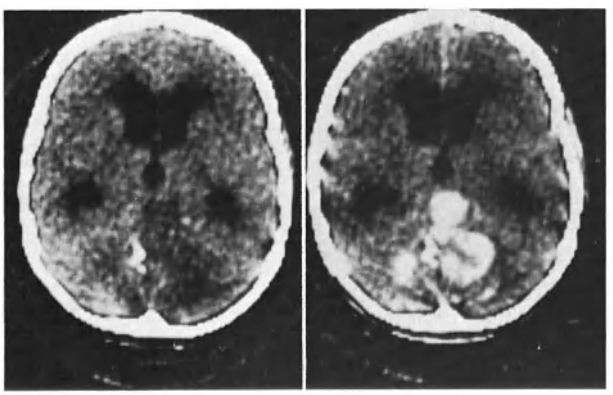

a b

Fig. 2a and b. Grade I astrocytoma: a) before contrast, b) after contrast

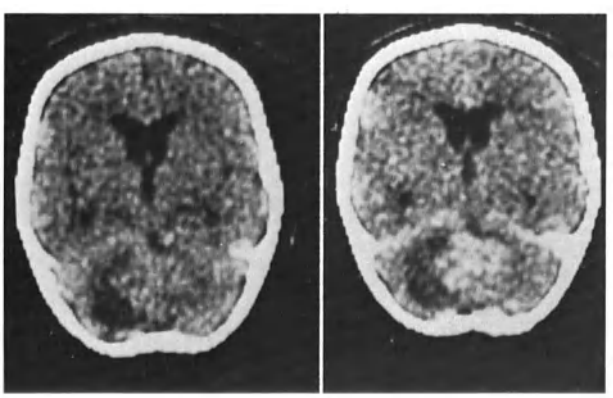

a b

Fig. 3a and b. Medulloblastoma: a) before contrast, b) after contrast

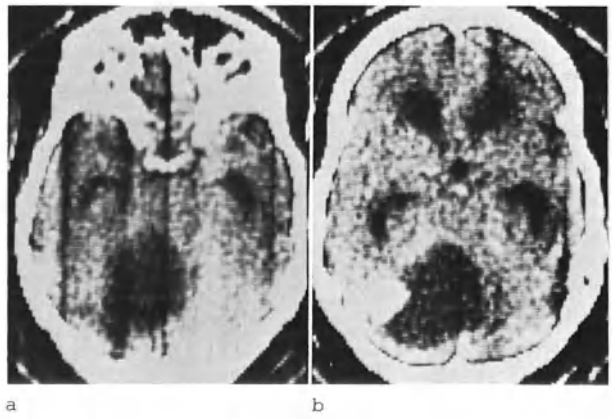

a b

Fig. 4a and b. Cystic haemangioblastoma: a) before contrast, b) after contrast

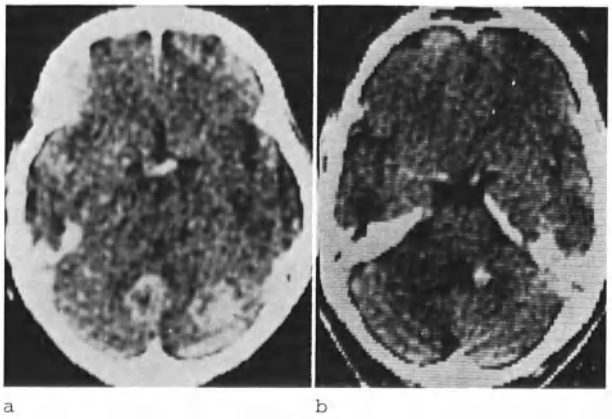

a b

Fig. 5. (a) Metastases from carcinoma of the breast - after contrast, (b) metastasis from bronchial carcinoma - after contrast

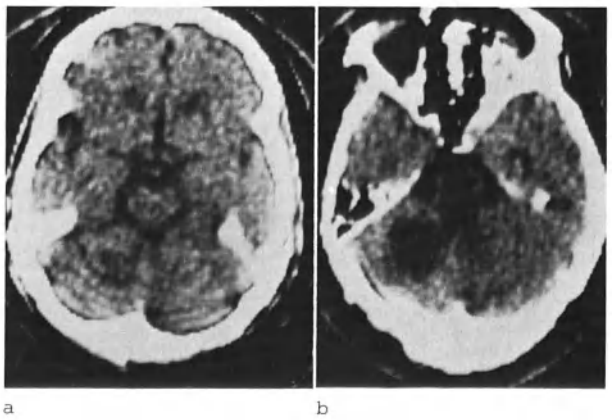

a b

Fig. 6. (a) L. cerebellar infarct and atrophy, (b) L. cerebellar infarct and brain-stem infarct

C.A.T. Scanning in Tumours of the Cerebellopontine Angle

T. T. King and J.A.E. Ambrose*

The most common tumour of the cerebellopontine angle is the acoustic neuroma. A great improvement in the diagnosis of this lesion has occurred in the last 15 years or so, owing to the work of House, who has demonstrated that the tumour can be detected when quite small. The technical advances which have brought this about are the elaboration of neuro-otological tests to distinguish between deafness of cochlear and of neural origin, improved tomographic techniques for the demonstration of enlargement of the internal auditory meatus, the use of tomography allied to air encephalography to show relatively small tumours in the cerebellopontine angle, and of positive contrast cisternography to show tumours confined to the internal auditory canal.

The effectiveness of these methods is shown by the fact that in the last 8 years the departments of otology and neurosurgery at the London Hospital have had experience with about 120 acoustic nerve tumours, about half of which would be regarded as small by previous standards. In the last 18 months we have carried out C.A.T. scans on 28 proven cases as an additional method of investigation, and this paper presents our experience with this tool, its advantages and its limitations. We have classified the tumours according to size into three groups, small tumours are confined to the internal auditory canal or just protrude through it into the cerebellopontine angle. Medium tumours extend into the intracranial cavity for up to 2.5 cm and clinically are accompanied only by eighth and sometimes seventh nerve abnormalities. Large tumours are 3 cm or more in diameter and usually, but not always, produce neurological abnormalities. All tumours with neurological findings on examination were in this group, but some tumours proven to be large radiologically and at operation had no neurological signs.

A large acoustic nerve tumour is easily recognised on the C.A.T. scan. Hydrocephalus, if present, is readily demonstrated, and the fourth ventricle is displaced towards the opposite side (Fig. 1), but it is difficult to recognise obliteration of the cerebellopontine angle cistern, owing to low-density artefacts in this region. The tumour may not be visible on the ordinary scan although it sometimes can be seen clearly (Fig. 6). Following the intravenous injection of 60 ml of meglumine iothalamate, the density and visibility of the tumour are enhanced (Fig. 2), though the extent to which this occurs varies a good deal (Fig. 3). For the purposes of this paper we have graded it roughly into two groups: slight and marked. Of 21 tumours detected, 5 enhanced poorly and 16 markedly (Table 1). The size of the tumour did not seem to be an important point in determining this.

The C.A.T. scan can give information about the anatomy and physical constitution of the tumour not available by any other method. The presence of a cyst within the tumour is easily recognised even without enhancement (Figs. 4 and 5) and this is a considerable help to the

*The Department of Neurosurgery, The London Hospital, London, E.1. and The Department of Radiology, Atkinson Morley's Hospital, London, S.W.20.

Table 1. Enhancement with conray

Poorly	Markedly
5	16

surgeon, as it suggests that the operation may be rendered easier. Knowledge of where the cyst lies within the tumour allows it to be emptied early in the procedure giving extra room when it is most needed. A finding which has emerged from C.A.T. scanning and which confirms an impression from operation, is that the anatomical disposition of the tumour may vary from case to case, that this is due to variation in the direction of growth of the tumour and that these variations in anatomical relationships may influence the difficulty of the operation, the postoperative course and the possibility of preserving the facial nerve in the case of large tumours. Figures 6 and 7 show a large tumour which enhances very well and which is seen to extend medially and forwards so that its inner border crosses the midline and comes very close to the median groove of the pons. The extent of distortion of the brain stem is easily seen, and one would expect that removal of such a mass would lead to considerable postoperative brain stem disorder, as indeed was the case. Figure 8 shows a tumour which has extended backwards more than it has medially, so that the principal indentation is in the cerebellum and middle cerebellar peduncle rather than the pons. The tumour also contains a cyst in its dorsal part. At operation the pons was less exposed at the end of the procedure than is usual, and the facial nerve was preserved with good function after the operation. Figure 9 shows a tumour of unusually elliptical cross-section having its long axis pointing medially and somewhat backwards.

An important point which needs to be known is the smallest size of tumour which can be detected. On general grounds one would expect that intracanalicular tumours would not be demonstrable. In this material, two small tumours were not seen and a third was reported as being visible, but review of the scan shows this to be a false positive. All the large tumours were demonstrated although not, as we have shown, with equal clarity. It is in the medium group which covers lesions from about 0.5 cm to about 2.5 cm in diameter in the cerebellopontine angle that the limit of resolution must lie. Our figures show that two-thirds of these were detected, usually quite easily (Fig. 10). Among the four that were missed, three were between 1 and 1.5 cm in diameter and a tumour of 2 cm was not seen, but retrospective studies suggested this was because the scans were made too high, for we have had a number of tumours of this size which were readily detected.

It looks as if somewhere between 1 and 1.5 cm is the limit of resolution and that the demonstrate tumours of 2 cm or so, care must be taken to get the cuts at the right level.

Summary

The C.A.T. scan has proved a valuable method of detecting acoustic nerve tumours of 2 cm or more in diameter, and obviates the need for air studies or other neuroradiological procedures in these cases. It has the advantage, too, of demonstrating the anatomical relationships of the tumour and brain stem, information not obtainable by any other method, and will inform the surgeon of the presence of a cyst within the tumour. We think that a negative C.A.T. scan in the presence of

Table 2. C.A.T. scans in 28 acoustic nerve tumours

Size of tumour	Number	Scans	
		Positive	Negative
Large	13	13	0
Medium	12	8	4
Small	3	0	3
Totals	28	21	7

a strong suspicion of a medium or small tumour is probably an indication for positive contrast cisternography rathern than an air study.

Acknowledgements. We are indebted to Mr. Andrew Morrison, under whose care the majority of these cases were admitted and to Dr. Ian Wylie for neuroradiology.

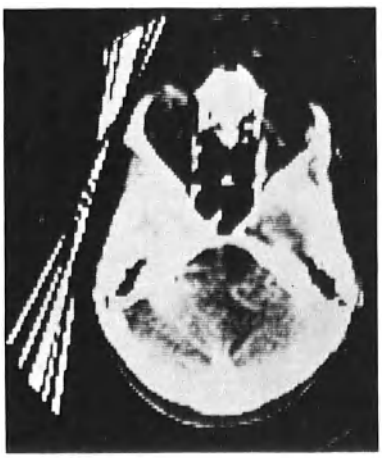

Fig. 3

Fig. 4

Fig. 1. Right sided tumour, invisible in unenhanced scan. Fourth ventricle displaced
Fig. 2. Same case as Fig. 1 with enhancement

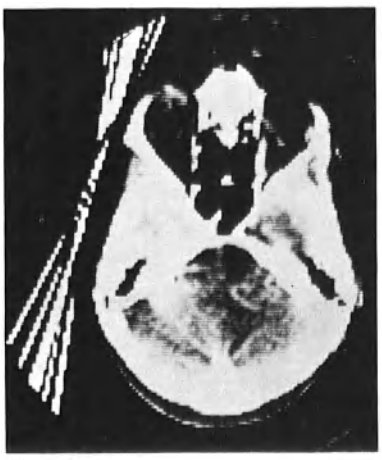

Fig. 3

Fig. 4

Fig. 3. Poorly enhanced right acoustic nerve tumour
Fig. 4. Cystic right tumour, unenhanced. Both low and high density areas are visible

Fig. 5

Fig. 6

Fig. 5. Same case as Fig. 4 with enhancement
Fig. 6. Large left tumour, visible without enhancement

Fig. 7

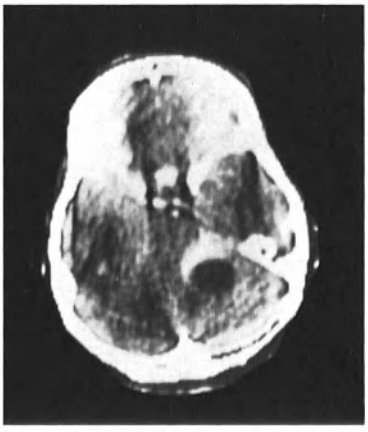

Fig. 8

Fig. 7. Same case as Fig. 6. Medial extension of tumour and distortion of brain stem is seen

Fig. 8. Cystic tumour, enhanced. It has grown mainly backwards, into cerebellum

Fig. 9

Fig. 10

Fig. 9. Poorly enhanced tumour, extending medially and backwards

Fig. 10. Tumour of 2 cm, enhanced

C.A.T. Studies of Tumours of the Skull Base and Face

J. M. Caillé, A. Dop, P. Constant, and J. L. Renaud-Salis*

Although C.A.T. has amply proved its effectiveness in exploration of the head, it is beginning to reveal its defects and inadequacies in other areas. With the skull base and the face, its performance is markedly inferior. Our study is concerned with the limitations of C.A.T. in these areas.

Material and Methods

All our patients were investigated using a Total Body Scanner (Acta Scanner) equipped in short scan with a 160 × 160 matrix. Each rotation provides two slices 7.5 mm thick and 3 mm apart. The theoretical spatial resolution is 1.5 mm and the densitometric resolution 0.5%. The density of water is 200 on a scale of 2048 levels.

We examined 32 patients who presented, or had presented, tumours of the skull base or the face. We excluded from the study intracranial extra-axial tumours near the base or invading the base: neurinomas, meningiomas, hypophyseal tumours, etc.

The C.A.T. problems posed by these tumours are essentially the same as those posed by intra-axial tumours. For the same reasons we excluded primarily intraorbital tumours, as embryology, anatomy, physiology and now C.A.T. all show that the fundus oculi is an organ indissociable from the brain itself.

Of these 32 patients, 11 were examined before and after injection with iodinated contrast medium; 4 were examined before and after radiotherapy; 4 were examined for the first time only after radiotherapy.

Results

The mean density of most of the tumours is compared to that of the lateral pterygoid muscles. The distribution of the densities of these tumours in relation to the density of the external pterygoid muscle is roughly symmetrical: 9 were more dense, 7 of the same density and 7 less dense (Fig. 1).

The density of the pterygoid muscle was taken as a reference level because the muscle is large, always visible no matter what window is used for reading the slices, usually situated near the tumoral process; it also provides an important reference point for evaluating tumoral extensions towards the pterygo-maxillary region.

---

*Service de Neuro-Radiologie: Centre Jean Abadie, Bordeaux(France).

After contrast injection (11 patients - Fig. 2) the distribution of densities changed:

Three tumours had a density above that of lateral pterygoid by, on average, 8 to 14 points.

Six tumours had the same density as that of the muscle.

Two tumours had a density lower by 4 to 6 points.

Thus most of the tumours (8 out of 11) had a density comparable to or only slightly below that of the lateral pterygoid.

Changes of Tumoral Density as Compared with Density of the Muscle after Contrast Injection

In four cases, initial density very much above that of the muscle diminished and became identical or very nearly identical to that of the muscle.

In one case, tumoral density compared to that of the muscle changed from +4 to -4 points. The contrast thus remained the same.

In one case, the density remained the same as that of the muscle both before and after injection.

In five cases, the density increased after injection:

in one case, it changed from -10 to -4, the new density being thus closer to that of the muscle after injection;

in one case, the increase was very slight (+ 2 points);

in three cases, the increase in contrast was significant, with final densities of +10, +14, +16.

Thus only four tumours became markedly more visible after contrast. They were: an angiosarcoma, an extracranial meningioma, a tumour of the cavum oris and a chordoma

Tumours and Radiotherapy (Fig. 3)

Four patients were examined before and after radiotherapy; four were examined only 6 months to 3 years after radiotherapy.

After radiotherapy only one of these tumours had a density equal to that of the lateral pterygoid muscle. The other 7 had a density very much below (-4 to -10 points).

The decrease in density for the 4 patients examined before and after radiotherapy was of 8 points on average. Contrast injection of these irradiated and apparently inactive tumours did not change their density.

Tumours of the Skull Base (12 Cases)

The majority of these cases were examined secondarily. C.A.T. was carried out in order to determine their extent as exactly as possible before treatment.

Tumours of the Sinuses (9 Cases) (Figs. 4, 5)

Out of eight cases of cancer of the maxillary sinus (six epidermoid carcinomas) in which tumoral and muscular density were compared, seven had a density equal to or below that of the muscle.

(Two cases - identical density and five cases - lower density).

After radiotherapy (four cases) the density was still 5 to 6 points below that of the muscle.

In the two cases the density which before radiotherapy had been the same as that of the muscle became, 2 and 6 months after therapy, lower by 6 to 8 points.

Tumours of the Cavum Oris (5 cases) (Fig. 6)

In these five cases, the existence of the primary tumour was not known before C.A.T. Three of them had already been irradiated for apparently primary cervical lymph node disease before C.A.T. Conventional X-rays were considered normal in all cases, and in 4 cases the pharyngoscopy was negative. C.A.T. allowed guided biopsy which thus confirmed the diagnosis.

The five patients were examined before and after contrast injection. In four cases the contrast of the tumour decreased or remained the same after injection of iodinated contrast agent: the difference of density remained the same or approached that of surrounding structures. In only one case did the injection allow diagnosis of a tumour: the density before injection was identical to that of the pterygoid muscle but after contrast injection was 10 points above it.

Discussion

The effectiveness of C.A.T. should be discussed under two headings: densitometric and morphological.

The achievements of this technique in the investigation of the brain can be explained by anatomical and physiological particularities. We are dealing with a symmetrical structure which if not homogeneous has at least very narrow variations of density. It is thus possible when reading slices of the brain to use small windows which show up density variations of 0.5 to 1% if the lesion is sufficiently large.

Moreover, most of the pathological processes investigated by C.A.T. are relatively easy to recognise by virtue of:

their effects on the fluid compartments (ventricular dilation or deformity);
the oedema which often accompanies them;
their own density.

There is a final factor which explains in large part the achievements of this technique. Very often there are changes in the blood-brain barrier: in a tumour of neural origin, on the periphery of a metastasis or an abscess, during the evolution of an infarct. These changes allow one, after injection of iodine, to opacify a tumour, an abscess, peri-metastatic oedema, etc. The tumoral vascular pool is only responsible

for a very small part of this opacification. It represents (as Gado) has well shown) only 6 to 7% of tumoral volume. This enhancement is easier to see since after contrast injection adjacent healthy parenchyma changes in density only very slightly (1 to 2%). The densitometric and optical contrasts thus become very clear. They are represented by 3 to 15 points difference on the density scale. The structures of the skull base and face are very heterogeneous and the densities vary considerably on the same slice (as between air-filled cavites, fat, muscular mass, bones). It is not possible, when studying all these structures together, to use narrow windows which show up small differences in density; however, when wide windows are used here, they smooth out the picture and mask small differences of density, thus decreasing the performance of the C.A.T.

Obviously, outside the head there is no blood-brain barrier and the only things to be taken into account in tumoral differentiation are the tumoral vascular pool and the possible diffusion of the iodine into the extra-cellular spaces - on condition that the density of the tumoral environment remains stable or changes in the reverse direction.

After contrast injection it is no longer possible, using C.A.T. alone, to recognise all tumoral processes (Fig. 7). The distribution of tumoral densities compared with that of the pterygoid muscles is roughly symmetrical. In nine cases the density is higher, in seven cases the same and in seven cases lower. In seven cases it is indissociable from its environment, in nine cases it is significantly more dense and in seven cases less so.

Out of 11 patients injected with contrast medium, in seven cases the density remained the same or approached that of the pterygoid muscles. After injection the muscular masses become more dense (+10 to +15 points) not so much because of the vascular pool of the muscle as because of the diffusion of iodine into the muscular mass through fenestrations in the capillaries (Pappenheimer). The tumoral vascular pool is in most cases incapable of producing a density increase equal or superior to that of the muscle. In three cases the density increase was clearly above that of the muscle. In one case there was an angioblastic sarcoma and although the vascular pool was considerable, there was certainly also some extravascular diffusion. One case was of extracranial meningioma. The ease with which contrast medium diffuses in healthy meninges and in meningiomas is well known: this diffusion explains the opacification. The last was a tumour of the cavum oris. We were not able to advance any explanation here. Thus, apart from certain cases in which the vascular pool and extravascular diffusion were particularly marked, injection of iodine masked rather than accentuated the tumoral mass.

Tumours Already Treated by Radiotherapy (Fig. 8)

Eight patients were examined after radiotherapy; four of them both before and after.

These densities were distributed in a very peculiar fashion since seven of them were 4 to 10 points below that of the pterygoid muscles and one had the same density. In the four cases examined both before and after radiotherapy, the density decrease was of 8 points on average. This decrease was explained by postradiological histology since the tissue had become fibrous and almost totally avascular. It should be noted that for the three patients who were injected, tumoral density did not vary after injection. Our series is of course too small to permit one to draw definitive conclusions but this would seem to be a possible

method for checking the evolution of an irradiated tumour. Any increase in density must give rise to fears of a resumption of tumoral activity.

Although C.A.T. with iodinated contrast medium seems to be less effective at the skull base than in the brain, morphological studies on the other hand would seem to be of considerable use. Conventional tomography demonstrates the bone structures very well but it does not show up endo- and extracranial prolongations, especially those in the pterygo-maxillary fossa. Also, the determination of target volume in radiotherapy makes the use of transverse axial slices desirable. For these reasons C.A.T. has seemed to us of the greatest usefulness in studying osseous tumours of the skull-base. If windows of width 150 to 200 units are used, the outline of the bone structures appears quite clearly, and two slices suffice to determine the tumoral volume. It is then easy to reproduce the picture in its real dimensions and to plot the iosodose curves. For the same reasons C.A.T. examination of tumours of the maxillary antrum is now performed as a matter of course. Destruction of the posterior wall, possible infiltration of the pterygo-maxillary fossa and extension upwards towards the skull base are easily studied on three slices (Figs. 5 and 6). In some cases we also used semi-axial slices which defined tumoral volume even more exactly.

The superiority of C.A.T. seem to us incontestable in the diagnosis of tumours of the cavum oris. Five patients presented, at examination, apparently primary cervical adenopathies and in four cases conventional radiology and pharyngoscopy were considered normal. C.A.T. showed deformity of the cavum oris and, in four cases, tumoral hyperdensity. Biopsy guided by C.A.T. allowed precise histological diagnosis to be made (Fig. 7).

Conclusions

C.A.T. is much less effective for tumours of the skull base than for intra- or extra-axial intra-cranial tumours both because wide windows are necessary to read the slice and because we do not possess a densitometric contrast product. In the brain, iodine highlights any breakdown of the blood-brain barrier, diffusing sufficiently into the extracellular spaces to opacify most tumours. This marker, non-selective but very useful where the brain is concerned, becomes more of a hindrance than a help when dealing with the face, because of the considerable intramuscular diffusion. However, from a morphological point of view the contribution of C.A.T. seemed to us substantial in that it allowed precise definition of tumoral volume and thus better adaptation of radiotherapy.

It would seem to be quite effective in the diagnosis of tumours of the cavum oris and in examination of apparently primary malignant cervical adenopathies.

Technological progress and the development of selective markers will doubtless allow the use of C.A.T. not only for its morphological contributions but also for its incontestably useful densitometric applications.

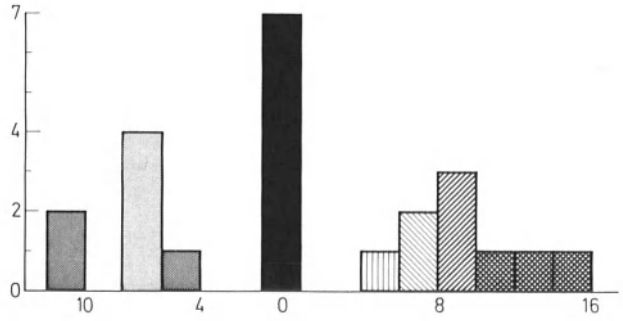

Fig. 1. Density of 23 soft-tissue tumours relative to lateral pterygoid muscle. Horizontal axis: density: greater than lateral pterygoid (*to right*) in ACTA number; lesser (*to left*); vertical axis: number of cases

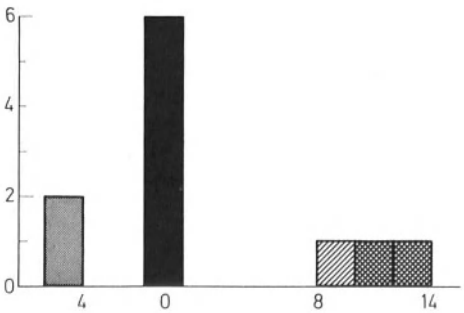

Fig. 2

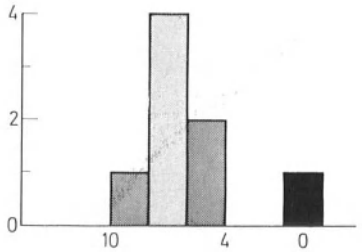

Fig. 3

Fig. 2. Density of 11 tumours relative to lateral pterygoid muscle after intravenous contrast medium injection (see Fig. 1 for explanation)

Fig. 3. Density of 8 tumours examined after radiotherapy, relative to lateral pterygoid muscle (see Fig. 1)

Fig. 4. Epidermoid carcinoma of the left maxillary sinus

Fig. 5. Enormous carcinoma of right maxillary sinus (3 slices give exact tumoral extension)

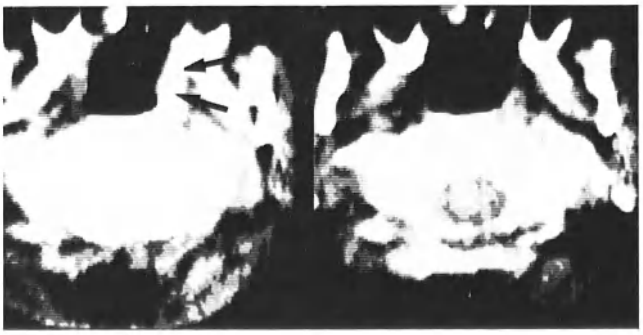

Fig. 6. Nasopharyngeal tumour: on the left, deformation and increased density of right lateral wall (arrows)

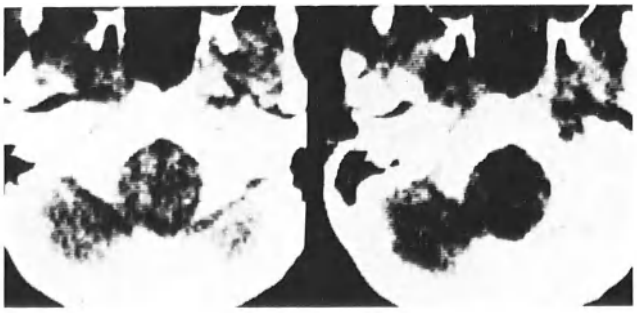

Fig. 7. Nasopharyngeal tumour before and after contrast medium injection: on the left, before injection: increased density easily visible; on the right, after injection, increased density no longer visible

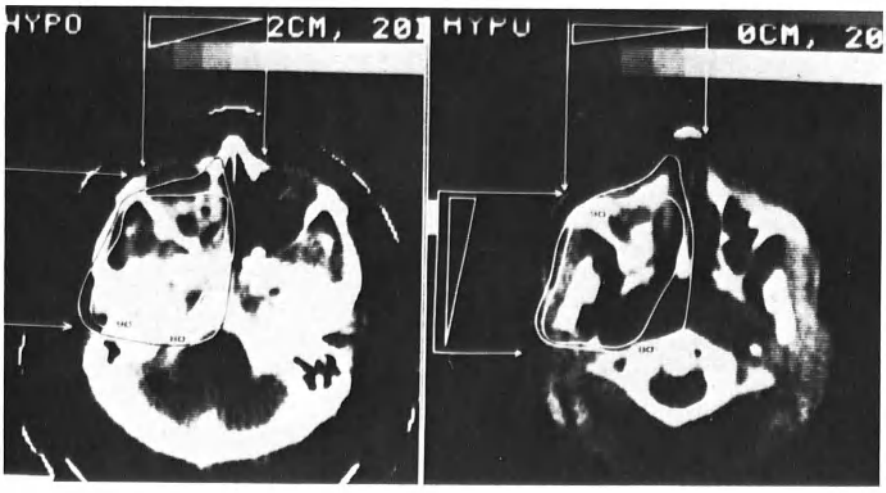

Fig. 8. After the determination of tumour volume isodose curves are plotted. Example of radiotherapy simulation in a case of left maxillary sinus carcinoma

Tumours and Other Lesions of the Visual Pathways

The Comparative Values of Various Neuroradiological Investigations in the Diagnosis of Intracranial Optic Pathway Lesions

P. Michotey*, I. F. Moseley**, G. Lecaque*, and P. Palmieri*

The purpose of this study is to establish the relative roles of the available neuroradiological procedures in the diagnosis of lesions of the intracranial optic pathways since the development of C.A.T.

Morphology and vascular anatomy together represent the basic radiological data required for definition of any lesion. In this paper, we shall assess the usefulness of C.A.T. and other neuroradiological methods in the various sites, rather than attempting to describe the large range of pathological appearances which may be encountered. From a clinical viewpoint, most of the patients examined for this study presented predominantly ophthalmological symptoms and signs, particularly field defects.

Four sections follow, corresponding to the various portions of the optic pathways, each necessitating a different detailed radiological approach: the optic chiasm, the optic tracts and lateral geniculate bodies, the optic radiations and the occipital cortex.

Intracranial Optic Nerves and Chiasm

A brief anatomical description will aid the understanding of lesions situated in the suprasellar region.

The chiasm is a quadrilateral plate of white matter, extending vertically upwards and backwards. It is formed by the conjunction of the two optic nerves, which constitute its anterior corners; the posterior corners are formed by the initial portions of the optic tracts. Lying in front of the third ventricle, the chiasm forms its anteroinferior wall. Differences in the position and length of the optic nerves and chiasm are numerous, and explain the variable effects of pituitary adenomas on the chiasm, giving rise to field defects, which are more pronounced when the optic nerves are short, or the chiasm is in a low position.

The chiasm is supplied by numerous small arteries: it lies between the terminal portions of the internal carotid arteries, and its lateral surfaces are supplied by small vessels arising from them. The two anterior cerebral arteries pass medially anterior to the optic nerves, and, together with the anterior communicating artery, vascularise the anterior segment of the chiasm. Finally, the posterior and inferior surfaces of the chiasm are supplied by small vessels arising from the posterior communicating artery.

---

*Radiologie Vasculaire et Neuroradiologie, Hôpital de la Timone Marseille.
**Lysholm Radiological Department, National Hospital for Nervous Diseases, London

This complex configuration, and the possible anastomoses uniting all these tiny arteries make it impossible to demonstrate the vascular supply of the chiasm on currently available angiograms.

Clinically, of course, each case is different; an ophthalmological examination on a patient with a chiasmatic lesion may show diminished visual acuity, often unilateral at first, with subsequent optic atrophy, and a visual field defect such as a bitemporal or unitemporal hemianopia; less frequently, scotomas or altitudinal defects may be observed.

Traditionally, the best neuroradiological examination for study of a suprasellar lesion has always been pneumoencephalography, frontal and lateral tomograms showing the chiasm lying in the subarachnoid space, surrounded by air. C.A.T. as currently available cannot reliably display the structures in the interpeduncular and suprasellar areas. Thinner frontal or sagittal C.A.T. sections, together with the injection of water-soluble contrast media into the CSF will improve the results in this region. Postioning of the head is important: it must be extended to an angle of 10 to 15° relative to the orbitomeatal plane, so that the C.A.T. sections pass through the plane of the intracranial optic structures; this is the same angulation used for the study of the orbits.

The radiological investigation of a suprasellar lesion must include plain radiographs, which may show bone destruction or sclerosis at the base of the skull, or the presence of calcification; pneumoencephalography is the best way to outline the lesion in the basal cisterns, and to show its relationship to the chiasm itself and the anterior end of the third ventricle, but often gives little clue as to the nature of the lesion. Selective internal and external carotid angiography may show either the deformity of the circle of Willis or the presence of tumoral or other pathological vessels, e.g. in an ateriovenous malformation or aneurysm. Angiography can, indeed, indicate the exact nature of the lesion in a number of cases; such techniques as that of the balloon catheter, allowing selective injection of, e.g., the ophthalmic artery, improve its diagnostic possibilities.

The contribution of C.A.T. is to demonstrate the space-occupying lesion in relation to the brain itself, to show its position, shape, size, its effects on the ventricles and the brain parenchyma, and finally, to suggest the exact nature of the lesion in many cases.

However, it should be pointed out that some lesions which are isodense with normal brain and which do not appear to be hypervascular after intravenous contrast medium injection can pass unobserved at C.A.T., while unequivocal abnormalities are found on both pneumoencephalography and arteriography (Fig. 1). Similarly, the exact nature of the lesion should be diagnosed with caution, taking into account the entire clinical picture, since there are a number of lesions having only slightly different C.A.T. appearances.

C.A.T. is of considerable value for identifying, e.g., the microcalcification present in a craniopharyngioma and invisible on plain radiographs, the hypervascularity of an optic chiasm glioma (Fig. 2), or the presence of a cyst within a tumour such as a pituitary adenoma.

These different procedures are, of course, not in competition with one another; each provides certain complementary information, but each also has its limitations, which should be recognised.

Optic Tracts and Lateral Geniculate Bodies

The optic tract stretches from the posterior angle of the chiasm to the lateral geniculate body, as a cord running around the cerebral peduncle and passing backwards in the choroid fissure. It is surrounded by cavities and cisterns: the anteroinferior part of the third ventricle, the optic and peduncular and crural cisterns. It is accompanied by two satellite vessels: the anterior choroidal artery and the basal vein of Rosenthal.

The lateral geniculate body is a small mass lying on the inferolateral surface of the pulvinar, with which it is continuous.

The blood supply of the initial section of the optic tract comes from numerous small branches of the internal carotid artery, the posterior communicating artery, the middle cerebral artery and the anterior choroidal artery. The posterior two-thirds of the optic tract and the lateral geniculate body are supplied by the anterior and posterolateral choroidal arteries and also by the thalamoperforating vessels.

On C.A.T. it is usually impossible positively to identify the optic tract or lateral geniculate body; however, the situation of these structures in relation to readily identifiable elements such as the third ventricle, cerebral peduncles and atrium of the lateral ventricle enables them to be localised with some precision. Clinically, it is most unusual to see an isolated lesion of the optic tract or lateral geniculate body, but adjacent lesions affect the optic pathways by compression or direct invasion.

The characteristic field defect is a homonymous lateral hemianopia, which is found with all optic retrochiasmatic lesions; it is thus difficult with large space-occupying lesions to distinguish between affection of the optic tracts and optic radiations.

The conventional neuroradiological work-up should take into account all available techniques, since with these deep cerebral lesions accurate diagnosis may be difficult. C.A.T. is of major use in the localisation of a lesion, and in further showing its morphology and density. It should therefore be the initial examination, other procedures being undertaken as indicated by the C.A.T. findings (Fig. 3). However, there are a number of cases in which, even with a complete neuroradiological investigation, a precise diagnosis of only the localisation is possible; the nature of the lesion must be established at surgery.

Thus, the lesions found in this area are radiologically complex; C.A.T. should be the initial investigation.

Optic Radiations

The optic radiations consist of a plate of white matter extending from the lateral geniculate body to the occipital cortex, beginning as a thick sheaf and widening progressively, passing around the atrium of the lateral ventricle in relation to the temporal horn, passing posteriorly on the lateral surface of the ventricle, and then going on to form an internal concavity, dividing towards the occipital pole into three tracts: a superior, to the superior lip of the calcarine fissure, an inferior to the inferior lip, and a posterior going on towards the occipital pole.

The vascularisation of the optic radiations as far as the paraventricular segment is by means of the perforating branches of the anterior and posterior choroidal arteries and lenticulostriate arteries; further back, the supply comes from deep branches of the middle cerebral artery and the posterior cerebral artery; they are respectively for the lateral, medial and inferior fibre tracts.

This anatomical arrangement explains why a space-occupying lesion must be of a certain size in order to be clearly seen on carotid or vertebral angiography, since the deep branches are invisible radiologically and the cortical arteries lie at a relatively large distance from the optic radiations. However, the ventricular cavities can rapidly be deformed by small lesions due to their proximity.

Technically, the C.A.T. cut passing through the optic radiation plane resembles that passing through the optic tracts; in fact, all the intracranial optic pathways from the chiasm to the calcarine fissure are found on the same plane, which can be explored by two adjacent cuts, depending upon the correct position of the head, which is extended to approximately 15^{o}.

These various technical and anatomical factors explain why C.A.T. is incontestably the best form for the neuroradiological examination of expanding lesions located at the level of the optic radiations. Their location, size, ventricular and parenchymal effects and densitometric aspects are evident. The indications for pneumoencephalography have completely disappeared whereas before, this examination was the best as a topographical landmark (Fig. 4).

Small lesions can go unobserved using traditional types of examination; in this case C.A.T. is the only procedure which assures a proper diagnosis. Again, however, one must be extremely careful in diagnosing the nature of the lesion.

Cerebral angiography still has an important role in the preparation for neurosurgery, since one can clearly see cerebral convolutions by cortical arteries; this preoperative system of localisation enables the choice of the best approach and the localisation of vessels which must be avoided. Angiography is, of course, also required when a vascular lesion is suspected (Fig. 5).

Precise definition of the vascular pedicles of an angioma must clearly be obtained, and it may be important to confirm that a hypodense C.A.T. image corresponds to a vascular accident and not a tumour.

Occipital Cortex

The occipital lobe is the smallest lobe of the cerebrum. It has a lateral surface, an inferior surface, and a medial surface which is excavated by the deep calcarine fissure separating the fusiform gyrus above from the lingual gyrus below. The calcarine fissure indents the internal side of the occipital horn of the lateral ventricle; just above this, another indentation represents the forceps major of the corpus callosum.

The principal visual cortex, the striate cortex, occupies both lips and the bottom of the calcarine fissure and overlaps to the lateral surface of the occipital lobe.

The vascularisation of the occipital lobe is given by the middle cerebral artery on the lateral surface, and the posterior cerebral artery on the inferior and medial surfaces. Here, the cortical branches of the posterior cerebral artery serve as a better landmark of the cortical structures (as with the calcarine fissure) than the C.A.T., the localising value of which is more limited.

From a pathological point of view it is unusual for a lesion to be strictly limited to the occipital cortex and in most cases an extension to the underlying white matter is evident. C.A.T. permits one to visualize, for example the existence of two abscesses, while angiography only shows the diagnosis of a single expanding lesion (Fig. 6). However, as with all other cerebral areas, angiography is an indispensable complement each time one suspects a vascular lesion.

Summary

With the given facts of neuroradiological anatomy, the combination of information from conventional neuroradiological examinations, and that from C.A.T. is of great interest.

To varying extents, each segment of the optic pathways, i.e., the optic nerve, the chiasm, the optic tracts, the lateral geniculate bodies, optic radiations and occipital cortex, can be either indirectly or sometimes directly seen. According to the level of the lesion of the optic pathway, each cannot be studied with the same precision and with the same technique: for example, small lesions of the optic nerve or the chiasm are diagnosed with far more finesse by the use of pneumoencephalography due to their extra-cerebral location; conversely, C.A.T. permits lesions situated in the deep white matter to be seen with more success than any other method.

One must not look upon different neuroradiological techniques as competitive, since they are in essence complementary factors in working towards a diagnosis which can often prove to be difficult.

References

1. AMBROSE, J.: Computerised transverse axial scanning (tomography): Part II. Clinical application. British J. of Radiology 46, 1023-1047 (1973).
2. BAKER, H.L., KEARNS, T.P., CAMPBELL, J.K., HENDERSON, J.W.: Computerized transaxial tomography in neuro-ophthalmology. Amer. J. of Ophthalmology 285-294 (1974).
3. HOUNSFIELD, G.N.: Computerised transverse axial scanning (tomography): PartI. Description of system. British J. of Radiology 46, 1016-1022 (1973).
4. PERRY, B.J., BRIDGES, C.: Computerised transverse axial scanning (tomography): Part III. Radiation dose considerations. British J. of Radiology 46, 1048-1051 (1973).
5. SANDERS, M.D., GAWLER, J.: Computerised tomographic scanning (EMI Scan) in neuro-ophthalmology. Transactions of the Ophthalmologic Society of the United Kingdom 95, 237-245 (1975).

Fig. 1a

Fig. 1b

Fig. 1a and b. Pituitary adenoma difficult to diagnose on C.A.T. (a) and quite evident on anteroposterior tomogram at pneumoencephalography (b)

Fig. 2

Fig. 3a

Fig. 3b

Fig. 2. Glioma of chiasm, clearly seen in interpeduncular fossa

Fig. 3a and b. Angiography was secondarily performed to confirm the vascular lesion observed on C.A.T. A very large aneurysm of the posterior cerebral artery was demonstrated

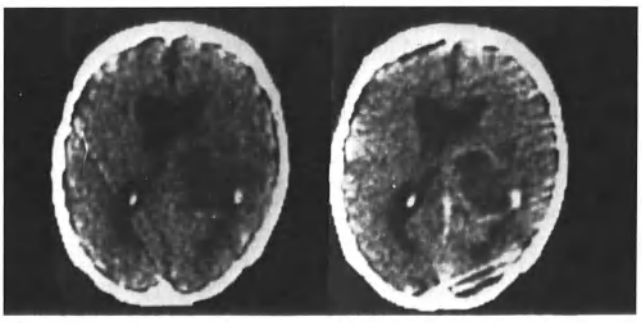

Fig. 4a

Fig. 4b

Fig. 5

Fig. 4a and b. Malignant tumour in the region of the optic radiation, showing peripherally increased density after contrast medium injection (b)

Fig. 5. Angioma vascularised by the branches of the middle cerebral artery and located at the level of the optic radiations

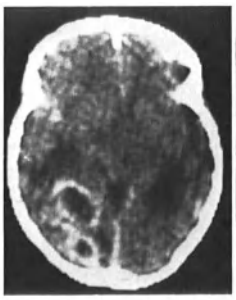

Fig. 6a

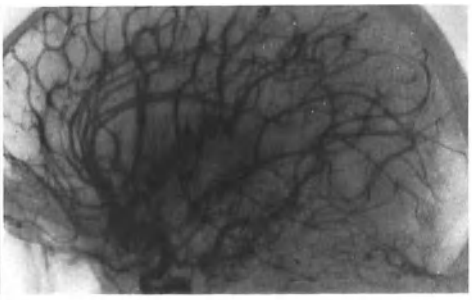

Fig. 6b

Fig. 6a and b. Two occipital cerebral abscesses well demonstrated by C.A.T. cuts (a), while the angiography is less precise (b)

An Evaluation of C.A.T. in the Diagnosis of Orbital Space-Occupying Lesions

G. A. S. Lloyd* and J. A. E. Ambrose**

The introduction of computerised tomography into clinical practice by AMBROSE and HOUNSFIELD in 1972 opened a new era in the diagnosis of soft-tissue tumours in the orbit. In a preliminary communication (1) the findings in the first 17 histologically proven primary tumours and granulomas examined by this technique were recorded. Progressive refinements in the apparatus (vide infra) and a 4-5-fold increase in the number of verified cases now allows a more mature assessment of C.A.T. scanning and its place in relation to other methods of orbital investigation.

Technique

The original EMI scanner employed an 80 × 80 matrix with a pixel size of 3 × 3 mm and a collimated slice thickness of 13 mm. In January 1974 a 160 × 160 matrix was introduced, reducing the pixel size to 1.5 × 1.5 mm. The majority of the patients in this series were examined by this version of the apparatus. More recently further refinements of the apparatus have incorporated:

1. Improved sensitivity and spatial resolution.

2. A 320 × 320 cell matrix reducing the pixel size to 0.75 × 0.75 mm using a collimated slice thickness of 8.5 mm.

3. Longitudinal and coronal plane reconstructions.(These are feasible but are at present limited because of high lens and corneal radiation dose).

Case Material

Over 120 patients with a clinically suspected orbital abnormality have been examined by C.A.T. scanning. Of these, 75 have been shown to have a primary orbital tumour, vascular anomaly or inflammatory process (Table 1). These were verified either by biopsy, surgical excision or, in the case of vascular anomalies, by angiography. Lesions with secondary extension to the orbit from adjacent structures in the middle fossa of the skull or paranasal sinuses were not included in the series, since these are for the most part readily diagnosed by established techniques. Although C.A.T. scanning has an important role to play in the diagnosis of secondary orbital disease, an assessment of this tech-

* Moorfields Eye Hospital, London.
** Atkinson Morley's Hospital, London.

Table 1. Diagnosis in 75 proven space-occupying lesions in the orbit

Pseudotumour (granuloma)	14
Meningioma	14
Lacrimal gland tumour	12
Haemangioma	9
Lymphoma	8
Venous malformation	2
Haemangiopericytoma	2
Malignant melanoma	2
Cystic hygroma of optic nerve	2
Blood cyst	2
Neurilemmoma	2
Metastasis	2
Optic nerve glioma	2
Arterio-venous malformation	1
Dermoid	1
Total	75

nique as far as the orbit is concerned must be based primarily upon its ability to show pathology originating in the orbital soft tissues.

The patients in the series were also examined by three other methods used in orbital investigation: orbital venography, ultrasonography and axial hypocycloidal tomography (2), enabling a direct comparison to be made between these techniques and C.A.T. scanning (Table 2). In

Table 2. Diagnostic accuracy in 75 proven primary orbital space-occupying lesions

C.A.T. scanning (Emiscan)	91%
Orbital venography	91%
Ultrasonography	86%
Axial hypocycloidal tomography	73%

The diagnostic accuracy was assessed as a simple positive/negative response.

only five instances was it found to be necessary to perform carotid angiography in the management of these patients prior to surgery, although some had had arteriography performed at other centres before referral to Moorfields.

Discussion

The overall diagnostic accuracy of C.A.T. scanning in this series in terms of a positive/negative response (is a lesion present or not?) was recorded as 91% (see Table 1). This compared with venography (91%), ultrasonography (86%) and axial hypocycloidal tomography (73%). One false positive Emiscan was recorded and five false negatives. The solitary false positive was encountered when the 80 × 80 matrix was in use, and it seems unlikely that this error would have been made had the fine matrix then been available. Of the five false negative scans, there were two with optic nerve abnormalities; two with masses in the orbital roof; and one patient with an orbital varix, proved at venography. This patient presented with intermittent proptosis, and despite the use of jugular compression to raise the venous pressure and produce

maximum filling of the varix during the examination, no abnormality was recorded on the scan. There was a single patient who was unable to tolerate the examination. With the introduction of the high-definition scans provided by the 320 × 320 matrix it seems unlikely that in future any significant optic nerve enlargements will be missed with the resolution now obtainable. Similarly, lesions missed above the rectus muscle cone in the orbital roof should be adequately demonstrated by the introduction of three-plane imaging.

Despite these errors, C.A.T. scanning has proved the optimum method of demonstrating a space-occupying lesion in the orbit, and its is expected that with further refinements of design, particularly three-plane imaging, the diagnostic performance in this respect should be improved. In the orbit, however, it is not enough to leave the diagnosis at the stage of a simple positive or negative indication for an orbital mass. Some idea of the likely histology is needed prior to treatment, which differs widely with the type of lesion present. For example, in a venous malformation, accounting in our practice for over 20% of intraconal space-occupying lesions in the orbit, deep surgical intervention is usually contraindicated (4). Cosmetic surgery to eliminate unsightly superficial varices is generally all that is required. On the other hand, benign encapsulated tumours in the orbit require surgical excision, while lymphomata and secondary malignancy should be treated by radiotherapy, and granulomas (pseudotumours) by steroid therapy.

There are three ways in which C.A.T. scanning might further the diagnosis and indicate the likely aetiology of a space-occupying lesion in the orbit:

1. By identifying the site of origin of the mass, for example the optic nerve or lacrimal gland

2. By its shape and density

3. By consideration of the absorption values before and after contrast medium injection.

The optic nerve tumours, both gliomata and meningiomata were clearly identified as arising from the optic nerve with scans made on the 160 × 160 matrix or 320 × 320 matrix scanner, and could be differentiated from other encapsulated tumours in the muscle cone such as haemangiomata. The latter tumours are also readily diagnosed on their typical morphology as depicted on the C.A.T. scan. They give a clear-cut image usually rounded, with well defined edges and even density values (Fig. 1). Another tumour arising within the muscle cone which may give similar appearances is a neurilemmoma. In our experience these are usually larger than the haemangiomata, and the size of the mass present may suggest the diagnosis. However, this differentiation is of little practical significance since the treatment is the same for both tumours, namely, excision by lateral orbitotomy.

The benign encapsulated tumours referred to above could be clearly differentiated by their clear-cut margins from infiltrative lesions in the muscle cone, such as granulomata, lymphomata or secondary tumours (Fig. 2). These latter space-occupying lesions typically showed an ill-defined mass of irregular outline and uneven density. The commonest lesion to present these features is the pseudotumour or granuloma in the orbit. Sometimes these masses may involve the lacrimal gland, extending both intraconally and extraconally, and the inflammatory process may involve a rectus muscle, causing local enlargement. This is, however, a non-specific sign. It was recorded 13 times in the series, and

in addition to its association with pseudotumour, was also observed in dysthyroid exophthalmos, and in two examples of lacrimal gland tumours in which the mass had extended into the lateral rectus muscle; it also occurred in one patient with an orbital varix in the muscle cone.

It was not found possible to differentiate the lymphomata occurring in the orbit from pseudotumours by the morphology of the lesion as depicted on C.A.T. Differentiation of inflammatory processes from true tumours in the orbit is particularly difficult when they occur in the orbital apex where all mass lesions have a very similar appearance on C.A.T. scans. However, a clue to the differentiation of granulomata from tumours in the orbit may sometimes be furnished by consideration of the absorption values. Figure 3 showes a series of histograms in which the absorption values of seven lymphomata, seven meningiomata and six cavernous haemangiomata have been summated. These comprise the total absorption values for the lymphomatous tissue, meningiomatous tissue and haemangiomatous tissue recorded in the series; the absorption values are recorded before intravenous contrast and after contrast. It can be appreciated that none of these values are in the negative range of the EMI scale; but if the summated absorption values of 10 pseudotumours from the series are considered (Fig. 4), it can be seen that some of these are in the negative range. It seems probable that this indicates that the inflammatory process is simply infiltrating the fat cells in the muscle cone (which give negative absorption values) and that the fat cells are being incorporated in the picture elements of the C.A.T. scan. The incorporation of normal fat cells from the muscle cone in pathological tissue can be shown histologically. Figure 5 shows a lymphomatous pseudotumour in which normal fat from the muscle cone is clearly incorporated in a mass of lymphocytes.

It can also be appreciated that in Figure 3 there is simply no difference between the distribution of absorption values in the three types of tumour recorded - the mean values before and after contrast are almost identical. The conclusion from this series is, therefore, that it seems unlikely that tissue recognition can be obtained from consideration of the absorption values as recorded on the numerical printout from the computer, other than indicating that the lesion is likely to be of an infiltrative nature.

It remains to discuss the role of the three other techniques used for the routine investigation of patients in this series. The most important of these is venography. There are two main reasons for performing this investigation routinely in patients with suspected orbital disease; firstly to demonstrate venous malformations which are by their nature best shown by this technique, and are important since in our experience they represent over 20% of all intraconal space-occupying lesions; secondly the investigation is important in the diagnosis of inflammatory processes in the orbit. A high proportion of venous obstruction in the rectus muscle cone are due to an inflammatory process (3) and in the absence of plain X-ray or clinical evidence of secondary neoplasia in the orbit, an intraconal obstruction without major venous displacement is strong evidence of an inflammatory process. Less essential as far as orbital soft-tissue diagnosis is concerned is conventional axial hypocycloidal tomography of the orbit; but the technique is very simple to perform, and is useful to exclude an expanding process arising in the sinuses such as an ethmoid mucocoele and also to show the integrity of the bony walls of the orbit prior to surgery.

The last method of soft tissue imaging, ultrasound, has the merit of being without radiation hazard, but generally the shape and location of masses in the orbit is not so obviously demonstrated as by C.A.T. scan. B-mode ultrasound is an easy examination to perform and carries

the diagnosis about as far as Emiscan, in that it is usually possible to differentiate between an infiltrative process in the orbit and an encapsulated tumour. In this series cross-sectional imaging of the optic nerve by C scan and ultrasonic holography provided information on some patients not given by C.A.T.

Conclusion

This study of 75 verified mass lesions in the orbit has shown that

1. C.A.T. scanning is the optimum method of demonstrating if there is or is not a mass in the orbit.

2. It can identify optic nerve tumours in nearly all patients, but other techniques, particularly unltrasonography, are sometimes needed for complete diagnosis.

3. It can identify benign neoplasms in the rectus muscle cone accurately, for example haemangioma or neurilemmoma; and in most patients it is possible to differentiate between these encapsulated tumours and an infiltrative process such as a pseudotumour, lymphoma or metastasis. From the present evidence, however, it seems unlikely that C.A.T. scanning will provide tissue identification beyond this simple differentiation.

4. Venography is still a necessary procedure in the investigation of orbital disease to identify venous malformations and also inflammatory conditions in the orbit.

References

1. AMBROSE, J.A.E., LLOYD, G.A.S., WRIGHT, J.E.: A preliminary evaluation of fine matrix computerized axial tomography (Emiscan) in the diagnosis of orbital space-occupying lesions. British Journal of Radiology 47, 747 (1974).
2. LLOYD, G.A.S.: Axial hypocycloidal tomography of the orbits. British Journal of Radiology 48, 460 (1975).
3. LLOYD, G.A.S.: Radiology of the Orbit. Philadelphia: W.B. Saunders 1975, p. 68.
4. WRIGHT, J.E.: Orbital vascular anomalies. Transactions of the American Academy of Ophthalmology and Otolaryngology 78, 606 (1974).

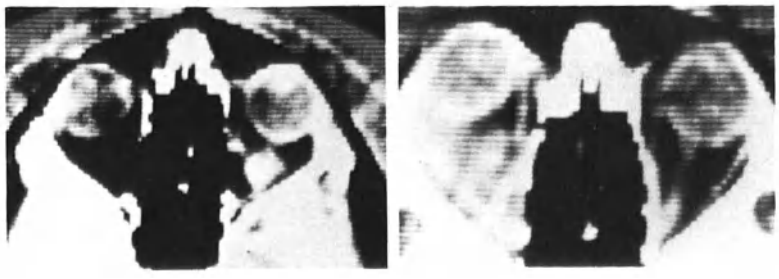

Fig. 1. Small, clearly defined mass in muscle cone (*right*), due to a cavernous haemangioma

Fig. 2. Diffuse mass in left orbit with ill-defined margins and uneven density due to a granuloma (pseudotumour)

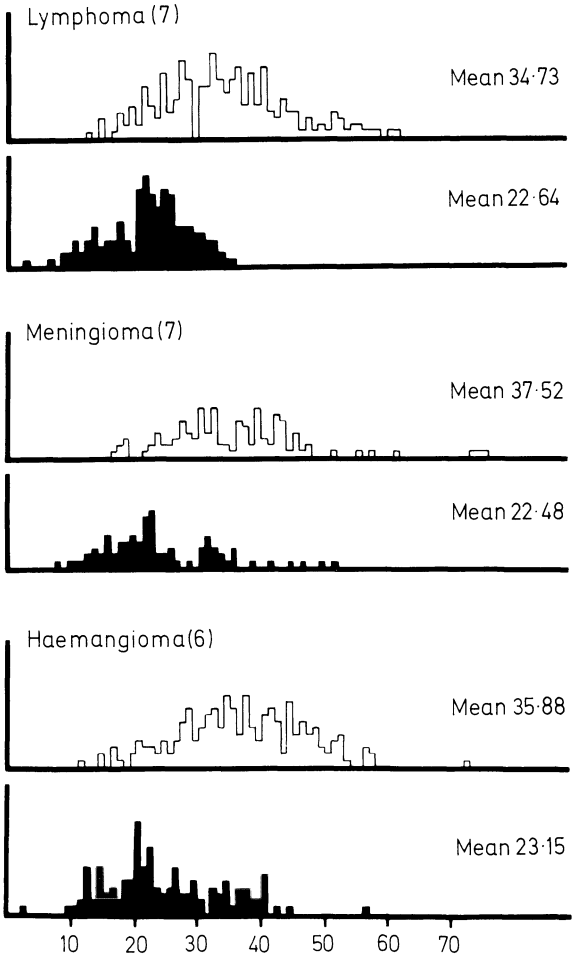

Fig. 3. Histograms of summated absorption values from seven lymphomata, seven meningiomata and six haemangiomata in the orbit
Black = pre contrast obsorption values; white = post contrast absorption values

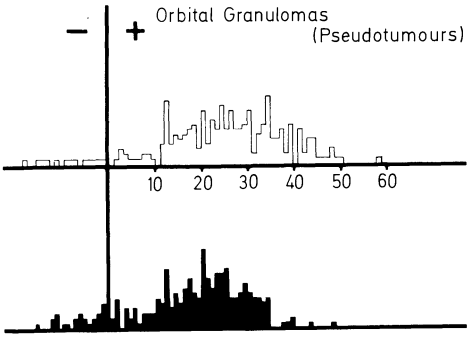

Fig. 4

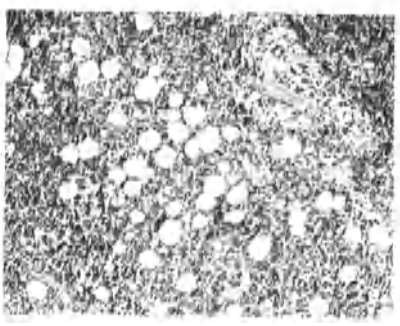

Fig. 5

Fig. 4. Summated absorption values recorded in 10 granulomata (pseudotumours) Black = pre-contrast absorption values; white = post-contrast absorption values

Fig. 5. Histology of lymphomatous pseudotumour: normal fat cells from muscle cone incorporated in a mass of lymphocytes

C.A.T. Scanning in Diseases of Children

Computerised Axial Tomography and Paediatric Neurosurgery

K. Till*

In this paper I shall concern myself with the considerable impact which C.A.T. has had upon the practice of paediatric neurosurgery. I shall try to emphasise the *clinical* importance of C.A.T. and its influence upon management of clinical problems rather than attending to the finer points of the technique itself.

I have been asked to describe mainly the importance of C.A.T. in intracranial tumours and I shall try to do so. It should be remembered, however, that paediatrics - and paediatric neurosurgery in particular - deals with the diseases of an age group and not with the disorders of a particular system within the body. It is especially in childhood that the CNS is involved in a multitude of disorders which, in many cases, are not primarily neurological. In my hospital, which is a *general* children's hospital dealing mainly with referrals from other hospitals, it is estimated that no less than 40% of all the patients have a significant CNS aspect of their illness. This is so, although the children have such varied disorders as those which involve cardiac or urological disease, immune deficiency, bleeding diatheses, leukaemias and so on. It is as if the smaller body of a child allows the more rapid dissemination of a disease so as to effect the CNS very commonly.

In attempting to keep to my brief, to concentrate on intracranial tumours, I must emphasise that there are many conditions in childhood which mimic or imitate brain tumours. The direct referral from other hospitals into the neurosurgical department tends to have signs of raised intracranial pressure, which is often assumed to mean intracranial neoplasm. The signs of localised brain disease which might justify this diagnosis of neoplasm are very often completely absent. To give some idea of the final diagnosis in nearly 1000 admissions of children with raised intracranial pressure, there follows an analysis of causes. On rarer occasions I have seen children with *only* raised intracranial pressure who proved to have uraemia, drug poisoning, tuberculous meningitis, leukaemia, renal disease, benign intracranial hypertension, etc.

Within the confines of a children's hospital, the referrals (and hence the use to which C.A.T. can be put) can be grouped as follows:

1. Metabolic disorders, often genetically determined

2. Bleeding diatheses, especially Factor 8 deficiency (haemophilia) and Factor 9 deficiency (Christmas disease)

3. Subarachnoid haemorrhage

4. Leukaemia

---

*Consultant Neurological Surgeon, Hospital for Sick Children, Great Ormond Street, London.

5. Endocrine disorders such as precocious puberty, reduced stature (dwarfism), diabetes insipidus and diabetes mellitus

6. Degenerative cerebral disease, especially those slow virus disorders which may mimic brain tumours of which subacute sclerosing panencephalitis is the main culprit

7. Congenital cardiac disease which in pre- and postoperative stages may be associated with cerebral oedema, infarction and cerebral abscess

8. Coma of unknown origin, of which lead and drug poisoning, unsuspected trauma, renal disease are all possible causes.

In general, the uses of C.A.T. in childhood diseases have been:

1. For diagnosis of intracranial disorder, and especially - something which does not attract attention or even mention in seminars and medical meetings - the *exclusion* of structural changes. Examples of this are the exclusion of suspected haematoma after head injury and the exclusion of a mass lesion when mimicked by a viral or degenerative cerebral disease.

2. Monitoring the changes in an intracranial tumour after operation, during radiotherapy and during later follow-up when tumour recurrence may be suspected; monitoring hydrocephalus after shunt treatment or when shunt malfunction or valve mismatching is suspected; monitoring the size of an intracranial abscess during treatment by aspiration.

3. Following the course of effects of intracranial bleeding from aneurysm or arteriovenous malformation leading to haematoma formation or hydrocephalus.

I propose to give examples chosen because they illustrate the effect of C.A.T. upon decision making and upon the management of certain types of intracranial disorders in childhood. I would remind you that the numerous occasions upon which a negative scan is obtained are equally important, since the exclusion of structural change in the brain often avoids the use of invasive techniques in serious diseases (such as leukaemia) where the risk of such investigations are by no means negligible.

Craniopharyngioma

A lesion characterised by calcification and cyst formation is clearly demonstrated by C.A.T. The extent and nature of its contents may influence the decision whether to operate. Typical C.A.T. appearances may show the surgeon's ideal case - of medium size and cystic, readily amenable to total excision.

Figure 1 shows a girl aged 15 years who for 5 years had remained in good health without diminution of visual fields or other ill effects, following a shunt operation for hydrocephalus. The large extension into the right frontal lobe was considered a contraindication to surgical intervention in such an otherwise healthy child. We have since learned that often the cystic contents have an absorption coefficient much higher than water - contrary to our expectations in view of the high cholesterol content. It may be, therefore, that such an extension is not solid tumour but an easily removed cyst.

Pineal Tumours

These are notoriously difficult to excise safely. A knowledge of the nature in addition to the extent will influence the surgeon's decision how to treat. The growth may be well defined and homogeneous - and amenable to excision. Figure 2, however, shows a complex pineal tumour. Plain radiographs showed a small area of calcification. The scan shows, however, that in addition to being very extensive, the lesion is very irregular in outline and is heterogenous, containing areas of calcification and at least three areas of low density, probably fat. Removal of such a teratoma would be highly dangerous and radiotherapy is far preferable.

Often Supratentorial Tumours

I have referred to the remarkable lack of neurological abnormality - so-called localising signs - in many children with raised intracranial pressure. C.A.T. often provides either a diagnosis or firm guidance towards the appropriate neuroradiological investigations.

Examples of frontal lobe tumours which did not cause neurological abnormality included a large cystic ependymoma, and a frontal tumour of heterogenous density, with much oedema, which was a rare neuroblastoma of undetermined origin (Fig. 3).

A 7-year-old child, alert and free from neurological abnormality but suffering from headache and vomiting with papelloedema, gave the C.A.T. appearance shown in Figure 4. The clear-cut edges of the cyst and absence of a tumour nodule or oedema suggested the correct diagnosis of hydatid cyst.

Raised intracranial pressure in a 4-year-old boy who had pulmonary infiltration suggested a diagnosis of tuberculous meningitis. Instead, his scan showed a cerebellar abscess (Fig. 5), a tuberculoma with caseous contents. Excision was required, rather than merely treatment of the hydrocephalus.

Monitoring by C.A.T. after tumour removal is, of course, far more easily carried out than by contrast studies. Even more important than the demonstration of persistent tumour is the recognition that a return of signs of raised intracranial pressure after tumour removal need not be due to recurrence. The child in Figures 6a, b had had a cerebellar medulloblastoma treated by partial excision and radiotherapy 1 year previously. The return of headache, vomiting, papilloedema and drowsiness was taken to indicate tumour regrowth. C.A.T. showed only hydrocephalus due to postoperative arachnoiditis *without* tumour. The treatment and prognosis were thus quite different.

A different situation obtains when neurological abnormalities are present suggesting the diagnosis of tumour, but C.A.T. serves to exclude it. The boy in Figure 7 developed head nodding and excessive head growth, suggesting hydrocephalus due to a suprasellar mass. Pneumoencephalography confirmed this. C.A.T. showed the lesion to contain only CSF. This arachnoid cyst was dealt with by direct attack as well as by shunt.

C.A.T. will undoubtedly provide much more information about the natural history of neoplastic processes in children. A baby aged 7 months was found to have hydrocephalus, which was successfully treated by shunt surgery. The pneumoencephalogram at that time showed a mass in the left lateral ventricle. For unknown reasons this diagnosis was ignored. *Twelve years* later, mild headache lead to C.A.T. scanning. The scan (Fig. 8) shows the same mass, which has grown in proportion to the child's brain and is assumed to be a choroid plexus papilloma.

Posterior Fossa Tumours

Posterior fossa tumours are treated by neurosurgeons in a variety of ways, some by preoperative reduction of raised intracranial pressure for days or weeks, some without such preparation. In all cases a confident diagnosis made without risking deterioration in the patient's condition is needed if mortality is to be minimised. C.A.T. provides such information about site and size of the tumour; cyst formation is shown and the site of a mural nodule demonstrated, while the degree of hydrocephalus and the presence of oedema or bleeding will influence the management.

The specific pathology of a solid tumour in the posterior fossa cannot be recognised with confidence. Although medulloblastoma has a tendency to be of high density and astrocytoma of low density there are many exceptions.

So far, we have operated upon 25 children with posterior fossa tumours using C.A.T. as the *only* investigation, believing that the surgical management is not influenced by angiography or encephalography. One case was mistakenly operated upon through misinterpretation of the scan.

Secondary deposits in the brain are very rare in children. A recent report from the Mayo Clinic showed that of 300 cases of solid tumour in kidney, liver, etc., only 16 secondaries were found in the brain, *always* accompanied by pulmonary deposits.

Cases most nearly resembling metastases in my experience are those with leukaemia, in which the onset of cerebral symptoms or sign may be due to abscess formation (so-called opportunist infection), viral encephalitis, leukaemic deposits, hydrocephalus and cerebral atrophy. Figure 9 shows at least two abscesses due to nocardial infection from a pulmonary abscess.

Overall Conclusions

1. Children do not usually present with evidence of brain tumour - only with evidence of raised intracranial pressure or local cerebral dysfunction, having a wide variety of possible causes. Careful history taking and examination and good plain radiographs remain an essential part of their investigation.

2. The non-invasive technique of C.A.T. serves as a very valuable screening method in a multitude of clinical situations, as a guide to further investigations in a lesser number, as a means of confident diagnosis of an expanding lesion in many cases of an intracranial tumour and as a means of pathological diagnosis in, so far, a minority.

3. The possibility of follow-up by C.A.T. is already providing a remarkable insight into the natural history of the effects of treatment on many conditions. The natural reluctance to investigate repeatedly children with intracranial tumours or hydrocephalus using contrast studies has long prevented us from studying progress in a disease or the response to treatment. Further experience, especially with closer studies of absorption coefficients, of enhancement methods and enhancement clearance velocities will enrich our understanding significantly.

Fig. 1

Fig. 2

Fig. 1. Cystic craniopharyngioma extending into right frontal lobe

Fig. 2. Pineal teratoma containing calcium and fat

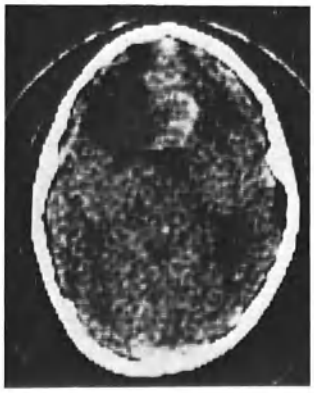

Fig. 3

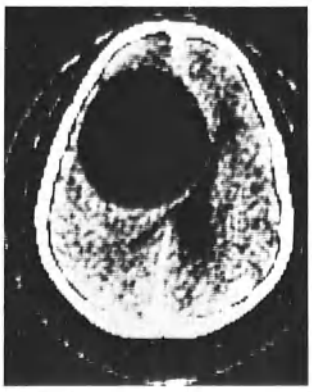

Fig. 4

Fig. 3. Secondary neuroblastoma causing no focal symptoms

Fig. 4. Hydatid cyst

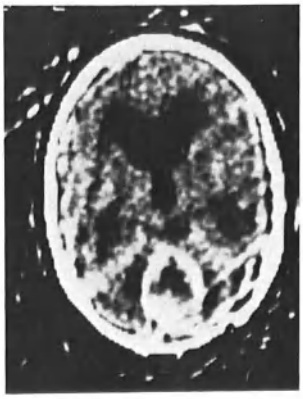

Fig. 5

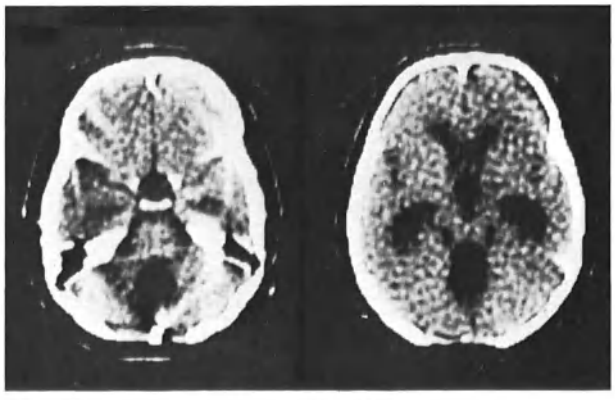

Fig. 6a Fig. 6b

Fig. 5. Tuberculoma, following enhancement with contrast

Fig. 6a and b. Postoperative hydrocephalus due to basal arachnoiditis

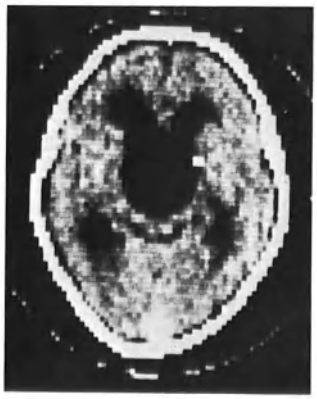

Fig. 7

Fig. 8

Fig. 7. Suprasellar arachnoid cyst

Fig. 8. Choroid plexus papilloma of left lateral ventricle

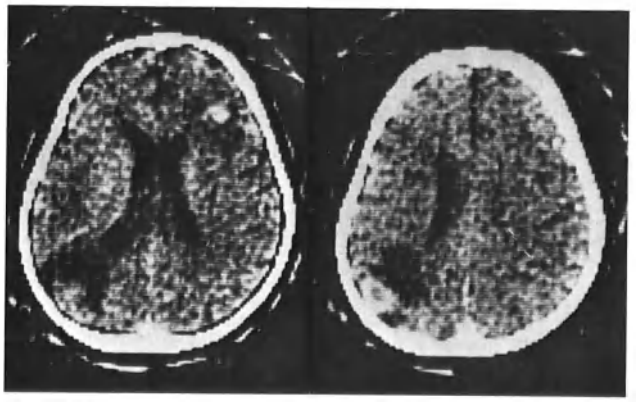

Fig. 9a

Fig. 9b

Fig. 9a and b. Multiple cerebral absesses due to *Nocardia*

C.A.T. in the Diagnosis and Management of Childhood Hydrocephalus

C. Raybaud, P. Farnarier*, P. Palmieri, N. Pinsard**, and M. Choux***

Hydrocephalus is the most frequent neurosurgical occurrence in children. It always indicates severe intracranial pathology, and raises important diagnostic problems concerning the cause of the increased ventricular pressure as well as the future of brain function. In the last two decades, prognosis has been considerably improved because of better surgical conditions and the possibility of placement of safely functioning ventricular drainage.

Neuroradiology has come a long way since DANDY (1), in 1918, described air ventriculography, allowing for the first time a direct diagnosis of hydrocephalus, of the site of the lesion, and an indirect means of recognising the pathology. Further development of ventriculography (with air or iodinated contrast media) and of angiography (2) has since then met the needs of modern neurosurgery. Although the diagnosis of hydrocephalus, with its causes and its consequences can be made with certainty by conventional means, the procedures are technically complex, and possibly hazardous.

The introduction of computerised tomography in 1972 (3, 5) was a significant step in simplifying the diagnostic approach. Indeed, C.A.T. can be applied without clinical restriction. Morphological demonstration of the whole of the ventricular cavities is easily obtained. Moreover, this specifically densitometric method yields very useful information about the brain parenchyma, as to whether it contains abnormal tissues or cystic cavities.

Clinical Material

Diagnostic problems of hydrocephalus in childhood can occur in various clinical contexts, i.e. acute, chronic, and during follow-up. In our centre, within 18 months we have studied 106 cases of which 21 were control scans after surgery. Of the remaining 85 cases, 33 (39%) presented with an acutely increased intracranial pressure, with fundoscopic abnormalities, opening of the cranial sutures, and symptoms related to the growth of a mass in the CSF pathway. Seven cases (8%) were neonates or infants with a rapid increase of head circumference and a bulging fontanelle. In 35 older children (41%) the problem was that of a macrocephaly, with or without mental or neurologic abnormalities, sometimes showing acute deterioration following minimal head trauma. Finally, 10 cases (12%) presented with clinical features suggesting a 'normal pressure hydrocephalus', after having suffered head trauma, meningitis or subarachnoid haemorrhage.

*Radiologie Vasculaire et Neuroradiologie, Hôpital de la Timone, Marseille.
** Clinique Pediatrique, Hôpital des Enfants de la Timone, Marseille.
*** Neurochirurgie Pediatrique. Hôpital des Enfants de la Timone, Marseille.

Tumoral Hydrocephalus

Tumoral hydrocephalus occurs when a space-occupying lesion obstructs the CSF pathway. The clinical features often combine those of an acute increase of the intracranial pressure and local symptoms related to the tumour. Although these patients are usually examined because of acute deterioration, the slow growth of the mass permits a relatively long-lasting evolution, with the progressive development of hydrocephalus.

Hydrocephalus is demonstrated on C.A.T. by the symmetrical enlargement of the lateral ventricles. The brain tissue around the ventricular cavities is still relatively thick, and the shape of the basal ganglia is preserved. Dilatation affects the frontal horns, which appear rounded, and even more so the ventricular atria. Temporal horns are also rounded. Typically, the margins of the ventricles are somewhat blurred, and the surrounding white matter appears of diminished density. This seems to indicate a subependymal resorption of CSF (4), quite frequent in those cases of acute obstructive hydrocephalus.

In addition to the ventricular dilation, C.A.T. demonstrates the causal lesion: posterior fossa tumour, in the brain stem, the fourth ventricle or the cerebellum; tumour of the third ventricle, of the caudate nucleus, of the thalamus or of the choroid plexus.

Hydrocephalus related to brainstem glioma is not constant, and always less marked than in other cases of posterior fossa mass, except when it occupies the ventricular lumen. The basal ganglia tumours often produce asymmetrical hydrocephalus, especially when the lesion is located around the foramen of Monro. Absence of communication between the ventricles can be indicated by differences of density between the lateral ventricles.

The usefulness of C.A.T. is especially well illustrated in cases of choroid plexus papilloma, which are much better delineated by this method than by any other neuroradiological approach. In the same way, the cystic nature of some brain stem gliomas or of the cerebellar astrocytomas can be shown, thus helping towards surgical appraisal.

However, a more precise anatomical evaluation necessitates completion of the investigation by the other neuroradiological procedures. It is essential for the surgeon to know feeding arteries and vascular landmarks of the brain. Anatomical relationships of the tumour to the adjacent structures, and the involvement of such critical areas as the floors of the fourth and the third ventricles are best demonstrated by positive contrast ventriculography. The introduction of air into the basal cisterns may also show extracerebral extension of the lesion.

Hydrocephalus in Infants

Hydrocephalus in infancy is also an urgent diagnostic problem. The brain at this age is extremely sensitive to the increase of pressure, but recovery is often possible if treatment is applied early. Clinical features are usually limited to a rapid increase of the head circumference, with a bulging fontanelle. Planning investigations raises particular problems in infants. Indeed, C.A.T. scanning (with the first generation of scanners) may necessitate general anaesthesia, or at least heavy sedation, while air ventriculography can be done merely

by puncturing the fontanelle, without anaesthesia. For this reason, in our department, we prefer not to begin investigation by C.A.T. However, when the ventricular dilation is huge, adequate filling of the cavities with air is difficult to obtain, and C.A.T. is the optimal method. On the other hand, analysis of the CSF pathway is better with air encephalography, for instance when aquaduct stenosis is associated with a Dandy-Walker malformation of the posterior fossa.

Macrocephaly in Children

Macrocephaly is a difficult problem in child neurology, especially when no neurological deficit is observed. Most physicians would be reluctant to prescribe procedures such as pneumoencephalography or ventriculography, since macrocephaly may be of no clinical significance. However, the possibility of chronic hydrocephalus, the necessity of preserving intellectual development and the prevention of acute decompensation, should lead to investigations. Because it is non-invasive, C.A.T. is the method of choice as a first diagnostic approach, and can be added to by other means whenever the scan is abnormal.

Most often, investigations reveal hydrocephalus associated with malformations. There may be an arachnoid cyst, or porencephalic cavities. The horizontal plane of the C.A.T. slices as well as the possibility of showing cavities which do not communicate freely with the CSF pool makes C.A.T. the most useful tool for diagnosing this type of lesion. Aqueduct stenosis can be diagnosed from the association of a triventricular dilation associated with a small fourth ventricle. However, the content of the posterior fossa as well as the aqueduct should be analysed by pneumoencephalography and/or ventriculography, in order to exclude other pathologies such as an Arnold Chiari malformation. In the same way, an air study should be performed in cases of communicating hydrocephalus in order to confirm the absence of an anomaly at the outlet of the fourth ventricle, and to show the level of the extracerebral block.

Normal Pressure Hydrocephalus

Patients suspected of 'normal pressure hydrocephalus' should be investigated by C.A.T.; the clinical grounds for considering such a diagnosis being deterioration after head injury or disease in the subarachnoid space. Confident differentiation between brain atrophy and hydrocephalus is impossible, though patency of CSF pathways may be ascertained on air studies alone. On C.A.T. scans, however, atrophy is also well demonstrated, while the ventricular size and the thickness of the cerebral mantle are well appreciated. Diagnosis of so-called normal pressure hydrocephalus still requires 24 to 48 hours' continuous recording of the intraventricular pressure though the disturbance of the CSF absorption process may also be analysed by studying the progression of intrathecally injected substances, either metrizamide followed by means of C.A.T., or radioisotopes followed on a gamma camera.

Postoperative Control

Follow-up of shunted patients necessitates repeated examinations in order to check up on the patency of the shunt, the possibility of local complications, the efficiency of the ventricular drainage, the recurrence of the pathology and the return to normality of the brain. Performing angiograms or air studies over and over again may be harmful, and is not accepted by most of the patients.

C.A.T. appears to be the procedure best suited for follow-up, since it provides all the information needed with a minimum of discomfort. In some cases, however, especially when symptoms of intracranial hypertension reappear, ventriculography, or radio-isotopic exploration of the patency of the ventricular drain may be added. Such complications as infection around the drain and ventricular collapse with shunt dependency and subdural collections are readily demonstrated on C.A.T. scans. Reconstitution of the cerebral mantle can be checked upon. It is worth noting that, in several cases, a disproportion remains between the frontal horns and the atria in the return to normality of ventricular size. This persisting enlargement of the atria indicates a deterioration of brian parenchyma in the posterior part of the hemispheres. The absence of a decrease in the ventricular size after shunting is of poor prognosis as far as brain function is concerned.

Arrested hydrocephalus is a particular clinical entity in which the ventricles have been enlarged by increased intracranial pressure, with a consequent enlargement of the head, but later on, a balance has occurred between the secretion of CSF and the compensatory absorptive mechanisms. This has resulted in the cessation of ventricular enlargement, with normalisation of the intraventricular pressure. The final appearance consists of large ventricles, with normal pressure and clinically without any cerebral dysfunction.

Summary

C.A.T. is certainly the best single procedure for the investigation of hydrocephalus in childhood. It is non-invasive. It demonstrates precisely the size of the ventricles and the thickness of the cerebral mantle, allowing a trustworthy comparison for follow-up studies. Repeated follow-up examinations are easy to perform without damage to the patient. Any associated pathology is demonstrated, and the level of obstruction can usually be precisely located.

Nevertheless, in our opinion, the relationships of a tumour to the surrounding structures, the cisternal involvement and the patency of the CSF pathway, should be investigated more thoroughly by a direct visualisation of the ventricles and the subarachnoid spaces. Thus, a thorough investigation of hydrocephalus, as a rule, necessitates the performance first of a complete C.A.T. scan, then appropriate procedures adapted to each case. The only exceptions to this rule are infants in whom direct puncture ventriculography can be done first, since it is very simple to carry out, and has the advantage of relieving intracranial pressure. Follow-up C.A.T. studies can be repeated harmlessly as often as required by the clinical condition of the patient.

References

1. DANDY, W.E.: Ventriculography following the injection of air into the cerebral ventricles. Annals of Surgery 68, 5-11 (1918).
2. HARWOOD NASH, D.C.F., FITZ, C.R.: Neuroradiological techniques and indications in infancy and childhood. In: Progr. Peadiat. Radiol. KAUFMANN, H.J. (ed.). Basel: Karger 1976, Vol. V, pp. 2-85.
3. HOUNSFIELD, G.N.: Computerised transverse axial scanning (tomography): Part I. Description of system. British Journal of Radiology 46, 1016-1022 (1973).
4. NAIDICH, T.P., EPSTEIN, F., LIN, J.P., KRICHEFF, I.I., HOCHWALD, G.M.: Evaluation of pediatric hydrocephalus by computed tomography. Radiology 119, 337-345 (1976).
5. NEW, P.F.J., SCOTT, W.R.: Computed Tomography of the Brain and Orbit. Baltimore: William and Wilkins Co. 1975.

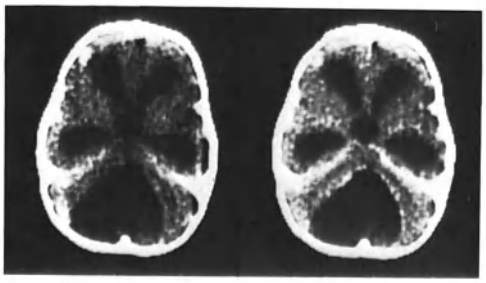

Fig. 1

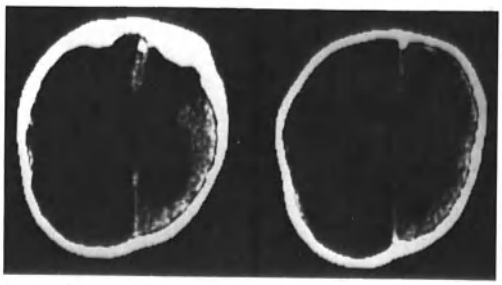

Fig. 2

Fig. 1. Tumoral hydrocephalus: C.A.T. shows marked ventricular dilation, with blurred ventricular margins and a low density in surrounding white matter. A cystic mass is demonstrated in the posterior fossa (astrocytoma)

Fig. 2. Huge chronic hydrocephalus: a typical case in which air studies fail to demonstrate adequately the ventricular cavities, while C.A.T. clearly shows ventricular enlargement and thickness of remaining cerebral mantle

Fig. 3. Postoperative scan: ventriculoperitoneal drainage has been efficient, while an arachnoid cyst still displaces brain tissue (unsatisfactory cystoperitoneal drainage)

Fig. 4. Arrested hydrocephalus: 13-year-old girl who presented with rapid head enlargement during first months of life; surgery was not performed at that time. This girl now lives normally and is quite a good pupil at school

C.A.T. in the Phakomatoses

D. P. E. Kingsley*

The phakomatoses, or neuroectodermal dysplasias, are a group of hereditary conditions characterised by the development of tumours in many organs, but notably in the skin and CNS. A number of conditions have been included under this heading, but only five occur with sufficient frequency to merit our attention here, and of these I do not intend to discuss ataxia telangiectasia, as we have only scanned one of these patients, and the examination was unsatisfactory.

Instead, it is intended to concentrate on four conditions: neurofibromatosis, tuberose sclerosis, Sturge Weber and von Hippel-Lindau disease.

Neurofibromatosis

During the past 3 years we have had the opportunity to scan 13 patients with neurofibromatosis and suspected intracranial abnormalities. One of these examinations was unsuccessful but the diagnoses of the intracranial abnormalities of the other 12 cases are shown in Table 1. The total number of abnormalities exceeds 12 since a number of patients had more than one abnormality.

Table 1. Neurofibromatosis

C.A.T. findings in 12 cases:	
Ventricular dilatation	7
Optic nerve glioma	2
Optic chiasm glioma	2
Hemihypertrophy	2
Absent orbital wall	1
Acoustic neuroma	2
Normal	2

Two main types of abnormality are seen in the skull and CNS: skeletal dysplasia and intracranial neoplasm.

Skeletal dysplasia may affect the skull, the commonest abnormality being a defect in the postero-superior wall of the orbit (Fig. 1). Patients with this abnormality frequently present with pulsating exophthalmos due to direct extension of the temporal lobe into the back of the orbit. It should be noted that the optic nerve is displaced medially (Fig. 1).

*Lysholm Radiological Department, The National Hospital, London.

Hemihypertrophy of the skull may also occur in the trigeminal distribution. Two such cases have been scanned. The hypertrophy involves not only the bony structures but also the intracranial contents. There is enlargement of the diploic spaces, sinuses and petrous bones and within the cranial cavity there is enlargement of brain tissue. Both cases were noted to have abnormally dilated ventricles, the involved side being the most prominently dilated. Heterotopic grey matter was also present in one case.

Mental retardation has been noted in approximately 10% of patients with neurofibromatosis and, of our patients, three were mentally retarded; in seven patients there was evidence of ventricular dilatation without any evidence of underlying obstruction.

Intracranial neoplasms occur with great frequency. In one study the incidence was as high as 47% (1). Tumours involve either the cranial nerve sheaths or may be frank gliomas, ependymomas or meningiomas.

Optic tumours may involve either the nerve or the chiasm. Thickening of the nerve is usually quite definite, but comparison with the opposite side may not be reliable since such tumours may be bilateral. Two optic nerve tumours, one involving the chiasm, and one primary chiasmal glioma have been scanned. The latter also involved the optic radiation on the left side (Fig. 2).

It is essential to obtain overlapping scans so that no part of the orbit or suprasellar cisterns is missed. The appearances are typical. The optic nerve tumour is shown as a thickened optic nerve, and may or may not enhance following intravenous contrast injection. Careful sections may enable the optic canal to be seen, but this is only possible with very careful scanning using 8 mm or finer collimators.

Optic chiasm tumours are demonstrated by the presence of a mass with a density the same as or greater than brain tissue lying within the suprasellar cistern (Fig. 2). Routine scan sections may fail to show the cistern and for this reason also a small lesion may be missed unless adequate scans are obtained. These tumours may also enhance.

Acoustic neuromas occur less commonly than optic gliomas; we have encountered two such cases. Unfortunately, the scans, undertaken during our early experience, were not diagnostic. In neurofibromatosis acoustic neuromas are frequently bilateral, as in one of our cases.

Tuberose Sclerosis

A total of 13 cases have been scanned, their ages ranging from 11 months to 32 years. All but one of the patients had cutaneous evidence of tuberose sclerosis at C.A.T. and consequently the diagnosis was suspected on clinical grounds alone. Table 2 shows the incidence of positive radiological features in these cases. Plain skull X-rays were undertaken in all patients but calcification was found in only six cases; in six cases the skull radiograph was normal. Raised intracranial pressure was noted in three patients and atrophy in two.

Air encephalography or ventriculography was undertaken in three patients. In only one were ventricular filling defects noted. One patient had evidence of atrophy, and in one patient with raised intracranial pressure there was obstruction at third ventricular level.

Table 2. Tuberose sclerosis

Findings in 13 cases (aged 11 months to 32 years)	
Clinical features present:	13
Skull X-ray	
Calcification	6
Raised pressure	3
Atrophy	2
Normal	6
C.A.T.	
Paraventricular masses	13
Calcified tubers	10
Coefficients >20	
Hydrocephalus	6
Astrocytomas	4

C.A.T. demonstrated abnormalities in all patients. All had at least one, and usually several, paraventricular masses (Fig. 3). Many of the masses were calcified with absorption coefficients of 30-40 units making them easy to identify. Others were presumably uncalcified and were only detected in retrospect. The smallest lesions detectable measured approximately 1.5-3.0 mm in diameter, i.e., one to two pixels, and had absorption coefficients only 2 or 3 units higher than the surrounding brain tissue. Uncalcified masses may lie proud of the ventricular wall, in which case they are easier to detect, or else they may manifest themselves only by being of slightly higher than brain tissue density, becoming evident only in later scans. In such a situation only a high index of suspicion will produce a positive diagnosis.

Microscopic calcification in tubers may be difficult to assess, for while absorption readings of 30-40 units are consistent with calcification too small to be detected on plain radiographs, tubers with absorption coefficients nearer to brain tissue density may still contain calcium. In our cases, absorption coefficients were below 20 in three patients, two of whom were under 1 year of age. Sequential scans undertaken in two patients over periods of 18 months showed no significant enlargement of the paraventricular nodules. Two patients were given intravenous contrast medium. It was found very difficult to assess the pre- and post-enhancement scans, as the cuts varied slightly. There did not appear to be any significant enhancement of these lesions.

Intracranial tumours other than subependymal nodules are encountered less commonly than in neurofibromatosis, but are said to occur in about 15% of patients (2). Dilated lateral ventricles were noted in six of our patients, signs of raised intracranial pressure being the presenting symptom in three. In all three, and in another patient without signs of raised pressure, giant cell astrocytomas were noted in the region of the foramen of Monro (Fig. 4).

Sturge Weber Syndrome

Ten cases of Sturge Weber syndrome have been examined by C.A.T.; four involved the right side, three the left, and three were bilateral (Table 3).

Table 3. Sturge Weber Disease

Findings in 10 cases (aged 4-16 years)	
Clinical features present:	10
Skull X-ray	
Calcification	9
Hemiatrophy	10
C.A.T.	
Calcification	10
Hemiatrophy	10
Dilated subarachnoid space	5

All 10 cases were diagnosed clinically, having the typical naevus in the trigeminal distribution. One patient had congenital glaucoma. At the time of the scan the patients' ages ranged from 4 to 16, although many patients had been diagnosed earlier.

On the plain skull radiograph, bony changes of hemiatrophy were noted in all patients, while the typical serpentine calcification was noted in all but one.

Changes on C.A.T. were most striking (Fig. 5). Hemiatrophy was well demonstrated on the affected side with enlargement of the frontal sinus.

Cortical calcification was well demonstrated, and was always in excess of that seen on the plain radiograph. In one patient small amounts of calcification were noted in left frontal and parieto-occipital regions which were not visible on the plain film; this showed merely hemiatrophy.

The calcification is dense, with absorption coefficients of 60-180 units. The calcified gyri are better demonstrated by increasing the window width to 200 with a window level of 50 (Fig. 5).

Widening of the subarachnoid space may occur over the calcified area and this was visible in five patients.

Von Hippel-Lindau Disease

Although this condition is included in the congenital hereditary diseases involving the CNS as well as many other organs, no case has been described before puberty.

The condition is said to constitute approximately 2% of brain tumours and 7-10% of posterior fossa tumours (3). We have scanned three patients with this diagnosis during the past 3 years, two of whom were mother and daughter.

The typical lesion is a haemangioblastoma lying in the cerebellar hemisphere or vermis with an associated cystic cavity (Fig. 6a). C.A.T. defines the low density cystic area well, and following contrast injection the mural haemangioblastoma shows intense enhancement (Fig. 6b).

Frequently, these haemangioblastomas are multiple, as was the case in all three of our patients. We were unable, however, to demonstrate the other lesions on C.A.T., and angiography was eventually required to localise the other lesions.

In rare cases, the haemangioblastomas occur supratentorially, but even in such circumstances there may be further tumours in the posterior fossa. We encountered one such patient with a large tumour in the left posterior temporal region. The posterior fossa tumours were not demonstrated.

The diagnosis can be made on C.A.T. only when the cystic lesion is typical and where other tumours are demonstrated. However, a high index of suspicion is required, and a family history of the disease should be sought after. In such circumstances multiple overlapping scans of the posterior fossa should be undertaken using contrast enhancement.

Summary

The role of C.A.T. in the diagnosis and management of the phakomatoses is difficult to assess. It is uncommon for C.A.T. scanning to make the initial diagnosis, since in most cases, with the possible exception of von Hippel-Lindau disease, the diagnosis is made on clinical grounds in the first instance. In neurofibromatosis small cranial nerve tumours involving the optic and acoustic nerves are readily demonstrable but, because of their size, multiple overlapping cuts are required to demonstrate them adequately. Other lesions such as gliomas and the bony abnormalities are, however, well demonstrated. In tuberose sclerosis C.A.T. is capable of demonstrating lesions as small as 1.5-3.0 mm in diameter. In the *forme-fruste* the diagnosis of this condition is likely to be made earlier by this method than by any other.

In Sturge Weber disease the diagnosis, not usually in doubt clinically, is confirmed, while in von Hippel-Lindau disease a high index of suspicion is required to make the diagnosis.

Contrast enhancement has not been of particular value in tuberose sclerosis, since it has been found difficult to achieve the same pre- and post-enhancement scan level. In Sturge Weber disease, patients in the early stage of the disease have not been scanned, while in the later stages calcification is such that enhancement would be unlikely to be of value. In neurofibromatosis contrast enhancement may sometimes be of value, while in von Hippel-Lindau disease it is essential.

Overall, C.A.T. undoubtedly offers an extremely high incidence of positive scans in these conditions and, as such, is probably the most useful single investigation from the point of view not only of confirming the diagnosis but also in their follow-up.

References

1. HORIE, A., SHIGEMI, V., FUKUSHIMA, T., TANAKA, K.: Neurofribromatosis complicated by intracranial tumours. Acta Pathologica Japonica 24, 705-716 (1974).

2. KAPP, J.P., PAULSON, G.W., ODOUR, G.L.: Brain tumours with tuberose sclerosis. Journal of Neurosurgery 26, 191-202 (1967).
3. MELMON, K.L., ROSEN, S.W.: Lindau's disease. Review of the literature and study of a large kindred. American Journal of Medicine 36, 595-617 (1964).

Fig. 1

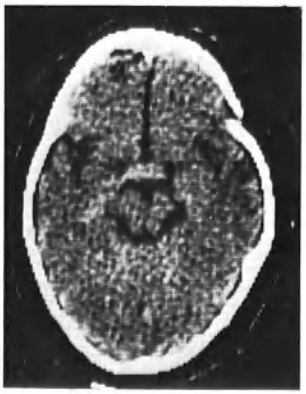

Fig. 2

Fig. 1. Absence of postero-lateral wall of L. orbit in neurofibromatosis

Fig. 2. Glioma of optic chiasm extending into L. optic radiation; case of neurofibromatosis

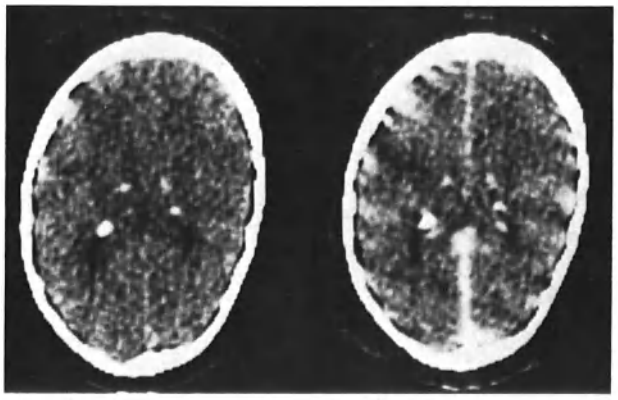

Fig. 3a

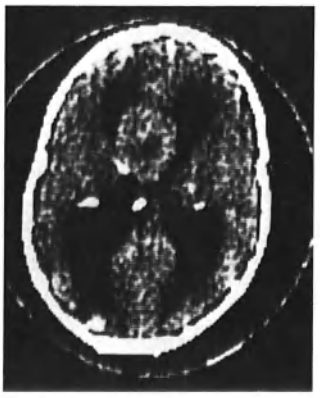

Fig. 3b

Fig. 4

Fig. 3a and b. Tuberose sclerosis before (a) and after intravenous contrast medium (b) with typical phakomata, showing no significant enhancement

Fig. 4. Tuberose sclerosis, showing hydrocephalus due to giant cell astrocytoma

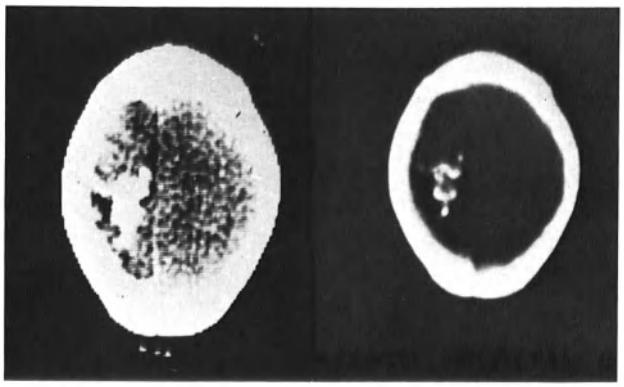

Fig. 5a and b. Sturge Weber disease showing left sided calcification and hemiatrophy. (a) Standard window width, (b) window width 200

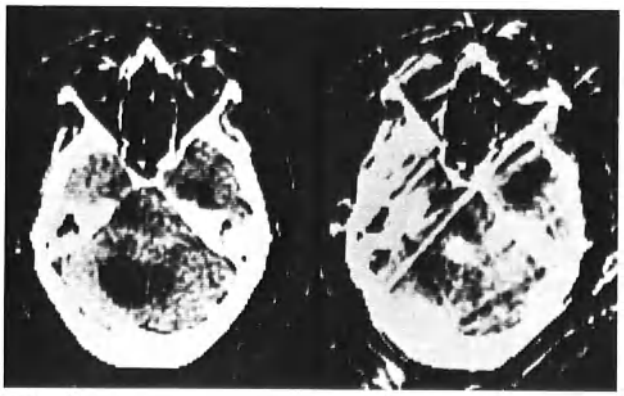

Fig. 6a Fig. 6b

Fig. 6a and b. Cystic haemangioblastoma of von Hippel-Lindau disease, before (a) and after intravenous contrast medium (b) showing marked enhancement of mural nodule

Diseases of the Brain Parenchyma, Atrophy and Hydrocephalus

The Role of C.A.T. in the Diagnosis and Management of Intracranial Infections

I. F. Moseley, L. E. Claveria, and G. H. du Boulay*

Conventional radiological and isotope investigations are of limited use in the diagnosis of intracranial infections. The diagnostic possibilities in meningitis and encephalitis are very limited (7), and cerebral abscesses, although they may produce certain well-documented changes in, e.g. the angiogram (5) or radioisotope study (3), are generally diagnosed clinically, with the radiological investigations confirming the presence of some disease processes compatible with the clinical diagnosis.

It rapidly became clear that C.A.T. was an extremely powerful agent for the diagnosis of cerebral abscess (2, 6), although its utility in other infections is less spectacular.

Material

Sixty patients suffering from intracranial abscess, encephalitis or meningitis have been studied at the National Hospital, Queen Square with the 160 × 160 matrix EMI Scanner (Table 1). In all of them the diagnosis has been confirmed by clinical, laboratory, biopsy or necropsy data.

Table 1. Case material - intracranial infections

Abscess		32
Bacterial	22	
Tuberculous	5	
Fungal	5	
Encephalitis		15
Focal (herpes)	7	
Generalised	8	
Meningitis		14
Bacterial	6	
Tuberculous	7	
Fungal	1	
Total		61

*Lysholm Radiological Department, National Hospital for Nervous Diseases, London.

Results

Intracranial Abscess

Pyogenic

Clinical Features. These cases included 19 cerebral, 2 cerebellar and 3 subdural abscesses, in 22 patients (2 patients each having a temporal and cerebellar or posterior fossa subdural abscess). Two-thirds of the patients were less than 30 years of age. In 18 cases some source of infection was found: cardiac in 5, postoperative in 5, and ear or paranasal sinuses also in 5; 2 patients had suffered recurrent meningitis, and the last had repeated chest infections. The most commonly affected region was the frontal lobe (9 cases).

Other Investigations. An EEG had been carried out in four cases; it correctly lateralised the lesion in three, two of whom also had focal neurological disturbance, and showed a diffuse abnormality in the remaining comatose and decerebrate patient, who had left temporal and left cerebellar hemisphere abscesses. *The skull radiograph* showed an abnormality in four cases: frontal and maxillary sinusitis, air within a temporal lobe; air within a subdural empyema (after tapping); calcification in the capsule of a chronic subdural empyema. In all of the remainder it was thought to be normal. *Carotid angiography* was carried out in only seven cases; in four it showed a mass lesion, which was avascular in three, but with some circumferential blush in the fourth. Once case showed only dilated ventricles; this was the patient with left temporal and cerebellar lesions - a vertebral angiogram was not performed. The remaining two examinations (one including vertebral angiography) were thought to be negative, even in retrospect: both patients had temporal lesions; thus it would appear that three temporal abscesses were missed in three cases, but in one of these the angiogram was carried out almost 3 weeks before the temporal abscess became manifest clinically (the patient also had a posterior fossa subdural empyema).

Radioisotope scans were carried out in three patients, and were positive in each case; two of these also had positive angiograms.

C.A.T. Data. One of the cerebellar lesions was not seen; the tomographic cuts were not low enough. A left temporal abscess was also not identified: this was the patient in whom the angiogram was also negative. All of the other intra-axial lesions were shown as irregular areas of lowered attenuation coefficients, with, in a few cases, a suggestion of a rim in which the coefficients were less reduced. There was clear oedema in 17 cases (Fig. 1) and in 18 there was evidence of a mass lesion. Intravenous contrast medium was injected in 16 patients, and in 14 produced a ring enhancement (Fig. 2) which was seen to be multilocular in 8. In one of the remaining patients, there was no enhancement, and the scan was wrongly interpreted as being normal, while in the other, in whom the brain had already been needled, enhancement was homogeneous.

Four cases showed hydrocephalus, and in four there was evidence of extension of the inflammatory process to the ventricular system.

The subdural empyemata appeared in different ways: the first as an area of lowered attenuation with marked enhancement of its periphery after contrast medium injection; the second as a calcified capsule surrounding material having the same attenuation coefficients as brain, and unchanged after contrast medium injection; and the third as a super-

ficial collection with coefficients slightly less than brain, containing bubbles of air (after aspiration), and with an irregularly enhancing capsule (Fig. 3a).

Tuberculous

Clinical Features. All five patients were immigrants; three were over 30 years of age. The past history was unknown in one child, but three of the four adults were known to have had tuberculous meningitis. Three patients presented with epilepsy, and in one of these the EEG showed a diffuse abnormality. Only two patients had single lesions, and the frontal lobe was the least commonly affected region (one lesion only).

Other Investigations. The EEG has been referred to above. *The skull radiograph* showed calcification in one case, and signs of raised intracranial pressure in a further patient presenting with appropriate symptoms. *Radioisotope scans* were performed on two patients; both were negative. *Angiography* showed a parietal mass lesion, indistinguishable from a tumour in one case, but was negative in another patient with tuberculomata in the brain stem and caudate nucleus. *Ventriculography* in the latter patient had suggested a cerebellar lesion; surgical exploration was negative.

C.A.T. Data. Abnormalities were demonstrated in all five patients, in three of whom two or more lesions were shown. In two cases there was calcification within the tuberculomata, but in the remainder the attenuation coefficients were either the same as those of normal brain, or reduced. Intravenous injection of contrast medium produced definite enhancement in all cases: ring-like in three, homogeneous also in two of these and a further patient, and irregular in the last. The latter lesion was diagnosed radiologically as a glioma, the clinical history being slowly progressive (Fig. 3b). Only two of the lesions showed mass effect, which was never gross. Oedema was present in both.

Fungal (Three Nocardial, Two Aspergillous)

Clinical Features. Four of the five patients were young adults, and all five were receiving immunosuppressive therapy. Three had suffered abscesses elsewhere. Two cases showed multiple intracranial abscesses. In every patient except one the frontal and/or parietal lobes were involved; in the remaining case the abscess was in the cerebellar hemisphere.

Other Investigations: An EEG was recorded in one case, showing a focal abnormality. *The skull radiographs* were normal in every case. In two cases, *radioisotope scans* were carried out: in the first, one only of three lesions was identified, while in the other the scan was equivocal, becoming definitely positive 2 weeks later - after burr-hole aspiration. Conventional neuroradiological contrast examinations were not carried out in any case.

C.A.T. Data. Eight abscesses were identified in the five patients, all as areas of lowered attenuation coefficients, although in two cases rims of less diminished density were seen. After contrast medium injection, five showed homogeneous uptake, and only three showed a typical ring pattern, which was multilocular in one case. All cases showed oedema, but in two this was unassociated with mass effect.

Encephalitis

Herpes Simplex

Seven proven cases have been examined, six of whom showed reduced attenuation coefficients in one or other temporal lobe (more often the left), with bilateral lesions in two (Fig. 4). Two patients with profound neurological deficits showed internal capsule lesions in addition, and in a third there was a frontal cortical lesion. Despite extensive disease, mass effect was not marked, and none of the cases showed displacement of the midline structures. Intravenous contrast medium given in two cases produced no change in the appearances.

Other radiological investigations in these patients were not contributory.

Other Encephalitides

Eight cases have been fully documented, with appropriate clinical history, CSF and EEG changes.

Conventional radiological examinations showed no abnormalities. In six cases the C.A.T. studies were interpreted as normal, but, with follow-up it became clear that in one case there had initially been a slight but definite - 2-3 EMI number - decrease in the attenuation coefficients of the cerebral white matter, which subsequently resolved. In another case there were more obvious areas of lowered coefficients in certain portions of the paraventricular white matter.

One proven case of toxoplasmosis was examined, the plain films of which showed definite parasellar calcification. C.A.T. confirmed the presence of much more extensive parasellar and paraventricular calcification than had been indicated by the conventional studies; it also demonstrated marked hydrocephalus (in association with microcephaly), and considerable alteration in the configuration of the lateral ventricles. The posterior fossa structures were preserved (Fig. 5). Similar appearances had been seen in a suspected case, which was however unproven, and is therefore not included in the present series (2).

Meningitis

Pyogenic

Six patients were examined by C.A.T.: three within the 1st week, and the remainder at least 3 weeks from the onset of symptoms. All these examinations were normal, as were radioisotope scans carried out on three of the patients. An angiogram carried out in one case demonstrated non-specific arteritic changes only.

Tuberculous

C.A.T. was carried out on seven cases, of whom four also had pulmonary tuberculosis; in five patients the results were quite normal, despite the fact that an air encephalogram had suggested lateral ventricular dilatation in one of them. Two patients were shown to have hydrocephalus by C.A.T. and in one of these there was also abnormal enhancement of the tissues surrounding the circle of Willis after contrast medium injection, indicative of a basal meningitis (Fig. 6). In one of the pa-

tients with a normal C.A.T. carotid angiography also demonstrated non-specific arteritic changes.

Fungal

A single case of cryptococcal meningitis showed no plain radiograph or C.A.T. abnormality; no other radiological examinations were performed.

Discussion

It is clear from our results that, whereas radiology in general has little part to play in the diagnosis and management of infective encephalitis and meningitis (with certain exceptions; *vide infra*), it is extremely important in cases of cerebral abscess. In published series of this condition the mortality has ranged from 27 to 53% (1, 4), while in the present series of 32 patients only 5 (16%) succumbed, and 22 (69%) made a good recovery. It seems reasonable to think that among the reasons for this improvement in the results the early confirmation of the clinical diagnosis and the precise localisation of the lesion obtained with C.A.T. have been significant.

As suggested above, cerebral abscess is generally diagnosed clinically, the role of radiological exploration being to confirm (or in a number of cases, to exclude) the clinical suspicion and to localise the lesion with sufficient precision as to facilitate burr-hole aspiration by the surgeon (4). Except in those rare cases in which gas is seen in an abscess, or calcification in a tuberculoma, the plain skull radiograph is too non-specific to fulfil either of these criteria. Angiography and air studies may permit more accurate localisation, although the distinction between the abscess itself and surrounding oedema is often impossible; 'specific' findings at angiography are only relatively so, and lacking in many cases (5). Angiography is arguably more useful for the exclusion of other types of lesion. The appearances of isotope scans are also non-specific in the large majority of cases, but localisation of the lesion is often excellent, with a clear demonstration of the abscess as distinct from the surrounding oedema (3).

In the present study, three lesions were not identified. Two of these were temporal lesions of at most 1.5 cm diameter, in patients examined very shortly after the onset of symptoms, and it is possible in both cases that no actual abscess had formed at the time of the C.A.T. The third non-visualised abscess was within the cerebellum in a patient who also had a temporal lobe abscess; the posterior fossa was not satisfactorily examined. In a fourth case an area of oedema was identified in the parietal region, but when the scan was repeated after contrast medium injection, the highest tomographic cut was still below the level of the superficially lying lesion. Thus, in this case, localisation was partially successful, but not pathological diagnosis; this was also true in two further cases, in which the nature of a subdural empyema was not appreciated and a tuberculoma was diagnosed as a glioma. Even in retrospect, this latter mistake could not have been avoided.

Thus, there were 9% of cases in which localisation was not successful and 9% in which the correct diagnosis was not made; using this single, non-invasive investigation, diagnosis and localisation were correct in 82%.

The adequacy of C.A.T. in this context is underlined by the small number of patients on whom radiological studies other than plain skull radiography were carried out: angiography in 9 (28%); radioisotope scans in 7 (22%) and an air study in 1 (3%). EEGs were recorded in 6 patients (19%).

The high proportion of abscesses showing enhancement with contrast medium injection (25 of 26 cases) and the greatly improved accuracy of localisation of the lesion thus obtained make it mandatory that injection should be carried out whenever the clinical diagnosis of abscess is raised. Of the 37 abscesses present in the 26 patients to whom contrast medium was given, 26 showed a ring of enhancement, and although similar appearances may be seen in a number of other conditions, given the appropriate clinical picture, this observation is most suggestive. Furthermore, the ring enhancement seen in other conditions can often be distinguished: thus, for example, the 'capsule' of tumours is usually thicker and irregular, with enhancement within it or associated solid nodules, and oedema may not be striking in the presence of considerable midline displacement, whereas with infarcts there is commonly little or no mass effect, and the ring enhancement occurs at the periphery of the lesion rather than within it. With both gliomas and metastases the attenuation coefficients may be increased above those of normal brain before enhancement, while, with the exception of two tuberculous lesions, all the abscesses were at most isodense with brain, usually being of lower density.

In addition to being an aid in the localisation of the abscess, the ability of C.A.T. to show after contrast medium injection the presence of multiple loculi may be of great assistance to the surgeon. We have found that clear demonstration of this characteristic may be obtained most satisfactorily by carrying out the post-enhancement C.A.T. 1 or 2 hours after injection of the contrast medium rather than immediately.

It was further observed in several of our cases that the "capsule" no longer enhanced after apparently successful aspiration of the abscess, whereas, in cases where enhancement was still seen, there was good clinical evidence that active infection was still present. For this reason, we would strongly suggest that no barium contrast medium be instilled into the abscess cavity at the time of drainage, not only because the high density of such contrast medium may create unwelcome artefacts on subsequent C.A.T. examinations, but because it may obscure uptake of the intravenous contrast medium. When C.A.T. is freely available for follow-up examinations, instillation is not necessary, and the introduction of a foreign body which the surgeon may later feel constrained to excise may thus be avoided.

When an abscess is suspected in postoperative cases, it is clear that C.A.T. will always show an abnormality; for the demonstration of an abscess in this situation, intravenous contrast medium must be used.

Five of the eight fungal abscesses have been noted as showing homogeneous enhancement rather than the typical ring pattern; this may be related to the more granulomatous nature of these lesions. The most important differential diagnostic feature in all these cases was perhaps their occurrence in patients receiving immunosuppressive drugs, while a previous history of tuberculous meningitis was obtained in the majority of patients with tuberculomata. These observations are significant in that the differentiation between these lesions and pyogenic abscesses was often impossible on C.A.T. criteria alone, except in the two cases in which tuberculomata were calcified. It may be remarked, however, that although half the patients with non-pyogenic abscesses

were observed to have multiple lesions, only 3 of the 22 other patients showed this feature.

The demonstration of C.A.T. abnormalities (areas of lowered attenuation coefficients, without space-occupying effect) in patients with encephalitis or meningitis is of interest, but not of great practical use. There is some hope, however, that observation of these changes in herpes simplex encephalitis may, with isotope and angiographic data (7) result in earlier diagnosis, and possibly thereby in improved prognosis. The late effects of this disease may also be documented by C.A.T.

C.A.T. also plays a part in the exclusion of other lesions, e.g. abscess or tumour, in patients with encephalitis or meningitis. In the latter condition, its main role is in the detection and management of such complications as hydrocephalus.

Conclusions

C.A.T. is the radiological method of choice for diagnosis, localisation and subsequent management of intracranial abscesses, and in many cases will render other forms of investigation unnecessary. It is the only non-invasive technique which will clearly demonstrate multilocular lesions, multiple small lesions and intraventricular rupture. It is also of use in the differential diagnosis of encephalitis and in the management of the complications of meningitis.

Addendum

A further case of aspergillous abscess has come to our attention. This patient had disseminated aspergilloma, was on large doses of steroids and had a cerebral lesion diagnosed as an infarct, but eventually shown at autopsy to be an abscess.

References

1. BELLER, A.J., SAHAR, A., PRAISS, I.: Brain abscess. A review of 89 cases over a period of 30 years. Journal of Neurology, Neurosurgery and Psychiatry 36, 757-768 (1973).
2. CLAVERIA, L.E., DU BOULAY, G.H., MOSELEY, I.F.: Intracranial infections: investigation by computerised axial tomography. Neuroradiology (1976) (in press).
3. DAVIS, D.O., POTCHEN, E.J.: Brain scanning and intracranial inflammatory disease. Radiology 95, 345-346 (1970).
4. GARFIELD, J.: Management of intracranial abscess. A review of 200 cases. British Medical Journal 1969/II, 7-11.
5. LEEDS, N.E., GOLDBERG, H.I.: Angiographic manifestations of cerebral inflammatory disease. Radiology 98, 595-604 (1971).
6. PACTON, R., AMBROSE, J.E.A.: The EMI Scanner. A brief review of the first 650 patients. British Journal of Radiology 47, 530-565 (1974).
7. PEXMAN, J.H.W.: The angiographic and brain scan features of acute Herpes simplex encephalitis. British Journal of Radiology 47, 179-184 (1974).

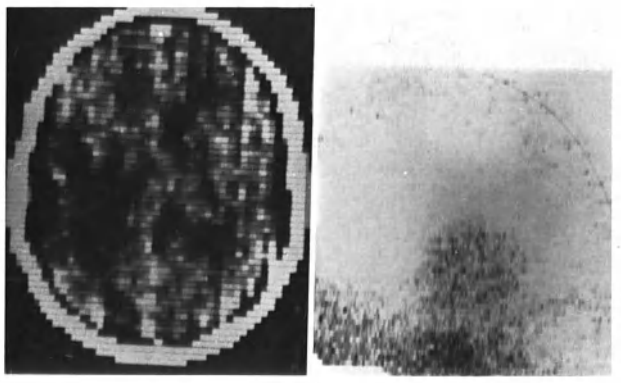

a b

Fig. 1a and b. Otogenic abscess (not included in present series). (a) 80 matrix C.A.T. (b) left lateral isotope scan. The C.A.T., made without contrast medium, does not separate abscess and oedema; scan shows only the former

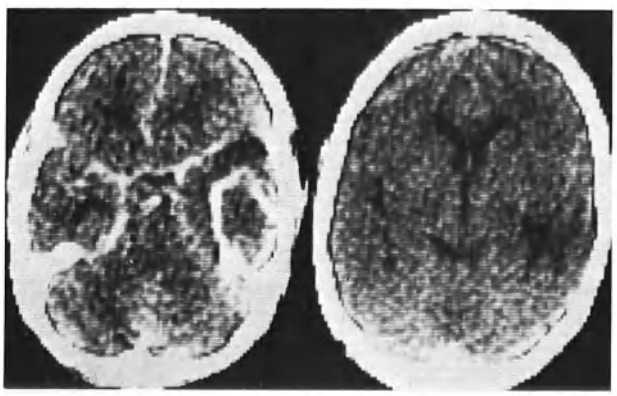

a b

Fig. 2a and b. Typical right temporal lobe abscess. (a) Enhancement of capsule by intravenous contrast medium. Anterior displacement of middle cerebral artery. (b) After successful treatment: oedema only; no enhancement

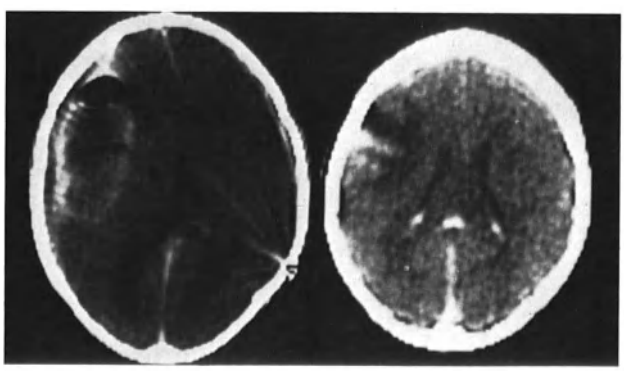

a b

Fig. 3. (a) Subdural empyema. Irregular enhancement of capsule. Contents loculated (air bubbles) and denser than CSF. (b) Frontoparietal tuberculoma mimicking a glioma (enhanced)

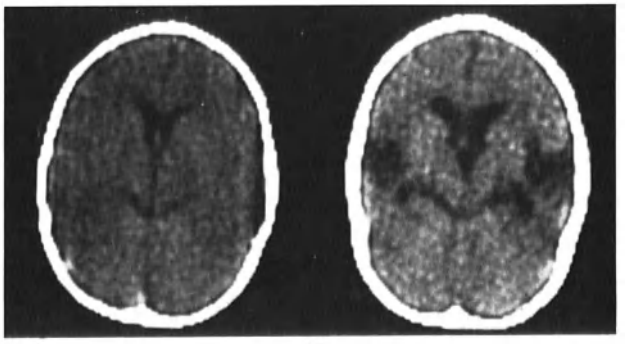

a b

Fig. 4a and b. Herpes simplex encephalitis. (a) Acute phase: vague left temporo-parietal low density. (b) One year later: necrosis of both temporal lobes, mild hydrocephalus. (There was also right frontal necrosis)

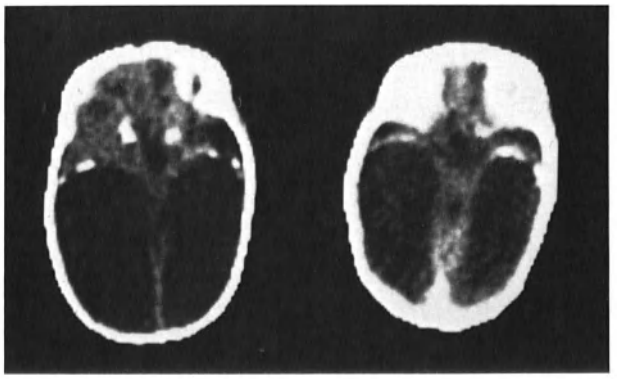

a b

Fig. 5a and b. Intrauterine toxoplasmosis. (a) Perisellar and periventricular calcification; gross hydrocephalus. (b) After contrast medium injection middle cerebral arteries lie free in CSF. Normal superior vermis in the midline

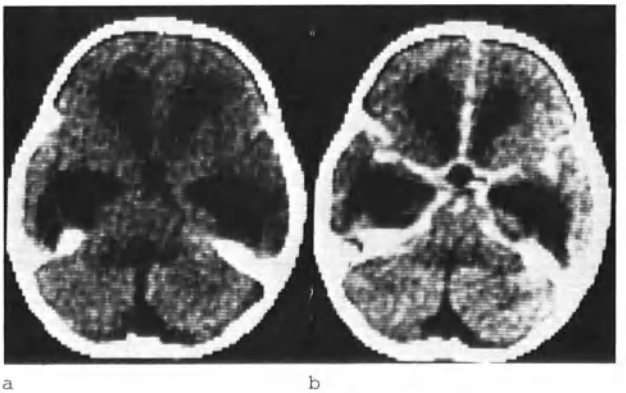

a b

Fig. 6a and b. Tuberculous meningitis. (a) Marked hydrocephalus. (b) Abnormal hypervascular tissues surround the circle of Willis, evidence of basal meningitis

C.A.T. in Leukodystrophy and Neuronal Degeneration

B. E. Kendall, L. E. Claveria, and W. Quiroga*

Conventional neuroradiology previously had a limited part to play in distinguishing the diseases grouped under the generic terms leukodystrophy and neuronal degeneration from tumours when the clinical presentation was atypical. Atrophy may occur in any of these conditions and its distribution is sufficiently distinctive to allow recognition of, for example, striatonigral and pontocerebellar degeneration and of progressive supranuclear palsy on pneumoencephalograms.

The attentuation characteristics of normal white and grey matter distinguish them on C.A.T. Extremes of normal variation of grey matter are 18-30 and of white matter 11-18. Attenuations extending outside these ranges are recognised visually as abnormal at usual window levels, but white matter in the low normal range may occasionally be difficult to distinguish without reference to the print-out. C.A.T. may be expected to show attenuation changes in addition to possible atrophy in some of the conditions being discussed (10). In order to assess the incidence and specificity of any abnormalities we have reviewed those patients who have been examined with the 160 × 160 matrix scanner in whom a diagnosis of one of these conditions has been established. The differential diagnosis is discussed in relation to other cases presenting with similar C.A.T. appearances over the same period. The results are set out in Tables 1-7.

Discussion

Leukodystrophies

Leukodystrophy is the generic term for a heterogeneous group of conditions which have in common several clinical and morphological characteristics. They include spongiform leukodystrophy (Canavan's diffuse sclerosis), Alexander's disease, metachromatic leukodystrophy, globoid leukodystrophy (Krabbe's disease) and sudanophilic leukodystrophy which includes adreno-leukodystrophy (7). They are usually inherited in an autosomal recessive manner. The myelin sheaths are abnormal and the white matter is replaced by glia, often of loose structure with increased fluid content, whereas the grey matter is relatively unaffected. The conditions are bilateral and symmetrical and the degeneration is progressive, sometimes leading in chronic cases to considerable atrophy before death. The usual presenting symptoms are symmetrical motor and sensory disabilities, the emphasis depending on the major site of pathology. Mental retardation and dementia often occur later but convulsions are not a prominent feature. The findings on our cases are shown in Table 1.

---

*Lysholm Radiological Department, The National Hospital, London.

Table 1. Leukodystrophies

Case	Diagnosis	Evidence	Associated condition	Sex and age	Family history	C.A.T. distribution	C.A.T. follow-up	Clinical course
1	Spongiform	Biopsy	-	M/16	+S	Generalised	Increased	Progressive
2	Spongiform	Sib. of case 1	-	M/6	+S	Generalised	Increased	Progressive
3	Metachromatic	Urine/enzyme	-	F/7	-	Generalised	-	Progressive
4	Metachromatic	Urine/enzyme	-	M/35	-	Frontal atrophy	-	Progressive
5	Adreno-leuko-dystrophy	Post mortem	-	M/6		General, occipital +	Increased	Progressive
6	Adreno-leuko-dystrophy	"	-	M/7	-	Occipital	-	Progressive
7	? Adreno-leuko-dystrophy	Clinical	Cataract/ glaucoma	M/8	-	General parietal and occipital + 'atrophy'	Increased	Progressive
8	Leuko-dystrophy	Clinical	-	M/6	C	Generalised	Increased	Progressive
9	Leuko-dystrophy	Clinical	-	M/3	+S	Generalised	Increased	Progressive
10	Leuko-dystrophy	Clinical	-	M/7	-	Generalised	Increased	Progressive

S = Sib affected
C = Parents consanguinous

Spongiform leukodystrophy (Canavan's diffuse sclerosis) is characterised pathologically by almost complete demyelination of cerebral white matter. It is replaced by a loose glial network which appears oedematous and contains large spaces between the glial fibres on histological examination. Our two cases were brothers, the disease in the elder being proven by biopsy. Megalencephaly, which is especially common in the infantile forms of this disease, was present in both patients and, as usual, neurological deterioration was continuous. C.A.T. showed identical changes in both siblings (Fig. 1); there was extensive symmetrical, low attenuation (7 Hounsfield units) throughout the white matter of both cerebral hemispheres, noticeably sparing the internal capsules. There was widening of the interhemispheric fissures indicating some atrophy. Similar findings have been reported and illustrated in a case report (2).

Alexander's disease presents an indistinguishable clinical syndrome and the macroscopic appearance of the brain is also similar. Microscopically, Rosenthal fibres massed around the blood vessels and adjacent to the ependyma and pia characterise the disease. Though we have not examined cases with C.A.T. it is probable that the appearances would be similar to those in spongiform degeneration.

Metachromatic leukodystrophy is associated with deficiency of the enzyme aryl sulphatase A which can be detected by examination of blood from affected subjects. There is accumulation of sulphatides in cells of the central and peripheral nervous system and in many viscera. This substance shows characteristic staining reactions and the disease can be most easily diagnosed by demonstrating the sulphatides in epithelial cells obtained from urinary sediment. In addition to the typical leukodystrophy the affected subjects may have peripheral neuropathy. Case 3 of our series was aged 7 and fairly rapidly progressive. There was generalised periventricular low attenuation most marked in the frontal region (Fig. 2a). Case 4, aged 35, had shown a history of slowly progressive mental deterioration since the age of 15 and was now severely demented and epileptic. In addition to low attenuation, which was considerably more marked in the frontal white matter than elsewhere, there was moderate dilatation of the lateral and third ventricles due to cerebral atrophy.

In *globoid cell leukodystrophy* or Krabbe's disease there is deficiency of the enzyme galactocerebrosidase which can be estimated in blood samples. There is accumulation of cerebroside, which can be detected by staining with PAS in epithelioid cells in the central and peripheral nervous system, causing a combined leukodystrophy and peripheral neuropathy. The disease mainly affects young infants and death usually occurs under 2 years of age. Though we have not examined cases with C.A.T. there is no reason to suspect that the appearances would not be similar to extensive involvement by other leukodystrophies.

Adrenoleukodystrophy is transmitted as an X-linked recessive, typically affecting boys of about 4-6 years. The leukodystrophy is most pronounced in the occipital lobes and the disease typically presents with cerebral blindness. There is breakdown of normal myelin resulting in a non-specific accumulation of sudanophil material in the affected regions. It is unknown why adrenal cortical atrophy is associated with this condition, but it aids in recognition when there is clinical or biochemical evidence of its presence such as increased skin pigmentation or high ACTH levels in the blood (1). In cases 5 (Fig. 2b) and 6 the diagnosis was proved at post-mortem. The low attenuation was most pronounced in the white matter of the occipital and parietal lobes and spared the frontal lobes. Identical changes have been illustrated in a case report (5).

There was no biopsy or biochemical proof of the diagnosis in our other four cases, but the progressive clinical picture was associated with a similar C.A.T. abnormality to that in the six proved cases and the extent of the C.A.T. abnormality increased after intervals ranging between several months and 1 year. In case 8, the parents were consanguinous and in case 9 a brother had a similar disease.

It appears, therefore, that this C.A.T. abnormality of well demarcated, symmetrical, low attenuation in the cerebral white matter, in association with an appropriate clinical syndrome, is highly suggestive of leukodystrophy and that the distribution of the abnormality may be of some help in suggesting the type of leukodystrophy.

Similar C.A.T. Appearances in Other Conditions

Demyelination Associated with or Following Systemic Illness

Of our 10 cases fitting into this category, 5 showed no abnormality on C.A.T. The typical lesion shown histologically in these conditions (6) are small perivenous demyelinations and cellular infiltrations similar to those which have been most extensively studied in postvaccinial encephalomyelitis (4) and which are too small to be shown on C.A.T. Only when these lesions become confluent or, for unknown reasons, are associated with unusually marked surrounding oedema, which can occasionally be sufficient to cause death from tentorial coning, will they be visible. Five of our patients, all with clinical evidence of diffuse or multifocal involvement of the CNS, showed one or more low-attenuation lesions which varied on serial C.A.T.s (Table 2). None of

Table 2. Encephalomyelitis

Sex and age	Presentation systemic illness	C.A.T. low attenuation	Follow-up C.A.T. low attenuation	Clinical progress
F/6	Intellectual Deterioration Brain stem signs	Cerebellum and Brain stem	2/12. L. Parietal	Improved
M/21	R. sensory disturbance, cord lesion	Normal	1/12. L. Parietal	Improved
F/5	R. hemiparesis	L. cerebellar	3/52. Cleared	Normal
F/23	Visual loss	L. parieto-occipital	3/52. R. parieto-occipital	Normal

the lesions showed enhancement following intravenous contrast injection. One of these patients is of particular interest because the initial C.A.T. showed diffuse low attenuation in the cerebral white matter similar to that in the leukodystrophies. During the following month the patient's condition improved from one of semi-coma with bilateral paresis to moderate confusion, but there was now a dense left hemiplegia. Repeat C.A.T. showed marked decrease in the extent of the bilateral low attenuation, but there was now enlargement of the lateral ventricles and a circumscribed low attenuation in the right internal capsule suggesting an infarct. At this time the patient also had evidence of a spinal cord lesion. After a further month the patient had recovered further, but had a residual left hemiparesis, and the C.A.T. showed

clearing of the periventricular low attenuation but persistence of the other features. This patient is grouped in Table 3 with two other patients in whom C.A.T. showed similar extensive, symmetrical, low attenuation in the cerebral white matter and who are considered to fit best into the group of post-infective or allergic demyelination. They both had subacute cerebral illnesses accosiated with a minor systemic illness. In one of them follow-up C.A.T. showed decrease in the abnormality, associated with clinical improvement (Fig. 3). The other patient completely recovered clinically, but there was no C.A.T. follow-up.

Table 3. Encephalomyelitis

Diagnosis	Evidence	Associated condition	Sex and age	Family history	C.A.T. distribution	C.A.T. follow-up	Clinical course
? Encephalitis	Large head, regression/ spastic	Diarrhoea, vomiting chest infection	M/1¼	-	General	Decreased	Improved
? Encephalitis	Headache/ ataxia	Pyrexia and vomiting	M/3	-	General	-	Recovered
Encephalomyelitis	Clinical	Fever and rash, CSF lymphocytosis	M/24	-	General	Decreased atrophy R. capsular infarct	Cord lesion

Low Attenuation in Patients with Muscular Dystrophies (Table 4)

There were two patients with muscular disorders, one muscular dystrophy with consanguinous parents, and one with myopathy (Fig. 4a) which was also present in the father and only sibling. Both children had evidence of a cerebral disorder and C.A.T. showed generalised low attenuation in the cerebral white matter without enhancement following intravenous

Table 4.

Clinical abnormality	Associated condition	Sex and age	Family history	C.A.T. distribution	C.A.T. Follow-up	Clinical course
Spasticity	Muscular	F/5/12	C	General	Decreased	Static 2 years
Large head, retarded, epileptic	Myopathy also in father and sister	F/8	-	General	-	Improved

contrast medium. One patient remained static clinically over 2 years and follow-up C.A.T. scan showed decrease in the low attenuation. The other patient also improved, but there has been no follow-up C.A.T. The nature of the cerebral pathology in these children is unknown; it could be merely fortuitous, but the association with muscular disorders

is documented for interest. Enlarged lateral ventricles and cortical atrophy have been reported on air encephalograms in patients suffering from spinal neurogenic muscular atrophy and muscular dystrophy (9). Neuropathological study in patients with Duchenne and myotonic muscular dystrophy (12) has revealed low brain weight and an increased number of ectopic nerve cells in subcortical white matter, best explained by decreased neuronal migration in foetal life. Mental deficiency is associated in an unusually large percentage of patients with muscular dystrophy.

Vascular Disorders (Table 5)

Table 5. Vascular Disorders

Diagnosis	Evidence	Associated condition	Sex and age	Family history	C.A.T. distribution	C.A.T. follow-up	Clinical course
Encephalopathy	-	BP240/140	M/2	-	General	-	Recovered
Encephalopathy	-	Hypertension 2 years	M/48	-	General	-	Improved
-	Dementia	Polycythaemia	M/55	-	General	-	Static
-	Dementia	Polycythaemia	F/60	-	General	-	Static

Generalised, well-demarcated, symmetrical, low attenuation in the central cerebral white matter was also found in two patients with hypertensive encephalopathy (Fig. 4b). Both were severely confused, with papilloedema. The blood pressure was reduced, in the first case following nephrectomy for unilateral renal artery stenosis associated with medullary sclerosis of the kidney and in the second by hypotensive drug therapy. The first case completely recovered and the other improved, but there were no follow-up C.A.T. scans.

Two patients with polycythaemia presented with severe dementia. There was markedly diminished cerebral blood flow in all regions, which was improved in one case following treatment but there was no concomitant improvement in the neurological condition and no follow-up C.A.T. has yet been performed. White matter degeneration in association with polycythaemia has been described (3) and is thought to be the result of ischaemia associated with slow cerebral blood flow. The possibility of its being associated with antimetabolite treatment has also been suggested but this has not been administered in our patients.

Disseminated Necrotising Leukoencephalopathy (Table 6)

C.A.T. scans have been performed on two patients in whom this diagnosis has been established at autopsy. Both had been subjected to cranial radiotherapy and to prolonged courses of intrathecal and systemic antimetabolite drugs, mainly methotrexate for malignant meningitis following lymphosarcoma and lymphoblastic leukaemia respectively. After initial improvement, both suffered a progressive cerebral illness. In the 54-year-old woman this was acute, and progressed to coma before

Table 6.

Diagnosis	Evidence	Associated condition	Sex and age	C.A.T. distribution	C.A.T. follow-up	Clinical course
Necrotising leukoencephalopathy	Autopsy	Lymphosarcoma D X T methotrexate	F/54	General	-	Progressive
Necrotising leukoencephalopathy	Autopsy	Lymphoblastic leukaemia D X T methotrexate	M/9	General with calcification	1/12 Static	Progressive

death. C.A.T. (Fig. 5a) showed extensive low attenuation throughout both cerebral hemispheres similar to that occurring in the leukodystrophies. At autopsy the brain was diffusely necrotic and oedematous.

The child had a much slower course, with increasing mental deterioration over 3 years before death from pneumonia. C.A.T. scans, in addition to showing the symmetrical low attenuation, also revealed linear symmetrical calcification in the cerebral white matter and basal ganglia (Fig. 5b). Our cases are similar to those reported at autopsy (13) which showed extensive multifocal coagulative necrosis extending to confluence with associated oedema. There is a notable absence of inflammatory and macrophage reaction. Microscopy shows demyelination with axonal damage, gliosis and focal status spongiosis. Mineralised debris has been noted in the necrotic foci (8, 11). The condition is thought to be due to disturbance of the blood-brain barrier by radiotherapy which allows antimetabolites to penetrate into the cerebral white matter. These probably interfere with the function of the oligodendrocytes with subsequent necrosis of the myelin.

C.A.T. abnormalities in our patients with neuronal degeneration are shown in Table 7. The main purpose of C.A.T. in these conditions is to exclude an underlying tumour, infarct or hydrocephalus in clinically atypical cases. Atrophy of expected distribution is frequently (Fig. 6b) though by no means invariably present. More specific changes were present in a few cases, such as cavitation in the basal ganglia in three cases with Parkinsonism (Fig. 6a). This is known to be more frequent and severe at autopsy in postencephalitic Parkinsonism, but it occurred in one case of each aetiology in our series.

In one of our three patients with Wilson's disease there was increased attenuation (up to 200 Hounsfield units) in the thalami. The other two were normal.

Many children with signs suggesting failure of normal cerebral development or of regression, progressive focal disturbances or epilepsy, have been examined with C.A.T. over the period of this survey, and C.A.T. has been useful in separating those with congenital abnormalities, tumours, infarcts and birth trauma from those which we have discussed. We are not aware of any cases of leukodystrophy which have not had an abnormal C.A.T. scan at first examination but, because similar appearances can occur in other conditions which are not necessarily progressive, we feel that follow-up C.A.T. is essential unless there

Table 7. Neuronal degeneration

Parkinsonism	Postencephalitic	7	Cavitation basal ganglia (1) Moderate atrophy (4) Normal (3)
	Ideopathic	2	Cavitation basal ganglia (1) Sylvian fissures enlarged (1) Normal (1)
	Shy-Drager	2	Brain stem atrophy (2) All ventricles enlarged (2) Cortical sulci and cerebellar sulci enlarged (2) Normal (O)
Striato-nigral atrophy	Ideopathic	2	Cavitation basal ganglia (1) Anterior horns enlarged (1) Normal (O)
	Birth injury	1	Cavitation basal ganglia (1) Cortical cerebellar atrophy (1)
Hepato-lenticular degeneration (Wilson)		3	Increased attenuation (200 Hounsfield units) (1) Normal (2)
Hereditary cerebellar ataxia		5	Brain stem atrophy (2) Enlarged fourth ventricle (3) Enlarged cerebellar sulci (2) Normal (2)
Progressive supra nuclear palsy (Steele-Richardson)		3	Moderate enlargement of lateral ventricles and cortical sulci (3) Brain stem normal (3) Normal (O)
Motor neurone disease		2	Moderate enlargement of lateral ventricles (1) Cortical sulci enlarged (1) Normal (1)

is clinical or histological confirmation of a leukodystrophy. During the same period we have examined several children with megalencephaly of unknown cause, (including three with Soto's disease) in whom the brain appeared normal or showed only slightly enlarged ventricles.

Summary

At the time of presentation, leukodystrophy is characterised by symmetrical, well-defined, low attenuation in the cerebral white matter. Early in its course each disease has a tendency to a particular distribution of changes, but the general appearances are similar in all the leukodystrophies. Similar C.A.T. appearances may occur in the other conditions which have been discussed. Some of these may regress spontaneously or be amenable to therapy, whereas the leukodystrophies are always progressive. All the diseases in which neuronal degeneration occurs may be associated with atrophy maximum in the appropriate distribution of the disease process, but frequently also more diffuse. C.A.T. is useful in distinguishing atypical cases from other pathologies.

References

1. BLAW, M.: Adrenoleukodystrophy. In: Handbook of Clinical Neurology. VINKEN, P.J., BRUYN, G.W. (eds.). Amsterdam: North-Holland 1973, pp. 128-133.
2. BOLTSHAUSER, E., ISLER, W.: Computersied axial tomography in spongy degeneration. Lancet 1976/I, 1123.
3. D'AGOSTINO, A.N., PEASE, G.L., KERNOHAN, J.W.: Cerebral demyelination associated with polycythaemia vera. Journal of Neuropathology and Experimental Neurology 22, 138-147 (1963).
4. DE VRIES, E.: Postvaccinial Perivenous Encephalitis. Amsterdam: Elsevier 1960, pp. 18-63.
5. DUDA, E.E., HUTTENLOCHER, P.R.: Computed tomography in adrenoleukodystrophy. Correlation of radiological and histological findings. Radiology 120, 349-350 (1976).
6. ELLSWORTH, C.A.: Acute disseminated encephalomyelitis and allergic neuroencephalopathies. In: Handbook of Clinical Neurology. VINKEN, P.J., BRUYN, G.W. (eds.). Amsterdam: North-Holland 1970, pp. 500-571.
7. ERDOHAZI, M.: The leukodystrophies. Proc. of the Roy. Soc. Med. 68, 561-562 (1975).
8. FLAMENT-DURAND, J., KETELBRANT-BALASSE, P., MAURUS, R., REGNIER, R., SPEHL, M.: Intracerebral calcifications appearing during the course of acute lymphatic leukaemia treated with methotrexate and X-rays. Cancer 35, 319-325 (1975).
9. HOVSTAD, L., LOCHEN, E., SJAASTAD, O.: Pneumoencephalographic findings in various primary and secondary muscular disorders. Acta Neurologica Scandinavia 53, 128-136 (1976).
10. LANE, B.: Cerebral white matter disease on CT scanning. Proceedings of 14th Annual Meeting of American Society of Neuroradiology. Neuroradiology 12, 43-55 (1976).
11. PRICE, R.A., JAMIESON, P.A.: The C.N.S. in childhood acute leukaemia. Subacute leukoencephalopathy. Cancer 35, 306-318 (1975).
12. ROSMAN, N.P., KAKULAS, B.A.: Mental deficiency associated with muscular dystrophy - a neuropathological study. Brain 89, 769-787 (1966).

13. RUBENSTEIN, L.J., HERMAN, M.M., LONG, T.F., WILBUR, J.R.: Disseminated necrotising leukoencephalopathy. Cancer 35, 291-305 (1975).

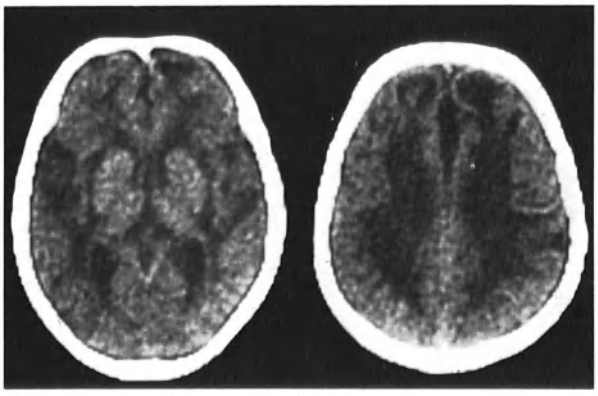

a b

Fig. 1. Case 1: Spongiform degeneration. Symmetrical low attenuation (average 7 Hounsfield units) in cerebral white matter. Note sparing of internal capsules. Widening of interhemispheric fissure due to atrophy

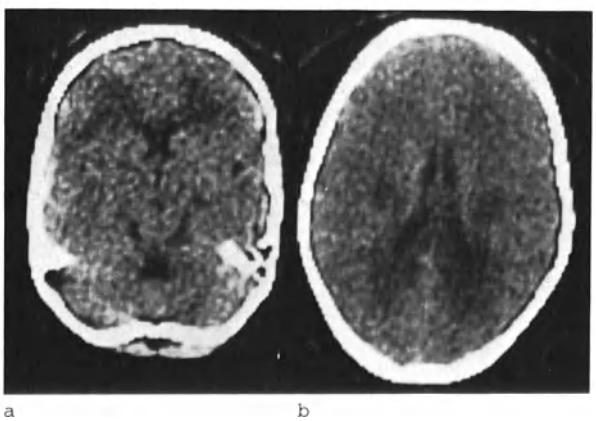

a b

Fig. 2. (a) Case 3: Metachromatic leukodystrophy. Symmetrical low attenuation in deep white matter, most prominent in frontal lobes. (b) Case 5: Adreno-leukodystrophy. Symmetrical low attenuation prominent in occipital lobes, sparing frontal lobes

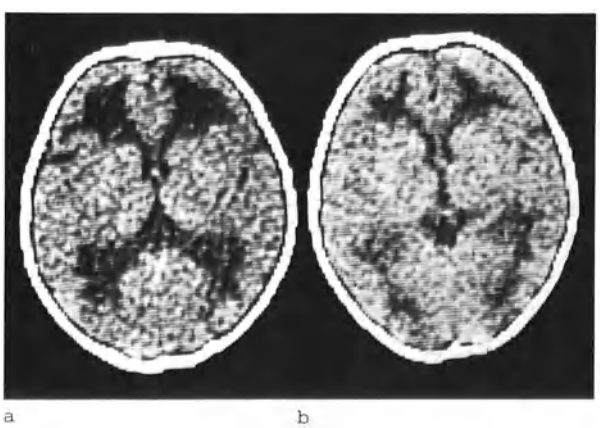

a b

Fig. 3a and b. Case 12: Encephalitis. (a) Symmetical low attenuation corona radiata. (b) 5 weeks later following clinical improvement, diminution in C.A.T. abnormality

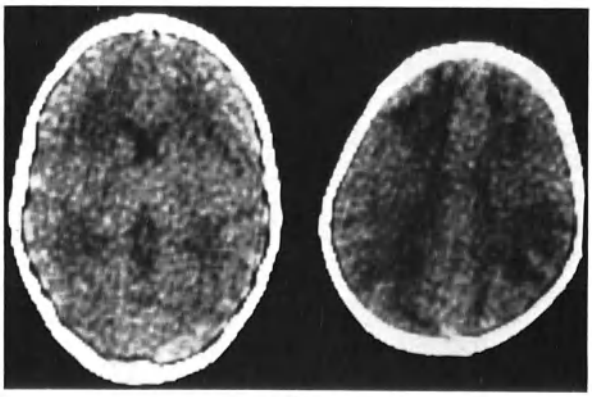

a b

Fig. 4a and b. Symmetrical low attenuation in corona radiata. (a) Case 11: Myopathy; (b) Case 18: Hypertensive encephalopathy (BP 240/140)

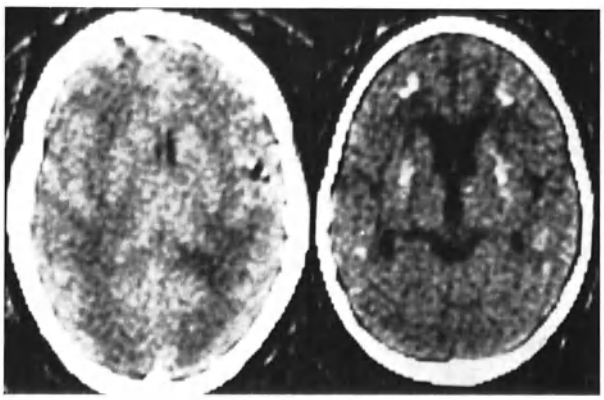

a b

Fig. 5. (a) Case 23: Acute necrotising leukoencephalopathy. Symmetrical low attenuation corona radiata. (b) Case 24: Necrotising leukoencephalopathy. Less extensive low attenuation; curvilinear calcification in white matter and in basal ganglia; minor dilatation of lateral ventricles and Sylvian fissures

a b

Fig. 6. (a) Post-encephalitic Parkinsonism. Symmetrical low attenuation suggesting cavitation in lentiform nuclei. Widening of Sylvian fissures. (b) Shy-Drager syndrome. Diffuse atrophy. Fourth ventricle and basal cisterns dilated. Brain stem small

C.A.T. in Multiple Sclerosis

C. Gyldensted*

One hundred and ten patients with clinically definite multiple sclerosis were examined with C.A.T. of the brain with the 160 × 160 matrix EMI scanner in the period September 1, 1974 to August 31, 1975.

Eighty-two areas of low X-ray attenuation around the ventricular system were found in 40 cases (36%), particularly adjacent to the anterior and posterior horns and trigones. These areas are postulated to represent the large periventricular plaques known to exist in multiple sclerosis.

Mean plaque volume was 1.26 cm^3 and mean attenuation was 9.5 EMI units. Intravenous injection of isotonic metrizoate (1.5 ml per kilo body weight) did not give further diagnostic information.

Periventricular plaques were associated with central and cortical atrophy of the brain, as only three plaque cases had normal measurements. A total of 49 patients (45%) with atrophy and no plaques were found, while only 20 cases (18%) had normal EMI scans.

No difference in duration of disease or age at onset could be statistically confirmed between the three different groups of multiple sclerosis patients.

A more detailed report will be published in Neuroradiology 11 (1976).

*Department of Neuroradiology, Rigshospitalet, Copenhagen, Denmark.

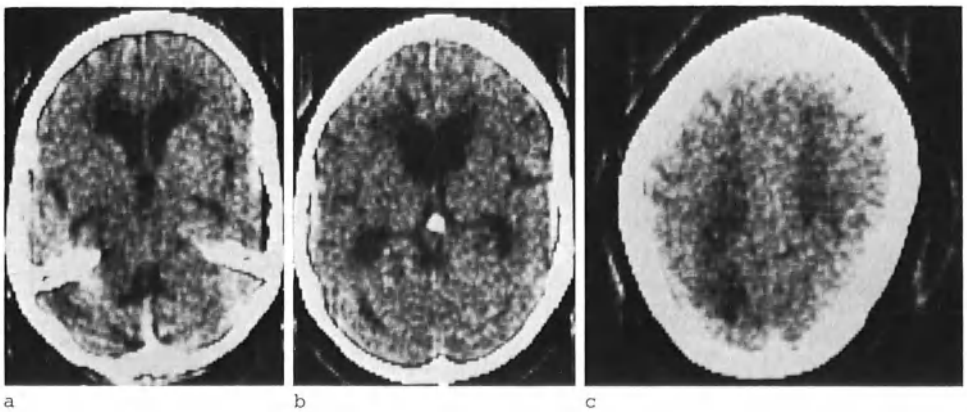

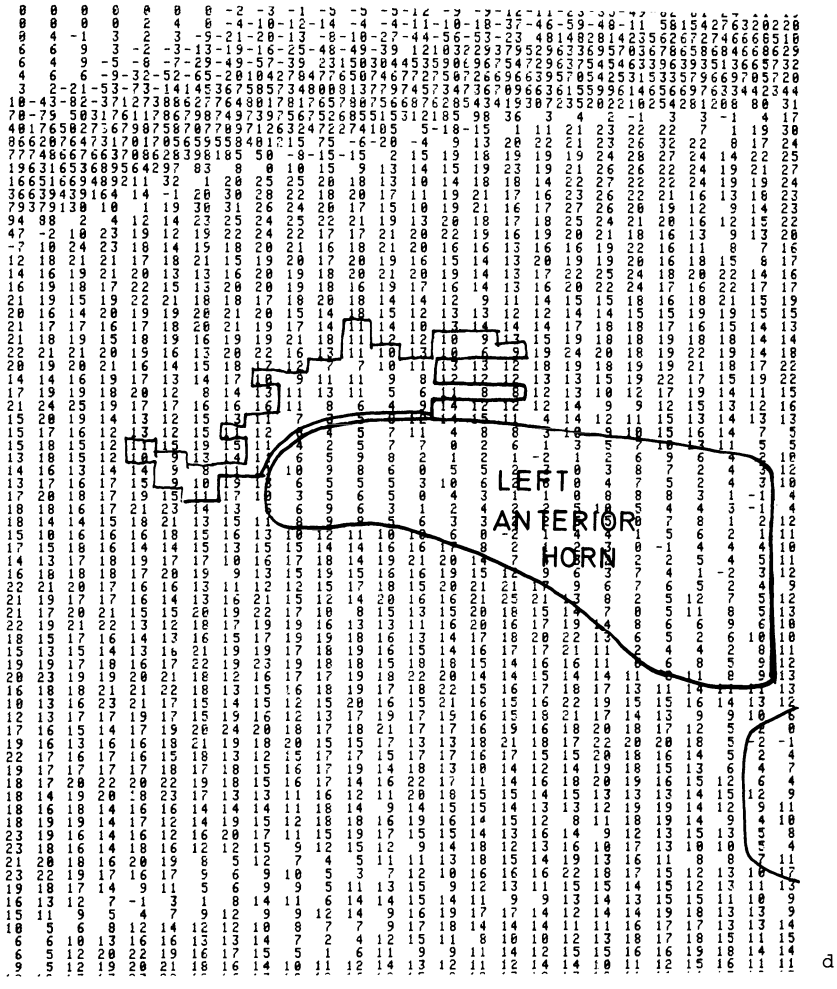

Fig. 1a-d. A.J. Female, age 58 years. MS for 40 years. Moderate ventricular enlargement and cortical atrophy. (a) and (b) Two contiguous sections showing large plaques at lateral angles of left and right anterior horns. Total plaque volume left side: 6.2 cc, right side 4.0 cc. (c) C.A.T. from the same patient at a higher level showing an area of pathologically low attenuation above the left occipital horn considered to be a cerebral plaque. Volume 2.8 cc. Mean attenuation 9.0 EMI units. (d) Detail of 160 × 160 pixel paper print corresponding to (a) showing plaque at left anterior horn

Hydrocephalus, Atrophy and Their Differential Diagnosis - CSF Dynamics Investigated by Computer Cisternography

T. Hindmarsh and T. Greitz*

The differential diagnosis between hydrocephalus and cerebral atrophy constitutes a challenge to the clinician. The concept of low pressure hydrocephalus introduced in the sixties has made this differentiation more important. Pneumoencephalography has offered some aid, but correlations between anatomical observations made at air studies (and at autopsy) and clinical findings have not been satisfactory. So far no reliable method has been found to select patients with hydrocephalus suitable for operation by a shunting procedure. The introduction of isotope cisternography has not brought about a significant improvement of this situation.

Computer assisted (C.A.) cisternography (1) has enabled us to study essentially the same physiological parameters as with isotope cisternography, taking advantage of a higher spatial resolution and a significantly reduced radiation dose to the spinal cord. The aim of the present paper is to correlate the physiological parameters with the anatomical findings observed at C.A.T. However, the clinical data available are not sufficient to make a comparison with the clinical symptoms possible.

Material and Methods

This work is mainly based on experiences in the examination of 51 adult patients referred to the Department of Neuroradiology because of clinical suspicion of communicating hydrocephalus. All these patients were demented. They were examined by computerised tomography using the 160 × 160 matrix. The CSF dynamics were investigated using isotope cisternography in 29 patients, C.A. cisternography in 12, and both methods in 10 patients.

As reference material, 10 patients were examined following lumbar myelography using metrizamide.

For isotope studies, 250 microcuries of 169 Ytterbium DTPA were injected in the lumbar area and scans were taken after 3, 24, and 48 h.

The technique of C.A. cisternography is as follows. The patient is placed in the lateral recumbent position with a firm pillow under his head. The head-end of the table is tilted down about 10°. A lumbar injection is made and 20 ml or metrizamide (Amipaque) in a solution containing 85 mg iodine per ml are injected. The position of the patient brings the bolus of the contrast medium up to the cervicodorsal junction. The patient is left in this position for about 30 min to allow the medium to be transported to the intracranial spaces by the CSF circulation. It is important to keep the head in a sufficiently high position

*Department of Neuroradiology, Karolinska Sjukhuset, Stockholm, Sweden.

to prevent the contrast medium from entering the head by gravity. Scans were usually taken after 3, 6, and 24 h. We have recently begun to give the patients 200 mg phenobarbital as a premedication orally the night before the examination, occasionally supplemented by an intravenous injection of the same amount immediately prior to the examination.

Results

Normal (reference) material. Cuts taken 3 h after the injection invariably demonstrate contrast medium within the cisterna magna, the basal cisterns and in most cases also within the fourth ventricle (Figs. 1 and 2). A definite enhancement of the third ventricle is rare in a normal group of patients. A slight increase in the attenuation of the lateral ventricles may be observed but stays below 10 EMI units, which means that the attenuation of the CSF remains below that of the brain. The attenuation of the basal cistern usually starts to decrease after 3 h. At the same time contrast medium of increased concentration appears in the Sylvian and interhemispheric fissures. In a normal case, at least in younger individuals, maximum concentration over the convexity is achieved after 12 h.

Patients with clinical hydrocephalus. At C.A. cisternography the same type of pathological change of the CSF circulation was observed as with isotope cisternography. A fairly common observation was that of *slow circulation* with or without a *non-persistent filling of the lateral ventricles* with contrast medium. Sometimes a transient enhancement of the CSF is revealed by the fact that the ventricles are difficult to observe because they are filled with contrast medium. As the contrast medium begins to reach the convexities, the area adjacent to the calvarium shows increased attenuation. At the same time dilated cerebral sulci may still be clearly visible high up on the convexity but after 24 h this is usually no longer the case. This eventual non-visualisation of cisterns and sulci at C.A. cisternography indicates that they have become filled with contrast medium of about the same density as that of the brain and affords a means of determining the maximum filling over the convexity and consequently the speed of the CSF circulation.

As with isotope cisternography a more *persistent and sometimes marked intraventricular uptake* may be observed. In these patients contrast filling over the convexities is usually poor and in three such cases a suggestion of contrast accumulation in the subependymal tissues around the lateral ventricles was observed (Fig. 3). This was thought possibly to be due to a leakage through the ependyma into the subependymal oedematous tissues.

In general a very good agreement was found between C.A.T. studies and isotope studies in the 10 patients who were examined with both methods. The same patients showed transient or persistent intraventricular filling or no intraventricular uptake respectively. When a relative block was observed in the posterior fossa using isotope cisternography, the same findings were made at C.A.T. cisternography.

In order to further elucidate the correlation between the two methods, the attenuation changes with time within the lateral ventricles were evaluated in the 10 patients who were examined with both methods. Curves were then plotted referring to patients with persistent uptake at isotope cisternography, to those with non-persistent uptake and to patients shown to have a normal CSF circulation using isotope cisternography.

These three groups were shown to differ with respect to the time course of the attenuation changes. This suggests a good agreement between the results of the two methods of cisternography. As seen from the curve (Fig. 4) there is a tendency for patients with a normal CSF circulation to have a continuous increase of the attenuation during the first 24 h as opposed to the other two groups.

It was considered important to correlate the anatomical changes with the physiological parameters observed, paying special attention to changes which - according to our experience from pneumoencephalography - could represent either atrophy or hydrocephalus. It was found that in general the same changes occurred as seen at air studies. In a normal case, using our technique, the sulci over the cerebral convexities are barely visible. Most of the Sylvian fissures are not seen at C.A.T. with the exception of their most anterior and lateral extensions. In most cases of hydrocephalus no sulci are seen high up on the convexity in the parietal area. However, as at pneumoencephalography, a marked dilatation of the Sylvian fissures and occasionally of the interhemispheric fissure may be seen. An extension of the dilated Sylvian fissures up into the parietal area is a rather frequent finding and should not be considered to be due to cortical atrophy. Dilatation of the temporal horns has been considered an important sign in pressure and low-pressure hydrocephalus. This dilatation may be observed at C.A.T. The size of the lateral ventricles was estimated by an anterior horn index and the width of the third ventricle was calculated.

The sulci over the convexity were classified as normal, i.e. barely or not visible, moderately enlarged or highly enlarged. Tables 1 and 2 show the results of an attempt to compare the anatomical changes with the physiological parameters observed. The data on CSF dynamics presented in these tables are obtained with either isotope cisternography or C.A. cisternography, or with both methods. As the results in the cases examined with both methods were in complete agreement, all data were pooled.

As seen from Table 1, patients in this selected material with no visualisation of the sulci over the convexities frequently showed an intraventricular uptake of isotope or contrast medium. Such uptake was observed in 70% of the 23 patients with absence of convexity sulci. In 48% the intraventricular uptake was persistent. This occurred only in 11% of patients with enlarged sulci. Persistent filling was also a common observation (52%) in patients with dilated temporal horns and occurred in 60% of patients with a triad consisting of dilated temporal horns, dilated Sylvian fissures and absence of visible sulci over the convexity, i.e. with the findings thought to be characteristic of communicating hydrocephalus. As seen from Tables 3 and 4, a significant positive correlation was observed between persistent filling and increasing width of the anterior horn and a significant negative correlation between the same parameter and a normal CSF circulation.

The size of the third ventricle showed a positive correlation to intraventricular uptake (Table 4).

Discussion

The high sensitivity of C.A.T. allows the subarachnoid spaces to be studied radiologically using iodinized contrast media of low concentration. This sensitivity is exemplified by the fact that an increase of the iodine content of the CSF by 1 mg per ml increases the attenuation

Tables 1-4. Correlations between anatomical changes observed at C.A.T. and physiological parameters studied either by isotope cisternography, by C.A. cisternography or by both methods. Figures indicate the percentage distribution of physiological parameters in patients all showing the same findings with regard to a given morphological parameter

		Normal circulation	Slow circulation	Ventricular filling Transient	Persistent	
Table 1						
Absence of convexity sulci						
23 cases	%	17	13	22	48	
Moderate dilatation of convexity sulci						
19 cases		11	32	47	11	
High grade dilatation of convexity sulci						
9 cases		33	11	44	11	%
Table 2						
Widened Sylvian fissures						
22 cases	%	5	23	36	36	
Widened temporal horns						
23 cases		5	13	30	52	
"Triad"						
10 cases		0	10	30	60	%
Table 3						
Index anterior horn						
<0.29						
16 cases	%	50	19	31	0	
0.29-035						
19 cases		0	32	42	26	
>0.35						
16 cases		6	6	31	56	%
Table 4						
Width of third ventricle						
≤7 mm						
24 cases	%	33	29	29	8	
>7 mm						
27 cases		4	11	41	44	%

of the CSF with 10 to 15 units. A prerequisite for a suitable contrast medium for use in cisternography is a relatively high molecular weight which prevents its rapid absorption from the subarachnoid space. Hence, methiodal sodium of low molecular weight is rapidly absorbed and will not be observed intracranially, while meglumine iocarmate (Dimer **X**) and metrizamide will remain within the subarachnoid space in a sufficient concentration. This difference in absorption is reflected in the time course of the concentration of iodine in the serum following

lumbar injection; a contrast medium of a high molecular weight reaches its peak more slowly than that of a low molecular weight. This difference may also be observed with regard to the renal excretion of the media.

The high frequency of fourth ventricle filling in normal cases is evidently not due to passive transport by gravity as this phenomenon also occurs in patients subjected to lumbar myelography who were kept in a slightly upright position following the examination. The difference in filling between the lateral ventricles and the fourth ventricle may be explained by the fact that the aqueduct to a certain extent constitutes a functional barrier against the ascent of contrast medium. The observed rim of contrast medium around the lateral ventricles of two hydrocephalic patients could be due to a leakage of the medium through the ependyma. Leakage of water into the subependymal tissues has been observed in experimental hydrocephalus, and a zone of low attenuation suggestive of subependymal oedema has been observed at C.A.T. (1).

However, these changes seem to be more frequent in patients with acute hydrocephalus. In patients who had a ventriculo-atrial shunt because of hydrocephalus, the attenuation around the lateral ventricles was higher before shunting than after (2). This suggests that several factors are operating which may change the attenuation around the ventricles in hydrocephalus. Changes in the water content as well as quantitative and qualitative changes of the components of the cerebral tissues such as myelin must be taken into consideration.

The tendency for normal patients examined with C.A. cisternography to have a continuous increase of the attenuation within the lateral ventricles during the first 24 h might possibly be due to the fact that iodine is secreted from the choroid plexus into the lateral ventricles or less likely to simple diffusion of a contrast medium into the ventricles. Although our results clearly demonstrate a correlation between the morphological changes observed at C.A.T. and the changes of the CSF dynamics observed by cisternography, yet no single sign or symptom nor any combination of signs have been found allowing a reliable differential diagnosis between cerebral atrophy and hydrocephalus. However, patients with a generalised widening of the sulci over the convexities, with or without dilatation of the lateral ventricles, tend to have a normal CSF circulation and patients with dilated ventricles having no or only few dilated sulci over the convexity, dilatation of the CSF pathways such as the interhemispheric and Sylvian fissures as well as of the parietal sulci tend to have a pathological CSF circulation and an intraventricular uptake at cisternography.

Conclusions

1. C.A. cisternography is a useful tool in the investigation of CSF dynamics.

2. Its high resolution has afforded new information on normal physiology and abnormal CSF circulation. Retrograde filling of the fourth ventricle is a normal finding.

3. A functional disturbance observed at cisternography may be correlated to anatomical observations of importance in the diagnosis of hydrocephalus and cerebral atrophy.

References

1. GREITZ, T. HINDMARSH, T.: Computer assisted tomography of intracranial CSF circulation using a water-soluble contrast medium. Acta Radiol. (Diagnosis) 15, 497-507 (1974).
2. HINDMARSH, T.: Changes of attenuation coefficient of the periventricular subependymal tissue in hydrocephalic patients. Paper presented at the International Symposium on Computer Assisted Tomography in Nontumoral Diseases of the Brain, Spinal Cord and Eye. Bethesda, Maryland, 1976.

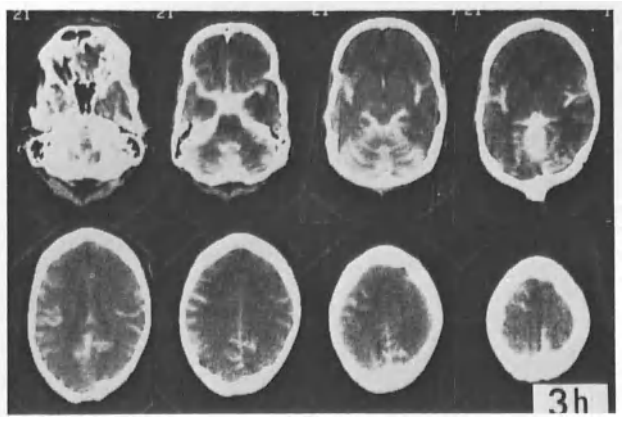

Fig. 1. C.A. cisternography. Normal case 3 h after intrathecal injection of metrizamide. Filling is obtained of fourth ventricle, basal cisterns and subarachnoid space around the cerebellum. Contrast medium begins to appear in Sylvian and interhemispheric fissures

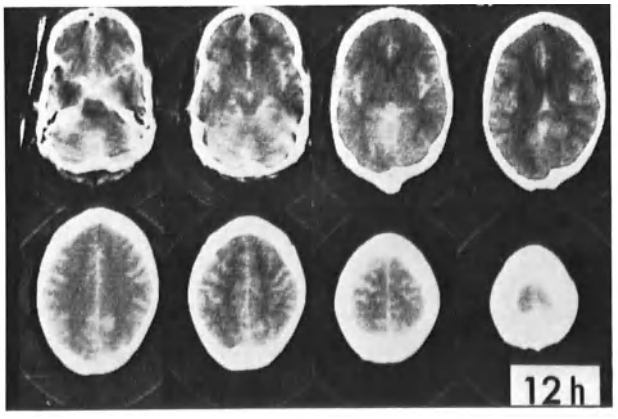

Fig. 2. Same case 12 h after injection. Contrast medium has reached the sulci of cerebral hemispheres

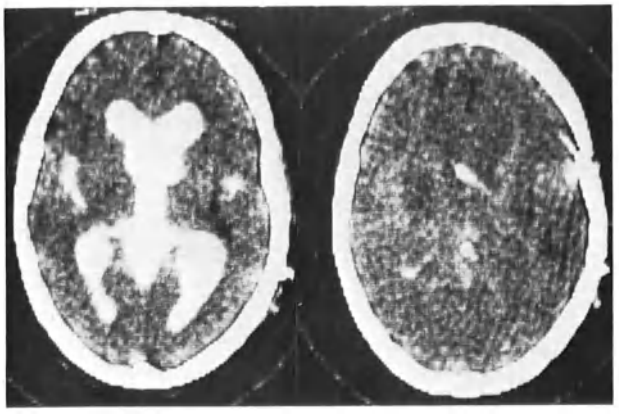

Fig. 3. Patient with communicating hydrocephalus showing persistent intraventricular uptake. Lateral ventricles difficult to observe in right hand picture taken 12 h after injection due to remaining contrast medium; a rim around the ventricles shows contrast enhancement possibly due to leakage into subependymal tissue

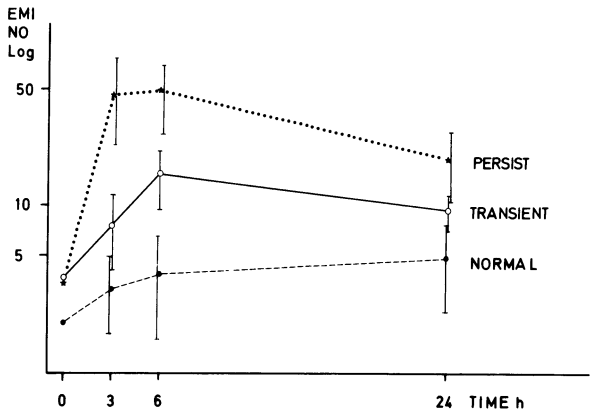

Fig. 4. Mean attenuation changes with time within the lateral ventricles at C.A. cisternography in three groups of patients. Upper curve refers to patients shown to have a persistent intraventricular uptake at *isotope* cisternography, middle curve to those with a transient uptake and bottom curve to those with a normal CSF circulation

The Clinical Significance of "Cerebral Atrophy" as Shown by C.A.T.

L. E. Claveria, I. F. Moseley*, and J. F. Stevenson**

Before the development of C.A.T., the only reliable way of demonstrating atrophic changes in the brain during life was by pneumoencephalography. From the early days of the use of this procedure, measurements have been made of the size of the ventricles (4), although there has been considerable discussion as to their validity (2). Even more difficulty has been encountered in the establishment of normal values for the size of the cerebral sulci, particularly in their relationship to clinical evidence of dementia (1, 3, 9, 11, 13); such correlation has been disappointing. One of the disadvantages has been the difficulty in filling the sulci in some patients without other evidence of convexity block, although some workers have suggested that this may represent a pathological rather than a technical feature (10).

With C.A.T. the morphology of the brain and its pathological modifications can be displayed, without any disturbance, as never before. Thus, it has been possible to show the cerebral sulci, the subarachnoid space around them and the ventricles in the 'natural' state; there is considerable evidence (17) that pneumoencephalography itself may cause significant alterations in e.g., ventricular size, and even (16) in the appearance of the sulci. This unprecedented ability to see with C.A.T. the cerebral structures may have led to an over-willingness to diagnose atrophic changes on the basis of clear visibility of the sulci when the brain was in fact normal. Thus, of the first 5000 C.A.T. examinations performed at the National Hospital, Queen Square, 85% were thought to be abnormal, of which 22% were regarded as showing cerebral atrophy.

Since the use of C.A.T. does provide such an excellent opportunity for the demonstration of normal and pathological anatomy, it was thought essential to attempt to correlate the appearances seen at C.A.T. with the results of psychometry and the clinical state of the patients.

Material and Methods

Eighty-one patients originally diagnosed on the basis of the C.A.T. as having cerebral atrophy were reviewed. Each had been examined with the EMI 160 matrix Scanner, and had had full psychometric assessment. The scans were compared with an arbitrarily graded set of standard C.A.T. studies showing the interhemispheric fissure, Sylvian fissure, basal cisterns and sulci and ranging from normal (Grade 0) to marked enlargement (Grade 4). The ventricular size was also measured, Evans' ratio (5) being calculated (i.e., the maximum diameter of the frontal horns of the lateral ventricles divided by the maximum transverse diameter of the skull, measured from inner table to inner table). In addition,

*Lysholm Department of Radiology and
**Psychology Department, The National Hospital for Nervous Diseases, London.

a Total Score was calculated, comprising the individual scores of the fissures, cisterns and sulci; this was then also graded as 0 to 4.

The scores for each of the structures assessed and the ventricular size were then correlated with the psychometric assessment (also graded 0 to 4 in ascending degrees of higher function loss) for the whole group, for patients presenting specifically with dementia as the initial symptom, for those with a long history (5 years or more) or slow onset of symptoms, and for patients whose ventricles were considered to be dilated (i.e., with an Evans' ratio of more than 0.30). Ventricular size and psychometry were also correlated.

Results

The results, analysed as indicated above, are shown in Figures 1-3. Although they appear to show a rough correlation between the signs of cortical atrophy and psychometric assessment, these are not statistically significant, owing to a wide scatter of values. Thus, for example, there were 23 patients of dementia grades 2, 3 or 4 with only minimally enlarged sulci (Grades 0 or 1), while 3 patients with obviously enlarged sulci (Grades 3 or 4) with little or no dementia (Grades 0 or 1). The correlation with the other atrophic features was no closer, and on Total Score 20 patients with grades 2 or 3 atrophy were normal on examination (16) or grade 1 demented (4). Grade 4 Total Score was, however, associated with marked intellectual impairment (2 Grade 3, 1 Grade 4).

Scatter about the 'ideal' (grade-for-grade) correlation was generally even, (31 above the line, 39 below; 1 : 1.3) for the whole group, and for the various subgroups, e.g. slow onset, with two notable exceptions: in patients with a long history, the atrophic signs were more marked than the degree of dementia (9 above the line, 14 below; 1 : 1.6) and in those with enlarged ventricles (Evans' ratio more than 0.3), the cortical atrophic signs were slight relative to the degree of dementia (16 above the line, 3 below; 5.3 : 1).

Discussion

It is clear that any study in which an attempt is made to seek a clinical correlation with alterations in normal structures which are not known *a priori* to be of pathological significance should include a control series. For both practical and ethical reasons it has not been possible for us to form such a series of 'normal' volunteers. A single such series has been reported (7, 8) as showing a slight but insignificant increase in the size of the sulci with age (from a mean diameter of 2.9 mm in the third decade to 4.3 mm in the seventh decade), and no significant change in Evans' ratio (0.27 and 0.28 respectively).

Our attempts to correlate mental function and C.A.T. appearances of cortical atrophy have been disappointing. Although there is in several instances a rough correlation between intellectual deficit and specific signs or total score, the level of significance achieved is low and there is sufficient individual variation as to render C.A.T. demonstration of atrophy of little use as a clinical parameter. Thus, a perfect, i.e. grade-for-grade correlation was present as follows: Sylvian fissure enlargement: 23%; interhemispheric fissure enlargement: 21%; basal

cistern size: 17%; cerebral sulci 20%. This last figure is particularly salutory.

Grade-for-grade correlations were even less good between total C.A.T. score in the groups presenting with dementia (14%, with a long history (12%), or with a slow onset of symptoms (11%).

The better correlation with ventricular size bears out the conclusions of earlier workers, using pneumoencephalography (14).

The inconstant relationship between cognitive function and brain morphology as shown by C.A.T. is of course similar to that encountered by other workers using techniques which are less reliable e.g., pneumoencephalography, or less physiological, e.g., necropsy.

Dementia is a difficult problem to approach clinically; although it is often clear even to an untrained observer that the patient is demented, dementia as a symptom or sign is protean in its manifestations. C.A.T. undoubtedly represents a very reliable screening procedure for the detection of structural lesions which declare themselves as dementia. But such lesions or recognised biochemical disorders together can be incriminated in only 15% of cases presenting in this way (12). In the large majority, therefore, a presumptive diagnosis of cerebral atrophy secondary to some 'degenerative process' will be made. Our results suggest that in the absence of a structural lesion, C.A.T. appearances are almost irrelevant to this diagnosis.

GAWLER (6) reviewed a series of patients seen at the National Hospital, Queen Square with a referring diagnosis of dementia. Five percent were shown to have no structural abnormality whotsoever (including manifestations of cerebral atrophy) on C.A.T.; of these, 46% showed profound deficits on psychometry. Conversely, less than 70% of the whole series had any C.A.T. evidence of atrophic changes. The results from this series, which in contrast to our own, had been approached primarily from the clinical viewpoint, were nevertheless largely in agreement with those of the present study. It is also noteworthy that Gawler's series and our own coincide very closely as to the frequency of the various final clinicopathological diagnoses.

Thus, the bipartite enigma of why intellectual functions are well preserved in patients having radiologically or pathologically demonstrated cerebral atrophy while other profoundly demented patients appear to have morphologically normal brains, both at the gross and microscopic level (3), remains. Pathophysiologically, the existence of the latter group is less surprising, but it is the patients of the former group who are disclosed by C.A.T.

In this paper it has been possible only to deal superficially both with the atrophic changes shown at C.A.T. and with the psychometric assessment. Further analysis may reveal unexpectedly significant findings. In passing, it must be noted that marked enlargement of cerebral sulci or the ventricles appears to occur with increased frequency in system degenerations such as Parkinsonism, Huntingdon's chorea and motor neurone disease as well as in idiopathic epilepsy (15) migraine and a number of other conditions.

Conclusions

C.A.T. permits easy demonstration of the cerebral ventricles and such structures whose enlargement has been thought to indicate, clinically significant cerebral atrophy, such as the fissures and sulci. It has not been possible to demonstrate other than a very approximate correlation of these atrophic changes with psychometric assessment.

We would thus emphasise that cerebral atrophy is a strictly morphological observation and that to accept its C.A.T. demonstration as indicating a significant clinical state would be to render a disservice to many patients.

References

1. BLESSED, G., TOMLINSON, B.E., ROTH, M.: The association between quantitative measures of dementia and of senile change in the cerebral grey matter of elderly subjects. The British Journal of Psychiatry 114, 797-811 (1968).
2. BRUIJN, G.W.: Pneumoencephalography in the Diagnosis of Cerebral Atrophy. Utrecht: Smits 1959.
3. CORSELLIS, J.A.N.: Mental illness and the ageing brain. Institute of Psychiatry - Maudsley monograph 9. Oxford University Press 1962.
4. DAVIDOFF, L.M., DYKE, C.G.: The Normal Encephalogram. 2nd ed. Philadelphia: Lea and Febiger 1946.
5. EVANS, W.A.: An encephalographic ratio for estimating ventricular enlargement and cerebral atrophy. Archives of Neurology and Psychiatry 47, 931-934 (1942).
6. GAWLER, J.: M.D. Thesis. London (in preparation).
7. GYLDENSTED, C., KOSTAELJANETZ, M.: Measurement of the normal hemisphere sulci with computer tomography: a preliminary study on 44 adults. Neuroradiology 10, 147-149 (1975).
8. GYLDENSTED, C., KOSTAELJANETZ, M.: Measurements of the normal ventricular system with computer tomography of the brain. Neuroradiology 10, 205-213 (1976).
9. HAUG, J.O.: Pneumoencephalographic studies in mental disease. Acta Psychiatrica Scandinavica. Suppl. 165, 38 (1962).
10. LYING-TUNELL, U., MARIONS, O.: Pneumoencephalographic findings in intellectual impairment. In: Cisternography and Hydrocephalus. Springfield, Ill.: Charles C. Thomas 1972, p. 357.
11. MANN, A.H.: Cortical atrophy and air encephalography: a clinical and radiological study. Psychological Medicine 3, 374-378 (1973).
12. MARSDEN, C.D., HARRISON, M.J.G.: Outcome of investigation of patients with presenile dementia. British Medical Journal 1972/II, 249-252.
13. McCORMACK, W.O.: A study of the relationship between dementia and radiologically diagnosed cerebral atrophy in elderly patients. D.P.M. Dissertation, University of London 1962.
14. MELCHIOR, J.C., DYGGVE, H.V., GYLSTORFF, H.: Pneumoencephalographic examination of 207 mentally retarded patients. Danish Medical Bulletin 12, 38-42 (1965).
15. MOSELEY, I.F., BULL, J.W.D.: Computerised axial tomography in epilepsy. Epilepsia (in press).
16. MOSELEY, I.F., LOH, L., DU BOULAY, G.H.: The effects of general anaesthesia on the size of the subarachnoid spaces at pneumoencephalography. Paper presented to the British Society of Neuroradiologists, Cambridge, September 1976.
17. MOSELEY, I.F., SONDHEIMER, F.K.: The 24 hour pneumoencephalogram. Clinical Radiology 26, 389-405 (1975).

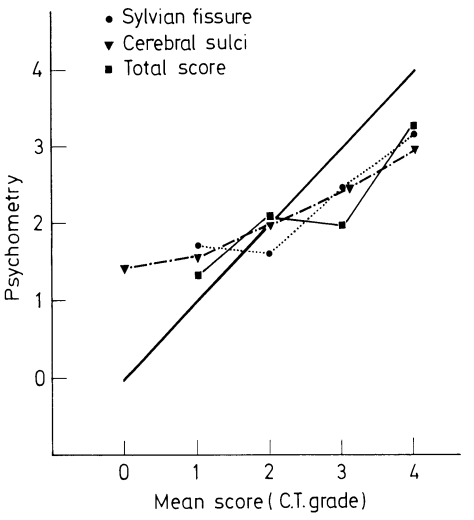

Fig. 1

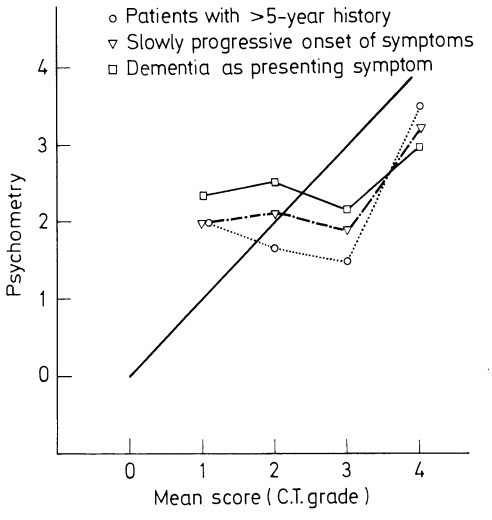

Fig. 2

Fig. 1. Correlation between psychometry and C.A.T. evidence of cortical atrophy. (Continuous straight line represents 'ideal' relationship)

Fig. 2. Total Score (see text) of C.A.T. evidence of cortical atrophy correlated with psychometry in three groups of patients

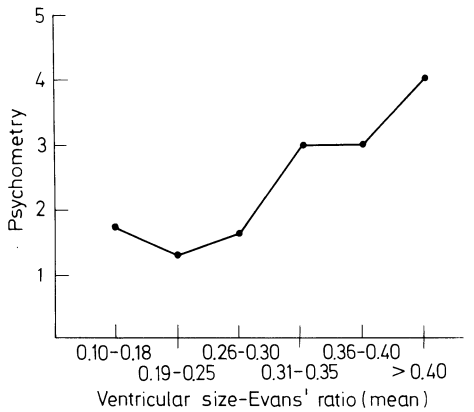

Fig. 3. Relationship of psychometry to ventricular size. Upper limit of normal for Evans' ratio: 0.30

Computerised Axial Tomography and Dementia in the Elderly

M. A. Roberts*, F. I. Caird*, J. L. Steven**, and K. W. Grossart**

Two separate studies have been carried out. In the first, measurements of the ventricular size and sulcal size in the computerised tomograms were compared with the appearances in the pneumoencephalograms of the same patients. In the second study the measurements of the ventricular size and sulcal size obtained from the computerised tomograms were used to assess the degree of atrophy, in a group of elderly patients, and the relationship between the degree of atrophy and intellectual performance was then investigated.

In the first study (8), ventricular size was assessed from the encephalogram by three methods. Firstly, an assessment was made independently by two experienced neuroradiologists who noted the size as normal, or slightly, moderately, or grossly dilated, scoring these respectively 0, 1, 2, and 3. The sum of these two radiologists' scores was termed the 'ventricular score'. Secondly, the width in millimetres of the lateral recesses of the cellae mediae of the ventricles was measured in a supine antero-posterior view and this was termed the 'ventricular span' (1, 2, 3). Thirdly, the maximum width of the third ventricle, the width of the lateral ventricles, the height of the lateral ventricles were measured, and termed the 'combined ventricular atrophy' (5). This was graded as absent, slight, moderate or severe. These measurements were made in 67 patients aged 18 to 64 years all of whom had both computerised tomograms and pneumoencephalograms during the same admission.

From the computerised tomograms ventricular size was taken from the 80 × 80 matrix digital print-out of the slice which showed the largest area of ventricle. The area representing ventricle was assumed to consist of all the cells of the matrix with a density of 9 units or less and this was measured by planimetry. The total area in cm^2 was termed the 'maximum ventricular area'.

The size of the cortical sulci was assessed from the encephalogram in two ways. Firstly, the two neuroradiologists graded the sulci as normal (0), showing focal dilatation (1), or general dilatation (2), and the two scores together made up the 'sulcal score'. Secondly according to the scheme of NEILSEN et al. (6), cortical atrophy was graded as absent, slight, moderate, or severe. From the computerised tomogram the degree of sulcal widening was measured from the 80 × 80 print-out of one of the higher slices which showed cortex but not ventricle. Two measurements were made; the total number of low density cells of 9 units or less, and the apparent maximum width in low density cells of the widest sulcus.

The results of this study are fully reported by ROBERTS et al. (8). There was agreement between the three methods of measuring ventricular size on the pneumoencephalogram, and there was also a clear general

---

*University Department of Geriatric Medicine, University of Glasgow.
**Department of Neuroradiology, Institute of Neurological Sciences, Glasgow.

relationship between the maximum ventricular area on the computerised tomogram and the ventricular score and also with the combined ventricular atrophy in the air study. We consider it reasonable to regard a maximum ventricular area of less than 10 cm^2 as normal, between 10 and 14 as showing slight dilatation, between 14 and 18 moderate dilatation, and greater than 18 as severe dilatation. We also found a highly significant relationship between the ventricular span on the pneumoencephalogram and the maximum ventricular area on the computerised tomogram. There is an acceptable level of agreement between the sulcal score and cortical atrophy in the pneumoencephalogram. However, the relationship between sulcal width as measured in the scan, and the degree of cortical atrophy as determined in the pneumoencephalogram, is less clear, but normal sulci and gross degrees of cortical atrophy can be readily identified. The apparent width of the widest sulcus on the scan is well related to the presence of considerable degrees of cortical atrophy as shown on the pneumoencephalogram, but lesser degrees are not so clearly shown.

In the second study (7), these scan measurements were used to assess the degree of cerebral atrophy in 66 geriatric patients, aged 62 to 90 years, 59 of them women; 17 were mentally normal. Only those patients who showed no clinical evidence of focal cerebral disease(other than that of their mental state as specified below) were included. Their mental state was assessed clinically as follows: 1, normal, where there was no evidence of mental abnormality apart from minor degrees of impairment of memory; 2, mild impariment, where there was definite impairment of memory and of calculating ability; 3, moderate impairment, as for mild impairment, but also disorientation for time and/or place; 4, severe impariment, as for moderate impairment but also difficulty with self-care, in particular with dressing; most could not walk unaided and many were incontinent of urine. All 66 were scored by the Crichton Geriatric Behavioural Rating Scale (9) and all but 5 by a 30-point memory and information test similar to that of ROTH and HOPKINS (10).

There was found to be a clear relationship between ventricular size and clinical assessment, although there was some overlap. It is interesting to note that even in the mentally normal the mean maximum ventricular area is 16 cm^2 as compared with the estimate we made of the upper limits of normal for younger subjects of 10 cm^2 or less. There was a statistically significant correlation between ventricular size and behavioral score and also between ventricular size and the memory and information test score. There was no clear relation between the severity of intellectual impairment and either the number of low density cells in the cortical slice or the width of the widest cortical sulcus.

Among the conclusions to be drawn from the studies are, firstly, that slight but definite ventricular enlargement is usual in the normal elderly, but it remains uncertain at what age this process becomes apparent. Secondly, that in the elderly patient without clinically obvious cerebrovascular disease or infarction there is a broad correlation between the degree of ventricular dilatation and the degree of intellectual impairment. Therefore, as suggested by HUCKMAN et al. (4), if there is a marked degree of intellectual impairment and only little or no ventricular dilatation, further consideration of the diagnosis is indicated. Conversely, if ventricular dilatation is greater than expected from the degree of intellectual impairment, obstructive or normal pressure hydrocephalus must be excluded. Thirdly, it would seem that the maximum ventricular area provides an adequate measure of ventricular size on computerised tomography. Lastly, we consider that the lack of clear relationship between mental state and evidence of cortical

atrophy on the scan may be due either to the inadequacies of measurement of widening, or the lack of any true relation in old age.

References

1. BRUIJN, G.W.: Pneumo-encephalography in the Diagnosis of Cerebral Atrophy. Utrecht: Smits 1959.
2. BURHENNE, H.J., DAVIES, H.: The ventricular span in cerebral pneumoencephalography. American Journal of Roentgenology, Radiotherapy and Nuclear Medicine 90, 1176-1184 (1963).
3. ENGESET, A., SKRAASTAD, E.: Methods of measurements in encephalography. Neurology (Minn.) 14, 381-385 (1964).
4. HUCKMAN, M.S., FOX, J., TOPEL, J.: The validity of criteria for the evaluation of cerebral atrophy by computed tomography. Radiology 116, 85-92 (1975).
5. NEILSEN, R., PETERSEN, O., THYGESEN, T., WILLANGER, R.: Encephalographic ventricular atrophy. Acta Radiol. (Diagnosis) 4, 240-256 (1966a).
6. NEILSEN, R., PETERSEN, O., THYGESEN, T., WILLANGER, R.: Encephalographic cortical atrophy. Acta Radiol. (Diagnosis) 4, 437-448 (1966b).
7. ROBERTS, M.A., CAIRD, F.I.: Computerised tomography and intellectual impairment in the elderly. Journal of Neurology, Neurosurgery and Psychiatry (To be published October 1976).
8. ROBERTS, M.A., CAIRD, F.I., GROSSART, K.W., STEVEN, J.L.: Computerised tomography in the diagnosis of cerebral atrophy. Journal of Neurology, Neurosurgery and Psychiatry (To be published September 1976).
9. ROBINSON, R.A.: Some problems of clinical trials in elderly poeple. Gerontologia Clinica 3, 247-257 (1961).
10. ROTH, M., HOPKINS, B.A.: Psychological test performance in patients over 60. Part 1: Senile psychosis and the affective disorders of old age. Journal of Mental Science 99, 439-450 (1953).

For relevant tables, graphs, illustrations and a fuller list of references, see papers by ROBERTS et al. (7 and 8).

Vascular Conditions

The Use of C.A.T. in Cerebral Infarction

M. J. G. Harrison*

It is the intention of this brief paper to discuss the major clinical problems facing the neurologist in the management of patients suffering from cerebral infarction; to indicate the questions that have to be asked in each case, and to suggest where the C.A.T. scan is and can be helpful.

Differential Diagnosis

Patients who sustain an acute hemiplegia or other focal deficit representing loss of function in a vascular territory will usually have suffered a cerebral infarct. The differential diagnosis however includes cerebral haemorrhage, tumours and subdural haematoma (10).

Cerebral haemorrhage can be reliably detected by the C.A.T. scan as an area of high tissue density (9) the scans proving positive immediately. Evidence of ventricular compression or shift (mass effect) will be present in the great majority (perhaps 75%). Blood will be visible within the ventricular system in some cases. The detailed findings in cerebral haemorrhage are discussed by MÜLLER (6). It is perhaps worth noting, however, that the ability of the C.A.T. scan to detect small haematomas has revealed that even some patients with transient neurological deficit have in fact had an extravasation of blood rather than an ischaemic lesion. This may alter our management of such minor episodes which are often assumed to be ischaemic and for which anticoagulation has therefore been considered.

The distinction between cerebral infarction and brain tumour is more difficult. As up to 5% of patients with an acute hemiplegia may prove to have a tumour (13), the possibility must be considered, and the differentiation is of pratical importance. Infarction causes an area of low density in C.A.T. scans within a vascular territory. If the area is large but there is no evidence of a mass effect, infarction is more likely than a tumour. The presence of a dilated ventricle on the side of the area of low density if the patient is scanned for the first time a few weeks after the onset of the hemiplegia is also much in favour of an infarct (Fig. 1). Other features which may prove helpful concern the characteristics of the associated oedema and of the enhancement that may follow the injection of Conray. Oedema may accompany tumours and infarcts and both may cause midline shift and evidence of mass effect (7). The oedema that accompanies a tumour may show a particular digital pattern since it follows the confines of the hemisphere white matter (Fig. 2). Infarct oedema does not appear to behave in this way. The mass effect of oedema around an infarct resolves after 2 to 3 weeks, so persistence of such a mass effect beyond this interval would favour a tumour.

---

*The Middlesex Hospital, London.

Enhancement of the area of low density by the injection of Conray can occur with either tumours or infarct (50%). Enhancement, however, does not appear to occur in the first 48 h of an infarct, so its presence on the day of onset of a hemiplegia would raise suspicions of a tumour. This is similar to the suspicion of tumour raised by the early positive isotope brain scan after hemiplegia. Enhancement of the low density area on a C.A.T. scan more than 6 weeks after the onset of a hemiplegia would also be more likely to indicate a tumour since the enhancement accompanying an infarct appears short-lived. A halo of low density astride a ring of enhancement may be an indication of a tumour.

As these remarks make clear, it may require a period of follow-up with serial scanning before the distinction between cerebral infarct and tumour can be made. This is the same situation as obtains with electroencephalography and isotopic encephalography. The management situation may require the question to be answered in a shorter time course, in which case angiography may be needed.

A subdural haematoma may occasionally present a problem in the diagnosis of the cause of a hemiparesis. The C.A.T. scan diagnosis is not always simple. The classical change would be of a peripheral crescent of low density (Fig. 3), but the only clue to the presence of a subdural haematoma may be of a mass effect without a hemisphere abnormality.

Vascular Territory

It is frequently important to know the territory of an infarct and accurate information which is now available from the C.A.T. scan can be of help in making an aetiological diagnosis and in planning treatment. If a patient makes a full recovery from a thromboembolic infarct the question may arise as to whether vascular surgery would be contemplated if there is a stenosis or atheromatous ulcer on the extracranial vessel feeding the territory of the recent infarct. The correlation of symptoms and extracranial atheromatous changes is at best only 65% (1). The ability to show whether an infarct is in the internal carotid territory (anterior cerebral artery; middle cerebral artery) (Fig. 1) or that of the posterior cerebral artery (vertebrobasilar supply((Fig. 4) can therefore be crucial to planning angiographic studies and interpreting the significance of abnormalities found in extracranial vessels.

Aetiology

Cerebral infarction may occur in watershed territories in the context of a hypotensive crisis for example after cardiac arrest. The demonstration by C.A.T. of an infarct in such a border zone (Fig. 5) may therefore give a clue to the haemodynamic nature of the causative event (11). If an infarct is shown to be in the territory of, say, the middle cerebral artery including a wedge of cortex, it is much more likely that local occlusion of the internal carotid, middle cerebral artery or one of its branches has occurred directing attention to the possibility of local atheromatous disease of the ipsilateral carotid artery as a cause for the event. Cardiac embolism might be considered more likely when a haemorrhagic infarct is seen in which areas of high density reflect the presence of petechial haemorrhages in an ischaemic low density areas (Fig. 6). Small, deeply placed areas of low density in the putamen, and near the internal capsule, are more likely to represent

the effects of hypertensive small vessel disease although I am not aware of any clinicopathological confirmation that recent lacunes as described by FISHER (4) have been recognisable on the C.A.T. The detection of small deep lacunar infarcts is an important goal, however, since their correct management involves control of the arterial pressure without the necessity to carry out angiography, and with no indication for anticoagulants.

Prognosis

The distinction of small hypertensive lacunes and haemorrhagic embolic infarctions would carry prognostic significance. The nature and extent of Conray enhancement of a cerebral infarct on C.A.T. may also have prognostic importance since it may reflect the presence of the phenomenon of luxury perfusion at the border of the damaged area, and this in turn has been thought to imply a better prognosis.

Pathophysiology

The contrast between the effectiveness of dexamethasone in the treatment of patients with cerebral tumours and the disappointing results in stroke victims has been clear for some years now (8). The C.A.T. scan is, I believe, helping to explain the difference. The oedema which accompanies a tumour can be seen on C.A.T. evidence to occupy the anatomical white matter corresponding to the variety of oedema thought to be vasogenic in origin (5) (i.e. due to a disturbance of the blood-brain barrier (B.B.B.) with spread of extravasated plasma constituents through the white matter). Serial scans in patients with infarcts show that the oedema never follows the same distribution, is more diffuse, and includes the grey matter. The oedema is visible within the first few hours in some cases whilst enhancement with Conray indicating a disordered B.B.B. is delayed (48 h). The implication of this evidence is that the early infarct oedema is cytotoxic rather than vasogenic (5). It is this fundamental pathological difference that I believe may underly the failure of dexamethasone to make a clear-cut difference to the mortality and morbidity of cerebral infarction despite the clear-cut role of oedema in the fatality of some infarcts (12).

Long-term Follow-up

Dilatation of the ipsilateral ventricle occurs in 85% of cases as a hemisphere infarct resolves, and AMBROSE (9) found that some cases showed symmetrical dilatation of the ventricular system. The significance of these changes to the development of multi-infarct dementia is as yet unknown. It will be of great interest to follow patients with cerebrovascular disease combining neuropsychological testing, C.A.T. scanning for evidence of ventricular size and multiple infarcts, and cerebral blood flow and metabolic studies. There are many other exciting possibilities for research. Most importantly, the epidemiological study of cerebrovascular disease can now be put on a secure footing. Hitherto it has been impossible in population studies to know whether cerebral haemorrhage and cerebral infarction were being confused. C.A.T. control of data such as that obtained in Framingham is

now a real possibility. There is evidence of a reduced risk for recurrent stroke with the treatment of hypertension (3), but we need to know for certain whether this is due to a change in the risk of recurrence of cerebral infarction or only of haemorrhage.

Finally, attempts at therapy such as treatment of oedema need the separation of cerebral haemorrhage from infarction that the C.A.T. scan can provide, and it would now be possible to carry out a controlled trial of an antioedema regime in just those infarcts that show the presence of oedema. A small significant benefit may have been lost in the groups of patients studied so far, due to the heterogeneity of the case material.

Though everybody has his own reason for being excited by the advent of C.A.T., a case can be made out that it is in cerebrovascular disease that its impact will be most impressive.

References

1. ALTER, M., KIEFFER, S., RESCH, J., ANSARI, K.: Cerebral infarction. Clinical and angiographic correlations. Neurology 22, 590-602 (1972).
2. AULICH, A.: 8th Salzburg Conference (1976).
3. BEEVERS, D.G., HAMILTON, M., FAIRMAN, J.E., HARPUR, J.E.: Antihypertensive treatment and the course of established cerebral vascular disease. Lancet 1973/I, 1407-1409.
4. FISHER, C.M.: Lacunes: small, deep cerebral infarcts. Neurology 15, 774-784 (1965).
5. KLATZO, I.: Neuropathological aspects of brain edema; presidential address. Journal of Neuropathology, and Experimental Neurology 26, 1-14 (1967).
6. MÜLLER, H.R.: Cerebral, cerebellar and pontine haemorrhages. This symposium, p. 249-254 (1977).
7. NG, L.K.Y., NIMMANNITYA, J.: Massive cerebral infarction with severe brain swelling. A clinicopathological study. Stroke 1, 158-163 (1970).
8. NORRIS, J.W.: Steroid therapy in acute cerebral infarction. Archives of Neurology 33, 69-71 (1976).
9. PAXTON, R., AMBROSE, J.: The EMI scanner: A brief review of the first first 650 patients. British Journal of Radiology 47, 530-565 (1974).
10. ROSS RUSSELL, R.W., HARRISON, M.J.G.: The completed stroke. British Journal of Hospital Medicine 10, 244-249 (1973).
11. MCAULEY, D., ROSS RUSSELL, R.W.: Vascular disease of the visual radiation and cortex. This symposium, p. (1977).
12. SHAW, C.M., ALVORD, E.C., BERRY, R.G.: Swelling of the brain following ischaemic infarction with arterial occlusion. Archives of Neurology 1, 161-177 (1959).
13. SILVERSTEIN, A.: Arteriography of stroke. I. Incidence of mass lesions in patients with clinical diagnosis of occlusive cerebrovascular disease. Archives of Neurology 12, 387-389 (1965).

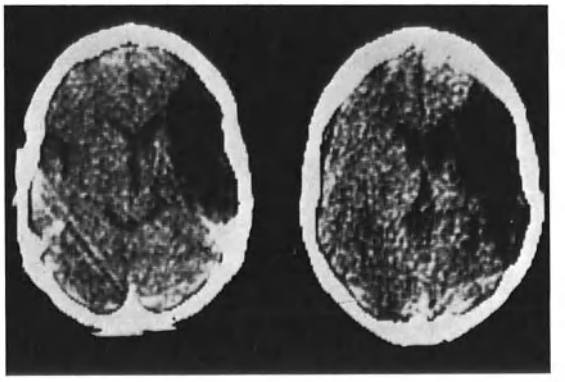

Fig. 1. Infarct in right middle cerebral artery of territory

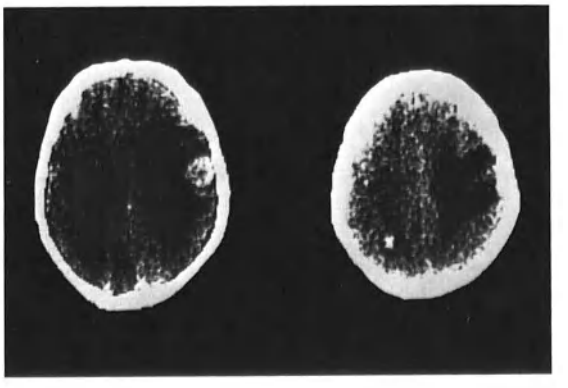

Fig. 2. Metastasis with right hemisphere oedema

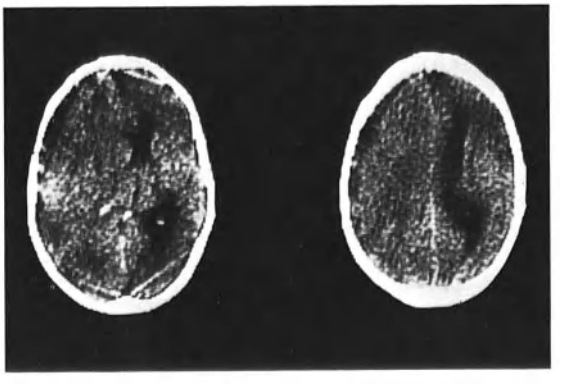

Fig. 3. Left-sided subdural haematoma

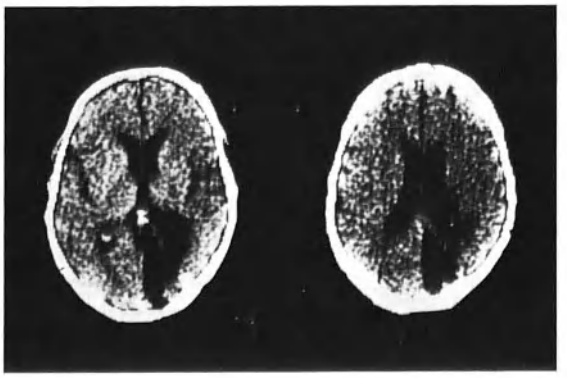

Fig. 4. Infarct in territory of right posterior cerebral artery

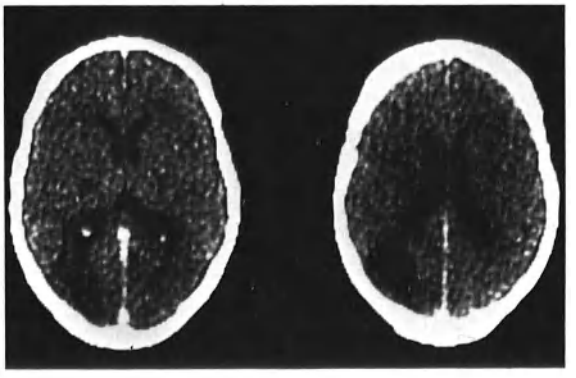

Fig. 5. Watershed infarct (in territory of middle cerebral artery - posterior cerebral artery)

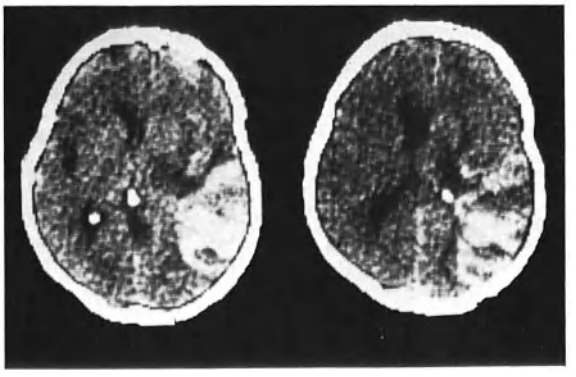

Fig. 6. Haemorrhagic infarct

C.A.T. Studies of Cerebral Ischaemia

P. Constant, A. M. Renou, J. M. Caillé*, and J. Vernhiet

For many years, investigation of cerebral ischaemia was possible only by means of angiography and scintigraphy. At the present time, however, to the investigation of the vascular component C.A.T. adds the direct visualisation of the cerebral parenchyma itself. Its innocuous nature makes it possible to follow the evolution of a lesion by repeated examinations. Our study compares the performances and respective applications of C.A.T. angiography. scintigraphy, and measurement of regional cerebral blood flow (rC.B.F.) in cerebral ischaemia.

Material and Methods

One hundred and fifty-eight patients were examined: 62 were females and 96 males. The age distribution of these patients is shown in Table 1.

Two hundred and eighty-seven C.A.T. studies were performed according to a time schedule shown in Table 2.

Table 1. Age (years)

≤ 20	21-40	41-50	51-60	61-70	≥ 70
3	9	21	34	48	43

Table 2. Two hundred and eighty-seven C.A.T. examinations

1st week	2nd week	3rd week	4th week	2nd month	>2 months
46	41	39	35	59	67

The number of C.A.T. studies varied from 1 to 10 per patient.

The C.A.T.s were performed with an Acta Scanner equipped with a 160 × 160 matrix. Slices were 7.5 mm thick, 3 mm apart. The slice plane was usually at 20° to the orbitomeatal plane.

In 105 patients, C.A.T. was repeated after injection of 2 ml per kg body weight of iodinated contrast medium (38%).

The number and topography of lesions and their effects on nearby structures were essessed.

*Service de Neuro-Radiologie, Centre Jean Abadie, Bordeaux.

The density values of these lesions were measured in Acta numbers which were related to the time relative to onset of symptoms for the patients taken as a whole and also divided into four clinical groups defined according to evolution:

1. Transient ischaemic attacks
2. Rapidly regressing attacks
3. Serious infarcts with clinical improvement
4. Serious infarcts without clinical improvement

The detection of these lesions and exact determination of their size is subject to certain limits, due essentially to:

1. Dense or light artefacts in the posterior fossa, the temporal fossae and the skull base
2. The partial volume effect
3. The volume of the lesion itself
4. Difficulties in reproducing the same slice from one examination to another in the same patient
5. The effects of the anti-oedema treatment

C.A.T. results were compared with those of angiography, scintigraphy and in some cases measurement of rC.B.F.

One hundred and ten patients underwent angiography, but only 70 of these examinations could be studied usefully:

30% were performed from the 1st to the 7th day
22% from the 8th to the 15th day
21% from the 16th to the 30th day
9% from the 31st to the 60th day
10% beyond that time

We looked for morphological and dynamic signs of circulatory arrest or slowing in the proximal or distal arteries (vascular holdup, a vascular area, delayed arterial filling, persisting arterial opacification, absence of localised venous drainage) and signs of functional changes (arterial opacification by anastomotic pathways, capillary blush, early venous drainage). Degree of atheroma of the blood vessels supplying the head was also assessed.

One hundred and thirty-one static isotope scans were performed as follows:

23 from the 1st to the 7th day
73 from the 8th to the 30th day
12 from the 31st to the 60th day
23 beyond the 60th day.

Only seven angioscintigraphies were carried out.

rC.B.F. was measured in 18 patients:

10 were measured once
7 were measured twice, a fortnight apart
1 was measured 3 times.

We looked for any increase or decrease in diffuse or regional blood flow. In five cases we tested vasoreactivity by administering Alfatesin. Autoregulation was not tested.

Results and Discussion

Low-Density Lesions

The average densities of all the lesions examined on the same day are shown in Figure 1. The histogram would seem to correlate satisfactorily with the anatomical evolution of the infarcted tissue.

There were no changes in the C.A.T. in the first few hours. Decrease in density is greatest during the 2nd week, showing the development of oedema linked with a progressively more marked liquefaction necrosis. Density increases slightly in the 3rd week because of regression of the oedema and progressive revascularisation of the infarcted area.

The secondary decrease shown on the histogram represents the formation of the cystic resorption cavity in infarcts with permanent sequelae. The liquid in this cavity has the same attenuation coefficient as CSF.

High-Density Lesions (8 Cases)

These lesions, which were always the result of the presence of clotted blood, were always associated with low density areas, the two areas together representing a haemorrhagic infarct. The haemorrhagic suffusion was located only in the white matter, but the absence of haemorrhagic lesions in the cortex was in fact a detection artefact. Blood was found in the ischaemic area from the 2nd to the 32nd day. The haemorrhagic area rarely appeared in the first ten days. Maximum density was reached from the outset. It decreased progressively and disappeared in 1 or 2 weeks. These lesions were always secondary to embolic obstructions.

Number of Lesions

Eighty-six patients had only one ischaemic lesion, while 36 patients had from 2 to 4 lesions. Multiple lesions could be the result of either the same accident or different accidents.

Topography

Seventy-nine lesions were on the right and 70 on the left. There were only 3 in the posterior fossa, this small number being related to our criteria for selecting patients. There were 146 hemispheric lesions, 8 rolandic, 52 frontal, 42 temporal, 67 parietal, 40 occipital, and 17 were in the basal ganglia. (The largest lesions are listed under several headings). In 36 cases the infarct corresponded obviously to a known vascular distribution.

Dimensions

In 32 cases the lesions were extensive, and in 90 cases more localised. They ranged from 1 cm in diameter to those which occupied the whole hemisphere.

Mass Effect

Mass effect was encountered in 32 cases and was shown by localised or diffuse compression of the ventricular wall, crushing of the cortical sulci and sometimes shift of the middle line. It disappeared progressively and was never found after the 3rd week. During the 2nd month, shrinkage of the infarcted area led to homolateral traction of the nearby structures, with enlargement of the cortical sulci as the only remaining evidence of the infarct after several months.

Diffuse Cortical Atrophy

Atrophy was frequently found but was very pronounced in 5 cases. In 61 cases there was bilateral and in 45 cases unilateral ventricular dolation - in the latter cases always on the same side as the infarct.

Effects of the Injection of Iodinated Contrast Agent

One hundred and five patients underwent contrast injection and in 27 cases the infarcted area enhanced. The numerical values were correlated with the time factor (Fig. 2). This histogram shows a peak of intensity at the end of the 2nd week. Opacification disappeared progressively and was very rarely found after 2 months. The enhanced area was variously located: in 13 cases it was on the periphery and in 6 cases only at the centre.

Infarct enhancement was connected with disturbances of the blood-brain barrier and the inflammatory reaction which increased circulatory flow. In rare cases it could have been linked to luxury perfusion or vascular necrosis, but only three haemorrhagic infarcts enhanced.

Together with the general results for all ischaemic lesions we studied the C.A.T. data for each of the previously defined clinical groups in conjunction with the angiographic, scintigraphic and blood flow data.

Transient Ischaemic Attacks

There were 16 patients (10%) in this group, 10 females and 6 males, varying in age from 26 to 71.

C.A.T.

Eighteen C.A.T.s were performed from the 1st day to the end of the 2nd year following the ictus. Sixteen of these were normal. In 2 cases there were low-density lesions corresponding to previous infarcts, unrelated to the present accident.

Scintigraphy

All 7 static scintigraphies were normal.

Angiography

Ten patients underwent angiography: two cases were normal, two cases had diffuse atheromatosis of the cerebral vessels, six cases had complete or nearly complete thrombosis of the internal carotid artery, which shows the great variation in clinical expression of this type of lesion.

rC.B.F.

Only one patient underwent measurement of rC.B.F., which was normal. (Certain authors have however found persistant focal disturbances over several months).

Overall, the C.A.T. and scintigraphic investigations were normal in transient ischaemic attacks. They would seem to be indicated only as means of detecting a different pathological process.

On the other hand, angiography combined with rC.B.F. is certainly indicated. These should be done as soon as possible, so as to show up changes connected with the ictus and the lesion responsible, which might need surgical treatment.

Rapidly Regressing Infarcts

This group contained 25 patients (16%) of whom 7 were female and 18 male, aged from 35 to 78.

C.A.T.

C.A.T. was normal in 8 cases: in 1 case it was performed on the 1st day and in 4 cases after the 3rd week.

C.A.T. was abnormal in 17 cases. The average density of the lesions assessed the same day and correlated with the time factor is given in Figure 3, which shows a clear parallel between rapid clinical improvement within the fornight and regression of the lesions.

Scintigraphy

In 17 cases scintigraphy was done, and in 3 cases was positive, on the 2nd, 7th and 43rd days. In 14 cases it was negative, even during the 2nd week.

Angiography

Thirteen patients underwent angiography: 31% of cases were normal; 76% were pathological, showing one or several infarcts.

rC.B.F.

Six patients were examined once or several times. In one case the result was normal, but the examination was done 6 months after the ictus. In five cases focal changes of blood flow directly related to the ictus were shown.

Static scintigraphy was an obvious failure with this type of accident. Even when it was positive, the lesions are always perfectly clear at C.A.T.

Serious Infarcts with Clinical Improvement

This group contains 66 patients (42%), 23 females and 42 males, aged from 34 to 84 years; 42 patients had at least one risk factor; 26 patients had from 2 to 10 C.A.T.s.

C.A.T.

C.A.T. was normal only once (2%), when carried out on the 1st day. It was abnormal in 65 cases (98%). On the density histogram (Fig. 4), fluctuations related to the time factor accord with the general evolution. Cystic resorption cavities are very large, showing the sequelae present in even these cases.

Scintigraphy

This was done in 60 cases, only 50% of which were abnormal.

Angiography

Of these examinations, 18% were normal, except for atheromatosis; 82% were abnormal, showing lesions affecting both the cerebral and carotid regions.

rC.B.F.

Twelve examinations were done, on seven patients. In all cases there were considerable disturbances connected with the ictus. In two cases there was complete recovery and in two cases considerable improvement.

Scintigraphy is thus a failure with this group also. There is, however, very satisfactory correlation and reciprocity between angiography and C.S.T.

Serious Infarcts without Clinical Improvement

This group includes 51 patients (32%), 22 females and 29 males, aged from 14 to 84 years; 29 had serious risk factors, and 12 of them died between the 2nd and 81st day.

C.A.T.

Figure 5 shows the density evolution of these lesions, which are of very low density at all stages of the evolution. Oedema and necrosis are more marked in this group than in the preceeding ones. In four cases C.A.T. did not show parenchymatous lesions connected with the present ictus. In one case C.A.T. was carried out on the 1st day and

in three the lesion was very small, as the clinical findings had suggested. In six cases there was enhancement after contrast medium injection, but there was no relation between the opacification and the gravity of the clinical picture. Three lesions were haemorrhagic.

Scintigraphy

Fifty static scintigraphies were carried out. Twenty-nine (58%) were abnormal and the C.A.T. data there were always closely concordant in topography with the C.A.T. Twenty-one (42%) were normal, but 15 of these were carried out after a fortnight.

Angiography

Twenty-six examinations were performed: 24 were abnormal (with, in 12 cases, complete thrombosis of the internal carotid); 2 were normal, but in one of these a cerebellar infarct was confirmed.

rC.B.F.

This was measured twice in two cases. In each case the grey flow was so low that it had to be measured stochastically. At the second measurement the flow was unchanged in one case and even lower in the other.

In general it is in this group that the most serious lesions were found. There were, however, a certain number of failures:

1. With C.A.T. because of the small size of some lesions
2. With angiography and scintigraphy because the examinations were not performed early enough

Conclusion

Scintigraphy is a partial failure in detecting ischaemic lesions. However, C.A.T., angiography and rC.B.F. are well adapted to these investigations and, used together, allow accurate morphological and functional assessment of parenchymatous and vascular lesions.

Comparison of density evolution in each of the four clinical groups shows a characteristic C.A.T. pattern for ischaemic cerebral lesions. The evolution in each group is parallel to the anatomical and clinical evolution.

The peak of low density in the 2nd week is similarly important in groups 2, 3 and 4: not only is this peak related to oedema but the oedematous reaction is much the same in all groups.

Within each group the density levels in the 1st week and beyond the 30th day differ little. However the levels do vary from group to group, the sequelae being in general more serious when the lowest density level is reached quickly.

The outline of each histogram is the result of 2 factors: (Fig. 6)

1. Necrosis, variable in extent from patient to patient at the outset, with subsequent evolution towards cavitation and thus density similar to that of cerebrospinal fluid

2. Oedema, showing a fairly stable peak of intensity in the 2nd week and disappearing totally before the 20th day

It would thus seem that initial and more or less permanent neuronal damage is related to the extent of the infarct. If the patient survives, the medium-term prognosis can be established beyond the 20th day, other things being equal.

Summary

One hundred and fifty-eight patients with cerebral ischaemia were divided into four clinical groups and studied at C.A.T. The results were correlated with those of angiography, scintigraphy and regional cerebral blood flow measurement. C.A.T. evolution was closely correlated with clinical and anatomical evolution.

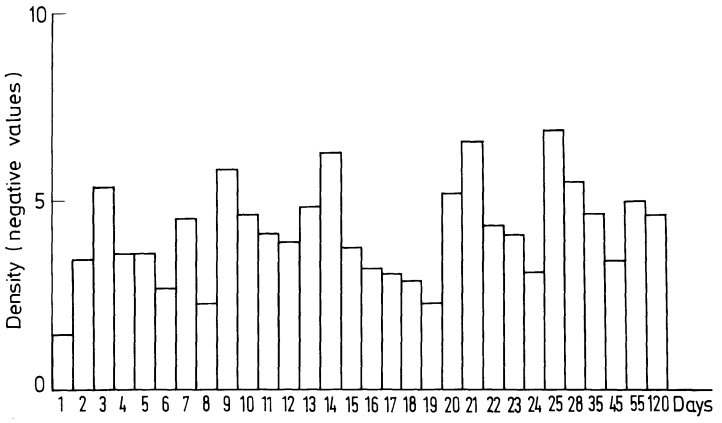

Fig. 1. General evolution in density of brain infarcts

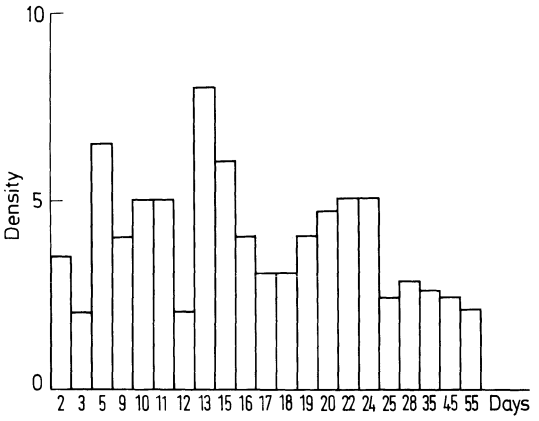

Fig. 2. Evolution in density of enhanced areas (after contrast medium injection)

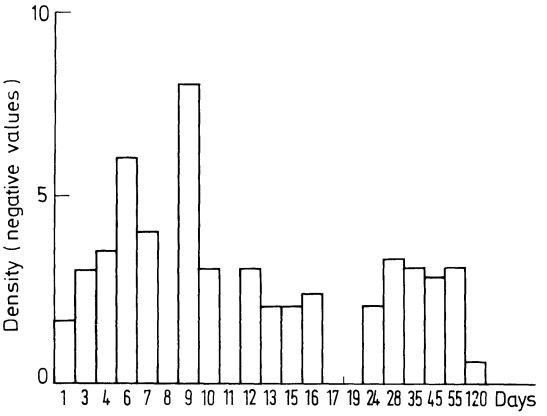

Fig. 3. Evolution in density of rapidly regressing attacks

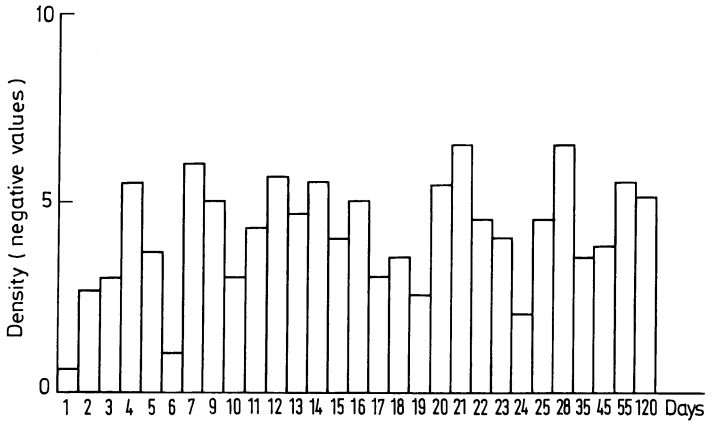

Fig. 4. Evolution in density of serious infarcts with clinical improvement

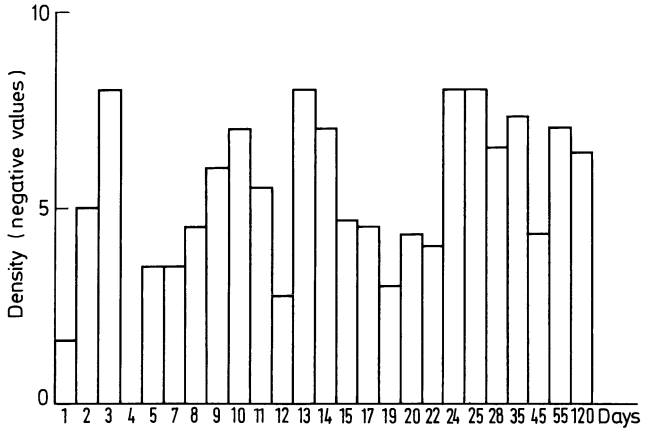

Fig. 5. Evolution in density of serious infarcts without clinical improvement

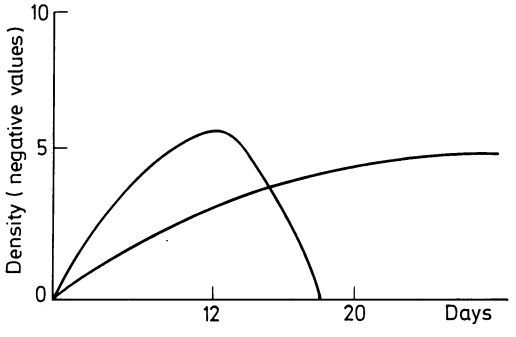

Fig. 6. The general evolution of whole histograms is the result of two phenomena:
- necrosis, - oedema (maximum within the 2nd week; disappears before the 20th day)

Jacksonian Epileptic Seizures as Inaugural Manifestations of Sylvian Infarctions Revealed by Computerised Axial Tomography (C.A.T.)

H. Gastaut, G. Boudouresques, J.-L. Gastaut, and B. Michel*

The existence of epileptic seizures in connection with cerebral arterial pathology was already known in the 19th century (FONTENEAU, 3; JACKSON, 5; GOWERS, 4). Yet, for the past 30 years such an aetiology was proposed with great reluctance, apart from some cases where the relation to a cerebral vascular accident was evident, such as seizures accompanying or appearing after a patent infarct or haemorrhage.

Now, certain authors, including BAROLIN (1), and the School of Strasbourg (2-6), insist once more on the relative frequency of epileptic seizures occurring during cerebral arterial pathology.

It now seems useful to consider this problem making use of the information given by C.A.T., limiting ourselves for the time being to cases of cerebral infarction.

Classically, we can distinguish three groups of epileptic seizures, according to the moment of their onset after a cerebral infarct:

1. Seizures preceding the infarction, which are exceptional
2. Seizures occurring simultaneously with the ischaemia
3. Seizures appearing after the infarction

Material and Results

Out of a population of 942 adult epileptics examined with C.A.T. we observed in 17 patients without any prior history of cerebrovascular accidents, a Sylvian infarction responsible for a syndrome evolving in three phases:

1. The initial episode is represented by one or several partial seizures with a Jacksonian progression, and in one-third of the cases by a Jacksonian status epilepticus.

2. A post-ictal episode (which can be absent in some cases) is represented during several hours or days by a focal deficiency syndrome with a corresponding delta focus on the EEG.

3. Sequelae are observed in only one-third of the cases and are represented by the persistence of a neurological deficiency syndrome and/or Jacksonian seizures.

The following five cases illustrate this syndrome.

---

*Service de Neurophysiologie Clinique, Groupe Hospitalier de la Timone, Marseille.

Case 1

A 30-year-old woman presented acutely on April 19, 1976, with somatomotor seizures of the right face and arm with Jacksonian extension and occuring in a repetitive manner. These seizures were followed by a post-ictal right hemiparesis which persisted for 36 h. The EEG showed slow abnormalities arising at the left centroparieto-occipital junction (Fig. 1). The C.A.T. performed on April 24 showed a left centroparietal infarct (Figs. 2a and b). A left carotid angiogram confirmed the existence of a thrombosis of the cortical branches of the Sylvian artery in the motor area. A control C.A.T., 5 weeks later, was unchanged. At this time EEG was normal (Fig. 1) and the clinical state of the patient was entirely satisfactory.

Case 2

A 70-year-old man presented a somatomotor seizure affecting the right face and arm with Jacksonian extension, on June 18, 1976. After the seizure there was a post-ictal right hemiplegia and aphasia which regressed in 24 h. The EEG of June 20, 1976, showed marked slowing of the electrical activity of the left hemisphere. The C.A.T. of June 25, 1976, revealed an infarction of the superficial and deep Sylvian regions of the left hemisphere in connection with a complete thrombosis of the internal carotid artery, as confirmed by angiography.

Case 3

A 66-year-old woman was admitted to the hospital on April 15 1976 because of repeated somatomotor seizures affecting the right face and arm with Jacksonian extension. A post-ictal right hemiplegia regressed to a large extent in a few days. An EEG performed on the day of admission to hospital allowed the recording of several seizures. In the following days, some abnormalities of the left hemisphere persisted. The C.A.T. of April 28 1976 showed an infarct in the deep and posterior part of the left frontal lobe, extending to the cortical region. A left carotid angiogram was normal. The EEG and the clinical state returned rapidly to normal.

Case 4

A 47-year-old man presented on July 28 1973 with six partial somatomotor seizures affecting the left face and arm. The neurological examination was normal, but the EEG showed irritative abnormalities of the fronto-Rolando-temporal region. Cerebral scintigraphy and a pneumoencephalogram were normal, but the right carotid arteriogram revealed obliteration of the right Rolandic artery. With barbiturate treatment, the patient has presented no more seizures and his neurological state has remained completely normal. Two C.A.T.s performed respectively on October 22 1975 and July 26 1976 (Fig. 3a) showed a hypodense cortical area in the pre-Rolandic region representing a mature infarct.

Case 5

A 64-year-old woman presented in 1974 a left somatomotor seizure affecting the upper limb and face with Jacksonian extension and followed by secondary generalisation. A post-ictal hemiparesis was rapidly regressive. On May 13 1976, the patient presented a clonic seizure of the left upper limb, and on May 29 she presented a somatosensory

seizure (numbness and dysaesthesiae of the left superior limb). Neurological examination revealed a right parietal lobe syndrome. The EEG showed some paroxysmal abnormalities in the right parietal area. The scintigraphy was normal, whereas the C.A.T. showed (Fig. 3b) marked sequelae of a right parieto-occipital ischaemia, most probably secondary to an embolus of cardiac origin in the Sylvian territory.

We will not describe the remaining 12 cases in detail, but remark only that they all follow exactly the same clinical course.

Inaugural Jacksonian seizures as described above do not represent the only variety of epileptic seizure in connection with Sylvian ischaemia. C.A.T. has enabled us to show that an isolated grand-mal seizure (or status epilepticus) can occasionally represent the inaugural manifestation of a sylvian infarction.

Similarly, we have seen cases of Jacksonian seizures or grand-mal seizures occurring months or years after an ictus, and in these cases the seizures mark the sequel and not the beginning of the infarction as revealed by C.A.T.

Discussion

We should like to emphasise the fact that in our work all the Jacksonian somatomotor seizures described as initial manifestations of a cerebral vascular accident were due to a cerebral infarction and that in no case was a cerebral hemorrhage diagnosed. This is in agreement with the works of ROHMER et al. (6) which showed that epileptic seizures occurring simultaneously with a cerebromeningeal hemorrhage are always generalised and not partial. Thus it seems that as far as arterial pathology is concerned Jacksonian seizures can be considered synonymous with ischaemic processes. However, this is not the opinion of BAROLIN et al. (1) who consider that Jacksonian seizures can occur not only during infarction but also during hemorrhages.

Secondly, only 3 out of our 17 patients presented status epilepticus whereas in the series of ROHMER et al. (6), 13 out of 21 patients presented this condition. This difference in frequency most certainly explains the difference which existed in the evolution of the two series. In fact, 8 out of the 21 patients of ROHMER et al. (6) died before the 15th day, but 6 of these patients presented a partial status epilepticus. On the other hand we had no fatalities in our series even among the 3 patients having presented status epilepticus. This great difference in the evolution is in agreement with BAROLIN et al. (1) who feel that the onset of isolated epileptic seizures represent a good prognosis during cerebral infarction (the possibility of survival being twice as high in these cases as comparted to cases where the patients have not presented epileptic seizures). According to these same authors the prognosis is quite unfavorable in cases of status epilepticus, this being most probably due to the aggravation of the cerebral ischaemic lesions due to the lasting electrical discharge of status epilepticus (1).

The advantage of C.A.T. in demonstrating the ischaemic origin of epileptic seizures is certainly superior to that of cerebral arteriography. According to the results of the Strasbourg group, angiography gave abnormal results in only 7 out of the 13 cases studied; this represents about 50% of the cases. According to BAROLIN et al (1) this percentage is only around 20%. C.A.T. is currently the only method allowing a visualisation of infarction in almost all cases and shows at the same

time the topography and extent of the lesions. This is not the case with angiography which shows only the topography and type of lesion of the corresponding artery (or arteries). Yet, we must not forget that in many cases angiography reveals no abnormality, whereas C.A.T. reveals the infarcted region as a hypodense zone whose evolution can be studied by further examinations.

In conclusion we would like to insist on the importance and autonomy of the syndrome we have described and on the role played by C.A.T. in this field. The interest of the isolation of such a syndrome is theoretical as well as practical. In fact we have been able to show with C.A.T. the existence of 30 tumours and 5 post-traumatic scars, out of the 942 patients examined, in epileptics presenting partial Jacksonian seizures with an entirely different electroclinical pattern. Hence it appears from our study that 57.5% of Jacksonian seizures in adults are of tumoral origin, 9.5% are of traumatic origin and 33% are due to Sylvian infarction.

Such a large number of epileptic seizures of ischaemic origin had not been suspected until now, and it is one of the merits of C.A.T. to have brought to our attention their relative frequency. We must finally remark that in the presence of a Jacksonian seizure of the adult, besides a tumoral origin (which we must always fear) there may be a partial Sylvian infarction in one-third of the cases, often responsible for only moderate sequelae or even clinically and electrically (EEG) not perceptible.

References

1. BAROLIN, G.S., SCHERZER, E., SCHNABERTH, G.: Die zerebro-vaskulär bedingten Anfälle. Bern: Hans Huber 1975.
2. COQUILLAT, G.: Crises épileptiques et pathologie vasculaire cérébrale (à propos de 107 observations). Thèse Médecine, Strasbourg (1973).
3. FONTENEAU, A.: Du ramollissement cérébral, au point de vue de l'embolie artérielle. Thèse Médecine, Paris (1861).
4. GOWERS, W.R.: Cited by LOUIS, S., MAC DOWEL, F.: Epileptic seizures in non embolic cerebral infarction. Archives of Neurology 17, 414-418 (1967).
5. JACKSON, J.H.: Selected Writings of John Hughlings Jackson. Vol. 1. On Epilepsy and Epileptiform Convulsions. London: Taylor J. Hodder and Stoughton 1931.
6. ROHMER, F., COLLARD, M., KURTZ, D., WARTER, J.M., COQUILLAT, G.: Les crises épileptiques au cours de la pathologie artérielle cérébrale. (Données cliniques). Revue Neurologique 131, 661-669 (1975).

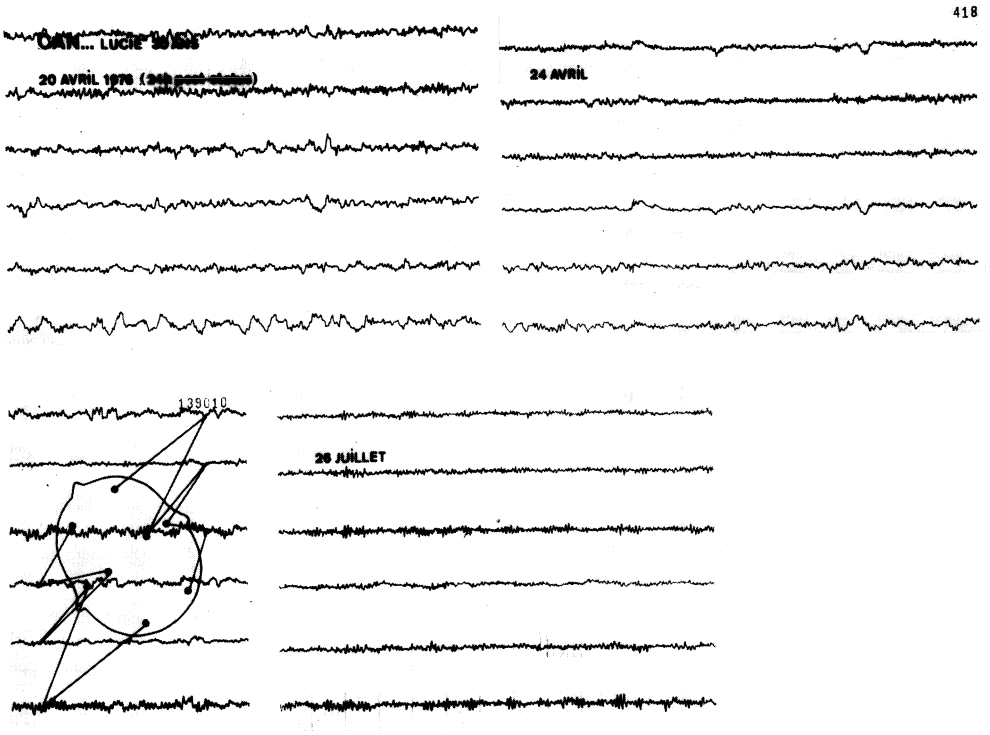

Fig. 1. Case 1: EEG of April 20 1976 shows numerous slow abnormalities in the left hemisphere. EEG of April 24 1976; the abnormalities still persist. EEG of July 26 1976; normal tracings

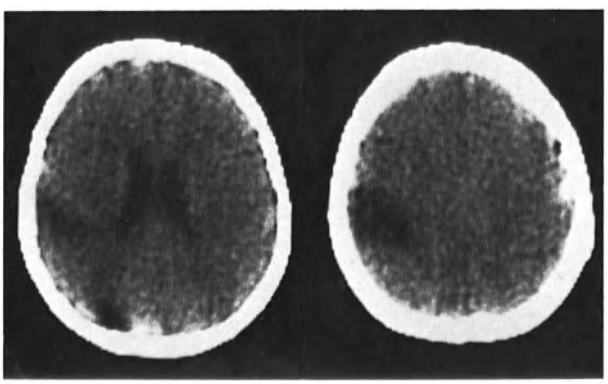

Fig. 2a and b. Same patient: C.A.T. of the brain passing through the lateral ventricles and the convexity and showing a triangular hypodense image in the left posterior parietal region

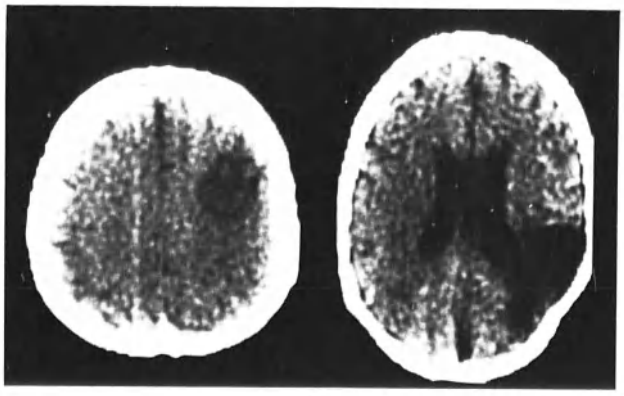

a b

Fig. 3. (a) Case 4. C.A.T. of the brain passing through the convexity and showing a hypodense area in the right prerolandic region. (b) Case 5. C.A.T. of brain passing through lateral ventricles and showing a hypodense area in the right superficial and deep parietal regions

Vascular Diasease of the Visual Radiation and Cortex

D. L. F. McAuley and R. W. R. Russell*

Until the development of the EMI-Scanner, there has been no useful method for demonstrating in life the anatomical extent of infarction in the brain. The scanner has added a new dimension to the investigation of such cases, and this is particularly true in lesions involving the occipital visual cortex where isolated lesions are common, this being the territory of the posterior cerebral artery. A unique opportunity exists to attempt to confirm established anatomical correlates in view of the known details of retinotopic projection on the primary visual cortex. This paper describes a small series of 24 patients suffering from a variety of visual defects secondary to ischaemic lesions.

Anatomy

The primary visual cortex in man, Brodman's area 17, is small and is disposed almost entirely on the medial aspect of the occipital lobe, a small amount extending onto the posteromedial aspect of the occipital pole. The extent of the visual cortex is extremely variable, as is the symmetry. The central 8-10^{o} of vision projects to the posterior pole, while the serial concentric zones of the retina from the macula to the periphery are represented from behind forwards above and below the calcarine fissure (2). Much of the cortex, particularly that representing the horizontal octants, is buried within the calcarine fissure.

The calcarine fissure runs upwards and forwards from the occipital pole so that the lowermost relevant slice of the computerised scan tends to show the macular cortex at the posterior pole, while the higher slices show the more anterior visual cortex, i.e. the more peripheral visual field. The higher slice would display cortex above the fissure representing the lower half field and vice versa. In the standard scanning procedure, approximately three slices cut through the visual cortex, the lowermost relevant slice including mainly the posterior pole.

Ten adult human brains were cut in 13 mm slices in the normal operating plane of the scanner. Accepting all the limitations of correct angulation in sectioning the brain and other factors, the extent of the visual cortex was marked out in each slice. These slices approximate roughly to IB, IIA, IIB and IIIA of the usual EMI-Scan notation and were made parallel to the orbitomeatal line. The striate cortex regularly showed up in at least two slices and in one brain in as many as four.

There is normally considerable variation in the anatomical features demonstrated in any one scan slice in different patients depending on the positioning of the patient, the shape of the patient's head and the centering heights above the orbitomeatal line. In the cadaver slices it was found that the major visual cortex representation occurs in the

*The National Hospital, London.

slice which includes the pineal. When viewed from the medial aspect, it contains the longest part of the calcarine fissure.

In the present series the scan slice most consistently involved is that in which the pineal is visualised and, as the scanner notation is irrelevant, a system of using the pineal slice as the reference has been adopted, the slices below the pineal being P-1, P-2 etc., and those above P+1, P+2 and so on. The P-1 slice will therefore contain most of the macular area, while slice P some, mainly upper, macula and P+1 little if any macula. From the original illustrations of BEEVOR (1), where the vascular sypply of the occipital pole was marked out in ascending horizontal slices, the posterior cerebral territory is known to be greatest lower down, and diminishes with higher cuts as the middle cerebral contribution increases. A watershed area between the posterior and middle cerebral arteries exists close to the occipital pole.

Present Series

The patients have been catergorized into four types of visual field defects (Table 1). All patients had cerebrovascular disease, migraine or cardiac emboli and had fixed field defects.

Table 1.

			Visual field defect	Scan slices showing infarct
Quadrantanopia				
Upper				
M	64	Hypertension, cerebrovascular disease	R. -	P-1, P
M	30	Migraine	R. -	P
M	65	Cerebrovascular disease	R. -	P-2, P-1, P
M	66	Mitral stenosis, cardiac embolus	R. Macular Sparing	P-1 (6. radiation)
F	32	Myocardial infarct, cardiac embolus	L. -	P-1, P, P+1
Lower				
M	65	Myocardial infarct, cardiac embolus	R. Mac. Sparing	P
M	65	Cerebrovascular disease	R. Mac. sparing	P+1 (O. radiation)
M	78	Atrial fibrillation, cardiac embolus	R. P.Mac. sparing	P+1
F	66	Hypertension, cerebrovascular disease	R. P.Mac. sparing	P+1, P+2 (also P+3 right)
M	50	Migraine	L. Mac. sparing	P+2 (O. radiation) (also P+1 left)
M	61	Atrial fibrillation, cardiac embolus	R. P.Mac sparing	Nil (?? P+1)
Complete Hemianopia				
F	74	Atrial fibrillation, cardiac embolus	L. -	P-1, P, P+1, P+2
M	68	Cerebrovascular disease	R. -	P, P+1, P+2
M	52	Hypertension, cerebrovascular disease	L. Mac. sparing	P-1, P, P+1, P+2
M	55	Cerebrovascular disease	L. Mac. sparing	Nil
M	63	Cerebrovascular disease	L. Mac. sparing	P-1, P, P+1
Homonymous scotoma				
M	62	Hypertension, cerebrovascular disease	L. Paracentral	Nil
F	57	Migraine	R. Upper quadrantic	P-1 (O. radiation)

Table 1. Continued

			Visual field defect	Scan slices showing infarct
M	65	Atrial fibrillation, cardiac embolus	L. Inferior quadrantic	Nil (?? P+1)
F	29	Migraine	R. -	P, P+1
Bilateral defect				
M	57	Cerebrovascular disease	R & L imp. visual localisation	(R) P-1, P, P+1 (O. radiation)
			Prosopagnosia, dyslexia, dysgraphia	(L) P+1
F	67	Hypertension Migraine	R & L visual agnosia agraphia, alexia,	(R) P-1, P
			prosopagnosia	(L) P-1, P
M	52	Hypertension, cerebrobascular disease	R & L tunnel vision	(R) P, P+1, P+2
				(L) P-1, P, P+1, P+2
F	57	Cerebrovascular disease	R & L inferior quadrantic Mac. sparing	(R) P, P+1
				(L) P, P+1

No attention has been paid to the details of the infarct evolution, most patients having been scanned only once as near to the time of the campimetry as possible.

Patients were scanned at various intervals, 20 days to 20 years after the onset of their lesion, and the standard 13 mm collimator was used with centring heights of 3.0, 5.5 and 8.0 cm above the orbitomeatal line. The criteria of infarct size were based on the limits of the low density area checked on the printout if necessary. An important normal variation which had to be considered when interpreting the scans was the size of the ventricular occipital horn. This extends a long way back into the occipital lobe, and, if it is asymmetrical or the patient is oblique, can lead to confusion with the low density area of the infarct and make delineation difficult.

Two patients had normal scans, 5 weeks and 5 months respectively after the onset of their lesions. Two others had equivocal scans. One of those with a normal scan surprisingly had a complete hemianopia while the other had a small homonymous central scotomatous defect. Of the two with equivocal low density occipital areas one patient had a small paracentral homonymous scotomatous defect while the other had a lower quadrantanopia with partial macular sparing. It is not surprising to find small scotomatous defects failing to show up on the scan, as this is clearly a question of size of lesion. However, it is more difficult to explain the normal scan with a major hemianopic defect.

Conversely there were two patients who had unsuspected infarcts in the occipital area without a corresponding visual field defect. Both were small and restricted to one scan slice; one was very high in the P+3 slice, and was very probably in the parastriate area (and therefore would not be expected to give rise to a visual field defect), while the other at the level of P+1 probably involved the posterior optic radiation rather than cortex.

The series also shows that occipital infarcts causing isolated visual field defects involve more than just primary visual cortex as several

cases clearly involved the para- and even peri-striate areas, together with the posterior optic radiations. This is to be expected from the distribution of the posterior cerebral artery.

Extent of Lesion

The first general question to be answered is whether a complete hemianopia is associated with a more extensive lesion (appearing in more slices) than a quadrantic or scotomatous defect. This appears to be true if the number of involved slices in each group are counted. The complete hemianopia have a mean of 3.5 slices while the upper quadrantanopias a mean of 2.0 and the lower of 1.2.

Location of Infarcts

Secondly, there was a difference in abnormal slices between those with an upper and those with a lower quadrantanopia. With an upper quadrantanopia the lesion involved slice P and below in all 5 cases (with only one also involving the P+1 slice), whereas in lower quadrantanopias none involved slices lower than slice P. Superiorly placed lesions therefore tend to produce inferior field defects and vice versa.

Macular Sparing

Thirdly, it is relevant to look at those patients who had a hemianopia and macular sparing to see if this corresponded to survival of the posterior pole. Although macular sparing has been extensively debated in the past there is still doubt about the explanation. In the case of occipital infarcts the explanation normally invoked is that the anastomotic blood supply to the occipital pole from the middle cerebral artery is sufficient to allow the macular cortex and corresponding radiation to survive.

Some of the patients in the present series who showed central sparing of 10^{o} had scans indicating survival of the posterior pole, but this was not a regular finding.

Quadrantanopias

In all the lower quadrantic defects at least partial macular sparing occurred. The scan on such a patient shows a low density area on the P slice only, indicating that little of the macula should be involved.

Scotomatous Defects

Two patients showed scotomatous defects, but with normal scans. Both scotomas, although small, were paracentral, causing the prominent symp-

toms in the patient. The lesions in these two cases were probably situated posteriorly in the macular area but are presumably smaller than the effective resolution of the scan, bearing in mind the possibly smaller alteration in X-ray attenuation.

One unusual scotomatous upper quadrantic visual field defect did not involve the occipital cortex at all, but rather was a posterior temporal lesion. The visual field defect is presumably explained as a partial lesion of the radiation, but does not conform well with the accepted anatomy of the visual pathways.

Bilateral Defects

One patient developed sudden cortical blindness which subsequently resolved, leaving constant visual distortion of shape, inability to read, loss of ability to recognize familiar objects and faces and loss of colour vision with relative preservation of central vision. This combination of defects is of great interest and has been well described. The associated lesions are usually bilateral, involving the inferior occipital lobes and radiations. The scan in this patient shows bilateral low-density lesions in the P-1 and P slices with survival of the posterior poles. The lesions extend laterally and clearly must also involve the lower radiations and parastriate areas.

Constricted fields can also be due to bilateral lesions. One patient showed infarction on the left extending from the P-1 slice anteriorly to include P and P+1 while on the right the lesion included P, P+1, P+2 and P+3. On both sides the occipital pole is spared while there is extensive damage to the rest of the visual cortex and beyond the primary visual area. The visual fields show true tunnel vision with preservation only of the central 5^{o} (using a large target) and the visual acuity was preserved to 6/5 on both sides - exactly what would be anticipated from the scan findings (Fig. 1).

The correlations which have been attempted in this paper are inexact, and it is possible to come only to general conclusions. The findings, however, are those which would be anticipated from a knowledge of the anatomy of the visual pathways. Perhaps when the resolution of the scanner is further improved and finer slice widths can be used it may be possible to develop this study. A particularly useful advance would be the ability to reconstruct the scan data and display images in other planes so that a 3-dimensional plot of the visual cortex lesion could be made.

References

1. BEEVOR, C.E.: On the distribution of the different arteries supplying the human brain. Philosophical Transactions of the Royal Society, Series B 200, 1-55 (1909).
2. HOLMES, G.: Disturbances of vision by cerebral lesions. British Journal of Ophthalmology 2, 353-384 (1918).

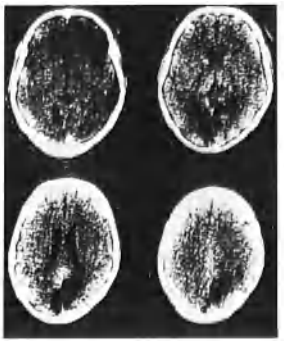

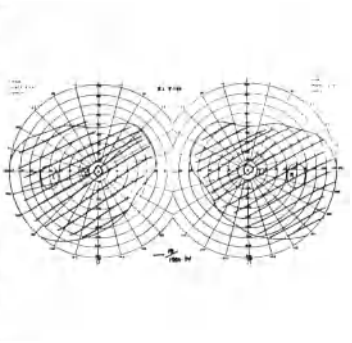

Cerebral, Cerebellar and Pontine Haemorrhages

H. R. Müller* and U. Wiggli**

Since its early description by AMBROSE (2) the C.A.T. pattern of cerebral haemorrhages has been well known, and except for the recognition of the underlying pathology, which is only occasionally evident from the scan, seldom gives rise to differential diagnostic problems. Besides thus providing a specific diagnosis, the method makes available a world of additional information, such as exact localisation and extent of the haematoma, perforation into the ventricular system and to the subarachnoid space, mass displacement and oedema.

The convenience with which these data are obtainable and the possibility to scan a patient repeatedly to follow the evolution of the lesion in time add further to the tremendous impact C.A.T. is having on the clinical management of these patients.

Early C.A.T. Appearance of the Intracerebral Haematoma

Recent intracerebral haematomas present on the C.A.T. scan as dense white areas with high absorption values (Fig. 1a).

In a series of 27 large haematomas, scanned within 24 h after onset of symptoms, and not being contaminated by artefacts on the scan, the mean values measured in the central area of the lesion were between 30 and 39 EMI units, the individual values ranging from about 15 to 47.

It has been shown experimentally that the erythrocytes are the main factor in producing the high absorption values of recent haematomas (1, 8). While circulating blood, measuring 13-28 EMI units according to SCOTT et al. (8), contributes to the absorption value of intact brain tissue only as a partial volume and, therefore, cannot be identified as such, the high absorption becomes evident if extravasation occurs and consequently full volumes are measured.

There is experimental evidence for clotting not being necessary for the production of the high absorption pattern found in recent haematomas. However, from experimental findings (8) as well as from measurements in vivo (5, 6) it appears that some increase in absorption values of the haematoma occurs during the first few hours after bleeding.

In order to demonstrate in vivo the role of the erythrocytes in the production of high absorption, the mean absorption was measured in the centre of 24 haematomas scanned within 24 h after bleeding, and the values obtained were plotted against the haemoglobin and haematocrit values measured on admission of these patients. On the resulting graph (Fig. 2) a weak linear correlation can be seen which proved, however,

*Neurosurgical Clinic, University of Basle, Kantonsspital.
**Institue of Medical Radiology, University of Basle, Kantonsspital.

not to be statistically significant. Haemodilution in some of the patients having received infusions before being admitted to hospital as well as individual variations of serum expulsion out of the clot may have interfered in this experiment.

Evolution in Time of the Haematoma Pattern

If the mean absorption of the whole haematoma area is followed, a decrease can be observed from the first week (Table 1). Conversely, the absorption measured in the central area remains high at least for two weeks (Table 2).

Table 1. Mean absorption (EMI scale) ±SD of total haematoma area in four cases followed up

	First day	after 1 week	2 weeks	4 weeks
1.	29.8 ±9.0	23.7 ±8.2	23.4 ±8.5	19.7 ±7.3
2.	29.3 ±8.7	27.0 ±7.9	24.2 ±7.3	23.4 ±5.2
3.	28.5 ±9.0	25.7 ±8.8	18.0 ±7.0	16.9 ±4.5
4.	26.9 ±7.9	24.1 ±8.4	18.4 ±5.3	

Table 2. Mean absorption (EMI scale) ±SD, central region of intracerebral haematomas. (Rectangular sample of 100 1.5 × 1.5 × 13 mm voxels)

Day 2 to 7	Day 8 to 14	Day 15 to 21
36.8 ±3.2	37.0 ±6.5	32.2 ±3.2
35.6 ±3.0	35.5 ±3.3	31.8 ±5.2
33.0 ±3.5	35.2 ±2.9	28.2 ±4.7
32.4 ±2.4	35.0 ±2.9	
32.2 ±3.2	34.8 ±3.9	
31.8 ±5.0	23.8 ±3.7	

Subsequently the mean absorption value of the total haematoma area falls progressively, at a rate which seems to be related to the size of the haematoma, the final stage being a lacuna of reduced size with various degrees of tissue retraction and ventricular widening.

The different time scale of absorptional behaviour of the central and the total haematoma area appears to be due to transformation of the haematoma beginning at its periphery.

A typical oedema pattern surrounding the high density zone is only exceptionally seen from the first day after bleeding. It usually becomes visible only during the first week, almost invariably increases in size during this period and may remain for several weeks. It is our impression, though no measurements are available, that the oedema zone remains smaller if steroid treatment is given and that it is usually more extensive in parietal and occipital haematomas than those in other locations.

In many haematomas a small border surrounds the high absorption area even on very early scans. It is not finger-shaped and may be due to serum migrating out of the clot rather than oedema.

In some subacute intracerebral haematomas a ring pattern can be seen after enhancement, which may, with an inappropriate or controversial history, give rise to the differential diagnosis of a tumor. Such a pattern, with a high central density, was observed in one chronic encapsulated intracerebral haematoma (Fig. 1b). In this case the capsule appeared to have organised too fast in relation to the natural degradation of the haematoma to allow the clearance of the high density degradation products.

Haematoma Location as Related to Aetiology

The following is a retrospective analysis of 123 consecutive observations of non-traumatic intracerebral, cerebellar and pontine haemorrhages including five cases of primary intraventricular bleeding.

Table 3. Non-traumatic haematomas examined by C.A.T. from Jan 1974 to Sept. 1976 (123 cases). Numbers in brackets indicate ventricular perforation

	No.	Hypertension	Hypertension + Anticoagulant	Anticoagulant therapy	Aneurysm	Arteriovenous malformation	Other
Frontal	22 (12)	1	-	1	11 (9)	4 (2)	5 (1)
Temporal (including trigonal)	22 (5)	2	3 (1)	6 (1)	1	1	9 (3)
Parietal	7	1	1	2	-	2	1
Occipital	7 (2)	1	-	4 (1)	-	1	1 (1)
Putaminal	28 (15)	18 (7)	2 (1)	2 (2)	3 (3)	-	3 (2)
Caudatal	3 (2)	1 (1)	1	1 (1)	-	-	-
Thalamic	16 (12)	11 (9)	2 (1)	2 (1)	-	1 (1)	-
Cerebellar	8 (3)	3 (1)	1 (1)	1 (1)	-	1	2 (0)
Pontine	5 (2)	2 (1)	1	1 (1)	-	1	-
Primary ventricular	5	-		3	-	-	2
Total	123 (53)	40 (19)	11 (4)	23 (8)	15 (12)	11 (3)	23 (7)

A total of 249 scans were done on these patients; 56 patients had angiography and 57 patients died, of whom 44 underwent autopsies.

The following main points emerged from the review of this case material:

Among the *lobar haematomas* as many as half of the frontal ones were caused by aneurysmal bleeding. On the other hand, haemorrhages caused by anticoagulant therapy showed a clearcut predilection for the temporo-occipital region and, particularly, the trigonal area. Only 5 of the 58 lobar bleedings were hypertensive. Contrariwise, 8 of the 11 intracerebral bleedings from arteriovenous malformation were lobar. Most of the

ventricular perforations occurred in the frontal haematomas, particularly with aneurysmal bleeding.

As would be expected, as many as two-thirds of the *basal ganglia haemorrhages* were purely hypertensive, but in this group too, anticoagulant therapy was quite an important bleeding cause. All putaminal haemorrhages rupturing into the ventricular system did so by reaching the frontal horn over the external and/or internal capsule. Haemorrhages within the thalamus ruptured either into the posterior part of the third or into the lateral ventricle.

A special feature of our case series is the observation of nine particularly small hypertensive paraganglionic haemorrhages (four putaminal, three thalamic and one caudate). Six of these survived with conservative treatment. These patients, presenting with motor or sensorimotor hemipareses of capsular type are particularly prone to be misdiagnosed clinically as ischaemic strokes. A special feature of thalamic bleeding was the showing of signs usually attributed to lobar lesions, such as a sensorimotor aphasia in one case and a parietal lobe syndrome in three.

Eighteen basal ganglionic haemorrhages of medium to large size, 9 of them having ventricular perforation, were operated and 14 survived. The operative mortality (22%) was thus even lower - with the criteria for operation adopted - than that of the 21 lobar haematomas operated in the same time period (33%). However, 7 patients of the basal ganglia group as opposed to two in the lobar group remained bedridden or severely handicapped.

Eight *cerebellar* and five *pontine haemorrhages* were observed, and there was no problem of detecting and localising these lesions (Fig. 3). Even pontine haematomas measuring less than 1.5 × 1.5 cm were clearly demonstrated. In five patients in whom a cerebellar or pontine haematoma had ruptured into the fourth ventricle, blood was present in both occipital horns.

Five patients having cerebellar haematomas were operated upon, and three survived. One of them was tetraplegic on admission and, thanks to early diagnosis by C.A.T., left the hospital ambulant 10 days after operation. Since the clinical pictures of cerebellar and pontine haemorrhages do not categorically exclude each other, the diagnosis by C.A.T. played a crucial role in improving the salvage rate of our patients suffering from cerebellar haematomas.

Discussion

The high accuracy of C.A.T. for the diagnosis of intracerebral haematomas, as reported by several authors (2, 5-8) has been confirmed by the retrospective analysis of our case material. Except for some subacute and late stages, where isodense patterns may occur (3) and except for some encapsulated chronic haematomas, which could be mistaken for tumours or thrombosed aneurysms, there seems to be no problem in identifying a haematoma as such.

Since bleeding sources such as arteriovenous malformations and aneurysms cannot be excluded even on enhanced scans, and since bleeding from them can produce any haematoma pattern, a deliberate use of angiography in patients whose C.A.T. shows an intracerebral haematoma is advisable. Angiography should be done for this reason even in patients primarily

scheduled for conservative treatment. Only cases judged from clinical and C.A.T. evidence to be fatal, and patients not allowing, from the rapidity of the clinical evolution, time for further investigations before surgery should be excluded from angiography.

An extensive use of C.A.T. in stroke patients is recommended since from our experience the proportion of intracerebral haematomas not be detected without C.A.T. is not negligible.

Finally, C.A.T. should lead us to reconsider the principles for conservative versus operative management. We are learning from this method that many lobar haematomas, even of large size, may do well under conservative treatment and that an expectant policy is certainly justified in all cases not primarily presenting with signs of brain stem compression or ventricular block. On the other hand basal ganglia haemorrhages, not considered so far by the majority of neurosurgeons to benefit from surgical treatment, are becoming, through the use of C.A.T., progressively successfully operable.

References

1. ALFIDI, R.J., MACINTYRE, W.J., MEANY, T.F., CHERNAK, E.S., JANICKI, P., TARAR, R., LEVIN, H.: Experimental studies to determine application of CAT scanning to the human body. The American Journal of Roentgenology 124, 199-207 (1975).
2. AMBROSE, J.: Computerised transverse axial scanning (tomography): Part 2. Clinical application. British Journal of Radiology 46, 1023-1047 (1973).
3. MESSINA, A.V., CHERNIK, N.L.: Computed tomography: the "resolving" intracerebral hemorrhage. Radiology 118, 609-613 (1975).
4. MÜLLER, H.R., WÜTHRICH, R., WÜGGLI, U., HÜNIG, R., ELKE, M.: The contribution of computerized axial tomography to the diagnosis of cerebellar and pontine haematomas. Stroke 6, 467-475 (1975).
5. MÜLLER, H.R., WÜTHRICH, R., LÉVY, A., HÜNIG, R., ELKE, M.: Diagnosis and localization of intracerebral haematomas using computerized axial x-ray tomography. Cerebral Vascular Disease, 7th International Conference Salzburg 1974. MEYER, J.S., LECHNER, H., REIVICH, M. (eds.). Stuttgart: Thieme 1976, pp. 55-60.
6. PAXTON, R., AMBROSE, J.: The EMI scanner. A brief review of the first 650 patients. British Journal of Radiology 17, 530-565 (1974).
7. PRESSMAN, B.D., KIRKWOOD, J.R., DAVIS, D.O.: Posterior fossa hemorrhage. Localization by computerized tomography. Journal of the American Medical Association 232, 932-933 (1975).
8. SCOTT, W.R., NEW, P.F., DAVIS, K.R., SCHNUR, J.A.: Computerized axial tomography of intracerebral and intraventricular hemorrhage. Radiology 112, 73-80 (1974).

a b

Fig. 1. (a) Putaminal haemorrhage from middle cerebral artery aneurysm. (b) Encapsulated chronic intracerebral haematoma within the temporal lobe. Ring pattern after enhancement (*right*)

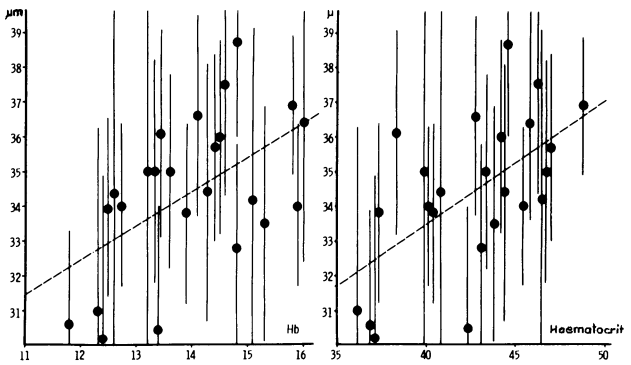

a b

Fig. 2a and b. Mean central absorption µm (EMI scale) of 24 fresh intracerebral haematomas versus (a) haemoglobin and (b) haematocrit (rectangular sample of 100 1.5 × 1.5 mm units)

a b

Fig. 3. (a) Cerebellar haematoma of right hemisphere. (b) Pontine haematoma ruptured into the fourth ventricle

Diagnosis of Subarachnoid Haemorrhage by Computerised Tomography in Intracranial Aneurysms

G. Scotti*, D. Melançon**, R. Ethier*, and K. Terbrugge***

The advent of computerised tomography has not yet really changed the diagnostic approach to subarachnoid haemorrhage. Four-vessel catheterisation remains absolutely necessary to visualise the ruptured aneurysm. However, computerised tomography has added some very useful information.

According to the few extensive papers published up to now on the use of computerised tomography in subarachnoid haemorrhage (1, 2, 3) the presence of extravasated blood may easily be recognized, as well as its extent and distribution. Sometimes the location of the aneurysm itself may be predicted by the pattern of distribution of blood in the subarachnoid spaces or the formation of a haematoma. The role of computerised tomography is particularly relevant in following the patient's clinical evolution: oedema due to spasm is clearly seen as are fresh bleeding and the development of hydrocephalus.

The aim of our work was to evaluate: first, the accuracy and reliability of C.A.T. in showing the subarachnoid haemorrhage and intracranial aneurysms; second, the possibility of predicting the location of the ruptured aneurysm on the basis of the pattern of distribution of extravasated blood.

Material and Methods

The C.A.T. scans of 46 patients admitted to the Montreal Neurological Institute for subarachnoid haemorrhage following rupture of an intracranial aneurysm were reviewed. The presence of one or more aneurysms was assessed by means of four-vessel angiography in all but one patient, in whom only post-mortem examination was available.

The location of aneurysms is listed in Table 1. Of the two unusual cases one was an aneurysm of the posterior pericallosal artery, the other was on a lenticulostriate artery.

In reviewing the scans, note was taken of: (a) presence of extravasated blood; (b) its pattern of distribution and the possibility of predicting the site of the ruptured aneurysm on this basis; (c) the rate of resorption of extravasated blood.

---

*Neurological Clinic, University of Milan, Italy.
**Montreal Neurological Institute, Canada.
***Toronto Western Hospital, University of Toronto, Canada.

Table 1. Characteristics of the group of 46 patients with subarachnoid haemorrhage and intracranial aneurysms

Location of aneurysm	Number of patients	C.A.T. evidence of extravasated blood
Anterior communicating	14	13
Internal carotid - posterior communicating	10	9
Middle cerebral	4	4
Basilar	2	2
Multiple	14	12
Unusual locations	2	2
Total	46	42

Results

Extravasated blood was recognised in 42 of the 46 patients; this gives 90% accuracy of C.A.T. in demonstrating extravasated blood. Its density ranges between 35 and 45 Hounsfield units.

Table 2. Localisation of subarachnoid blood in cases of ruptured aneurysm

	Total	Supra-sellar	Interhemi-spheric	Sylvian	Interpe-duncular	Ambient	Quadri-geminal
Anterior communicating	13	9	13	6	3	3	
Internal carotid - posterior communicating	9	5	3	5	2	2	1
Middle cerebral	4		2	4			
Basilar	2	1	2		1	1	1
Multiple	12	5	9	6	1	2	2

Table 3. Haematomas and intraventricular haemorrhages in cases of ruptured aneurysm

	Total	Intra-ventricular	Intra-cerebral	Septal	Sylvian	Inter-front	Subdural	Others
Anterior communicating	13	2	1	1		1		
Internal carotid - posterior communicating	9	1	1		1			2
Middle cerebral	4	1	1		2		2	
Basilar	2	2						
Multiple	12	2	1	1	1			1
Unusual	2	1	2					

Tables 2 and 3 show the preferential distribution of extravasated blood according to the site of the ruptured aneurysm; some patterns are characteristic but not necessarily diagnostic of each group since frequent overlap exists. Anterior communicating artery aneurysms tend to bleed almost invariably into the suprasellar cisterns and the interhemispheric fissure (Fig. 1). Blood is frequently seen around the brain stem and in the Sylvian fissures. Callosal and cingulate sulci may be outlined by blood. This pattern, although very common for anterior communicating aneurysms is, however, not pathognomonic since it may also be seen in ruptured internal carotid or posterior communicating aneurysms. In the last group, however, blood is less frequently present in the interhemispheric fissure and more frequently in the Sylvian fissure where it may collect to form a haematoma (Fig. 3). Middle cerebral artery aneurysms almost invariably bleed into the Sylvian fissure, usually unilaterally. Our experience with ruptured basilar aneurysms is limited. In cases of multiple aneurysms the pattern of extravasated blood depends on the one that had ruptured and the location may be suggested when it is typical.

When the location of the haematoma is taken into consideration certain typical patterns are found. The only pathognomonic localising finding is the septal haematoma (Fig. 2) which occurs only with ruptured anterior communicating artery aneurysms (1). Frontal haematomas are seen in anterior communicating and internal carotid artery aneurysms. Sylvian haematomas may indicate either a ruptured middle cerebral artery aneurysm on that side, or an internal carotid or posterior communicating artery aneurysm (Fig. 3).

Temporal or basal ganglia haematomas occur with ruptured aneurysm in the same location. In some cases a small haematoma just around the aneurysm may indicate exactly its location.

The two subdural haematomas in our series were found in ruptured middle cerebral artery aneurysms. Intraventricular haemorrhage may be seen in any group.

In the few patients in which the C.A.T. scan was repeated every other day in order to study the rate of resorption of extravasated blood, it was found no longer to be recognizable after the 6th to the 10th day following the bleed.

Discussion

The use and value of computerised tomography in the diagnosis of subarachnoid haemorrhage are obvious from the results of our retrospective analysis and have already significantly modified our diagnostic approach to patients with this symptom.

Extravasated blood was demonstrated in 90% of subarachnoid haemorrhages; the percentage rises to 100% if one considers only the cases in which the scan was done within the first 7 days after a bleed.

Lumbar puncture may, in our experience, be avoided and will probably remain an historical manoeuvre in subarachnoid haemorrhage. C.A.T. gives much information unobtainable from angiography by showing the extent of bleeding into the subarachnoid spaces, the ventricles, brain parenchyma and subdural spaces. The location of the ruptured aneurysm may frequently be predicted and this is particularly useful in cases of multiple aneurysms. The initial C.A.T. scan carried out to diagnose

the subarachnoid haemorrhage may also become a very important baseline for follow-up C.A.T.

The frequency of complications in subarachnoid haemorrhage is well known and often necessitates repeated angiography. C.A.T. scans will probably eliminate this need since they clearly show recurrence of bleeding, oedema due to ischaemia following vasospasm and the presence and formation of hydrocephalus. The mechanism of development of hydrocephalus will probably be better understood.

References

1. HAYWARD, R.D., O'REILY, G.V.A.: Intracerebral haemorrhage. Accuracy of computerised transverse axial scanning in predicting the underlying etiology. Lancet 1976/I, 4.
2. KENDALL, B.E., LEE, B.C.P., CLAVERIA, L.E.: Computerised tomography and angiography in subarachnoid haemorrhage. The British Journal of Radiology 49, 483-501 (1976).
3. SCOTTI, G., ETHIER, R., MELANÇON, D., TERBRUGGE, K., TCHANG, S.: Computerized tomography in the evaluation of intracranial aneurysms and subarachnoid hemorrhage. Radiology (1976) (in press).

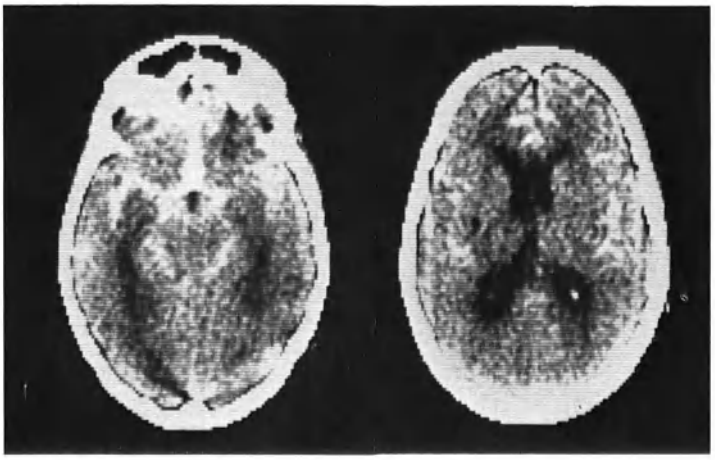

a b

Fig. 1a and b. Subarachnoid haemorrhage following rupture of anterior communicating artery aneurysm; increased density is seen in the basal cisterns, crural and ambient cisterns, Sylvian fissures, interhemispheric fissure, callosal and cingulate gyri

Fig. 2. Septal haematoma, a pathognomonic picture of ruptured anterior communicating aneurysm

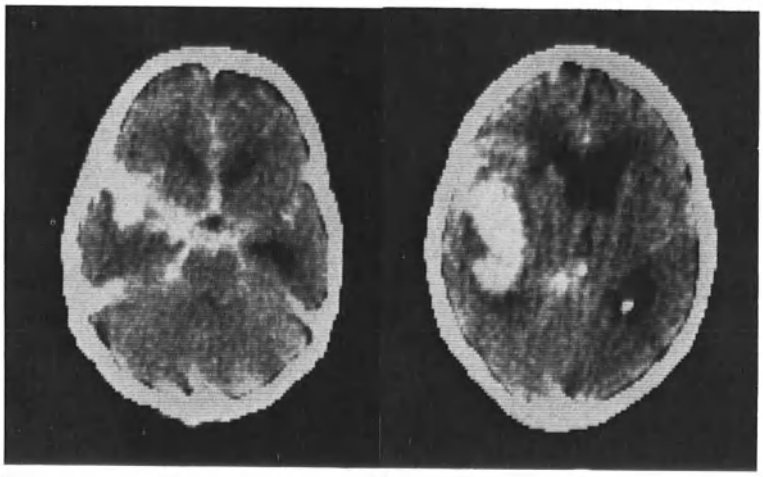

a b

Fig. 3a and b. Sylvian haematoma following rupture of an internal carotid artery aneurysm

The Use of Computerised Axial Tomography (C.A.T.) for the Diagnosis and Management of Intracranial Angiomas

B. E. Kendall and L. E. Claveria*

In a recent publication (3) we analysed all the proven cases of intracranial angioma which had been examined by computerised axial tomography (C.A.T.) and also all those cases in which a proven C.A.T. diagnosis of angioma had been made, using a 160 × 160 matrix EMI head scanner at The National Hospital, Queen Square, since December, 1974. We have added a further 10 cases, bringing the total number of angiomas in our series examined by C.A.T. to 50, and present a review of the value and limitations of C.A.T. in the diagnosis and management of angiomatous malformations based on this series and on cases reported in the literature.

The results of anaylsis of our series of 50 angiomatous malformations are presented in Tables 1-6.

Classification

Arteriovenous Malformations (avm's)

The majority of intracranial angiomas detected by neuroradiological methods are avm's involving the brain parenchyma and sometimes the overlying meninges; 46 of our series were of this type. There were two dural avm's, both shunting into the transverse sinuses, neither of which caused any enlargement of cerebral vessels nor produced any focal changes on the computed tomograms. Pathologically enlarged meningeal channels were present on the plain X-rays of both these patients and suggested the diagnosis prior to angiography.

Cavernous Angiomas

Cavernous angiomas are composed of dilated venous spaces without intervening brain parenchyma; calcification may be present in the walls of the abnormal vessel. The one cavernous angioma in this series was illustrated in our previous publication (Fig. 11) (3). It showed as a circumscribed rounded lesion of increased attenuation similar to that of an intracerebral haematoma and was explored without further contrast studies. The correct diagnosis was only made by histological examination.

Venous Malformations

The so-called venous malformations are in fact avm's in which the feeding arteries are of normal size and shunting is relatively slow, so that the conspicuous components of the malformation are dilated

*Lysholm Radiological Department, The National Hospital, London.

venous channels which are separated by cerebral substance. They are well shown with modern angiographic techniques. The one case in this series showed calcification in the brain parenchyma adjacent to the malformation, and dilated subependymal veins draining from it were shown after contrast enhancement (Fig. 1). Several cases of Sturge-Weber syndrome have been examined but will be reported separately (5).

Telangiectases

Intracranial angiomas also include capillary telangiectases, which are mentioned for completeness. These lesions, however, are too small to be detected on C.A.T. and, although they are responsible for some apparently spontaneous intraparenchymal haematomas, they cannot usually be recognised prior to post-mortem examination.

Clinical Features

The presenting features, age and sex of our patients are set out in Table 1. It differs from other series in two features. Firstly, 54% of our patients presented initially with subarachnoid haemorrhage whereas usually only about 40% of patients present in this way (6). Many of our patients were referred from other hospitals into our neurosurgical units, which accounts for this prevalence of subarachnoid haemorrhages. Secondly, the average age (33 years) of patients presenting with haemorrhage is considerably greater than that usually recorded in the lit-

Table 1. Cerebral angiomas

1. Total 50	27 presenting with subarachnoid haemorrhage 23 presenting with other symptoms		
2. Age range	6-63 *Mean* 33	3. Sex:	25 female 25 male

(a) Presenting as subarachnoid haemorrhage - Age range 6-63 Mean 33 - (a) 13 female 14 male
(b) Presenting miscellaneous - Age range 13-63 Mean 33 - (b) 12 female 11 male

erature; for example it was 15-20 years in the review by PERRETT and NISHIOKA (9). The majority of children in our region are referred to a specialised paediatric unit which probably accounts for this discrepancy. We do not consider that this selection has significantly influenced the C.A.T. findings in our series.

An important distinction is made between cases presenting with subarachnoid haemorrhage (group 1) and those presenting with other symptoms but without subarachnoid haemorrhage (group 2). In the first group the primary purpose of the scan has been to show the site of bleeding so that detailed selective angiography can be directed towards showing the precise anatomy of any underlying lesion and its connections to the cerebral vessels. We believe it is reasonable to omit scanning after intravenous contrast injection if this information is given by the plain scans. In the other group also, plain scanning may strongly suggest the diagnosis and, especially when a haematoma is shown, angiography will probably be indicated. However, in circumstances where it

is evident that an angioma would be best managed conservatively regardless of its precise anatomy, either because of the risks of surgical approach in a particular location or because of the condition of the patient, angiography may be considered unnecessary if C.A.T. supplemented by other non-invasive studies, such as in gamma encephalography (10, 12), can definitely establish the diagnosis. In this group rescanning after intravenous contrast medium should not usually be omitted. Of the total series all the patients were scanned without intravenous contrast injections and 74% were rescanned after contrast injection.

Localisation

The localisation of the angiomas in this series is shown in Table 2. Apart from the dural avm's, the position of the malformation had no definite influence on the possibility of visualising the lesion though it is evident that small malformations adjacent to bone may be difficult to detect because of partial volume defects.

Table 2. Cerebral angiomas

Localisation	With haemorrhage	%	% of total	No haemorrhage	%	% of total	Total	%
Frontal	6	22	12	5	22	10	11	22
Temporal	4	15	8	3	13	6	7	14
Parietal	7	26	14	7	30	14	14	28
Occipital	4	15	8	2	9	4	6	12
Deep	2	7	4	1	4	2	3	6
Posterior fossa	1	4	2	3	13	6	4	8
Intraventricular	2	7	4	1	4	2	3	6
Dural	1	4	2	1	4	2	2	4

Right and left hemispheres equally affected.

The attenuation value of blood is proportional to the haemoglobin level (8); with a normal level of around 15 g percent of haemoglobin the attenuation value is 28 EMI units, which is higher than that of brain substance and considerably greater than that of CSF. Large vessels of an angioma are only directly visible because of the volume of the blood which they contain and hence the angiomatous complex is usually slighter denser than the adjacent brain. The precise appearance of the vessels will vary, depending on their angle relative to the tomogram cut; they will be tubular or vermiform when cut longitudinally and oval or rounded when they are transected. Multiple vessels separated by brain and CSF spaces give an appearance of mottled density. Enlarged feeding arteries and draining veins are frequently evident. These features are considered to be typical of angiomatous malformations (Fig. 2). The incidence of secondary effects and complications of avm's in this series is shown in Table 3. Mass effect was not a prominent feature, in the absence of haemorrhage, but it did occur with large avm's. Low density adjacent to the avm's, usually recognisable as atrophy though occasionally in-

Table 3. C.A.T. Findings

	Presenting as sub-arachnoid haemorrhage	%	% of total	Presenting with other neurology	%	% of total	Total	%
Calcification	2	7	4	7[a]	32	14	9	18
Hydrocephalus	8	30	16	2	9	4	10	20
Mass effect	10	37	20	4	18	8	14	28
Focal atrophy/ infarct	4	15	8	11	50	22	15	30
Associated haematoma	15	56	30	2[b]	9	4	17	34

[a] Including 1 venous angioma.
[b] Including 1 thrombosed cavernous angioma.

distinguishable from infarction on a single scan, was particularly common in group 2. Calcification in the walls of the angiomatous vessels, in the draining veins or in the parenchyma is shown on plain films in between 15% (2) and 29.5% (11). Calcification should be more readily detected on C.A.T. but in the present series it was only visible in 18%. It may be obscured by adjacent haemorrhage at the window levels usually employed.

Rescanning after Intravenous Contrast Injection

Attenuation of the blood, including that in the angiomatous malformation, is increased by intravenous contrast medium. About 20% of avm's, which were not visible or showed only slight or non-specific changes before intravenous contrast injection, become typical after enhancement as the increased density of blood overcame the partial volume effect of the brain which was previously masking them. Seven cases with typical appearances prior to enhancement are confirmed and further features of the malformations, such as connecting vessels and more precise outlining of the extent of the lesion, are usually apparent after enhancement (Fig. 3). A malformation draining through transparenchymal veins has a typical wedge shape tapering towards the subependymal

Table 4.

C.A.T. changes	Presenting with subarachnoid haemorrhage	Presenting without clinical haemorrhage	Total
Vessels shown on C.A.T. without contrast	12 (44%)	10 (43%)	22 (44%)
Atypical density C.A.T. without contrast	8 (30%)	4 (17%)	12 (24%)
Vessels shown after contrast only	7 (26%)	3 (11%)	10 (20%)
Others	2 (7%)	4 (17%)	6 (12%)

region, which may be recognised if the wedge lies in the axis of the C.A.T. cut. Our 50 patients can be subdivided into four groups as shown in Table 4.

Typical C.A.T. Appearances without Intravenous Contrast Injection

Twenty two of our cases (44%) showed typical changes on C.A.T. without contrast injection. Rescanning after contrast was performed in 13 of them and typical appearances were confirmed in 12 (Figs. 2 and 3). The other one failed to enhance, and because of this we made a mistaken diagnosis of a glioma, despite the typical pre-contrast scan and absence of any mass effect. The lesion did not opacify at angiography and only at surgery was it eventually established that the C.A.T. appearances were due to completely thrombosed vessels of an avm. Similar cases have been described (13) and it should be noted that C.A.T. is the best pre-operative means of showing a totally thrombosed avm.

Typical C.A.T. Appearances Only after Intravenous Contrast Injection (Table 5)

Table 5.

	Group 1	Group 2	Total
Typical C.A.T. only after intravenous contrast	7	3	10
Findings on Plain C.A.T.:			
Normal	3	1	4
Focal high density	2	1	3
Focal low density	2	0	2
Focal atrophy	0	1	1

In the 10 cases (20%) in which the typical appearances of an avm were seen only after contrast enhancement, 7 presented with subarachnoid haemorrhage and four of these showed a focal abnormality on the pre-contrast scan (Fig. 3). Of the three presenting without haemorrhage, one showed focal atrophy and another showed a high density adjacent to the left side of the third ventricle, deforming it and causing hydrocephalus. There was marked enhancement of the lesion and it is evident in retrospect that it was composed of tubular structures connecting with the dilated vein of Galen. Despite these typical features and the absence of any marked mass effect or surrounding oedema, the lesion was misdiagnosed as a glioma on C.A.T. It has been illustrated in a previous paper (3).

Focal High Attenuation Lesion

In the remaining 18 patients (36%) typical appearances due to the angioma itself were not evident. In 12 cases (24%) there was a focal high attenuation lesion on the unenhanced scan and in 10 of these patients, 8 of whom presented with subarachnoid haemorrhage, this was

due to an intraparenchymal haematoma. In 1 case the density was proved at surgery to be due to the thrombosed cavernous haemangioma which has been discussed. In the 12th case the density was due to calcification adjacent to a venous angioma (Fig. 1). Intravenous contrast medium was given to 5 of the cases in this group and enhancement adjacent to the haematoma occurred in 4 of them. There was, however, no typical appearance of enlarged vessels and it should be noted that cases have now been reported in which enhancement has occurred adjacent to a resolving spontaneous or traumatic haematoma (7, 14). Thus rim enhancement is non-specific, though it may well have been due to the angioma itself in our cases. In the 5th patient there was no enhancement in a small cerebellar avm which filled well on angiography. It is uncertain now why even in retrospect it could not be detected, but this was possibly due to its small size and its proximity to the tentorium, so that enhancement of that structure following intravenous contrast medium may have obscured that of the malformation.

Significance of Position of a Haematoma

The relationship between the site of the haematoma on C.A.T. and the probable aetiology of a haemorrhage has been previously discussed (1, 3), and the value of C.A.T. in localising the site of origin of subarachnoid haemorrhage has also been discussed (4). In brief, the likelihood of an underlying avm may be suggested by clinical features, such as a relatively young patient, the absence of systemic causes for spontaneous haemorrhage and by a haematoma in an unusual site for aneurysmal or spontaneous haemorrhage. The former extend to the common sites of berry aneurysms close to the circle of Willis; anterior communicating aneurysms tend to involve the frontal lobes, interhemispheric or callosal region; middle cerebral aneurysms tend to involve the temporal lobes, more lateral parts of the frontal lobes and para-sylvian region; and distal carotid-posterior communicating aneurysms tend to bleed into the temporal lobes. Spontaneous haemorrhages may occur in any position but haematomas within the centrum semi-ovale and parietal lobes are more usually spontaneous. Focal haematomas immediately adjacent to the ventricular walls and bulging into the ventricular cavities (Fig. 3) are especially suggestive of avm's and a sufficient number of haematomas in the thalami and subcortical regions are due to avm's to warrant angiography unless a systemic cause for them is evident. The combined clinical and radiological features suggested an avm in all eight of these cases presenting with subarachnoid haemorrhage and a parenchymal haematoma, and detailed angiographic investigations showed an avm adjacent to the lesion in every case.

Focal Low Attenuation or Normal Scans

In the remaining six cases (12%) the probability of an angioma could not have been suggested on the C.A.T. findings alone. One patient showed a low attenuation lesion which showed central enhancement indistinguishable from an infarct prior to angiography (Fig. 4). Slight focal atrophy was present in another patient who was not rescanned after intravenous contrast. No focal abnormality was present in the other four patients. Two of these had dural avm's which have previously been discussed, and intravenous contrast medium was not given to the other two patients.

Mistaken Diagnosis of avm (Table 6)

Table 6. Misdiagnosis of lesion on C.A.T.

Reported C.A.T. diagnosis	Correct diagnosis
Glioma	avm
Infarct	avm
Glioma	avm thrombosed
Haematoma	Cavernous angioma
Angioma or glioma	Venous angioma
avm	Recent infarct (3)
avm	Empyema

During the period of the study over 4500 C.A.T. scans were performed and among these there were four cases in which a low density lesion showed a tubular pattern of partial enhancement which caused us to make a mistaken diagnosis of angiomatous malformation, though in all cases the appearances were atypical. Three of these were infarcts between 1 and 4 weeks old, and there is no doubt that the distinction from an avm could have been made by repeat scanning after an interval of 3 or 4 weeks. The fourth case has already been reported in detail (3); in brief, the C.A.T. scan showed a well-circumscribed low-density lesion below the left side of the tentorium which showed marked marginal enhancement continuous with the straight sinus after intravenous contrast medium. An avm was suspected, but this was ruled out by vertebral angiography. After 1 month the C.A.T. demonstrated increase in the size of the subtentorial lesion, with marginal enhancement of even thickness around a low density centre suggesting an abscess; at surgery this was shown to be an infratentorial subdural empyema. In retrospect, the only reason for confusion on the first scan was the proximity of the enhancing margin of the lesion to the straight sinus which was naively interpreted as drainage of a vascular malformation into the sinus. No cerebral tumours were mistakenly diagnosed as avm's. It should be noted that none of these misdiagnosed lesions was of increased density prior to enhancement, nor did any of them show the tubular or mottled densities of enlarged vessels after enhancement which are so suggestive of an angiomatous malformation.

Value of C.A.T. in Management

C.A.T. appearances which should have suggested the presence of an angioma were present in 64% of these cases and in a further 24% a focal high-density lesion was shown which, in the clinical context, again suggested the possibility of an underlying angioma. The value of C.A.T. in diagnosis of these lesions is therefore apparent. If C.A.T. is negative, plain film examination is of particular importance in cases with subarachnoid haemorrhage, since detection of enlarged vascular channels may give pre-angiographic indication of a dural avm and the nature of any calcification is better assessed on plain films than on C.A.T. if it is visible on the former.

C.A.T. should be performed prior to angiography because, by showing the position and extent of any abnormality, it may lead to modification of further diagnostic studies. Thus, if the lesion is shown to be extensive, for example, involving a whole hemisphere (Fig. 5) or to be sit-

uated centrally within the brain stem, it may be considered surgically inaccessible and angiography, therefore, may be avoided. Again, the precise position of the lesion indicates which vessels should be examined in detail to elucidate the nature of the malformation and the anatomy of its arterial supply and venous drainage. Even though angiography is the only means of showing these features of an angioma and is indicated on clinical grounds, C.A.T. should not be ommitted because it shows more accurately the extent of any haemorrhage, infarction or oedema and the relationship of the malformation to these changes and to the cerebral parenchyma and ventricular system. C.A.T. and angiography are thus complementary in determining the feasibility of surgery and sometimes in determining the best surgical approach.

C.A.T. is valuable in elucidating the mechanism of any clinical deterioration occurring spontaneously or during the postoperative period. Thus infarction or bleeding (Fig. 2) may be distinguished from hydrocephalus and the cause of the latter may be shown, whether it be obstructive due, for example, to large vessels or blood clot occluding the aqueduct, or communicating due to previous haemorrhage.

Summary

C.A.T. showed typical changes due to an angioma itself in 44% of unenhanced scans. In 20%, typical vessels were only shown after contrast injection. A focal or lateralising high attenuation due to bleeding, thrombosed vessels or calcification was present in a further 24%. C.A.T. failed to show any focal abnormality in 8% of this series, but in two of these cases (4%) C.A.T. was not repeated after intravenous contrast.

C.A.T. shows the relationship of the malformation to the brain parenchyma and ventricular system, and complications such as parenchymal and intraventricular haematoma, infarction, hydrocephalus, calcification, focal atrophy and cyst formation. It is thus of great value in determining the cause of a clinical state both before and after surgery and in controlling management. C.A.T. does not elicit the exact nature of the malformation, nor show the site of a shunt, nor the precise anatomy of the arterial supply and venous drainage. Thrombosed angiomas, which do not fill at angiography, may be recognised on C.A.T.

References

1. HAYWARD, R.D.,O'REILLY, G.C.A.: Intracerebral haemorrhage. Lancet 1976/I, 1-4.
2. HOUDART, R., LE BESNERAIS, Y.: Les anévrysmes artério-veineux des hémisphères cérébraux. Paris: Masson 1963.
3. KENDALL, B.E., CLAVERÍA, L.E.: The use of computed axial tomography (CAT) for the diagnosis and management of intracranial angiomas. Neuroradiology (in press).
4. KENDALL, B.E., LEE, B.C.P., CLAVERÍA, E.: Computerised tomography and angiography in subarachnoid haemorrhage. British Journal of Radiology 49, 483-501 (1976).
5. KINGSLEY, D.P.E.: Computed tomography in the phakomatoses. Proceedings of First European Seminar on Computerised Axial Tomography in Clinical Practice, London 11th-15th October, 1976.
6. KRAYENBÜHL, H., YASARGIL, M.G.: Das Hirnaneurysma. Basel: Geigy 1958.

7. MESSINA, A.V.: Computed Tomography: Contrast enhancement in intracerebral haemorrhage. Proceedings of 14th Annual Meeting of American Society of Neuroradiology. Neuroradiology 12, 43-55 (1976).
8. NEW, P.F.J., SCOTT, W.R.: Computed Tomography of the Brain and Orbit (EMI Scanning). Baltimore: Williams and Wilkins 1975, pp. 263-265.
9. PERRETT, G., NISHIOKA, H.: Report on the co-operative study of intracranial aneurysms and subarachnoid haemorrhage. Section: Arteriovenous malformation; an analysis of 545 cases of cranio-cerebral arteriovenous malformations and fistulae reported to the co-operative study. Journal of Neurosurgery 25, 467-490 (1966).
10. PLANIOL. T.H., AKERMAN, M.: La gamma-encéphalographie dans les anévrysmes artério-veineux sustentoriels. Etude de 54 cas. Presse médicale 73, 2205-2210 (1965).
11. RUMBAUGH, C.L., POTTS, D.G.: Skull changes associated with intracranial arteriovenous malformations. American Journal of Roentgenology 98, 525-534 (1966).
12. WALTINO, O., EISTOLA, P., VUOLIO, M.: Brain scanning in the detection of intracranial arteriovenous malformations. Acta neurologica scandinavica 49, 434-442 (1973).
13. WING, S.D., KRAMER, R., NORMAN, D., NEWTON, T.H.: The detection of arteriographic occult angiomatous malformations by Cranial Computed Tomography. Proceedings of 14th Annual Meeting of American Society of Neuroradiology. Neuroradiology 12, 43-55 (1976).
14. ZIMMERMAN, R., LEEDS, N.E., NAIDICH, T.P.: Ring blush associated with intracerebral haematoma. A new CT finding. Proceedings of 14th Annual Meeting of American Society of Neuroradiology. Neuroradiology 12, 43-55 (1976).

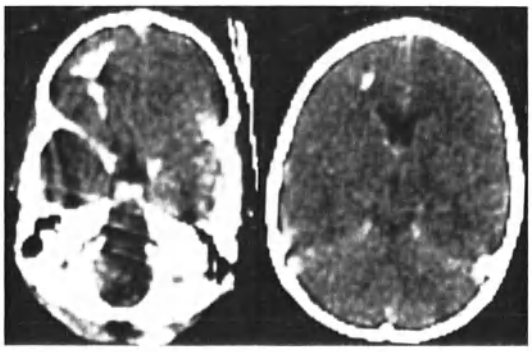

a b

Fig. 1a and b. Venous angioma. (a) Plain scan. Calcification left frontal lobe with linear extension towards anterior horn. (b) After intravenous contrast medium. Enlarged anterior caudate vein extending from malformation

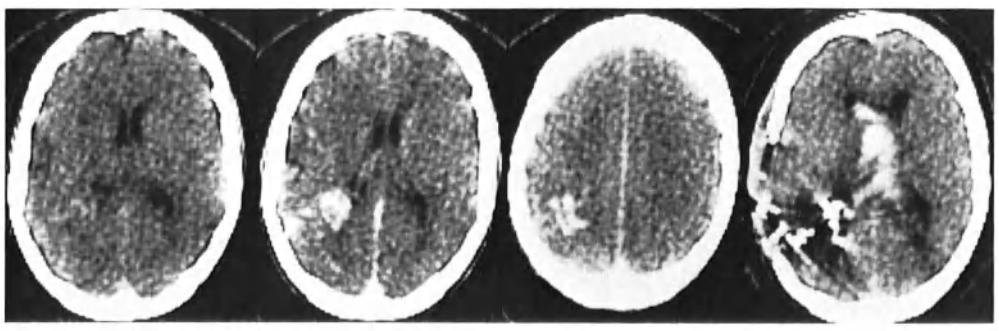

a b c d

Fig. 2. (a) Unenhanced scan. Typical left parietal avm. Curvilinear increased attenuation (28 Hounsfield units) suggesting enlarged vessels cut longitudinally. (b) and (c) adjacent cuts after intravenous contrast medium. The increased attenuation renders the vessels of the avm obvious. Those cut longitudinally cause curvilinear densities and those cut transversely are round or oval. (d) Same patient. Sudden clinical deterioration after excision of avm. Scan after intravenous contrast medium. Multiple silver clips at site of completely removed avm. Haematoma in left lateral ventricle and displacement of ventricular system to right

a b

Fig. 3. (a) Unenhanced scan. Haematoma projecting into body of right lateral ventricle. Moderate hydrocephalus. (b) After intravenous contrast medium. Rim enhancement. Linear densities of enlarged vessels draining avm to subependymal veins of right lateral ventricle

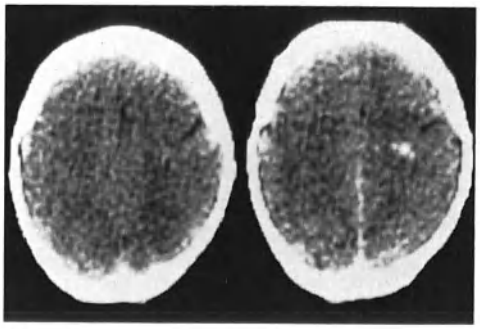

Fig. 4a

Fig. 4b

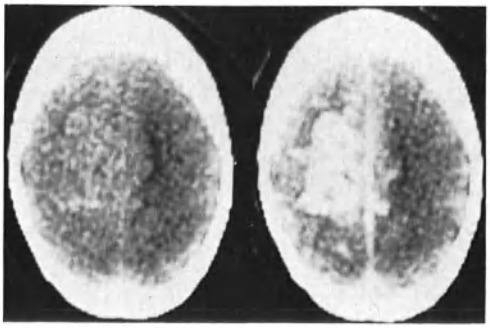

Fig. 5a

Fig. 5b

Fig. 4a and b. Right parietal avm. (a) Plain scan. Slightly low attenuation R. parietal region. (b) After intravenous contrast medium. Non-specific small area of enhancement in low density region

Fig. 5. (a) Plain scan. (b) After intravenous contrast medium. Very extensive avm involving most of left parietal lobe and medial part of right parietal lobe

The Study of Cerebral Blood Volume by C.A.T. and a Comparison with Other Methods

M. Gado, J. Eichling, C. Higgins, and M. Currie*

Introduction

Computerised Tomography (C.A.T.) has been utilised by some investigators (7) to measure the regional cerebral blood volume (rCBV). The method depends on obtaining the numerical attenuation values computed by the scanner for the cerebral tissue before and after intravenous injections of iodinated contrast material.

The attenuation values of a medium computed by the EMI scanner are derived from the equation: Attenuation value (EMI number) = $\frac{\mu x - \mu w}{\mu w} \times 500$ where μx and μw are the linear attenuation coefficients of the medium and water respectively. Blood samples are taken at the time of the pre-contrast and post-contrast scans. These are then scanned and the numerical attenuation values are obtained. The increase in attenuation by the tissue divided by the increase in attenuation by the systemic blood yields the value of the regional rCBV after correction for the difference between the haematocrit of the systemic and cerebral blood.

For the latter conclusion to be correct there are several conditions that have to be fulfilled. One of these is the assumption that the iodinated molecule is confined to the blood space. The purpose of this work is twofold. First, to compare the mean CBV measured by this method with measurements in the same animal under the same conditions by another method using positron emission transaxial tomography (P.E.T.T.) and to test the response of rCBV to $PaCO_2$ changes by both methods. Second, to verify the assumption that contrast material injected intravenously remains confined to the blood space in the normal brain.

Material and Methods

A 13 1b. male Rhesus monkey was premedicated by sernylan and atropine, heparinized by 3000 I.U. initially and 2000 I.U. 2 h later. A 17 gauge PE catheter was introduced into the left brachial artery for the purpose of obtaining arterial blood samples for $PaCO_2$ and systemic blood iodine measurements. A similar catheter was introduced into the left femoral vein for the purpose of administration of medication, tracer or iodinated contrast material. The animal was paralysed with Flaxedil, intubated and ventilated by a pump delivering 125 cc of 100% oxygen per stroke at a rate of 12 strokes/min to attain normocarbic arterial blood level or approximately $PaCO_2$ = 38-40 mm Hg. Moderate hypercarbia was produced by reducing the stroke volume and rate. Marked hypercarbia

*Mallinckrodt Institute of Radiology, Washington University School of Medicine, St. Louis, Missouri.

was obtained by ventilating the animal with 90% oxygen and 10% carbon dioxide delivering 125 cc/stroke at 12 strokes/min. For low $PaCO_2$, 200 cc of 100% oxygen were delivered per stroke at 15 strokes/min. The measurement of rCBV by positron C.A.T. scanning was achieved with a positron emission transverse tomograph (P.E.T.T.) (6) subsequent to an intravenous infusion of "CO-haemoglobin ("C: $T_{1/2}$ = 20.3 min). The data collection was initiated after a 10-min blood equilibration period and serial samples of arterial blood were withdrawn during the 8-min scans in order to establish the mean blood activity. The mean CBV for a region of interest was computed from the equation

$$rCBV = \frac{(CPS/cc\ tissue) \times 100}{(CPS/g\ blood)\ \rho \times f} \quad (cc/100cc)$$

where (CPS/cc tissue) is the mean computed activity per unit volume of in vivo tissue comprising the region of interest. This quantity is obtained by correlating the response of the P.E.T.T., i.e., reconstructed data, to the measured activity concentrations contained in a five-chamber phantom. (CPS/g blood) is the mean activity per unit volume of sampled blood during the study, ρ blood is the physical density of blood (ρ blood = 1.05-1.06 g/ml) and f is the ratio of mean cerebral haematocrit and large-vessel haematocrit for the region of interest, i.e., $f = HcT_C/Hct_{LV}$. Although it is well established that the mean haematocrit of vascular beds is less than that of large vessels, only a few studies have attempted to determine this parameter. An f value of 0.85 was used in the present study. The area selected for computing mean CBV on the P.E.T.T. image was selected according to the C.T.T. image (see below).

After the P.E.T.T. measurement of rCBV was completed, the animal was transfered to the EMI scanner. The head was adjusted in position and a test image of one slice was obtained to adjust the level to a plane very similar to the one imaged by P.E.T.T. A C.A.T. scan of this slice was taken as a baseline under normocarbic conditions. The animal then received an intravenous injection of Meglumine Iothalamate (282 mgm of iodine/1 cc). A dose of 1 cc/1b was injected over a 4-min period. The scan was started 1 min later. A 4.5-min scan was obtained. Several blood samples were taken at the beginning and during the scan to ensure constant $PaCO_2$ level. Only one blood sample (3.5 cc + 0.5 cc of heparin) was drawn at 2 min after the beginning of the scan. Mild and marked hypercarbia were induced as described above and the same procedure was repeated. A dose of 1 cc/1b of Conray 60 was given before each of the two scans done under moderate and marked hypercarbia to maintain a high blood level of iodine in this particular experiment. Hyperventilation was induced and a scan done under hypocarbic conditions after the injection of 0.5 cc/1b body weight of Conray 60. Polaroid images and numerical printouts were obtained for each of the five images taken for the same brain slice under the conditions described above. A rectangular area of the left cerebral hemisphere was marked excluding the region of the tentorium cerebelli where the iodinated contrast material is not confined to the blood pool (Fig. 1). A narrow rim of parietal convexity cortex was also excluded to avoid reconstruction artefacts. The area thus mapped out corresponded to a tissue volume of 25 cc. The mean attenuation value was calculated for the same area in each of the baseline and the three post-contrast scans. The blood samples corresponded to a tissue volume of 25 cc. The mean attenuation value was calculated for the same area in each of the baseline and the three post-contrast scans. The blood samples corresponding to the five scans consisting each of 3.5 cc of blood + 0.5 cc Heparin were collected in a 10-cc plastic syringe where each was diluted with normal saline to the volume of 7 cc necessary for imaging. Each syringe had a diameter of 15 mm. The syringes filled with diluted blood were scanned inside a

plexiglass phantom full of water built for this purpose. A 4.5-min scan was performed at the same KV and mA settings as the head scans. Numerical printouts were obtained with a matrix of 160 × 160 picture elements. On the printout, an area of 5 × 5 picture elements within each syringe was outlined. This corresponded to 9 × 9 mm and excluded the zone of partial volume effect between the syringe wall and its contents. The mean of the attenuation values in the 5 × 5 picture elements was computed for each blood sample and multiplied by 2 to correct for dilution.

It was then possible to calculate the difference between the mean attenuation value of the left cerebral hemisphere on the baseline scan and any given post-contrast scan. This difference was defined as the brain enhancement under the conditions of that particular scan. A similar value was calculated for enhancement of the blood drawn at the time of the scan. From these two values, the mean rCBV for the hemisphere under the circumstances of that particular scan was calculated from the equation: $\frac{\text{Mean Value of Enhancement of the Brain}}{\text{Mean Value of Enhancement of the Blood}} \times 100 \times 0.85$ The value 0.85 corrects for the lower mean cerebral haematocrit compared to large-vessel haematocrit. The value of mean rCBV calculated with this method is in units of cc/100 cc of brain tissue.

In order to determine the distribution of iodinated contrast material in relation to the blood space in the normal brain and to compare it with other tissues, the following experimental procedure was undertaken. Eight adult rabbits weighing between 6.5 and 8.5 pounds were selected. On the day prior to the experimental procedure 3 cc of the animal's blood were drawn, labelled with 20 μCi of ^{51}Cr and re-injected intravenously. On the next day 4 cc of Meglumine Iothalamate labelled with ^{125}I containing 100 μCi of activity were injected into the ear vein. Ten minutes later the animal was sacrified, and samples of several tissues were taken into previously weighed and marked test tubes. The samples taken were from brain, dura, muscle, kidney, liver, and heparinised blood. The test tubes were weighed to determine the weight of the sample to the nearest 0.0001 g. The weight of the samples was 0.7554 g (± 0.15) blood, 0.6649 (± 0.22) brain, 0.0486 (± 0.02) dura, 0.6015 (± 0.2) muscle, 0.4987 (± 0.26) kidney, 0.5166 (± 0.19) liver. The activity in the samples was counted using a semiconductor detector for ^{125}I, window set at 26-29 KeV (Te K_{α} X-rays) and a NaI(Tl) well detector for ^{51}Cr, window set at 300-340 KeV. The background for ^{51}Cr was counted over 3000 s and the background in counts/min computed. The counting time for ^{125}I varied from 80 s in blood to 3000 s in brain. The activity of ^{51}Cr expressed as the number of counts/min/g of each sample was calculated. This was divided by the counts/min/g of blood to obtain the tissue blood ratio of ^{51}Cr activity. Similarly the tissue/blood ratio of ^{125}I activity was calculated.

'Space' is defined as the apparent volume obtained by dividing the amount retained by the concentration of the tracer in the plasma. Therefore the $\frac{\text{tissue blood ratio of } ^{125}I}{\text{tissue blood ratio of } ^{51}Cr}$ equals the ratio between ^{125}I space and ^{51}Cr space in the tissue specified. This ratio was computed for each of the tissue samples in each animal. This ratio was corrected twice for the difference between the mean cerebral haematocrit and large vessel haematocrit. The reason for two fold correction is that the ratio is calculated between a plasma tracer (^{125}I) and an RBC tracer (^{51}Cr).

Results

The data obtained for six P.E.T.T. determinations of the mean cerebral blood volume of the left hemisphere of the scanned slice as a function of arterial pCO_2 are shown in Table 1 and Figure 1.

Table 1.

pCO_2 (mm Hg)	rCBV (ml/100 g)
38	2.79
38	2.71
55	3.64
53	3.50
67	4.21
71	4.00

Table 2.

Scan No.	Brain attenuation	Brain enhancement	Blood attenuation	Blood enhancement	rCBV	CO_2
1	20.05	-	27.3	-	-	40
2	21.54	1.49	58.3	31	4.09	42.5
3	22.26	2.21	68.3	41	4.58	53.5
4	23.38	3.33	77.3	50	5.66	62
5	22.2	2.15	72.1	44.7	4.09	25

The data obtained by transmission C.A.T. (EMI scanner) are shown in Table 2. The baseline mean attenuation value for the brain was 20.05 EMI scale units, and for the blood 27.3 units. After contrast injection, and under approximately the same normocarbic condition, there was an observed enhancement of 1.49 and 31 EMI units for the brain and the systemic blood respectively. The mean rCBV of the left hemisphere was thus 4.09 cc/100 cc. When $PaCO_2$ was elevated to 53.5 mm Hg and the blood enhancement boosted to 41 EMI units, the brain enhancement rose to 2.21 EMI units accounting for an increase of mean rCBV to 4.58 cc/100 cc. A further increase in mean rCBV to 5.66 cc/100 cc was noted at $PaCO_2$ of 62 mm Hg. When $PaCO_2$ was dropped to 25 mm Hg the mean rCBV dropped to 4.09 cc/100 cc.

The values of mean rCBV of the left hemisphere calculated by both the transmission and emission C.A.T. methods and the response of CBV to alterations in $PaCO_2$ by both methods, with the equations for rCBV are as follows:

Transmission C.A.T. rCBV = $0.049\ PaCO_2 + 2.18$
Emission C.A.T. rCBV = $0.042\ PaCO_2 + 1.25$

The results of the ^{125}I space to ^{51}Cr space ratio in the tissue samples obtained from each of the eight experimental animals are shown in Table 3. The tissue/blood ratio of ^{51}Cr reflects the blood volume in the tissue. The ratio was 1.48% for brain. The tissue/blood ratio of ^{51}Cr for the dura was high due to the small weight of the sample (less than 0.1 g) with contamination of the surface by extravasated blood. This anomaly, however, was normalised when the similarly high value of the

Table 3. Calculation of the ratio between the ^{125}I-space and the ^{51}Cr space (rabbit)

Tissue	No.	Tissue/blood ratio of ^{51}Cr	No.	Tissue/blood ratio of I	^{125}I space/ ^{51}Cr space	Corrected for haematocrit
Brain	5	1.48 (± 0.4)	6	2.5 (± 0.9)	1.69	1.2
Dura	5	51.3 (±20.9)	6	152.7 (±26)	2.98	2.2
Muscle	5	1.0 (± 0.4)	6	14.3 (± 2.9)	14.3	10.3
Kidney	6	9.9 (± 2.4)	6	610.5 (±142)	61.67	44.4
Liver	6	19.3 (± 6.5)	6	96.2 (±33.5)	4.98	3.7

ratio for ^{125}I was divided by the ratio for ^{51}Cr and the resultant value for ^{125}I space to ^{51}Cr space ratio is therefore reliable. The muscle had the lowest blood volume (1.0%). The highest blood volume was in the liver (19.3%). The value 610.5% for the tissue/blood ratio of ^{125}I in the kidney sample reflects the concentration of I_2 by the kidney. The value of the ratio between the ^{125}I space and the ^{51}Cr space in the brain was 1.22. In other viscera the values were much higher, 10.3 for muscle and 44.4 for the kidneys.

Discussion

The results of CBV measurement by different methods by different investigators (1, 3, 4, 5) are shown in Table 4 and Figure 3. The normobarbic CBV at $PaCO_2$ 38-40 varies from 2.7 to 5.8 cc/100 cc. The varia-

Table 4.

Method	Investigator	Experimental animal	Normocarbic CBV	Equation for rCBV and $PaCO_2$
Mark IV	KUHL et al.	Baboon	4.7	0.049 $PaCO_2$ + 2.88
Transit time (outflow)	SMITH et al.	Goat	4.9	0.043 $PaCO_2$ + 3.18
Transit time (residue)	EICHLING et al.	Rhesus monkey	3.5	0.041 $PaCO_2$ + 2.0
Fluorescence	PHELPS et al.	Rhesus monkey	5.8	0.046 $PaCO_2$ + 4.06
Emission C.A.T.	The authors	Rhesus monkey	2.7	0.049 $PaCO_2$ + 2.18
Transmission C.A.T.	The authors	Rhesus monkey	4.1	0.042 $PaCO_2$ + 1.25

tion probably reflects different parts of the blood pool 'included' by different methods since the slopes of the linear relationships are in excellent agreement. It is estimated that blood volume is distributed in the circulatory bed in the following percentages: veins 60-70%, arteries 20-30% and capillaries 10%. It is therefore conceivable that major superficial veins excluded from the calculation by the C.A.T. methods and the fluorescence method (4) may account for much of the variation. We have to date determined the mean rCBV of the scanned slice for four Rhesus monkeys as a function of arterial pCO_2. The data obtained for 15 determinations is shown in Table 5 and Figure 3. The values in the current experiment are consistent with previous data.

Table 5.

Monkey	$PaCO_2$* (mm Hg)	rCBV (ml/100 g)
1	25	2.18
	28	2.17
2	38	2.79
	38	2.71
	55	3.64
	53	3.50
	67	4.21
	71	4.00
3	41	2.93
	48	3.08
	25	2.35
	20	2.20
4	42	2.87
	42	2.98
	68	4.68

Of interest is the fact that the value measured for the whole hemisphere by transmission C.A.T. occupies a median position between the range of CBV values. The slope of the response of the CBV to changes in $PaCO_2$ shows a high degree of similarity between the different methods of measurement.

In the current work the same animal was studied by emission C.A.T. and transmission C.A.T. Both methods have a high regionality. The resolution of emission C.A.T. is much lower (picture element = 10 mm) than transmission C.A.T. (picture element = 1.5 mm). Because of the small size of the monkey's brain it was not possible to obtain regional values by emission C.A.T. This however can be obtained in human subjects.

Although both methods utilise computer reconstruction imaging, there is a fundamental difference between emission and transmission C.A.T. in measuring CBV. The blood label in emission C.A.T. is a red cell label (carboxyhaemoglobin). It is therefore bound to the blood space. The tracer (iodine) used in CBV measurement by transmission C.A.T. is a plasma tracer. The second part of this experimental work was designed to validate its use as a blood indicator. As shown in the last column in Table 3, the brain differed from other organs in that the ratio between ^{125}I space and ^{51}Cr space was close to unity. This finding is an expression of the function of the blood-brain barrier. These observations are in agreement with those of PHELPS et al. (4), who found that similar values of CBV were obtained by iodine fluorescence in life and ^{51}Cr activity measured in brain and blood when the animal was sacrified. ZILKHA et al. (7) described computer subtraction in conjunction with C.A.T. in order to expedite the computation of rCBV in several regions in man. They found that values in the frontal and temporal regions were lower than the mean hemisphere value (4.9 ± 0.7) and higher in the occipital region. The left hemisphere showed a higher CBV than the right.

It seems, therefore, that CBV in the normal brain with intact function of the blood-brain barrier lends itself to measurement by C.A.T. The measurements made in pathological conditions have to be analysed with extreme caution due to the possible presence of iodine in the extra-

vascular space. GADO et al. (2) have found that measurements made with transmission C.A.T. in patients with tumours have yielded in some instances values that are unrealistically high such as 130% due to extravascular egress of iodine. They also found similar observations in tumours removed surgically from patients whose blood had been tagged with ^{51}Cr-labelled RBC_s and in whom a plasma label $R^{125}1SA$ was injected at the time of surgery. They found that high tissue/blood ratios of iodine obtained by C.A.T. in those patients corresponded more with the $R^{125}1SA$ values than the ^{51}Cr values, the latter being more indicative of the blood volume of the tumour. They concluded by drawing an analogy between the phenomenon of contrast enhancement on C.A.T. and increased uptake of radionuclide activity by lesions with defective blood-tissue barrier.

The experimental model presented here is a method by which it will be possible to evaluate with certainty the validity of the use of iodinated contrast material as a blood tracer for CBV measurements by C.A.T. The effect of the dose of contrast material on the accuracy of the method can also be evaluated.

Conclusions

Measurements of mean rCBV of the hemisphere of Rhesus monkey brain were made by computerised transmission tomography (C.A.T.) using iodinated contrast material and compared with measurements made on the same animal by P.E.T.T. The response of RCBV to $PaCO_2$ changes, as measured by C.A.T. was in the same direction as that measured by P.E.T.T. The model represents a method for evaluation of the reliability of C.A.T. with iodinated contrast material for haemodynamic studies.

References

1. EICHLING, J.O.: Circulation Research 37, 707-713 (1975).
2. GADO, M.H.: Radiology 115, 107-112 (1975).
3. KUHL, D.E.: Circulation Research 36, 610-618 (1975).
4. PHELPS, M.E.: Journal of Applied Physiology 35, 274-279 (1973).
5. SMITH, A.L.: Journal of Applied Physiology 31, 701-707 (1971).
6. TER-POGOSSIAN, M.M.: Radiology 114, 89-98 (1975).
7. ZILKHA, E.: British Journal of Radiology 49, 330-334 (1976).

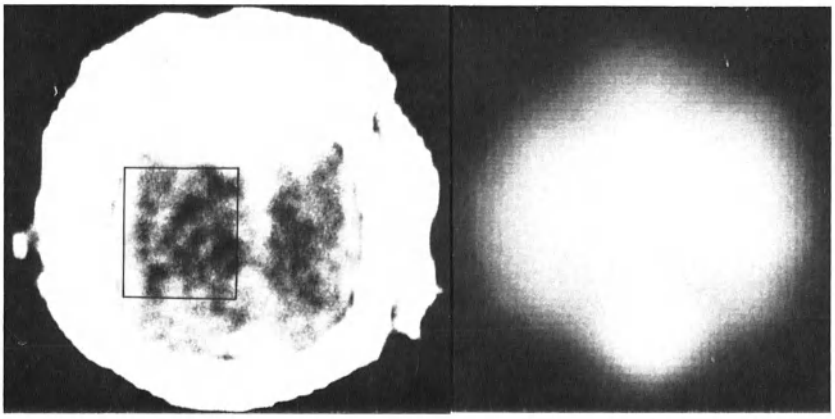

a b

Fig. 1a. C.A.T. of monkey. b) P.E.T.T. The area for computing the left hemispheric mean rCBV was outined

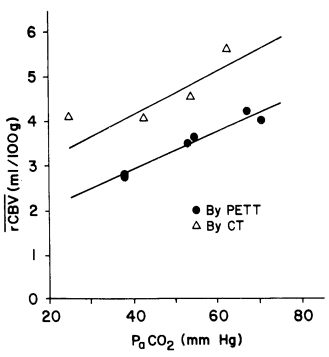

Fig. 2

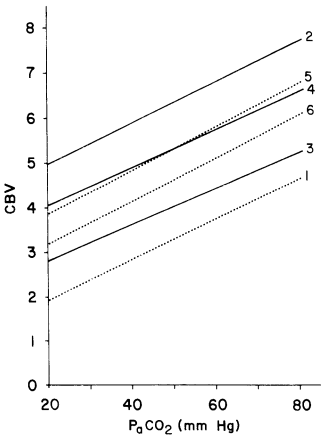

Fig. 3

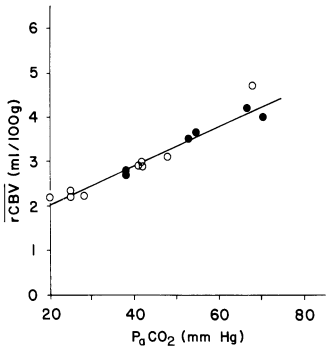

Fig. 4

Fig. 2. Values of left hemispheric mean rCBV measured in same animal by C.A.T. and P.E.T.T. under different levels of $PaCO_2$

Fig. 3. Comparison of the present data with those reported by other investigators using other methods of measurements *1*. P.E.T.T. *2*. X-ray fluorescence *3*. $\overline{T}$ (Residue) *4*. $\overline{T}$ (outflow) *5*. Mark IV *6*. C.A.T. See text

Fig. 4. Data from fifteen CBV determinations by P.E.T.T. in 4 Rhesus monkeys. The open circles are the present data

Measurements: Physical Considerations

Electron Density and Atomic Number Determination - Methods, Limitations and a Study of Colloid Cysts

I. Isherwood*, R. A. Rutherford**, and F. A. Strang***

Introduction

EMI scanners are capable of precise measurements of the attenuation coefficient of small elements of tissue in vivo at X-ray voltages ranging from 100 kVp to 140 kVp. Substances of which the densities differ by 1 part in 1000 can be differentiated (3, 6).

The linear attenuation coefficient, μ, of a substance depends on

1. Effective number of atoms per unit volume, N*.
2. Effective atomic number, Z*.
3. Effective energy of X-ray beam employed, E*.

The effective number of electrons per unit volume, N*Z*, is the effective electron density and is very nearly equal to the real electron density of the material.

Despite the polychromatic nature of the X-ray beam, the computer algorithm implemented by the machine calculates attenuation values that relate linearly to the linear attenuation coefficient of the material at particular energies, i.e. 62 keV for the 100 kVp beam, 70 keV for the 120 kVp beam and 74 keV for the 140 kVp beam (6) (Fig. 1).

A mathematical relationship can be obtained between μ, N* and Z* incorporating the effective energy E*.

Attenuation coefficients can be measured at two different beam energies and from such data it is possible to obtain separate measurements of electron density and effective atomic number of materials.

The validity of the method has been checked by comparing measured effective atomic number, Z*, and effective electron density, N*Z*, with similar values calculated from known composition of material (7) (Fig. 2). A mean variation between actual and predicted values of atomic number, Z, was less than 1%.

The feasibility of extracting mean atomic number and electron density in the clinical situation has previously been investigated (7). In order to reduce noise, values of EMI number have been obtained by averaging over 25 elements progressively across the scan. Electron density determined in this way is accurate to 0.5% and the effective atomic number accurate to 3%. This disparity is due to the fact that at the beam energies currently employed the dominant interaction is Compton scattering which is an interaction between X-rays and electrons and which therefore depends very little on the type of atom present.

---

*Department of Diagnostic Radiology, University of Manchester.
**Department of Medical Biophysics, University of Manchester.
***Department of Neurological Surgery, University of Manchester.

Relevance of Electron Density and Effective Atomic Number Measurement

Certain questions need to be considered if the measurement of Z* and N*Z* is to prove a worthwile application of computerised tomography.

(A) Physical
1. How accurately can N* and Z* be measured?
2. With what precision can N* and Z* be measured?

(B) Clinical.
3. Can an accurate measurement of N* and Z* to the precision currently attainable detect the small chemical changes which may accompany disease?
4. Will a measurement of N* and Z* affect clinical management?

Accuracy

Accurate measurements of Z* should be produced by accurate measurements of μ, the linear attenuation coefficient of the material under investigation at two distinct energies. It is essential, therefore, that an accurate correction for the fact that the X-ray beam is polychromatic can be made (1, 3). An accurate correction appears to have been implemented in the EMI brain scanner programme (7).

Information needed to calculate Z* is to be derived from the change in attenuation values when X-ray beam energy is changed from 100 kVp to 140 kVp. This difference is small. The measurement of Z* is therefore extremely sensitive to errors in the measurement of μ. Such errors may arise due to:

1. Artefacts
2. Patient movement
3. Patient position in sequential scans
4. Position of material within the depth of a C.A.T. section

Precision

It has already been shown that if the 100 kVp and 140 kVp beams are employed, Z* may be measured to a precision of about 3% ($\pm$ 0.2) for a 25 element region, or 5% ($\pm$ 0.1) for a 100-element region (7).

Precision can be improved by employing beam energies that are further apart. Measurement of Z* to 1 part in 400 ($\pm$ 0.02) for a 25 element region may be achieved by use of beam energies of 40 keV and 80 keV provided that an accurate correction for the polychromaticity of the beam can be made at these energies (8).

Chemical Change in Disease

It is important to recognise that electron density, N*Z*, and effective atomic number, Z*, are measures of mean composition of material. This is so whether the material is contained within 1 or 25 elements.

A number of factors may influence the effective atomic number, Z*. The effect of different concentrations of various atoms on Z* has been modelled. The assumption has been made that atoms are added to water and that the concentration of water molecules remains unchanged (Fig. 3). The concentrations of those atoms which might be detected if Z*

Table 1. The limits of detection if Z* can be measured to ± 0.1

Element	Concentration mg/ml
Sodium	19.9
Potassium	2.6
Calcium	2.0
Iron	0.93
Copper	0.69
Krypton	0.42
Iodine	0.11

could be measured to a precision of ± 0.1 are considered in Table 1. It is clear that concentrations of atoms below the limits considered would not produce a measurable change in Z*.

Higher atomic number materials, as might be expected, are more readily detectable. It is known that the administration of iodine to the vascular system will raise the average attenuation level of blood by 12-15 Hounsfield units per 1 mg/ml increase in iodine concentration at 120 kVp (5). If a change in Z* is due solely to the presence of iodine or other high atomic number element it should be possible to estimate the amount of such an element in tissue with accuracy and precision. This is not usually the case - both normal and pathological tissue contain a variety of elements, many of which are of low atomic number. The mean Z* will be affected by the relative proportions of high and low atomic number elements. Subtle changes may therefore be difficult to detect.

Clinical Management

There is no doubt that C.A.T. scanning of the brain has significantly affected clinical management by visual demonstration of density differences to be found in normal brain and pathological processes which affect it.

The role of N* and Z* measurement in clinical management will need therefore to be in the improvement of detectability of disease, the more accurate differentiation of disease process or the study of biological pathways.

Colloid Cysts of the Third Ventricle

Colloid cysts comprise 0.55% of all intracranial tumours (4). Diagnosis by clinical and traditional neuroradiological methods may be difficult. A recent series (10) describes 38 cases in most of which the diagnosis was made by conventional neuroradiological methods. In this series the most useful investigation was pneumography.

The value of C.A.T. in the diagnosis of colloid cysts has been more recently appreciated (2, 7, 9).

Colloid cysts of the third ventricle have a characteristic high density (Fig. 4). The high attenuation value has been shown to be due to an increased electron density rather than any contribution from high atomic number elements (7) (Fig. 5).

Material and Methods

Twenty-three patients with colloid cysts have been investigated and treated in the Departments of Neuroradiology and Neurological Surgery in Manchester Royal Infirmary over the years 1940 to 1976. These patients are the subject of a separate clinical review (11).

Fifteen patients (65%) were treated solely by bilateral Torkildsen's ventriculo-cisternostomies. Thirteen, i.e. 86% of this group, are alive and well (Table 2). Of these survivors, 12 have been located and 11 recalled for double energy C.A.T. In 9 of these patients it was possible to calculate the electron density and effective atomic number of the colloid cyst. Movement between successive scans made such calculation impracticable in two patients.

Table 2. Colloid cysts: 23 patients 1940-1976. Three died before treatment

Treatment	Number	Died
Ventriculo-cisternostomy only		
- bilateral	14	1
- unilateral	1	1
Surgical removal	3	1
Ventriculo-cisternostomy and removal	2	0

Survivors of by-pass group = 13 (86%)

One patient (C.L.) died before treatment, and was also diagnosed by C.A.T. The colloid cyst subsequently removed at post-mortem was rescanned at two beam energies and was also the subject of histological and chemical analysis.

Results and Discussion

The clinical details of 12 patients with ventriculo-cisternostomies and the 1 patient who died before treatment are contained in Table 3.

Eight patients were male and the age range at the time of operation was from 22 to 59 years (mean 40.4 years).

Postoperative survival periods ranged from 1-23 years which with an added estimation of duration of symptoms indicated a possible tumour age of up to 27 years.

The definitive diagnostic radiological procedure in the present group of patients was myodil ventriculography in seven (Fig. 6b), air ventriculography in one, air encephalography in one (Fig. 6a) and C.A.T. in four.

Results indicating estimated size in pixels and attenuation values at two energies together with electron density and effective atomic number estimations for colloid cysts in nine survivors and one specimen tumour are recorded in Table 4.

Table 3.

Patient	Age (1976)	Sex	Duration of symptoms pre-operative (years)	Post-operative survival (years)	Definitive radiological procedure
J.K.	55	M	2	23	MV
J.H.	53	M	5	22	MV
A.B.	62	F	3	20	AV
P.G.	56	M	10 days	17	MV
H.D.	71	F	0.5	12	MV
P.K.	40	M	1.5	8	MV
J.E.	57	M	0.25	7	AEG
S.H.	34	F	3	4	MV
R.H.	55	F	0.25	4	MV
V.S.	47	F	15	2	C.A.T.
G.L.	53	M	2	2	C.A.T.
C.C.	23	M	0.5	1	C.A.T.
C.L.[a]	32	M	0.6	-	C.A.T.

MV - Myodil ventriculogram, AV - Air ventriculogram, AEG - Air encephalogram, C.A.T. - Computerised axial tomography

[a]Excised specimen.

Table 4.

Patient	Size (pixels)	EMI No. 100 kV mean ± S.E.	EMI No. 140 kV mean ± S.E.	Mean electron density (± 0.01) 10^{23}	Mean effective atomic number (Z*) (± 0.1)
J.K.	44	19.7 ± 0.6	17.9 ± 0.5	3.461	7.40
J.H.	62	31.0 ± 0.4	26.8 ± 0.4	3.495	7.68
A.B.	146	43.3 ± 0.7	38.3 ± 0.6	3.577	7.65
P.G.	38	35.5 ± 1.0	31.3 ± 0.9	3.532	7.62
H.D.	44	23.0 ± 0.6	26.3 ± 0.6	Movement	
P.K.	164	36.3 ± 0.5	33.0 ± 0.4	3.555	7.51
J.E.	42	13.5 ± 0.4	12.0 ± 0.4	3.409	7.51
S.H.	38	32.8 ± 0.8	30.9 ± 0.7	3.553	7.37
V.S.	135	37.0 ± 0.6	34.5 ± 0.6	3.575	7.41
G.L.	77	32,8 ± 0.9	28.6 ± 0.7	Movement	
C.C.	76	28.7 ± 0.6	25.3 ± 0.4	3.492	7.60
C.L.[a]	60	21.2 ± 0.6	17.8 ± 0.5	3.433	7.67

[a]Excised specimen

Size does not appear to have any relation to estimated age of tumour. An attempt was made to calculate size from the original conventional neuroradiological investigations but this proved to be unreliable. Subjective impressions do not suggest any significant change in size or shape in any individual patient from initial diagnosis to current C.A.T. scan.

Attenuation values of colloid cysts in 11 patients and 1 post-mortem specimen range from 13.5 to 43.3 (mean 29.56) at 100 kVp and 12.0 to 38.3 (mean 26.89) at 140 kVp.

Electron density of 12 colloid cysts expressed as a function of attenuation value at 140 kVp demonstrates a consistent relationship between the two. Effective atomic number, however, has no relationship (Fig. 7).

Chemical analysis of the excised colloid cyst specimen is given in Table 5. There was no evidence of high atomic number material within the cyst. Histological analysis confirmed the nature of the lesion.

Table 5. Chemical analysis

Water	88.7 %
Carbon	5.6 %
Nitrogen	1.41%
Hydrogen	0.78%
Sodium, Chlorine, Potassium, Oxygen	3-4%
Iodine	nil
Calcium	nil

The colloid cyst of one patient (C.C.) was not detected at the initial C.A.T. examination. Dilatation of the ventricular system was noted. The lesion was readily identified 2 weeks after bilateral Torkildsen's ventriculo-cisternostomy (Fig. 8). The explanation for this phenomenon is almost certainly that the initial sections were not sufficiently low to include the tumour. The colloid cyst may itself have been displaced inferiorly by the dilated lateral ventricles. It is important to emphasise, therefore, that sections must include the suprasellar structures and where clinical suspicion of a colloid cyst exists with associated hydrocephalus, a repeat scan following ventricular drainage may be of value.

The long-term survival of patients treated solely by bilateral Torkildsen's ventriculo-cisternostomies together with the evidence that colloid cysts do not change in size or chemical character over long periods suggests that this simple surgical approach to the problem is safe and effective (11).

Summary

The feasibility of extracting electron density and effective atomic number measurements from tissue in vitro and in vivo has previously

been reported. The method requires scans to be obtained at two different beam energies. Optimisation of these energies at 40 keV and 80 keV could enable a variation of 1 part in 400 of effective atomic number to be detected. The method is subject to certain limitations related to accuracy and sensitivity. The effect of varying the concentrations of certain atoms has been modelled, demonstrating the limits below which variation in effective atomic number is unlikely to be detectable.

A series of 12 patients with colloid cysts has been considered. All were treated by bilateral ventriculo-cisternostomy from 1-23 years ago. Nine of these patients and the colloid cyst of one additional patient who died before treatment could be instituted have been subjected to double-energy scanning. The results suggest that the high attenuation values observed in colloid cysts are due to increased electron density and not to any increase in high atomic number elements. The cysts do not appear to change in size or content over long periods.

Acknowledgments

The authors wish to thank Miss H. Jarvis and the radiographic staff of the Department of Neuroradiology for their support. Thanks are also due to Mrs. G.E.H. Shawcross for the preparation of illustrative material and to Mrs. M. Tipton for her helpful secretarial assistance.

References

1. BROOKS, R.A., DI CHIRO, G.: Beam hardening in x-ray reconstructive tomography. Physics in Medicine and Biology 21, 390-398 (1976).
2. ISHERWOOD, I., RUTHERFORD, R.A., PULLAN, B.R.: Measurement of electron density and effective atomic number. First International Symposium on Computer Tomography. Bermuda, 1975.
3. McCULLOUGH, E.C., BAKER, H.L., HOUSER, O.W.: An evaluation of the quantitative and radiation features of a scanning x-ray transverse axial tomography. Radiology 111, 709-715 (1974).
4. POPPEN, J.L., REYES, V., HORRAX, G.: Colloid cysts of the third ventricle. Journal of Neurosurgery 10, 242-263 (1953).
5. RIDING, M., BERGSTRÖM, M., BERGVALL, U., GREITZ, T.: Computer intravenous angiography. Acta Radiologica Suppl. 346, 82-90 (1975).
6. RUTHERFORD, R.A., PULLAN, B.R., ISHERWOOD, I.: Calibration and response of an EMI scanner. Neuroradiology 11, 7-13 (1976).
7. RUTHERFORD, R.A., PULLAN, B.R., ISHERWOOD, I.: Measurement of effective atomic number and electron density using an EMI scanner. Neuroradiology 11, 15-21 (1976).
8. RUTHERFORD, R.A., PULLAN, B.R., ISHERWOOD, I.: X-ray energies for effective atomic number determination. Neuroradiology 11, 23-28 (1976).
9. SACKETT, J.F., MESSINA, A.V., PETITO, C.K.: Computed tomography and magnification vertebral angiotomography in the diagnosis of colloid cysts of the third ventricle. Radiology 116, 95-100 (1975).
10. SAGE, M.R., McALLISTER, V.L., KENDALL, B.E., BULL, J.W.D., MOSELEY, I.F.: Radiology in the diagnosis of colloid cysts of the third ventricle. British Journal of Radiology 48, 708-723 (1975).
11. STRANG, F.A., ISHERWOOD, I.: Colloid cysts of the third ventricle. (In press).

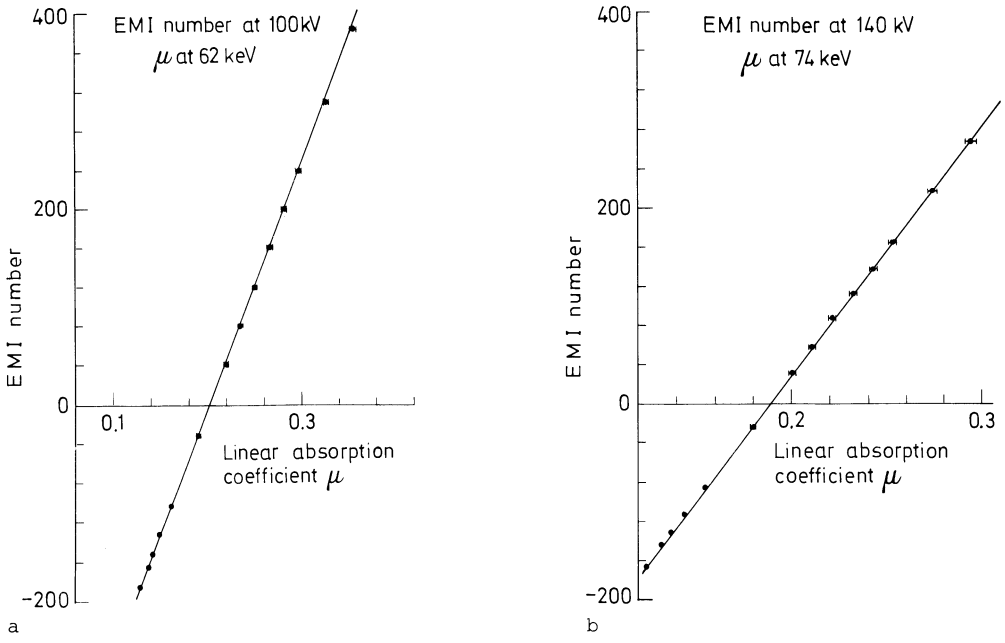

Fig. 1a and b. Variation of EMI number. (a) At 100 kVp with μ as calculated at 62 keV. (b) At 140 kVp with μ as calculated at 74 keV

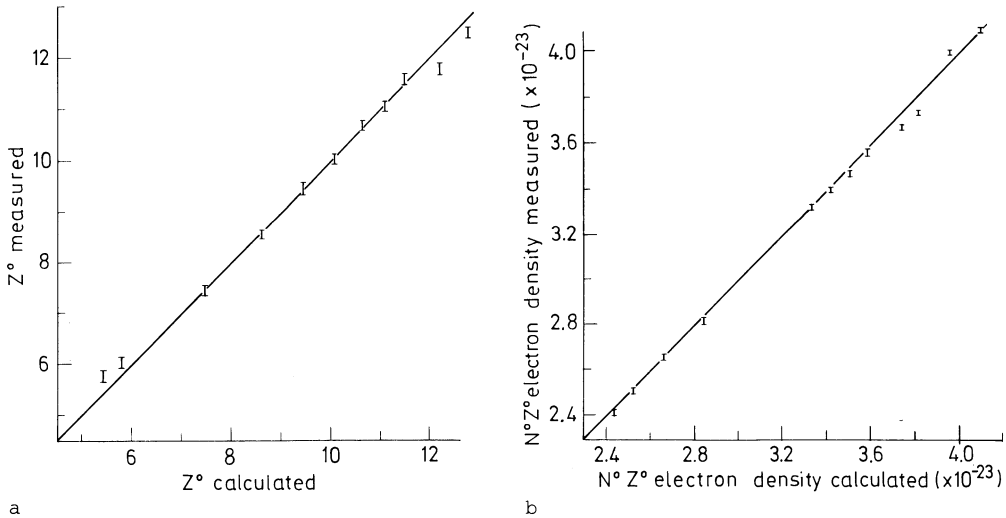

Fig. 2a and b. Comparison of (a) measured effective atomic number Z* and (b) measured electron density N*Z* with similar values calculated from known composition of material

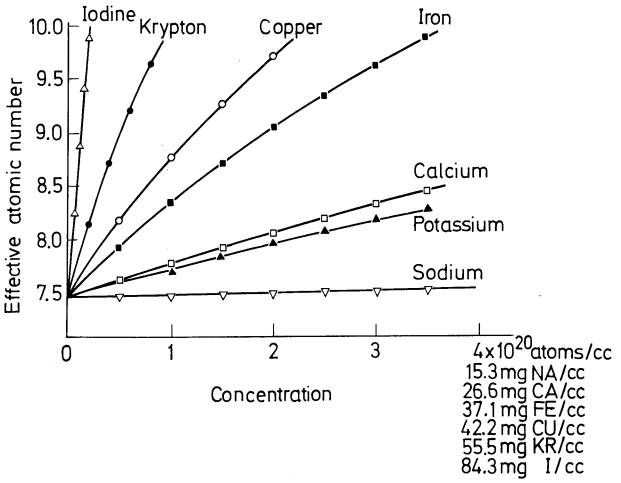

Fig. 3

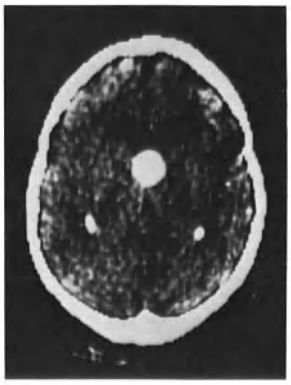

Fig. 4

Fig. 3. Effect of different concentrations of various atoms on effective atomic number Z*

Fig. 4. C.A.T. Characteristic high density of colloid cyst

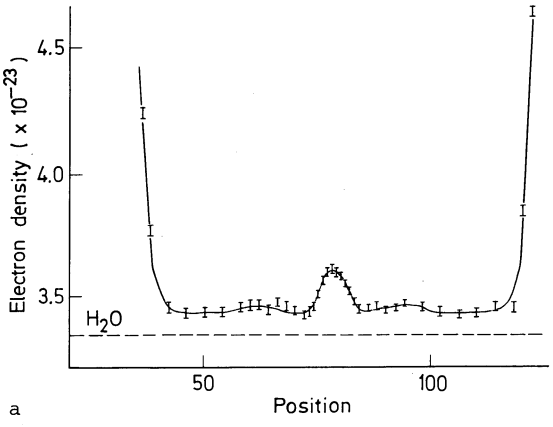

a

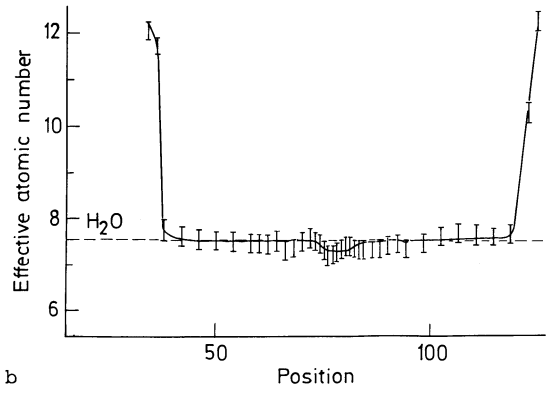

b

Fig. 5. (a) Electron density and (b) effective atomic number as functions of position across a colloid cyst

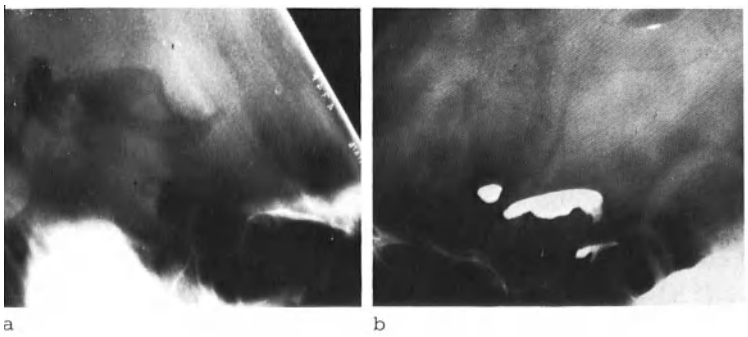

Fig. 6a and b. Colloid cysts demonstrated by (a) air encephalogram - sagittal tomogram. (b) Myodil ventriculogram

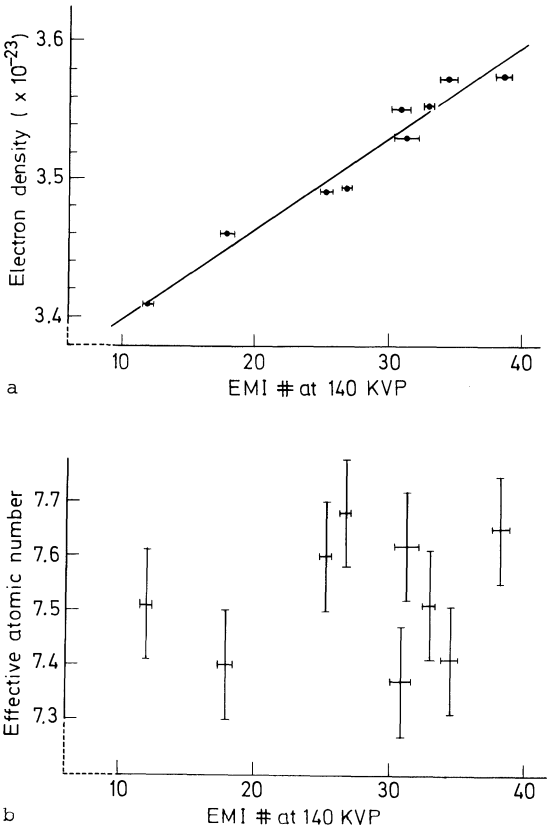

Fig. 7. (a) Electron density and (b) effective atomic number expressed as functions of attenuation value at 140 kVp

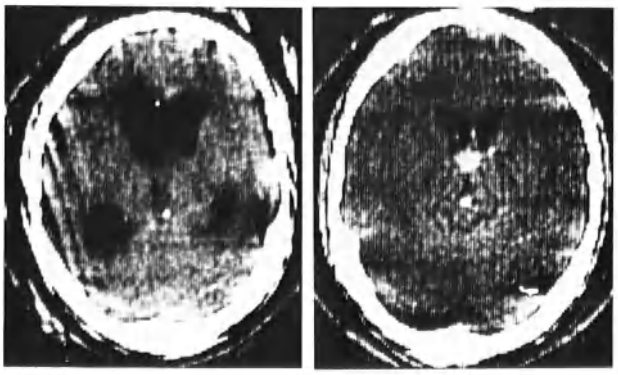

Fig. 8a and b. C.A.T. scan (patient C.C.). (a) Before and (b) after ventricular drainage

Bone Mineral Estimation Employing Computer Assisted Transverse Axial Tomography - A Preliminary Study

I. Isherwood*, B. R. Pullan**, R. A. Rutherford**, and P. H. Adams***

Introduction

The skeleton is a dynamic tissue, continually reconstituted and remodelled by bone resorption and reformation. A net loss in total bone mass occurs with advancing years (19) and bone loss occurs in all women after the menopause (2, 21). There is almost certainly great individual variation in the rate of such loss and the development of osteoporosis (21). The importance of the recognition of bone loss lies in the prevention of those fractures which occur at sites containing predominantly trabecular bone (18), namely vertebral bodies, the femoral neck and the wrist.

The management of patients with metabolic bone disorders would be facilitated if a technique capable of making serial measurements of mineral content in those skeletal sites containing trabecular bone with precision and reproducibility were available (5).

An ideal method would be non-invasive and allow:

1. Separate measurement of bone mass and bone mineral in both trabecular and cortical bone

2. Measurement in critical skeletal sites, in particular the vertebral bodies

3. Measurement independent of individual bone shape and size variation and independent of extrinsic and intrinsic "soft tissue", notably fat.

Clinical methods of evaluating patients with metabolic bone diseases are available ranging from external metabolic balance studies to bone biopsy. All provide useful information, but all have limitations.

The application of quantitative bone measurement in the study of metabolic bone disorders is well recognised, and many techniques are available. They vary widely in accuracy and precision.

Measurement by non-invasive technique is currently achieved by:

1. Neutron activation analysis

2. Interaction of bone with electro-magnetic radiation, either X- or gamma-rays

Neutron activation analysis is the only available method for the direct measurement of total skeletal calcium (8).

---

*Department of Neuroradiology, Manchester Royal Infirmary.
** Department of Medical Biophysics, Univesity of Manchester.
*** Department of Medicine, Manchester Royal Infirmary.

Methods employing X- or gamma-rays depend upon direct measurement of the linear attenuation coefficient of material during sampling at one or more skeletal sites. The attenuation coefficient can be related to bone mass and bone mineral.

The simplest techniques require direct measurements from radiographs either by morphological measurement or densitometry (4, 10, 11, 14, 20, 28). These methods have been employed extensively but may be subject to considerable inter- and intra-observer error (1).

Absorptiometric mineral determination employing gamma rays, i.e., monochromatic photon radiation, together with appropriate scintillation-counting detectors, is a more sensitive technique (6, 23). This method, whilst free of the errors due to variation in X-ray tube output and film emulsion, has a reproducibility of the order of 2-5% due to statistical fluctuations and repositioning errors. Precision as high as 2% has however been claimed (27, 29).

Techniques employing an X-ray source and crystal detection devices have been employed (3, 13). An additional detector to monitor the tube output permits tube fluctuation errors to be compensated. Radiation fluxes are higher than those obtained with an isotope source, with consequent reduction in statistical fluctuation errors. The reproducibility of this method is claimed to be 2%.

The disadvantages of all these methods are twofold:

1. They do not differentiate between cortical and trabecular bone mineral content.

2. They are influenced by adipose tissue both within the bone and subcutaneously (30, 31).

Methods developed by GARNETT et al. (12), CLARKE and VAN DYKE (7) and OLKKONEN and KARJALAINEN (22) utilise the measurements of both transmitted and scattered photons from a gamma-ray source to obtain a measure of electron density within a small volume of bone at a particular location. Bone density within the trabecular space has then been determined. The reproducibility of in vivo measurement is uncertain. The method may not be a sensitive indicator of mineral content in the trabecular space.

Computerised transverse axial tomography (C.A.T.) allows measurement of the distribution of attenuation coefficients within the cross-section of an object (15). The attenuation coefficients in a cross-section of known thickness are computed from a set of X-ray transmission measurements using an X-ray source and detector system. The method has been widely employed in the investigation of brain abnormalities and has been used in our own clinic to investigate more than 6000 patients with neurological disorders. Computation of the derived data from the EMI brain machine enables 25,600 absorption values of material to be obtained within each slice usually 8 mm or 13 mm in depth. The absorption values are presented on a 160 × 160 matrix of 25,000 picture elements (pixels). The numerical values of these picture elements indicate mean attenuation coefficient of material for a volume of tissue (voxel) of 1.5 × 1.5 × 13 mm.

The accuracy and precision of the measurement capability of the method has been investigated. Variations of density of one part in 1000 and variations in atomic number of one part in 400 are just detectable for volumes of tissue approximately 1 cubic centimetre (24).

Material and Methods

A simple modification to the EMI brain scanner has been produced which has enabled cross sections of the forearm to be obtained and the remarkable precision of the reconstruction method to be exploited (16, 17).

A tank was constructed in perspex (Fig. 1) and then inserted into the headbox assembly of the scanner. The tank contained a hand grip and three sample solutions of calcium chloride. The latter were of known attenuation coefficient to enable the X-ray tube characteristics to be monitored. The tank was filled with water, air bubbles removed and the subject under investigation asked to grip the perspex bar at the end of the tank. The forearm then rested along the floor of the tank. A marker was placed on the forearm prior to immersion in the tank. This marker indicated the position of the ulnar styloid and allowed external reference to the plane of cross-section.

Two simultaneous contiguous cross-sectional scans were obtained of the forearm 1.3 cm proximal to the ulnar styloid employing a 13-mm collimator at 100 kVp and 60 mA and 140 kVP and 28 mA. These energies were selected to enable atomic number determinations to be obtained in the hope that bone mineral changes could be distinguished from bone mass changes (25).

Four groups of measurements were obtained:

1. Cadaver forearm
2. Repeated measurements on a male volunteer
3. Postmenopausal female volunteers
4. Young adult male medical student volunteers

Computational Methods

A matrix of numbers can be printed out from which the distribution of attenuation coefficients can be deduced (25) (Fig. 2) or presented by analogue conversion as a grey-scale picture (Fig. 3).

An important feature of analysis depends upon an accurate definition of bone edge. No threshold value of attenuation coefficient can be determined below which bone can be excluded with certainty because of the partial volume effect within the voxel of tissue close to the bone edge. Hence a set of thresholds were determined above which values were known to correspond to bone, i.e. 20, 40, 60 and 80 units. The sum of all attenuation values above these thresholds in the region of the bone was then taken and a linear extrapolation carried out to determine the projected sum of attenuation values at zero threshold (Fig. 4).

The sum of attenuation values so obtained was used as the measure of bone mineral content.

A measure of trabecular bone content was determined by obtaining the sum of a 4 × 4 matrix of values at the centre of the trabecular space.

Transformation and interpolation of the rectangular matrix onto a polar system of co-ordinates whose origin is the approximate centre of the bone (Fig. 5) has enabled additional parameters, including volume, thickness of bone cortex and mean radius of bone, to be obtained. If

h is a maximum absorption value at a particular region of the cortex, the inner boundary of the cortex was defined as the contour of values equal to 3 h/4 which was always above values corresponding to trabecular space. The outer boundary of the cortex was defined as the contour of values equal to h/2. The thickness of cortex was then the mean distance between these two contours. Volume was defined as the number of voxels contained within a cylinder enclosed by the two contours. The radius of bone was defined as the mean distance in matrix units of the contours from the origin.

Results

The results from the four groups of measurements are given in Tables 1-4.

Table 1. Repeat bone measurements on a cadaver arm

Scan No.	Sum of EMI No. within bone	Volume of cortex (voxels)	Thickness of cortex (matrix units)	Radius of bone (matrix units)
1	41440	54.44	2.65	3.22
2	41378	54.78	2.64	3.23
3	41430	54.70	2.64	3.24
4	41247	54.49	2.58	3.32
Mean	41374 ± 91	54.60 ± 0.2	2.63 ± 0.03	3.25 ± 0.04

Table 2a. Repeat bone measurements on a volunteer with a peak tube voltage of 100 kV

Scan No.	Sum of EMI No. within bone	Volume of cortex (voxels)	Thickness of cortex (matrix units)	Radius of bone (matrix units)
1	25990	54.49	3.29	2.61
2	26900	54.36	3.32	2.60
3	26890	59.62	3.53	2.68
4	26335	48.01	4.79	2.06
5	27300	62.32	3.73	2.67
Mean	26683 ± 518	55.76 ± 5.5	3.73 ± 0.62	2.52 ± 0.26

Table 2b. Repeat bone measurements on a volunteer with a peak tube voltage of 140 kV

Scan No.	Sum of EMI No. within bone	Volume of cortex (voxels)	Thickness of cortex (matrix units)	Radius of bone (matrix units)
1	19815	54.61	3.26	2.65
2	19815	56.18	3.57	2.49
3	20225	65.46	3.65	2.83
4	19885	53.92	3.27	2.59
5	20535	59.93	3.67	2.64
Mean	20055 ± 317	58.02 ± 4.8	3.48 ± 0.21	2.64 ± 0.12

The reproducibility of the measurement of bone mass in the cadaver arm is about 0.2%. This represents the reproducibility of the technique for a situation in which the bone is in exactly the same position for each scan.

Table 3. Bone measurements on a group of post-menopausal females

Subject	Age	Sum of EMI No. within bone		Mean EMI No. within a region of trabecular bone	
		100 kV	140 kV	100 kV	140 kV
H.W.	63	15930	13600	4.7	-20.1
W.	70	12209	10878	8.5	9.4
P.	68	12273	10155	36.3	25.8
M.W.	65	13201	13433	61.9	57.2
Q.	69	15555	12139	15.6	2.3
Mean	67	13834 ± 801	12041 ± 681	25.4 ± 10.6	14.9 ± 12.9

Table 4. Bone measurements on a group of young male students

Subject	Age	Sum of EMI No. within bone		Mean EMI No. within a region of trabecular bone	
		100 kV	140 kV	100 kV	140 kV
M.J.	20	15608	15033	89.8	67.5
M.S.	20	18083	13865	57.2	44.4
R.C.	21	28180	21394	36.3	24.0
P.B.	21	14789	12367	84.1	57.9
R.P.	21	25394	19406	94.3	70.1
Mean	20.6	20411 ± 2695	16413 ± 1711	72.3 ± 11.1	52.8 ± 8.5

Repositioning introduces the most significant error, as illustrated in Tables 2a and b. Five scans on a volunteer obtained over a period of 7 days show a reproducibility at 100 kV of about 2% and at 140 kV of 1.4%. The difference between these reproducibilities is not statistically significant. The reproducibilities of the other parameters, namely cortical volume, cortical thickness and bone radius are approximately 7%, 5% and 4% respectively. The usefulness of these parameters is uncertain at present.

The results shown in Tables 3 and 4 are illustrated in Figures 6a and b. The difference between the means of the 'total bone' measurement of each group is significant at $p = 0.03$ for both 100 kV and 140 kV. The difference between the means of the trabecular bone measurement is significant at $p = 0.01$ at 100 kV and $p = 0.02$ at 140 kV.

Discussion

Preliminary studies obtained by C.A.T. suggest that the method has not only the capability to produce a cross-section of trabecular structure in the distal radius but has notably increased precision of measurement compared with other methods. Trabecular bone changes much more rapidly with age than total or cortical bone. The EMI scanning approach to bone densitometry has therefore the dual advantages of very high precision and an ability to measure that part of the bone which will change most rapidly with age or disease. Potential reproducibility within the limitations of this preliminary study was good and it was certainly possible to demonstrate a significant difference between mineral content of trabecular bone in a group of elderly ladies and

young male students. The positioning technique was simple but not ideal and improvements in this aspect should lead to reproducibilities close to those obtained in cadaver arm.

The mineral content of distal radius and ulna even when obtained with accuracy and precision may not necessarily reflect the bone mineral content of those skeletal sites with higher proportions of trabecular bone, notably the vertebral bodies (9, 26). Now that C.A.T. is available for the whole body it may be possible to employ the accuracy and precision of the technique not only to shed further light on this subject but also for the first time directly to make observations concerning trabecular bone in the vertebral bodies.

Summary

By minor modification of an EMI brain scanner C.A.T. has been utilised to determine measurements of bone mineral content in distal radius and ulna. Such measurements are possible, independent of subcutaneous adipose tissue and irrespective of bone contour.

Preliminary studies suggest that the accuracy and precision justify further longitudinal studies in the exploration of trabecular bone within vertebral bodies by whole body C.A.T.

Acknowledgments

The authors wish to thank Miss H.Jarvis and the Radiographic staff of the Department of Neuroradiology for their support in enabling this study to be undertaken in a busy service Department. Thanks are also due to the Department of Medical Illustration and Mrs. G.E.H. Shawcross for preparation of illustrative material and to Mrs. M. Tipton for her valuable secretarial assistance.

References

1. ADAMS, P., DAVIES, G.T., SWEETMAN, P.: Observer error and measurements of the metacarpal. British Journal of Radiology 42, 192 (1969).
2. ADAMS, P., DAVIES, D.P., SWEETMAN, P.: Osteoporosis and the effects of ageing on bone mass in elderly men and women. Quarterly Journal of Medicine 39, 601-615 (1970).
3. ARCHER-HALL, J.A., CARPENTER, P.B., EDWARDS, J.P.M., FRANCOIS, D.E.: A new method of bone mineral estimation using a conventional x-ray set. British Journal of Radiology 46, 375-380 (1973).
4. BARNETT, E., NORDIN, B.E.C.: The radiological diagnosis of osteoporosis - a new approach. Clinical Radiology 11, 166-174 (1960).
5. Editorial: Management of osteoporosis. British Medical Journal 1975/IV, 307-308.
6. CAMERON, J.F., SORENSON, J.: Measurement of bone mineral in vivo: an improved method. Science 142, 230-232 (1963).
7. CLARKE, R.L., VAN DYKE, G.: A new method for measurement of bone mineral content using both transmitted and scattered beams of gamma rays. Physical and Medical Biology 18, 532-539 (1973).

8. COHN, S.H., DOMBROWSKI, C.S.: Measurement of total body calcium, sodium chlorine, nitrogen and phosphorus in man by in vivo neutron activation analysis. Journal of Nuclear Medicine 12, 499-505 (1971).
9. DOYLE, F.: Clinical Endocrine Metabolism 1, 143-167 (1972).
10. DOYLE, F.H.: Ulnar bone mineral concentration in metabolic bone diseases. British Journal of Radiology 34, 698-712 (1961).
11. GARN, S.M.: An annotated bibliography on bone densitometry. American Journal of Clinical Nutrition 10, 59-67 (1962).
12. GARNETT, E.S., KENNETT, T.J., KENYON, D.B., WEBSTER, C.F.: A photon scattering technique for the measurement of absolute bone density in man. Radiology 106, 209 (1973).
13. GUSTAFSSON, L., JACOBSON, B., KUSOFFSKY, L.: X-ray spectrophotometry for bone mineral diterminations. Medical and Biological Engineering 113-119 (1974).
14. HORSMAN, A., SIMPSON, M.: The measurement of sequential changes in cortical bone geometry. British Journal of Radiology 48, 470-476 (1975).
15. HOUNSFIELD, G.M.: Computerised transverse axial scanning (tomography). British Journal of Radiology 46, 1016-1022 (1973).
16. ISHERWOOD, I., PULLAN, B.R., RUTHERFORD, R.A.: Quantitative aspects of computer tomography. 1st International Symposium on Computer Tomography. Bermuda, 1975.
17. ISHERWOOD, I., RUTHERFORD, R.A., PULLAN, B.R., ADAMS, P.H.: Bone mineral estimation employing computer assisted transverse axial tomography. Lancet 1976/II, 712-715.
18. KNOWELDEN, J., BUHR, A.J., DUNBAR, O.: Incidence of fractures in persons over 35 years of age. A report to the M.R.C. Working Party on Fractures in the Elderly. British Journal of Preventive Social Medicine 18, 130 (1964).
19. MERZ, A.L., TROTTER, M., PETERSON, P.R.:Estimation of skeleton weight in the living. American Journal of Physical Anthropology 14, 589-609 (1956).
20. MORGAN, D.B., SPIERS, F.W., PULVERTAFT, C.N., FOURMAN, P.: The amount of bone in the metacarpal and the phalanx according to age and sex. Clinical Radiology 18, 101-108 (1967).
21. NORDIN, B.E.C., GALLAGHER, J.C., AARON, J.E., HORSMAN, A.: Postmenopausal osteopenia and osteoporosis. Frontiers of Hormone Research 3, 131-149 (1975).
22. OLKKONEN, H., KARJALAINEN, P.: A ^{170}Tm gamma scattering technique for the determination of absolute bone density. British Journal of Radiology 48, 594-597 (1975).
23. REED, G.W.: British Empire Cancer Campaign Annual Report 38, 489 (1960).
24. RUTHERFORD, R.A., PULLAN, B.R., ISHERWOOD, I.: Calibration and response of an EMI scanner. Neuroradiology 11, 7-13 (1976).
25. RUTHERFORD, R.A., PULLAN, B.R., ISHERWOOD, I.: Measurement of effective atomic number and electron density using an EMI scanner. Neuroradiology 11, 15-21 (1976).
26. SHAPIRO, J.R., MOORE, W.T., JORGENSEN, H., REID, J., EPPS, C.H., WHEDON, D.: Osteoporosis: evaluation of diagnosis and therapy. Archives of Internal Medicine 135, 563-567 (1975).
27. SORENSON, J.A., CAMERON, J.R.: A reliable in vivo measurement of bone mineral content. Journal of Bone and Joint Surgery 49, 481-497 (1967).
28. VIRTAMA, P., HELELA, T.: Acta Radiologica (Suppl.) 293 (1969).
29. WEST, R.R., REED, G.W.: Measurement of bone mineral in vivo by photon beam scanning. British Journal of Radiology 43, 886-893 (1970).
30. WOOTEN, W.W., JUDY, P.F., GREENFIELD, M.A.: Analysis of the effects of adipose tissue on the absorptiometric measurement of bone mineral mass. Radiology 8, 84-89 (1973).

31. ZEITZ, L.: Effect of subcutaneous fat on bone mineral content measurements with the "single energy" photon absorptiometric technique. Acta Radiologica 11, 401-410 (1972).

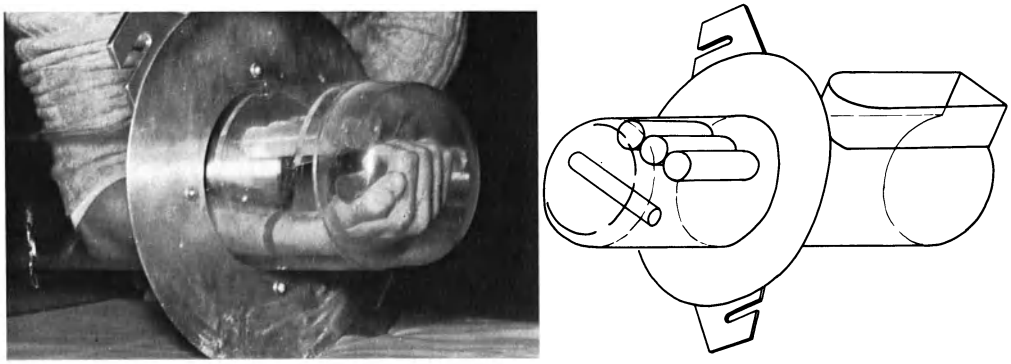

a b

Fig. 1a and b. A perspex water tank for insertion into the EMI head box assembly enabling cross sections of the forearm to be obtained

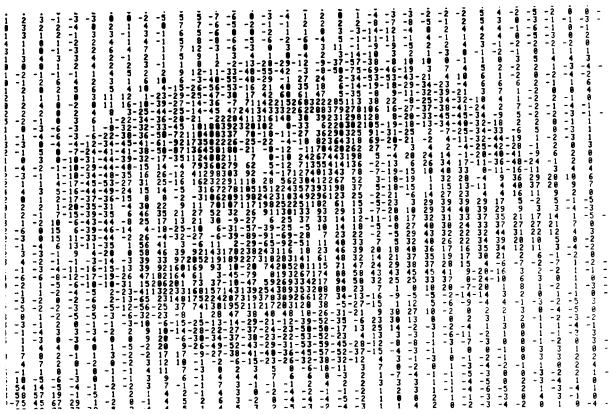

Fig. 2. Numerical print-out of the distribution of linear attenuation coefficients following C.A.T. scan of the forearm

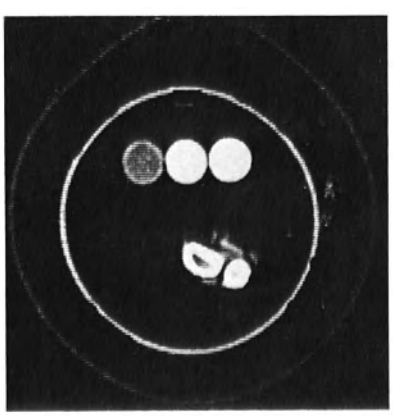

Fig. 3

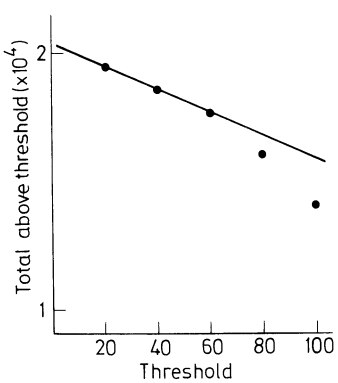

Fig. 4

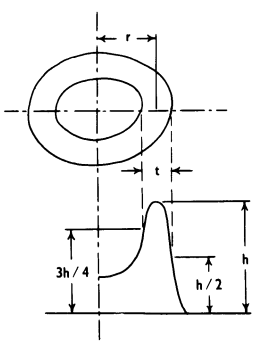

Fig. 5

Fig. 3. Grey-scale picture of forearm cross section

Fig. 4. Projected sum of attenuation values at zero threshold

Fig. 5. Transformation of rectangular index on to polar system of co-ordinates

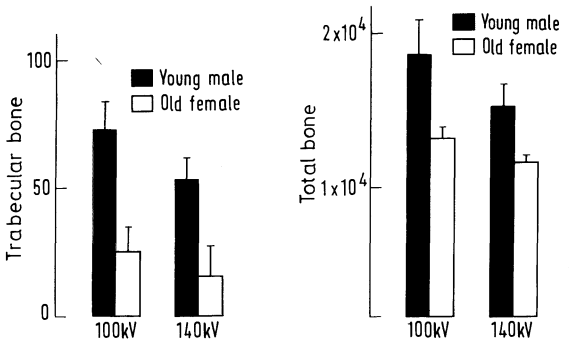

Fig. 6 a and b. Mineral content of 'trabecular bone' (a) and 'total bone' (b) in elderly ladies and young male volunteers

The Physical Performance of a Prototype CT5000 EMI Body Scanner

R. A. Rutherford*, B. R. Pullan*, and I. Isherwood**

Introduction

It has been pointed out by various authors (1, 2, 4) that there exists a trade-off between three of the parameters usually used to describe the diagnostic quality of a C.A.T. scan.

These are:

1. The radiation dose
2. The spatial resolution
3. The noise levels in the reconstructed picture.

The relationship between these parameters can be described crudely as:

$$\text{Dose} \propto \frac{(\text{Signal to noise})^2}{(\text{Resolution})^3}$$

The term 'resolution', referred to in the above trade-off equation, is the smallest possible resolution achievable for objects of high contrast. This is normally set by the size of the matrix element (pixel) for which values of absorption coefficient are calculated.

Measurements of radiation dose, spatial resolution and noise levels have been made for a prototype EMI CT5000 scanner, currently installed in the Department of Diagnostic Radiology at the University of Manchester, to determine the type of trade-off that has been implemented. It is important to be clear that these results are for a particular prototype machine and may not reflect the performance of production machines or other prototype machines.

In addition to these measurements, an assessment has been made of:

4. The long-term reliability of the EMI numbers calculated by the algorithm

5. The efficacy of carrying out C.A.T. brain scans on the CT5000 body machine rather than on the CT1000 brain machine

*Department of Medical Biophysics, University of Manchester.
**Department of Diagnostic Radiology, University of Manchester.

Dose

Material and Methods

The CT5000 can be used to scan objects of 13 in. or 10 in. diameter depending on the mode of scanning chosen. The dose to the skin administered by these two modes was assessed using a Vibron Electrometer with a 0.6 cc thimble chamber. The chamber was positioned at the circumference of a cylindrical container of water (13 in. or 10 in. diameter) which was placed in the patient support. The chamber was irradiated by allowing the X-ray tube to traverse and index around the water cylinder as it would in a normal scan of 20 s duration. The measurement was repeated by scanning in the reverse direction. The whole procedure was repeated for a variety of positions of the chamber around the circumference of the cylinder.

The effect of taking multiple slices was investigated using a thermoluminescent powder, lithium fluoride. Small capsules of the powder were positioned at 1-centimetre intervals along a thin perspex rod which was attached at right angles to one end of and along the axis of the 13 in. cylinder.

The cylinder was positioned in the patient support so that the first capsule was at the centre of the X-ray beam. Without changing the position of the cylinder, 50 slow scans were carried out. The equipment that was available for processing the LiF samples necessitated this number of scans. The scans were carried out without being processed by the computer.

Results

Figures 1 and 2 show the variation of skin dose as a function of position around the circumference of the water cylinders. The distance of a point from the origin represents the dose in these polar diagrams. The maximum skin doses measured were 2.7 rads (13 in. scan) and 4.2 rads (10 in. scan).

These values were obtained for:

Fast Scan (20 s)

A slow scan (approximately 80 s) will produce doses that are approximately four times higher.

A Single Slice

Multiple slice studies, discussed below, can give rise to larger doses.

Figure 3 is a graph of the dose along the axis of the 13 in. cylinder as a function of the distance from the centre of the section and shows how the irradiation of a slice affects neighbouring areas of tissue.

It can easily be shown that if a set of nine scans is carried out at one centimetre intervals, then the dose to the central slice is about 4.8 times the dose of a single slice.

A slight difference in the doses measured for clockwise and anti-clockwise scans was observed.

Discussion

The scanning motion of the X-ray tube results in maximum skin doses on the side of a patient which faces the X-ray tube. The opposite side receives less dose because of the shielding effect of the patient's own body. If mechanical problems can be overcome, it would seem advisable to arrange for the X-ray tube to index underneath the patient so that the radiation dose can be minimised to critical areas such as the orbits and gonads. The alternative to this is to scan certain patients in a prone position but this is obviously undersirable from the patient's point of view.

The pile-up factor of 4.8 for nine scans is large and is probably due to poor design of the collimator that is currently installed. The pile-up can probably be reduced by a factor of two by better collimator design.

It should still be noted, however, that a series of slow 10 in. scans on a suitably modified machine could build up X-ray doses of up to 80 rads if scans are repeated with contrast medium present. Such a series of scans should therefore be carried out with caution and after some assessment of the likely benefits.

Spatial Resolution

Materials and Methods

The spatial resolution was assessed by scanning wires at different positions within the phantom. Precautions were taken to ensure that the wires were perpendicular to the plane of the section. The size of the wires was such that they occupied only a fraction of one pixel.

The method for extracting the impulse response of the scanner was similar to that described previously (5) except that the position of the wire was assessed by taking the 'centre of gravity' of the 3 × 3 matrix of numbers surrounding the highest value.

The response along the axis of the scanner was measured using a method described previously (5).

Results

Figure 4a shows the averaged impulse responses for the 13 in. and 10 in. scanning modes. The EMI value of a particular pixel is plotted as a function of its distance from the wire.

Figure 4b shows the response along the axis of the scanner at both the centre and edge of the field of view.

Discussion

The spatial resolution measured in this way is, within experimental error, equal to that expected from the size of the matrix. Changing from the 13 in. to the 10 in. scanning mode definitely results in an improvement in high contrast resolution.

To avoid regions of reduced sensitivity Figure 4b indicates that scans should be spaced at approximately 1 cm intervals.

Noise

Methods and Results

Fast and slow scans were carried out on the 13 in. and 10 in. water cylinders. The noise level was taken to be the standard deviation of the EMI numbers within a 20 × 20 box at the centre of the matrix.

The results are given in Table 1:

Table 1.

Scan type	Standard deviation
13 in. normal	9.12 ± 0.33
13 in. slow	4.83 ± 0.17
10 in. normal	5.81 ± 0.21
10 in. slow	3.10 ± 0.11

Discussion

The results in Table 1 show the noise levels obtained with each scanning mode.

A slow scan takes 4 times longer than a fast scan (3.5 times if the slow scan is reduced to 70 s as on current production machines). The number of photons contributing to a particular transmission measurement therefore increases by a factor of four and one would expect from the theory of three-dimensional reconstruction that the noise in a slow scan would be reduced by a factor of two.

The experimental results support this theory and suggest that most of the noise in the reconstructed picture is due to the random fluctuations in the number of detected photons.

Long-Term Reliability of the EMI Numbers

Method and Results

The radiographers operating the CT5000 machine were asked to include in as many sections as they could, a small bottle containing distilled water. A numerical print out was obtained for the region containing the bottle and the mean EMI number calculated for a 10 × 10 box at the centre of the water sample.

The variation of EMI number obtained for water is shown in Figure 5. The numbers labelling the X-axis indicate the patient code number and the date of the scan.

Discussion

The variation in the EMI value is clearly larger than one would expect from the random fluctuations in the imaging process.

The errors could be due to a number of factors:

1. The patient may be larger than the 13 in. for which the computer calculates values.

2. Over-ranging saturates the detectors and leads to the inaccurate measurement of projection values.

3. The polychromatic correction may be inadequate.

4. Assorted errors too numerous to mention.

Unless the reliability of the EMI numbers can be increased, precise quantitative work such as that described by RUTHERFORD et al. (6) will not be possible.

Brain Scans on the CT5000

Materials and Methods

The phantom used to assess the quality of brain scans on the body machine is illustrated in Figure 6. The five cylindrical samples had densities ranging from 2 parts in 1000 less than water to 2 parts in 1000 greater than water. The phantom 'skull' consisted of three layers of simulated skull of thicknesses 3 mm, 8 mm and 11 mm and was filled with water.

This phantom was scanned by the CT5000 (slow and fast scan modes) and also by the CT1000 brain machine currently installed in the Department of Neuroradiology at Manchester Royal Infirmary.

The phantom was scanned at each skull thickness and a numerical printout obtained for each scan.

The accuracy of the polychromatic correction was assessed and a value for the signal to noise ratio obtained for each scan type. The latter was defined as the difference between the EMI number of the most dense and least dense cylinder divided by the uncertainty in that difference.

Results

Figures 7, 8, 9 show the scans obtained. Each picture has been photographed at the same settings, namely: window level = 9 units, window width = 50 units.

Figures 10 and 11 demonstrate the distortion in the reconstructed values due to the presence of skull. The EMI values for the water are plotted as a function of distance from the skull edge. Clearly the CT1000 (with water box) achieves a better 'spectral' correction.

The signal to noise levels for each scan type are given in Table 2:

Table 2.

Scan type	Skull thickness	Signal to noise
	3 mm	18.6
Brain machine	8 mm	13.2
	11 mm	12.4
	3 mm	10.9
Body machine normal	8 mm	8.6
10 in.	11 mm	6.8
Body machine slow	3 mm	17.0
10 in.	8 mm	12.6
	11 mm	15.8

It can be seen that the signal to noise levels for the brain machine can only be matched by the 10 in. slow scan on the CT5000.

Discussion

If a comprehensive theory of visual detection and recognition were available, it would be possible to describe the quality of an image purely in physical terms such as resolution and noise levels and to use these to assess the relative quality of two image forming methods. Even though such a theory does not exist, it is possible to compare the CT5000 and the CT1000 by generating ROC curves by means of a psychophysical experiment (3).

This study has not yet been carried out, but certain points can already be made.

There is little evidence at present to suggest that abnormalities in the soft tissue of the brain can be seen more clearly on the 320 × 320 matrix. GODFREY HOUNSFIELD himself has suggested that 160 × 160 may be the ideal matrix size for scanning the head (1).

The sample cylinders may seem more sharply defined on the CT5000 scans than on the CT1000 scans due to the increased resolution, but tumours and other soft-tissue abnormalities do not have sharp edges and so the ability to detect them is not likely to be enhanced by high resolution studies.

The penalty for higher resolution is, according to the trade-off equation, either a higher patient dose or a lower signal-to-noise ratio or both. A slow 10 in. scan produced on the CT5000 has a signal-to-noise ratio comparable to that of the CT1000 brain machine, but at a cost of an eightfold increase in patient dose. Figures 12 and 13 show examples of comparable brain sections taken with these two scanning modes to show that even this eightfold increase in patient dose may not produce pictures of as good diagnostic quality as those of the CT1000.

Until 160 × 160 brain sections can be produced optimally on the CT5000, it would seem inadvisable to use the machine for scanning heads. The diagnostic quality per unit radiation dose seem too low.

This highlights the need for a CT scanner which is sufficiently flexible to allow optimum scanning modes to be chosen for particular clinical situations.

Conclusion

The trade-off equation is fundamental to the design of C.A.T. scanners.

The higher resolution scans obtained by the CT5000 are formed at the expense of higher radiation dose and lower signal to noise ratios, and for slow 10 in. scans of the head the radiation dose may be intolerably high.

It remains to be seen whether the diagnostic quality of the images produced by the CT5000 justifies the higher radiation dose to the patient.

An improved collimator, recently intalled on the Manchester CT5000 scanner, has resulted in significantly lower skin doses for single slice scans and also significantly smaller pile-up factors for multiple slice scans.

Acknowledgments

We would like to thank the Science Research Council for providing a studentship for Mr. R.A. Rutherford. We would also like to thank Mr. J.B. Massey and Mr. P. Williams, of the Regional Department of Physics and Bioengineering for their help with the thermoluminescent dosimetry; the radiographic staff in the Department of Diagnostic Radiology for their assistance; Mrs.G.E.H. Shawcross for the preparation of illustrative material and finally to Miss B.K. Holt for her secretarial assistance.

References

1. HOUNSFIELD, G.N.: Picture quality of computed tomography. American Journal of Roentgenology 127, 3-9 (1976).
2. McCULLOUGH, E.C., PAYNE, J.T.: Performance evaluation and quality assurance of computed tomography scanners, with illustrations from the E.M.I., ACTA,and Delta Scanners. Radiology 120, 173-188 (1976).
3. METZ, C.E., STARR, S.J., LUSTED, L.B., ROSSMANN, K.: Progress in evaluation of human observer visual detection performance using the ROC curve approach. Presented at the IVth International Conference on Information Processing in Scintigraphy. Orsay, France. July 1975 (published in the proceedings).
4. PULLAN, B.R., RUTHERFORD, R.A., ISHERWOOD, I.: Computerised transaxial tomography. Presented at the 7th L.H. Gray Conference. Leeds, England. April 1976 (to be published in the proceedings).
5. RUTHERFORD, R.A., PULLAN, B.R., ISHERWOOD, I.: Calibration and response of an E.M.I. scanner. Neuroradiology 11, 7-13 (1976).
6. RUTHERFORD, R.A., PULLAN, B.R., ISHERWOOD, I.: Measurement of effective atomic number and electron density using an E.M.I. scanner. Neuroradiology 11, 15-21 (1976).

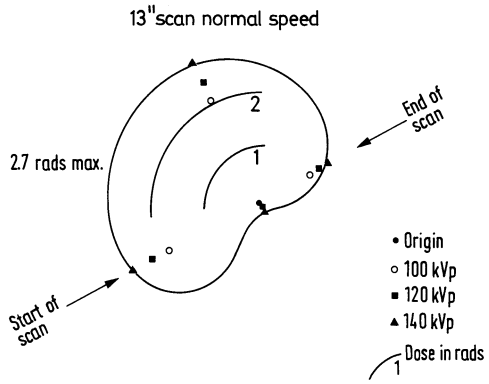

Fig. 1

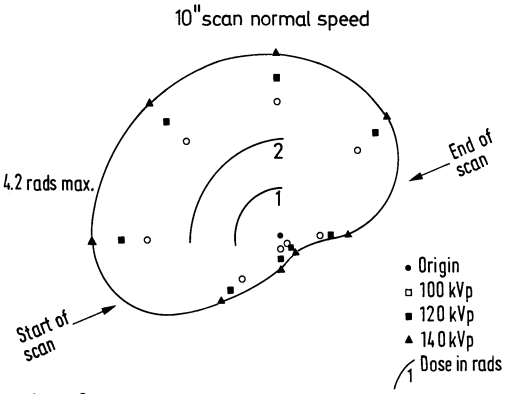

Fig. 2

Fig. 1. Patient dose for a single 13 in. scan
Fig. 2. Patient dose for a single 10 in. scan

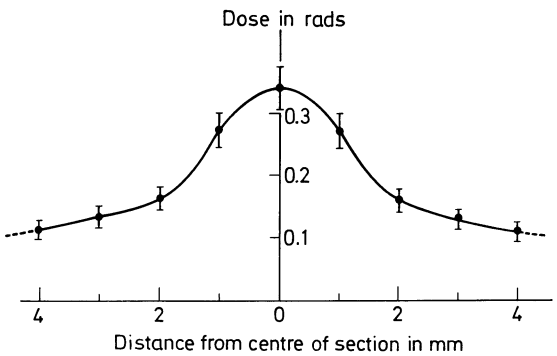

Fig. 3. Variation of dose with distance from centre of scanned section

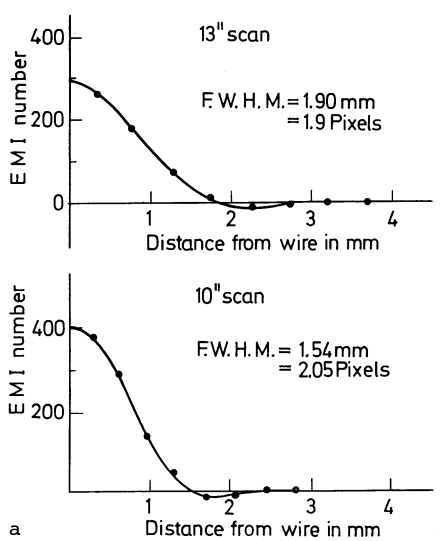

a

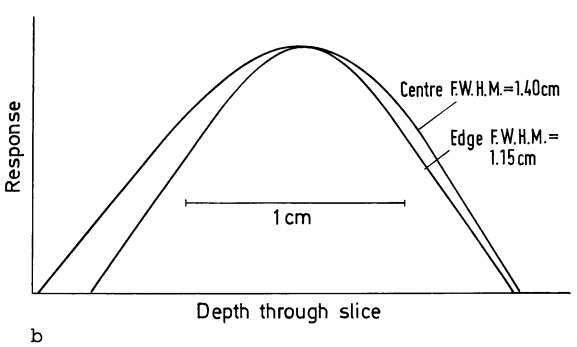

b

Fig. 4. (a) Impulse response. (b) Response along axis of scanner

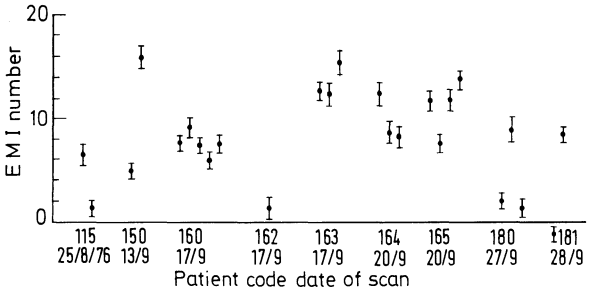

Fig. 5. Mean EMI number for a sample of water for a variety of scans

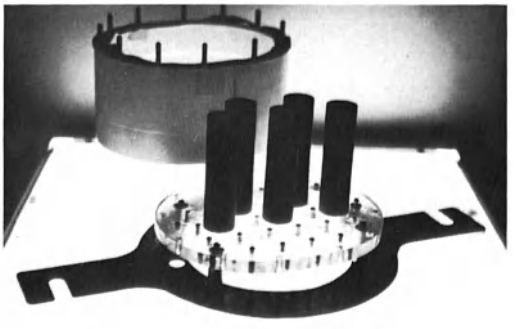

Fig. 6. Phantom used to test quality of head scans

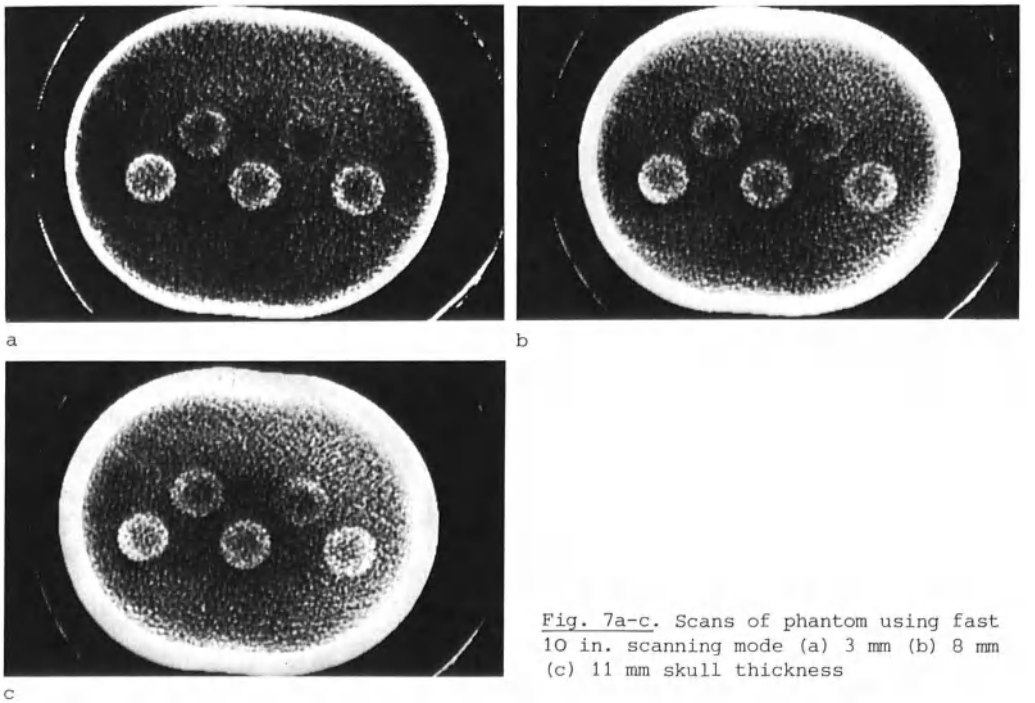

Fig. 7a-c. Scans of phantom using fast 10 in. scanning mode (a) 3 mm (b) 8 mm (c) 11 mm skull thickness

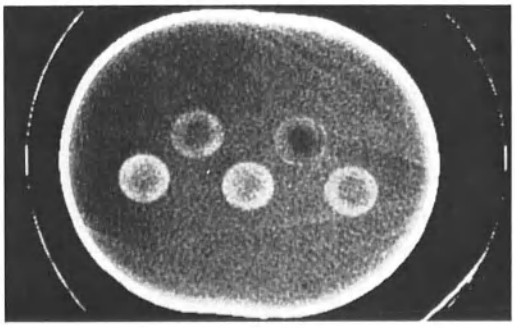

a

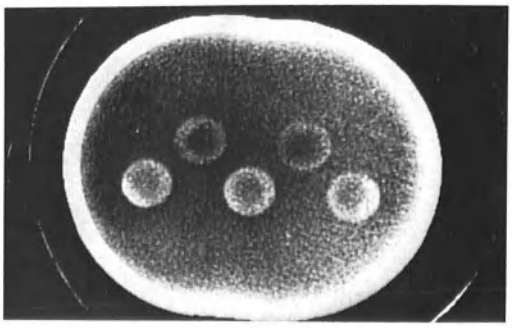

b

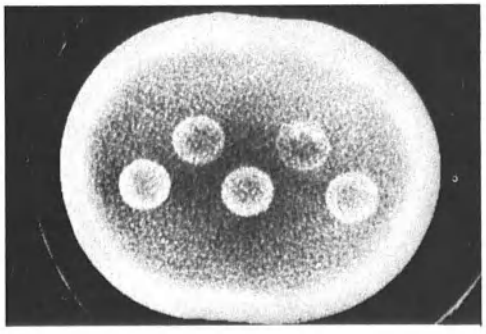

c

Fig. 8a-c. Scans of the phantom using the slow 10 in. scanning mode (a) 3 mm (b) 8 mm (c) 11 mm skull thickness

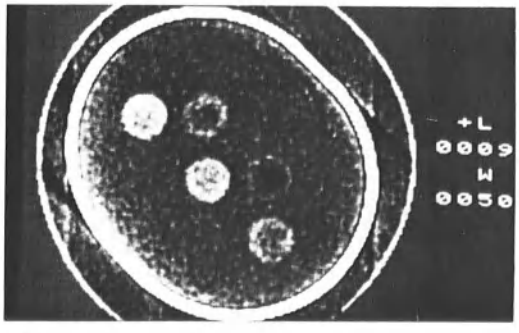

a

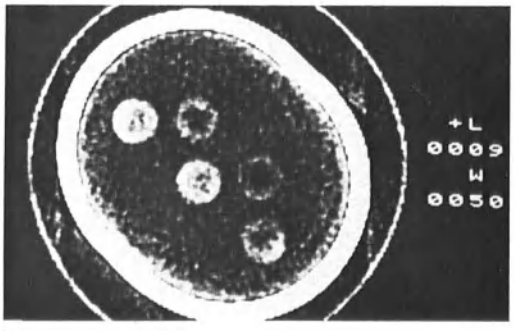

b

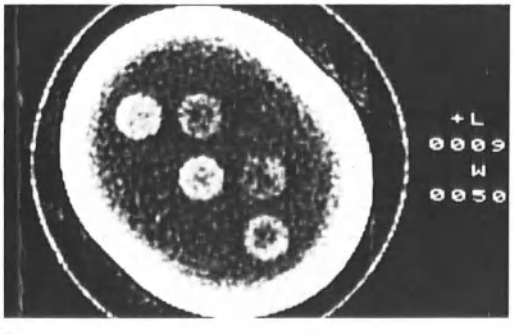

c

Fig. 9a-c. Scans of the phantom using the CT1000 brain scanner (a) 3 mm (b) 8 mm (c) 11 mm skull thickness

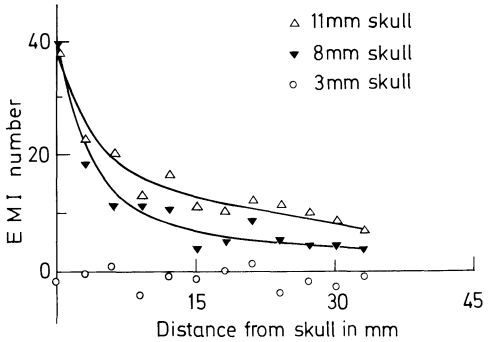

Fig. 10.

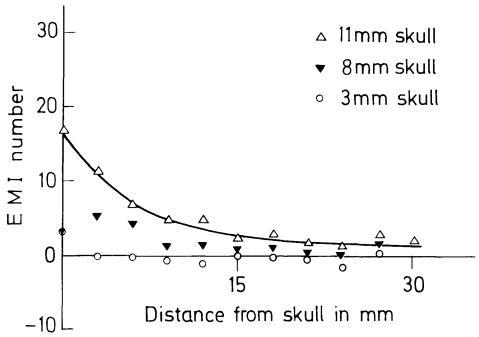

Fig. 11

Fig. 10. Skull correction for body machine
Fig. 11. Skull correction for brain machine

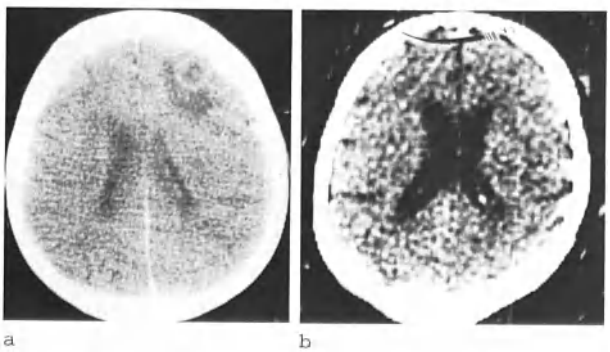

Fig. 12a and b. Comparable brain sections taken using (a) slow 10 in. scan mode (b) brain machine

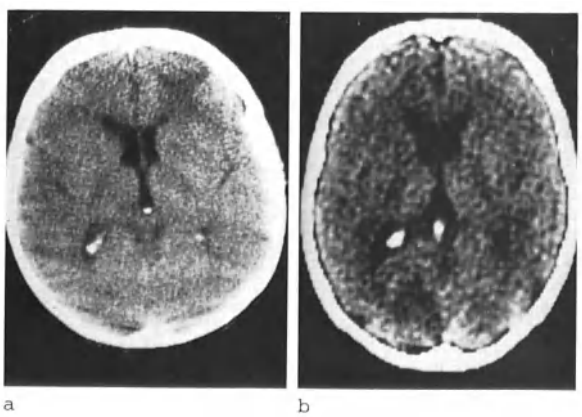

Fig. 13a and b. Comparable brain sections taken using (a) slow 10 in. scan mode (b) brain machine

The Body Scanner in Neurological Disease

The Total Body Scanner in Neurological Disease

M. Gado, J. Eichling, and M. Currie*

Computerised tomography of the brain was developed in 1973. A considerable volume of experience has accumulated during this time to allow evaluation of the technique in the investigation of patients with intracranial disease. On the other hand, total body scanning is a more recent development and the experience with the technique is much more limited. The purpose of this communication is to summarise our experience with a prototype EMI total body scanner installed at the Mallinckrodt Institute of Radiology for the investigation of neurological disease. The subject will be dealt with in two parts: (1) versatility of the total body scanner and its value in clinical practice and (2) a comparison between the prototype total body scanner and the dedicated head scanner in brain imaging, including analyses of the difference in performance of the two scanners and its effect on the brain image.

Versatility of the Total Body Scanner

There are two main features that distinguish the total body scanner from the dedicated head scanner. These are the removal of the water bag and the larger size of the aperture of the body scanner which can accomodate the torso of an adult patient. The aperture measures 17 in. in diameter compared to 12 in. in the dedicated head unit. As a result, the body scanner acquired the ability to examine parts of the body below the base of the skull. In patients with neurological disease, these parts are particularly the facial bones, the neck and the spine.

Patients with Large Head Size

Out of the first 8000 patients requiring C.A.T. of the brain in our institution, there were 7 whose heads were too large to fit into the aperture of the head scanner. There were 2 patients with Paget's disease, 1 with aqueduct stenosis presenting in late adult life and 3 with no evidence of cranial or intracranial abnormality. The 7th patient had bilateral herniation from two craniotomy defects for subdural haematoma followed by brain swelling.

Other Projections of the Brain

The large diameter of the aperture of the body scanner allows imaging of the brain with the neck hyperextended while the patient lies in the prone or supine position. A CT scan in a plane near to the coronal plane can be obtained (Fig. 1). Because of the fixed vertical position of the gantry of the scanner, the degree of hyperextension necessary for obtaining an image in the true coronal plane may be too uncomfortable

*Mallinckrodt Institute of Radiology, Washington University School of Medicine, St. Louis, Missouri.

for a patient with a short of stiff neck. In these cases, a 'sub-coronal' scan is obtained.

The coronal CT image provides another projection of the relationship between a lesion and the ventricular system. We believe that this projection has a potential in the visualisation of lesions in the suprasellar region although we have not had the opportunity to test it in a lesion smaller than 3 cm in diameter.

Facial Bones and Base of the Skull

We have examined the facial bones and the base of the skull in coronal and horizontal CT scans of 12 patients. In 5 of them there was no evidence of disease in this region and in the remaining 10 patients the histologically proven diagnoses were as follows:

Nasopharyngeal angiofibroma	1
Maxillary sinus carcinoma	2
Nasopharyngeal carcinoma	1
Mucocoele of the sphenoid sinus	3

Each of the patients who had pathological lesions was examined also by polytomography. The facial bones were well visualised by CT (Fig. 2) as well as by polytomography and bone destruction was equally well demonstrated by both techniques. The CT images were much clearer in delineating the tumour outline. The contrast between the soft-tissue shadow of the lesion and air was not as well demonstrated by polytomography.

The Spinal Canal

We examined the lumbar spine in seven patients before myelography. The final diagnoses were:

Herniated lumbar disc	2
Stenosis of the lumbar spinal canal	2
Intraspinal lipoma	1
Cervical cord swelling	2

We also examined the lumbar spine in 25 CT scans done for the lower abdomen in patients in whom there was no evidence of compression of the lumbar nerve roots.

In none of the cases was it possible to visualise the nerve roots of the cauda equina. It was impossible to see any evidence of the herniated disc material inside the spinal canal in either of the two patients who showed large disc herniation with significant defects on positive contrast conventional myelography. In the patient with the intraspinal lipoma of the lumbosacral region, the nature of the lesion was identified on the C.A.T. image by the very low density of fat compared with the other contents of the spinal canal (Fig. 3).

In order to evaluate the value of C.A.T. in the diagnosis of stenosis of the lumbar spinal canal, we measured the sagittal and the widest transverse diameters of the spinal canal on the C.A.T. image. We also measured the area of the spinal canal using a loop calibrated to 0.1 mm. Measurements of the same parameters were taken for the vertebral body on the same image to account for variations in patient's size. We then calculated the ratio between the areas of the spinal canal and the vertebral body and we compared these data with measurements of the

Table 1. C.A.T. and radiographic measurements in four patients with backache and sciatica

Case No.		1	2	3	4
Diagnosis		Disc	Herniation	Narrow	Canal
a-p diameter of canal (mm)	C.A.T.	3	3.5	2.5	2.5
	X-ray	19	21	18	19
Transverse diameter of canal (mm)					
	C.A.T.	5.5	5.5	4.5	5.5
	X-ray	30	29	29	35
Area of canal (mm^2)	C.A.T.	10.5	12.5	5.5	8.5
Area of vertebral body (mm^2)	C.A.T.	67	65	66	72.6
Canal/body ratio (%)	C.A.T.	15.7%	19%	8.3%	11.7%

sagittal and interpedicular diameters on the plain radiographs. The results are shown in Table 1. The measurements of the sagittal and the widest transverse diameters of the spinal canal on the C.A.T. image corresponded to those taken from the radiographs with a minification factor of 6:1 on the C.A.T. image. In both patients with narrow canals these diameters were slightly smaller, but they were still at the lower limit of the normal variants. In both patients however, there was a significant decrease in the canal to body ratio on the C.A.T. image compared to the patients with disc herniation. In the 25 patients included as controls, the canal to body ratio varied from 14.2 to 22.3%. The mean was 17% with a standard deviation of ± 2.5.

Discussion

Although the number of patients included in this series is small, the analysis of the data shows that the total body scanner has addressed computerised tomography to two new major areas of neuroradiological application: 1. The skull base and the nose and throat 2. the spinal canal. It has also demonstrated the potential of scanning the brain in different projections.

With the use of transaxial CT alone a mental process on the part of the viewer is required in order to appreciate the spatial relationships between anatomical structures and/or lesions in the vertical plane. The actual visualisation of images of the same structures in both the horizontal and vertical planes may facilitate the process and increase the level of confidence in localisation. This may prove particularly useful in mapping a craniotomy flap or in radiotherapy planning.

Lesions at the base of the brain, lesions of the the skull base and those extending intracranially are best suited for accurate localisation by the combined transaxial and vertical approach.

Lesions in the region of the sella generally fall in this category. We did not have the opportunity to test the value of coronal CT in small suprasellar lesions. We have noticed however, in the small number of patients examined in the coronal plane for other reasons, that the resolution of the suprasellar cistern is impaired by reconstruction artefacts at the interface between bone and air in the sphenoid sinus.

The quality of the C.A.T. images of the base of the skull and the facial bones by the total body scanner are superior. This is due to the capability of the C.A.T. body scan system to handle a wide range of varia-

tions in X-ray attenuation and the high inherent contrast in the structured examined. Polytomography has been extremely useful in the study of this region. In the comparison between the two techniques in this small number of patients, both methods yielded the same result. The clarity of soft tissue visualisation on the C.A.T. image, is due to the absence of blur from any overlying structures as the X-ray beam 'views' only the structures included in the image. In this small number of patients we did not recognize any compromise in the information on C.A.T. image as a result of the limitations on resolution imposed by the thickness of the slice (13 mm) and the size of the picture element (0.7 mm) compared to polytomography. A study including a larger number of patients is under way, and the results will be the subject of a separate communication.

The data on the spinal canal indicate that the resolution and contrast capabilities (resolving power) of the system are not yet sufficient for visualisation of the spinal cord, the cauda equina, the nerve roots or herniated disc material. The imaging of these structures remains within the field of conventional myelography with positive or air contrast. Structures of high inherent contrast such as fat can be visualized on C.A.T. and their nature can be identified. This was the case in the one patient with intraspinal lipoma in our small series.

The evaluation of the bony spinal canal itself by transaxial CT seems to be promising. It has been shown in the past that the typical appearance of a narrow spinal canal on myelography may be present in the face of normal measurements on plain radiography. It has been well recognised that encroachment by the laminae rather than shortness of the sagittal diameter is the offending cause in these cases. It has not been possible to obtain this information preoperatively by conventional radiography. Polytomography in the transaxial plane has been tried but there are serious limitations in regard to dose, technique and image quality.

With the use of transaxial CT the area of the spinal canal can be evaluated regardless of the measurements of the sagittal or interpedicular diameter. We recommend the use of the ratio between the area of the spinal canal and the area of the vertebral body at the same level is used rather than the absolute value of the canal area. This allows for variations in patient's size and for any fluctuation in the minification factor on the display or on the polaroid copy. In our two patients with the syndrome of narrow canal, the canal-to-body ratio was significantly different from the ratio in the two patients with herniated disc and the 25 controls. Both patients underwent extensive lumbar laminectomy with good clinical result. Further work is required to determine the minimum canal-to-body ratio in patients with no clinical symptoms.

The Brain Image by the Total Body Scanner: the Performance of the Scanner

Material

In order to compare the performance of the total body scanner with the dedicated head scanner in brain imaging we examined six patients by both scanners within 2 days. We also reviewed 15 scans on different patients studied by the body scanner and a similar number studied by the head scanner. A total of 36 C.A.T. brain scans constitute the material of this comparison.

In order to compare objectively the performance of the two scanners, and for the purpose of correct interpretation of the observations, we constructed three phantoms. The first phantom consisted of plastic syringes 11 cm in diameter filled with different dilutions of Conray 60 and surrounded with water in a plexiglass container. The iodine concentrations varied from 105 to 1408 mg/100 cc. The second phantom consisted of 3 and 15 mm diameter rods of four plastics: nylon, polystyrene, H.D. polyethylene and L.D. polyethylene. The rods were surrounded with water in the plexiglass container. The 3-mm rods were intended to test resolution. The 15-mm rods were intended to obtain the true EMI number reconstructed by each scanner from the numerical printout. The third phantom contained eight syringes filled with calcium acetate solutions in water with different concentrations containing from 0.25 to 5.0 g of calcium/100 cc. The syringes were surrounded with water in the plexiglass container. Each phantom was scanned by the two scanners respectively in the same day. Scans at 100 kV and 120 kV were obtained in each instance. The slice thickness was 13 mm. Polaroid copies were taken at comparable window settings to compare the images. When necessary, window settings were changed to obtain the same image quality and the settings were then compared. A numerical printout was obtained for each scan (160 × 160 for head scanner, 320 × 320 for body scanner). The EMI numbers of water, plastics and solutions of Conray and calcium were obtained by calculating the mean and standard deviation (S.D.) of 25 numerical values from the centre of the syringe of the rod, avoiding the peripheral partial volume effect of the syringe material in the case of the solutions and the surrounding water in the case of the rods. These values were then compared for evaluation of noise (S.D.), spatial uniformity, linearity and alteration with kV change.

Results

1. Brain images: There were two patients who were uncooperative and were included in the study for evaluation of motion artefacts. They showed less on the images taken by the total body scanner (20 s scanning time) than with the head scanner (4.5 min scanning time).

There was one patient who had surgical metallic clips inserted intracranially at a previous craniotomy. The images obtained from both scanners showed the typical star-like linear artefacts radiating from the site of the metallic object. There was one patient who had droplets of Pantopaque (Myodil) in the intracranial subarachnoid space from a previous myelogram. The images from both scanners showed the opacities of the iodized oil, but no linear artefacts were seen in either image.

There were two patients who were cooperative and did not show undue movements during the scanning time. No motion artefacts were seen in either scan. There was sharper delineation of the margins of the intracranial structures in the images of the body scanner (matrix size 320 × 320). There was, however, some degree of non-uniformity of the contrast in the same slice on the images of the body scanner in more than 50% of the cases (Fig. 4). This took several forms. In some images it appeared as a broad halo of decreased density deep to the inner table of the skull. In other patients it appeared as unilateral decreased density. In others it appeared as a slight increased density towards the centre of the slice. The images of the body scanner were grainy overall and there was a tendency to show a flatter tone indicating a generalised decrease of contrast.

2. Phantom images. Table 2 shows the mean and S.D. of the attenuation values of water obtained by the head and body scanners at nine positions

Table 2. Comparison of EMI head and body scanners: uniformity and noise (S.D.)

Position	Water attenuation (S.D. at 120 kV) Head scanner	Body scanner
1	0.1 (2.9)	15.0 (3.8)
2	0.4 (3.4)	20.0 (4.5)
3	0.6 (2.1)	9.2 (3.9)
4	0.3 (2.8)	15.6 (3.3)
5	0.9 (3.1)	27.5 (3.4)
6	0.8 (1.6)	12.1 (3.2)
7	1.3 (3.3)	7.6 (4.7)
8	1.8 (2.1)	9.0 (5.1)
9	2.2 (3.9)	5.0 (3.9)

within the 10 in. scans of the head and body scanners. The mean values from the numerical printout of the head scanner varied from -2.2 to 0.1. The S.D. varied from 1.6 to 3.9. The corresponding mean values for the body scanner ranged from 5.0 to 27.5 and the standard deviation ranged from 3.2 to 5.1.

The attenuation of the Conray solutions showed a linear relationship with the iodine content (Fig. 5) on the head scanner at 120 kV. The values at 100 kV showed also a linear relationship and a shift upwards. The shift of the attenuation values was also linearly related to the iodine content (Table 3).

Table 3. The relationship between the shift of attenuation values with kV and the iodine content head unit

I (mg %)	kV Shift (100-120)
105	2.7
176	6.5
211	6.4
352	8.6
423	13.6
564	16.2
704	17.6
846	23.1
1408	40.3

On the body scanner there was also a linear relationship between the attenuation values and the iodine content although the scatter was much more marked than with the head scanner. For iodine concentrations below 625 mg % the body scanner attenuation values at 120 kV were higher than the head scanner values (Fig. 5). The opposite was true for iodine concentrations above 625 mg. Moreover, when the graph was extrapolated, the attenuation value from the head scanner at 0 concentration of iodine was 0 but the value from the body scanner was 21 EMI units. The alteration of attenuation values with shift of kV in the case of the body scanner showed also an unexpected pattern. When kV was changed from 120 to 100 the attenuation values *dropped* for iodine concentrations below 790 mg %. The expected increase was only observed when the iodine concentrations were more than 790 mg %. When the graph was extrapolated the attenuation value at 0 concentration of iodine at 100 kV was 3 EMI units.

We were able to correct the discrepancies shown in the attenuation values computed by the body scanner by a two step manoeuvre. First step: the scale was displaced by 21 units for the 120 kV to correct for the attenuation value of water = 0. The second step: the slope of the line was corrected by multiplying each value by 1.3. A similar correction was required for 120 kV values with one difference, namely the scale had to be displaced by 3 units only to correct for water = 0.

Similar observations were found with the phantom containing the calcium acetate solutions and the phantom containing the plastic rods (Fig. 6). In the latter case scans were obtained at 120 kV only.

Discussion

Three conclusions were drawn from the experimental data of the iodine solution scans and may be used to explain some of the findings described in the brain scans: (1) The body scanner in its prototype available to us is not programmed for scanning the same object at different kV setting. (2) The percent contrast scale of the body scanner is 30% larger than that of the head scanner. Two more conclusions were drawn from the water scans described above: (1) The body scanner images have a higher noise level (S.D.) (2) The body scanner images have less uniformity.

The analysis of the images of the six patients who each had a C.A.T. scan of the brain by both the head scanner and the body scanner indicates that there are some favourable and some unfavourable features of the body scanner performance, reflected in the brain image produced.

The short scanning time eliminates to a great extent motion artefacts and therefore eliminates the need for heavy patient sedation. To our experience this has been a serious problem with the head scanner in infants, particularly the group with perinatal intracranial haemorrhage who required repeated C.A.T. scans for evaluation of ventricular size.

The larger matrix of the body scanner image allows sharper delineation of anatomical structures.

The undesirable features of performance of the body scanner include the high noise level, lack of uniformity, and the higher percent contrast scale. The noise level is reflected in the graininess of the image.

Lack of uniformity was demonstrated in our experimental data using the water-filled phantom. These data serve as the basis for explaining the asymmetry of brain density in apparently normal patients examined by the prototype body scanner. These experimental and in vivo observations were not seen in the images of the head scanner with the water bag filling the space between the surface of the head and the limits of the field of the reconstructed image. We are currently testing the efficacy of various methods of reducing the effect of the large air gap caused by the smaller size of the head, particularly in the transverse diameter.

For an overall assessment of the performance of the body scanner in brain imaging, one has to consider both the favourable and unfavourable features discussed above. A thorough evaluation requires a larger number of patients of different age groups and disease conditions. It also requires a double blind study with independent observers. However, a general statement can be made based upon this small series, that for most clinical purposes of C.A.T. brain imaging the body scanner can

serve as an alternative to the dedicated head scanner, widely used at the present time. On the other hand, the dedicated head scanner is superior in situations where quantitative analysis is required. This is particularly the case in dynamic studies with contrast material, comparative assays of water content, demyelination etc. In these cases the accuracy, low noise and the capability to scan the same object with different kV settings are indispensable even if sedation is required for proper imaging.

Dose Considerations

The absorbed doses delivered to selected points of a Rando-Alderson human phantom were evaluated employing thermoluminescent dosimeters (TLD). Surface-absorbed dose measurements utilised small teflon LiF TLD discs (5 mm diameter) while internal measurements were made with small cylinders composed of tissue equivalent material (4 mm diameter × 9 mm) and containing LiF powder. Several dosimeters of each type were calibrated with (1) 140 kV_p + 1.0 cm Al added filtration and (2) 140 kV_p + 1.0 Al and 3.0 cm water added filtration by concurrent measurement of the radiation exposure response of the dosimeters and a Victoreen 651 thimble ionization chamber. A rad-to-roentgen ratio of 0.94 was used.

Absorbed doses were obtained subsequent to EMI scans of both the head and torso. For a typical brain study of three scans providing six tomographic reconstructions the maximum skin-absorbed dose is approximately 1 rad. For the same study the absorbed dose imparted to a central region of the brain was found to be approximately 80 millirads. Thus, the data indicate a total energy deposition, i.e., integral dose, for the brain comparable to that delivered by a single skull film.

However, absorbed doses obtained subsequent to EMI scans of the torso are significantly higher. The maximum skin-absorbed dose to a slice due to a scan of that slice is of the order of 4 rads for a standard scan 20 s duration through 180° with 140 kV and 28 mA. Furthermore, contributions to the same slice from other tomographic cuts are such that a set of five slices will increase the maximum skin-absorbed dose to about 6 rads. Similarly, the interior-absorbed doses within a central slice of tissue will vary from a minimum of some 2 rads to the maximum of 6 rads. This corresponds to an integral dose for the central slice of a five-slice set of some 1700 g-rads. As a comparison, a typical chest film will deliver an entrant skin absorbed dose of approximately 0.040 rads and an integral dose of about 13 g-rads per centimeter slice. Similarly, image-intensifier fluoroscopy will typically impart about 5-10 rads/min to the skin and deliver an integral dose of about 1500-3000 g-rads/min per centimeter slice. Thus, the total energy deposition subsequent to a C.A.T. study is approximately that incurred from a minute of fluoroscopy for similar imaged areas of the subject.

The measured gonadal absorbed doses are cause of even greater concern. The measured gonadal doses were 90 millirads due to a single scan of the upper chest and 270 millirads due to a single scan of the lower abdomen. Hence, a C.A.T. study consisting of five slices delivers an absorbed dose to the gonads in the range of 0.5-1 rad depending on the anatomy scanned. This value compares unfavourably with gonadal-absorbed doses from conventional X-ray procedures.

Thus, it appears that the radiation absorbed dose imparted to subjects undergoing C.A.T. studies with a body scanner is of such magnitude to preclude its use as a widespread diagnostic screening tool of the torso.

Fig. 1. Normal coronal CT scan of the brain and facial bones

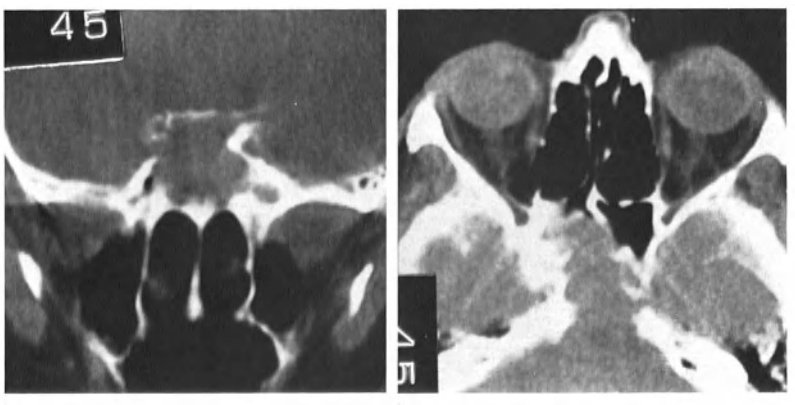

a b

Fig. 2a and b. Pyocoele of the sphenoid sinus (a) Coronal CT (b) Transaxial CT. There is expansion and opacity of the sphenoid sinus with erosion of the roof and posterior wall

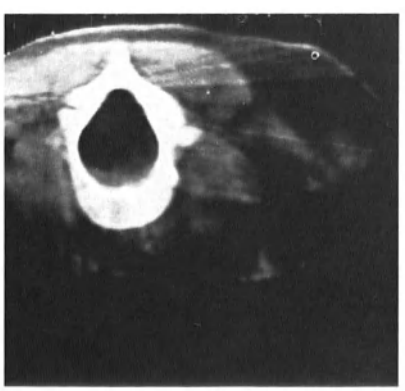

Fig. 3. Intraspinal lipoma. Lesion is distinguished on the image by low density of fat

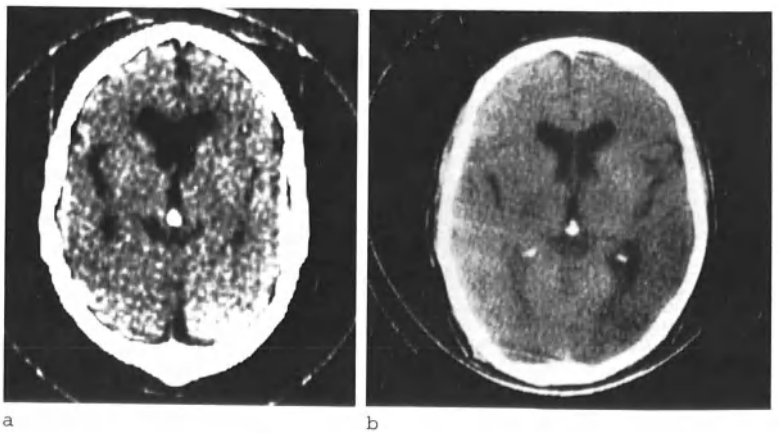

Fig. 4a and b. C.A.T. of same patient (a) Dedicated head unit (b) Body scanning unit

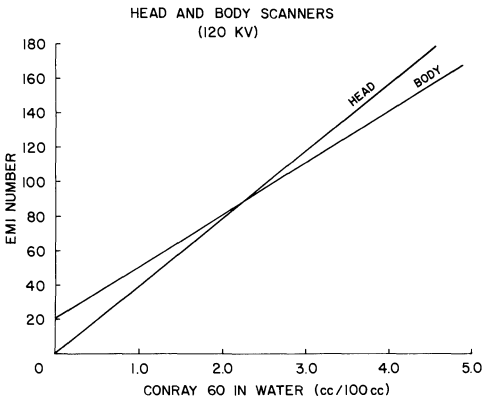

Fig. 5

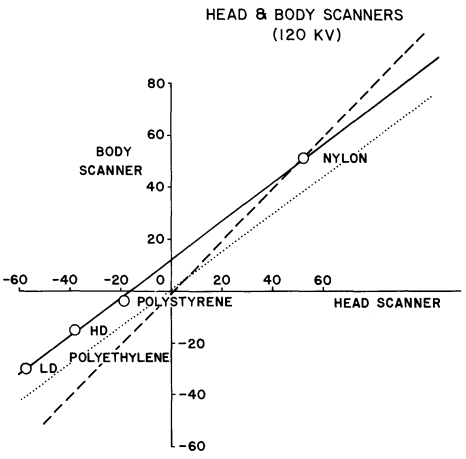

Fig. 6

Fig. 5. Attenuation values obtained by head and body scanners for the same phantom containing several dilutions of Conray 60 in distilled water

Fig. 6. Attenuation values of four different plastics, obtained by the body scanner plotted against those obtained by the head scanner (solid line). Dotted line shows the correction introduced by displacing scale of body scanner. Dashed line is the meridian

Computer Tomography of the Spine

A Preliminary Report

I. Isherwood*, R. A. Fawcitt*, J. R. L. Nettle*, J. W. Spencer*, and B. R. Pullan**

Introduction

The unique advantages of computer tomography so successfully exploited in the cranial cavity are now, with the advent of the Whole Body Scanner, available for the investigation of the spine and neural axis. Cross-sectional anatomical studies together with detection of tissue attenuation differences will, it is anticipated, enable not only the morphology of the bony spine, the intervertebral articulation system, the spinal canal, the neural axis and associated structures to be investigated but also the physiology of the CSF circulation in the spinal subarachnoid space.

Evaluation of spinal morphology and pathology is of course available against a detailed background of adjacent body organs including major vessels and muscles.

Studies of the axial anatomy of the spine including its articulation system have previously, in vivo, been carried out by conventional transverse axial tomography (4, 10, 15). The possible advantages of computer tomography in the bony spine have only recently been outlined (11).

Estimation of bone mass and mineral in vertebral trabecular bone will also be possible. Adaptation of the EMI Brain Scanner to obtain cross-sections of the forearm have clearly demonstrated the ability of the method to determine with accuracy and reproducibility bone mass and mineral estimation in the appendicular skeleton (9).

The availability of Metrizamide, the water soluble, non-ionic, iodine-containing contrast medium of low osmolality for examination of the CSF pathways has, in conjunction with whole body scanning, added a further dimension to the investigation of the spine and neural axis (2).

Material and Methods

All investigations have been carried out on the EMI CT 5000 which has been operational in the Department of Diagnostic Radiology in the Stopford Medical School, University of Manchester, since June 1976. All C.A.T. sections are 13 mm in depth and presented on a 320 × 320 matrix with an alternative 160 × 160 matrix quadrant display.

1. Two hundred patients have been investigated. A variety of clinico-radiological protocols are at present under study. The majority of pa-

*Department of Diagnostic Radiology, University of Manchester.
**Department of Medical Biophysics, University of Manchester.

tients so examined reveal coincidental information concerning the spine and related structures.

2. Computer tomographic study of a reconstructed, disarticulated pair of lumbar spinal segments has been undertaken to determine the normal anatomical features in an 'ideal' horizontal transverse axial plane. Two disarticulated segments were sealed together with plasticine containing metal markers at the disc margins. Cross-sectional views were obtained by both computed tomography and hypocycloidal tomography.

3. Computer tomographic study of a cadaver lumbar spine has been undertaken to determine the effect of postural and positional variations on sectional anatomy. An articulated spine with covering soft tissue was investigated by computer tomography in the longitudinal, transverse and a variety of inclined planes, to simulate anteroposterior and lateral spinal tilts.

4. Ten patients have been the subject of a special protocol related to the study of the movement and absorption of Metrizamide in the spinal canal.

10 ml of Metrizamide at a concentration of 170 mg iodine per ml have been injected by lumbar puncture prior to conventional lumbar myelography in the Department of Neuroradiology. The patients have been transported in the sitting position and subsequently allowed to remain in a horizontal supine position with a standard pillow. Computer tomographic scans have been obtained at levels corresponding to the basal cisterns, C3, T6, T12 and L3 at 1, 2, 3, and 6 h after injection.

5. To determine the effect of spectral filtering by surrounding high-density material on the attenuation values within the spinal cord, a phantom of the spinal cord and surrounding subarachnoid space has been constructed (Fig. 1). The concentric cavities of the phantom were filled with water, varying concentrations of Metrizamide and varying concentrations of calcium chloride. The attenuation value of the central water has been studied as a function of varying concentrations of Metrizamide.

Results and Discussion

C.A.T. of the spine provides not only an additional radiographic projection capable of demonstrating topographical anatomy and bone pathology in the vertebral body and neural arch but also a detailed display of paravertebral structures (Fig. 2). Identification of the position and articular margins of the apophyseal joints together with their relationship to spinal canal contents enables a more detailed analysis of spinal canal narrowing (Fig. 3). An assessment of the influence of such joint disease on nerve entrapment syndromes should then be possible.

Constraints

Despite the obvious advantages afforded by computer tomography of the spine and its associated structures, there are significant constraints limiting its full exploitation:

Anatomical

Spinal curvature may occur in either a-p or lateral planes. Such curvature may be a normal feature or due to posture or pathological change (Fig. 4).

Radiological

(a) Accurate registration of a section 13 mm in depth in different patients or re-registration in the same patient despite clinical and conventional radiological identification of level is a significant difficulty. Anatomical, postural and positional reproducibility compound this particular problem. (b) Accurate identification of a structural margin is extremely difficult due to the 'partial volume' effect, i.e., an interface passing obliquely through a computed volume ('voxel') of tissue.

Physical

Spatial resolution and sensitivity with existing radiation dose levels of the EMI CT 5000 are such that significant statistical fluctuations occur in the quantitative data relating to bone and spinal canal contents (13). Identification of neural tissue, in particular, without recourse to contrast material in the subarachnoid space, is unreliable. (b) Sensitive quality control is impeded by the computing time of 200 seconds per section and a disc capacity of 8 sections.

Disarticulated Reconstructed Lumbar Spine Segments

C.A.T. sections of conventional depth, i.e. 13 mm through a disarticulated bony specimen in an 'ideal' position, i.e., without spinal curvature, have demonstrated appearances which may be related to the level of section (Fig. 5).

Upper Segment of Vertebral Body

The lumbar spinal canal at this level has a continuous bony contour formed by the concave posterior margin of the vertebral body, the vertically orientated pedicles, the caudally convergent laminae and the base of the spinous process. The spinal canal is triangular in shape with an interlaminar notch at the apex. The transverse processes are well seen. The cortico-medullary boundary zone in the vertebral body is indistinct.

Centre of Vertebral Body

The lumbar spinal canal may retain its bony continuity, but the intervertebral foramina play an increasingly prominent part in the lateral margins. The dorsolateral walls are formed by the inferior articular process and the pars interarticularis. The spinal canal is triangular. The section is usually below the transverse processes. The cortico-medullary boundary zone is clearly identifiable together with a dense cortical anterior margin to the vertebral body. Trabecular bone is most accessible at this level.

Lower Segment of Vertebral Body

The bony ring of the spinal canal is discontinuous due to the intervertebral foramina forming the lateral walls. The superior articular facets of the adjacent caudal segment form the dorsal margins of the intervertebral foramina and are therefore ventrally situated at the apophyseal joints. The upper aspect of the apophyseal joints, situated at an approximate angle of 50^{o} to the coronal plane, the inferior articular facets and the laminae form the dorsal margin of the spinal canal. The spinal canal appears at its most capacious but is clearly influenced by the articular segments. The lower margin of the vertebral body may be ill-defined at the disc margin.

Intervertebral Disc

The intervertebral foramina form the lateral wall of the spinal canal which therefore appears discontinuous. The apophyseal joints and the laminae form the dorsal margins. A section through and in the same plane as the intervertebral disc incorporates the bony margins of the adjacent vertebral bodies which therefore appear indistinct, especially anteriorly.

Cadaver Lumbar Spine

Computer tomography of the cadaveric specimen in the sagittal plane (Fig. 6) together with the schematic illustrations of a scoliotic spine (Fig. 4) demonstrate the problems introduced by spinal curvature in accurate transverse axial reconstruction.

Upward and downward tilt of the specimens simulating lordosis and kyphosis (Fig. 7) demonstrate the apparently changing relationships between vertebral body, intervertebral disc and neural arch when represented in a transverse axial section of finite depth.

Ten-degree angulation of the long axis of the specimen to right and left simulating scoliosis (Fig. 8) demonstrates the apparently changing shape and contour of the vertebral segment as the section traverses structures obliquely. Some bony features, e.g., transverse process or lateral aspect of the posterior neural arch, may in these circumstances be ill-defined and their margins appear to be eroded. Correlation with several adjacent sections in addition to conventional radiology is essential.

Computer Assisted Myelography

The contour of the spinal canal though subject to the physical constraints discussed earlier is normally identifiable. Isodensity of structures within the spinal canal together with statistical fluctuation in attenuation values makes differentiation between both normal and abnormal contents difficult. It is necessary therefore to introduce a suitable contrast material into the subarachnoid space.

Metrizamide, a non-ionic glucose-amide with a molecular weight of 789.1, is a water soluble contrast medium containing 3 iodine atoms. It has

a low osmolality and in a concentration of 170 mg iodine per ml is isotonic with CSF.

Metrizamide has been extensively studied as a myelographic agent (7, 12, 14), and also employed in conjunction with computer tomography as a means of studying the cerebrospinal fluid flow and intracranial absorption pathways (5). Metrizamide introduced by the lumbar route for myelographic purposes appears in the intracranial cerebrospinal fluid spaces in 1 to 2 h and over the hemispheres in 24 h (5, 6, 8). Because of the much increased sensitivity of computer tomography the contrast medium is detectable in much lower concentrations than would be possible by conventional radiology at these sites. In CSF 1 mg of iodine per ml is sufficient to raise the attenuation value as measured by the EMI scanner by 12.5 Hounsfield units (6). The study of Metrizamide in the spinal subarachnoid space has been referred to by DI CHIRO as computer assisted myelography (2).

Metrizamide was identifiable in this present series of patients at all levels - in the thoraco-lumbar spine at 1 h, and in the cervical and intracranial subarachnoid spaces at 1-2 h (Fig. 9). No untoward reactions have occurred. Identification of anatomical features together with heterogeneity of composition of tumour is possible, as in the brain (Fig. 10a and b).

The pattern of movement and diffusion of Metrizamide introduced by the lumbar route is related to:

1. Circulation of CSF, i.e., the 'third' circulation (1)

2. Dilution of contrast medium in the total CSF volume (say 150 ml)

3. Initial layering of dense contrast medium

4. Posture

5. Variation in intrathoracic and intra-abdominal pressure transmitted by the epidural venous plexus

6. Diffusion into neural tissue

Typical results of 4 of the 10 patients studied are presented in Table 1. Attenuation values in the cord have been increased uniformly by 20 units to ensure that negative values were not obtained. All values have been normalised to unity at the first measurement in the accompanying graphs (Fig. 11). The levels of unity for Metrizamide in the CSF space and for cord (+20) are stated at each base line.

The following features are worthy of comment:

1. Metrizamide has a density of 1.184 at a concentration of 170 mg of iodine per ml (7) which is responsible for initial layering. Variation in posture or intra-body cavity pressure may result in contrast being directed to a region in the spinal canal distant to the injection site, e.g. cervical spine (Fig. 11b).

Several patterns of behaviour which can only be related to a combination of posture, density of contrast and gravity occur in the first 2 h. Following this, an overall dilution pattern occurs which is accompanied by an anticipated reduction in iodine level within the CSF.

Table 1. Mean attenuation values of spinal cord and CSF containing Metrizamide at four anatomical levels at 1-, 2-, 3-, and 6-h intervals in four patients

Patient	Level	C3				T6				T12				L3			
	Time (hours)	1	2	3	6	1	2	3	6	1	2	3	6	1	2	3	6
C.K.	CSF (mean)	41.5		35	29.9	124.5	76	42.5	24.5	51	101.5	65.5	52.5	315.5	112	68.5	21.5
	Cord (mean +20)	32	65	32.5	26.5	42	32	17	16	18	59	40	36				
L.A.	CSF (mean)	36	70.5	91	54.5	244.5	132	80.5	81.5	246.5	96	90.5	83.5	75	148.5	101.5	78.5
	Cord (mean +20)	15.5	55.5	51.5	39.5	109.5	81.5	55.5	65	116	28.5	43.5	58.5				
K.L.	CSF (mean)	33.5		11		76.5	28.5	27.5	38.5	86.5	27.5	34		111	98.5	56	19
	Cord (mean +20)	30.5	37	10		41.5	32	30.5	41	62	11.5	22	25.5				
M.R.	CSF (mean)	20.5	89.5	83.5	72	130.5	102.5	99.5	51	156.5	117.5	100	76	173.5	145.5	78.5	93.5
	Cord (mean +20)	15.5	49	51	47.5	70	69	63	25.5	52.5	55.5	69.9	48	193.5		103	113.5

2. The dorsal spinal cord is anteriorly located during computer assisted myelography supporting the belief (7) that this situation is the true one under physiological conditions (Fig. 9b).

3. Attenuation values of spinal cord fall consistently from 1-6 h, suggesting that Metrizamide has entered the spinal cord within the 1st hour. The dilution pattern of Metrizamide in the cord follows that in the CSF space. Entry is presumably effected along perivascular channels into the extracellular space of the spinal cord.

4. A secondary rise of attenuation values within the spinal cord at 3-6 h observed in some patients, e.g. Fig. 11d, leads to speculation that a second compartment, possibly intracellular, may be concentrating iodine. Problems of cord margin identification, lack of knowledge concerning attenuation levels of cord before intraduction of Metrizamide together with variable noise levels make such observations no more than speculative. Further studies are currently being undertaken to investigate the pattern of behaviour of Metrizamide in the 1st hour after injection.

5. Dependence of the attenuation values of simulated 'spinal cord' on the circumferential concentrations of Metrizamide suggest that the results observed in the living could only be effected at high Metrizamide concentrations (Fig. 12). If the volume of CSF in the spinal canal were only 100 ml, then the effective concentration in clinical circumstances would be 1.70 mg of iodine per ml. At this level spectral filtering does not appear to be influencing reconstruction values.

Problems of registration and of obliquity in the plane of CT section make it necessary to interpret bony landmarks with caution.

Water-soluble contrast, e.g. Metrizamide, in the subarachnoid space is necessary to demonstrate neural tissue with certainty.

It is well known that changes in the blood-spinal cord barrier are a result of osmotic factors - the degree of capillary permeability rising with hypertonicity and any resultant damage probably compounded by hypotension or gravitational effect (3). High molecular weight substances, e.g. Metrizamide, injected into the subarachnoid space have been demonstrated (6) to be excreted primarily by the arachnoidal villi intracranially. Some nevertheless is almost certainly excreted via the meningeal membranes of the spinal canal, and there seems little doubt from the present study that an initial partition with the extracellular space in the cord occurs.

Whilst the toxicity of Metrizamide is very low (7) CT of the spinal canal is beginning to provide the opportunity to study not only the movement and absorption of this contrast medium in the CSF pathways but also its behaviour in neural tissue.

Summary

Two hundred patients have been examined on the EMI CT 5000 Whole Body Scanner.

Studies have been made of disarticulated and cadaver spine to identify (1) normal anatomical features in cross-sectional slices of 13 mm depth and (2) the effect of normal and abnormal curvature of the spine on these features.

Patients have been studied by CT following lumbar injection of Metrizamide. The distribution, flow pattern and dilution of Metrizamide have been investigated in detail in 10 patients. This preliminary study suggests that Metrizamide is (1) necessary in the spinal canal to visualise the neural axis and pathological processes which affect it; (2) may appear in the subarachnoid space of the head and upper cervical spine in 1 h; (3) enter the extra-cellular space of the spinal cord in the 1st hour; (4) achieve a uniform diffusion and dilution pattern in the subarachnoid space and spinal cord from 3-6 h; (5) may concentrate in a second compartment, possibly intracellular, from 3-6 h.

The effect of spectral filtering by Metrizamide on the attenuation values of the spinal cord has been modelled and shown not to be significant at the anticipated dilution of contrast medium in the CSF space of the spinal canal.

Acknowledgments

The authors would like to thank Miss G.S. Lord, Superintendent Radiographer, for valuable support, and the Department of Medical Illustration and Mrs. G.E.H. Shawcross for the preparation of illustrative material. They would also like to express their gratitude to Mrs. M. Tipton for her patient and expert secretarial assistance.

References

1. DI CHIRO, G.: The 'Third Circulation". Nuclear Medicine. WAGNER, H.N. (ed.). New York: H.P. Publishing Co. 1975, pp. 103-111.
2. DI CHIRO, G., SCHELLINGER, D.: Computed tomography of spinal cord after lumbar intrathecal introduction of Metrizamide (computer assisted myelography). Radiology 120, 101-104 (1976).
3. FUNQUIST, B., OBEL, N.: Effect on the spinal cord of subarachnoid injection of water soluble contrast medium. An experimental study in dogs. Acta Radiologica (Diag.) 56, 449-465 (1961).
4. GARGANO, F.P., JACOBSEN, R.E., ROSOMOFF, H.L.: Transverse axial tomography of the spine. Neuroradiology 6, 254-258 (1974).
5. GREITZ, T., HINDMARSH, T.: Computer assisted tomography of intracranial C.S.F. circulation using a water soluble contrast medium. Acta Radiologica (Diag.) 15, 497-507 (1974).
6. HINDMARSH, T.: Elimination of water soluble contrast medium from the subarachnoid space. Investigation with computer tomography. Acta Radiologica Supp. 346, 45-50 (1975).
7. HINDMARSH, T.: Myelography with the non-ionic, water soluble contrast medium Metrizamide. Acta Radiologica (Diag.) 16, 417-435 (1975).
8. HINDMARSH, T., GREITZ, T.: Computer cisternography in the diagnosis of communicating hydrocephalus. Acta Radiologica Supp. 346, 91-97 (1975).
9. ISHERWOOD, I., RUTHERFORD, R.A., PULLAN, B.R., ADAMS, P.H.: Bone mineral estimation employing computer assisted transverse axial tomography. Lancet 1976/II, 712-715.
10. JACOBSEN, R.E., GARGANO, F.P., ROSOMOFF, H.L.: Transverse axial tomography of the spine. Journal of Neurosurgery 42, 406-411 (1975).
11. KREEL, L., OSBORN, S.: Transverse axial tomography of the spinal column: a comparison of anatomical specimens with EMI scan appearances. Radiography 42, 73-80 (1976).

12. Metrizamide, a non-ionic water soluble contrast medium - Experimental and preliminary clinical investigations. Acta Radiologica Supp. 335, 1-390 (1975).
13. RUTHERFORD, R.A., PULLAN, B.R., ISHERWOOD, I.: Performance of an EMI Body Scanner. (In press).
14. SKALPE, I.O., AMUNDSEN, P.: Lumbar radiculography with Metrizamide, a non ionic water soluble contrast medium. Radiology 115, 91-95 (1975).
15. TAKAHASHI, S.: Atlas of Axial Transverse Tomography and its Clinical Applications. Berlin-Heidelberg-New York: Springer 1969.

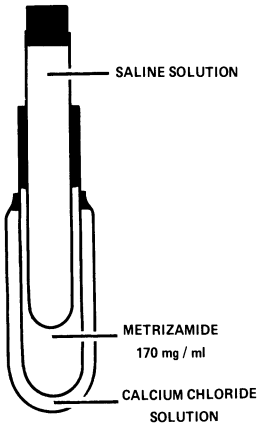

Fig. 1. Phantom employed to determine effect of spectral filtering. Concentric tubes represent spinal cord, subarachnoid space and bone

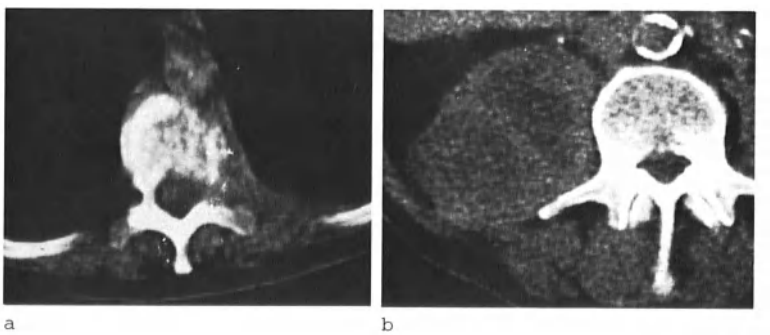

Fig. 2a and b. CT sections demonstrating: (a) Pedicular and vertebral bone erosion in paravertebral lymphoma. (b) Staphylococcal psoas abscess (note calcified aorta)

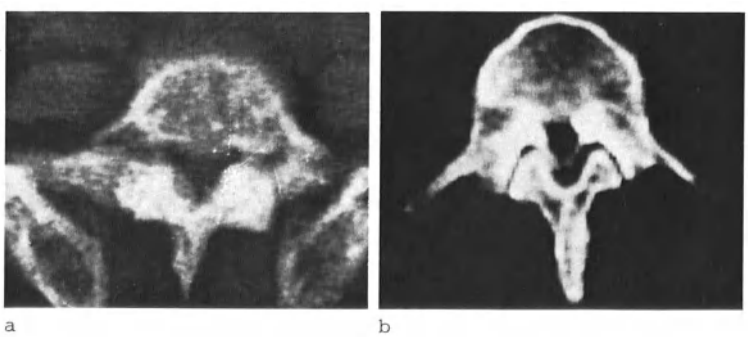

Fig. 3a and b. CT section demonstrating spinal canal narrowing: (a) Paget's disease. (b) Achondroplasia

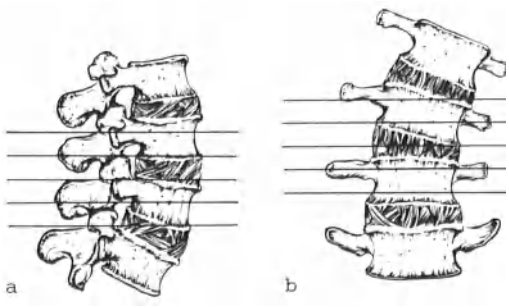

Fig. 4a and b. Effect of spinal curvature on CT sections of lumbar spine. (a) Lateral. (b) Anteroposterior

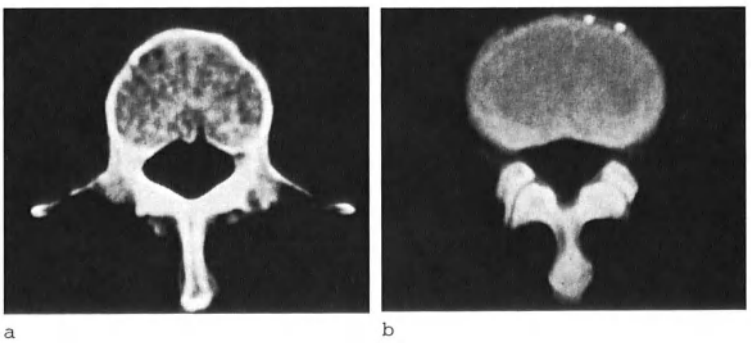

Fig. 5a and b. Horizontal CT sections of disarticulated spine. (a) Upper segments of vertebral body. (b) Intervertebral disc level

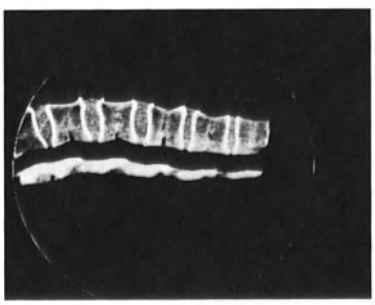

Fig. 6. Sagittal CT section of cadaver lumbar spine

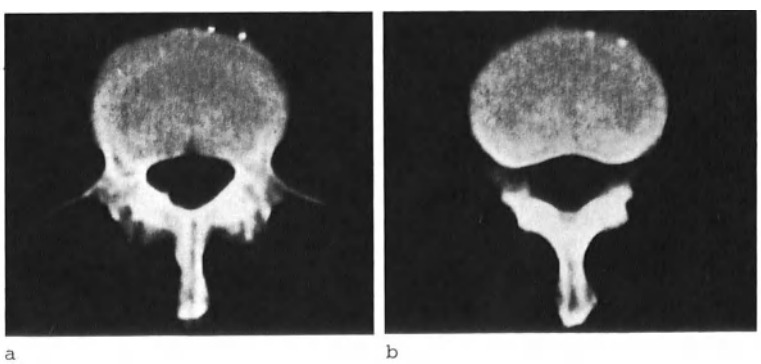

Fig. 7a and b. Horizontal CT sections of cadaver lumbar spine. (a) Upward tilt. (b) Downward tilt

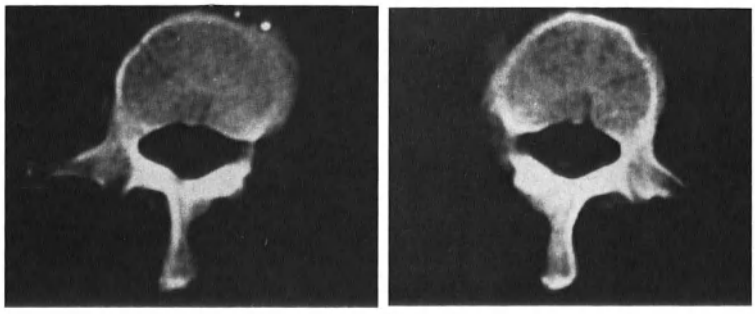

a b

Fig. 8a and b. Horizontal CT sections of cadaver lumbar spine with 10° angulations. (a) To the left. (b) To the right

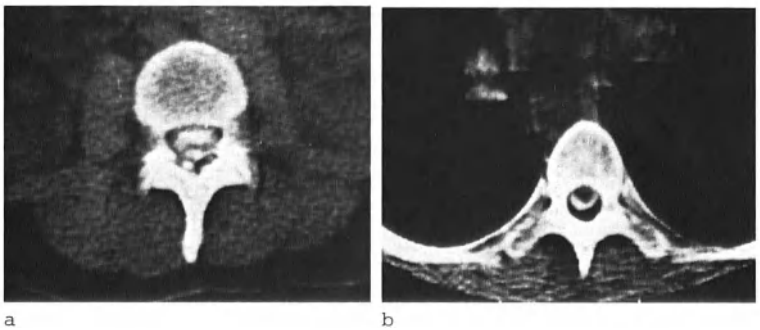

a b

c

Fig. 9a-c. Computer assisted myelography at 1 h demonstrating: (a) Cauda Equina at L3. (b) Anterior location of spinal cord at T6. (c) Central location of spinal cord at T1

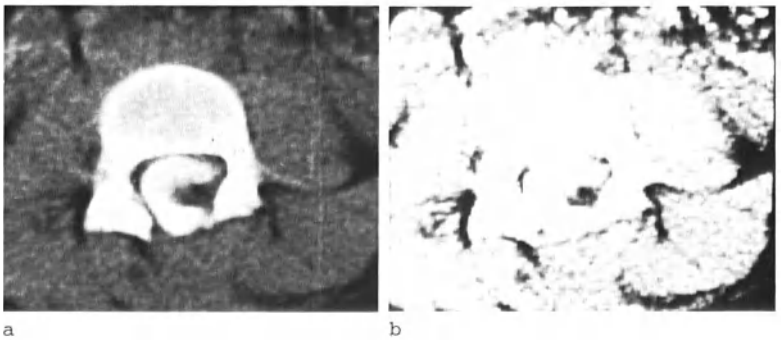

a b

Fig. 10a and b. Computer assisted myelography. Postoperative scan in spinal dysraphism. Residual lipoma within a tethered spinal cord at L5

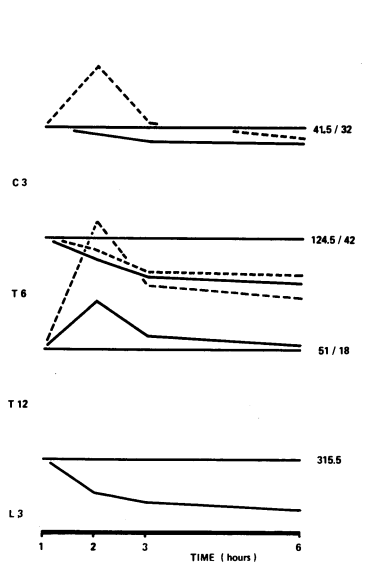

a

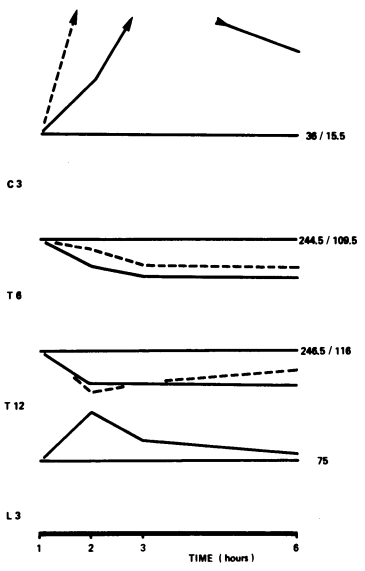

b

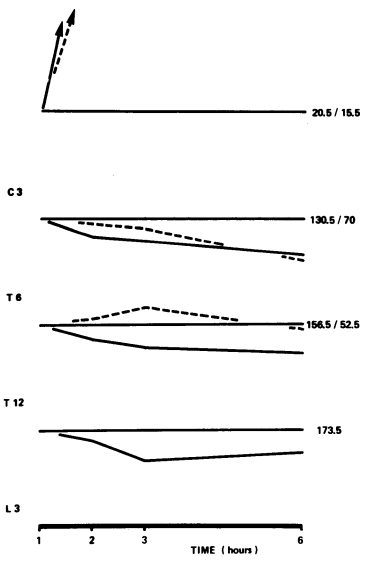

c

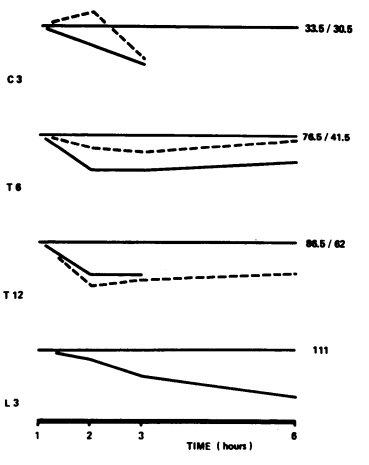

d

Fig. 11a-d. Normalised attenuation values of subarachnoid space and spinal cord as a function of anatomical level and of time in 4 typical patients (C.K., L.A., M.R., K.L.). These graphs are representations of the data in Table 1. Dotted lines represent cord attenuation values. Solid lines show CSF attenuation

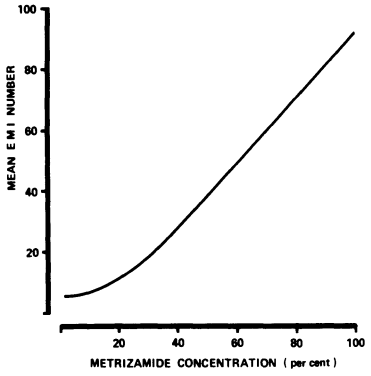

Fig. 12. Phantom study of attenuation values of 'spinal cord' as a function of Metrizamide concentration in the "subarachnoid space"

C. A. T. of the Body

Anatomy

Some Anatomical Problems of Computerised Axial Tomography

L. Kreel*

The study of anatomy has been inherent in medical training for centuries if not millenia. This knowledge has become part and parcel of diagnosis and anatomical fluency is almost a prerequisite for radiology. These detailed studies must neither be forgotten nor ignored if there is to be a correct appreciation of C.A.T. displays of axial anatomy. By 1850, anatomical texts had not only reached present day standards of accuracy but were far superior in their presentation and beauty. Modern illustrations cannot compare with the hand-tinted lithographs of, say, Quain's anatomical atlas (6), which even contains occasional axial views.

Answers to very specific points related to computerised tomography may on occasion also be found. The clear view of muscle bundles given by C.A.T. scanning means, of course, that sooner or later radiologists will be required to know them by name. This in itself is no particular problem, except at the shoulder and upper arm. In this region, conventional anatomical texts provide descriptions and illustrations with the upper limbs lying alongside the body. However, in examining a patient on the scanner the arms are extended, lying near the head. Anatomical texts for artists and some older anatomy books (1) do provide the necessary illustrations which allow a correct interpretation of C.A.T. views of these muscles.

Even without an alteration in the conventional position of the body the knowledge of muscle relationships can be important. In the lower part of the neck, the sterno-cleido mastoid and sterno-thyroid produce two ovoid shadows above the sternum which can easily be taken for vessels. However, at this level the common carotid and subclavian arteries and the internal jugular veins lie much more posteriorly near the posterior margin of the soft-tissue density of the thyroid. Anatomy illustrations show these relationships clearly enough for correct interpretation of C.A.T. scans.

One difficulty encountered with conventional axial anatomy books is that they view the body from above, so that the heart appears on the viewer's right and the liver on the viewer's left (2, 4). A mirror image of these pictures is therefore needed to relate them to the appearances of C.A.T. and ultrasound scans. Fortunately, TAKAHASHI'S beautiful book (5) on axial tomography, produced for conventional radiographic axial tomograms, views the body from below and can easily be related to the pictures of C.A.T. The idealised diagrams are extremely detailed and show many structures not normally visible by C.A.T. scanning. This is hardly a defect but, on the contrary, can be important, as in placing the phrenic nerve in relationship to mediastinal pathology.

One drawback of all anatomical texts is the impossibility of showing the numerous variations encountered in radiological practice and par-

*Division of Radiology, Clinical Research Centre and Northwick Park Hospital, Harrow.

ticularly in axial anatomy when based on sections of a single body. As an example, the raised right hemidiaphragm will change the alignment of the liver. The right kidney and gall bladder are then often at a higher level as well as the colon. When this occurs, axial sections may be misinterpreted as showing atrophy or absence of the left lobe of the liver.

There are, however, at least two aspects of anatomical displays which are unique to computerised tomography. Firstly, if there is no adipose tissue and this applies to subcutaneous, retroperitoneal, mediastinal and mesenteric regions, the various structures will not be demarcated (Fig. 1). In computerised tomography the fat planes are essential for defining boundary lines between organs, unless their tissue density is such that they can be distinguished. Even in the absence of fat planes the liver can usually be delineated because it is of greater density then neighbouring organs and within the confines of the liver margin the gall bladder is visible because bile has a much lower radiographic density.

Movement artefacts will, of course, also blur outlines of various organs making their definition difficult or impossible. At present, this also applies to the heart where ventricles and atria merge into an area of uniform tissue density (Fig. 2b).

The other aspect of C.A.T. sections is that it is not possible to display the full range of tissue densities on one picture (Fig. 2). If the pulmonary blood vessels are shown then the soft tissues cannot be seen and conversely, if the soft tissues are displayed, then the lungs appear black. At the other extreme, the detail of vertebral bodies cannot be shown together with soft tissues of lung fields. One can, of course, overcome this difficulty by photographic or electronic techniques or by displaying these sections at differing window levels side by side.

The various organs will be recognised by their size, shape and position. This applies equally to conventional radiographs and even in anatomical dissections. But with computerised tomography the bowel and especially the small bowel can present a very real problem in recognition. The small bowel is mobile and when filled with its normal fluid content has a tissue density similar to major abdominal blood vessels, pancreas and lymph nodes. Small bowel can therefore look like pancreas, and particularly the tail of the pancreas, or like lymph nodes lying on the aorta. It can also mimic a tumour, especially if dilated by effects of an anticholinergic given to stop movements. It may then have a diameter of up to 4 cm.

Axial sections are localised according to their spinal level because of the varying position of organs within the body with respiration and with changes from the erect to horizontal. The use of the preliminary 'scanogram' radiograph, as previously described (3), allows this to be done but it must be recognised that at any one vertebral level the sections can appear very different. An axial section taken through D3 may show the aortic arch or be well above it, and quite clearly in these circumstances the two axial sections of D3 will look quite unlike each other. This applies even more so to the levels between D9 and 11 where there is such a variable position of the diaphragm.

Four particular aspects of axial anatomy, namely the mediastinum, liver, pancreas and spine, will be considered in this paper because these have produced problems in interpretation.

The Mediastinum

The anatomy of the mediastinum is relatively unfamiliar to radiologists as this cannot be shown except by contrast examination. Intravascular contrast tends to display the venous or arterial system separately and their three dimensional relationships are not obvious, nor usually relevant to particular clinical problems. Pneumo-mediastinography on the other hand tends to distort the tissue planes and, in the anterior mediastinum, alters the position of the thymus. C.A.T. sections of the lower cervical region and mediastinum may therefore initially present something of a problem.

In the lower part of the neck and superior mediastinum the tissues are disposed along the coronal plane but at the level of the aorta the mediastinum is aligned sagittally. As the apex of the lungs appear on the sections they lie posteriorly and the mediastinum between becomes triangular in shape. The left subclavian artery is the most posterior of the major aortic branches and can produce a bulge on the mediastinal border lateral to the oesophagotracheal approximation or to the oesophagus itself. The left common carotid lies anterior to the subclavian artery and the brachiocephalic (innominate) artery is to the right of the left common carotid. However, the internal jugular, at the level of the thyroid is lying postero-laterally in its relation to the common carotid but just below the thyroid it curves forward as the brachiocephalic vein to take up an immediately retrosternal position.

It is important to be able to identify these vascular structures because they appear circular or ovoid and therefore resemble lymph nodes which are not normally visible at these levels.

The central trachea and oesophagus are approximately midway between the sternum and spine. The oesophagus frequently contains air, making it clearly visible. At higher window levels the adjacent walls of the trachea and oesophagus are not visible, so that the central air space has an elongated shape made up of the oesophagus posteriorly and trachea anteriorly. The fact that the oesophagus so frequently contains air is surprising and may be related to the administration of anticholinergics in those patients who also have an abdominal scan.

Just above the aortic arch the anterior mediastinum is usually rectangular with the superior vena cava bulging its right margin anterolateral to the trachea.

The aortic arch usually lies at the level of D4 taking up an exclusive position in the mediastinum and curving around the trachea. The right lung is then in close apposition to the lateral wall of the trachea. Lying anterior to the aortic arch is a small triangular or slit-like portion of areolar tissue which contains the thymus or thymic remnant and is attached anteriorly to the posterior sternal margin.

At the bifurcation of the trachea (approximately D5 level) the pulmonary artery trunk lies slightly anterior and to the left of the circular ascending aorta. The posterior and rightward sweep of the pulmonary artery appears just caudal to this level and proceeds in front of the right main bronchus (Fig. 3). The descending aorta is the most posterior structure being closely applied to the left anterior aspect of the vertebral body. On the right side, the lungs appear to indent the mediastinum behind the right main bronchus and pulmonary artery where it often reaches to the midline. The lateral bulge of the superior vena cava is still a prominent feature on the lateral wall of the mediastinum slightly behind the ascending aorta.

As the heart chambers come into view, the mediastinum appears globular or ovoid, being of course more prominent towards the left anterior quadrant. At present the heart chambers cannot be seen separately from each other and their positions must be surmised rather than identified.

There is, however, one "chamber" which is consistently delineated lying on the right posterior margin of the heart contour at about the level of D9/D10 (Fig. 4). On conventional radiographs, especially on tomography, a faint curved density is seen overlying or just to the right of the spine and has been described as the pulmonary venous inflow chamber. However, axial anatomy texts, particularly that of TAKAHASHI, show this as the inflow of the inferior vena cava into the right atrium. It appears that the inflow tract of the pulmonary veins lies just cranial to the inflow of the inferior vena cava and both produce a somewhat similar appearance on the C.A.T. scan. The level at which the cut is taken is the main distinguishing feature with pulmonary venous inflow chamber appearing at a more cranial level than the inferior vena cava inflow tract.

The Liver

The partial volume effect is well illustrated in the most cranial sections through the liver and cupola of the right hemidiaphragm. The peripheral base of the right lung decreases until it forms a posterior crescent between the diaphragmatic cupola and its retroperitoneal attachment. The peripheral diaphragm is seen as a thin band curving over and enclosing the aorta.

The true tissue density of the liver becomes apparent only as the sections lie below the lung base and particularly when the upper poles of the kidneys appear. It is then obvious that normal liver density (circa 35 Hounsfield units) is considerably higher than that of kidney, muscles or pancreas (circa 25 H. units), but similar to that of the spleen.

The liver encloses the inferior vena cava, which appears as a lesser density ovoid just to the right of the aorta and behind the quadrate lobe of the liver. The portal vein at the hilum is of similar density to the inferior vena cava and its branches appear as it proceeds towards the periphery of the liver (Fig. 5). At cuts above and below this level the portal vein branches appear in cross section as small round areas of about 0.5-0.75 cm in diameter. The major hepatic ducts lie anterior to the portal vein in the hilum and cannot be distinguished unless contrast medium is used (Fig. 6).

On the more cranial sections the right lobe of the liver and spleen are seen but proceeding caudally the left lobe occupies the anterior aspect of the abdomen. The outer curved margin is closely applied to the inner margin of the abdominal wall. It becomes obvious that even small peritoneal effusions are visible as a crescent of low density (circa 1 H. unit) interposed between the liver and inner margin of the abdominal wall.

The falciform and gastrohepatic ligaments can normally be identified and frequently the coeliac axis, branching into the hepatic and splenic arteries. The hepatic vein may also be identified as it merges with the inferior vena cava, but normal bile ducts have not been seen. However, dilated bile ducts appear as low-density branching or well-defined round areas and the normal gall bladder is shown as a low density round area surrounded by the denser liver parenchyma. Between the vis-

ible vascular structures the liver substance is homogeneous, except for the occasional band artefact of 'lower density' which lies along the line of the posterior intercostal spaces.

In the more caudal cuts the left lobe is smaller, and finally only Reidel's lobe remains visible.

The Pancreas

It takes at least two and frequently four to six sections at 1-cm intervals to show the pancreas (Fig. 7). Before starting the C.A.T. scan, the pancreas is localised by reference to the position of the duodenal loop or the common bile duct on conventional radiographs. If these are not available, localisation of the gastric antrum and duodenum is attempted on the 'scanogram' using contained gas as the marker.

In most cases some form of contrast medium is needed to separate duodenum and jejunum from pancreas. The head of the pancreas tends to be ovoid and is seen alongside the superior mesentric artery. The body of the pancreas curves over the proximal part of the superior mesenteric artery. The inferior margin of this shadow can often be shown to be the splenic vein.

The tail of the pancreas runs towards the angle between the left kidney and the spleen, behind the gastric fundus and in front of the left suprarenal. Its margin may be either smooth or undulating and is frequently closely approximated to the jejunum which, without contrast medium in it, can make the tail of the pancreas appear enlarged or tumorous.

The pancreas is clearly seen when surrounded by retroperitoneal fatty tissue, but if these fat planes are lost, the pancreas cannot be seen separately from surrounding structures.

The Spine

The wealth of detail that has become manifest in soft tissues with computerised tomography is matched by that found in bone and particularly in the spine. The bony limits of the spinal canal and the apophyseal joints are clearly visible, and cortex is well demarcated from medulla (Figs. 8, 9).

To locate an axial section accurately it is often not suffucient to know just the level with reference to a particular vertebral body, but also to know whether it is in the upper, middle or lower thirds or at an intervertebral disc space. The axial anatomy of the vertebral body is recognisably different at thse different levels, and allows for more accurate localisation.

When a section is taken through the upper or lower third of the vertebral body or through an intervertebral disc space, there is little or no compact bone with no real distinction between cortex and medulla of the vertebral body (Fig. 9). In the middle third of a vertebral body a clear, well-defined cortex is present and is clearly distinguished from medulla (Fig. 8). Similarly, the pedicles are attached to the upper half of the vertebral body with the vertebral foramina in its lower

half. In the dorsal region the costovertebral joints are in line with the upper third of the vertebra, the proximal oblique part of the rib lies opposite the upper intervertebral disc and the posterior horizontal part of the rib lies at the level of the lower third of the vertebral body above.

In the lumbar region, where the spinous process lies more horizontally than in the dorsal region, its appearance is also very helpful in localisation. The thin, well-corticated compact part of the spinous process is at the middle third of the body, while the broad, poorly corticated part of the spinous process is at the lower third or intervertebral disc space. This, of course, presupposes that there is no tilt of the vertebral body and is by and large true for the L2/3 region, but fails when the axis of the vertebra is changed due to a lordosis or kyphosis.

Similarly, the shape of the spinal canal varies and is largest at the level of the intervertebral disc with a dome-shaped posterior part as it lies caudal to the neural arch, but is smallest at the upper third appearing triangular anterior to the neural arch. This again will to a certain extent depend on the tilt of the spine.

The change in alignment of the apophyseal joints from the coronal plane in the upper dorsal region to almost a sagittal lie in the lower lumbar region, is also clearly visible. The densest or most compact bone lies in the region of the apophyseal joints and laminae.

Summary and Conclusions

Our knowledge of axial anatomy is based by and large on a transposition from the frontolateral plane. True axial anatomical studies are relatively infrequent and tend not to cover the many inherent variations. Our knowledge of the anatomy on computerised tomography reflects this, but the appearances specific to this mode of presentation must be recognised.

Special consideration has been given to the mediastinum, liver, pancreas and spine because of the problems associated with clinical practice in the interpretation of C.A.T. sections.

Acknowledgements

Grateful acknowledgement is made to the Department of Health and Social Security whose far-sighted and generous help has assisted greatly in the development of this project. The assistance and considerable help from Mr. John Twydle, who has been managing the machine, is also gratefully acknowledged.

References

1. CHESELDEN, W.: The Anatomy of the Human Body. 7th ed. London: Hitch & Dodsley 1750.

2. EYCLESHYMER, A.C., SCHOEMAKER, D.M.: A Cross-Section Anatomy. New York: Appleton-Century-Crofts (1970).
3. KREEL, L.: The E.M.I. Whole Body Scanner: An interim clinical evaluation of the prototype. British Journal of Clinical Equipment 1, 220-227 (1976).
4. ROY-CAMILLE, R.: Coupes Horizontales du Tronc. Paris: Masson 1959.
5. TAKAHASHI, S.: An Atlas of Axial Transverse Tomography and its Clinical Application. Berlin-Heidelberg-New York: Springer 1969.
6. QUAIN, J., WILSON, E.: A series of Anatomical Plates. London: Taylor & Walton 1842-1848.

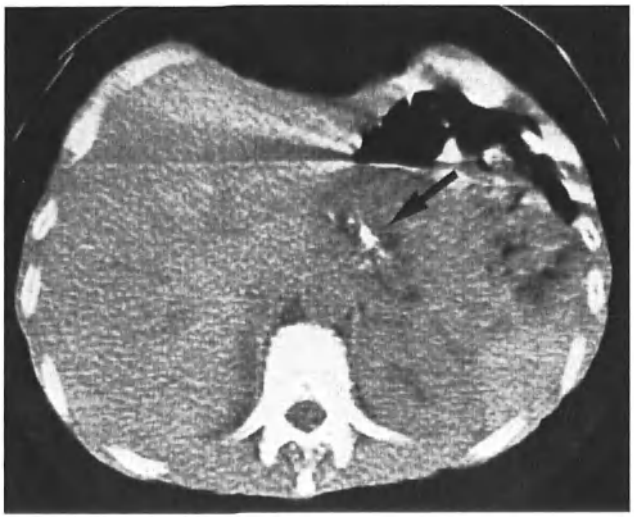

Fig. 1. Section through tail of pancreas from a patient with chronic calcific pancreatitis and malabsorption. Lack of fat planes makes it difficult to demarcate the various organs. The liver (*arrow*) is defined because it has a slightly higher density than adjacent tissue

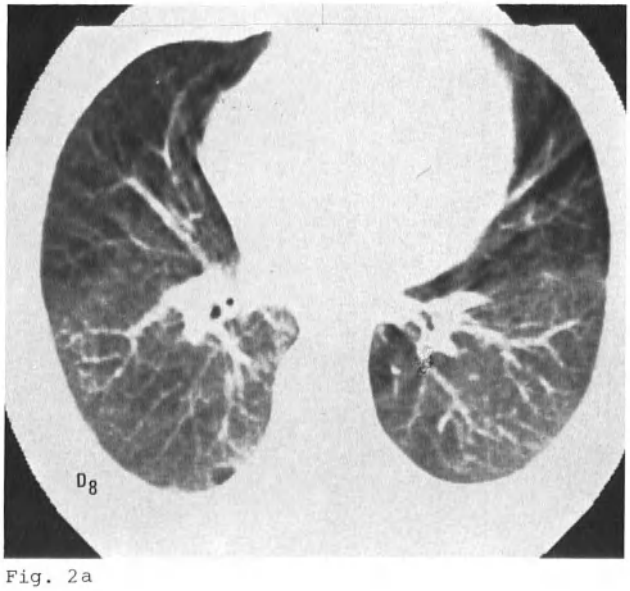

Fig. 2a

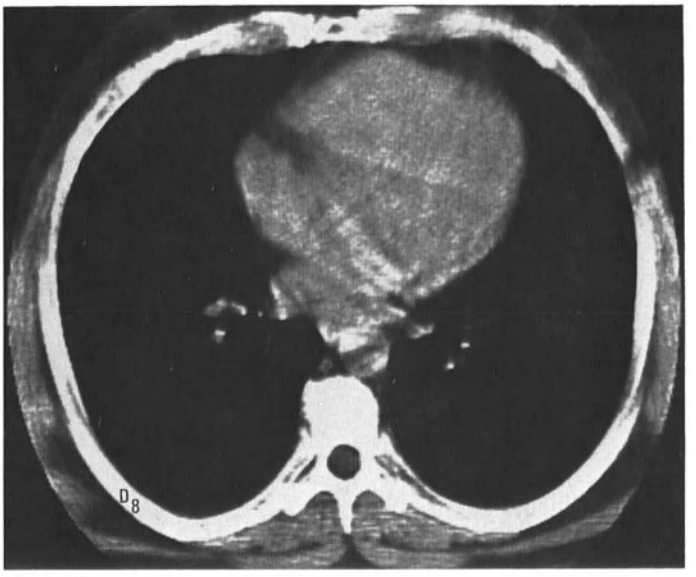

Fig. 2 b

Fig. 2c

Fig. 2a-c. Sections taken though D8, (a) to show lung fields (W.W. 400; W.H. -415), (b) soft tissues (W.W. 150; W.H. -015) and (c) bone (W.W. 400; W.H. +065), which cannot all be shown on one picture because of the different tissue densities

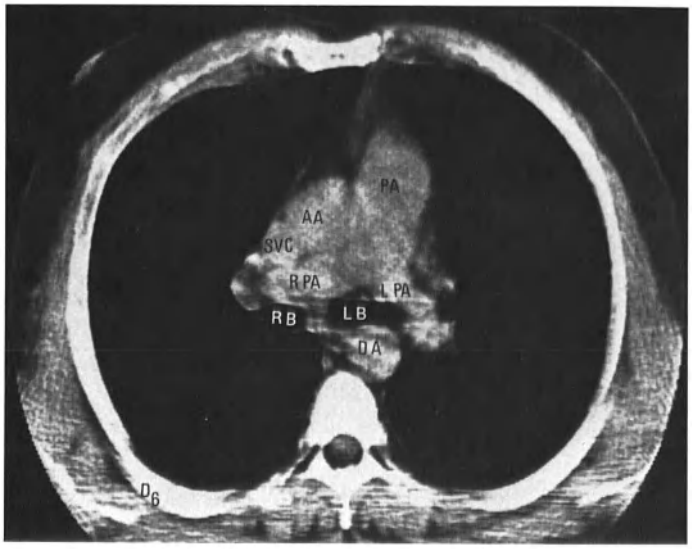

Fig. 3. Section through D5 at the tracheal bifurcation (AA - Ascending Aorta, PA - Pulmonary Artery, RPA - Right Pulmonary Artery, LPA - Left Pulmonary Artery, RB - Right Bronchus, LB - Left Bronchus, SVC - Superior Vena Cava)

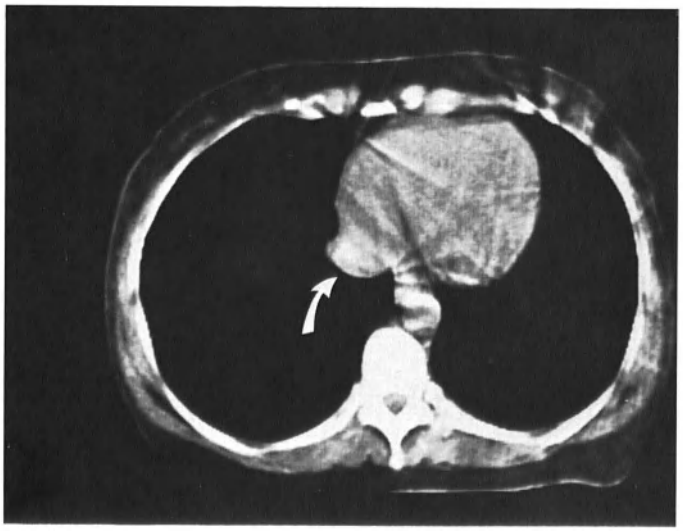

Fig. 4. The protrusion of the right posterior margin of the heart (*arrow*) is the inflow of pulmonary veins, which lies just cranial to the inflow of inferior vena cava into right atrium

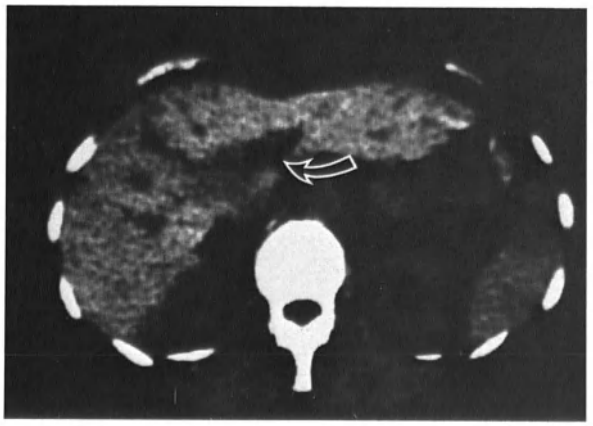

Fig. 5. Liver section through hilum showing portal vein and branches. Branches appear as round 'defects' in liver substance

Fig. 6. Same patient after calcium ipodate (Solubiloptin) given orally. Hepatic duct forms the most anterior part of the lesser density hilum of liver which cannot be distinguished without contrast medium

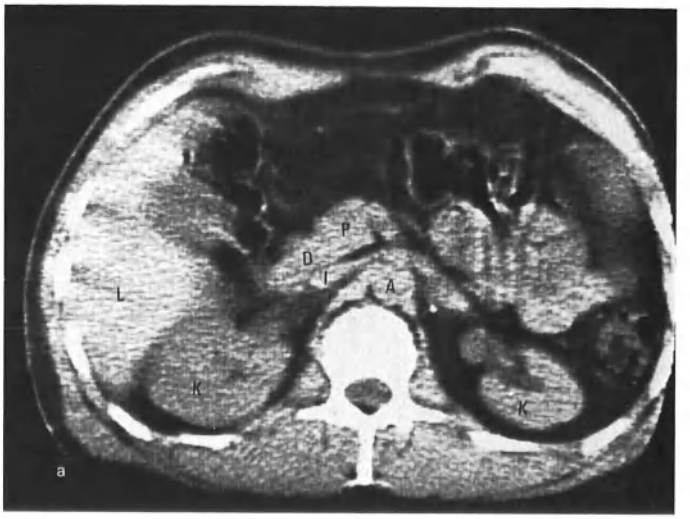

Fig. 7a

Fig. 7b

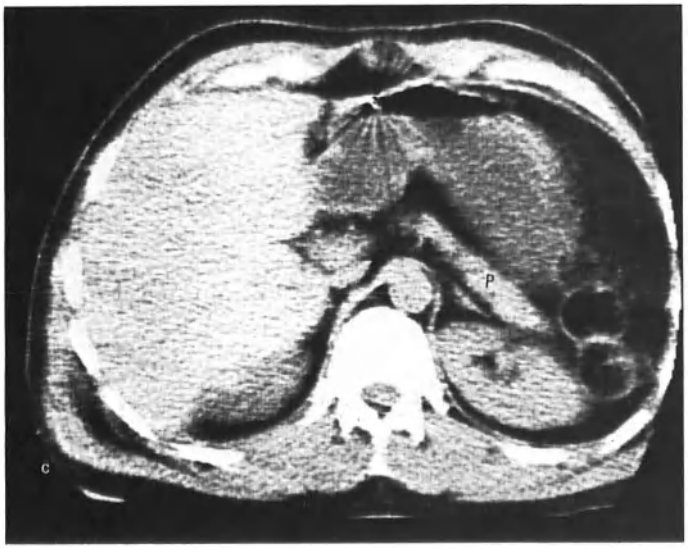

Fig. 7c

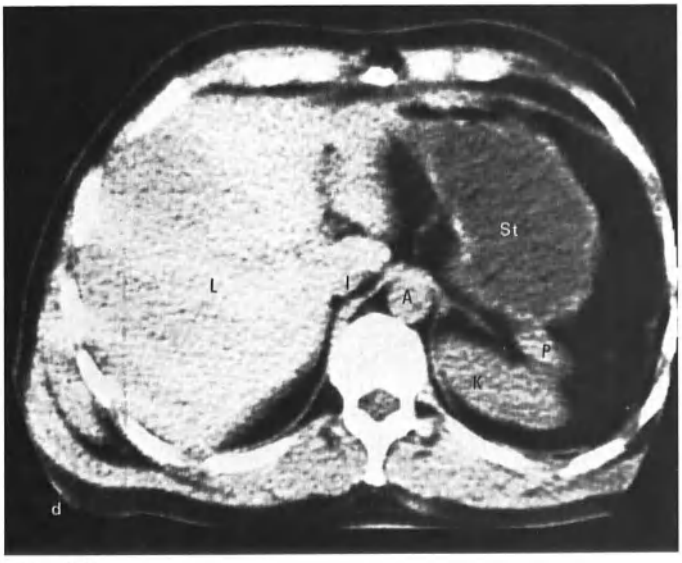

Fig. 7d

Fig. 7a-d. Four sections at 1 cm intervals showing the pancreas (P). (a) head, (b) body, (c) tail, (d) tail. (L - liver, D - duodenum, K - kidney, A - aorta, I - inferior vena cava, St - stomach)

Fig. 8. L4 vertebral body, section through middle third showing thin well-defined cortex and transverse processes

Fig. 9. Section through upper third of L5 showing ill-defined cortex, intervertebral foramina and apophyseal joints

Computerised Tomography of Abdominal Blood Vessels

H. C. Redman*

The advent of whole body computerised tomography presents a new method for evaluation of the abdominal vasculature. For years, angiography has been the only technique for studying blood vessels and it still gives the most detailed information. Grey-scale and real time ultrasound are also used in the evaluation of the aorta, inferior vena cava and the splenic, hepatic and portal veins. Abdominal C.A.T. scanning routinely visualises the abdominal aorta (1, 3) and inferior vena cava. Branch arteries including the coeliac, superior mesenteric and iliac arteries are generally demonstrated. The renal arteries and veins are regularly seen, but are not always separable. The splenic, superior mesenteric and portal veins can also be demonstrated occasionally. Identification of these abdominal vessels helps in localisation of other intra-abdominal structures. Abnormalities of vessels are also seen and occasionally can be seen only at C.A.T. scanning.

The aorta normally lies anterior to the spine, to the left of midline (Fig. 1). It is usually clearly distinguishable at all levels, though it is more difficult to define in very thin patients, or in the presence of adjacent inflammation or infiltrating neoplasm (Fig. 2). The diameter of the aorta can be measured, and is seen to diminish as the major visceral arteries arise. Calcification in the aortic wall may be seen which is not demonstrated on abdominal radiographs. Such calcification is generally discontinuous and is often adjacent to arterial origins. Elongation of the abdominal aorta can be detected.

The coeliac artery arises from the anterior surface of the aorta, usually at the level of vertebral bodies T12 to L1 (Fig. 3). When the xyphoid is used as a marker, the coeliac artery will generally be seen on one or more cuts done 1 to 4 cm caudad to the tip of the xyphoid. It courses in a ventral direction for 1 to 4 or 5 centimetres and then branches into the common hepatic and splenic arteries which may be seen coursing to the right and left respectively. We have not yet demonstrated the left gastric artery, which has a small diameter. The frequency of demonstration of splenic and hepatic arteries is increased by overlapping the scanning sections, but is largely dependent on the course of each artery, the amount of surrounding fat and the presence of calcification. Incidence of visualisation should increase when E.C.G. gating is possible.

The superior mesenteric artery also arises from the anterior surface of the aorta 1 to 3 centimetres caudad to the coeliac artery (Fig. 4). It arises dorsal to the pancreas and is most frequently visualised on cuts made between 3 and 7 centimetres distal to the xyphoid tip (2). Its ventral course is variable and generally shorter than that of the coeliac artery. It may simply be seen in cross-section dorsal to the pancreas or ventral to the third portion of the duodenum. Its branches are not often identified.

---

*Mt. Zion Hospital and Medical Center, San Francisco, University of California, School of Medicine, and Stanford University School of Medicine.

The renal arteries arise laterally from the aorta at, or slightly caudad to, the origin of the superior mesenteric artery (Fig. 5). When a renal vessel can clearly be seen to arise from the aorta, it can be definitely identified as a renal artery. Frequently, however, both the renal artery and vein are seen on the same cut and cannot be completely separated. The renal veins, of course, enter the inferior vena cava and the left passes anterior to the aorta, factors which help to identify the veins.

The inferior mesenteric artery generally arises from the anterior surface of the aorta at the level of the third lumbar vertebral body. It is normally quite small, measuring less than 5 mm in diameter in most patients. It is not often identified at C.A.T. scanning. The iliac arteries are seen anterior to the spine, generally arising about vertebral body L4. They then course laterally into the pelvis.

It should be remembered that arterial vascular anatomy is highly variable so that examinations made to demonstrate specific vascular structures must be tailored to the patient, rather than relying on a routine approach.

The inferior vena cava lies to the right of the aorta against the spine for much of its course through the abdomen (Fig. 6), but moves ventrally as it becomes intrahepatic. Unless contrast material is infused, it becomes difficult to distinguish within the liver. In the supine patient it usually has a flat-oval configuration. When the patient is prone, it may become more rounded.

The iliac veins can sometimes be identified on high pelvic scans as they course medially to form the inferior vena cava. The junction generally occurs 1 to 3 cm distal to the aortic bifurcation.

The renal veins can be identified when they are seen to enter the inferior vena cava or when the left renal vein is seen anterior to the aorta. Their course is generally not exactly parallel to that of the corresponding renal artery. They are larger in diameter and they are frequently located cephalad to the renal arteries. However, it is not always possible to separate renal arteries and veins at C.A.T. scanning.

The splenic, superior mesenteric and portal veins can occasionally be identified (Fig. 7). The straighter course and larger calibre of these veins aids in distinguishing them from arteries.

At present, angiography still provides the most detailed information about vascular structures and has a much finer resolution than C.A.T. scanning. However, position and size of the major abdominal vessels can be determined by C.A.T. scanning and patency can be judged by use of a contrast medium infusion. Calcifications can also be detected which are below the resolution of conventional radiographs. Future technological developments will undoubtedly increase the vascular detail obtainable at C.A.T. scanning. The current state of the art can define some pathology such as aneurysms and calcification. Contrast medium enhancement, E.C.G. gating or very fast scan times and variable section thicknesses should all increase the information available.

References

1. ALFIDI, R.J., HAAGA, J., MEANEY, T.F., MACINTYRE, W.J., GONZALEZ, L., TARAR, R., ZELCH, M.G., BOLLER, M., COOK, S.A., JELDEN, G.:

Computerized tomography of the thorax and abdomen; a preliminary report. Radiology 117, 257-264 (1975).
2. HAAGA, J.R., ALFIDI, R.J., ZELCH, M.G., MEANY, T.F., BOLLER, M., GONZALEZ, L., JELDEN, G.L.: Computed tomography of the pancreas. Radiology 120, 589-595 (1976).
3. SAGEL, S., STANLEY, R.J., EVENS, R.L.: Early clinical experience with motionless whole-body computed tomography. Radiology 119, 321-330 (1976).

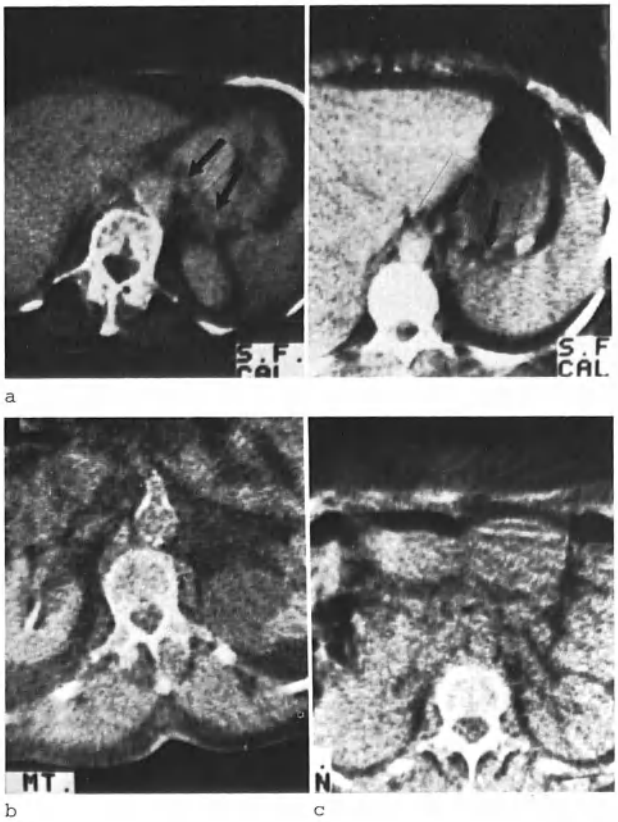

Fig. 1a-c. Aorta. (a) Aorta at the xyphoid. It is to the left of midline. Splenic artery (*arrows*) is seen many times as it enters and leaves the plane of the section. (b) Aorta at 4 cm caudad to the xyphoid. Patchy aortic calcification is seen at origin of the superior mesenteric artery. (c) Aorta at level of origin of renal arteries in a thin patient

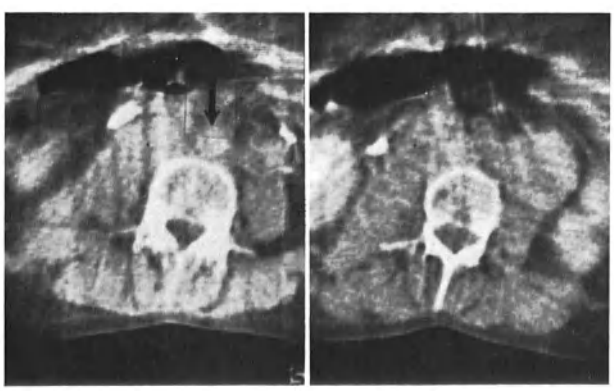

Fig. 2a and b. Metastatic ovarian carcinoma obscuring aorta and inferior vena cava. (a) Section at the umbilicus reveals a retroperitoneal mass engulfing inferior vena cava. Aorta is identified (*arrow*). (b) Section 3 cm cephalad to the umbilicus. Retroperitoneal mass is more extensive and has almost completely obscured the aorta

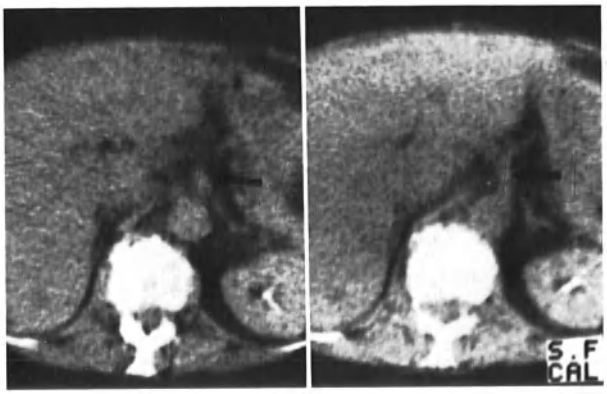

Fig. 3. Coeliac artery. Two cuts made at 3 cm below the xyphoid. Coeliac artery (*arrows*) arises from anterior surface of aorta. It runs ventral and then divides into common hepatic and splenic arteries

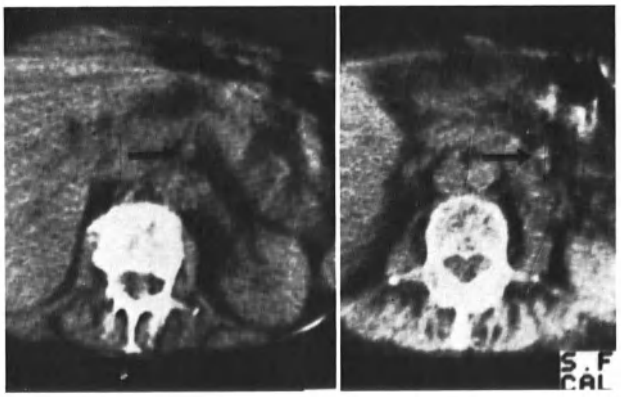

Fig. 4a and b. Superior mesenteric artery. (a) Superior mesenteric artery (*arrow*) is seen immediately ventral to the aorta and dorsal to the pancreas. Left renal artery is seen. (b) Cut performed 3 cm caudad shows superior mesenteric artery (*arrow*) ventral to fourth portion of duodenum

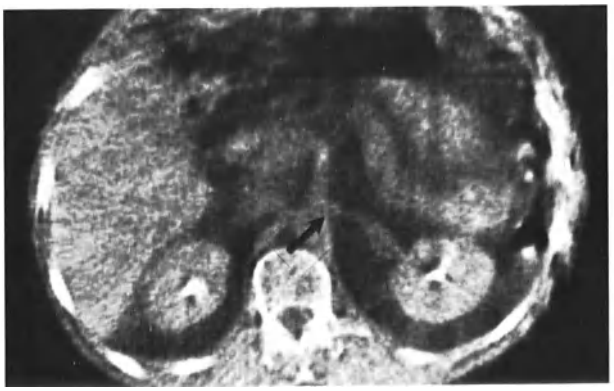

Fig. 5. Left renal artery. Left renal artery (*arrow*) is seen arising from aorta at the same level as superior mesenteric artery. Right renal artery arose at a lower level

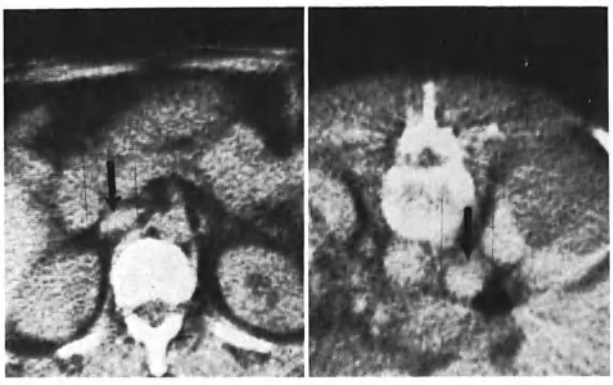

Fig. 6a and b. Inferior vena cava. (a) Supine. Inferior vena cava (*arrow*) is seen to the right of aorta. It has a typical oval shape. Superior mesenteric artery is seen arising from aorta. (b) Prone. Inferior vena cava (*arrow*) often assumes a rounded shape when patient is prone. Right renal cyst is seen

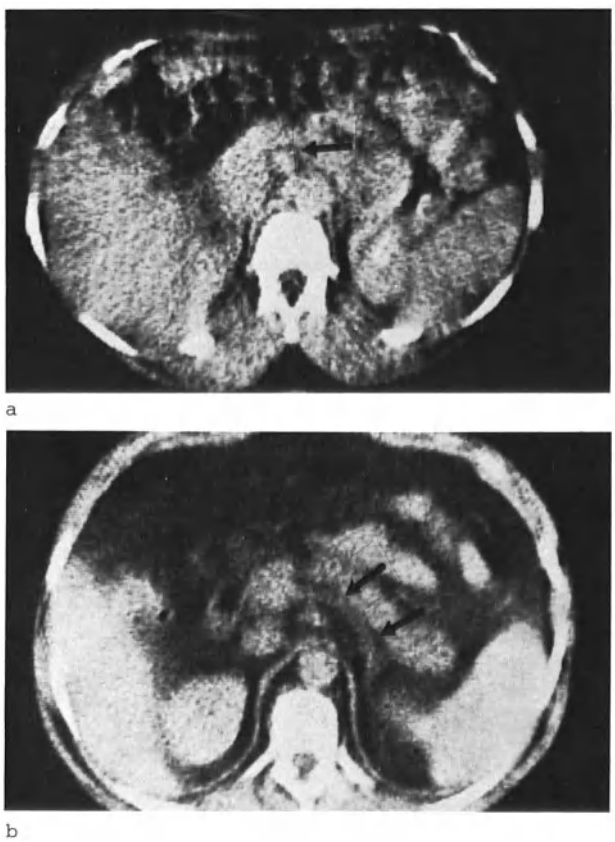

Fig. 7. (a) Superior mesenteric vein (*arrow*) is seen dorsal to pancreas. It generally lies to the right of superior mesenteric artery and is larger in diameter. (b) Splenic vein (*arrows*) is seen coursing dorsal to pancreas and entering portal vein

C.A.T. in the Pelvis

H. C. Redman*

Pelvic masses, whether in the female or male, are not easy to evaluate fully by palpation, and ultrasound has proved invaluable in this situation, since it can readily distinguish solid from cystic masses and can demonstrate free fluid. Often, the specific nature of the mass can be suggested. Ultrasound also has the advantage of not being ionising, a feature especially important in the child-bearing age. There are some limitations to pelvic ultrasound, however. First, unless the bladder can be adequately distended, evaluation of the pelvis is generally quite limited. Neurological problems, radiation cystitis and large masses pressing on the urinary bladder all may make filling difficult. Patients who may not take fluids by mouth are sometimes difficult to hydrate enough to distend the bladder fully. Also, since ultrasound does not penetrate either bowel gas or bone, the ultrasonic evaluation of the side walls of the pelvis is limited. Finally, smaller structures such as the ureters cannot be identified at ultrasound. Therefore, there is a place for C.A.T. in certain patients, to study the pelvic structures not demonstrable by ultrasound or other methods.

The bladder can be evaluated by C.A.T., although the indications for such a study are few (2). Demonstration of the bladder is improved by intravenous injection of 10-20 cc of 60% iodine-containing contrast material. Both prone and supine scanning ensure complete demonstration of the bladder walls. If the position of the ureters is of primary importance, an infusion of 300 cc of 30% contrast material will make persistent ureteric filling likely. However, such a large amount of contrast material obscures detail of the bladder and, with progressive bladder distension, leads to obscuration of structures adjacent to the bladder, such as the prostate, uterus and ovaries. Bladder wall neoplasm can be demonstrated as a mass or thickening of the bladder wall (Fig. 1). More importantly, since the primary tumour is usually known to be present, extension beyond the bladder wall can also be detected, aiding in the staging of these neoplasms. Direct tumour extension can be demonstrated and nodal metastases are seen if enlargement has occurred. Intrinsic nodal abnormalities are not yet routinely detectable. Since staging of bladder carcinomas is difficult, C.A.T. may have a significant contribution to make in these patients.

The uterus is seen as a homogeneous soft-tissue mass dorsal to the bladder. Its position and configuration are variable, depending on the degree of bladder distension and on whether anteversion or retroversion is present. Angulation of the gantry may permit scanning of the uterus in cross-section, if desired. Uterine masses can be identified by distortion of uterine shape and size (Fig. 2) and masses surrounding the uterus can often be identified as such, but the information derived is rarely more, and often less than that derived from pelvic ultrasound, when this can be successfully accomplished.

---

*Mt. Zion Hospital and Medical Center, San Francisco, University of California School of Medicne, and Stanford University School of Medicine.

The ovaries are often not distinguished from other pelvic soft tissues when they are normal, although they are occasionally seen laterally, adjacent to the bladder (Fig. 3). When abnormally enlarged, a cystic or solid mass is seen (Fig. 4). Once again, ultrasound provides this information without radiation risk when the bladder can be distended, and should therefore be attempted first.

The prostate can be identified between the bladder and the rectum. In older men, calcifications are sometimes seen and enlargement can be detected (Fig. 5). An over-opacified bladder will obscure the prostate and 10-20 cc of 60% contrast material should be used in these patients.

Evaluation of the lateral pelvic soft tissues is better accomplished by C.A.T. scanning than by any other noninvasive technique (1), since the muscles and lymph nodes can easily be demonstrated. Node masses are easily identified and can be followed during therapy (Fig. 6). If a lymphogram has been performed, C.A.T. will show residual nodal contrast when it is no longer detectable by radiography. While enlargement of nodes is the primary abnormality detectable at C.A.T., nodes which have been opacified previously may have an identifiable filling defect which is seen as a bizarre configuration.

An important application of C.A.T. in the pelvis is the demonstration of the position of the ureters in a complex pelvic mass or in the post-operative patient. An infusion of about 300 cc of 30% contrast medium, prior to and during the scanning, will generally lead to consistent filling of the ureters. The ureters are demonstrated running antero-lateral to the psoas muscles and then running laterally at the pelvic brim and finally converging towards the trigone. In the presence of endometriosis or extensive inflammation or neoplasm, incorporation of a ureter into the lesion is sometimes seen, or it may be simply displaced or compressed by the mass (Fig. 7). This information is valuable to the surgeon and cannot be obtained in any other fashion.

Summary

The uses of C.A.T. in the pelvis are still being defined. At present, ultrasound remains the primary diagnostic tool in the pelvis, both because it does not require ionising radiation and because the information it provides is equal to or better than C.A.T. in most situations. There are, however, several circumstances in which C.A.T. should be considered. These include: patients who cannot adequately distend the urinary bladder, thus limiting the ultrasound; staging or follow-up of lateral pelvic masses which are not well demonstrated at ultrasound, and the need to demonstrate the position of the ureters relative to a complex pelvic mass.

References

1. ALFIDI, R.J., HAAGA, J., MEANEY, T.F., MACINTYRE, W.J., GONZALEZ, L., TARAR, R., ZELCH, M.G., BOLLER, M., COOK, S., JELDEN, G.: Computed tomography of the thorax and abdomen; a preliminary report. Radiology 117, 257-264 (1975).
2. SAGEL, S., STANLEY, R.J., EVENS, R.G.: Early clinical experience with motionless whole-body computed tomography. Radiology 119, 321-330 (1976).

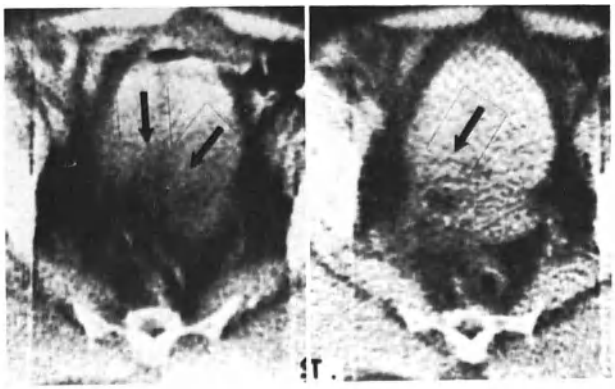

Fig. 1

Fig. 2

Fig. 1. Bladder tumour. Two C.A.T. sections demonstrate intraluminal tumour (*arrow*) as well as tumour extension to right lateral pelvic sidewall

Fig. 2. Uterine leiomyomata. Uterus is enlarged and has a distorted contour. Uterine cavity (*arrow*) is demonstrated, a somewhat unusual occurrence due to the multiple leiomyomata

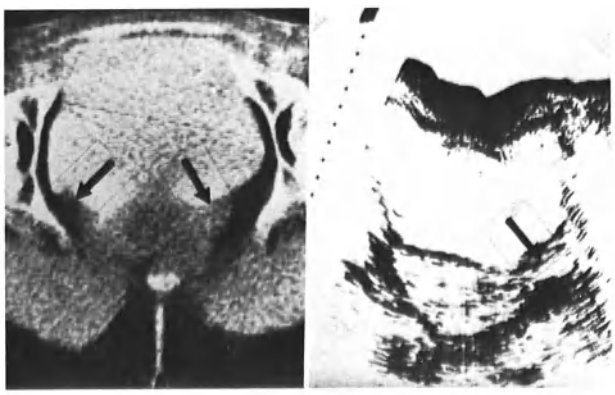

a b

Fig. 3a and b. Ovaries. (a) C.A.T. scan performed 5 cm cephalad to the symphysis demonstrates both ovaries (*arrows*) lateral to the bladder. Uterus is largely obscured by contrast material in bladder. (b) Transverse ultrasound in same patient 5 cm cephalad to symphysis demonstrates uterus better. Only one ovary is seen (*arrow*)

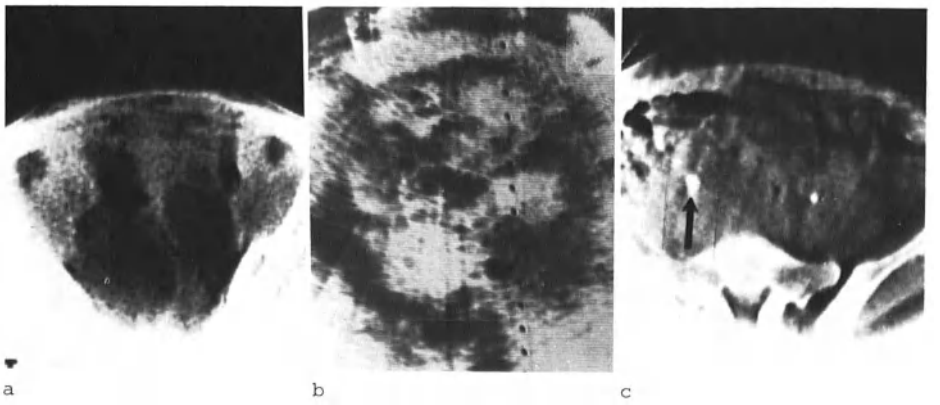

Fig. 4a-c. Ovarian carcinoma. (a) Soft tissue mass is seen involving entire pelvis on a section 5 cm cephalad to the symphysis. Both cystic and solid components are seen. Bowel is intimately related to mass. (b) Transverse ultrasound at same level also reveals complex nature of mass. At surgery, massive bilateral cystadenocarcinoma of ovaries was found which was unresectable. (c) C.A.T. section 8 cm cephalad to the symphysis demonstrates right hydroureter (*arrow*). Tumour mass extended cephalad at least 3 more centimetres

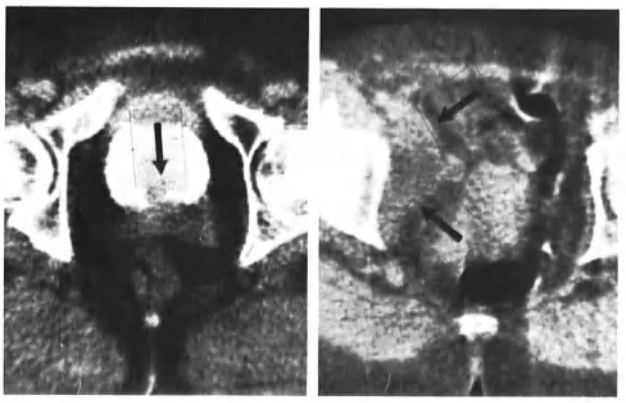

Fig. 5 Fig. 6

Fig. 5. Prostatic enlargement. Enlarged prostate is seen impressing dorsal surface of bladder (*arrow*) on a section 1 cm cephalad to the symphysis. Regions of the seminal vesicles and rectum are also demonstrated

Fig. 6. Recurrent ovarian carcinoma, 5 months following resection and radiation. Patient was unable to distend her bladder for ultrasound. C.A.T. demonstrates recurrent tumour mass (*arrow*) along pelvic sidewall. Adjacent enlarged nodes are seen. Scans done in the lower abdomen revealed tumour involvement of para-aortic chain bilaterally

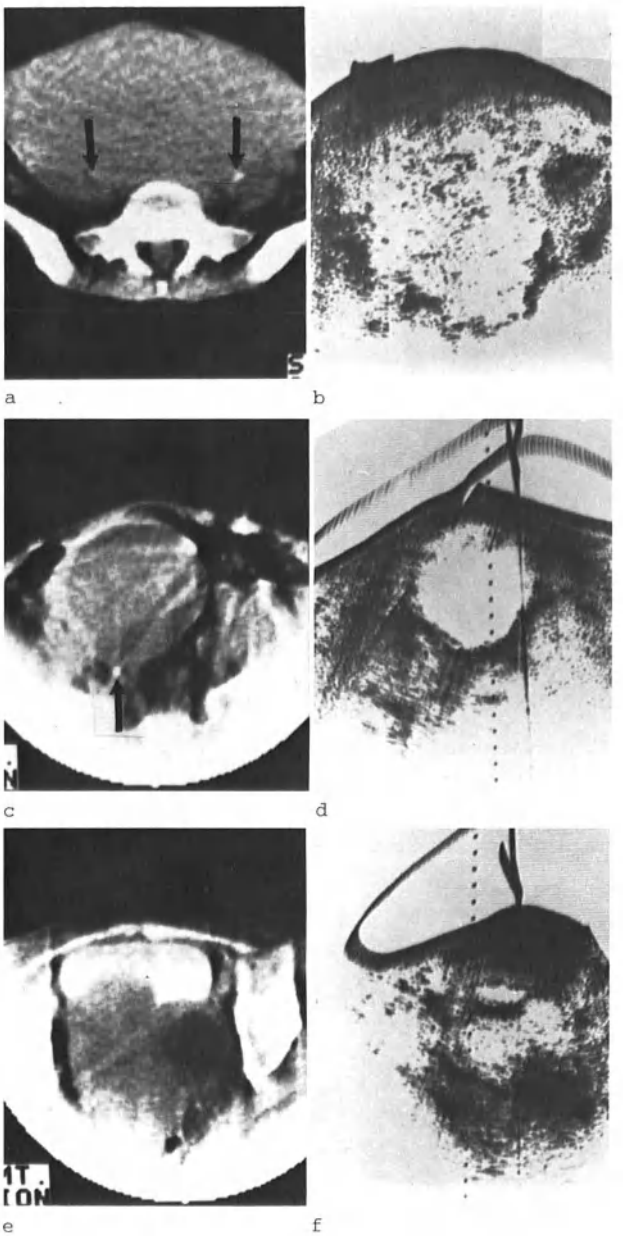

Fig. 7a-f. Ureters. (a) Large uterine leiomyoma is demonstrated to displace but not involve both ureters (*arrows*). (b) Ultrasound at same level reveals more about internal architecture of mass but does not demonstrate ureters. (c) C.A.T. section 9 cm cephalad to the symphysis in a patient with extensive endometriosis, reveals that right ureter (*arrow*) has been incorporated in the wall of a large cystic mass. (d) Ultrasound of cyst. (e) C.A.T. 3 cm above the symphysis demonstrates a smaller cyst as well as a soft tissue mass engulfing uterus and impressing bladder. (f) Ultrasound at this level shows both cystic and solid components but does not suggest the extensiveness of the abnormality quite as fully

C.A.T. of the Soft Tissues

H. C. Redman*

The ability of C.A.T. scanners to detect slight differences in tissue density allows the radiologist to evaluate the various soft tissues of the body, an opportunity never before available. Not only does this present new diagnostic possibilities for most radiologists, it means relearning soft tissue anatomy in cross-section. The variety of lesions which can theoretically be evaluated is legion.

The soft tissues of the lower extremities are easily studied and provide their own internal control. The upper extremities present a slightly greater technical problem and often must be studied positioned lateral to the torso. An alternative is to place them fully extended above the head, a position difficult to maintain for many people. The muscle masses within the extremities are well demonstrated, and diffuse swelling can be distinguished from a discrete mass or haematoma (Fig. 1). Lipomas can be identified (Fig. 2) but it is unlikely that the histological nature of other soft tissue masses will be specifically determined with current technology since there is significant overlap in the tissue densities of the various lesions.

The thoracic and abdominal wall musculature and that of the retroperitoneum and pelvis are also well seen at C.A.T. scanning. Tumour occurring in a scar can generally be distinguished from exuberant scar tissue or inflammation (Fig. 3). Neoplastic invasion of the psoas muscles and other muscles of the retroperitoneum and pelvis is seen as asymmetrical enlargement (Fig. 4). Extent of tumour involvement can be defined, aiding in radiation therapy planning, since the configuration of the tumour can be determined in three dimensions.

In summary, C.A.T. scanning has the capability of evaluating soft tissues never before accessible to diagnostic radiology. The information available can be used to determine surgical and radiation treatment plans.

---

*Mt. Zion Hospital and Medical Center, San Francisco, University of California School of Medicine, and Stanford University School of Medicine.

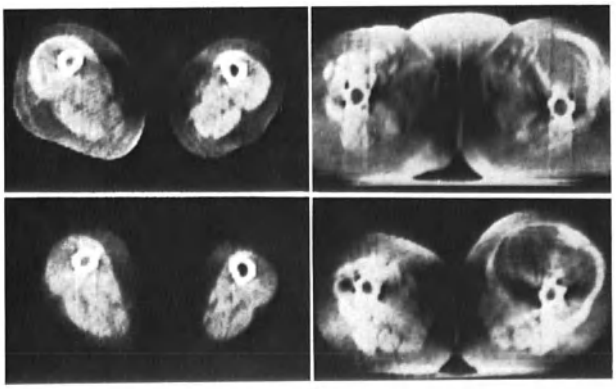

a b

Fig. 1. (a) Diffuse swelling right thigh following total hip prosthesis. Comparison with opposite thigh shows that each muscle belly is enlarged and no discrete haematoma is demonstrated. (b) Haematoma following total hip prosthesis. Muscle bellies are displaced and distorted by an extensive haematoma which involved much of the thigh

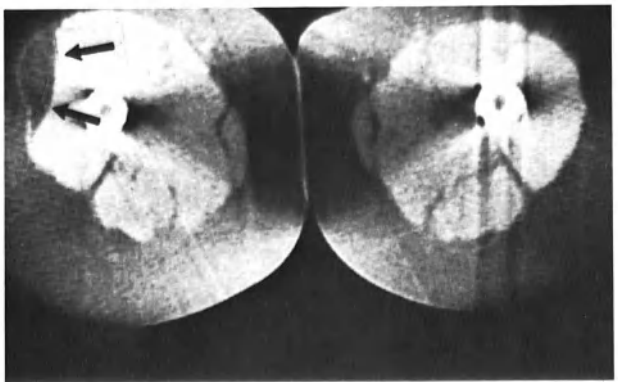

Fig. 2. Lipoma of the thigh. Low density lesion (*arrows*) is seen lateral to the muscles of right thigh. A smaller lipoma is present dorsally on the left thigh

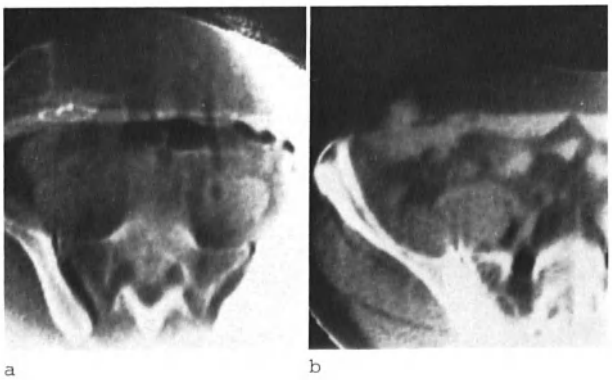

a b

Fig. 3a and b. Anterior abdominal wall pathology. (a) Scar in anterior abdominal wall following surgery and radiation therapy for neoplasm. Palpation had raised the question of tumour recurrence near incision. (b) Tumour recurrence in anterior abdominal wall. A nodule is seen in the soft tissues and there is involvement of muscular wall, which is irregular and distorted

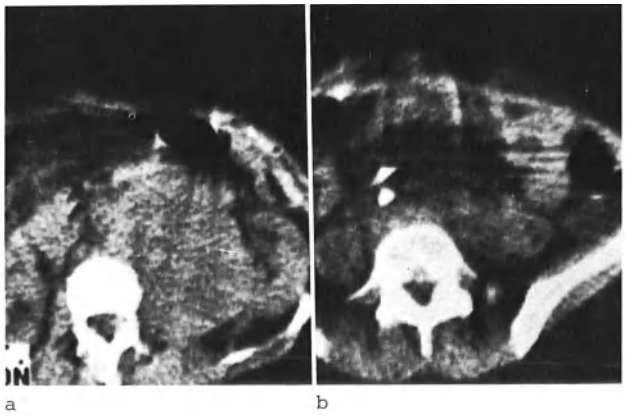

Fig. 4a and b. Retroperitoneal xanthosarcoma. (a) Section 9 cm caudad to the xyphoid reveals a large left retroperitoneal mass displacing left kidney laterally. Aorta is completely obscured. (b) Section 3 cm caudad to umbilicus. The mass, though smaller, is distorting left psoas muscle

The Liver and Pancreas

Imaging the Liver and Pancreas - A Clinician's View

P. B. Cotton*

When considering the potential role for computed tomography of the abdomen, it is appropriate to consider the extent to which current diagnostic techniques satisfy clinical demands. Any review must have a strong personal bias. With so many possible techniques and refinements, a comprehensive and objective assessment is impossible. The literature is full of contradiction and confusion, largely because many results depend as much upon the workman as on his tools.

In the context of hepatic and pancreatic disease there are several common questions:

1. Jaundice - medical or surgical?
2. Does the liver contain metastases?
3. Is the pancreas normal or abnormal?
4. Pancreatic disease - is it cancer or pancreatitis?
5. Relapsing pancreatitis - is there a local lesion which may require surgery?

Jaundice

The clinician's main concern is to detect those patients with extrahepatic obstruction, who need surgery, and those without, who must be protected from surgery. In many patients this distinction between medical and surgical jaundice is difficult. The critical discriminating test is a cholangiogram, for which many routes are now available. However, precedence is usually given to non-invasive methods including plain radiography, barium studies and isotopic liver scanning. Unfortunately, these are rarely helpful. Radio-opaque gallstones and pancreatic calcification may be apparent on a plain radiograph, but do not absolutely define the cause of jaundice. Demonstration of varices on a barium meal is obviously of relevance, and a definite abnormality of the duodenal loop suggests that a pancreatic lesion is present. Finer abnormalities of the duodenal loop and the papillary region are more difficult to interpret. Hypotonic duodenography is more accurate, but this technique is being superseded by fibreoptic duodenoscopy, at which specimens can be taken for histology or cytology. One disadvantage of a barium meal is that residual barium in the intestine may delay further radiology. Standard isotopic liver scanning has proved rather disappointing. Demonstration of a small liver and enlarged spleen is good evidence for chronic liver disease, and large filling defects in the liver are obviously relevant. However, clinical experience dictates that reports of less definite abnormalities should be interpreted with caution. In particular, attempts to diagnose large duct obstruction from a hilar scan defect are liable to observer variation and error.

---

*Gastrointestinal Unit, The Middlesex Hospital, London.

Dynamic isotopic scans are of more interest and potential value. Radioactively labelled BSP, Rose Bengal, and experimental pharmaceuticals can be followed by sequential scanning through the liver, gallbladder, bile duct and intestine, and an isotopic cholangiogram can be constructed (11). A high degree of accuracy has been claimed for this technique in the differential diagnosis of jaundice, and further evaluation is awaited.

In many centres the diagnostic approach to obscure jaundice has consisted mainly of prolonged observation and eventual laparotomy. This expensive and potentially hazardous method is no longer appropriate or necessary. Cholangiograms can be obtained by many routes: percutaneous transhepatic (PTC), transjugular, transumbilical, or laparoscopic. Recently it has become possible to cannulate the bile duct via the papilla of Vater under direct vision using a fibreoptic duodenoscope (ERCP) (3). We have provided a definitive diagnosis in 89 of our last 100 jaundiced patients, without any complications. However, ERCP is not an easy technique to learn, and its use in jaundice has recently been challenged by the increasing popularity of fine needle PTC. In expert hands this technique has high success rates for both dilated and normal duct systems, and it also provides a method for preoperative biliary decompression which may improve surgical results. One randomised comparison showed that fine needle PTC was most effective when ducts were dilated, and ERCP more accurate when they were not (6). A method for pre-selection would be helpful; this is precisely the potential role for computed tomography, and indeed for grey-scale ultrasonography (13). An imaging technique which can demonstrate dilated intrahepatic ducts with or without a dilated gallbladder would short-cut the diagnostic process.

Does the Liver Contain Metastases?

This question arises in two main contexts - preoperative assessment of patients with primary malignancy, particularly in the gastrointestinal tract, and as part of the diagnostic process in patients with general malaise and disturbed liver function. Diagnosis or exclusion of hepatic metastases is often a crucial factor in patient management and clinicians need reliable information. In practice this usually means liver histology, taken by needle puncture, or during laparoscopy or open operation. British use of angiography in this context is strictly limited. An accurate non-invasive technique would be preferable. Isotopic liver scans can demonstrate space-occupying lesions, but resolution is not sufficient to allow clinical reassurance from a normal scan report. Preliminary assessments of grey-scale ultrasonography (13) and computed tomography are of considerable interest, and new studies are awaited.

Pancreatic Imaging and Diagnosis

The assessment of diagnostic tests in patients with liver disease and jaundice is relatively simple, since most patients come quickly to an independent diagnostic conclusion. This is not so in pancreatic disease, particularly chronic pancreatitis. A diagnosis based on histology is available only in patients with disease severe enough to require surgery. Pancreatic calcification is an excellent marker, but is also a late phenomenon. Thus the efficiency of diagnosis of chronic pancre-

atitis in any institution can be expressed as the reciprocal of the percentage of such patients who have calcification. Any assessment of the accuracy of a diagnostic method (scanning or function testing) based on the clear end-point of pancreatic calcification is clinically totally irrelevant. At this stage the diagnosis is already established and diagnostic tests are unnecessary. They are needed in the grey area of clinical doubt, in less severe disease, where there may be no immediate and independent diagnostic arbiter. Indeed sometimes the test being assessed is even used as one of the criteria for the final diagnosis. The literature on pancreatic diagnostic tests is further confused by the important factor of individual skill. The results of pancreatic function testing, isotope scanning, ultrasonography, arteriography and pancreatography all depend as much upon the experience and diligence of the investigator as upon the technique used. The author uses the same golf clubs as Jack Nicklaus but does not always achieve the same results.

Tests must be assessed in the clinical context. In patients with obscure pain, the clinician needs a method which will document pancreatic normality or abnormality; either ability is useful, and both are rare. When a patient is known to have pancreatic disease (a mass, or pain with raised serum amylases) the question is different: is it cancer or pancreatitis? Thirdly, in patients with relapsing pancreatitis the question concerns the demonstration or exclusion of a local lesion such as duct obstruction or a pseudocyst for which surgery might be appropriate. Different tests may be relevant to different questions.

An abnormal result from a carefully performed pancreatic function study indicates pancreatic disease, but cannot separate pancreatitis from cancer, unless cytology is added. A normal result does not exclude painful pancreatitis or distal cancer. In relapsing acute pancreatitis a low bicarbonate output suggests duct obstruction.

Pancreatic isotope scanning is easy for patients and generally available, but overall results have been disappointing. An abnormal scan is meaningless. Most proponents of isotope scanning rest their case on the contention that a perfectly normal isotopic image virtually excludes chronic pancreatic disease. This was certainly true in one British study (12), but other large surveys have found false negatives in up to 21% of scans (1). Our most recent assessment of pancreatic isotope scanning has led us to discontinue its use. Amongst 30 patients with an unequivocally normal scan, there were 14 with definite pancreatic disease.

Arteriography is one field where the effect of individual expertise is apparent. Some individuals achieve results of high accuracy (7), but these are available in few British centres. Vascular alterations indicate advanced pancreatic disease, and give guidance concerning the surgical approach. However, a normal arteriogram does not exclude chronic pancreatitis or carcinoma and their radiographic distinction may be difficult.

The author confesses a bias towards pancreatography, of which he has the most experience. An individual offering a particular technique will often see the worst results of other techniques - not only because he wishes to do so, but also because the failure of other techniques may have led to the patient's referral. Pancreatography is only part of endoscopic retrograde cholangio-pancreatography (ERCP) (3). A method which allows a complete survey of the stomach, duodenal loop, papilla, biliary and pancreatic duct systems is a powerful tool in the investigation of obscure abdominal pain. In experienced hands a pancreatogram

can be obtained in over 90% of patients - failures usually being attributable to local disease or surgery.

Pancreatitis is a condition with a spectrum of severity, from a single acute attack with complete histological and functional recovery to end-stage disease with a destroyed and calcified gland. The incidence of abnormal pancreatograms (as well as arteriograms and scans) depends where chronic pancreatitis is defined within this spectrum. In many patients with relapsing acute pancreatitis the pancreatogram is normal. In late disease with abnormal function, all pancreatograms are abnormal. Between these extremes lie the majority of patients with relapsing pancreatitis. Pancreatograms usually show duct abnormalities such as strictures or complete obstruction, and provide a vital map on which to plan surgical triumphs. In this context a normal pancreatogram is not misleading. Indeed it is helpful in guiding patients and clinicians away from surgery. When a pancreatogram is normal and the diagnosis of pancreatitis remains in doubt, pure pancreatic juice can be collected from within the duct system at ERCP. This technique has considerable diagnostic and research potential (4).

Most pancreatic cancers are advanced and incurable at the time of clinical presentation. ERCP provides an accurate method of diagnosis, particularly of tumours of the papilla which may have a good prognosis. ERCP has allowed a firm diagnosis in 82% of our last 55 cases of pancreatic cancer. Failures included 3 patients with equivocal radiology, and 7 where cannulation failed. In 1 patient the main pancreatic duct system was normal. When a pancreatogram shows complete obstruction, the distinction between chronic pancreatitis and carcinoma may be difficult on the radiographic appearances alone. Endoscopic histology or cytology (9) may be diagnostic, but in some cases the clinical history is the major discriminator.

Patients with subacute pancreatitis or chronic problems following an acute attack may have a pseudocyst. Pancreatography is not an appropriate diagnostic method; cysts are rarely visualised, since less than half connect with the duct system. When contrast enters the cyst, there is a significant risk of sepsis.

Ultrasound scanning has been used for many years for the detection of pancreatic psuedocysts. The newer grey-scale technique allows more detailed pictures and should be a routine procedure in all patients with recurrent pancreatitis. In the hands of experts high accuracy is now also claimed for the diagnosis of cancer and chronic pancreatitis (2, 5, 10). A striking development is percutaneous pancreatic biopsy using ultrasonic guidance (8).

For clinicians interested in pancreatic diagnosis, the main interest over the next few years will be the developing interface between grey-scale ultrasonography and computed tomography. Both must be judged in the clinical context, and in their answers the specific clinical questions. The final test for any technique is not its performance in the hands of pioneer experts, but its everyday results in routine departments; its success can then be judged by the number of requests. No technique can claim to be of clinical value unless it is actually available to the patient.

References

1. BARON, J.H.: Pancreatic function tests. In: Topics in Gastroenterology. TRUELOVE, S.C., GOODMAN, J. (eds.). Oxford: Blackwell 1975, Vol. III, pp. 129-152.
2. BURGER, J., BLAUENSTEIN, U.W.: Current aspects of ultrasonic scanning of the pancreas. American Journal of Roentgenology 122, 406-412 (1974).
3. COTTON, P.B.: Progress Report ERCP 76. Gut (in press).
4. COTTON, P.B., HEAP, T.R.: The analysis of pancreatic juice. British Journal of Hospital Medicine 14, 659-666 (1975).
5. DOUST, B.D.: The use of ultrasound in the diagnosis of gastroenterological disease. Gastroenterology 70, 602-610 (1976).
6. ELIAS, E., HAMLIN, A.N., JAIN, S., LONG, R.G., SUMMERFIELD, J.A., DICK, R., SHERLOCK, S.: A randomised trial of percutaneous transhepatic cholangiography with the chiba needle versus endoscopic retrograde cholangiography for bile duct visualisation in jaundice. Gastroenterology 71, 439-443 (1976).
7. GOLDSTEIN, H.M., NEIMAN, H.L., BROOKSTEIN, J.J.: Angiographic evaluation of pancreatic disease. Radiology 112, 275-282 (1974).
8. HANCKE, S., HOLM, H., KOCH, F.: Ultrasonically guided percutaneous fine needle biopsy of the pancreas. Surgery, Gynaecology and Obstetrics 140, 361-364 (1975).
9. HATFIELD, A.R.W., SMITHIES, A., WILKINS, R., LEVI, A.J.: Assessment of endoscopic retrograde cholangio-pancreatography (ERCP) and pure pancreatic juice cytology in patients with pancreatic disease. Gut 17, 14-21 (1976).
10. LÜTH, H., PETZOLDT, R., HOFMANN, K.P., RÖSCH, W.: Ultraschalldiagnostik bei Pankreaserkrankungen. Klinische Wochenschrift 53, 419-424 (1975).
11. RONAI, P.M., BAKER, R.J., BELLEN, J.C., COLLINS, P.J., ANDERSON, P.J., LANDER, H.: Technetium 99m pyridoxylideneglutamate: a new hepatobiliary radiopharmaceutical. II. clinical ascpects. Journal of Nuclear Medicine 16, 728-737 (1975).
12. SPENCER, A.M., PATEL, M.P., SMITS, B.J., WILLIAMS, J.D.F.: Pancreatic scanning as a diagnostic tool in the district general hospital. British Medical Journal 1974/IV, 153-156.
13. TAYLOR, K.J.W.: Grey-scale ultrasound B-scanning for assessment of the liver and the kidney. British Journal of Clinical Equipment 1, 113-121 (1976).

C.A.T. of the Pancreas

J. Husband and L. Kreel*

Introduction

Computerised tomography is a new development in the non-invasive imaging of intra-abdominal disease. Anatomical structures are displayed in a way which has not been possible previously.

The normal pancreas is clearly shown in the majority of patients. This is a study of 82 patients with suspected pancreatic disease examined by computerised tomography using the EMI whole body scanner. The aims of the study were to define the radiological signs of pancreatic disease and to assess the accuracy of this technique in the demonstration of pancreatic lesions.

Material and Methods

Eighty two patients with suspected pancreatic disease were examined by computerised tomography using the EMI whole body scanner.

All patients reveived a low residue diet for 3 days prior to the examination to reduce the amount of bowel gas and received oral calcium phosphate (400 mg t.d.s.) for a similar period to show the position of the colon. Propantheline (30 mg i.m.i.) was given 10 min before the examination to overcome streak artefacts caused by gas in moving bowel.

A slit beam radiograph of the chest and abdomen was taken in the supine position. This film is known as the 'scanogram'. Lead markers were placed on the skin of the patient so that the level of each tomographic slice could be related to the exact anatomical site of the 'scanogram'. The position of the pancreas was determined by review of previous radiological studies. Gas in the duodenal loop on the 'scanogram' was also a helpful localising sign. Scans were taken at 1-cm intervals through the pancreas and at 1.5-cm intervals through the liver.

Results

Table 1 shows the final diagnosis achieved by laparotomy, post-mortem or biochemical analysis in 76 patients with suspected pancreatic disease. In 4 patients the lesion demonstrated remains unconfirmed and in 2 artefacts obscured the pancreas.

---

*Division of Radiology, Clinical Research Centre and Northwick Park Hospital, Harrow.

Table 1. Suspected pancreatic disease final diagnosis in 76 patients

Normal	26
Pancreatitis[a]	25
Tumours[a]	26

[a]One patient included in two groups.

Normal Pancreas - 26 Patients

A normal pancreas was clearly shown by computerised tomography in 26 patients. In one of these patients the head showed a scalloped contour subsequently shown to be a separate ventral head of pancreas.

Table 2. False positive examinations

Clinical diagnosis	C.A.T.	Final diagnosis
1. ? Tumour in tail	Mass in tail	Laparotomy normal
2. ? Tumour in tail	Mass in tail	Laparotomy normal
3. Chronic pancreatitis	Enlarged body and tail	Laparotomy normal
4. ? Pancreatitis	Irregular pancreas	No laparotomy
	Chronic pancreatitis	U/S normal

In 3 patients the C.A.T. scan was incorrectly interpreted and in 1 patient the interpretation was probably incorrect (Table 2). Three of these false positive examinations were due to incorrect diagnosis in the region of the tail of the pancreas.

Pancreatitis - 25 Patients (Table 3)

Table 3. Signs of pancreatitis - 25 patients

			No. of patients
Pancreas enlarged	'Mass'	(1)	8
	Localised	(6)	
	Diffuse	(1)	
Inflammatory change			8
Calcification			6
Pseudocyst	Well defined	(2)	6
	Ill defined	(1)	
	Extra pancreatic effusion	(3)	
Normal scan			1

Radiological signs of pancreatitis were demonstrated by computerised tomography in 24 patients. In one patient the C.A.T. scan was normal but laparotomy revealed histological evidence of pancreatitis. Eight

patients showed more than one sign of pancreatitis. Enlargement of the pancreas was seen in 8 patients. One patient presented with obstructive jaundice due to a 'mass' in the head of the pancreas. This was clearly shown by computerised tomography and also by ultrasound, but it was impossible to exclude a tumour. Follow-up examination 4 weeks later showed complete resolution of the mass. Localised enlargement was seen in a further 6 patients. Diffuse enlargement of the whole pancreas was shown in 1 patient (Fig. 1).

Inflammatory change was demonstrated in eight patients. Signs of inflammation included irregularity of the borders of the pancreas, infiltration of surrounding fat by strands of tissue and thickening of the mesentery, diaphragm and peritoneum.

Severe loss of body fat was shown in four patients. All these patients showed other signs of pancreatitis. These included pancreatic calcification, localised enlargement and fat replacement in the head. Although chronic calcific pancreatitis was suspected in seven patients (Table 4), in two the calcification, demonstrated by conventional radiography,

Table 4. Calcification - 8 patients

Pancreatic	
1. Early calcific pancreatitis	1
2. Dense calcific pancreatitis	5
Extra-pancreatic	
In lymph nodes	2

was shown by C.A.T. to be extra-pancreatic. In both these cases the calcification was shown to be in lymph nodes and in one calcification was also present in a large gastric ulcer. In one patient calcification was demonstrated by computerised tomography but this had not been shown on the plain abdominal film.

In five patients dense calcification was present in the pancreas which was clearly visible by conventional techniques. In one further patient fine calcification was demonstrated in the head of the pancreas which was not visible on the plain films of the abdomen (Fig. 2). In addition to calcification other signs of pancreatitis were also shown in this group of patients. These signs included loss of body fat, fat replacement in the head surrounding the calcification, localised enlargement, inflammatory change and dilatation of the pancreatic duct (Fig. 3).

'Pseudocysts' were shown in 6 patients. These have been divided into three types for descriptive purposes.

Type I. Circumscribed cysts with a well-defined wall were shown in two patients. One was in the head of the pancreas and one in the tail (Fig. 4). There was no difficulty in distinguishing these low-density lesions from tumours.

Type II. A large ill-defined cyst with an irregular outline was demonstrated in one patient who had presented with acute pancreatitis. The C.A.T. also showed moderate ascites.

Type III. Extra-pancreatic collections of fluid were shown in three patients. In two of these the fluid collections were situated in the abdomen adjacent to the psoas muscle. An unsuspected mediastinal effusion

was demonstrated in the third patient, who also had a loculated right-sided pleural effusion.

Tumours - 26 Patients

Tumours of the pancreas were composed of carcinomas and endocrine tumours. One patient had a mucoid adenocarcinoma of the colon with diffuse peritoneal infiltration (Table 5). Carcinoma of the pancreas was unequivocally demonstrated by computerised tomography in all 19 patients. In 17 patients the lesion was in the head of the pancreas and

Table 5. Tumours - 26 patients

		No. of patients
Carcinoma	Head - 17 Body - 2	19
Endocrine	Gastrinoma - 3 Insulinoma - 2 Glucagonoma - 1	6
Mucoid adenocarcinoma of colon		1

in 2 it was situated in the body. In one patient a carcinoma in the head of the pancreas was shown to be associated with dilatation of the gall bladder and intrahepatic bile ducts (Fig. 5). The stomach was also dilated due to partial obstruction of the duodenum.

Carcinomas were shown to have only a very slightly higher density than normal pancreatic tissue. The smallest carcinoma demonstrated in this series was 4 cm in diameter (Fig. 6).

Endocrine tumours were diagnosed in six patients on clinical and biochemical grounds. There were three gastrinomas, two insulinomas and one glucagonoma. Computerised tomography failed to demonstrate the primary lesion in five patients. However, two of these patients were shown to have possible secondary deposits in the liver after contrast enhancement. In one patient a large cystic glucagonoma in the head of the pancreas was demonstrated, as well as chronic calcific pancreatitis in the tail.

Miscellaneous Group - Five Patients

1. Secondary deposits were demonstrated in two patients. One had small peripheral deposits in the lungs and the other large deposits in the liver.

2. A final diagnosis of primary biliary cirrhosis was made in two patients, and in both of these patients the C.A.T. scans showed marked diffuse enlargement of the pancreas. These findings are unconfirmed.

3. Artefacts obscured the pancreas in two patients but no gross lesion was visible.

Comments

The results of computerised tomography in this study of 82 patients are shown in Table 6. The correct diagnosis was made in 66 patients. There were four false positive examinations (Table 2). The lesion was not demonstrated in 6 patients, of whom 5 had endocrine tumours. The diagnosis remains unconfirmed in 4.

Table 6. Results - computerised tomography of the pancreas

Total	Correct diagnosis	False + ve	False - ve	Lesion unconfirmed	Technical failures
82	66	4	6	4	2

Discussion

The normal pancreas is clearly shown by computerised tomography in the majority of patients. A layer of fat surrounds the pancreas and helps to differentiate it from adjacent small bowel, which has the same density as pancreatic tissue. However, in some patients difficulty does arise in distinguishing the head of the pancreas from the duodenum and the tail from the jejunum. In our series of 82 patients three false positive examinations were due to misinterpretation of appearances of the tail of the pancreas which appeared to be enlarged because of adjacent jejunum. In an attempt to overcome this important problem a positive contrast medium is being routinely used to act as a marker in the duodenum and jejunum. Ten minutes before the examination, 2.5 ml sodium/meglumine diatrizoate (Gastrografin) diluted in 500 ml water is given orally. Although our experience is limited, we have already found this preparation most valuable.

The radiological signs of pancreatitis are well shown by computerised tomography. Although there is little difficulty in making the diagnosis of chronic calcific pancreatitis by conventional techniques, computerised tomography has revealed additional signs of disease not shown by other methods of investigation. These include inflammatory change around the pancreas, loss of body fat, fat replacement in the head of the pancreas and dilation of the pancreatic duct. Fine calcification, not demonstrated by ultrasound or conventional radiology, was shown in the head of the pancreas in one patient (Fig. 2). Chronic calcific pancreatitis had been diagnosed in two patients who showed evidence of calcification on plain films of the abdomen. However, computerised tomography showed that the calcification was extra-pancreatic; the pancreas in both patients was unequivocally normal. This information was extremely valuable in further management of these patients.

The diagnosis of pseudocyst is important as surgery is indicated. For descriptive purposes we have divided pseudocysts into three types. Type I is the well-defined circumscribed lesion with a definite wall. Type II is an ill-defined irregular cyst. This type of lesion was seen in one patient who also had moderate ascites. A possible explanation of these appearances is that the cyst had ruptured, producing ascites, and leaving an incompletely filled cavity in the pancreas. Extra-pancreatic collections of fluid (Type III) were demonstrated in three patients. One patient was known to have a right-sided pleural effusion. Computerised tomography demonstrated a large unsuspected mediastinal effusion

surrounding the oesophagus. Collections of fluid adjacent to the psoas muscle were demonstrated in two further patients.

Evidence of pancreatitis without cyst formation or calcification was demonstrated in 13 patients. The diagnosis was confirmed by abnormal pancreatic function tests and laparotomy. Computerised tomography was valuable in these patients because pseudocyst formation and calcification were reliably excluded.

The C.A.T. scan may certainly be normal in the presence of pancreatitis as was shown by one patient with histological evidence of disease. However, C.A.T. scanning in these cases is concerned with excluding pseudocysts, calcification and tumours.

Large tumours of the head of the pancreas present no difficulty in diagnosis by conventional techniques. Computerised tomography not only shows the exact size and site of the primary mass but also demonstrates secondary changes in other organs (Fig. 5). These include metastases in the liver, dilatation of the gall bladder and intrahepatic bile ducts. It is important to note that all this information is gained from a single non-invasive examination by computerised tomography.

It has been reported that the density of carcinoma of the pancreas does not differ significantly from normal pancreatic tissue (1). However, we have found that tumours do appear a little denser than the normal pancreas, but the recognition of tumours depends largely on the abnormal contour of the gland produced by these lesions. The smallest carcinoma diagnosed in this series was 4 cm in diameter. The lesion was situated in the body of the pancreas and projected posteriorly, overlying the superior mesenteric artery.

Endocrine tumours are usually very small and do not alter the contour of the pancreas. We have been unable to demonstrate the majority of these lesions up to the present time, but it is hoped that future developments in the use of contrast media or in computerised tomography may overcome this problem.

Primary biliary cirrhosis was diagnosed in two patients by the demonstration of mitochondrial antibodies and other confirmatory clinical evidence. Both ultrasound and computerised tomography demonstrated a diffusely enlarged pancreas in each of these patients. The significance of these findings is not clear and further investigation of patients with biliary cirrhosis is necessary before a definite conclusion can be made from these observations.

Preparation of the patient is important in reducing the incidence of artefacts caused by bowel movement and includes the reduction of bowel gas and the use of anticholinergics. Artefacts, particularly those due to movement, obscure the pancreas and the examination is therefore of little value.

At the present time, it therefore seems likely that computerised tomography will have an important role in the demonstration and diagnosis of pancreatic disease.

Summary

Eighty two patients with suspected pancreatic disease have been examined by C.A.T. using the EMI whole body scanner. The patients were divided

into three main groups according to the final diagnosis obtained by laparotomy, post-mortem or biochemical analysis. The aims of the study were to determine the radiological signs of pancreatic disease shown by computerised tomography and to assess the accuracy of this technique in the demonstration of pancreatic lesions. Results demonstrate that pancreatic lesions are clearly shown in the majority of patients. There were six false negative examinations, of which five were in patients with endocrine tumours; these tumours are usually too small to be recognised by computerised tomography. Three of the four false positive examinations were due to misinterpretation of appearances in the region of the tail of the pancreas.

It is hoped that these errors will be considerably reduced in the future as further experience in computerised tomography is gained.

Acknowledgements

Grateful acknowledgement is made to the Department of Health and Social Security whose far-sighted and generous help has assisted greatly in the development of this project. The assistance and considerable help from Mr. John Twydle, who has been managing the machine, is also gratefully acknowledged. We are also grateful to Dr. Peter Cotton, who referred many of the patients to us for investigation.

References

1. SHEEDY, P.F.: Computed tomography of the body: initial clinical trial with the EMI prototype. Amer. J. Roentgenol. 127, 23-51 (1976).

Fig. 1. Pancreatitis - diffuse enlargement of the pancreas (*arros*)

Fig. 2. Chronic pancreatitis - calcification in the head of the pancreas (*arrows*)

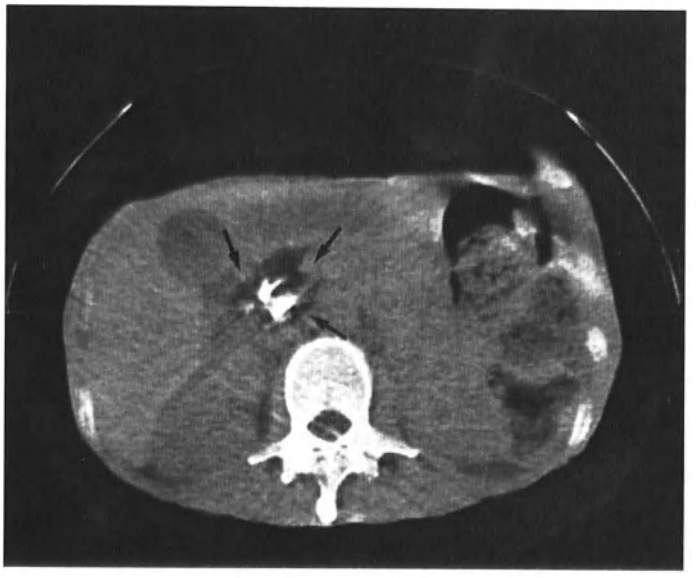

Fig. 3. Chronic calcific pancreatitis. Calcification and fat replacement in head of pancreas (*arrows*); loss of intra-abdominal fat

Fig. 4. Pseudocyst in tail of pancreas (*arrows*)

Fig. 5. Carcinoma of head of pancreas (*short arrows*). Dilated intrahepatic bile ducts (*long arrow*). G.B.: gall bladder

Fig. 6. Carcinoma of body of pancreas (*arrows*)

C.A.T. in Acute and Chronic Pancreatitis

A. L. Baert, E. Ponette, J. Pringot, G. Marchal, A. Dardenne, and Y. Coenen*

Introduction

Not longer than 15 years ago the only available morphological information about the pancreas was given by radiographs of the abdomen, the stomach, the duodenum and the biliary system.

From about 1960 onwards several other methods were developed: pancreatic scanning with ^{75}Se- (selenomethionine) arteriography, ultrasound and endoscopic retrograde cholangiopancreaticography (E.R.C.P.).

However, arteriography and E.R.C.P. pose technical problems, and the quality of the image obtained by pancreas scanning with isotopes and by ultrasound has the intrinsic limits of these methods (4).

With respect to C.A.T. we will try to answer two questions:

1. Is C.A.T. able to visualise the pancreas?
2. What is the value of C.A.T. in the diagnosis of pancreatitis?

Patients

From May 1976 onwards we examined the pancreas in 81 patients; in 3 of them a follow-up examination was performed.

The criteria for the final diagnosis were either the findings from surgical intervention or from a combination of clinical and biochemical data, conventional X-ray examination, ultrasound, E.R.C.P. and anteriography.

The pancreas was considered to be normal according to these criteria in 31 of the patients examined. In 28 patients the diagnosis was pancreatitis; 11 had acute and 17 chronic pancreatitis. In 8 patients with chronic pancreatitis, calcifications were present. It should be pointed out that the patients with pseudocysts have been included in these numbers. Three of these pseudocysts were complications of acute pancreatitis whereas the 2 remaining developed in the context of a chronic pancreatitis (Table 1).

*Dept. of Radiology K.U.L. (Dir. Prof. A. Baert) and Dept. of Radiology U.C.L. (Dir. Prof. P. Bodart).

Table 1. Final diagnosis in patients referred for C.A.T. of the pancreas

Number of patients		81
Normal pancreas	31	
Pancreatitis		
- acute	11	
- chronic: calcified	8	
non-calcified	9	
- with pseudocyst	(5)	
Tumour	7	
Miscellaneous	3	
Inconclusive	12	

Methods

The patients were routinely examined in a fasting state of at least 12 hours.

The examination was begun in the supine position. One mg. Glucagon was injected intravenously in order to decrease bowel movements. Initially, this was followed by intravenous administration of an uro-angiographic contrast medium, in order to improve the X-ray absorption by visceral organs. It is, however, our experience that the gain in intra-abdominal contrast differences obtained by this method was not very impressive. Moreover, scattering artefacts due to excessive contrast in the renal pelvicalyceal system frequently reduced the quality of the limage.

The display of the head, body and tail of the pancreas in a single plane was obtained more easily by tilting the scanner 10-15° in the cranio-caudal direction, as foreseen by HAAGA (1).

A second series of scans was performed after turning the patient on the right side and after oral ingestion of a 5% solution of Gastrografin.

This technique, also described by HAAGA (1), offers the following advantages:

1. A decrease of the respiratory movements of the right diaphragm and consequently of the liver and the pancreatic head.

2. The Gastrografin solution opacifies the gastric and duodenal lumen, distinguishing them from the pancreatic parenchyma so that a very satisfactory outline of the pancreas is obtained.

In this way artefacts due to air in the stomach, disturbing the anterior margin of the pancreas can be avoided. However, it is important that a sufficient quantity of Gastrografin should be ingested. Otherwise, the intragastric air-fluid level is not situated sufficiently high, so that the image of the tail of the pancreas is disturbed.

3. The relationship between stomach, duodenum, liver and pancreas changes, decreasing the artefacts due to superimposition of these organs.

Pseudotumoral images caused by small intestinal loops adjacent to the pancreas in the supine position can disappear in the right decubitus position.

In some instances we performed C.A.T. of the pancreas combined with intravenous cholangiography. It was then possible to assess the spatial relationship between the common bile duct, the head of the pancreas and the medial border of the descending duodenum, which is opacified by the presence of the cholangiographic contrast medium in some patients.

The analysis of the results of our technique demonstrates that the pancreas was more frequently visualised in right decubitus in association with Gastrografin then in dorsal decubitus. The best results have, however, been obtained with a combination of both techniques. In this way the success rate was 85% (Table 2).

Table 2. Success ratio in visualising the pancreas by C.A.T.

(1) Dorsal decubitus	(2) Right decubitus with Gastrografin	Combination of (1) and (2)
49%	59%	85%

Results

Morphological Anomalies

In the analysis of the C.A.T. images of the pancreas the following parameters have been studied:

1. We measured the antero-posterior diameter of the head, body and tail of the pancreas in relation to the transverse diameter of the vertebral body, as proposed by HAAGA (1). In addition, his criteria of the dimensions of the normal pancreas have been used.

2. An obvious irregularity of the contour of the pancreas was considered as a pathological sign.

3. An obliteration of the fat plane which separates the dorsal surface of the pancreas from the mesenteric vessels, aorta and vena cava was also considered to be pathological.

4. A non-homogenous density in the pancreas was considered to be pathological in so far as it was caused either by calcifications or by a visible area of hypodensity, confirmed by numerical densitometry.

Acute Pancreatitis

In biochemically proven cases of acute pancreatitis, enlargement of the pancreatic gland was the most frequently observed pathological sign.

This enlargement can be diffuse or localised (Fig. 1).

However, we found that a normal volume of the gland can be present in patients with acute pancreatitis. Two other features can occur in acute

pancreatitis: (1) irregularity of the pancreatic borders (2) and/or disappearance of the surrounding peripancreatic fat planes.

Chronic Pancreatitis

It is well known from histopathological studies that the volume and general configuration of the pancreas can vary in relation to the degree of fibrosis and oedema (2).

When the dorsal fat plane completely disappears and the great vessels are no longer visible in a pancreas with enlarged head and irregular contour, the preferential diagnosis should be a malignant tumour. However, C.A.T. is unable to distinguish localised enlargement due to chronic pancreatitis from a neoplasm which has not invaded the surrounding structures.

On the other hand, we found that a decrease of the dorsal pancreatic fat plane is not necessarily caused by a tumour but can also occur in pancreatitis.

A decrease in the size of the gland can occur in chronic pancreatitis.

Hitherto we did not observe proven pancreatic calcifications on C.A.T. which were not visible on conventional radiographs.

In the presence of calcifications of larger size, considerable increase in artefacts may occur (Fig. 2).

However, it is obvious that C.A.T. will be very helpful to prove the exact intra- or extrapancreatic location of upper abdominal calcifications observed in conventional radiographs.

Pseudocysts

Due to the obvious differences in density in comparison with the surrounding tissues, pseudocysts can be demonstrated very easily by C.A.T. (3).

The pseudocyst can be so large that residual gland tissue is no longer seen (Fig. 3). In other cases the transition between the cyst and the gland can easily be seen.

The wall of the pseudocyst is rather thick and its lining is very regular.

A fluid-filled stomach can mimic a cyst, but the study of the relationship with the pancreas will prevent that error.

We were surprised by the fact that the density values in these pseudocysts were always in the range of 15 to 35 delta units, which is distinctly higher than in renal cysts. This can be explained by the fact that no clear liquid is present but a mixture of liquid, necrotic material and fibrin.

It should be pointed out that a pseudocyst may also develop in the pancreatic area, proximal to a neoplastic process.

Statistical Analysis

In a total number of 31 examinations in patients with pancreatitis, C.A.T. scan demonstrated pathological findings in 68%. All cases with pseudocysts were correctly diagnosed. There were no false positive examinations and the rate of false negatives was 16% (Table 3).

Table 3. Diagnostic value of C.A.T. in pancreatitis

Number of examinations: 62	- normal:	31
	- pancreatitis:	31
False positive	0/31	0%
Agreement - normal:	23/31	74%
- pancreatitis	21/31	68%
(pseudocyst: 6/6)		
False negative	5/31	16%
Inconclusive	12/62	21%

Table 4. Comparative diagnostic value of C.A.T. and upper gastrointestinal X-ray series in pancreatitis

Number of examinations: 45	- normal	21
	- pancreatitis:	24
	C.A.T.	Upper gastro-intestinal
False positive	0/21	3/21
Agreement - normal	16/21	18/21
- pancreatitis	17/24	16/24
False negative	3/21	6/24
Inconclusive	9/45	2/45

Table 5. Comparative diagnostic value of C.A.T. and ultrasound in pancreatitis

Number of examinations: 36	- normal:	17	
	- pancreatitis:	19	
	(1) C.A.T.	(2) Ultrasound	Combination (1) and (2)
False positive	0/17	1/17	1/17
Agreement - normal	13/17	11/17	15/17
- pancreatitis	14/19	12/19	17/19
False negative	2/19	5/19	1/19
Inconclusive	7/36	7/36	1/36

On the basis of our limited sample the comparison between C.A.T. and the upper gastrointestinal X-ray series points toward a larger number of incorrect diagnoses with the latter method (Table 4).

With ultrasound, we also found somewhat more false negatives and false positives than with C.A.T. A combination of both methods enabled us to increase the rate of correct diagnosis (Table 5).

Conclusions

C.A.T. is a good technique for visualisation of the pancreas! The success rate in our series was 85%. We encountered no false positive results.

In detecting pseudocysts the results were excellent.

Similar results to those of conventional X-ray technique were obtained in the diagnosis of chronic calcified pancreatitis. In the non-calcified form the method permits the visualisation of a decrease of the volume of the pancreatic gland, but in cases of local enlargement the differentiation from a neoplastic process is difficult.

In acute pancreatitis a diffuse or local enlargement is generally observed.

References

1. HAAGA, J.R., ALFIDI, R.S., ZELCH, M.G., MEANY, T.F., BOLLER, M., GONZALEZ, L., JELDEN, G.L.: Computed tomography of the pancreas. Radiology 120, 589-596 (1976).
2. HOWARD, J.M., NEDWICH, A.: Correlation of the histologic observations and operative findings in patients with chronic pancreatitis. Surgery, Gynecology and Obstetics 132, 387-395 (1971).
3. KREEL, L.: Preliminary evaluation of the EMI whole body scanner. Journal Belge de Radiologie 59, 267-280 (1976).
4. STUBER, J.L., TEMPLETON, A.W., BISHOP, K.: Sonographic diagnosis of pancreatic lesions. Amer. J. Roentgenol. 116, 406-412 (1972).

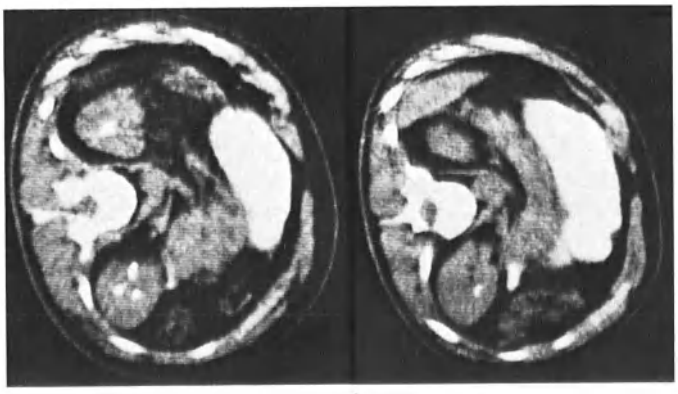

a b

Fig. 1a and b. Acute pancreatitis. Right lateral decubitus position. Note diffuse enlargement of head, body and tail of the pancreas

Fig. 2

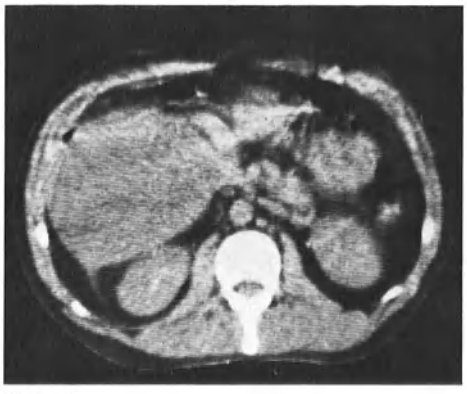

Fig. 3

Fig. 2. Chronic pancreatitis. Right lateral decubitus position. Presence of multiple calcifications in enlarged head of pancreas

Fig. 3. Pancreatitis with pseudocyst. Presence of a large rounded low density (delta numbers 20-25) mass in left hemiabdomen, situated anterior to left kidney. Note linear streak at dorsal side running through the retroperitoneal fat tissue in direction of left psoas muscle which may be due to enzymatic fat dissection along prexisting anatomical fascial planes

Oncology

The Whole Body C.A.T. Scanner and the Oncologist

S. Dische*

My task is not to talk of the interesting new shapes, all in shades of grey, revealed by the whole body scanner, but to give some impression of the effect of its presence upon patient management in oncology.

The clinician looks to the radiologist for aid with regard to:

1. Initial diagnosis of malignant disease

2. The extent of

a) the primary tumour
b) the immediate spread
c) regional metastases
d) distant metastases

3. The response to treatment, particularly after radiotherapy and cytotoxic chemotherapy

4. The detection of recurrence or metastasis in follow-up

Will the body scanner significantly increase the information which the radiologist can give us?

During the past 12 months, Dr. Kreel has detailed his findings using the Northwick Park C.A.T. scanner in our patients with malignant disease, and I shall be quoting extensively from his reports. Patients presenting certain tumours or problems were referred to Dr. Kreel at Northwick Park and we have attempted to compare the contribution of the body scanner in association with and in comparison to other methods of investigation. We determined not to be too easily swayed by an exciting new piece of equipment, but to be cautious in modifying management because of the findings in these early days when experience is being gained.

The body scanner seemed likely to contribute knowledge in patients with testicular tumour, and all eight newly presenting cases seen in a 9-month period were studied at Northwick Park by the scanner as well as by lymphography.

The first patient presented in August 1975 with a history of a swelling of the left testis of 5 months duration. He was otherwise a fit man of 38 years. An orchidectomy was performed and the histology was seminoma. The lymphogram showed some abnormalities, but no definite evidence for the presence of deposits in para-aortic nodes; but the body scan showed evidence for nodes extending from L4 up to D12. In addition to this valuable information, there were changes in the seventh and eight dor-

*Regional Radiotherapy Centre, Mount Vernon Hospital, Northwood, Middlesex, and Northwick Park Hospital, Harrow, Middx.

sal vertebrae arousing the suspicion of metastasis. Conventional radiographs of this area showed normal texture of the bones. He was given radiotherapy to all the nodes from the left inguinal region up to the left supraclavicular fossa. He was perfectly well in follow-up and at the beginning of June 1976 repeat C.A.T. was performed. There was now no evidence of enlarged nodes in the para-aortic region, but the bony abnormalities seen previously were even more clearly seen. Shortly after this the patient complained of pain across the lower neck and in the right shoulder, and an isotope bone scan gave dramatic evidence for multiple bony deposits. Conventional radiographic examination of the skeleton still showed no abnormality. His condition rapidly deteriorated and he was admitted to hospital for intensive chemotherapy, but died. A post-mortem showed multiple small metastases throughout the vertebral column.

In this case the body scanner showed at presentation secondary nodes in the para-aortic region not defined in the lymphogram. There was at that time no change in the X-rays of the dorsal spine to suggest any metastases being present. It took 9 months for symptoms to develop and for confirmation of the diagnosis. It might have been possible in his case to have commenced cytotoxic chemotherapy at a much earlier stage, but we were at the time sceptical as to the true significance of the body scanner findings in the spine.

The second patient with testicular tumour actually presented with pain in the back going down the right leg and the only positive finding initially was a node above the left clavicle. Histological examination of this showed an anaplastic tumour compatible with testicular origin. On questioning he did report an alteration in the relative size of his testes. There was much resistance in the epigastrium and although a mass could not be defined because of this we felt that there were many nodes in the para-aortic region infiltrating the lumbar nerve roots on the right side to give the pain in the leg. Lymphogram and intravenous pyelogram gave clear evidence of metastatic disease in the aortic nodes, but the true extent was dramatically shown using the body scanner. The scanner also showed bony deposits at a time when conventional X-rays and isotope bone scan showed no abnormality and also a number of small subpleural rounded lesions which were thought to be metastatic deposits. The patient was treated with cytotoxic chemotherapy and radiotherapy. The two follow-up scans were performed at 3 and 7 months. They showed resolution of the pulmonary lesions and considerable regression of the para-aortic nodes.

Here the scanner gave fuller information about the extent of massive para-aortic node involvement. It revealed small bony and pulmonary deposits not shown in any other way. The radiotherapy was planned with greater precision because of the knowledge revealed, and regression of tumour was monitored in follow-up studies.

In another case where lymphogram and body scan showed para-aortic nodes, the scan also revealed a node high in that region beneath the crura of the diaphragm at the level of D10, a most inaccessible position for any other type of investigation. It is, however, an important level for the radiotherapist, for he tends to make this the juncture of the fields of treatment for chest and abdomen - there is always risk of a gap or a low dose area just at this site.

The findings in the eight patients presenting testicular tumours are summarised in Table 1. With regard to para-aortic node involvement, it can be seen that in four cases information gained by lymphography and by body scan was similar. In two cases (3 and 8) no abnormal nodes were demonstrated by either test; in case 7 both revealed the presence

Table 1. Detection of metastasis in testicular tumours

Case No.	Histology	Para-aortic nodes		Lung and mediastinum		Bone	
		Pyelogram Lympho-gram	Body scanner	Radiographs Tomograms Lymphogram	Body scanner	Radiographs Isotope bone scan	Body scanner
1	Seminoma	?	+	-	-	-	+
2	Anaplastic teratoma	++	+++	-	+	-	+
3	Meso-thelioma	-	-	-	+	-	-
4	Anaplastic teratoma	+	++	+	++	-	-
5	Seminoma and ana-plastic teratoma	?	?	-	-	-	-
6	Anaplastic teratoma	+	++	-	-	-	+
7	Seminoma	+	+	-	-	-	+
8	Anaplastic teratoma	-	-	?	+	-	+

of secondary nodes while in case 5, both showed some nodal abnormality, thought not to be of significance. In the remaining four cases considerably greater information was gained with the body scan. In one the lymphogram result was equivocal, whereas the scan clearly showed involved nodes - our first patient, already described. In the remaining three, a greater impression of the full extent of secondary tumour in the para-aortic nodes was gained. It is important to note with regard to the para-aortic nodes that in no case did the lymphogram give us information that was not demonstrated by the scan, while the scan in half the cases gave greater information than was revealed by the lymphogram.

Looking at the lung or mediastinum, there was no sign by any method of examination of disease in this area in five of the eight cases. In one, our second case described, there was evidence of small lung deposits on the scan not revealed by other radiological techniques. In case 4 both radiographs and body scan showed pulmonary deposits, but these were revealed in greater number and with greater clarity by the scan. In case 8 there was equivocal evidence for nodes in the mediastinum by lymphogram but clear evidence for their presence by body scan.

If we turn to bony deposits, we find that in no case was there any evidence at initial presentation for bony metastases by conventional radiography. However, in five the body scanner has given evidence suggesting their presence. With the first two patients, the clinical course has fully confirmed the correctness of this diagnosis. We are closely following the other three patients, who have been rather more recently studied.

The body scanner appears to be making a major contribution to the investigation and management of our patients with testicular tumour.

The body scanner seemed likely to make a contribution in the investigation of the malignant lymphomas. The Regional Centre for Radiotherapy and Oncology at Mount Vernon gathers a large number of such cases from the 2 million population it serves. Over 50 cases presenting to my colleagues and myself have been studied by Dr. Kreel at Northwick Park and the results are at present being analysed. Some individual case histories can illustrate the contribution which the scanner appears to be making.

A boy, 8 years old, presented in January 1976 with a 6-week history of a lump in the left groin. A large mass of femoral and inguinal nodes was found and biopsy excision of one performed. A malignant histiocytosis - a highly malignant form of non-Hodgkin's lymphoma - was the final histological diagnosis. When we saw him, examination showed a fit boy with a recent scar in the left groin. There was an obvious mass above and below the scar, tumour appearing to extend into the left iliac fossa. Apart from a slight upper abdominal distension, no other abnormality could be found. Blood studies gave results within normal limits. Right iliac bone trephine showed no sign of tumour.

A lymphogram showed lymphocyst in the upper part of the left thigh with an obstruction above considered to be due to the recent surgery. Some altered pattern was noted in the right external iliac lymph nodes, but this was considered of dubious significance. No evidence of aortic node invasion was seen.

Displacement of the left ureter in the pyelogram showed that the mass in the left pelvis was extending higher than could be palpated. The scan showed the nodes in the left pelvis that were palpable clinically, but also aortic lymph node involvement at the level of L1 and L2. A surprise finding was an enlargement of the medial aspect of the spleen which in fact compressed the left kidney. Metastases in bone were also demonstrated. We decided that in view of the widespread disease cytotoxic chemotherapy was the first line of treatment. He has now completed six courses of combination chemotherapy, the agents including cylophosphomide, adriamycin, vincristine and prednisone. Clinically, all disease has regressed - none can be detected by examination in the clinic or by routine radiography. A scan, however, repeated six months after the original, gave a mixed picture. Certainly the nodes in the left pelvis appeared to have completely regressed but there was evidence for residual disease in the para-aortic area and although the spleen was smaller it remained considerably enlarged. The bony metastases were again demonstrated. In the light of this information it was decided to pursue further chemotherapy and five more cycles are planned after which we will repeat the body scan, as an important part of the review of management. Determination of the extent of disease and the monitoring of the response to treatment have been much aided by the body scanner in the case of this small boy.

Detection of recurrence of Hodgkin's disease often presents considerable problems as, or course, does its management once further disease is proven. A girl of 23 years first received radiotherapy to the nodes in the upper half of her body and later to those in the lower half when disease was proven there 2 years later. All went well, but in the following year she complained of pain high in the epigastrium. The only clinical abnormality was some resistance in this area. When a patient has been treated in this fashion we take great care not to over- or underlap our fields of treatment for fear on the one hand of radiation damage in spinal cord or bowel, or on the other of leaving an area untreated. This is the same problem we have considered with testicular tumour. If symptoms and signs develop later on related to this borderline area it is vitally important to determine whether post-radiation change

or recurrence is responsible. It is an extremely difficult area to visualise by any radiographic technique and even at laparotomy it may not be possible to see all that is going on up to the level of the diaphragm. The girl has already undergone laparotomy and splenectomy prior to the irradiation of the lower-half nodes. The scan however showed clearly the presence of recurrence of Hodgkin's disease. We have been able to bring this girl through six courses of intensive chemotherapy and now a repeat scan shows no evidence for disease.

A case of recurrence presenting different problems was that of a girl of 21 who presented in May 1974 with a 2.5-year history of a lump in the right neck. The histology was nodular sclerotic Hodgkin's disease. Radiographic examination of the chest showed an anterior mediastinal group of nodes and lymphography revealed nodal invasion in all the areas from inguinal to para-aortic region. Laparotomy and splenectomy was performed. The spleen was histologically involved, but the liver and bone marrow were free.

It was decided to treat by chemotherapy using nitrogen mustard, procarbazine, vincristine and prednisone. After six courses there was still radiologically some residual disease in the chest and para-aortic areas, as well as clinically the right neck, so four more were given. When these were finally completed in October 1975 there was no evidence of disease. We were pleased with her progress and no further chemotherapy was planned.

In May 1976, however, a node become palpable in the left lower neck, and a chest X-ray showed evidence for mediastinal and hilar gland enlargement. A lymphogram was performed at Northwick Park and showed no evidence for pelvic or para-aortic node enlargement at this time, but a body scan showed enlarged nodes not filled with contrast media in the para-aortic region from D11 to L3. Several vertebral bodies showed areas of increased density which were thought possibly to represent deposits. The enlarged mediastinal hilar nodes observed in the chest X-ray were clearly seen. It was decided that now we should use radiotherapy to all areas involved and that intially we should treat the upper half of her body. Because of the extensive mediastinal disease, the amount of lung shielding possible was limited. It was decided to give half of her radiotherapy and then wait an interval for regression to occur, perform another scan, and with its aid restrict the volume for further treatment. This plan has been pursued and good regression was obtained, enabling us to reduce the field for treatment. In this case of recurrence there was by lymphography no evidence for para-aortic nodes but clear evidence from the scan. This has also been of great value in clearly defining the mediastinal disease and enabling us to carefully define the volume to be irradiated and to restrict the volume for the final phase of her treatment to the mediastinum and spare a considerable volume of her lung.

We have begun to explore the use of the scanner in the staging of gynaecological tumours, in particular carcinoma of the cervix. It has been interesting to correlate the findings at examination under anaesthesia with those seen on the body scanner in the pelvis. In those studies so far there has been a good correlation. More important perhaps in an area beyond palpation were the demonstration of common iliac nodes and even more so the infiltration of the psoas muscle from them. Although the nodes were shown by lymphography, such extension was of course not revealed. Gross invasion of para-aortic nodes was seen in one patient treated 2 years previously for a stage III carcinoma of cervix. Invasion of the underlying lumbar spine was dramatically shown, but this was also by the time of this examination revealed by simple radiography. We are exploring the relative merits of lymphography and

body scanner in the detection of para-aortic nodes in carcinoma of the cervix.

Turning to other tumours, we have investigated two patients presenting similar problems who have both been treated previously for carcinoma of the bladder, by radiotherapy and then by cystectomy.

After a period of 2 years when all was going well, the patient first reported haematuria, some swelling of the right leg, which later subsided and left loin pain. The pyelogram showed a curious irregularity of the left ureter. Under anaesthesia there was some resistance in the left para-aortic area and we suspected the presence of secondary nodes. A body scan initially showed no definite evidence for recurrence. At laparotomy however, after division of considerable adhesions, an enlarged para-aortic node was found on the left side adherent to the ureter and left kidney. Biopsy showed a fairly undifferentiated carcinoma compatible with bladder origin. When Dr. Kreel re-examined the scan he did demonstrate an opacity smaller than expected but at the site of the nodes.

In the second case, where the interval after surgery was 18 months, the patient returned with swelling of both legs and some disturbance of bowel function. Examination under anaesthesia showed a resistance in the lower para-aortic area possibly due to nodes and some diffuse pelvic induration. An inferior vena cavagram performed at Northwick Park showed evidence of obstruction at the lower end of the inferior vena cava with a gross collateral circulation. The scan showed that this was due to large masses of secondary tumour. The findings were confirmed by laparotomy and biopsy. With courses of radiotherapy, in both cases some palliation has been achieved.

Our knowledge as to tumour involvement of the posterior abdomen in all types of malignant disease will surely be furthered as experience is gained.

In malignant disease a strong clinical suspicion for recurrence is usually followed by confirmation but in a considerable number of cases when investigations are complete recurrence of tumour is not responsible for new symptoms and the prognosis is, of course, much altered..

A man, aged 73, underwent an abdominoperineal resection for carcinoma of the rectum 3 years previously. It was a poorly differentiated adenocarcinoma, penetrating the muscle coat, and when he presented in February 1976 complaining of severe pelvic pain of 4 months duration a local recurrence in the pelvis seemed more than likely. Clinical examination, however, showed a fit man and no masses could be found even under anaesthesia. An intravenous pyelogram showed bilateral hydronephrosis with the site of obstruction on the pelvic brim. In the body scan no evidence for any mass in the pelvis could be found. In these circumstances exploration seemed justified. At laparotomy there was only fibrosis in the pelvis to account for the ureteric compression. Unfortunately, as yet symptomless hepatic deposits were discovered. At least in his case he was saved a needless and useless course of radiotherapy to the pelvis in the treatment of a local recurrence which had not apparently occurred.

Looking once again at the list of ways in which we ask for help from the radiologist, we can see that the whole body scanner is showing great promise as an investigation of value in patients with malignant disease. The scanner has proved most helpful in determining the extent of primary tumours and of their immediate and regional metastatic spread. Distant metastases, small in size, have been demonstrated in

lung, lymph nodes and bone where other investigations have yielded normal results. Of special importance is the discovery of bony deposits at a time when radiographs of the skeleton and the isotope bone scan yield normal results, and this may well have fundamental influence upon the approach to treatment in many patients. We have already seen this in patients with testicular tumour and with lymphomas; full investigation of other types of malignant disease may reveal similar findings.

Much help has been given in the careful planning of treatment and valuable data as to tumour response has been obtained. In oncology, it may well be that with the whole body scanner more information will be obtained than with any other single or combination of studies which the radiologists may employ upon our patients. It is possible that in some situations the body scanner may permit us to simplify the investigation and dispense with other procedures such as lymphography; on some occasions a patient may be spared a laparotomy. We need to make a careful assessment of those situations in oncology requiring investigation so as to fully compare the findings with the body scanner with those of the alternative methods of study.

We can conclude that the body scanner would seem likely to further knowledge as to disease in many individual cases and also to further fundamental knowledge as to tumour growth and response to treatment. We ought however, carefully to assess and report the benefit given to those unfortunate individuals who suffer malignant tumours so that the community as a whole can decide whether its resources should be used to provide such units.

C.A.T. of the Lymphomas

C.A.T. Scanning in Lymph Node Disease

L. Kreel*

The evaluation of the extent of disease in lymphoma and testicular tumour patients by computerised tomography has proved to be a most valuable contribution in patient management. The present paper is devoted mainly to cases of lymphoma and melanoma, but a small number of other cases are also included mainly because of their individual interest (Table 1).

Table 1.

Diagnosis	No. of cases	No. of scans	No. of lymphangiograms
Lymphoma	35	43	32
Reticulum cell sarcoma			
a. Stomach			
b. Failed exam	2	1	2
Myeloid leukaemia	1	1	0
Melanoma	6	6	6
Retroperitoneal or soft tissue sarcoma	3	5	0
Carcinoma - bladder or penis	3	4	1
	50	60	41

Material and Methods

The findings on all cases of histologically proven lymphoma of whatever type and of melanoma referred for computerised tomography were reviewed. Particular attention was given to features not demonstrated by other radiological examinations and more specifically to comparison with the findings on lymphangiography (Table 2). This was done as a retrospective study for the obvious reason that there was no real way of predicting in which cases the C.A.T. findings would add additional information.

For purposes of this study, lymph nodes were considered to be enlarged on C.A.T. scanning only when the findings were unequivocal. Where there has been any doubt about the interpretation the finding has not been included in the positive groups, and therefore at this point in time it is not possible to make an assessment of the false positive or false negative results. This is thus a crude analysis of the unequivocally positive findings, mainly to show which signs are likely to be encountered an their relative frequency.

*Division of Radiology, Clinical Research Centre and Northwick Park Hospital, Harrow.

Table 2.

All cases (lymphoma, melanoma, miscellaneous) Lymphangiogram negative or positive		Extra nodes in abdomen
(i)	Pelvis	2
(ii)	Common iliac and para-aortic up to L2	1
(iii)	Para-aortic above L2	13
(iv)	Mesenteric	5
(v)	Paraspinal (post diaphragmatic)	1
(vi)	Porta hepatis	1
Extra-nodal disease		
	Soft tissues	
	Liver	4
	Spleen	3
	Other	1
	Bone	11
Thorax		
	Retrosternal nodes	5
	Medistinal nodes	11
	Thymus	3
	Lateral inner thoracic wall	1
	Axillary nodes	5
	Pulmonary nodules	3
	Pulmonary 'infiltration'	3
	Pleural effusion (s)	1
	'Pulmonary oedema'	3
	Hypostatic pulmonary change	3

Some of the patients have been scanned more than once to assess their response to treatment. In two cases brain scans only were performed, but these are not included in the statistics. No attempt has been made to assess the value of axillary palpation against C.A.T. scanning.

The incidental findings are included even though these may have been shown by other means or were irrelevant to the management of the patient.

Bone densities were considered to be metastases only when they were greater than 0.5 cm in diameter and not recognisable as normal variants or incidental abnormalities such as calcified Schmorl's nodes. This is at present a rather subjective assessment, but detailed studies are proceeding to resolve this point.

Results

Lymphoma Cases (Table 3)

Forty-four C.A.T. examinations were performed on 37 patients. Additional lymph nodes not shown by lymphography were seen in 13 cases and in most of these were above the level of L2. Mesenteric nodes were detected in 5, retrosternal nodes in 6 and the thymus was assessed as

Table 3. Lymphoma and first degree lymph node disease

Number of cases	37
Number of scans	44
Extra-iliac and para-aortic nodes	13
Mesenteric nodes	5
Retrosternal nodes	5
Thymus infiltration	4
Liver second degree	4
Bone second degree	10
Axillary nodes	4

being involved in 3 patients. Liver metastases were seen in 4 patients, the spleen was enlarged in 3 and bone metastases diagnosed in 10, while axillary nodes could be seen in 4 cases.

C.A.T. Signs of Lymphoma Disease - Lymph Node Enlargement

Abdomen

Pelvis. A group of enlarged lymph nodes in the pelvis shows as a soft-tissue mass along the lateral wall of the pelvis lying on the ilio-psoas muscles. Within this mass there is often a small number of lymph nodes containing contrast medium if a lymphogram had been performed previously. The lymph node masses will displace adjacent bowel especially rectum and sigmoid colon if unilateral or if bilateral, compress adjacent bowel (Fig. 1). In lesser degrees of lymph node enlargement, a smaller rounded soft-tissue mass in the line of the iliac vessels is seen on the C.A.T. scan.

Common Iliac and Para-aortic Region up to L2. In only one case examined to date has it been found that when common iliac or para-aortic lymph nodes are obviously abnormal no additional lymph node enlargement has been shown in the area. The same, however, does not apply to lymph node enlargement above the level of obstruction to the flow of contrast or to 'non-visualised' lymph nodes. (The latter being defined as 'absent' lymph nodes when compared with the contralateral group.)

Para-aortic Lymphoma above L2. In 12 of the 35 patients who had lymphograms additional nodes were shown above the level of L2 on the C.A.T. scans. In these cases only a very small part of the lymph node mass showed contrast medium in lymph nodes, often amounting to no more than 5-10% of the total mass.

In these cases the margins of the inferior vena cava and aorta were lost and the mass itself would spread both laterally and/or anteriorly. Hydronephrosis due to ureteric obstruction occurred in two of these cases.

Mesenteric Group. In five cases obvious mesenteric lymph node masses could also be seen (Fig. 2). Contrast material was not seen in relation to mesenteric lymph nodes and in two cases there was a clear line of demarcation between mesenteric and para-aortic nodes. In this series no case of enlarged mesenteric nodes in the absence of para-aortic node enlargement was encountered.

Discrete Nodal Enlargement. In one case a group of nodes lying around the aorta and inferior vena cava were identified as rounded, discrete structures of soft tissue density.

Porta Hepatis. Localised discrete nodes were also identified in the same patient in the region of the porta hepatis.

Post-Diaphragmatic, Paraspinal Region. Replacement of the adipose tissue by tissue of higher density representing spread of malignant disease was encountered in one patient (Fig. 3).

Thorax

Retrosternal. Enlargement of lymph nodes immediately behind the sternum was encountered in five patients. These nodes show as rounded areas bulging into the medial anterior aspects of the periphery of the lung fields (Fig. 4).

Mid-mediastinal. Enlargement of mid-mediastinal lymph nodes were shown in 11 patients. Mediastinal lymph node enlargement was visible on chest radiographs in 8 of these cases. Contrast medium, after lymphography, was seen in 8 of these on chest radiographs and additonal nodes identified in all of these cases.

Thymus. An anterior mediastinal density having the 'shape of thymus' was encountered in three cases (Fig. 5).

Lateral Thoracic Wall. A soft-tissue mass was shown on the lateral thoracic wall separate from the mediastinum in one case.

Axillae. Enlarged lymph nodes in the axillae were shown in four cases and appeared as a single discrete lymph node, as multiple discrete nodes or as a lymph node mass.

Pulmonary Nodules. Pulmonary nodules shown as small round, well-defined opacities in the lung were shown in two cases.

Pulmonary 'Infiltration'. Opacities running into the lung fields were seen in three patients, all of whom had had radiotherapy.

Pulmonary 'oedema' or 'Hypostatic' Changes. In six patients hazy shadowing in the dependent parts of the lung fields or actual thick band shadows of interstitial oedema were detected. In one case an effusion was detected.

Extra-Nodal Disease

Liver (Fig. 6). Metastases in the liver were shown in four patients, in two as a single, discrete, round 'filling defect' with a density of circa 17 Hounsfield units or as multiple, coalescing areas with ill-defined borders in two cases. In one patient after contrast medium the density of the lesion was circa 38 Hounsfield units.

Spleen. The spleen was grossly enlarged in one patient and moderately so in another. The spleen substance appeared homogeneous with no visible filling defects. In a third case the medial part of the spleen was enlarged and was compressing the left kidney.

Bone. Rounded densities in vertebral bodies were detected, varying in size from 0.25 cm to 1 cm. These dense nodules have not been detected in patients who have been investigated for non-malignant conditions. In 10 cases these densities were found to be greater than 0.5 cm in diameter.

Miscellaneous Observations (Table 4). As mentioned previously, hydronephrosis due to ureteric obstruction by lymph node masses was shown on two occasions. Incidental findings included an ovarian cyst, renal cyst, a pneumothorax, bullous formation and a possible splenic artery aneurysm or spleniculus.

Table 4. Incidental findings

Diagnosis	No. of cases
Hydronephrosis	2
Renal cyst	2
Ovarian cyst	1
Pulmonary bullae	2
? Splenic artery aneurysm	1

Discussion. The introduction of lymphography was a major advance in showing the extent of lymphomatous disease, particularly in the previously hidden area of the abdomen. With time this procedure gained a major role in diagnosis but was, to a certain degree, supplanted by combined laparotomy, splenectomy and liver biopsy as a staging procedure.

The initial use of C.A.T. in lymphoma has shown that there are many areas where disease may be present and remain undetected by lymphography. In the abdomen this includes the pelvis, the mesentery, nodes above the level of L2, porta hepatis and retrodiaphragmatic nodes. The surprise is not so much that there are areas of undetected nodes on lymphography but the large size of these masses and the small number of nodes within these masses that take up the contrast.

C.A.T. examinations have the added advantage that they also show intrahepatic disease and provide a more accurate method of assessing splenic enlargement.

Additional disease over and above that shown by lymphography was surprisingly frequent. In one-third of patients extra lymph nodes were shown above the level of L2 and in about one-fifth there was evidence of mesenteric node involvement. An added advantage was the ease with which hydronephrosis is detected.

In the thorax the display of enlarged nodes in the retrosternal region and in the axillae has also proved helpful. Another major advantage of C.A.T. is the ability to monitor the effects of treatment. The three-dimensional view of the disease process is of considerable help in radiotherapy planning.

At present certain aspects of diagnosis with C.A.T. scanning must be considered equivocal. This applies particularly to the more minor changes in bone, such as the dense spots found in vertebral bodies particularly when under 0.5 cm in size. In a number of cases the larger densities have subsequently been shown to represent metastases. Further information on this point is likely to be forthcoming as patients have follow-up examinations and as the results in other conditions such as breast carcinoma emerge.

Similarly, the delineation of densities in the mediastinum which appear to be the thymus and the finding of small nodules in lungs will require final confirmation. Thus the C.A.T. scanner has made the problem

of radiological-pathological correlations even more acute, pointing the way to many future studies.

However, in some cases, even with obvious bone involvement, further information may become available on computerised tomography, as in one case where not only was the soft tissue mass in front of the sternum and the bone erosion defined but also the extension into the retrosternal space (Fig. 7).

The experience with the other tumours mentioned in this paper is much more limited. Nevertheless, some observations are warranted. Retroperitoneal masses other than lymph nodes have also been demonstrated. Retroperitoneal sarcoma, although a relatively uncommon tumour, is so well displayed that it is worth a special mention.

The appearances in the lung fields suggesting hypostatic changes, alveolar pulmonary oedema and interstitial oedema will also require further elucidation. This is under active investigation but will almost certainly take longer to solve than the bone changes.

Summary and Conclusions

Computerised tomography undoubtedly shows enlarged lymph nodes not demonstrated by other diagnostic methods, thus providing a more complete appraisal of the extent of lymphomatous disease in both the abdomen and thorax. This is extremely valuable in planning treatment and in monitoring the effects of such treatment. Present knowledge of the radiological appearances of lesser grades of lymphomatous disease is deficient and will need rapid expansion if computerised tomography is to be used to its maximum advantage.

Acknowledgements

Grateful acknowledgement is made to the Department of Health and Social Security whose far-sighted and generous help has assisted greatly in the development of this project. The assistance and considerable help from Mr. John Twydle, who has been managing the machine, is also gratefully acknowledged.

Fig. 1. Lymph node enlargement deep in pelvis in a patient with bladder carcinoma. Only a very small amount of contrast medium is present in relationship to the lymph node masses

Fig. 2. Enlargement of para-aortic (P-a) and mesenteric (M) lymph nodes. No contrast medium is taken up by the mesenteric nodes

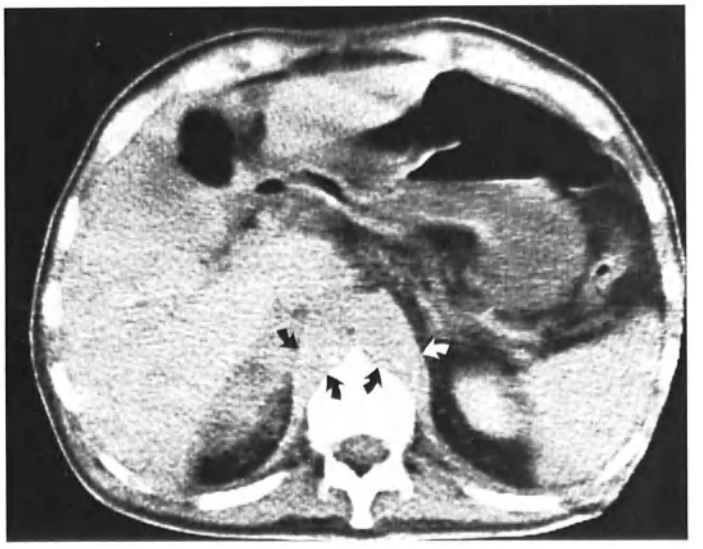

Fig. 3. Enlarged nodes behind diaphragm, obscuring aortic margin

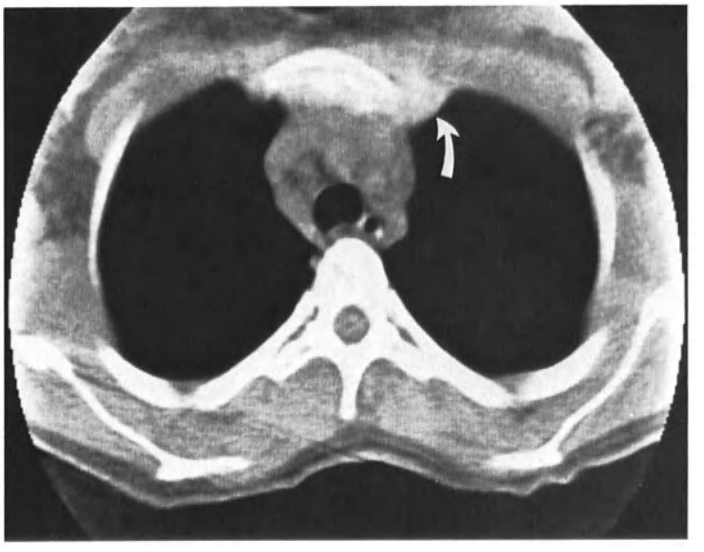

Fig. 4. Enlarged retrosternal and mediastinal nodes

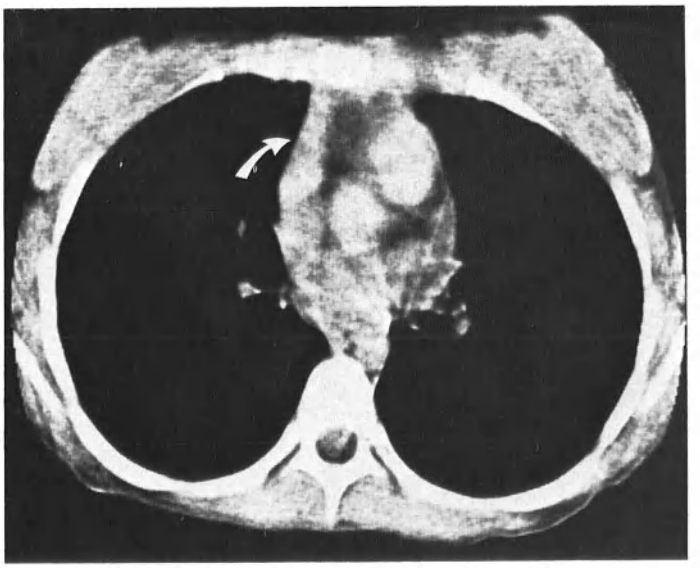

Fig. 5. Infiltration of right lobe of thymus

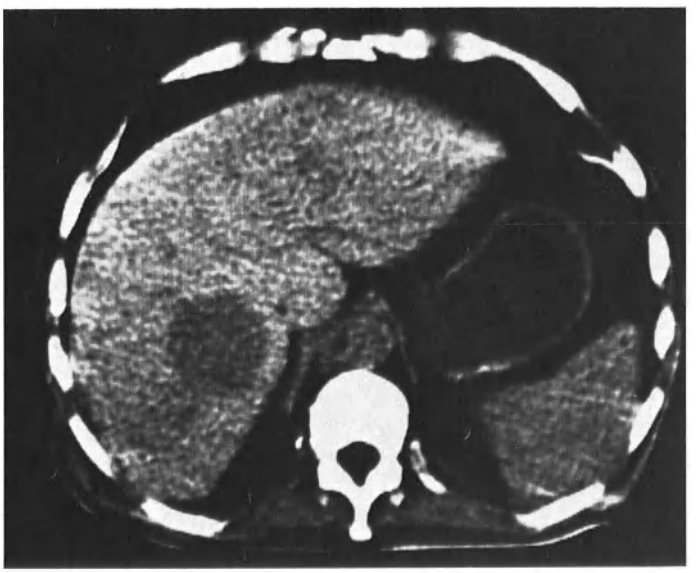

Fig. 6. Lymphoma metastasis in liver

Fig. 7. Presternal mass eroding bone; there is in addition a retrosternal mass

Evaluation of Normal and Abnormal Lymph Nodes at Computerised Tomographic Scanning of the Abdomen and Pelvis

H. C. Redman*, W. A. Federal*, R. A. Castellino**, and E. Glatstein*

Lymphography is a well established procedure for evaluation of the para-aortic nodes and is very accurate in staging lymphomas and in the detection of gross nodal metastases. Ultrasound is useful as a survey technique for massive para-aortic adenopathy and can sometimes detect isolated enlarged nodes or groups of nodes in other areas of the abdomen. The development of computerised tomographic (CT, C.A.T.) scanning has presented the diagnostician with an entirely new means to demonstrate lymph nodes. In theory, C.A.T. should be capable of demonstrating nodes in the mesentery and in the hepatic portal and splenic hilar regions, which are not visualised at lymphography and are not consistently evaluated at ultrasound. If such nodes could be demonstrated and abnormalities reliably detected, then C.A.T. scanning would clearly have a significant role in the staging and treatment planning of several neoplasms.

In conjunction with the Department of Radiology at Stanford Medical Center, a study has been undertaken to determine the role of C.A.T. in the staging of Hodgkin's disease and lymphomas. In addition, a series of abdominal scans has been evaluated to determine how often lymph nodes can be identified in the abdomen and pelvis.

Material and Methods

Patients being staged for Hodgkin's disease and lymphomas at Stanford University Medical Center were referred for C.A.T. scanning of the abdomen and upper pelvis. The C.A.T. scans were performed on a prototype ACTA scanner. Scanning time for each pair of 7.5 mm sections was 4.5 or 5.5 min. Scan pairs through the liver and spleen were performed at 2 cm intervals and those through the remainder of the abdomen and upper pelvis, at 3 cm intervals. Intravenous contrast medium was used in most patients to demonstrate the ureters; glucagon, 2 mg/i.m. was used to decrease peristalsis when needed and some patients were studied in the prone position to decrease respiratory motion. All patients underwent lymphography either prior to or following the C.A.T. scan. All also underwent coeliotomy with multiple liver biopsies, splenectomy and para-aortic node biopsies. The hepatic hilus and pelvic nodes were explored, but not routinely biopsied.

A series of 50 recent C.A.T. scans of the pelvis and abdomen was reviewed to determine: (1) if normal nodes could be identified, (2) the frequency of such identification, (3) the factors influencing such identification.

---

*Dept. of Radiology, Mt. Zion Hospital and Medical Center, San Francisco.
**University of California Medical Center, San Francisco.
***Department of Radiology, Standford University Medical Center, Palo Alto, California.

Results

In the 20 patients with Hodgkin's disease or a lymphoma in whom complete data was available, the liver was called normal in 18 at C.A.T. and this was confirmed at surgery. One patient had a low-density mass in the left lobe of the liver at C.A.T. which was found to be a benign fibrous nodule at surgery, and one had diffuse lymphomatous involvement which was not seen at C.A.T. Enlarged hepatic hilar nodes were demonstrated in one patient at C.A.T.; at coeliotomy, the patient had extensive abnormal nodes throughout the entire abdomen. Normal hepatic hilar nodes were not routinely identified at C.A.T. scanning.

One patient had had a prior splenectomy for trauma. In the remaining 19, the spleen was called enlarged at C.A.T. scanning in 4; these spleens weighed more than 275 gm at splenectomy. The remainder of the spleens weighed less than 217 gm. Nodules, measuring from 0.1 to 2.5 cm, were found pathologically in seven spleens. Nodules were seen at C.A.T. scanning in 4 of these patients, the smallest measuring about 1 cm. Abnormal splenic hilar nodes were not observed at C.A.T. scanning, though normal nodes were felt to be demonstrated in 6 patients. Splenic hilar nodes containing tumour were found at surgery in only 1 patient. These were not enlarged.

Para-aortic nodes and nodes in the upper pelvis were evaluated in all 20 patients (Fig. 1). The C.A.T. examination generally did not include the lower iliac and inguinal nodes. Lymphograms had been performed on 12 patients prior to C.A.T.; the remainder had the lymphogram later. In 16 patients the C.A.T. and lymphographic findings were in agreement. Pathological confirmation was available for 15 of these; in the last the precise nodes called abnormal at C.A.T. scanning and by lymphography were not the nodes which were biopsied. One C.A.T. scan was said to show adenopathy, but the nodes, though up to 2 cm in size, were normal at lymphography and pathology. Two patients were called normal at C.A.T. scanning, while lymphography and pathology demonstrated normal sized nodes containing tumour. In one case, both the C.A.T. scan and the lymphogram were called normal, but at coeliotomy unenlarged lymph nodes revealed lymphoma. In 2 patients, low pelvic nodes were abnormal at lymphography, but were not evaluated at C.A.T. scanning. The remainder of the studies in thse 2 patients were in agreement.

Mesenteric nodes could not be identified at C.A.T. scanning in any of the 20 patients. At laparotomy, 2 patients had mesenteric nodes which contained lymphoma.

The review of the last 50 pelvic and abdominal scans in which no nodal abnormality was expected, revealed that normal nodes were seen in the para-aortic region in 30 of the 40 abdominal scans and in the pelvis in 10 of the 15 cases in which this area was scanned. Normal nodes were felt to be identified in 7 patients in the splenic hilum and in three in the liver hilum. Mesenteric nodes were not identified.

Discussion

The actual frequency of liver abnormality in this series is 10%. Therefore, the precise role of C.A.T. in the evaluation of lymphomatous involvement of the liver cannot yet be defined. The 5.5 min scanner used in this study limits the size of an hepatic abnormality which can be demonstrated, since respiratory motion will obscure small lesions of

slight tissue density difference. Suspended respiration scans should regularly demonstrate nodules of less than 1 cm in size, thereby aiding surgical biopsy. Enlarged hepatic hilar nodes can be demonstrated with current C.A.T. scanning equipment. Normal nodes are sometimes seen but are difficult to differentiate from portal vessels.

Nodules in the spleen were seen when they were greater than 1 cm in size. Once again, suspended respiration scanning should markedly improve the demonstration of smaller nodules. Determination of splenomegaly was accurate at C.A.T. scanning. The criteria used for spleen size were projection of the spleen well anterior to the lumbar aorta, spleen size determination should be ultimately possible with C.A.T. Splenic hilar nodes can be seen at C.A.T. scanning. Enlargement, however, is the only criterion for abnormality.

Evaluation of lymph nodes at C.A.T. is primarily dependent on size. Internal architecture and small filling defects cannot be detected with the present equipment. In patients studied following lymphography, an unusual configuration of the opacified nodes suggested internal pathology, but the type could not be defined. Nodal evaluation was difficult in the thin patient, probably because of the absence of fat separating the nodes from other retroperitoneal structures. Abnormal nodes do not invariably obliterate fat planes, however.

In this study enlarged nodes could be seen cephalad to the cisterna chyli and involvement of hepatic hilar nodes was demonstrated once. Prior to exploration, therefore, C.A.T. can give additional information about upper abdominal nodes which is not available by other modalities.

The demonstration of the extent of adenopathy is also more complete with C.A.T. than at lymphography, and this may have a future practical application in planning the radiation therapy field. In patients with extensive nodal involvement, the cross sectional C.A.T. scan can demonstrate abnormal nodes dorsal to those opacified at lymphography.

The fact that normal nodes can be identified in 75% of abdominal C.A.T. scans and 66% of pelvic scans suggests that more sophisticated computer programs may permit evaluation of intrinsic nodal architecture in the future. Nodes are difficult to identify in very thin patients and in those with extensive peristaltic artefacts. Those in the pelvis are more difficult to identify with certainty than those in the para-aortic region. Normal nodes in the hepatic and splenic hila proved difficult to differentiate from blood vessels. Absence of contrast medium enhancement during an intravascular infusion is useful in making this distinction. Our current inability to identify mesenteric nodes is disappointing. With suspended respiration scanning and better resolution of structures at the mesenteric root, this may become possible.

Abdominal C.A.T. also provides information that might not be obtained in the usual staging work-up. In one patient, a diffusely enlarged pancreas was demonstrated which was felt to be due to chronic pancreatitis at surgery. In the same patient, bony involvement by the lymphoma was seen. Another finding was the fibrous liver nodule already mentioned. Since the entire abdomen is surveyed, renal and upper pelvic abnormalities should be detected.

At present, C.A.T. cannot replace any of the established diagnostic techniques used in staging lymphomas. It does give added information in many cases and has a potential for becoming a primary diagnostic modality when more subtle tissue density differences can be resolved with suspended respiration scanning.

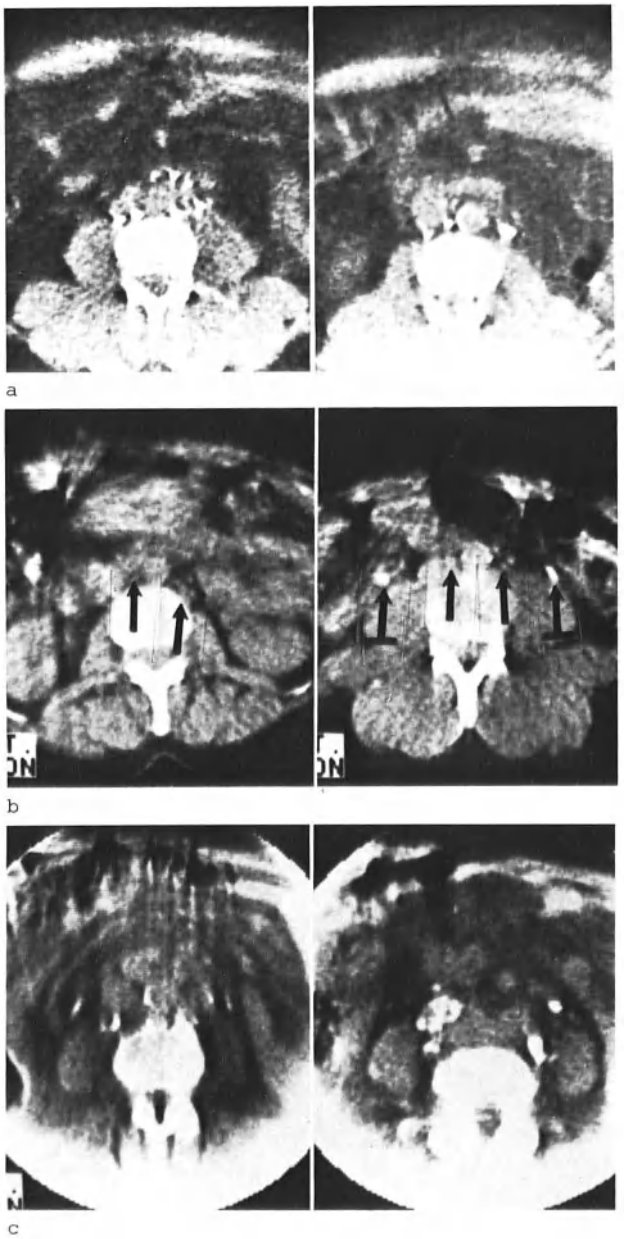

Fig. 1. Normal and abnormal nodes at C.A.T. scanning. (a) Normal nodes following a lymphogram. (b) Normal nonopacified nodes (*arrows*) in two patients. Ureters (*crossed arrows*) are opacified. (c) Abnormal nodes, partly opacified by lymphogram, are partially obscuring the other retroperitoneal structures. (d) A mantle of enlarged nodes (*arrows*) is present ventral to the aorta and inferior vena cava

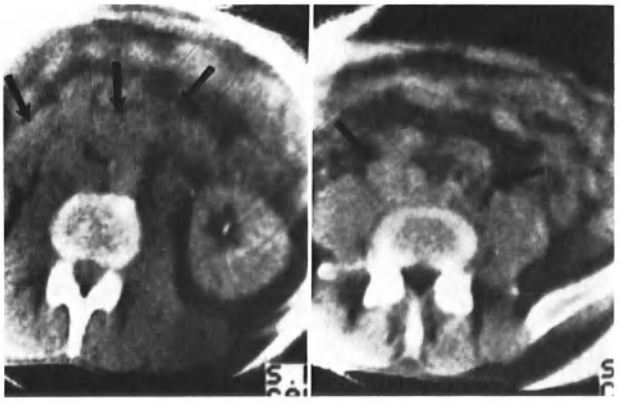

d

"The Manchester Experience"

J. J. K. Best and I. Isherwood*

Introduction

Hodgkin's disease, of all the malignancies, has probably shown the greatest improvement in results and treatment, which can be attributed to improvements in staging. Laparotomy is an essential part of the programme of investigations carried out for staging, but it carries a real risk. It was thought possible that C.A.T. could provide some if not all of the information acquired by laparotomy without the same risk.

The majority of patients with Hodgkin's disease in the North Western Region are seen by members of the Lymphoma Group working in the Manchester teaching hospitals. Most of these patients, amounting to perhaps 100 per year, are being entered into three trials which were started in February 1975.

The first trial (HD1) is for patients with supradiaphragmatic disease, Stage Ia through to II and including IIb, and the second trial (HD2) is for patients with nodal disease on both sides of the diaphragm but without constitutional upset, Stage IIIa. Investigation of all patients in these two trials includes lower limb lymphography followed by a staging laparotomy. This procedure involves sampling of nodes from iliac, para-aortic, mesenteric, coeliac and splenic hilar regions with marking of the biopsy sites by tantalum clips. This is followed by splenectomy, wedge biopsy of the liver and bone biopsy.

The patients entering the two trials are scanned (a) on admission, (b) following lymphography, (c) following laparotomy.

The trial is designed to assess (i) if there are characteristic CT features in lymph glands involved by lymphoma; (ii) if the presence of lymphoma in the liver and spleen, together with mesenteric, coeliac and splenic hilar lymph nodes can be detected; (iii) if scanning following lower limb lymphography will allow evaluation of lymphography in assessing abdominal involvement by lymphoma.

In the first 5 months of 1975 only seven patients were entered into the HD1 and HD2 trials. Because of this samll number the trial with CT scanning was opened to the third Hodgkin's disease trial (HD3), for patients with Stage IIIb and Stage IV disease and the non-Hodgkin's lymphoma trial groups.

---

*Department of Diagnostic Radiology, University of Manchester.

Material and Methods

Patients were referred for C.A.T. using the EMI CT5000 Whole Body Scanner which has been operational in the Department of Diagnostic Radiology in the Stopford Medical School, University of Manchester, since June 1976. All patient referrals were made using a special referral form (Fig. 1). Unless a special request for C.A.T. of another region was made, the examination was limited to the upper abdomen. The patients were scanned lying supine wearing their underclothes and a dressing gown. The patients' arms were either at their sides or above their head. The 32 cm ring was used and the area to be reconstructed not occupied by the patient was filled by bolus bags supported by a restraining strap. The patients were scanned at 140 kVp at normal scan speed (20 s).

The scan levels were measured from anterior anatomical surface landmarks which were assigned numbers arbitrarily, i.e. external auditory meatus = 100, sternal angle = 200, xiphisternal joint = 300, anterior superior iliac spine = 400, pubic symphysis = 500. The scan levels were measured in centimetres to the nearest anatomical landmark and the section coded by that measurement, e.g. 306 indicates a scan 6 cm below the xiphisternal joint.

For the upper abdominal survey in this trial a series of eight scans was made, starting at the level of the diaphragmatic crura and scanning caudally.

In selected patients the scans were repeated following injection of intravenous contrast, sodium iothalamate 420 mg iodine per ml (Conray 420) and 200 ml Gastrografin 5% taken orally. Patients were given either hyoscine butylbromide (Buscopan) 20 mg i.v. or propantheline bromide (Pro-Banthine) 30 mg i.v. at the beginning of each series of scans.

It was sometimes found advantageous to position patients in the lateral decubitus position, left side up.

The position of the patient on the table was recorded carefully and in those patients where the extent of the lesion might be used for radiotherapy treatment planning, the relevant anatomical surface marking was tattooed using sterile artist's pigment and tattooing needle. (Note: eight scans is the limit of one systems disc in the EMI CT5000 Whole Body Scanner.)

Results and Discussion

Forty-seven patients have been examined in the Lymphoma Trial by the end of September 1976. Seven of the patients in the trial fall into the Hodgkin's Trial group. The success of C.A.T. from the beginning of the trial in demonstrating upper abdominal lymph node enlargement and in elucidating the nature of paravertebral masses made it impossible to ignore the implications of C.A.T. on the management of those patients.

C.A.T. may demonstrate:

1. Upper abdominal lymph nodes and their enlargement (Fig. 2)

2. Paravertebral masses in the upper abdomen and dorso-lumbar region (Fig. 3)

3. Bony involvement where evidence of this is not suggested by conventional radiographs (Fig. 4)

4. Prevertebral lymph nodes (Fig. 5)

It may be used to assess:

1. The size and extent of a lesion

2. The progress of the disease, by monitoring the size of known lesions under treatment.

C.A.T. has an immediate and self-evident role in radiotherapy field planning to demonstrate not only the size, position and extent of lesions but also the changing positions of radiosensitive organs.

The method has not been capable of demonstrating any abnormality in the liver and spleen of patients with lymphomatous involvement of those organs except enlargement and in one patient a large metastatic deposit in the liver.

It is intended that the original trial of C.A.T. in patients with Hodgkin's disease should continue to assess its original aims. With the experience already obtained in the trial so far it is recognised that it may prove impossible to characterise lymphomatous involvement of the liver and psleen by intrinsic changes in the appearances of the organs. It is therefore intended to make a special study of (a) the prevertebral space and (b) the anatomy of the splenic hilum.

Because of the unintended but quite necessary influence that C.A.T. has been seen to have in the treatment and management of some patients, it is proposed to assess a simple method of providing information for radiotherapy treatment planning.

Acknowledgments

The authors would like to thank all the members of the Manchester Lymphoma Group and Dr. B. Eddleston, Consultant Radiologist, Christie Hospital, for their valuable assistance; Miss G.S. Lord and The Radiographic staff of the Department of Diagnostic Radiology, Stopford Medical School for their help; Mrs. G.E.H. Shawcross for the preparation of illustrative material and Mrs. M. Tipton for her secreterial help.

UNIVERSITY OF MANCHESTER DEPARTMENT OF DIAGNOSTIC RADIOLOGY

The Medical School, Stopford Building, Oxford Road, Manchester M 13 9 PT

Tel: o61 - 273 8241, extension 61
and
MANCHESTER LYMPHOMA GROUP

COMPUTER TOMOGRAPHY REFERRAL FORM FOLLOWING:-
(Please tick appropriate heading)

1. ADMISSION
2. LYMPHOGRAPHY
3. LAPAROTOMY
4. OTHER

NAME

DATE OF BIRTH

AGE

SEX

HOSPITAL

WARD

WARD NO.

REFERRING HOSPITAL NO.

OUT PATIENT

REFERRING DOCTOR

REFERRAL INFORMATION *(Please use diagram)*

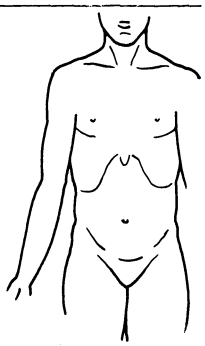

SPLENOMEGALY/SPLENECTOMY

HEPATOMEGALY

LYMPHADENOPATHY

OTHER RELEVANT INFORMATION

SPECIAL REASONS FOR REQUEST

DIAGNOSIS

HISTOLOGY

FOLLOW UP: UNDER INVESTIGATION/TREATMENT

O.P. PERIODIC FOLLOW UP

(Please tick appropriate heading)

SIGNED

DATE

Fig. 1. Referral form

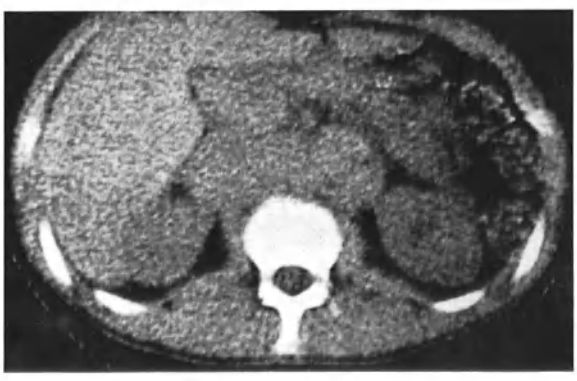

Fig. 2. Enlarged abdominal lymph nodes

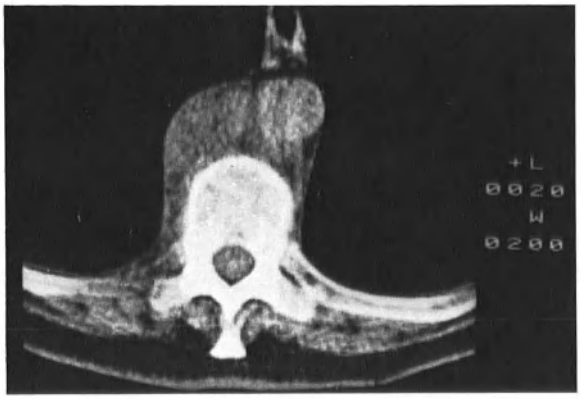

Fig. 3. Paravertebral mass in dorsolumbar region

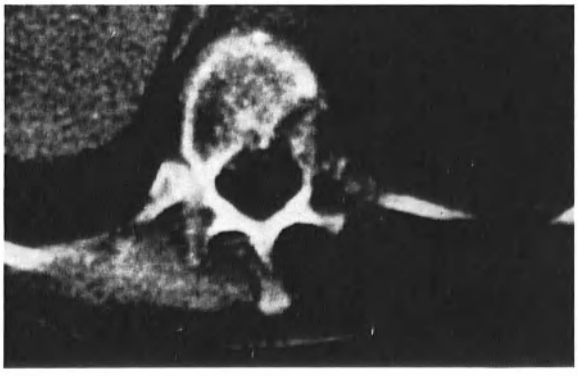

Fig. 4. Bone destruction by lymphoma

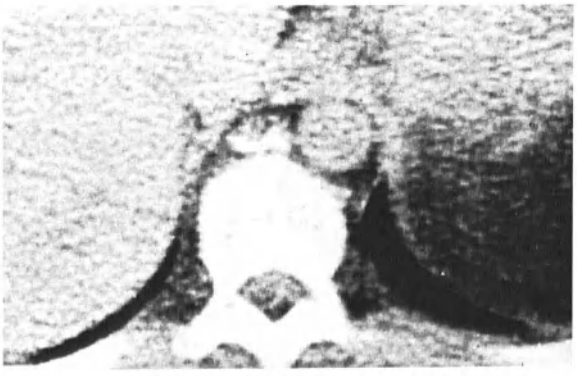

Fig. 5. Prevertebral lymph node

Computed Tomography of the Breast. A Report of a Pilot Study

J. J. K. Best*, D. L. Asbury*, W. D. George***, R. A. Sellwood***, and I. Isherwood*

Introduction

Carcinoma of the breast is an important cause of death in women. The results of a New York survey (13) suggest that population screening gives early detection with consequent improvement in survival figures. The screening consisted of clinical and mammographic examinations. Microcalcification is the single most important conventional radiological sign in the diagnosis of carcinoma of the breast. It may be detected in 30% to 61% of breast carcinomas (3, 7, 13). The success in detection is related to the recording medium, the most successful being xerography with rates of detection approaching and equal to that of histological examinations (9, 13).

The success of computerised tomography (C.A.T.) in detecting changes in tissue attenuation values in normal brain and the pathological changes affecting brain is well known (1). Changes in attenuation values of 1 part in 1000 are detectable (10). The expectation of success in detecting microcalcification using C.A.T. suggested the use of the technique as a screening method for carcinoma of the breast.

The results of the first 30 patients of a pilot sudy of C.A.T. of the breast are presented. The aim of the study is to evaluate C.A.T. as a screening procedure for carcinoma of the breast and to compare the results with conventional mammography of the same patients.

Material and Methods

The patients were referred for C.A.T. scans from a breast clinic at the University Hospital of South Manchester with clinical findings consistent with either malignant or benign breast disease. The patients were scanned the day following clinic attendance and admitted to hospital the next day.

The patients were scanned with the EMI CT5000 Whole Body Scanner which has been operational in the Department of Diagnostic Radiology in the Stopford Medical School, University of Manchester, since June 1976. The patients were scanned in the supine position wearing a dressing gown and underclothes. The patients were positioned with their arms at their sides or above their heads. Two patients were too large to be scanned lying supine and were positioned slightly rotated with the affected breast uppermost.

*Department of Diagnostic Radiology, University of Manchester.
**Department of Diagnostic Radiology, University Hospital of South Manchester.
***Professorial Surgical Unit, University Hospital of South Manchester.

The level of the lesion was identified by palpation and inspection of the mammograms. The 32 cm ring was used and that part of the area to be reconstructed not occupied by patient was filled by bolus bags. The patients were scanned at 140 kVp at normal scan speed (20 s). The first scan was made just caudad to the lesion. The patient was scanned at 1 cm intervals moving towards the head for a total of 8 scans. If the axillae had not been scanned in this first series, further scans were made.

One patient was rescanned after intravenous injection of sodium iothalamate 420 mg iodine/ml (Conray 420).

All but 2 patients had undergone mammography. The mammograms were taken using a vacuum packed screen film technique (2), or were xerograms.

All the C.A.T. scans were reviewed using hard copy and interaction with the Diagnostic Display Console (D.D.C.). They were reviewed retrospectively in the light of the accumulated experience of the series by one observer (J.J.K.B.) and assigned to one of three categories:

a) Lesion not seen
b) Malignant
c) Benign

The mammograms were reported routinely. All patients had histological confirmation of their diagnoses.

Results

Table 1 correlates the results of mammography, histology and C.A.T.

Table 1.

Patient	Mammography	Histology	C.A.T.
E.McC.	M	M	M
A.B.	M	B	M
R.P.	M	M	M
I.H.	B	B	M
N.C.	M	M	-
E.B.	M	M	SU
M.L.	B	B	M
J.W.	NM	M	M
K.K.	M	M	-
C.M.	M	M	M
I.C.	B	M	M
A.McG.	M	M	M
B.K.	M	B	M
H.McL.	M	B	B
M.T.	M	M	M
L.W.	M	M	M
M.A.	M	M	M
J.S.	M	M	-
C.G.	M	M	M
E.S.	B	M	-
F.L.	B	B	B
N.D.	M	M	B
A.McD.	B	B	-

Table 1. Continued

Patient	Mammography	Histology	C.A.T.
E.M.	B	B	B
B.O'R.	M	M	M
J.D.	NM	B	SU
A.W.	B	B	-
M.D.	M	M	M
M.M.	M	M	SU
D.G.	M	B	-

M - Malignant, B - Benign, - Lesion not seen, NM - No mammograms, SU - Scan unsatisfactory

Table 2.

	Lesions detected	Correct diagnosis	False positive	False negative
Mammography[a]	28/28	22/28	4/28	2/28
C.A.T.[b]	20/27	15/27	4/27	1/27

[a]Two patients did not have mammograms.
[b]Three patients are not included as their scans were technically unsatisfactory.

Table 2 presents the results in terms of the lesions detected, the correct diagnoses, the false positive and false negative rates for both mammography and C.A.T.

Three patients had unsuccessful scans. The scans of two patients failed to reconstruct due to technical faults. The scans of the third patient were so degraded by movement artefact as to make them unreportable.

A normal pattern of breast periductal tissue, fibrous stroma and fat was recognised (Fig. 1). Benign lesions were identified as mass lesions of the same radio-density as the fibrous stroma of the breast with a clearly defined edge (Fig. 2). Malignant lesions caused more disruption of the stromal and periductal patterns with loss of definition between the fat and fibrous tissue (Fig. 3).

Microcalcification associated with carcinomas could not be recognised either by interaction with the D.D.C. or by examination of the printout of EMI numbers.

One unequivocal C.A.T. sign of malignancy was demonstrated: the presence of a mass lesion with an axillary mass identified as enlarged lymph nodes (Fig. 4).

In one patient the diagnosis of necrotic carcinoma was correctly made because of a mass lesion with lower EMI number in the centre and associated axillary lymph nodes (Fig. 5).

Discussion

The results presented show that C.A.T. using the technique described and the Manchester EMI CT5000 Whole Body Scanner detects carcinoma of the breast less well than conventional mammography. It is recognised that the technique used is open to criticism, but it was chosen for simplicity and to allow as large a number of patients as possible to be examined using an appointment system so as to reproduce the type of workload of a screening facility.

It had been expected that C.A.T. would be capable of detecting calcification in the breast, but in the patients in whom microcalcification was demonstrated by conventional mammographic or xerographic methods, calcium was not detected either by inspection of the hard copy or by interaction with the data on the D.D.C. In the one patient where calcium was detected this was distant from the mass and the histology of the specimen showed calcification in a region of duct ectasia separate from the lesion.

It is thought that the failure to identify microcalcification is due to the small size of the calcifications, diameter 100 μm-300 μm[9]. This is smaller than the spatial resolution of the EMI CT5000 scanner, which is in the order of 1.0 mm. The microcalcifications will affect the mean attenuation value for the computed volume of tissue ("voxel") by a small amount which may be within the variation due to noise.

An expected advantage of whole body C.A.T. over conventional mammography and C.A.T. using special mammographic C.A.T. scanners, was the opportunity to detect carcinoma spread to axillary lymph glands. In this study unenlarged lymph glands could not be reliably identified. It is thought that this is because lymph nodes contain quantities of fat, some with only a rim of lymphoid tissue (Fig. 6) and are embedded in axillary fat. Because of the limitations of spatial resolution, as previously discussed, and the 'partial volume' effect, i.e. an interface passing obliquely through a voxel of tissue, lymph nodes may not be visualised.

Lymph nodes in which malignant cells are detected by histology may be only partially replaced by malignant cells. In three patients in this study enlarged lymph nodes were identified.

An important consideration when employing a screening procedure using ionizing radiation is the dose to the patient. It has been concluded that 6-monthly mammographic examinations over a 10-year period might induce a risk of breast cancer unless the dose per examination is reduced below 2 rads (5). The maximum skin dose with the vacuum packed screen film technique used for this study was in the order of 0.2 rads (2). Xeromammography delivers a skin dose reported to be approximately 5 rads for a single view exposure (4, 12). The absorbed dose received in a C.A.T. examination is the dose delivered in one scan together with contributions due to "pile up" from adjacent scans. The accumulated dose for the centre scan of 5 scans is in the order of 5 rads (8). Work presented at this seminar (11) suggests that the accumulated dose may be even higher.

It is realised that the numbers in this pilot study are too small for any great significance to be attached to them. If the rates of malignancies missed by mammography and C.A.T. are compared (Table 3) it may be seen that the difference is due to the eight carcinomas that were not detected by C.A.T.

Table 3. Malignancies missed

Mammography	2/18[a]	(6/60)	11%	(10%)
C.A.T.	6/17[b]	(19/60)	35%	(31.7%)

The figures in parentheses relate to results reported using the G.E. CT/M (REESE, 1976).
[a]One patient did not have a mammogram.
[b]Two patients are omitted from the C.A.T. total as two of the unsatisfactory scans were in patients with carcinoma.

It is thought that C.A.T., with its unique facility for quantifying variations in attenuation values of tissue, has a role to play in the diagnosis of breast carcinoma. It is intended to continue the trial scanning three groups of patients:

1. Patients with abnormal mammograms but with normal clinical findings

2. Patients whose mammograms show dense fibrous stroma which makes interpretation of mammography difficult

3. Patients with possible secondary spread, as shown by positive radio-isotope bone scans, but with negative X-rays

It is intended to modify the technique and use intravenous contrast to investigate the role of contrast enhancement as a reliable guide to the nature of lesions (Fig. 7). It is hoped to undertake statistical evaluation of the scan data and, following evaluation of the noise characteristics of the CT5000 scanner, it may prove possible to use the autocorrelation function to characterise changes in breast tissue and its response to disease (11).

In conclusion, it is felt that C.A.T. using the technique which was adopted for this pilot study does not provide a useful screening technique for carcinoma of the breast. This conclusion is based on the limitations of C.A.T. to detect carcinoma of the breast, as have been discussed, and on the considerations of radiation dose to the patient. It is thought this latter factor alone may preclude its use as a screening tool. If the cost effectiveness of the procedure is also considered, this reinforces the conclusion.

Acknowledgments

The authors are grateful to Miss G.S. Lord, Superintendent Radiographer, and the Radiographic staff of the Department of Diagnostic Radiology for their assistance. Thanks are also due to Mrs. G.E.H. Shawcross for preparation of illustrative material, to the Radiographic staff of the University Hospital of South Manchester and to Mrs. S. Andrews, Mrs. B. Fowler and Mrs. M. Tipton for secretarial help.

References

1. AMBROSE, J.: Computerised transverse axial scanning (tomography) Part 2. Clinical application. British Journal of Radiology 46, 1023-1047 (1973).

2. ASBURY, D.L., BARKER, P.G.: Radiation dosage to the breast in well women - screening surveys. British Journal of Radiology 48, 963-967 (1975).
3. BLACK, J.W., YOUNG, B.: A radiological and pathological study of the incidence of calcification in diseases of the breast and neoplasms of other tissues. British Journal of Radiology 38, 596-598 (1965).
4. BOAG, J.W., STACEY, A.J., DAVIS, R.: Radiation exposure to the patient in Xeroradiography. British Journal of Radiology 49, 253-261 (1976).
5. ELLIS, R.E.: Breast cancer following irradiation. British Journal of Radiology 45, 795 (1972).
6. FISHER, E.R., GREGORIO, R.M., FISHER, B.: A syllabus derived from findings of the National Surgical Adjuvant Breast Project (Protocol No. 4). Cancer 36, 1-84 (1975).
7. LEVITAN, L.H., WITTEN, D.M., HARRISON, E.G.: Calcification in breast disease, mammographic-pathological correlation. Amer. J. Roentgenol. 92, 29-39 (1964).
8. McCULLOUGH, E.C., PAYNE, J.T., BAKER, H.L., HATTERY, R.R., SHEEDY, P.F., STEPHENS, D.H., GEDGAUDUS, E.: Performance evaluation and quality assurance of computed tomography scanners, with illustrations from the EMI, ACTA and Delta scanners. Radiology 120, 173-188 (1976).
9. MILLIS, R.R., DAVIS, R., STACEY, A.J.: The detection and significance of calcifications in the breast, a radiological and pathological study. British Journal of Radiology 49, 12-26 (1976).
10. RUTHERFORD, R.A., PULLAN, B.R., ISHERWOOD, I.: Calibration and response of an EMI scanner. Neuroradiology 11, 7-13 (1976).
11. RUTHERFORD, R.A., PULLAN, B.R.: European Seminar on Computerised Axial Tomography in Clinical Practice, 1976.
12. RUZICKA, F.F., KAUFMAN, L., SHAPIRO, G., PEREZ, J., GROSSI, C.: Xeromammography and film mammography. Radiology 85, 260-269 (1965).
13. SHAPIRO, S., STRAX, P., VENET, L.: Periodic breast cancer screening in reducing mortality of breast cancer. Journal of the American Medical Association 215, 1777-1785 (1971).
14. TONGE, K.A., DAVIS, R., MILLIS, R.R.: The problems of discrimination in mammography. Arguments for using a biological test object. British Journal of Radiology 49, 678-685 (1976).

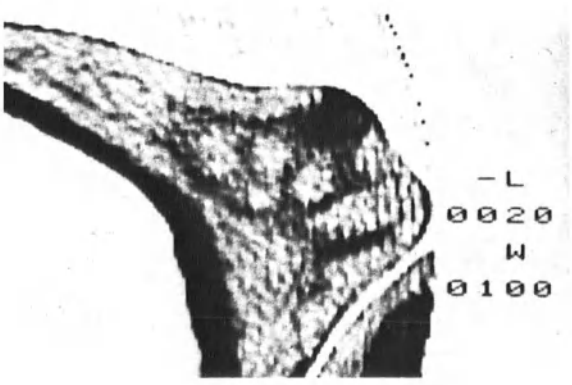

Fig. 1. Normal breast pattern

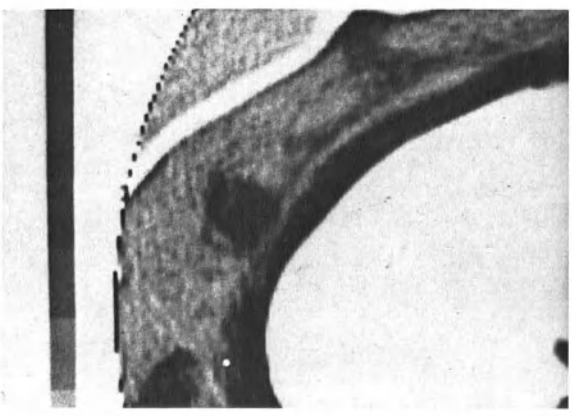

Fig. 2. Benign breast lesion

Fig. 3. Malignant breast lesion

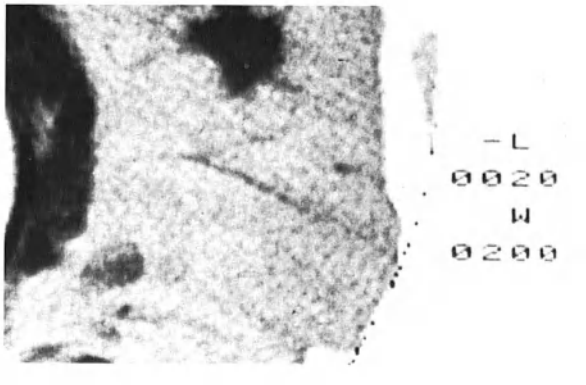

Fig. 4. Malignant lesion and enlarged axially lymph node

Fig. 5. Carcinoma with central necrosis

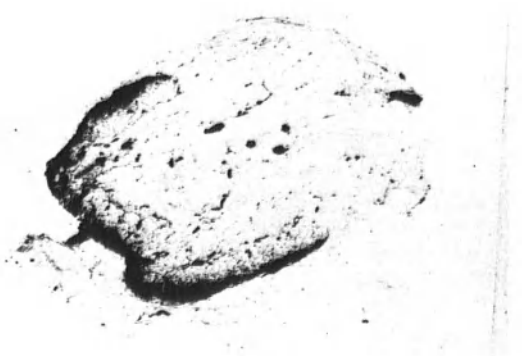

Fig. 6. Lymph node containing fatty tissue (histological section)

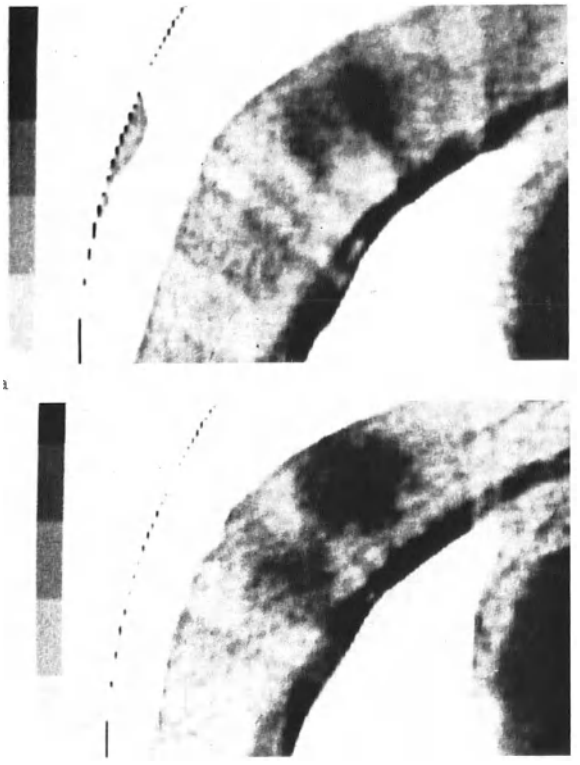

Fig. 7a and b. Carcinoma of breast (a) before contrast enhancement; (b) with contrast enhancement

Subject Index

FURTHER TITLES

S. Takahashi, S. Sakuma
Magnification Radiography
59 figures. VII, 110 pages. 1975
ISBN 3-540-07238-1

G. Salamon, Y.P. Huang
Radiologic Anatomy of the Brain
In cooperation with numerous experts
282 figures in 463 separate illustrations. XII, 404 pages. 1976
ISBN 3-540-07528-3
Distribution rights for Japan: Nankodo Co. Ltd., Tokyo

M.A. Meyers
Dynamic Radiology of the Abdomen
Normal and Pathologic Anatomy
With a Contribution Ultrasonography by E. Kazam
638 figures, including 14 color plates. LVI, 351 pages. 1976
ISBN 3-540-90178-7

Computerized Axial Tomography
An Anatomic Atlas of Serial Sections of the Human Body
Anatomy - Radiology - Scanner
By J. Gambarelli, G. Guérinel, L. Chevrot, M. Mattèi
With the technical collaboration of R. Galliano, S. Nazarian, Drawings by J.P. Jacomy, Photographies by D. Amy, M. Solor
550 figures (some in color), Approx 305 pages. 1977
ISBN 3-540-07961-0
This atlas will also be published in German

Advances in Cerebral Angiography
Anatomy - Stereotaxy - Embolization - Computerized Axial Tomography
INSERM-Symposium Marseille, May 13-16, 1975
Editor: G. Salamon
222 figures, 8 tables. XVI, 375 pages. 1975
ISBN 3-540-07569-0
Distribution rights for Japan: Nankodo Co. Ltd., Tokyo

S. Wende, E. Zieler, N. Nakayama
Cerebral Magnification Angiography
Physical Basis and Clinical Results
With the collaboration of K. Schindler
141 figures. VII, 150 pages. 1974
ISBN 3-540-06651-9
Distribution rights for Japan: Igaku Shoin Ltd., Tokyo

Springer-Verlag Berlin Heidelberg New York

A.S. Takahashi
An Atlas of Axial Transverse Tomography and its Clinical Application
576 figures. VII, 329 pages. 1969
ISBN 3-540-04730-1

A. Wackenheim
Roentgen Diagnosis of the Craniovertebral Region
500 figures, XXII, 601 pages. 1974
ISBN 3-540-06615-2
Distribution rights for Japan: Igaku Shoin Ltd., Tokyo

B. Schlesinger
The Upper Brainstem in the Human
Its Nuclear Configuration and Vascular Supply
With a Foreword by H. Ferner
326 figures, some in color, 10 tables. XVI, 266 pages. 1976
ISBN 3-540-07497-X

Radiological Exploration of the Ventricles and Subarachnoid Space
By G. Ruggiero, J. Bories, A. Calabrò, G. Christi, G. Scialfa, F. Smaltino, A. Thibaut
With the cooperation of G. Gianasi, G. Maranghi, C. Philippart, E. Signorini
90 partly colored (279 separate illustrations). XIV, 152 pages. 1974
ISBN 3-540-06572-5
Distribution rights for Japan: Igaku Shoin Ltd., Tokyo

Cranial Computerized Tomography
Proceedings of the Symposium Munich, June 10-12, 1976
Editors: W. Lanksch, E. Kazner
Editorial Board: T. Grumme, F. Marguth, H.R. Müller, H. Steinhoff, S. Wende
620 figures. XIV, 478 pages. 1976
ISBN 3-540-07938-6
Distribution rights for Japan: Nankodo Co. Ltd., Tokyo

IN PREPARATION
R. Djindjian, J.-J. Merland
Super-Selective Arteriography of the External Carotid Artery
With collaboration of J. Théron
Translated from the French by I.F. Moseley. - Preface by P.R. Houdart
1068 figures, 5 plates, some in colour, Approx. 990 pages. 1977
ISBN 3-540-08118-6

G. Szikla
Angiography of the Human Brain Cortex

Springer-Verlag Berlin Heidelberg New York